

X69-77591 c1

**GEORGE C. MARSHALL SPACE FLIGHT CENTER**

# SATURN

MPR-SAT-FE-69-4

MAY 5, 1969

## SATURN V LAUNCH VEHICLE FLIGHT EVALUATION REPORT-AS-504 APOLLO 9 MISSION

LIBRARY

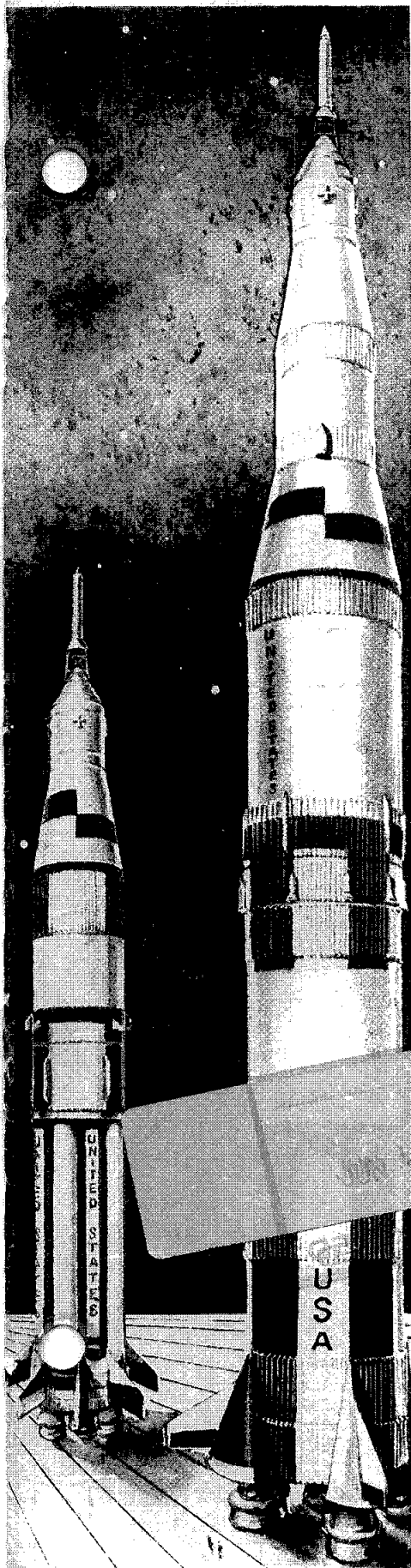
MAY 19 1969

MANNED SPACECRAFT CENTER  
HOUSTON, TEXAS

PREPARED BY  
SATURN FLIGHT EVALUATION WORKING GROUP



NATIONAL AERONAUTICS AND SPACE ADMINISTRATION

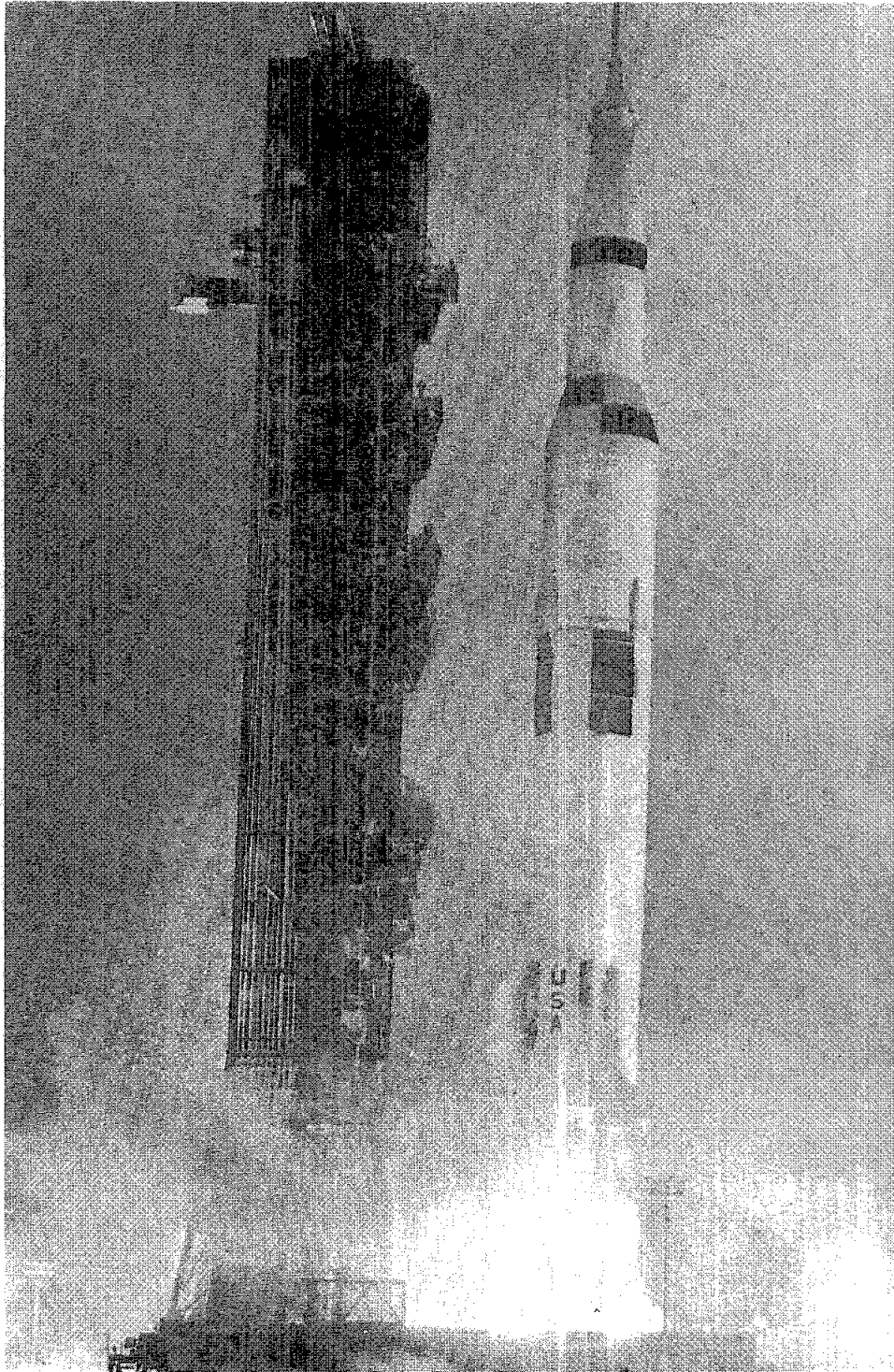


**GEORGE C. MARSHALL SPACE FLIGHT CENTER**

**MPR-SAT-FE-69-4**

**SATURN V LAUNCH VEHICLE  
FLIGHT EVALUATION REPORT - AS-504  
APOLLO 9 MISSION**

**PREPARED BY  
SATURN FLIGHT EVALUATION WORKING GROUP**



AS-504 LAUNCH VEHICLE

MPR-SAT-FE-69-4

SATURN V LAUNCH VEHICLE FLIGHT EVALUATION REPORT - AS-504  
APOLLO 9 MISSION

BY

Saturn Flight Evaluation Working Group  
George C. Marshall Space Flight Center

ABSTRACT

Saturn V AS-504 (Apollo 9 Mission) was launched at 11:00:00 Eastern Standard Time on March 3, 1969, from Kennedy Space Center, Complex 39, Pad A. The vehicle lifted off on schedule on a launch azimuth of 90 degrees east of north and rolled to a flight azimuth of 72 degrees east of north.

The S-IVB Third Burn test under contingency start conditions was not completely normal; however, it was successful in increasing the S-IVB/IU energy to attain escape velocity. The S-IVB/IU entered a solar orbit with a period of 325.8 days.

The principal Detailed Test Objective (DTO) of this mission was completely accomplished. Nine of the eleven secondary DTO's were completely accomplished, and two partially accomplished. No failures, anomalies or deviations occurred that seriously affected the flight or mission.

Any questions or comments pertaining to the information contained in this report are invited and should be directed to:

Director, George C. Marshall Space Flight Center  
Huntsville, Alabama 35812  
Attention: Chairman, Saturn Flight Evaluation  
Working Group, S&E-AERO-F (Phone 453-0357)

## TABLE OF CONTENTS

Section		Page
	TABLE OF CONTENTS	iii
	LIST OF ILLUSTRATIONS	xiii
	LIST OF TABLES	xxiii
	ACKNOWLEDGEMENT	xxviii
	ABBREVIATIONS	xxix
	MISSION PLAN	xxxiii
	FLIGHT TEST SUMMARY	xxxv
1	INTRODUCTION	
	1.1 Purpose	1-1
	1.2 Scope	1-1
2	EVENT TIMES	
	2.1 Summary of Events	2-1
	2.2 Variable Time and Commanded Switch Selector Events	2-3
3	LAUNCH OPERATIONS	
	3.1 Summary	3-1
	3.2 Prelaunch Milestones	3-1
	3.3 Countdown Events	3-1
	3.4 Propellant Loading	3-2
	3.4.1 RP-1 Loading	3-2
	3.4.2 LOX Loading	3-2
	3.4.3 LH <sub>2</sub> Loading	3-2
	3.4.4 Auxiliary Propulsion System Propellant Loading	3-3

TABLE OF CONTENTS (CONTINUED)

Section		Page
3.5	S-II Insulation, Purge and Leak Detection	3-3
3.5.1	Forward Bulkhead Insulation/Forward Bulkhead Uninsulated Circuits	3-3
3.5.2	Forward Skirt	3-3
3.5.3	Sidewall	3-4
3.5.4	Cylinder 1, Bolting Ring and J-Ring Combined Circuits	3-4
3.5.5	Common Bulkhead	3-4
3.5.6	Feedline Elbow	3-5
3.6	Ground Support Equipment	3-5
3.6.1	Ground/Vehicle Interface	3-5
3.6.2	MSFC Furnished Ground Support Equipment	3-6
4	TRAJECTORY	
4.1	Summary	4-1
4.2	Tracking Data Utilization	4-2
4.2.1	Tracking During the Ascent Phase of Flight	4-2
4.2.2	Tracking During Orbital Flight	4-2
4.2.3	Tracking During S-IVB Second Burn Phase of Flight	4-3
4.2.4	Tracking During S-IVB Third Burn Phase of Flight	4-3
4.3	Trajectory Evaluation	4-3
4.3.1	Ascent Trajectory	4-3
4.3.2	Parking Orbit Trajectory	4-9
4.3.3	S-IVB Second Burn Trajectory	4-10
4.3.4	Intermediate Orbit Trajectory	4-14
4.3.5	S-IVB Third Burn Trajectory	4-14
4.3.6	Escape Orbit Trajectory	4-14
5	S-IC PROPULSION	
5.1	Summary	5-1
5.2	S-IC Ignition Transient Performance	5-1
5.3	S-IC Main Stage Performance	5-3
5.4	S-IC Engine Shutdown Transient Performance	5-7

TABLE OF CONTENTS (CONTINUED)

Section		Page
	5.5 S-IC Stage Propellant Management	5-8
	5.6 S-IC Pressurization Systems	5-9
	5.6.1 S-IC Fuel Pressurization System	5-9
	5.6.2 S-IC LOX Pressurization System	5-10
	5.7 S-IC Pneumatic Control Pressure System	5-14
	5.8 S-IC Purge Systems	5-14
	5.9 POGO Suppression System	5-14
6	S-II PROPULSION	
	6.1 Summary	6-1
	6.2 S-II Chillover and Buildup Transient Performance	6-2
	6.3 S-II Main Stage Performance	6-4
	6.4 S-II Shutdown Transient Performance	6-13
	6.5 S-II Stage Propellant Management	6-13
	6.6 S-II Pressurization Systems	6-16
	6.6.1 S-II Fuel Pressurization System	6-16
	6.6.2 S-II LOX Pressurization System	6-18
	6.7 S-II Pneumatic Control Pressure System	6-21
	6.8 S-II Helium Injection System	6-24
7	S-IVB PROPULSION	
	7.1 Summary	7-1
	7.2 S-IVB Chillover and Buildup Transient Performance for First Burn	7-2
	7.3 S-IVB Main Stage Performance for First Burn	7-6
	7.4 S-IVB Shutdown Transient Performance for First Burn	7-9
	7.5 S-IVB Parking Coast Phase Conditioning	7-9

TABLE OF CONTENTS (CONTINUED)

Section		Page
7.6	S-IVB Chilldown and Restart for Second Burn	7-11
7.7	S-IVB Main Stage Performance for Second Burn	7-19
7.8	S-IVB Shutdown Transient Performance for Second Burn	7-26
7.9	S-IVB Intermediate Orbit Coast Phase Conditioning	7-26
7.10	S-IVB Engine Chilldown and Buildup Transient Performance for Third Burn	7-26
7.11	S-IVB Main Stage Performance for Third Burn	7-30
7.12	S-IVB Shutdown Transient Performance for Third Burn	7-38
7.13	S-IVB Stage Propellant Management	7-39
7.14	S-IVB Pressurization System	7-40
7.14.1	S-IVB Fuel Pressurization System	7-40
7.14.2	S-IVB LOX Pressurization System	7-47
7.15	S-IVB Pneumatic Control Pressure System	7-50
7.16	S-IVB Auxiliary Propulsion System	7-61
7.17	S-IVB Orbital Safing Operation	7-63
7.17.1	Fuel Tank Safing	7-63
7.17.2	LOX Tank Dump and Safing	7-64
7.17.3	Cold Helium Dump	7-66
7.17.4	Ambient Helium Dump	7-66
7.17.5	Stage Pneumatic Control Sphere Safing	7-66
7.17.6	Engine Start Tank Safing	7-66
7.17.7	Engine Control Sphere Safing	7-66
8	HYDRAULIC SYSTEMS	
8.1	Summary	8-1
8.2	S-IC Hydraulic System	8-1
8.3	S-II Hydraulic System	8-1
8.4	S-IVB Hydraulic System	8-1



TABLE OF CONTENTS (CONTINUED)

Section		Page
9	STRUCTURES	
	9.1 Summary	9-1
	9.2 Total Vehicle Structures Evaluation	9-1
	9.2.1 Longitudinal Loads	9-1
	9.2.2 Bending Moments	9-2
	9.2.3 Vehicle Dynamic Characteristics	9-4
	9.3 Vibration Evaluation	9-8
	9.3.1 S-IC Stage and Engine Evaluation	9-8
	9.3.2 S-II Stage and Engine Evaluation	9-13
10	GUIDANCE AND NAVIGATION	
	10.1 Summary	10-1
	10.1.1 Flight Program	10-1
	10.1.2 Instrument Unit Components	10-1
	10.2 Guidance and Navigation System Description	10-1
	10.2.1 Flight Program Description	10-1
	10.2.2 Instrument Unit System Description	10-3
	10.3 Guidance Comparisons	10-3
	10.4 Navigation and Guidance Scheme Evaluation	10-10
	10.4.1 Flight Program Performance	10-10
	10.4.2 Attitude Error Computations	10-11
	10.4.3 Program Sequencing	10-11
	10.5 Guidance System Component Evaluation	10-11
	10.5.1 LVDC Performance	10-11
	10.5.2 LVDA Performance	10-11
	10.5.3 Ladder Outputs	10-14
	10.5.4 Telemetry Outputs	10-14
	10.5.5 Discrete Outputs	10-14
	10.5.6 Switch Selector Functions	10-14
	10.5.7 ST-124M-3 Inertial Platform Performance	10-14
11	CONTROL SYSTEM	
	11.1 Summary	11-1
	11.2 Control System Description	11-2

## TABLE OF CONTENTS (CONTINUED)

Section		Page
11.3	S-IC Control System Evaluation	11-2
11.3.1	Liftoff Clearances	11-2
11.3.2	S-IC Flight Dynamics	11-3
11.4	S-II Control System Evaluation	11-10
11.4.1	Attitude Control Dynamics and Stability	11-10
11.4.2	Liquid Propellant Dynamics and Their Effects on Flight Control	11-16
11.5	S-IVB Control System Evaluation	11-16
11.5.1	Control System Evaluation During First Burn	11-18
11.5.2	Control System Evaluation During Parking Orbit	11-18
11.5.3	Control System Evaluation During Second Burn	11-18
11.5.4	Control System Evaluation During Intermediate Orbit	11-37
11.5.5	Control System Evaluation During Third Burn	11-37
11.6	Instrument Unit Control Components Evaluation	11-47
SEPARATION		
12.1	Summary	12-1
12.2	S-IC/S-II Separation Evaluation	12-1
12.2.1	S-IC Retro Motor Performance	12-1
12.2.2	S-II Ullage Motor Performance	12-2
12.2.3	S-IC/S-II Stage Separation	12-2
12.3	S-II Second Plane Separation Evaluation	12-9
12.4	S-II/S-IVB Separation Evaluation	12-9
12.4.1	S-II Retro Motor Performance	12-9
12.4.2	S-IVB Ullage Motor Performance	12-9
12.4.3	S-II/S-IVB Separation Dynamics	12-9
12.5	S-IVB/IU/LM/CSM Separation Evaluation	12-10
12.6	Lunar Module Ejection Evaluation	12-10

TABLE OF CONTENTS (CONTINUED)

Section		Page
13	ELECTRICAL NETWORKS	
	13.1 Summary	13-1
	13.2 S-IC Stage Electrical System	13-1
	13.3 S-II Stage Electrical System	13-4
	13.4 S-IVB Stage Electrical System	13-4
	13.5 Instrument Unit Electrical System	13-21
14	RANGE SAFETY AND COMMAND SYSTEMS	
	14.1 Summary	14-1
	14.2 Range Safety Command Systems	14-1
	14.3 Command and Communications System	14-2
15	EMERGENCY DETECTION SYSTEM	
	15.1 Summary	15-1
	15.2 System Evaluation	15-1
	15.2.1 General Performance	15-1
	15.2.2 Propulsion System Sensors	15-1
	15.2.3 Flight Dynamics and Control Sensors	15-2
16	VEHICLE PRESSURE AND ACOUSTIC ENVIRONMENT	
	16.1 Summary	16-1
	16.2 Surface Pressures and Compartment Venting	16-1
	16.2.1 S-IC Stage	16-1
	16.2.2 S-II Stage	16-5
	16.3 Base Pressures	16-5
	16.3.1 S-IC Base Pressures	16-5
	16.3.2 S-II Base Pressures	16-5
	16.4 Acoustic Environment	16-9
	16.4.1 External Acoustics	16-9
	16.4.2 Internal Acoustics	16-12
17	VEHICLE THERMAL ENVIRONMENT	
	17.1 Summary	17-1
	17.2 S-IC Base Heating and Separation Environment	17-1

TABLE OF CONTENTS (CONTINUED)

Section		Page
	17.2.1 S-IC Base Heating	17-1
	17.2.2 S-IC/S-II Separation Environment	17-6
	17.3 S-II Base Heating and Separation Environment	17-7
	17.4 Vehicle Aeroheating Thermal Environment	17-12
	17.4.1 S-IC Stage Aeroheating Environment	17-12
	17.4.2 S-II Stage Aeroheating Environment	17-16
18	ENVIRONMENTAL CONTROL SYSTEM	
	18.1 Summary	18-1
	18.2 S-IC Environmental Control	18-1
	18.3 S-II Environmental Control	18-4
	18.4 IU Environmental Control	18-6
	18.4.1 Thermal Conditioning System	18-6
	18.4.2 Gas Bearing Supply System	18-11
19	DATA SYSTEMS	
	19.1 Summary	19-1
	19.2 Vehicle Measurements Evaluation	19-1
	19.2.1 S-IC Stage Measurement Analysis	19-2
	19.2.2 S-II Stage Measurement Analysis	19-2
	19.2.3 S-IVB Stage Measurement Analysis	19-7
	19.2.4 IU Measurement Analysis	19-8
	19.3 Airborne Telemetry Systems	19-8
	19.3.1 S-IC Stage Telemetry System	19-9
	19.3.2 S-II Stage Telemetry System	19-9
	19.3.3 S-IVB Stage Telemetry System	19-9
	19.3.4 IU Telemetry System	19-10
	19.4 Airborne Tape Recorders	19-11
	19.4.1 S-IC Stage Recorder	19-11
	19.4.2 S-II Stage Recorders	19-11
	19.5 RF Systems Evaluation	19-12
	19.5.1 Telemetry System RF Propagation Evaluation	19-13
	19.5.2 Tracking Systems RF Propagation Evaluation	19-14
	19.5.3 Command Systems RF Evaluation	19-16
	19.6 Optical Instrumentation	19-20

## TABLE OF CONTENTS (CONTINUED)

Section		Page
20	VEHICLE AERODYNAMIC CHARACTERISTICS	20-1
21	MASS CHARACTERISTICS	
	21.1 Summary	21-1
	21.2 Mass Evaluation	21-1
22	MISSION OBJECTIVES ACCOMPLISHMENT	22-1
23	FAILURES, ANOMALIES AND DEVIATIONS	
	23.1 Summary	23-1
	23.2 System Failures and Anomalies	23-1
	23.3 System Deviation	23-1
24	SPACECRAFT SUMMARY	24-1
Appendix		
A	ATMOSPHERE	
	A.1 Summary	A-1
	A.2 General Atmospheric Conditions at Launch Time	A-1
	A.3 Surface Observations at Launch Time	A-1
	A.4 Upper Air Measurements	A-1
	A.4.1 Wind Speed	A-1
	A.4.2 Wind Direction	A-1
	A.4.3 Pitch Wind Component	A-2
	A.4.4 Yaw Wind Component	A-2
	A.4.5 Component Wind Shears	A-2
	A.4.6 Extreme Wind Data in the High Dynamic Pressure Region	A-2
	A.5 Thermodynamic Data	A-2
	A.5.1 Temperature	A-2
	A.5.2 Atmospheric Pressure	A-2
	A.5.3 Atmospheric Density	A-3
	A.5.4 Optical Index of Refraction	A-3
	A.6 Comparison of Selected Atmospheric Data for all Saturn Launches	A-3

TABLE OF CONTENTS (CONTINUED)

Appendix		Page
B	AS-504 VEHICLE DESCRIPTION	
	B.1 Summary	B-1
	B.2 S-IC Stage	B-1
	B.2.1 S-IC Configuration	B-1
	B.3 S-II Stage	B-6
	B.3.1 S-II Configuration	B-6
	B.4 S-IVB Stage	B-9
	B.4.1 S-IVB Configuration	B-9
	B.5 Instrument Unit (IU)	B-14
	B.5.1 IU Configuration	B-14
	B.6 Spacecraft	B-14
	B.6.1 Spacecraft Configuration	B-14

## LIST OF ILLUSTRATIONS

Figure		Page
2-1	Telemetry Time Delay	2-2
4-1	Ascent Trajectory Position Comparison	4-4
4-2	Ascent Trajectory Space-Fixed Velocity Comparison	4-9
4-3	Ascent Trajectory Acceleration Comparison	4-10
4-4	Dynamic Pressure and Mach Number	4-11
4-5	Acceleration Due to Venting - Parking Orbit	4-11
4-6	Ground Track	4-13
4-7	S-IVB Second Burn Phase Space-Fixed Velocity Comparison	4-13
4-8	S-IVB Second Burn Phase Acceleration Comparison	4-16
4-9	Acceleration Due to Venting - Intermediate Orbit	4-16
4-10	S-IVB Third Burn Phase Space-Fixed Velocity Comparison	4-17
4-11	S-IVB Third Burn Phase Acceleration Comparison	4-17
4-12	APS Velocity Increment	4-18
5-1	S-IC Start Box Requirements	5-2
5-2	S-IC Engine Buildup Transient	5-3
5-3	S-IC Steady State Operation	5-5
5-4	S-IC Outboard Engine Cutoff Deviations	5-7
5-5	S-IC Engine Shutdown Transient Performance	5-8
5-6	S-IC Fuel Ullage Pressure	5-10
5-7	S-IC Fuel Pump Inlet Pressure, Engine No. 2	5-11
5-8	S-IC Helium Bottle Pressure for Fuel Pressurization	5-11
5-9	S-IC LOX Tank Ullage Pressure	5-12
5-10	S-IC LOX Suction Duct Pressure, Engine No. 2	5-13
5-11	S-IC LOX Suction Duct Pressure, Engine No. 5	5-13
5-12	S-IC Center Engine LOX Suction Line Pressure	5-15
5-13	S-IC Control Sphere Pressure	5-16

## LIST OF ILLUSTRATIONS

Figure		Page
5-14	S-IC Prevalve Liquid Level, Typical Outboard Engine	5-17
6-1	S-II Thrust Chamber Jacket Temperature	6-2
6-2	S-II Engine Start Tank Performance	6-3
6-3	S-II Engine Pump Inlet Start Requirements	6-5
6-4	S-II Engine Thrust Buildup	6-6
6-5	S-II Steady State Operation	6-8
6-6	S-II LOX NPSP History	6-11
6-7	S-II Inflight LOX Level History	6-12
6-8	S-II Engine Shutdown Transient	6-14
6-9	S-II Stage Thrust Decay	6-14
6-10	S-II PU Valve Position	6-16
6-11	S-II Fuel Tank Ullage Pressure	6-18
6-12	S-II Fuel Pump Inlet Conditions	6-19
6-13	S-II Engine No. 1 LH <sub>2</sub> Inlet Pressure	6-20
6-14	S-II Engine No. 5 LH <sub>2</sub> Inlet Pressure	6-20
6-15	S-II LOX Tank Ullage Pressure	6-20
6-16	S-II LOX Pump Inlet Conditions	6-22
6-17	S-II Engine No. 1 LOX Inlet Pressure	6-23
6-18	S-II Engine No. 5 LOX Inlet Pressure	6-23
6-19	S-II Pneumatic Control Pressures	6-24
7-1	S-IVB Start Box and Run Requirements - First Burn	7-3
7-2	S-IVB Fuel Injector Temperature - First Burn	7-4
7-3	S-IVB Start Tank Performance - First Burn	7-5
7-4	S-IVB Buildup Transient - First Burn	7-6
7-5	S-IVB Steady State Performance - First Burn	7-8
7-6	S-IVB Shutdown Transient Performance - First Burn	7-12
7-7	S-IVB CVS Performance	7-13
7-8	S-IVB Ullage Conditions During Repressurization Using O <sub>2</sub> /H <sub>2</sub> Burner - First Restart	7-16
7-9	O <sub>2</sub> /H <sub>2</sub> Burner LH <sub>2</sub> Pressurant Coil Discharge Conditions - First Restart	7-17
7-10	S-IVB O <sub>2</sub> /H <sub>2</sub> Burner Thrust and Thrust Chamber Conditions - First Restart	7-18



## LIST OF ILLUSTRATIONS (CONTINUED)

Figure		Page
7-11	S-IVB Start Box and Run Requirements - Second Burn	7-20
7-12	S-IVB Fuel Lead - Second Burn	7-21
7-13	S-IVB Buildup Transients - Second Burn	7-22
7-14	S-IVB Start Tank Performance - Second Burn	7-22
7-15	S-IVB Steady State Performance - Second Burn	7-23
7-16	S-IVB Shutdown Transient Performance - Second Burn	7-27
7-17	LH <sub>2</sub> and LOX Ambient Repressurization Sphere Pressures and LH <sub>2</sub> Ullage Pressure	7-28
7-18	S-IVB O <sub>2</sub> /H <sub>2</sub> Burner Thrust and Thrust Chamber Conditions - Second Burn	7-29
7-19	S-IVB Start Box and Run Requirements - Third Burn	7-31
7-20	S-IVB Start Tank Performance - Third Burn	7-32
7-21	Effects of Extended S-IVB LH <sub>2</sub> Lead - Third Burn	7-33
7-22	S-IVB Buildup Transient - Third Burn	7-34
7-23	S-IVB Transient Chamber Pressure and LH <sub>2</sub> Injection Temperature - Third Burn	7-35
7-24	S-IVB Steady State Performance - Third Burn	7-37
7-25	Flow Diagram, Summary of S-IVB Third Burn Anomalies	7-40
7-26	S-IVB Third Burn Sequence of Events	7-41
7-27	S-IVB Gas Generator Chamber Pressure - Third Burn Start Transient	7-42
7-28	S-IVB Thrust Chamber Jacket and Engine Area Ambient Temperatures - Third Burn	7-43
7-29	S-IVB Engine Regulator Outlet Pressure	7-44
7-30	S-IVB Control Sphere Pressure - Third Burn	7-45
7-31	S-IVB Engine Valve Position - Third Burn	7-46
7-32	S-IVB Shutdown Transient Performance - Third Burn	7-48

## LIST OF ILLUSTRATIONS (CONTINUED)

Figure		Page
7-33	S-IVB LH <sub>2</sub> Ullage Pressure - First Burn and Parking Orbit	7-48
7-34	S-IVB LH <sub>2</sub> Ullage Pressure - Second and Third Burn	7-50
7-35	S-IVB Fuel Pump Inlet Conditions - First Burn	7-51
7-36	S-IVB Fuel Pump Inlet Conditions - Second Burn	7-52
7-37	S-IVB Fuel Pump Inlet Conditions - Third Burn	7-53
7-38	S-IVB LOX Tank Ullage Pressure - First Burn and Parking Orbit	7-54
7-39	S-IVB LOX Tank Ullage Pressure - Second Burn, Intermediate Coast and Third Burn	7-55
7-40	S-IVB LOX Pump Inlet Conditions - First Burn	7-56
7-41	S-IVB LOX Pump Inlet Conditions - Second Burn	7-57
7-42	S-IVB LOX Pump Inlet Conditions - Third Burn	7-58
7-43	S-IVB Pneumatic Control Performance	7-59
7-44	S-IVB APS Propellant Remaining Versus Mission Time - Module No. 2	7-63
7-45	S-IVB APS Propellant Remaining Versus Mission Time - Module No. 1	7-64
7-46	S-IVB Cold Helium Supply History	7-67
7-47	S-IVB Ambient Helium Repressurization Spheres Safing	7-68
7-48	S-IVB Start Tank Safing	7-68
7-49	S-IVB Pneumatic Safing History	7-69
8-1	S-IVB Hydraulic System Actuator Positions - Third Burn	8-2
8-2	S-IVB Hydraulic System Actuator Performance - Third Burn	8-4
8-3	S-IVB Hydraulic Reservoir Performance - Third Burn	8-5
8-4	S-IVB Hydraulic System Temperature - Third Burn	8-6
8-5	S-IVB Pitch Actuator Signal and Position - Third Burn	8-7

LIST OF ILLUSTRATIONS (CONTINUED)

Figure		Page
8-6	S-IVB Yaw Actuator Signal and Position - Third Burn	8-7
9-1	Longitudinal Loads at Maximum Bending Moment, Center Engine Cutoff, and Outboard Engine Cutoff	9-2
9-2	Longitudinal Structural Dynamic Response Due to Outboard Engine Cutoff	9-3
9-3	Maximum Bending Moment Near Max Q	9-4
9-4	First Longitudinal Modal Frequencies and Amplitudes During S-IC Powered Flight	9-5
9-5	S-II Stage Response/Frequency Characteristics	9-7
9-6	AS-504 Lateral Analysis/Measured Modal Frequency Correlation	9-8
9-7	S-IC Stage Structure Vibration Envelopes	9-10
9-8	S-IC Stage Engine Turbopump Vibration Envelope	9-11
9-9	S-IC Stage Components Vibration Envelopes	9-11
9-10	S-IC Vibration Measurement Locations	9-12
9-11	S-II Stage Structure Vibration Envelopes	9-15
9-12	S-II Stage Engine Vibration Envelopes	9-17
9-13	S-II Stage Component Vibration Envelopes	9-18
10-1	Tracking and ST-124M-3 Platform Velocity Comparison (Trajectory Minus Guidance)	10-4
10-2	Attitude Commands During Active Guidance Period	10-13
11-1	Pitch Plane Dynamics During S-IC Burn	11-4
11-2	Yaw Plane Dynamics During S-IC Burn	11-5
11-3	Roll Plane Dynamics During S-IC Burn	11-6
11-4	Normal Acceleration During S-IC Burn	11-8
11-5	Pitch and Yaw Plane Wind Velocity and Free Stream Angle-of-Attack During S-IC Burn	11-9
11-6	S-IC Engine Deflection Response to Propellant Slosh	11-11
11-7	Pitch Plane Dynamics During S-II Burn	11-12

## LIST OF ILLUSTRATIONS (CONTINUED)

Figure		Page
11-8	Yaw Plane Dynamics During S-II Burn	11-13
11-9	Roll Plane Dynamics During S-II Burn	11-14
11-10	S-II Engine Deflection Response to Propellant Slosh	11-17
11-11	Pitch Attitude Control During S-IVB First Burn	11-19
11-12	Yaw Attitude Control During S-IVB First Burn	11-20
11-13	Roll Attitude Control During S-IVB First Burn	11-21
11-14	Pitch Attitude Control During Maneuver to TD&E Attitude	11-22
11-15	Yaw Attitude Control During Maneuver to TD&E Attitude	11-23
11-16	Roll Attitude Control During Maneuver to TD&E Attitude	11-24
11-17	Pitch Attitude Control During Hard Dock	11-25
11-18	Yaw Attitude Control During Hard Dock	11-26
11-19	Roll Attitude Control During Hard Dock	11-27
11-20	Pitch Attitude Control During LM Ejection	11-28
11-21	Yaw Attitude Control During LM Ejection	11-29
11-22	Roll Attitude Control During LM Ejection	11-30
11-23	Pitch Attitude Control During Alignment of S-IVB to Local Horizontal Prior to Second Burn	11-31
11-24	Yaw Attitude Control During Alignment of S-IVB to Local Horizontal Prior to Second Burn	11-32
11-25	Roll Attitude Control During Alignment of S-IVB to Local Horizontal Prior to Second Burn	11-33
11-26	Pitch Attitude Control During S-IVB Second Burn	11-34
11-27	Yaw Attitude Control During S-IVB Second Burn	11-35
11-28	Roll Attitude Control During S-IVB Second Burn	11-36
11-29	Pitch Attitude Control During S-IVB Third Burn	11-39
11-30	Yaw Attitude Control During S-IVB Third Burn	11-40
11-31	Roll Attitude Control During S-IVB Third Burn	11-41

LIST OF ILLUSTRATIONS (CONTINUED)

Figure		Page
11-32	Measured and Calculated Engine Positions at Start of S-IVB Third Burn Prior to Oscillation Buildup	11-43
11-33	Measured and Calculated Engine Positions at End of S-IVB Third Burn Oscillation Period	11-44
11-34	S-IVB Roll Torque - Third Burn	11-46
11-35	S-IVB Slosh Frequencies and Heights During Third Burn	11-48
12-1	AS-504 Command Module Accelerations	12-4
12-2	Instrument Unit Longitudinal Accelerometer	12-5
12-3	Longitudinal Acceleration at Command Module During S-IC Thrust Cutoff (AS-503 and AS-504)	12-6
12-4	Longitudinal Acceleration at Command Module During S-IC/S-II Separation (AS-502 and AS-501)	12-7
12-5	Average S-IC OECO Thrust Decay, AS-501 Through AS-504	12-8
12-6	AS-504 and AS-503 S-IC Intertank - Longitudinal Acceleration	12-10
13-1	S-IC Stage Battery No. 1 Voltage and Current, Bus 1D10	13-2
13-2	S-IC Stage Battery No. 2 Voltage and Current, Bus 1D20	13-3
13-3	S-II Stage Main DC Bus Voltage and Current	13-5
13-4	S-II Stage Instrumentation Bus Voltage and Current	13-5
13-5	S-II Stage Ignition DC Bus Voltage and Current	13-6
13-6	S-II Stage Recirculation DC Voltage and Current	13-7
13-7	S-IVB Stage Forward Battery No. 1 Voltage, Current, and Temperature	13-8
13-8	S-IVB Stage Forward Battery No. 2 Voltage, Current, and Temperature	13-11
13-9	S-IVB Stage Aft Battery No. 1 Voltage, Current, and Temperature	13-14

LIST OF ILLUSTRATIONS (CONTINUED)

Figure		Page
13-10	S-IVB Stage Aft Battery No. 2 Voltage, Current, and Temperature	13-17
13-11	IU Battery 6D10 Voltage, Current, and Temperature	13-22
13-12	IU Battery 6D30 Voltage, Current, and Temperature	13-23
13-13	IU Battery 6D40 Voltage, Current, and Temperature	13-24
16-1	S-IC Engine Fairing Compartment Pressure Differential	16-2
16-2	S-IC Compartment Pressure Differentials	16-3
16-3	S-IC Compartment Pressure Loading	16-4
16-4	S-II Forward Skirt Pressure Loading	16-6
16-5	S-IC Base Pressure Differential	16-6
16-6	S-IC Base Heat Shield Differential Pressure	16-7
16-7	S-II Thrust Cone and Base Heat Shield Forward Face Pressures	16-8
16-8	S-II Heat Shield Aft Face Pressures	16-8
16-9	Vehicle External Overall Sound Pressure at Liftoff	16-9
16-10	S-IC External Overall Fluctuating Pressure Level	16-10
16-11	S-IC and S-II External Overall Fluctuating Pressure Level	16-11
16-12	S-II External Overall Fluctuating Pressure Level	16-11
16-13	S-IC Heat Shield Panels Internal Acoustic Environment	16-12
16-14	S-IC Intertank Internal Acoustic Environment	16-13
16-15	S-II Internal Acoustics History	16-13
17-1	S-IC Base Heat Shield Thermal Environment	17-3
17-2	F-1 Engine Thermal Environment	17-3
17-3	S-IC Heat Shield Forward Surface Temperature	17-4
17-4	S-IC Heat Shield Bondline Temperature	17-4

## LIST OF ILLUSTRATIONS (CONTINUED)

Figure		Page
17-5	S-IC Base Heat Shield Measurement Locations	17-5
17-6	S-IC Temperature Under Insulation, Inboard Side Engine No. 1	17-6
17-7	S-IC Upper Compartment Ambient Air Temperature During S-IC/S-II Stage Separation	17-7
17-8	S-II Heat Shield Base Region Heating Rates	17-8
17-9	S-II Thrust Cone Heating Rate	17-9
17-10	S-II Base Gas Temperature	17-10
17-11	S-II Heat Shield Aft Face Temperatures	17-11
17-12	S-II Heat Shield Forward Face Temperature	17-13
17-13	S-IC Intertank Aerodynamic Heating	17-14
17-14	S-IC Forward Skirt Aerodynamic Heating - Measurement C64-120	17-15
17-15	S-IC Forward Skirt Aerodynamic Heating - Measurements C322-120 and C323-120	17-15
17-16	Forward Location of Separated Flow	17-16
17-17	S-IC LOX Tank Skin Temperature	17-17
17-18	S-IC Fuel Tank Skin Temperature	17-17
17-19	S-IC Intertank Skin Temperature	17-18
17-20	S-IC Forward Skirt Skin Temperature	17-18
17-21	S-II Aft Interstage Aeroheating Environment	17-19
17-22	S-II Aft Interstage Aeroheating Environment, Ullage Motor Fairing	17-20
17-23	S-II LH <sub>2</sub> Feedline Aft Fairing Heating Rates	17-21
17-24	S-II LH <sub>2</sub> Feedline Forward Fairing Heating Rates	17-23
17-25	S-II Body Aeroheating Environment, Forward Skirt	17-23
17-26	S-II Body Structural Temperature, Forward Skirt Skin	17-24
17-27	S-II Aft Interstage Structural Temperature, Ullage Motor Fairing	17-24
17-28	S-II Body Structural Temperature, LH <sub>2</sub> Tank Insulation Surface	17-25

## LIST OF ILLUSTRATIONS (CONTINUED)

Figure		Page
18-1	S-IC Forward Compartment Canister Temperature	18-2
18-2	S-IC Forward Compartment Ambient Temperature	18-3
18-3	S-IC Aft Compartment Temperature Range	18-5
18-4	IU Environmental Control System Schematic	18-7
18-5	Thermal Conditioning System Methanol/Water Control Temperature	18-8
18-6	IU Sublimator Performance During Ascent	18-8
18-7	Thermal Conditioning System GN <sub>2</sub> Pressure	18-9
18-8	Selected Component Temperatures	18-10
18-9	Inertial Platform GN <sub>2</sub> Pressures	18-12
18-10	Gas Bearing System GN <sub>2</sub> Pressure	18-12
19-1	Telemetry Format	19-10
19-2	LVDC/LVDA Computer Word Flow	19-11
19-3	VHF Telemetry Coverage Summary	19-15
19-4	C-Band Radar Coverage Summary	19-17
19-5	Command and Communication System Coverage Summary	19-21
A-1	Scalar Wind Speed at Launch Time of AS-504	A-10
A-2	Wind Direction at Launch Time of AS-504	A-11
A-3	Pitch Wind Speed Component ( $W_x$ ) at Launch Time of AS-504	A-12
A-4	Yaw Wind Speed Component at Launch Time of AS-504	A-13
A-5	Pitch ( $S_x$ ) and Yaw ( $S_z$ ) Component Wind Shears at Launch Time of AS-504	A-14
A-6	Relative Deviation of Temperature and Density From PAFB (63) Reference Atmosphere, AS-504	A-15
B-1	Saturn V Apollo Flight Configuration	B-2
B-2	S-IC Stage Configuration	B-3
B-3	S-II Stage Configuration	B-7
B-4	S-IVB Stage Configuration	B-11
B-5	Instrument Unit Configuration	B-15
B-6	Apollo Spacecraft	B-18



## LIST OF TABLES

Table		Page
2-1	Time Base Summary	2-3
2-2	Significant Event Times Summary	2-5
2-3	Variable Time and Commanded Switch Selector Events	2-16
4-1	Total Velocity Deviations During S-IC/S-II Burn	4-5
4-2	Comparison of Significant Trajectory Events	4-6
4-3	Comparison of Cutoff Events	4-7
4-4	Comparison of Separation Events	4-8
4-5	Stage Impact Location	4-12
4-6	Parking Orbit Insertion Conditions	4-12
4-7	Intermediate Orbit Insertion Conditions	4-15
4-8	Escape Orbit Injection Conditions	4-15
4-9	Comparison of Heliocentric Orbit Parameters	4-18
5-1	S-IC Engine Performance Deviations	5-6
5-2	S-IC Stage Propellant Mass History	5-9
6-1	S-II Engine Performance Deviations (ESC +61 Seconds)	6-9
6-2	S-II Flight Reconstruction Comparison with Simulation Trajectory Match Results	6-10
6-3	S-II Propellant Mass History	6-17
7-1	S-IVB Engine Start Sequence Events - First Burn	7-7
7-2	S-IVB Steady State Performance - First Burn (STDV +60-Second Time Slice at Standard Altitude Conditions)	7-9
7-3	Comparison of S-IVB Stage Flight Reconstruction Data with Performance Simulation Results - First Burn	7-10
7-4	S-IVB Burn Time Deviations	7-11

LIST OF TABLES (CONTINUED)

Table		Page
7-5	S-IVB Engine Start Sequence Events - Second Burn	7-19
7-6	S-IVB Steady State Performance - Second Burn (STDV +60-Second Time Slice at Standard Altitude Conditions)	7-24
7-7	Comparison of S-IVB Stage Flight Reconstruction Data with Performance Simulation Results - Second Burn	7-25
7-8	S-IVB Engine Start Sequence Events - Third Burn	7-36
7-9	S-IVB Steady State Performance - Third Burn (STDV +60-Second Time Slice at Standard Altitude Conditions)	7-38
7-10	S-IVB Third Burn Performance Comparison	7-39
7-11	Comparison of S-IVB Stage Flight Reconstruction Data with Performance Simulation Results - Third Burn	7-47
7-12	S-IVB Stage Propellant Mass History	7-49
7-13	S-IVB Pneumatic Helium Bottle Mass	7-61
7-14	S-IVB APS Helium Bottle Mass	7-62
7-15	S-IVB APS Propellant Consumption	7-65
7-16	S-IVB Pneumatic Safing Conditions	7-69
9-1	S-IC Stage Vibration Summary	9-9
9-2	S-II Stage Maximum Overall Vibration Levels	9-14
10-1	Inertial Platform Velocity Comparisons	10-6
10-2	Guidance Comparisons	10-8
10-3	Start and Stop Times for IGM Guidance Commands	10-12
10-4	Parking Orbit Insertion Parameters	10-12
11-1	AS-504 Misalignment Summary	11-3
11-2	Maximum Control Parameters During S-IC Boost Flight	11-7
11-3	Maximum Control Parameters During S-II Boost Flight	11-15
11-4	Maximum Control Parameters During First Burn	11-37
11-5	Maximum Control Parameters During Second Burn	11-38

LIST OF TABLES (CONTINUED)

Table		Page
11-6	Maximum Control Parameters During S-IVB Third Burn	11-42
12-1	S-IC/S-II Separation Event Comparison AS-503 Versus AS-504	12-3
13-1	S-IC Stage Battery Power Consumption	13-3
13-2	S-II Stage Battery Power Consumption	13-7
13-3	S-IVB Stage Battery Power Consumption	13-20
13-4	IU Battery Power Consumption	13-25
14-1	Command and Communications System, Commands History, AS-504	14-3
15-1	Performance Summary of Thrust OK Pressure Switches	15-3
15-2	Maximum Angular Rates	15-4
15-3	EDS Associated Discretes	15-4
16-1	Sound Pressure Level Comparison of AS-504 With AS-501, AS-502 and AS-503 Data	16-14
18-1	TCS Coolant Flowrates and Pressures	18-6
19-1	AS-504 Flight Measurement Summary	19-2
19-2	AS-504 Flight Measurements Waived Prior to Launch	19-3
19-3	AS-504 Measurement Malfunctions	19-4
19-4	AS-504 Flight Measurements with Improper Range	19-7
19-5	AS-504 Questionable Flight Measurements	19-7
19-6	AS-504 Launch Vehicle Telemetry Links	19-8
19-7	Tape Recorder Summary	19-12
19-8	Signal Strength at Goldstone	19-19
21-1	Total Vehicle Mass- S-IC Burn Phase- Kilograms	21-3
21-2	Total Vehicle Mass- S-IC Burn Phase- Pounds Mass	21-4
21-3	Total Vehicle Mass - S-II Burn Phase - Kilograms	21-5
21-4	Total Vehicle Mass - S-II Burn Phase - Pounds Mass	21-6
21-5	Total Vehicle Mass - S-IVB First Burn Phase - Kilograms	21-7
21-6	Total Vehicle Mass - S-IVB First Burn Phase - Pounds Mass	21-8

LIST OF TABLES (CONTINUED)

Table		Page
21-7	Total Vehicle Mass - At Spacecraft Separation - Kilograms	21-9
21-8	Total Vehicle Mass - At Spacecraft Separation - Pounds Mass	21-10
21-9	Total Vehicle Mass - S-IVB Second Burn Phase - Kilograms	21-11
21-10	Total Vehicle Mass - S-IVB Second Burn Phase - Pounds Mass	21-12
21-11	Total Vehicle Mass - S-IVB Third Burn Phase - Kilograms	21-13
21-12	Total Vehicle Mass - S-IVB Third Burn Phase - Pounds Mass	21-14
21-13	Flight Sequence Mass Summary	21-15
21-14	Mass Characteristics Comparison	21-17
22-1	Mission Objectives Accomplishment Summary	22-2
23-1	Hardware Criticality Categories for Flight Hardware	23-1
23-2	Summary of Failures and Anomalies	23-2
23-3	Summary of Deviations	23-3
A-1	Surface Observations at AS-504 Launch Time	A-3
A-2	Solar Radiation at AS-504 Launch Time, Launch Pad 39A	A-4
A-3	Systems Used to Measure Upper Air Wind Data	A-4
A-4	Maximum Wind Speed in High Dynamic Pressure Region for Saturn 1 Through Saturn 10 Vehicles	A-5
A-5	Maximum Wind Speed in High Dynamic Pressure Region for Apollo/Saturn 201 Through Apollo/Saturn 205 Vehicles	A-5
A-6	Maximum Wind Speed in High Dynamic Pressure Region for Apollo/Saturn 501 Through Apollo/Saturn 504 Vehicles	A-6
A-7	Extreme Wind Shear Values in the High Dynamic Pressure Region for Saturn 1 Through Saturn 10 Vehicles	A-6

LIST OF TABLES (CONTINUED)

Table		Page
A-8	Extreme Wind Shear Values in the High Dynamic Pressure Region for Apollo/Saturn 201 Through Apollo/Saturn 205 Vehicles	A-7
A-9	Extreme Wind Shear Values in the High Dynamic Pressure Region for Apollo/Saturn 501 Through Apollo/Saturn 504 Vehicles	A-7
A-10	Selected Atmospheric Observations for Saturn 1 Through Saturn 10 Vehicle Launches at Kennedy Space Center, Florida	A-8
A-11	Selected Atmospheric Observations for Apollo/Saturn 201 Through Apollo/Saturn 205 Vehicle Launches at Kennedy Space Center, Florida	A-9
A-12	Selected Atmospheric Observations for Apollo/Saturn 501 Through Apollo/Saturn 504 Vehicle Launches at Kennedy Space Center, Florida	A-9
B-1	S-IC Significant Configuration Changes	B-5
B-2	S-II Significant Configuration Changes	B-10
B-3	S-IVB Significant Configuration Changes	B-13
B-4	IU Significant Configuration Changes	B-16

## ACKNOWLEDGEMENT

This report is published by the Saturn Flight Evaluation Working Group-- composed of representatives of Marshall Space Flight Center, John F. Kennedy Space Center, and MSFC's prime contractors--and in cooperation with the Manned Spacecraft Center. Significant contributions to the evaluation have been made by:

George C. Marshall Space Flight Center

Science and Engineering

Aero-Astroynamics Laboratory  
Astrionics Laboratory  
Computation Laboratory  
Astronautics Laboratory

Program Management

John F. Kennedy Space Center

Manned Spacecraft Center

The Boeing Company

McDonnell Douglas Astronautics Company

International Business Machines Corporation

North American Rockwell/Space Division

North American Rockwell/Rocketdyne Division

## ABBREVIATIONS

ACN	Ascension	DCS	Digital Command System
ANT	Antigua	DTO	Detailed Test Objective
AOS	Acquisition of Signal	EBW	Exploding Bridge Wire
APS	Auxiliary Propulsion System	ECO	Engine Cutoff
ASI	Augmented Spark Igniter	ECP	Engineering Change Proposal
AUX	Auxiliary	ECS	Environmental Control System
BDA	Bermuda	EDS	Emergency Detection System
BSC	O <sub>2</sub> /H <sub>2</sub> Burner Start Command	EMR	Engine Mixture Ratio
CCS	Command and Communications System	ESC	Engine Start Command
CDDT	Countdown Demonstration Test	EST	Eastern Standard Time
CECO	Center Engine Cutoff	EVA	Extra-Vehicular Activity
CG	Center of Gravity	FCC	Flight Control Computer
CIF	Central Instrumentation Facility	FM/FM	Frequency Modulation/ Frequency Modulation
CKAFS	Cape Kennedy Air Force Site	GBI	Grand Bahama Island
CM	Command Module	GFCV	GOX Flow Control Valve
CNV	Canaveral	GDS	Goldstone
COR	Carnarvon	GG	Gas Generator
CSM	Command and Service Module	GMT	Greenwich Mean Time
CSP	Control Signal Processor	GOX	Gaseous Oxygen
CVS	Continuous Vent System	GRR	Guidance Reference Release
CYI	Grand Canary Island	GSE	Ground Support Equipment
DEE	Digital Events Evaluator	GTI	Grand Turk Island

GWM	Guam	MAD	Madrid
GYM	Guaymas	MCC-H	Mission Control Center-Houston
HAW	Hawaii	MER	Mercury (ship)
HDA	Holddown Arm	MFV	Main Fuel Valve
HEP	Hardware Evaluation Program	MILA	Merritt Island Launch Area
HFCV	Helium Flow Control Valve	MLV	Main LOX Valve
HSK	Honeysuckle (Canberra)	MOV	Main Oxidizer Valve
IGM	Iterative Guidance Mode	MR	Mixture Ratio
IP&C	Instrumentation Program and Components	MSC	Manned Spacecraft Center
IRIG	Inter-range Instrumentation Group	MSFC	Marshall Space Flight Center
IS	Interstage	MSFN	Manned Space Flight Network
IU	Instrument Unit	MSS	Mobile Service Structure
KSC	Kennedy Space Center	MTF	Mississippi Test Facility
LES	Launch Escape System	NPSP	Net Positive Suction Pressure
LET	Launch Escape Tower	NASA	National Aeronautics and Space Administration
LIEF	Launch Information Exchange Facility	OAT	Overall Test
LM	Lunar Module	OCP	Orbital Correction Program
LOS	Loss of Signal	ODOP	Offset Frequency Doppler
LUT	Launch Umbilical Tower	OECO	Outboard Engine Cutoff
LV	Launch Vehicle	OMNI	Omni Directional
LVDA	Launch Vehicle Data Adapter	PAM/ FM/FM	Pulse Amplitude Modulation/ Frequency Modulation/Frequency Modulation
LVDC	Launch Vehicle Digital Computer	PAFB	Patrick Air Force Base



PCM	Pulse Code Modulation	SPS	Service Propulsion System
PCM/ FM	Pulse Code Modulation/ Frequency Modulation	SRSCS	Secure Range Safety Command System
PMR	Programmed Mixture Ratio	SS	Switch Selector
PSD	Power Spectral Density	SS/FM	Single Sideband/Frequency Modulation
PTCS	Propellant Tanking Control System	STDV	Start Tank Discharge Valve
PTL	Prepare to Launch	STP	Special Test Pattern
PU	Propellant Utilization	SV	Space Vehicle
PVC	Pressure Volume Compensator	T <sub>1</sub>	Time Base 1
RCS	Reaction Control System	T <sub>1</sub> I	Time to go in 1st Stage IGM
RDM	Remote Digital Multiplexer	T <sub>2</sub> I	Time to go in 2nd Stage IGM
RED	Redstone (ship)	TAN	Tananarive
RF	Radio Frequency	TD&E	Transposition, Docking & Ejection
RMS	Root Mean Square	TDM	Time Division Multiplexer
RP-1	Designation for S-IC Stage Fuel (kerosene)	TEL 4	Cape Telemetry 4
RPM	Revolutions Per Minute	TEP	Telemetry Executive Program
SA	Service Arm	TEX	Corpus Christi (Texas)
SEC	Seconds	TLI	Translunar Injection
SLA	Spacecraft LM Adapter	TM	Telemeter, Telemetry
SM	Service Module	TMR	Triple Modular Redundant
SMC	Steering Misalignment Correction	TSM	Tail Service Mast
SNR	Signal to Noise Ratio	TVC	Thrust Vector Control
SPL	Sound Pressure Level	UHF	Ultra High Frequency
		USB	Unified S-Band

UT Universal Time  
VAB Vehicle Assembly Building  
at KSC  
VAN Vanguard (ship)  
VHF Very High Frequency  
WHS White Sands

## MISSION PLAN

AS-504 (Apollo 9 mission) was the fourth flight of the Apollo Saturn V flight test program. It was to be the second manned Apollo Saturn V vehicle with the spacecraft including, for the first time, the lunar module (LM). The basic purpose of the flight was to demonstrate the capability of the manned Apollo Command and Service Modules (CSM) in earth orbit, particularly to evaluate LM systems capabilities, LM active rendezvous techniques, and combined CSM/LM functions. Additionally, two S-IVB restarts were scheduled to evaluate S-IVB restart capability to simulate lunar mission requirements. The crew consisted of Air Force Col. James A. McDivitt, Air Force Col. David R. Scott, and Russell L. Schweickart.

The space vehicle was composed of the AS-504 launch vehicle consisting of the S-IC, S-II, S-IVB and Instrument Unit (IU) stacked stages and spacecraft consisting of the Spacecraft Lunar Module Adapter (SLA), LM-3, and CSM-103.

The vehicle was to be launched from Complex 39, Pad A, of the Kennedy Space Center. The flight azimuth was to be 72 degrees east of north.

The vehicle mass at launch was to be about 2,940,728 kilograms (6,483,195 lbm). The S-IC and S-II stage powered flight times were to be approximately 160 and 370 seconds, respectively. The planned S-IVB first burn was to be about 114 seconds. The S-IVB/IU/LM/CSM was to be inserted into a 185.2 kilometer (100 n mi) altitude (referenced to the earth's equatorial radius) circular parking orbit. The vehicle mass at parking orbit insertion was to be about 134,895 kilograms (297,393 lbm).

About 10 seconds after insertion, the S-IVB/IU was to assume a local horizontal attitude until the maneuver to transposition, docking, and spacecraft ejection attitude at about 2 hours, 34 minutes range time. Following SLA jettisoning and separation, the CSM was to undergo transposition and docking with the LM early in the third revolution. LM ejection was expected to occur at approximately 4 hours and 10 minutes range time. For a nominal mission the S-IVB/IU was to revert to a local horizontal attitude and initiate the S-IVB second burn at about 4 hours, 46 minutes range time. The 63 second S-IVB second burn was to place the S-IVB/IU in a 2998 by 196 kilometer (1619 by 106 n mi) intermediate orbit. The launch vehicle was to coast for approximately 80 minutes to demonstrate the S-IVB engine ability to cool down sufficiently prior to a restart within one revolution. At approximately

6 hours and 7 minutes range time the S-IVB was to ignite for the third time and burn for about 242 seconds. The third S-IVB burn was to propel the launch vehicle into an earth escape trajectory (solar orbit). Following third burn, the stage safing sequence, which included dumping residual propellants, was to be initiated.

The CSM was to perform four Service Propulsion System (SPS) burns prior to LM activation. After LM activation, a CSM/LM docked descent propulsion system burn and extra-vehicular activities were to be performed. A fifth SPS burn was to circularize the orbit for the LM active rendezvous sequence. After the LM active rendezvous, the LM was to be jettisoned, and the ascent propulsion system would then burn to depletion. The CSM was to perform additional deorbit shaping SPS burns, then was to perform navigation sightings and other experiments prior to the deorbit. An SPS burn was to deorbit the spacecraft, and CM splashdown was to occur approximately 25 minutes later in the mid-Atlantic. Range time from liftoff was to have been about 238 hours and 12 minutes to splashdown.

## FLIGHT TEST SUMMARY

The second manned Saturn V Apollo space vehicle, AS-504 (Apollo 9 Mission), was launched at Kennedy Space Center (KSC), Florida on March 3, 1969 at 11:00:00 Eastern Standard Time (EST) from Launch Complex 39, Pad A. This fourth launch of the Saturn V Apollo was the first Saturn V/Apollo Spacecraft in full lunar mission configuration and carried the largest payload placed in orbit. The one principal, and nine of the eleven secondary Detailed Test Objectives (DTO's) were completely accomplished. The other two DTO's, S-IVB 80-minute restart and LOX/LH<sub>2</sub> dump, were partially accomplished.

The launch countdown was completed without any unscheduled countdown holds. Ground systems performance was highly satisfactory. The relatively few problems encountered in countdown were overcome such that vehicle launch readiness was not compromised.

The vehicle was launched on an azimuth of 90 degrees east of north and after 13.3 seconds of vertical flight, the vehicle began to roll into a flight azimuth of 72 degrees east of north. Actual trajectory parameters of the AS-504 were close to nominal except for the space-fixed velocity at S-II Engine Cutoff (ECO) and the escape orbit injection parameters. Space-fixed velocity at S-IC Outboard Engine Cutoff (OECO) was 29.33 m/s (96.23 ft/s) lower than nominal. At S-II ECO the space-fixed velocity was 81.70 m/s (268.04 ft/s) lower than nominal. At S-IVB first cutoff the space-fixed velocity was 0.87 m/s (2.86 ft/s) greater than nominal. The altitude at S-IVB first burn cutoff was 0.31 kilometers (0.17 n mi) lower than nominal, and the surface range was 66.77 kilometers (36.06 n mi) greater than nominal. The space-fixed velocity at insertion was 0.61 m/s (2.00 ft/s) greater than nominal. At intermediate orbit insertion the total space-fixed velocity was 18.67 m/s (61.25 ft/s) greater than nominal. The escape orbit injection parameters deviated significantly from nominal. The value of  $C_3$  was 824,712 m<sup>2</sup>/s<sup>2</sup> (8,877,126 ft<sup>2</sup>/s<sup>2</sup>) which was 30,470,506 m<sup>2</sup>/s<sup>2</sup> (327,981,795 ft<sup>2</sup>/s<sup>2</sup>) lower than nominal.

All S-IC propulsion systems performed satisfactorily. However, the combined thrust of the five F-1 engines was lower than predicted. At the 35 to 38-second time slice, average engine thrust reduced to standard pump inlet conditions was 1.21 percent lower than predicted. Average reduced specific impulse was 0.174 percent lower than predicted. Center Engine Cutoff (CECO) was initiated by the Instrument Unit as planned. Outboard engine cutoff was initiated by LOX low level sensors 2.8 seconds later than predicted but well within the 3 sigma limit.

The S-II propulsion system performed satisfactorily during the entire flight. Total stage thrust at 61 seconds after Engine Start Command (ESC), was 0.20 percent below the prediction. Average specific impulse was 0.25 percent above prediction at this time slice. Average engine mixture ratio was 0.33 percent above predicted. Low frequency performance oscillations were experienced by the center engine near the end of S-II burn and were similar to those on AS-503. Corrective action being planned for AS-505 is to cut off the center engine before the oscillations are expected. As sensed by the engines, ESC occurred at 164.17 seconds and engine cutoff was at 536.22 seconds with a burn time only 2.27 seconds longer than predicted.

The S-IVB J-2 engine operated satisfactorily throughout the operational phase of first and second burns with normal shutdowns. S-IVB first burn time was 123.84 seconds which was 10.3 seconds longer than predicted. The engine performance during first burn, as determined from standard altitude reconstruction analysis, deviated from the predicted Start Tank Discharge Valve (STDV) +60-second time slice by 0.764 percent for thrust and -0.117 percent for specific impulse. The Continuous Vent System (CVS) performed nominally during parking orbit, and the Oxygen/Hydrogen ( $O_2/H_2$ ) Burner satisfactorily achieved  $LH_2$  repressurization for restart. Repressurization of the LOX tank was not required. Engine restart conditions were within specified limits. The restart was successful with no indications of any problem. S-IVB second burn time was 62.06 seconds and was cut off by a timer. The engine performance during second burn, as determined from the standard altitude reconstruction analysis, deviated from the predicted STDV +60-second time slice by -0.587 percent, for thrust and -0.182 percent for specific impulse. The CVS performed nominally during the intermediate orbit, and the  $O_2/H_2$  Burner successfully achieved restart prior to third burn. Subsequently, the  $LH_2$  tank was satisfactorily repressurized by the ambient repressurization system. Repressurization of the LOX tank was not required. Engine conditions for the second restart (third burn) were unusual as a result of the extended fuel lead experiment. This was a planned experiment to evaluate the mission rule concerning failure of both LOX and  $LH_2$  chilldown systems. The restart was successful; however, the chamber pressure did indicate abnormal conditions during the start transient. Mainstage performance was not as predicted due to various anomalies which occurred during the burn. Third burn had a timed cutoff as expected. The stage was properly safed; however, propellant dump was not accomplished due to the third burn anomaly. During the early stages of launch countdown the regulator discharge pressure was high and was controlled by the backup system. Subsequently, the regulator pressure was high during boost and coast phase, however, there were no adverse effects on components or system functioning. The Auxiliary Propulsion System (APS) pressurization system developed a helium leak in module No. 2 at 4 hours and 25 minutes which ceased at 7 hours. However, the ullage pressures in the APS were acceptable throughout the mission.

The hydraulic systems on all stages performed satisfactorily throughout the flight, however, during S-IVB third burn the yaw actuator experienced abnormal oscillations of 3 degrees peak-to-peak amplitude at 0.65 hertz.

The structural loads and dynamic environment experienced by the AS-504 launch vehicle were well within the vehicle structural capability. The high altitude winds for this flight were the highest measured during any previous Saturn launch. However, due to a wind bias trajectory, the structural loads for AS-504 were well below the design limit values. There was no evidence of an unstable coupled thrust-structure-feed system oscillation (POGO) during S-IC powered flight. The low frequency (16 to 19 hertz) oscillation anomaly observed on AS-503 also occurred on AS-504 near the end of S-II stage burn. The oscillations reached a maximum level of approximately  $\pm 12.0$  g at the center of the S-II thrust structure crossbeam.

The guidance and navigation system performed satisfactorily during all periods for which data are available. The boost navigation and guidance schemes were properly executed, and the desired parking orbit insertion parameters were achieved with good accuracy. The third burn of the S-IVB stage placed the S-IVB/IU in a heliocentric orbit. All target parameters were satisfactorily achieved and all orbital operations were nominal. System performance was unaffected by either the unexpected change in thrust level during S-IVB third burn, or the failure to dump residual propellants following the burn. The Launch Vehicle Digital Computer (LVDC), the Launch Vehicle Data Adapter (LVDA), and the ST-124M-3 inertial platform functioned satisfactorily.

The AS-504 Flight Control Computer (FCC), Thrust Vector Control (TVC) and the APS satisfied all requirements for vehicle attitude control during boost and orbital control modes. The preprogrammed S-IC boost phase yaw, roll and pitch maneuvers were properly executed. The S-IC outboard engine radial cant was accomplished as planned. S-IC/S-II first and second plane separations were accomplished with no significant attitude deviations. At Iterative Guidance Mode (IGM) initiation, pitch-up transients occurred that were similar to those seen on AS-501 and AS-502. S-II/S-IVB separation occurred as expected and without producing any significant attitude deviations. During first and second S-IVB burns, satisfactory control was maintained over the vehicle. During the Command and Service Module (CSM) separation from the S-IVB/Instrument Unit (IU) and during the Transposition, Docking, and Ejection (TD&E), the control system maintained a fixed inertial attitude to provide a stable docking platform. During the S-IVB third burn the control system experienced high amplitude oscillations in the yaw plane for the first 100 seconds of burn. These oscillations were also evident in the pitch and roll planes. LOX and LH<sub>2</sub> sloshing was coupled to the control oscillations. After the performance shift, these oscillations damped out and pitch and yaw attitude control

was near nominal. However, a large roll torque had been developing and it peaked at 386 N-m (285 lbf-ft). At the performance shift the torque changed from bidirectional to unidirectional (counter-clockwise). APS control was as expected, except for the large demands placed upon the system by the control oscillations. The APS propellants were depleted as planned by an ullage burn after third burn.

In general, all AS-504 launch vehicle electrical systems performed satisfactorily. Data indicated that the redundant Secure Range Safety Command System (SRSCS) on the S-IC, S-II, and S-IVB stages were ready to perform their functions properly on command if flight conditions during the launch phase had required vehicle destruct. The system properly safed the S-IVB SRSCS on command from Bermuda (BDA). The performance of the Command and Communications System (CCS) in the IU was satisfactory, except for a degraded power amplifier output occurring late into the flight.

The Emergency Detection System (EDS) performance was nominal; no abort limits were reached. The AS-504 EDS configuration was essentially the same as AS-503.

The vehicle internal, external, and base region pressure environments were generally in good agreement with the predictions and compared well with previous flight data. The pressure environment was well below design levels. The measured acoustic levels were generally in good agreement with the liftoff and inflight predictions, and with data from previous flights.

The AS-504 vehicle thermal environment was similar to that experienced on earlier flights with the exception of minor changes due to trajectory differences.

The Environmental Control Systems performed satisfactorily during the AS-504 countdown. The IU Environmental Control System (ECS) exhibited satisfactory performance throughout the flight.

The data system for the AS-504 launch vehicle consisted of 2179 active flight measurements, 17 telemetry links, 3 tape recorders and tracking by Offset Frequency Doppler (ODOP), C-Band and Command Communication System (CCS). All elements of the data system performed satisfactorily except for 4 telemetry deviations which did not adversely affect required data. The propagation of Radio Frequency (RF) transmissions from the vehicle was satisfactory. The C-Band radar was commanded off at 27,213.5 seconds (7:33:03.5) and final loss of CCS signal was reported by Goldstone (GDS) to have occurred at 48,066 seconds (13:21:06). The 87 ground engineering cameras provided good data during the launch. However, dense cloud coverage precluded the acquisition of tracking camera data between 30 and 50 seconds.



## SECTION 1

### INTRODUCTION

#### 1.1 PURPOSE

This report provides the National Aeronautics and Space Administration (NASA) Headquarters, and other interested agencies, with the launch vehicle evaluation results of the AS-504 flight test. The basic objective of flight evaluation is to acquire, reduce, analyze, evaluate and report on flight test data to the extent required to assure future mission success and vehicle reliability. To accomplish this objective, actual flight malfunctions and deviations must be identified, their causes accurately determined, and complete information made available so that corrective action can be accomplished within the established flight schedule.

#### 1.2 SCOPE

This report presents the results of the early engineering flight evaluation of the AS-504 launch vehicle. The contents are centered on the performance evaluation of the major launch vehicle systems, with special emphasis on failures, anomalies, and deviations. Summaries of launch operations and spacecraft performance are included for completeness.

The official George C. Marshall Space Flight Center (MSFC) position at this time is represented by this report. It will not be followed by a similar report unless continued analysis or new information should prove the conclusions presented herein to be significantly incorrect. Final stage evaluation reports will, however, be published by the stage contractors. Reports covering major subjects and special subjects will be published as required.

## SECTION 2

### EVENT TIMES

#### 2.1 SUMMARY OF EVENTS

Range zero time, the basic time reference for this report is 11:00:00 Eastern Standard Time (EST) (16:00:00 Universal Time [UT]). This time is based on the nearest second prior to S-IC tail plug disconnect which occurred at 11:00:00.6 EST. Range time is calculated as the elapsed time from range zero time and unless otherwise noted, is the time used throughout this report. The actual and predicted range times are adjusted to ground telemetry received times. Figure 2-1 shows the time delay/lead of ground telemetry received time versus Launch Vehicle Digital Computer (LVDC) time and indicates the magnitude and sign of corrections applied to range time in Tables 2-1, 2-2 and 2-3.

Guidance Reference Release (GRR) occurred at -16.97 seconds and start of Time Base 1 ( $T_1$ ) occurred at 0.67 seconds. GRR was established by the Digital Events Evaluation (DEE-6) and  $T_1$  was initiated at detection of liftoff signal provided by de-energizing the liftoff relay in the IU at IU umbilical disconnect.

Range time for each time base used in the flight sequence program and the signal for initiating each time base are presented in Table 2-1.

Start of  $T_2$  was within nominal expectations for this event. Start of  $T_3$ ,  $T_4$  and  $T_5$  was initiated approximately 2.8, 5.1 and 16.0 seconds later than predicted, respectively, due to longer than expected S-IC, S-II and S-IVB burns. Reasons for the longer than expected burn times are discussed in Sections 5, 6 and 7 of this document. Start of  $T_6$ , which was initiated by the LVDC upon solving the restart equation, was 5.3 seconds later than predicted. Start of  $T_7$ ,  $T_8$  and  $T_9$  was 5.3, 6.1 and 6.0 seconds later than predicted, primarily because of the impact of the late start of  $T_6$ .

A summary of significant events for AS-504 is given in Table 2-2. Since not all events listed in Table 2-2 are IU commanded switch selector functions, deviations are not to be construed as failures to meet specified switch selector tolerances. The events in Table 2-2 associated with guidance, navigation and control have been identified as being accurate to within  $\pm 0.5$  seconds or accurate to within a major computation cycle.

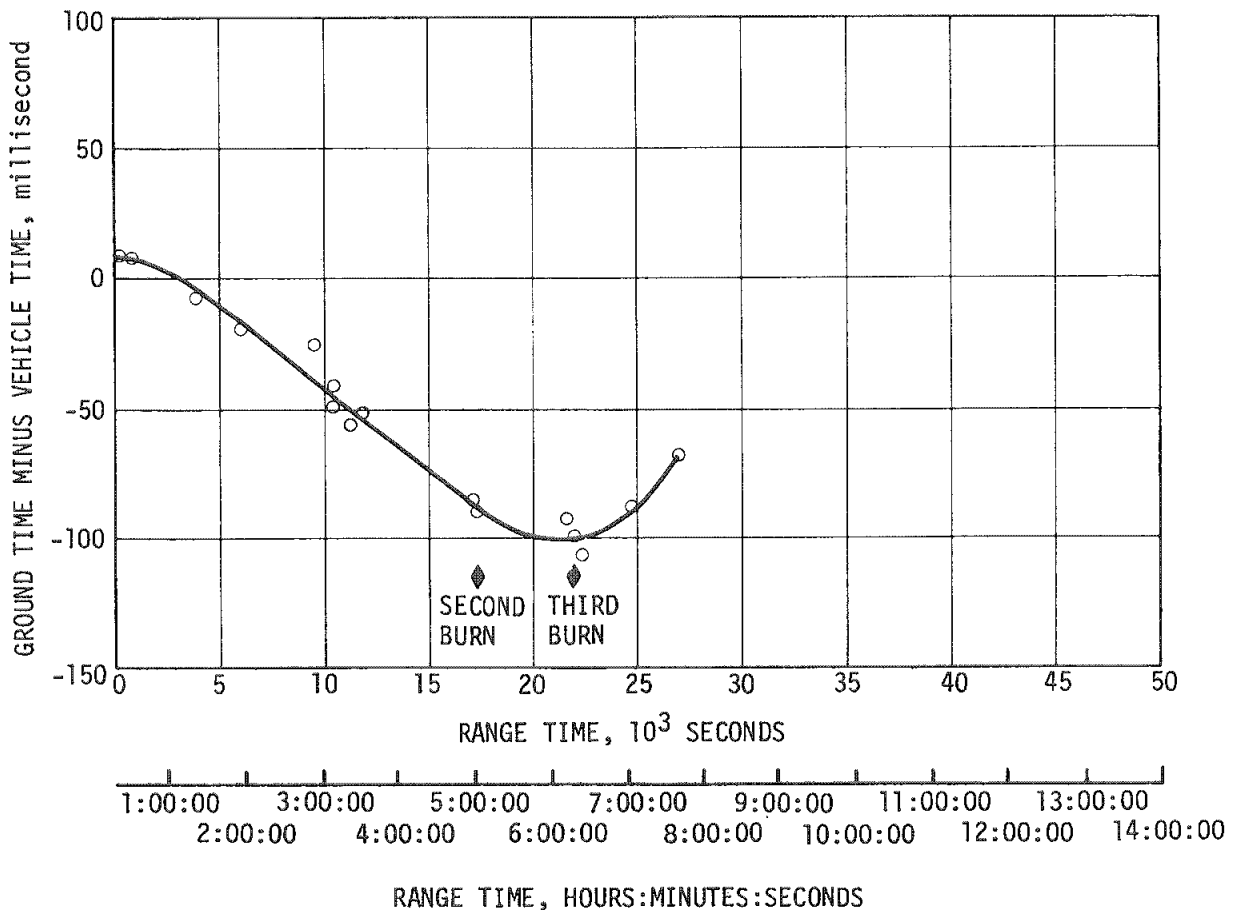


Figure 2-1. Telemetry Time Delay

The predicted times for establishing actual minus predicted times in Table 2-2 have been taken from 40M33640, "Interface Control Document Definition of Saturn SA-504 Flight Sequence Program" and from the "AS-504 Mission Launch Vehicle Operational Trajectory," dated 13 February 1969, as revised by S&E-AERO-FMT-48-69. The following times were changed:

- a. "S-II Mainstage" was used rather than "S-II Engine at 90 percent Thrust". S-II mainstage is defined as occurring 3 seconds after engine start command.
- b. "S-IVB Mainstage" was used rather than "S-IVB Engine at 90 percent Thrust" for all three burns. S-IVB mainstage is defined as occurring 2.5 seconds after engine ignition.

Table 2-1. Time Base Summary

TIME BASE	RANGE TIME SEC (HR:MIN:SEC)	SIGNAL START
T <sub>0</sub>	-16.97	Guidance Reference Release
T <sub>1</sub>	0.67	IU Umbilical Disconnect Sensed by LVDC
T <sub>2</sub>	134.28	S-IC CECO Commanded by LVDC
T <sub>3</sub>	162.30	S-IC OECO Sensed by LVDC
T <sub>4</sub>	536.25	S-II ECO Sensed by LVDC
T <sub>5</sub>	664.87	S-IVB ECO (Velocity) Sensed by LVDC
T <sub>6</sub>	16,577.24 (4:36:17.24)	Restart Equation Solution
T <sub>7</sub>	17,217.82 (4:46:57.82)	S-IVB ECO Commanded by LVDC
T <sub>8</sub>	21,580.98 (4:46:57.82)	Initiated by LVDC 5003.0 seconds after equation con- vergence (T <sub>6</sub> +5003.0 sec)
T <sub>9</sub>	22,281.53 (6:11:21.53)	S-IVB ECO Commanded by LVDC

- c. The "Helium Heater Off" times were changed in T<sub>6</sub> to reflect the same flight sequence event used in T<sub>8</sub>.
- d. The predicted start of T<sub>7</sub> and T<sub>9</sub> were changed to make these predictions compatible with the switch selector cutoff commands which initiate these time bases.

## 2.2 VARIABLE TIME AND COMMANDED SWITCH SELECTOR EVENTS

Table 2-3 lists known switch selector events which were issued during flight but which were not programmed for specific times. The Water Coolant Valve Open and Close switch selector commands were issued based upon the condition of two thermal switches in the Environmental Control System (ECS). The outputs of these switches were sampled once every 300 seconds, beginning at 480 seconds, and a switch selector command was issued to open and close the water valve to maintain proper temperature control.

Table 2-3 also contains the special sequence of switch selector events which were programmed to be initiated by telemetry station acquisition and included the following calibration sequence:

<u>FUNCTION</u>	<u>STAGE</u>	<u>TIME (SEC)</u>
Telemetry Calibrator In-Flight Calibrate On	IU	Acquisition +60.0
TM Calibrate On	S-IVB	Acquisition +60.2
TM Calibrate Off	S-IVB	Acquisition +61.2
In-Flight Calibrate Off	IU	Acquisition +65.0

In addition, known ground commands sent to the LVDC are included in this table.

Table 2-2. Significant Event Times Summary

EVENT	RANGE TIME		TIME FROM BASE	
	ACTUAL SEC	ACT-PRED SEC	ACTUAL SEC	ACT-PRED SEC
1. Guidance Reference Release (GRR)	-16.97	0.02	T <sub>1</sub> -17.63	0.63
2. S-IC Engine Start Sequence Command	-8.9	0.0	T <sub>1</sub> -9.6	0.0
3. S-IC Engine No. 1 Start	-6.0	0.0	T <sub>1</sub> -6.7	0.0
4. S-IC Engine No. 2 Start	-5.7	0.0	T <sub>1</sub> -6.4	0.0
5. S-IC Engine No. 3 Start	-6.1	0.0	T <sub>1</sub> -6.8	0.0
6. S-IC Engine No. 4 Start	-6.0	0.0	T <sub>1</sub> -6.7	0.0
7. S-IC Engine No. 5 Start	-6.3	0.0	T <sub>1</sub> -7.0	0.0
8. All S-IC Engines Thrust OK	-1.3	0.2	T <sub>1</sub> -2.0	0.2
9. Range Zero	0.0	-	T <sub>1</sub> -0.7	-
10. All Holddown Arms Released (First Motion)	0.3	0.0	T <sub>1</sub> -0.4	0.0
11. IU Umbilical Disconnect Start of Time Base 1 (T <sub>1</sub> )	0.67	0.01	T <sub>1</sub>	-
12. Begin Tower Clearance Yaw Maneuver	1.7*	0.1	1.1*	0.1
13. End Yaw Maneuver	9.7*	0.0	9.0*	0.0
14. Begin Pitch and Roll Maneuver	13.3*	1.8	12.6*	1.7
15. S-IC Radial Engine Cant	20.6	0.0	20.0	0.0
16. End Roll Maneuver	33.0*	2.7	32.3*	2.7

\*Accurate to within ±0.5 second.

Table 2-2. Significant Event Times Summary (Continued)

EVENT	RANGE TIME		TIME FROM BASE	
	ACTUAL SEC	ACT-PRED SEC	ACTUAL SEC	ACT-PRED SEC
17. Mach 1 Achieved	68.2	2.8	67.5	2.8
18. Maximum Dynamic Pressure (Max Q)	85.5	4.1	84.8	4.1
19. Start of Time Base 2 (T <sub>2</sub> )	134.28	0.07	T <sub>2</sub>	-
20. S-IC Center Engine Cutoff (CECO)	134.34	0.07	0.06	-0.01
21. End Pitch Maneuver (Tilt Arrest)	158.0*	1.0**	23.7*	1.0**
22. S-IC Outboard Engine Cutoff (OECO)	162.76	2.80	28.48	2.73
23. Start of Time Base 3 (T <sub>3</sub> )	162.80	2.83	T <sub>3</sub>	-
24. Start S-II LH <sub>2</sub> Tank High Pressure Vent Mode	162.9	2.8	0.1	0.0
25. S-II LH <sub>2</sub> Recirculation Pumps Off	163.0	2.8	0.2	0.0
26. S-II Ullage Motor Ignition	163.27	2.8	0.47	-0.03
27. S-IC/S-II Separation Command to Fire Separation Devices and Retro Motors	163.45	2.77	0.65	-0.05
28. Separation EBW Fire Signal	163.45	2.77	0.65	-0.06
29. S-IC Retro Motor EBW Fire Signal	163.46	2.77	0.66	-0.06
30. S-IC Retro Motor Burn Time Initiation (Thrust Buildup Begin)	163.47	2.77	0.67	-0.13

\*Accurate to within ±0.5 second.  
 \*\*Actual or predicted time is accurate to major computation cycle dependent upon length of computation cycle.

Table 2-2. Significant Event Times Summary (Continued)

EVENT	RANGE TIME		TIME FROM BASE	
	ACTUAL SEC	ACT-PRED SEC	ACTUAL SEC	ACT-PRED SEC
31. S-II Engine Start Command (ESC)	164.17	2.79	1.37	-0.04
32. S-II Engine Ignition (STDV Opens, Avg. of 5)	165.16	2.78	2.36	-0.03
33. S-II Mainstage	167.17	2.79	4.37	-0.04
34. S-II Ullage Motor Burn Time Termination (75 percent Thrust)	167.4	2.5	4.6	0.4
35. S-II Chardown Valves Close	169.2	2.8	6.4	0.0
36. Activate S-II PU System	169.7	2.8	6.9	0.0
37. S-II Second Plane Separation (Jettison S-II Aft Interstage)	193.5	2.8	30.7	0.0
38. Launch Escape Tower (LET) Jettison	198.3†	2.1	35.5†	0.7
39. Iterative Guidance Mode (IGM) Phase 1 Initiated	204.6*	3.3**	41.8*	0.5**
40. S-II LOX Step Pressurization	262.8	2.8	100.0	0.0
41. S-II Low Engine Mixture Ratio (EMR) Shift (Actual)	452.5	9.2	289.7	6.4
42. Guidance Sensed EMR Shift; IGM Phase 2 Initiated and Start of Artificial Tau Mode	461.5*	15.2**	298.7*	12.4**

\*Accurate to within  $\pm 0.5$  second.  
 \*\*Actual or predicted time is accurate to major computation cycle dependent upon length of computation cycle.  
 †Based on real-time report.



Table 2-2. Significant Event Times Summary (Continued)

EVENT	RANGE TIME		TIME FROM BASE	
	ACTUAL SEC	ACT-PRED SEC	ACTUAL SEC	ACT-PRED SEC
43. S-II LH <sub>2</sub> Step Pressurization	462.8	2.8	300.0	0.0
44. End of Artificial Tau Mode	492.7**	16.7**	329.9**	13.9**
45. Begin Chi Freeze; End of IGM Phase 2	527.1*	-3.1**	364.3*	-6.0**
46. S-II Engine Cutoff (ECO)	536.22	5.06	373.42	2.23
47. Start of Time Base 4 (T <sub>4</sub> )	536.25	5.09	T <sub>4</sub>	-
48. S-IVB Ullage Motor Ignition	537.1	5.2	0.8	0.1
49. S-II/S-IVB Separation Command to Fire Separation Devices and Retro Motors	537.2	5.2	0.9	0.1
50. S-II Retro Motor Burn Time Initiation (Thrust Buildup Begins)	537.3	5.3	1.04	0.3
51. S-IVB Engine Start Command (ESC)	537.28	5.08	1.03	0.01
52. S-IVB Fuel Chilldown Pump Off	538.4	5.1	2.2	0.0
53. S-IVB Engine Ignition (STDV Open)	540.82	5.66	4.57	0.57
54. S-IVB Mainstage	543.32	5.66	7.07	0.57
55. S-IVB PU Mixture Ratio 5.5 On	545.2	5.0	9.0	0.0
56. S-IVB Ullage Case Jettison	549.0	5.1	12.8	0.0
<p>*Accurate to within <math>\pm 0.5</math> second.  **Actual or predicted time is accurate to major computation cycle dependent upon length of computation cycle.</p>				

Table 2-2. Significant Event Times Summary (Continued)

EVENT	RANGE TIME		TIME FROM BASE	
	ACTUAL SEC	ACT-PRED SEC	ACTUAL SEC	ACT-PRED SEC
57. End of Chi Freeze; IGM Phase 3 Initiated and Start of Artificial Tau Mode	551.0*	12.0**	14.7*	6.9**
58. End of Artificial Tau Mode	552.9**	3.4**	16.6**	-1.8**
59. Begin Chi Bar Steering	631.4*	15.4**	95.2*	10.3**
60. Begin Chi Freeze; End of IGM Phase 3	657.8*	16.3**	121.6*	11.2**
61. S-IVB Velocity Cutoff Command (Guidance Cutoff)	664.65	15.93	T <sub>5</sub> -0.23	-0.03
62. S-IVB Engine Cutoff (ECO)	664.66	15.93	T <sub>5</sub> -0.21	-0.01
63. Start of Time Base 5 (T <sub>5</sub> )	664.87	15.95	T <sub>5</sub>	-
64. S-IVB APS Ullage Engine Ignition	665.2	15.9	0.3	0.0
65. S-IVB LOX Tank Pressurization Off	666.2	15.9	1.4	0.0
66. Parking Orbit Insertion	674.65	15.93	9.78	-0.02
67. Command Maneuver to Local Horizontal Attitude	684.9*	15.9**	20.0*	-0.1**
68. S-IVB LH <sub>2</sub> Continuous Vent On (CVS)	723.8	15.9	59.0	0.0
69. S-IVB APS Ullage Engine Cutoff	751.9	15.9	87.0	0.0

\*Accurate to within ±0.5 second.

\*\*Actual or predicted time is accurate to major computation cycle dependent upon length of computation cycle.

Table 2-2. Significant Event Times Summary (Continued)

EVENT	RANGE TIME		TIME FROM BASE	
	ACTUAL SEC	ACT-PRED SEC	ACTUAL SEC	ACT-PRED SEC
70. First Orbital Navigation Calculations	767.7**	10.7**	102.8*	-5.3**
71. Maneuver to Separation Attitude	9241.0*	12.0**	8576.1	-4.0**
72. CSM/LM S-IVB Separation Command	9676.0	93.1	9011.1	77.1
73. CSM/LM S-IVB Docking	10,927+	504	10,262+	488
74. PU Inverter and DC Power On	13,264.8++	15.9	12,600++	0.0
75. CSM/LM Ejection from S-IVB	14,886+	-97	14,221+	-113
76. Command Maneuver to Local Horizontal Attitude	15,905.1*	12.2**	15,240.2	-3.9**
77. Restart Maneuver Enable (Ground Command)	16,452+	-	15,787+	-
78. Begin S-IVB First Restart Preparations; Start of Time Base 6 (T <sub>6</sub> )	16,577.24	5.30	T <sub>6</sub>	-
79. Begin Powered Flight Navigation	16,582 ⊙	16**	15,917 ⊙	0.0
80. S-IVB O <sub>2</sub> /H <sub>2</sub> Burner LH <sub>2</sub> On	16,618.5	5.3	41.3	0.0
81. S-IVB O <sub>2</sub> /H <sub>2</sub> Burner Exciters On	16,618.8	5.3	41.6	0.0
82. S-IVB O <sub>2</sub> /H <sub>2</sub> Burner LOX On (Helium Heater On)	16,619.2	5.3	42.0	0.0
<p>*Accurate to within +0.5 second.  **Actual or predicted time is accurate to major computation cycle dependent upon length of computation cycle.  +Based on real-time report.  ++Derived Time  ⊙ Accurate to within ±2.0 seconds.</p>				

Table 2-2. Significant Event Times Summary (Continued)

EVENT	RANGE TIME		TIME FROM BASE	
	ACTUAL SEC	ACT-PRED SEC	ACTUAL SEC	ACT-PRED SEC
83. S-IVB LH <sub>2</sub> Vent Off (CVS Off)	16,619.4 <sup>++</sup>	5.3	42.2 <sup>++</sup>	0.0
84. S-IVB LH <sub>2</sub> Repres- surization Control On	16,625.3	5.3	48.1	0.0
85. S-IVB LOX Repres- surization Control On	16,625.5	5.3	48.3	0.0
86. S-IVB Aux Hydraulic Pump Flight Mode On	16,796.2	5.3	219.0	0.0
87. S-IVB LOX Chilldown On	16,826.2	5.3	249.0	0.0
88. S-IVB LH <sub>2</sub> Chilldown ON	16,831.2	5.3	254.0	0.0
89. S-IVB Prevalves Closed	16,836.2	5.3	259.0	0.0
90. S-IVB PU Mixture Ratio 4.5 On	17,027.4	5.3	450.2	0.0
91. S-IVB APS Ullage Engine Ignition	17,073.6	5.3	496.3	0.0
92. S-IVB O <sub>2</sub> /H <sub>2</sub> Burner LH <sub>2</sub> Off	17,074.0	5.3	496.8	0.0
93. S-IVB O <sub>2</sub> /H <sub>2</sub> Burner LOX Off (Helium Heater Off)	17,078.5	5.3	501.3	0.0
94. Prevalves Close Off	17,136.3	5.3	559.4	0.0
95. S-IVB LH <sub>2</sub> Chilldown Off	17,146.6	5.3	569.4	0.0
96. S-IVB LOX Chilldown Off	17,146.8	5.3	569.6	0.0
97. S-IVB Engine Re- start Command (2nd ESC-Fuel Lead Initiation)	17,147.20	5.26	569.96	-0.05
<sup>++</sup> Derived Time.				

Table 2-2. Significant Event Times Summary (Continued)

EVENT	RANGE TIME		TIME FROM BASE	
	ACTUAL SEC	ACT-PRED SEC	ACTUAL SEC	ACT-PRED SEC
98. S-IVB APS Ullage Cutoff	17,150.3	5.3	573.0	0.0
99. S-IVB 2nd Ignition (STDV Open)	17,155.54	5.80	578.30	0.50
100. S-IVB Mainstage	17,158.04	5.80	580.80	0.50
101. PU Programmed Mixture Ratio Off	17,160.2	5.3	583.0	0.0
102. Freeze Inertial Attitudes	17,161.5*	8.6**	584.1*	3.1**
103. S-IVB Engine Cutoff (2nd ECO)	17,217.60	5.26	T <sub>7</sub> -0.22	-0.02
104. Start of Time Base 7 (T <sub>7</sub> )	17,217.82	5.28	T <sub>7</sub>	-
105. S-IVB APS Ullage Engine Ignition	17,218.0	5.3	0.2	0.0
106. S-IVB LH <sub>2</sub> Vent On (CVS)	17,218.2	5.2	0.4	0.0
107. Intermediate Orbit Insertion	17,227.60	5.26	9.78	-0.02
108. First Orbital Navigation Calculations	17,234.2	6.7**	16.3	1.3**
109. S-IVB APS Ullage Engine Off	17,236.8	5.3	19.0	0.0
110. Command Maneuver to Local Horizontal Attitude	17,238.6*	5.9**	20.4*	0.2**
111. Restart Maneuver Enable (Ground Command)	20,417+	-	3199+	-
112. Begin Powered Flight Navigation	21,579.0*	17.4**	4361.1*	12.0**

+Based on real-time report.  
 \*Accurate to within +0.5 second.  
 \*\*Actual or predicted time is accurate to major computation cycle dependent upon length of computation cycle.

Table 2-2. Significant Event Times Summary (Continued)

EVENT	RANGE TIME		TIME FROM BASE	
	ACTUAL SEC	ACT-PRED SEC	ACTUAL SEC	ACT-PRED SEC
113. Begin S-IVB Re-start Preparations; Start of Time Base 8 (T <sub>8</sub> )	21,580.98	6.06	T <sub>8</sub>	-
114. S-IVB Aux Hydraulic Pump Flight Mode On	21,679.9	6.0	99.0	0.0
115. S-IVB LOX Chill-down On	21,709.9	6.0	129.0	0.0
116. S-IVB LH <sub>2</sub> Chill-down On	21,714.9	6.0	134.0	0.0
117. S-IVB Prevalves Closed	21,720.0	6.0	139.0	0.0
118. S-IVB PU Mixture Ratio 4.5 On	21,781.2	6.0	200.2	0.0
119. S-IVB O <sub>2</sub> /H <sub>2</sub> Burner LH <sub>2</sub> On	21,826.9	6.0	246.0	0.0
120. S-IVB O <sub>2</sub> /H <sub>2</sub> Burner Exciters On	21,827.2	6.0	246.3	0.0
121. S-IVB O <sub>2</sub> /H <sub>2</sub> Burner LOX On (Helium Heater On)	21,827.6	6.0	246.7	0.0
122. S-IVB APS Ullage Engines Ignition	21,956.9	6.0	376.0	0.0
123. S-IVB O <sub>2</sub> /H <sub>2</sub> Burner LH <sub>2</sub> Off	21,957.4	6.0	376.5	0.0
124. S-IVB O <sub>2</sub> /H <sub>2</sub> Burner LOX Off (Helium Heater Off)	21,962.0	6.0	381.0	0.0
125. S-IVB LH <sub>2</sub> Vent Off (CVS)	21,965.3	6.0	384.4	0.0
126. S-IVB Engine Re-start Command (3rd ESC-Fuel Lead Initiation Ground Command)	21,987.35	7.42	406.37	1.36

Table 2-2. Significant Event Times Summary (Continued)

EVENT	RANGE TIME		TIME FROM BASE	
	ACTUAL SEC	ACT-PRED SEC	ACTUAL SEC	ACT-PRED SEC
127. S-IVB LH <sub>2</sub> Chill-down Off	22,030.3	6.0	449.4	0.0
128. S-IVB LOX Chill-down Off	22,030.6	6.0	449.6	0.0
129. S-IVB APS Ullage Engine Cutoff	22,033.9	6.0	453.0	0.0
130. S-IVB 3rd Ignition (STDV Open)	22,039.26	6.47	458.28	0.48
131. S-IVB 3rd Mainstage	22,041.76	6.47	460.78	0.48
132. PU Programmed Mixture Ratio Off	22,043.9	6.0	463.0	0.0
133. Freeze Inertial Attitudes	22,044.6*	9.1**	463.5*	2.9**
134. S-IVB Engine Cutoff (3rd ECO)	22,281.32	5.99	T <sub>g</sub> -0.21	-0.01
135. Start of Time Base 9 (T <sub>g</sub> )	22,281.53	6.00	T <sub>g</sub>	-
136. Escape Orbit Injection	22,291.32	5.99	9.79	-0.01
137. First Orbital Navigation Calculation	22,298.0*	7.5**	16.35*	1.3**
138. Command Maneuver to Local Horizontal Attitude	22,302.0*	7.3**	19.4*	-0.8**
139. S-IVB Start Bottle Vent On	22,341.5	6.0	60.0	0.0
140. S-IVB Start LOX Dump	22,371.5	6.0	90.0	0.0
141. S-IVB Engine Helium Control Valve Open	22,371.7	6.0	90.2	0.0

\*Accurate to within ±0.5 second.  
 \*\*Actual or predicted time is accurate to major computation cycle dependent upon length of computation cycle.

Table 2-2. Significant Event Times Summary (Continued)

EVENT	RANGE TIME		TIME FROM BASE	
	ACTUAL SEC	ACT-PRED SEC	ACTUAL SEC	ACT-PRED SEC
142. S-IVB Start LH <sub>2</sub> Dump	23,051.3	6.0	769.8	0.0
143. S-IVB Engine Helium Control Valve Open	23,051.5	6.0	770.0	0.0
144. S-IVB Aux Hydraulic Pump Flight Mode Off	24,147.5++	6.0	1866.0++	0.0
145. S-IVB Engine Pneumatic System Vent On	24,157.5++	6.0	1876.0++	0.0
146. S-IVB Engine Pneumatic System Vent Off	24,757.5	6.0	2476.0	0.0
147. C-Band Radar Off	27,214.7	-	4933.1	-
148. S-IVB APS Ullage Engine No. 1 Ignition	27,244.6	-	4963.1	-
149. S-IVB APS Ullage Engine No. 2 Ignition	27,245.8	-	4964.2	-
150. S-IVB APS Ullage Engine No. 2 Depletion	27,671	-	5389.5	-
151. S-IVB APS Ullage Engine No. 1 Depletion	27,713	-	5431.5	-

++Derived Times.



Table 2-3. Variable Time and Commanded Switch Selector Events

FUNCTION	STAGE	RANGE TIME (SECONDS)	TIME FROM BASE (SECONDS)	REMARKS
Telemetry Calibrator Inflight Calibration On	IU	2286.2	T <sub>5</sub> +1621.4	TAN Rev 1
TM Calibrate On	S-IVB	2286.4	T <sub>5</sub> +1621.6	TAN Rev 1
TM Calibrate Off	S-IVB	2287.4	T <sub>5</sub> +1622.6	TAN Rev 1
Telemetry Calibrator Inflight Calibrate Off	IU	2291.2	T <sub>5</sub> +1626.4	TAN Rev 1
Telemetry Calibrator Inflight Calibrate On	IU	3198.2	T <sub>5</sub> +2533.3	CRO Rev 1
TM Calibrate On	S-IVB	3198.4	T <sub>5</sub> +2533.5	CRO Rev 1
TM Calibrate Off	S-IVB	3199.4	T <sub>5</sub> +2534.5	CRO Rev 1
Telemetry Calibrator Inflight Calibrate Off	IU	3203.1	T <sub>5</sub> +2538.3	CRO Rev 1
Telemetry Calibrator Inflight Calibrate On	IU	5366.1	T <sub>5</sub> +4701.3	GYM Rev 1
TM Calibrate On	S-IVB	5366.3	T <sub>5</sub> +4701.5	GYM Rev 1
TM Calibrate Off	S-IVB	5367.3	T <sub>5</sub> +4702.5	GYM Rev 1
Telemetry Calibrator Inflight Calibrate Off	IU	5371.1	T <sub>5</sub> +4706.3	GYM Rev 1
Telemetry Calibrator Inflight Calibrate On	IU	7822.2	T <sub>5</sub> +7157.3	TAN Rev 2
TM Calibrate On	S-IVB	7822.4	T <sub>5</sub> +7157.6	TAN Rev 2
TM Calibrate Off	S-IVB	7823.4	T <sub>5</sub> +7158.6	TAN Rev 2
Telemetry Calibrator Inflight Calibrate Off	IU	7827.2	T <sub>5</sub> +7162.4	TAN Rev 2
Telemetry Calibrator Inflight Calibrator On	IU	8790.1	T <sub>5</sub> +8125.3	CRO Rev 2
TM Calibrate On	S-IVB	8790.3	T <sub>5</sub> +8125.5	CRO Rev 2
TM Calibrate Off	S-IVB	8791.4	T <sub>5</sub> +8126.5	CRO Rev 2
Telemetry Calibrator Inflight Calibrate Off	IU	8795.1	T <sub>5</sub> +8130.3	CRO Rev 2
IU Command System Enable	IU	8795.6	T <sub>5</sub> +8130.8	CRO Rev 2
Telemetry Calibrator Inflight Calibrate On	IU	10,318.1	T <sub>5</sub> +9653.3	HAW Rev 2

Table 2-3. Variable Time and Commanded Switch Selector Events (Continued)

FUNCTION	STAGE	RANGE TIME (SECONDS)	TIME FROM BASE (SECONDS)	REMARKS
TM Calibrate On	S-IVB	10,318.3	T <sub>5</sub> +9653.5	HAW Rev 2
TM Calibrate Off	S-IVB	10,319.3	T <sub>5</sub> +9654.5	HAW Rev 2
Telemetry Calibrator Inflight Calibrate Off	IU	10,323.1	T <sub>5</sub> +9658.3	HAW Rev 2
Telemetry Calibrator Inflight Calibrate On	IU	10,958.1	T <sub>5</sub> +10,293.3	GDS Rev 2
TM Calibrate On	S-IVB	10,958.3	T <sub>5</sub> +10,293.5	GDS Rev 2
TM Calibrate Off	S-IVB	10,959.3	T <sub>5</sub> +10,294.5	GDS Rev 2
Telemetry Calibrator Inflight Calibrate Off	IU	10,963.1	T <sub>5</sub> +10,298.3	GDS Rev 2
Telemetry Calibrator Inflight Calibrate On	IU	14,374.1	T <sub>5</sub> +13,709.3	CRO Rev 2
TM Calibrate On	S-IVB	14,374.3	T <sub>5</sub> +13,709.5	CRO Rev 3
TM Calibrate Off	S-IVB	14,375.3	T <sub>5</sub> +13,710.3	CRO Rev 3
Telemetry Calibrator Inflight Calibrate Off	IU	14,379.1	T <sub>5</sub> +13,714.3	CRO Rev 3
Telemetry Calibrator Inflight Calibrate On	IU	15,870.1	T <sub>5</sub> +15,205.3	ARIA 3 Rev 3
TM Calibrate On	S-IVB	15,870.3	T <sub>5</sub> +15,205.5	ARIA 3 Rev 3
TM Calibrate Off	S-IVB	15,871.3	T <sub>5</sub> +15,206.5	ARIA 3 Rev 3
Telemetry Calibrator Inflight Calibrate Off	IU	15,875.1	T <sub>5</sub> +15,210.3	ARIA 3 Rev 3
TM Calibrate Off	S-IVB	16,575.4	T <sub>5</sub> +15,910.6	GDS Rev 2
Water Coolant Valve Open	IU	17,315.2	T <sub>7</sub> +96.4	LVDC Function
Water Coolant Valve Closed	IU	17,615.8	T <sub>7</sub> +397.9	LVDC Function
Command PCM Coaxial Switch Low Gain Antenna	IU	20,595.3	T <sub>7</sub> +3376.5	Ground Command Sequence
Command CCS Switch Low Gain Antenna	IU	20,595.3	T <sub>7</sub> +3376.5	Ground Command Sequence
Water Coolant Valve Open	IU	21,526.9	T <sub>7</sub> +4309.0	LVDC Function
Chilldown Shutoff Valve Close Off	S-IVB	21,710.0	T <sub>8</sub> +129.1	Ground Command Sequence for 2nd S-IVB Restart
Fuel Chilldown Pump Off	S-IVB	21,729.2	T <sub>8</sub> +148.2	Begin Ground Command Sequence for 2nd S-IVB Restart
LOX Chilldown Pump Off	S-IVB	21,730.0	T <sub>8</sub> +149.0	Ground Command Sequence for 2nd S-IVB Restart
Water Coolant Valve Closed	IU	21,828.6	T <sub>8</sub> +247.6	LVDC Function
Chilldown Shutoff Valve Close Off	S-IVB	21,952.8	T <sub>8</sub> +371.8	Ground Command Sequence for 2nd S-IVB Restart
Prevalves Close Off	S-IVB	21,953.5	T <sub>8</sub> +372.6	Ground Command Sequence 2nd S-IVB Restart
S-IVB Engine Cutoff Off	S-IVB	21,954.3	T <sub>8</sub> +373.3	Ground Command Sequence for 2nd S-IVB Restart

Table 2-3. Variable Time and Commanded Switch Selector Events (Continued)

FUNCTION	STAGE	RANGE TIME (SECONDS)	TIME FROM BASE (SECONDS)	REMARKS
Engine Ready Bypass	S-IVB	21,955.1	T <sub>g</sub> +374.1	Ground Command Sequence for 2nd S-IVB Restart
S-IVB Engine Start On	S-IVB	21,987.3	T <sub>g</sub> +406.4	Ground Command Sequence for 2nd S-IVB Restart
Telemetry Calibrator Inflight Calibrate On	IU	22,698.1	T <sub>g</sub> +416.5	GWM Rev 4
TM Calibrate On	S-IVB	22,698.3	T <sub>g</sub> +416.7	GWM Rev 4
TM Calibrate Off	S-IVB	22,699.3	T <sub>g</sub> +417.7	GWM Rev 4
Telemetry Calibrator Inflight Calibrate Off	IU	22,703.1	T <sub>g</sub> +421.5	GWM Rev 4
Engine Mainstage Control Valve Open Off	S-IVB	22,976.9	T <sub>g</sub> +695.2	GWM Rev 4
Engine He Control Valve Open Off	S-IVB	22,977.7	T <sub>g</sub> +696.1	GWM Rev 4
Engine He Control Valve Open On	S-IVB	22,993.4	T <sub>g</sub> +711.6	GWM Rev 4
Passivation Enable	S-IVB	22,993.6	T <sub>g</sub> +712.0	GWM Rev 4
Engine Mainstage Control Valve Open On	S-IVB	22,994.1	T <sub>g</sub> +712.8	GWM Rev 4
Start Bottle Vent Control Valve Open On	S-IVB	23,042.6	T <sub>g</sub> +761.0	GWM Rev 4
Engine Ignition Phase Control Valve Open Off	S-IVB	23,156.2	T <sub>g</sub> +874.6	GWM Rev 4
Engine He Control Valve Open Off	S-IVB	23,157.0	T <sub>g</sub> +875.4	GWM Rev 4
Passivation Enable	S-IVB	23,172.5	T <sub>g</sub> +890.9	GWM Rev 4
Engine Ignition Phase Control Valve Open On	S-IVB	23,173.2	T <sub>g</sub> +891.6	GWM Rev 4
Engine He Control Valve Open On	S-IVB	23,175.1	T <sub>g</sub> +893.4	LVDC Function
S-IVB Engine Cutoff Off	S-IVB	24,770.0	T <sub>g</sub> +2488.4	LVDC Function
Engine Ready Bypass	S-IVB	24,770.9	T <sub>g</sub> +2489.4	LVDC Function
Prevalves Close Off	S-IVB	24,771.9	T <sub>g</sub> +2490.3	LVDC Function
S-IVB Engine Start On	S-IVB	24,772.8	T <sub>g</sub> +2491.3	LVDC Function
Water Coolant Valve Open	IU	24,883.4	T <sub>g</sub> +2551.9	LVDC Function
Water Coolant Valve Closed	IU	25,134.9	T <sub>g</sub> +2853.4	LVDC Function
Command PCM Coaxial Switch Omni Antenna	IU	27,010.1	T <sub>g</sub> +4728.5	Ground Command Sequence
Command CCS Coaxial Switch Omni Antenna	IU	27,010.1	T <sub>g</sub> +4728.6	Ground Command Sequence
Command PCM Coaxial Switch High Gain Antenna	IU	27,109.1	T <sub>g</sub> +4827.5	Ground Command Sequence

Table 2-3. Variable Time and Commanded Switch Selector Events (Continued)

FUNCTION	STAGE	RANGE TIME (SECONDS)	TIME FROM BASE (SECONDS)	REMARKS
Command CCS Coaxial Switch Failure Safe High Gain Antenna	IU	27,109.1	T <sub>g</sub> +4827.6	Ground Command Sequence
Command PCM Coaxial Switch Fail Safe Low Gain Antenna	IU	27,163.7	T <sub>g</sub> +4882.1	Ground Command Sequence
Command CCS Switch Low Gain Antenna	IU	27,163.7	T <sub>g</sub> +4882.2	Ground Command Sequence
Command Inhibit C-Band Transponder No. 1	IU	27,191.0	T <sub>g</sub> +4909.4	Ground Command Sequence
Command Inhibit C-Band Transponder No. 2	IU	27,214.7	T <sub>g</sub> +4933.1	Ground Command Sequence
S-IVB Ullage Engine No. 1 On	S-IVB	27,244.6	T <sub>g</sub> +4963.0	LVDC Function
S-IVB Ullage Engine No. 2 On	S-IVB	27,245.8	T <sub>g</sub> +4964.2	LVDC Function

## SECTION 3

### LAUNCH OPERATIONS

#### 3.1 SUMMARY

The AS-504 Apollo 9 terminal countdown (-28 hours) was started at 22:00:00 Eastern Standard Time (EST), February 26, 1969. However the launch countdown was recycled to -42 hours because of the astronauts medical condition. The count was resumed at 2:30:00 EST, March 1, 1969.

The ground systems supporting the Apollo 9 countdown and launch performed exceptionally well. There were no significant failures or anomalies. Several systems experienced component failures and malfunctions, but these problems did not cause any holds or significant delays in the scheduled sequences of launch operations.

Damage to the complex and support equipment as a result of the AS-504 launch was minor and the slightest yet experienced.

#### 3.2 PRELAUNCH MILESTONES

Launch vehicle checkout at Kennedy Space Center (KSC) began with the arrival of the S-II-504 stage on May 15, 1968. The S-IC stage and the IU arrived on September 30, 1968, and the S-IVB stage arrived on September 12, 1968. The Lunar Module (LM) -3 arrived June 14, 1968 and was reassigned to this mission on August 19, 1968. The Command and Service Module (CSM) -103 arrived on October 5, 1968. After satisfactory checkout, the spacecraft was mounted atop the launch vehicle on December 3, 1968. The space vehicle was transferred to Launch Complex 39A on January 3, 1969. Space vehicle checkout operations at the pad proceeded without any significant problems that would impact launch readiness; however, because the astronauts developed colds, the terminal countdown initiated on February 26, 1969 was interrupted. After medical clearance of the crew, recycle countdown was started on March 1, 1969, and the Apollo 9 was successfully launched without any unscheduled holds, at 11:00:00 EST, March 3, 1969.

#### 3.3 COUNTDOWN EVENTS

The AS-504 Apollo 9 terminal countdown was picked up at 22:00:00 EST, February 26, 1969 (-28 hours). At 10:00:00 EST, February 27, 1969 (-16 hours) the scheduled 3-hour hold began, but at 10:30:00 EST during this

hold, the space vehicle was recycled to -42 hours because of the astronauts medical condition. Count pickup time was 2:30:00 EST, March 1, 1969.

The recycle countdown proceeded through launch scheduled as follows:

- a. -28 hours, 5.5-hour built-in hold
- b. -16 hours, 3-hour built-in hold
- c. -9 hours, 6-hour built-in hold

Launch occurred at 11:00:00.6 EST, March 3, 1969.

### 3.4 PROPELLANT LOADING

#### 3.4.1 RP-1 Loading

The RP-1 system successfully supported the AS-504 launch countdown. Replenish operations for launch were started at -13:10:00 and were completed 44 minutes later at -12:26:00. Level adjustment operations were initiated at -51 minutes and completed at -31 minutes, establishing the required S-IC flight mass of RP-1. Approximately 802.6 m<sup>3</sup> (212,035 gal) of RP-1 was consumed in support of the launch countdown. Following level adjustment, liquid sensor No. 1 failed to indicate a steady dry condition. Consequently, the transfer line automatic drain and inerting sequence was terminated before the transfer line was completely drained and purged. Drain and purge of the transfer line was completed manually. As was the case with all previous launches, the dry chemical fire extinguisher system in Launch Umbilical Tower (LUT) Room 4A activated during liftoff, covering RP-1 system components with powder.

#### 3.4.2 LOX Loading

The LOX system supported the launch countdown satisfactorily. All phases of the LOX loading operation were completed successfully and without incident. The LOX fill sequence was started at -8:19:00, with all stage replenish normal mode attained 2:57:00 later. Approximately 2203.1 m<sup>3</sup> (582,000 gal) of LOX was consumed in support of the launch countdown. Several facility measurements which indicate operational status for the LOX replenish pump were lost or exceeded redlines. However, in each instance sufficient backup measurements were available to verify satisfactory pump operation without interrupting the loading sequence. Launch damage to the LOX system was minor. A LUT control distributor was split open and some internal components damaged. In addition, several electrical cables were damaged by blast and must be replaced.

#### 3.4.3 LH<sub>2</sub> Loading

The LH<sub>2</sub> system successfully supported the launch countdown with no major incidents. The fill sequence began with initiation of S-II loading at

-4:45:00 and was terminated 88 minutes later upon achieving 100 percent S-IVB LH<sub>2</sub> load. A nominal loading time of 81 minutes was planned, but both S-II and S-IVB fast-fill modes were terminated early, apparently by a logic discrepancy. The Propellant Tanking Control System (PTCS) was programmed to terminate fast-fill for S-II and S-IVB at 96 and 97 percent, respectively. However, the fast-fill modes were terminated at 93 (S-II) and 94 (S-IVB) percent of flight mass by signals from the stage stop fill discretes. The early termination of fast-fill did not significantly affect the loading operation. Approximately 1854.9 m<sup>3</sup> (490,000 gal) of LH<sub>2</sub> was consumed in support of the launch countdown. Launch damage to the LH<sub>2</sub> system was minor. A seam was split open on the LH<sub>2</sub> disconnect tower control distributor, but there was no damage to internal components.

#### 3.4.4 Auxiliary Propulsion System Propellant Loading

Propellant loading of the S-IVB Auxiliary Propulsion System (APS) was accomplished satisfactorily. Total propellant mass in both modules at liftoff was 182 kilograms (401.2 lbm) of Nitrogen Tetroxide (N<sub>2</sub>O<sub>4</sub>) and 116 kilograms (255.8 lbm) of Monomethyl Hydrazine (MMH).

### 3.5 S-II INSULATION, PURGE AND LEAK DETECTION

The S-II-504 stage was the first to utilize improved joint closeouts of the external insulation. The joint closeouts for the insulation panels were of the nylon wet-layup configuration and replaced the rubber doublers used as closeouts on previous stages. The rubber doublers were susceptible to excessive cracking at low temperatures. A marked improvement in performance of the external insulation during ground hold and flight reflected the improved quality of the new insulation. Hazardous gas concentrations were low in all purge circuits.

#### 3.5.1 Forward Bulkhead Insulation/Forward Bulkhead Uninsulated Circuits

The forward bulkhead purge circuits were set to provide a stage inlet pressure of 1.0 N/cm<sup>2</sup> (1.5 psig). The forward bulkhead insulation circuit and uninsulated circuit were interconnected as on the previous flight vehicle. During propellant tanking the insulation circuit inlet pressure remained steady at approximately 1.0 N/cm<sup>2</sup> (1.5 psig) and the outlet pressure was slightly positive at approximately 0.01 N/cm<sup>2</sup> (0.015 psig) until launch. Inlet pressure of the forward bulkhead uninsulated circuit was steady at 1.5 N/cm<sup>2</sup> (2.2 psig).

#### 3.5.2 Forward Skirt

The forward skirt inlet pressure decreased from 0.7 N/cm<sup>2</sup> (1.0 psig) at the beginning of LOX loading to 0.5 N/cm<sup>2</sup> (0.7 psig) at the beginning of LH<sub>2</sub> loading. This loss of pressure was caused by the LH<sub>2</sub> tank chilling during LOX loading. After LH<sub>2</sub> loading the inlet pressure remained steady at 0.4 N/cm<sup>2</sup> (0.6 psig) until launch.

### 3.5.3 Sidewall

From an ambient set-up value of  $1.47 \text{ N/cm}^2$  (2.14 psig), the sidewall inlet pressure declined gradually to  $1.2 \text{ N/cm}^2$  (1.8 psig) during LH<sub>2</sub> tank chill-down. During LH<sub>2</sub> fill, the pressure further declined to  $1.0 \text{ N/cm}^2$  (1.5 psig) but at the completion of LH<sub>2</sub> loading it had recovered to  $1.2 \text{ N/cm}^2$  (1.8 psig) where it remained until launch.

Following nearly the same profile as the inlet, the sidewall outlet pressure decreased gradually from  $1.2$  to  $0.7 \text{ N/cm}^2$  (1.8 to 1.0 psig) during LH<sub>2</sub> tank chilldown. At the beginning of LH<sub>2</sub> fill the pressure changed from  $0.82 \text{ N/cm}^2$  (1.2 psig) to a minimum of  $0.23 \text{ N/cm}^2$  (0.34 psig) but recovered to  $0.4 \text{ N/cm}^2$  (0.6 psig) in approximately 20 minutes, continuing to increase to  $0.6 \text{ N/cm}^2$  (0.8 psig) at launch. There were no insulation discrepancies identified by operational television inspection nor was back purge required at any time.

Sidewall external temperature measurements generally ranged from 266 to 278°K (20 to 40°F) with two measurements as low as 236 and 228°K (-25 and -50°F). Because of the high relative humidity, a heavy frost layer formed on the insulation. Maximum temperature indicated in flight was 300°K (80°F). Total heat flow into the hydrogen during flight was 164,479,000 watt-seconds (156,000 Btu), well below contract requirements.

### 3.5.4 Cylinder 1, Bolting Ring and J-Ring Combined Circuits

Outlet pressure remained positive at approximately  $0.03 \text{ N/cm}^2$  (0.05 psig) indicating integrity of the cylinder 1 bonded foam-block insulation which was replaced prior to shipment to KSC. This repair utilized Lefkowied 109 adhesive supported by a glass carrier cloth to bond the preformed foam blocks to the tank wall. Inlet pressure remained steady at approximately  $1.2 \text{ N/cm}^2$  (1.8 psig).

### 3.5.5 Common Bulkhead

Inlet pressure remained at approximately  $2.5 \text{ N/cm}^2$  (3.6 psig) during the period the bulkhead was purged.

The outlet pressure decreased from approximately  $1.9$  to  $1.7 \text{ N/cm}^2$  (2.7 to 2.4 psig) during LOX loading but recovered normally. At the start of LH<sub>2</sub> loading the pressure decreased to  $-2.1 \text{ N/cm}^2$  (-3 psig) before recovering after approximately 20 minutes. This is normal and is the result of thermal shrinkage of the purge gas.

Evacuation of the bulkhead was started approximately 3:40:00 prior to launch. The redline limit of  $2.1 \text{ N/cm}^2$  (3 psia) was reached in approximately 45 minutes. Pressure at liftoff was  $0.21 \text{ N/cm}^2$  (0.3 psia) and did not exceed  $0.34 \text{ N/cm}^2$  (0.5 psia) during flight.



### 3.5.6 Feedline Elbow

The feedline elbow circuit consisted of internal grooves cut into the bolting support rings that retained the stainless steel elbows.

Inlet pressure varied between 1.9 and 2.0 N/cm<sup>2</sup> (2.8 and 2.9 psig) throughout the countdown. The outlet pressure remained reasonably steady at 0.6 N/cm<sup>2</sup> (0.8 psig) during the countdown.

## 3.6 GROUND SUPPORT EQUIPMENT (GSE)

### 3.6.1 Ground/Vehicle Interface

Ground systems performance was highly satisfactory. The Holddown Arms (HDA), Tail Service Masts (TSM), Service Arms (SA), and all other ground equipment functioned well in support of AS-504 launch.

All HDA were released pneumatically. All HDA release occurred at 0.3 second. The drop and lanyard pull for each arm was sufficiently fast to preclude detonation of the explosive nuts. The HDA service arm control switches functioned properly. Blast damage to the HDA consisted mainly of warped protective hoods and removal of some of the ablative coating. The grout under the base of HDA No. 3 was blown in, allowing flames to scorch some of the electrical cables inside the base.

TSM retraction was normal and all protective hoods closed properly. Mast retraction times were 2.53 seconds for TSM 1-2, 2.09 seconds for TSM 3-2, and 2.34 seconds for TSM 3-4, measured from umbilical plate separation to mast retract indication. The ablative coating applied to the TSM provided adequate blast protection; only a top coating will be required to restore the ablative protection.

SA systems performed within design limits during the launch sequence and retraction was normal. Damage to the SA at launch was the slightest yet experienced. There was some hydraulic fluid leakage in the SA No. 1 control console, however, there were no fires.

The SA No. 1 latchback "latched" indication was not displayed, and the "unlatched" indication was not extinguished, on the firing room control panel following liftoff. Postlaunch data reviews revealed that the unlatched signal went off at 1.73 seconds and that the latched signal went on at 1.77 seconds. Accordingly, it has been concluded that latchback of the arm to the tower was achieved in the expected manner.

The accumulator level switch in SA No. 4 hydraulic withdrawal system did not respond properly during performance of the automated pressure and level check program from -14 to -8 minutes. The hydraulic level low indication was so rapid that it was not sensed by the computer and the accumulator bleed valve was therefore not commanded closed. The program

halted for corrective instruction after a 90-second lapse without sensing low level. The bleed valve control switch was positioned manually. To insure a full charge in the system, the charging valve control switch was manually placed in the open position for 3 seconds and was then returned to the automatic mode.

### 3.6.2 MSFC Furnished Ground Support Equipment

3.6.2.1 S-IC Stage Oriented. The S-IC stage GSE performed satisfactorily during countdown and launch. Blast damage to the mechanical support equipment was minor. LUT storage racks incurred slight structural damage and activation of the dry chemical fire extinguishing system covered the hydraulic supply and checkout unit with white powder. There was no appreciable launch damage to the electrical support equipment.

The only mechanical support equipment anomaly occurred during charging of the the S-IC Gaseous Nitrogen ( $\text{GN}_2$ ) control bottles at -6:20:00. The high pressure fill regulator overshot the set pressure of  $2172 \pm 34.5 \text{ N/cm}^2$  ( $3150 \pm 50$  psig) and the  $\text{GN}_2$  bottles were pressurized  $34.5 \text{ N/cm}^2$  (50 psi) over the  $2275 \text{ N/cm}^2$  (3300 psig) redline. The vent valve was cycled and the bottles repressurized to  $2186 \text{ N/cm}^2$  (3170 psig). Bottle pressure stabilized at this value and the repressurization sequence was considered satisfactory for continuation of the countdown.

An electrical support equipment anomaly occurred during S-IC pneumatic systems preparation for launch. A relay in the LOX fill and drain heater circuit failed and caused shorting of an adjacent relay in the engine igniter circuit. The power module, containing both relays, was replaced and the circuit retested with no recurrence of the problem.

3.6.2.2 S-II Stage Oriented. The S-II stage GSE satisfactorily supported countdown and launch. There were no significant failures or anomalies. One minor problem was a defective relay in an amplifier sequencer rack (leak detection circuit) that was removed and replaced prior to -28 hours. Another minor discrepancy was a pneumatic control console (S-II insulation purge) feedline flowmeter output drop to zero during telemetry checks. It was determined that S-II telemetry transmitters caused Radio Frequency (RF) interference in the flowmeter circuitry, however, the flowmeter output is not mandatory during this brief telemetry check period. Only very minor damage was incurred to the S-II GSE during launch.

3.6.2.3 S-IVB Stage Oriented. Overall performance of the S-IVB stage GSE was satisfactory. The only system problems encountered were failures of two dome regulators and a helium relief valve in the pneumatic console. During prelaunch preparations, the  $2206 \text{ N/cm}^2$  (3200 psi) dome regulator located in the pneumatic supply console was replaced because of leakage.

The new regulator also failed after two operational cycles. At the same time the 2206 N/cm<sup>2</sup> (3200 psi) ambient helium relief valve failed open. Both the regulator and relief valve required replacement. Blast damage to the support equipment was generally minor. However, several LUT equipment storage racks received considerable damage such as cracked welds, broken latches and bent doors.

3.6.2.4 IU Stage Oriented. The Instrument Unit (IU) GSE performance during countdown was satisfactory although a few minor anomalies occurred. One of these was valve leakage in the GN<sub>2</sub> supply system. Valve leakage was detected in the GN<sub>2</sub> high pressure system during the pneumatic console regulator adjustment at -20 hours. The adjustment sequence was terminated and the system repressurized for component isolation and inspection. The leakage did not recur although the hardware was cycled a number of times. The system also functioned properly through the rest of the count and subsequent recycle. There was no launch damage sustained by the mechanical or electrical support equipment.

## SECTION 4

### TRAJECTORY

#### 4.1 SUMMARY

The vehicle was launched on an azimuth of 90 degrees east of north. At 13.3 seconds, the vehicle started a roll maneuver to a flight azimuth of 72 degrees east of north. The space-fixed velocity at S-IC Outboard Engine Cutoff (OECO) was 29.33 m/s (96.23 ft/s) lower than nominal. The space-fixed velocity at S-II Engine Cutoff (ECO) was 81.70 m/s (268.04 ft/s) lower than nominal. The space-fixed velocity at S-IVB first engine cutoff was 0.87 m/s (2.86 ft/s) greater than nominal. The altitude at S-IVB first burn cutoff was 0.31 kilometer (0.17 n mi) lower than nominal and the surface range was 66.77 kilometers (36.06 n mi) greater than nominal.

The parking orbit insertion conditions were very close to nominal except for the time of insertion itself. This was due primarily to the below normal performance of the S-IC and S-II stages. Parking orbit insertion time was 15.93 seconds later than nominal. The space-fixed velocity at insertion was 0.61 m/s (2.00 ft/s) greater than nominal and the flight path angle was 0.0049 degree lower than nominal. The eccentricity was 0.000133 greater than nominal. The apogee and perigee were 1.26 kilometer (0.68 n mi) greater than nominal and 0.49 kilometer (0.27 n mi) lower than nominal, respectively.

The intermediate orbit insertion conditions were very close to nominal except for the space-fixed velocity which was 18.67 m/s (61.25 ft/s) greater than nominal. The flight path angle at intermediate orbit insertion was 0.041 degree lower than nominal. The eccentricity was 0.00503 greater than nominal.

The escape orbit injection parameters deviated significantly from nominal. The value of  $C_3$  was 824,712 m<sup>2</sup>/s<sup>2</sup> (8,877,126 ft<sup>2</sup>/s<sup>2</sup>) which was 30,470,506 m<sup>2</sup>/s<sup>2</sup> (327,981,795 ft<sup>2</sup>/s<sup>2</sup>) lower than nominal. The eccentricity was 0.6532 less than nominal, the inclination angle was 0.054 degree less than nominal, and the descending node was 0.242 degree greater than nominal. Required escape velocity for the actual altitude reached at escape orbit injection was 9,596.22 m/s (31,483.66 ft/s). The actual velocity reached at escape orbit injection was 9,637.73 m/s (31,619.85 ft/s) which was 41.51 m/s (136.19 ft/s) greater than required.

The total space-fixed velocity was 1,520.20 m/s (4,987.53 ft/s) lower than nominal and the altitude was 106.05 kilometers (57.26 n mi) higher than nominal.

The actual impact locations for the spent S-IC and S-II stages were determined by a theoretical free-flight simulation. The surface range for the S-IC impact point was 32.10 kilometers (17.33 n mi) less than nominal. The surface range for the S-II impact point was 6.23 kilometers (3.36 n mi) less than nominal.

## 4.2 TRACKING DATA UTILIZATION

### 4.2.1 Tracking During the Ascent Phase of Flight

Tracking data were obtained during the period from the time of first motion through parking orbit insertion.

The ascent trajectory was established by merging the launch phase trajectory with the best estimate trajectory. The launch phase trajectory was established by integrating the telemetered body-fixed accelerometer data, and verified by Offset Frequency Doppler (ODOP) tracking data. The best estimate trajectory utilized telemetered guidance velocities as the generating parameters to fit data from six different C-Band tracking stations. These data points were fit through a guidance error model and constrained to the insertion vector obtained from the orbital solution. Comparison of the ascent trajectory with data from all the tracking systems yielded reasonable agreement.

### 4.2.2 Tracking During Orbital Flight

Orbital tracking was conducted by the NASA Manned Space Flight Network (MSFN). C-Band radar stations furnished data for use in determining the parking orbit, intermediate orbit, and escape orbit. There were also considerable S-Band tracking data available during these periods of flight which were not used due to the abundance of C-Band radar data.

The orbital trajectories were obtained by integrating corrected insertion/injection conditions forward. The insertion/injection conditions, as determined by the Orbital Correction Program (OCP), were obtained by a differential correction procedure which adjusted the estimated insertion/injection conditions to fit the C-Band radar tracking data in accordance with the weights assigned to the data. After all the C-Band radar tracking data were analyzed, some stations and passes were eliminated completely from use in the determination of the insertion/injection conditions.

#### 4.2.3 Tracking During S-IVB Second Burn Phase of Flight

C-Band radar data were obtained from the stations located at Patrick Air Force Base, Merritt Island, and Grand Bahama Island. These tracking data were found to be incompatible with the restart and intermediate orbit insertion vectors determined by the OCP, and were not used for the trajectory determination.

The S-IVB second burn trajectory was obtained by integrating the corrected restart vector forward utilizing telemetered guidance velocities. The corrected restart vector was determined by a procedure which adjusted the estimated restart vector in order to arrive at the same state vector at intermediate orbit insertion as determined from the intermediate orbital solution.

#### 4.2.4 Tracking During S-IVB Third Burn Phase of Flight

C-Band radar data were obtained from Carnarvon during the period from S-IVB second restart through escape orbit injection.

The S-IVB third burn trajectory was obtained by integrating the corrected second restart vector forward utilizing telemetered guidance velocities. The corrected second restart vector was determined by a procedure which adjusted the estimated restart vector to fit the tracking data in a best estimate sense utilizing the telemetered guidance velocities as generating parameters. Comparison of the second restart vector and the resulting escape orbit injection vector with those determined by orbital solutions yielded reasonable agreement.

### 4.3 TRAJECTORY EVALUATION

#### 4.3.1 Ascent Trajectory

Actual and nominal altitude, surface range, and cross range for the ascent phase are presented in Figure 4-1. Actual and nominal space-fixed velocity and flight path angle during ascent are shown in Figure 4-2. The velocity deviation at S-II Engine Cutoff (ECO) of 81.70 m/s (268.0 ft/s) less than nominal was outside the 3-sigma tolerance of -69.5 m/s (-228.0 ft/s). Lower propulsion performance levels than predicted on both the S-IC and S-II stages were the primary contributors to this velocity deviation. A breakdown of the individual contributing sources is presented in Table 4-1. This table shows that trajectory conditions at the start of the S-II operation were a major contributor to reduced S-II stage performance. The altitude deviation of -2.89 kilometers (-1.56 n mi) was within the  $-3\sigma$  value of -3.27 kilometers (-1.77 n mi). The major contributor to the lower propulsion performance on both stages are discussed in paragraph 5.3 (S-IC Propulsion) and paragraph 6.3 (S-II Propulsion). Comparisons of total inertial accelerations are shown in

Figure 4-3. The maximum acceleration during S-IC burn according to the postflight trajectory was 3.85 g. The accuracy of the trajectory at S-IVB first cutoff is estimated to be  $\pm 1.0$  m/s ( $\pm 3.3$  ft/s) in velocity components and  $\pm 500$  meters ( $\pm 1640$  ft) in position components.

Mach number and dynamic pressure are shown in Figure 4-4. These parameters were calculated using measured meteorological data to an altitude of 73.00 kilometers (39.42 n mi). Above this altitude the measured data were merged into the U. S. Standard Reference Atmosphere.

Actual and nominal values of parameters at significant trajectory event times, cutoff events, and separation events are shown in Tables 4-2, 4-3, and 4-4, respectively.

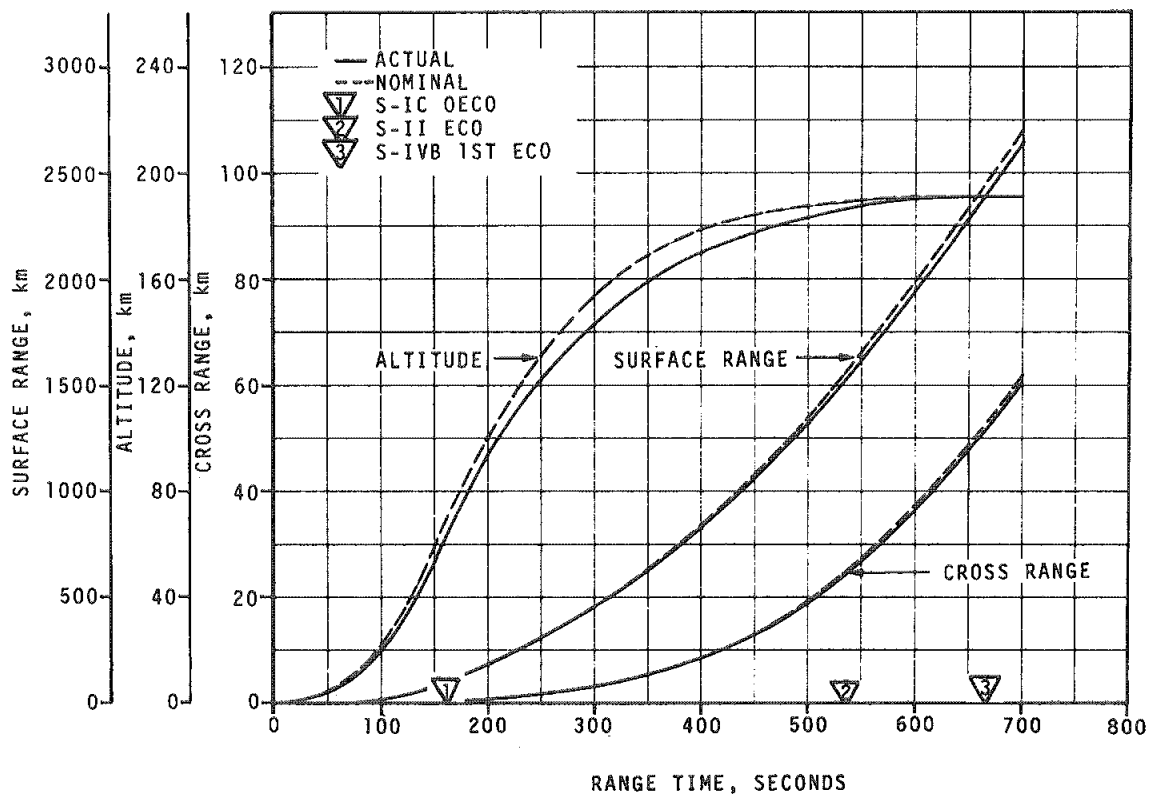


Figure 4-1. Ascent Trajectory Position Comparison

Table 4-1. Total Velocity Deviations During S-IC/S-II Burn

	Δ V DEVIATIONS	
	ACTUAL m/s (ft/s)	3 SIGMA LIMIT m/s (ft/s)
S-IC Stage		
Winds and Atmospheric Density	5 (16)	
Stage Performance (Engine Tag Values and Drag Coefficient)	-14 (-46)	
Mixture Ratio (+0.62 Percent)	-13 (-43)	
Fuel Density (+0.46 Percent)	3 (10)	
LOX Load at Holddown Arm Release -2150 kg (-4740 lbm)	-4 (-13)	
LOX Residuals 2561 kg (5645 lbm)	-6 (-20)	
Total S-IC Stage (Both Calculated and Observed)	-29 (-96)	-44.5 (-146.0)
S-II Stage		
Initial Conditions (Including S-IC ΔV, Low Altitude, and 1.0 Degree Δ Flight Path Angle)	-58.3 to -61.3 (-191.3) to (-201.1)	
S-II Propulsion Performance	-12.2 to -15.2* (-40.0) to (-49.9)	
Increased S-II GOX Pressurant Residual of 343 kg (756 lbm) at ECO	} -6.1 to -9.1 (-20.0) to (-29.9)	
Increased Upper Stage Weight of 450 kg (992 lbm)		
Total Calculated	-76.6 to -85.6 (-251.3) to (-280.9)	
Total Observed	-81.7 (-268.0)	-69.5 (-228.0)
*Only 3 to 5 m/s (10 to 16.5 ft/s) verified to be due to difference in predicted and actual propulsion performance.		



Table 4-2. Comparison of Significant Trajectory Events

EVENT	PARAMETER	ACTUAL	NOMINAL	ACT-NOM	
First Motion	Range Time, sec	0.3	0.3	0.00	
	Total Inertial Acceleration, $m/s^2$ (ft/s <sup>2</sup> )	10.78 (35.37)	11.01 (36.12)	-0.23 (-0.75)	
Mach 1	Range Time, sec	68.2	65.4	2.8	
	Altitude, km (n mi)	7.86 (4.24)	7.78 (4.20)	0.08 (0.04)	
Maximum Dynamic Pressure	Range Time, sec	85.5	81.4	4.1	
	Dynamic Pressure, $n/cm^2$ (lb/ft <sup>2</sup> )	3.020 (630.740)	3.285 (686.087)	-0.265 (-55.347)	
	Altitude, km (n mi)	13.76 (7.43)	13.32 (7.19)	0.44 (0.24)	
Maximum Total Inertial Acceleration: S-IC	Range Time, sec	162.84	159.96	2.88	
	Acceleration, $m/s^2$ (ft/s <sup>2</sup> )	37.72 (123.75)	38.50 (126.31)	-0.78 (-2.56)	
	S-II	Range Time, sec	536.31	531.25	5.06
	Acceleration, $m/s^2$ (ft/s <sup>2</sup> )	19.61 (64.34)	20.37 (66.83)	-0.76 (-2.49)	
	S-IVB 1st Burn	Range Time, sec	664.74	648.81	15.93
	Acceleration, $m/s^2$ (ft/s <sup>2</sup> )	7.84 (25.72)	7.68 (25.20)	0.16 (0.52)	
	S-IVB 2nd Burn	Range Time, sec	17,217.68	17,212.41	5.27
	Acceleration, $m/s^2$ (ft/s <sup>2</sup> )	12.16 (39.90)	11.79 (38.68)	0.37 (1.22)	
	S-IVB 3rd Burn	Range Time, sec	22,133.00	22,274.41	-141.41
	Acceleration, $m/s^2$ (ft/s <sup>2</sup> )	16.58 (54.40)	35.61 (116.83)	-19.03 (-62.43)	
	Maximum Earth-Fixed Velocity: S-IC	Range Time, sec	163.45	160.67	2.78
		Velocity, m/s (ft/s)	2,388.99 (7,837.89)	2,407.41 (7,898.33)	-18.42 (-60.44)
S-II		Range Time, sec	536.45	531.96	4.49
Velocity, m/s (ft/s)		6,535.25 (21,441.11)	6,618.93 (21,715.65)	-83.68 (-274.54)	
S-IVB 1st Burn		Range Time, sec	674.66	658.71	15.95
Velocity, m/s (ft/s)		7,390.30 (24,246.39)	7,389.71 (24,244.46)	0.59 (1.93)	
S-IVB 2nd Burn		Range Time, sec	17,218.20	17,214.06	4.14
Velocity, m/s (ft/s)		8,056.65 (26,432.58)	8,038.53 (26,373.13)	18.12 (59.45)	
S-IVB 3rd Burn		Range Time, sec	22,283.50	22,275.56	7.94
Velocity, m/s (ft/s)		9,120.68 (29,923.49)	10,646.93 (34,930.87)	-1,526.25 (-5,007.38)	
Apex: S-IC Stage		Range Time, sec	266.03	270.26	-4.23
		Altitude, km (n mi)	109.70 (59.23)	118.88 (64.19)	-9.18 (-4.96)
	Surface Range, km (n mi)	319.22 (172.37)	333.15 (179.89)	-13.93 (-7.52)	
	S-II Stage	Range Time, sec	593.58	563.26	30.32
	Altitude, km (n mi)	189.83 (102.50)	190.07 (102.63)	-0.24 (-0.13)	
	Surface Range, km (n mi)	1,900.81 (1,026.36)	1,745.11 (942.28)	155.70 (84.08)	

Table 4-3. Comparison of Cutoff Events

PARAMETER	ACTUAL	NOMINAL	ACT-NOM	ACTUAL	NOMINAL	ACT-NOM
	S-IC CECO (ENGINE SOLENOID)			S-IC OECO (ENGINE SOLENOID)		
Range Time, sec	134.34	134.27	0.07	162.76	159.96	2.80
Altitude, km (n mi)	41.59 (22.46)	45.14 (24.37)	-3.55 (-1.91)	64.47 (34.81)	67.36 (36.37)	-2.89 (-1.56)
Surface Range, km (n mi)	45.56 (24.60)	47.38 (25.58)	-1.82 (-0.98)	95.56 (51.60)	93.56 (50.52)	2.00 (1.08)
Space-Fixed Velocity, m/s (ft/s)	1,929.23 (6,329.49)	2,008.72 (6,590.29)	-79.49 (-260.80)	2,747.38 (9,013.71)	2,776.71 (9,109.94)	-29.33 (-96.23)
Flight Path Angle, deg	22.577	23.468	-0.891	18.539	19.610	-1.071
Heading Angle, deg	76.420	76.153	0.267	75.335	75.271	0.064
Cross Range, km (n mi)	0.20 (0.11)	0.10 (0.05)	0.10 (0.06)	0.43 (0.23)	0.22 (0.12)	0.21 (0.11)
Cross Range Velocity, m/s (ft/s)	7.18 (23.56)	2.97 (9.74)	4.21 (13.82)	9.40 (30.84)	7.44 (24.41)	1.96 (6.43)
	S-II ECO (ENGINE SOLENOID)			S-IVB 1ST ECO (ENGINE SOLENOID)		
Range Time, sec	536.22	531.16	5.06	664.66	648.73	15.93
Altitude, km (n mi)	186.56 (100.73)	189.14 (102.13)	-2.58 (-1.40)	191.04 (103.15)	191.35 (103.32)	-0.31 (-0.17)
Surface Range, km (n mi)	1,538.09 (830.50)	1,539.29 (831.15)	-1.13 (-0.61)	2,401.63 (1,296.78)	2,334.86 (1,260.72)	66.77 (36.06)
Space-Fixed Velocity, m/s (ft/s)	6,935.28 (22,753.54)	7,017.17 (23,022.21)	-81.70 (-268.04)	7,791.90 (25,563.98)	7,791.03 (25,561.12)	0.87 (2.86)
Flight Path Angle, deg	0.918	0.464	0.454	-0.007	-0.002	-0.005
Heading Angle, deg	81.872	81.872	0.000	86.979	86.545	0.434
Cross Range, km (n mi)	24.29 (13.12)	23.91 (12.91)	0.38 (0.21)	51.58 (27.85)	48.45 (26.16)	3.13 (1.69)
Cross Range Velocity, m/s (ft/s)	168.91 (554.17)	170.60 (559.71)	-1.68 (-5.51)	260.12 (853.41)	250.89 (823.13)	9.23 (30.28)
	S-IVB 2ND ECO (ENGINE SOLENOID)			S-IVB 3RD ECO (ENGINE SOLENOID)		
Range Time, sec	17,217.60	17,212.34	5.26	22,281.32	22,275.33	5.99
Altitude, km (n mi)	200.30 (108.15)	200.94 (108.50)	-0.64 (-0.35)	2,283.40 (1,232.94)	2,172.88 (1,173.26)	110.52 (59.68)
Space-Fixed Velocity, m/s (ft/s)	8,455.77 (27,742.03)	8,438.20 (27,684.38)	17.57 (57.65)	9,628.38 (31,589.17)	11,150.11 (36,581.73)	-1,521.73 (-4,992.56)
Flight Path Angle, deg	0.384	0.429	-0.045	-1.007	1.093	-2.100
Heading Angle, deg	112.544	112.921	-0.377	56.509	56.737	-0.228
Eccentricity	0.17952	0.17477	0.00475	1.01443	1.66680	-0.65237
$C_3^*$ m <sup>2</sup> /s <sup>2</sup> (ft <sup>2</sup> /s <sup>2</sup> )	-49,748,466 (-535,488,031)	-50,023,056 (-538,443,694)	274,590 (2,955,663)	664,476 (7,152,360)	31,092,572 (334,677,660)	-30,428,096 (-327,525,300)
Inclination, deg	32.303	32.490	-0.187	33.824	33.869	-0.045
Descending Node, deg	41.658	41.271	0.387	41.624	41.387	0.237

\*  $C_3$  is twice the specific energy of orbit

$$C_3 = v^2 - \frac{2\mu}{R}$$

where  $v$  = Inertial Velocity

$\mu$  = Gravitational Constant

$R$  = Radius vector from center of earth

Table 4-4. Comparison of Separation Events

PARAMETER	ACTUAL	NOMINAL	ACT-NOM
	S-IC/S-II SEPARATION		
Range Time, sec	163.45	160.68	2.77
Altitude, km (n mi)	65.09 (35.15)	68.02 (36.73)	-2.93 (-1.58)
Surface Range, km (n mi)	97.06 (52.41)	95.10 (51.35)	1.96 (1.06)
Space-Fixed Velocity, m/s (ft/s)	2,761.27 (9,059.28)	2,786.48 (9,141.99)	-25.21 (-82.71)
Flight Path Angle, deg	18.449	19.508	-1.059
Heading Angle, deg	75.337	75.268	0.069
Cross Range, km (n mi)	0.44 (0.24)	0.23 (0.12)	0.21 (0.12)
Cross Range Velocity, m/s (ft/s)	9.92 (32.55)	7.56 (24.80)	2.36 (7.75)
Geodetic Latitude, deg N	28.872	28.868	0.004
Longitude, deg E	-79.657	-79.676	0.019
S-II/S-IVB SEPARATION			
Range Time, sec	537.2	532.0	5.2
Altitude, km (n mi)	186.67 (100.79)	189.18 (102.15)	-2.51 (-1.36)
Surface Range, km (n mi)	1,544.19 (833.80)	1,544.43 (833.93)	-0.24 (-0.13)
Space-Fixed Velocity m/s (ft/s)	6,937.94 (22,762.27)	7,021.96 (23,037.93)	-84.02 (-275.66)
Flight Path Angle, deg	0.906	0.457	0.449
Heading Angle, deg	81.907	81.901	0.006
Cross Range, km (n mi)	24.45 (13.20)	24.05 (12.99)	0.40 (0.21)
Cross Range Velocity, m/s (ft/s)	169.43 (555.87)	171.10 (561.35)	-1.67 (-5.48)
Geodetic Latitude, deg N	31.802	31.806	-0.004
Longitude, deg E	-64.979	-64.976	-0.003
S-IVB/SPACECRAFT FINAL SEPARATION			
Range Time, sec	14,886.0	14,983	-97.0
Altitude, km (n mi)	194.89 (105.23)	193.54 (104.50)	1.35 (0.73)
Space-Fixed Velocity, m/s (ft/s)	7,792.22 (25,565.03)	7,793.29 (25,568.54)	-1.07 (-3.51)
Flight Path Angle, deg	0.028	0.037	-0.009
Heading Angle, deg	60.373	58.985	1.388
Geodetic Latitude, deg N	-14.315	-10.638	-3.677
Longitude, deg E	135.624	141.644	-6.020

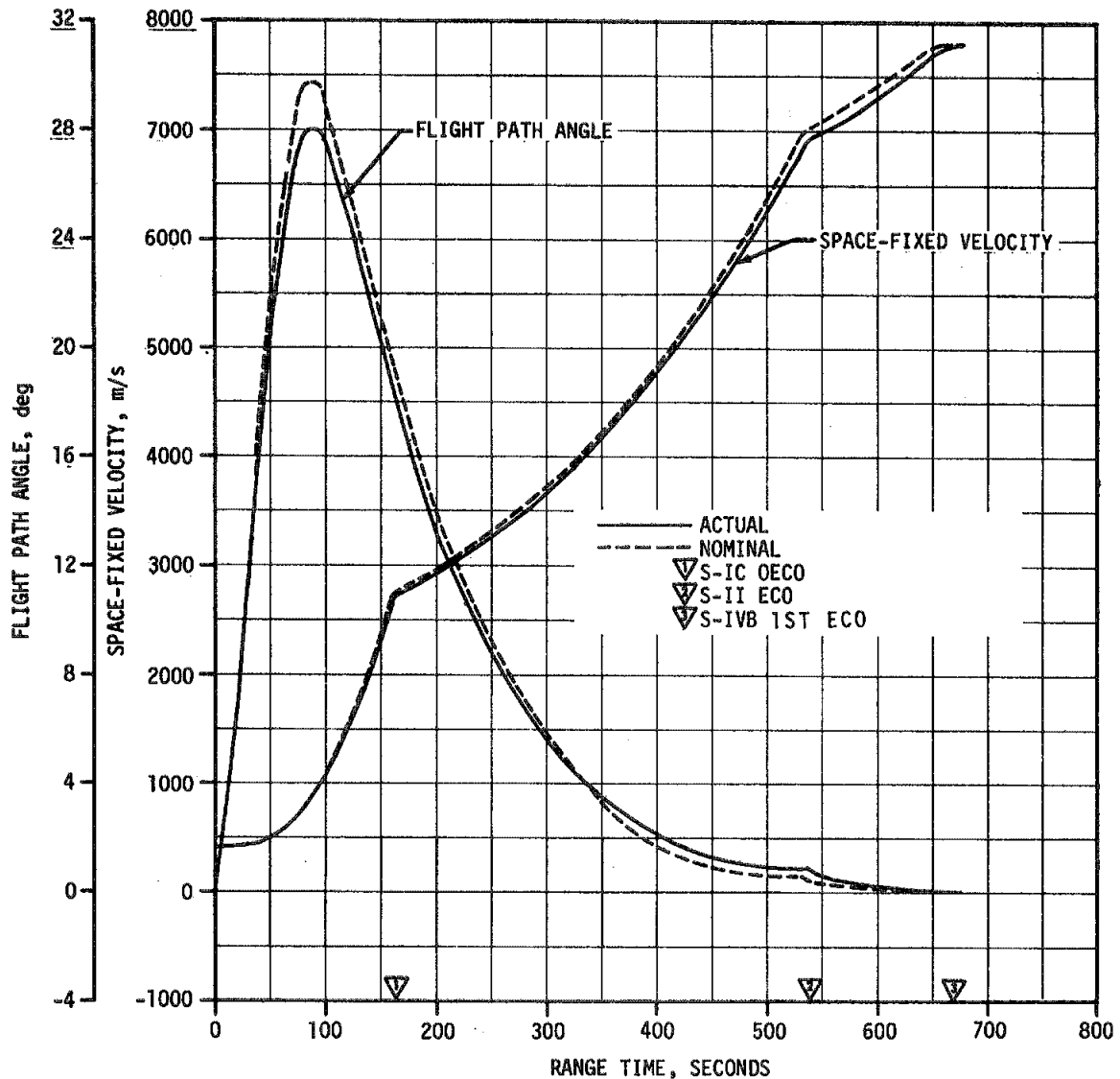


Figure 4-2. Ascent Trajectory Space-Fixed Velocity Comparison

The free-flight trajectories of the spent S-IC and S-II stages were simulated using initial conditions from the final postflight trajectory. The simulation was based upon the separation impulses for both stages and nominal tumbling drag coefficients. No tracking data were available for verification. Table 4-2 presents a comparison of free-flight parameters to nominal at apex for the S-IC and S-II stages. Table 4-5 presents a comparison of free-flight parameters to nominal at impact for the S-IC and S-II stages.

#### 4.3.2 Parking Orbit Trajectory

The acceleration due to venting during parking orbit is presented in Figure 4-5. These accelerations were obtained by differentiating the telemetered guidance velocity data and removing accelerometer biases and the effects of drag.

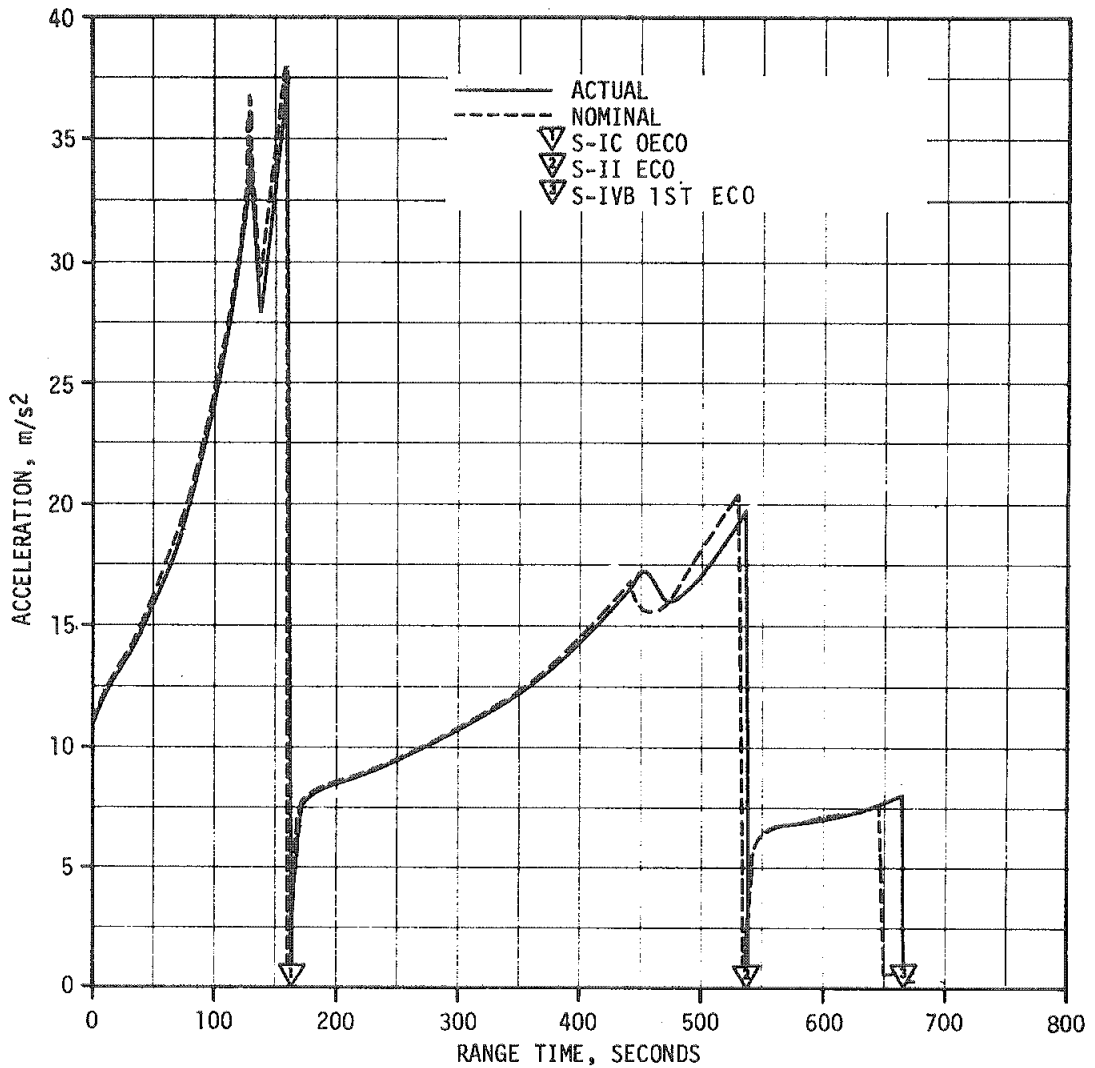


Figure 4-3. Ascent Trajectory Acceleration Comparison

A family of values for the insertion parameters was obtained depending upon the combination of data used and the weights applied to the data. The solutions that were considered reasonable had a spread of about  $\pm 500$  meters ( $\pm 1640$  ft) in position components and  $\pm 1.0$  m/s ( $\pm 3.3$  ft/s) in velocity components. The actual and nominal parking orbit insertion parameters are presented in Table 4-6. The ground track from liftoff to escape orbit injection plus 5650 seconds is given in Figure 4-6.

#### 4.3.3 S-IVB Second Burn Trajectory

Comparisons between the actual and nominal total space-fixed velocity and flight path angle are shown in Figure 4-7. The actual and nominal total inertial acceleration comparisons are presented in Figure 4-8. Throughout

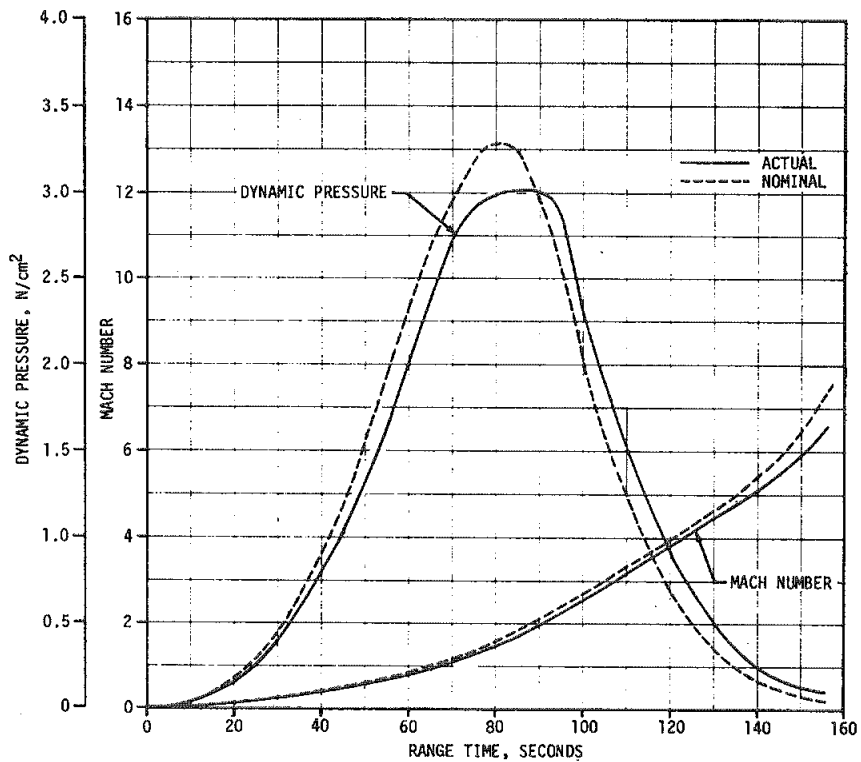


Figure 4-4. Dynamic Pressure and Mach Number

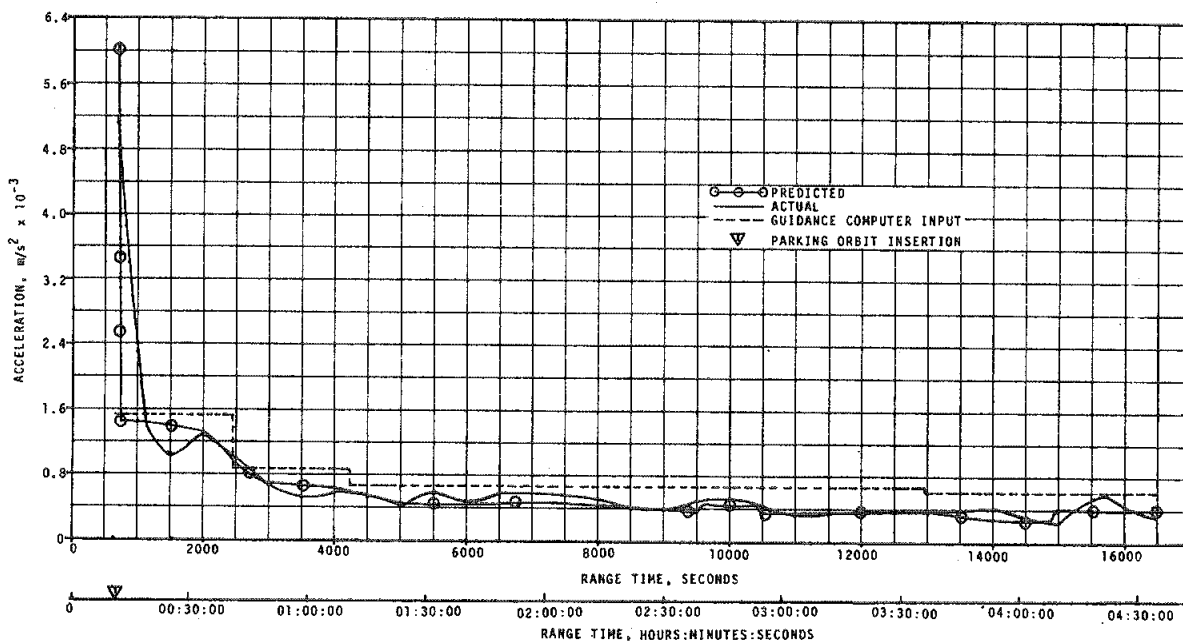


Figure 4-5. Acceleration Due to Venting - Parking Orbit

Table 4-5. Stage Impact Location

PARAMETER	ACTUAL	NOMINAL	ACT-NOM
S-IC STAGE IMPACT			
Range Time, sec	536.44	547.00	-10.56
Surface Range, km (n mi)	641.97 (346.64)	674.07 (363.97)	-32.10 (-17.33)
Cross Range, km (n mi)	7.61 (4.11)	7.51 (4.06)	0.10 (0.05)
Geodetic Latitude, deg N	30.183	30.258	-0.075
Longitude, deg E	-74.238	-73.917	-0.321
S-II STAGE IMPACT			
Range Time, sec	1,225.35	1,216.40	8.95
Surface Range, km (n mi)	4,469.24 (2,413.20)	4,475.47 (2,416.56)	-6.23 (-3.36)
Cross Range, km (n mi)	146.39 (79.04)	145.60 (78.62)	0.79 (0.42)
Geodetic Latitude, deg N	31.462	31.462	0.000
Longitude, deg E	-34.041	-33.977	-0.064

Table 4-6. Parking Orbit Insertion Conditions

PARAMETER	ACTUAL	NOMINAL	ACT-NOM
Range Time, sec	674.65	658.72	15.93
Altitude, km (n mi)	191.04 (103.15)	191.36 (103.33)	-0.32 (-0.18)
Space-Fixed Velocity, m/s (ft/s)	7,793.67 (25,569.78)	7,793.06 (25,567.78)	0.61 (2.00)
Flight Path Angle, deg	-0.0058	-0.0009	-0.0049
Heading Angle, deg	87.412	86.977	0.435
Inclination, deg	32.552	32.561	-0.009
Descending Node, deg	42.538	42.570	-0.032
Eccentricity	0.000149	0.000016	0.000133
Apogee*, km (n mi)	186.57 (100.74)	185.31 (100.06)	1.26 (0.68)
Perigee*, km (n mi)	184.61 (99.68)	185.10 (99.95)	-0.49 (-0.27)
Period, min	88.20	88.20	0.00
Geodetic Latitude, deg N	32.629	32.605	0.024
Longitude, deg E	-55.166	-55.877	0.711

\* Based on a spherical earth of radius 6378.165 km (3443.934 n mi)

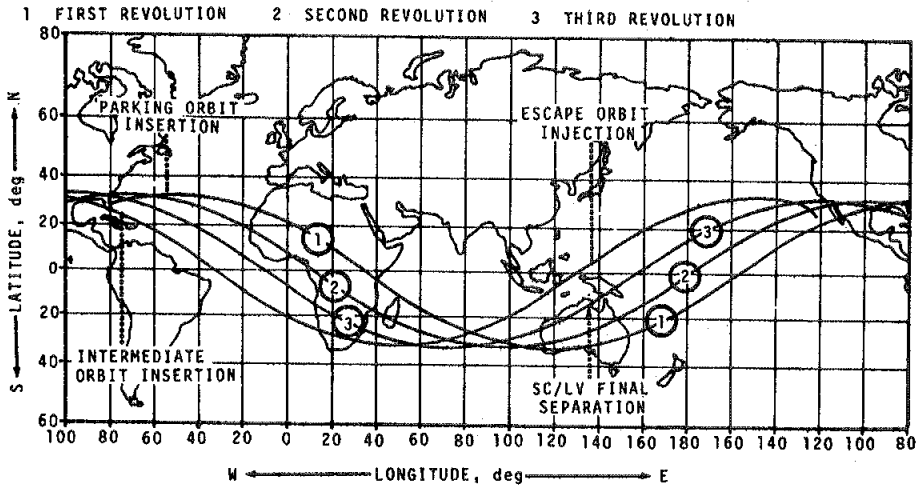


Figure 4-6. Ground Track

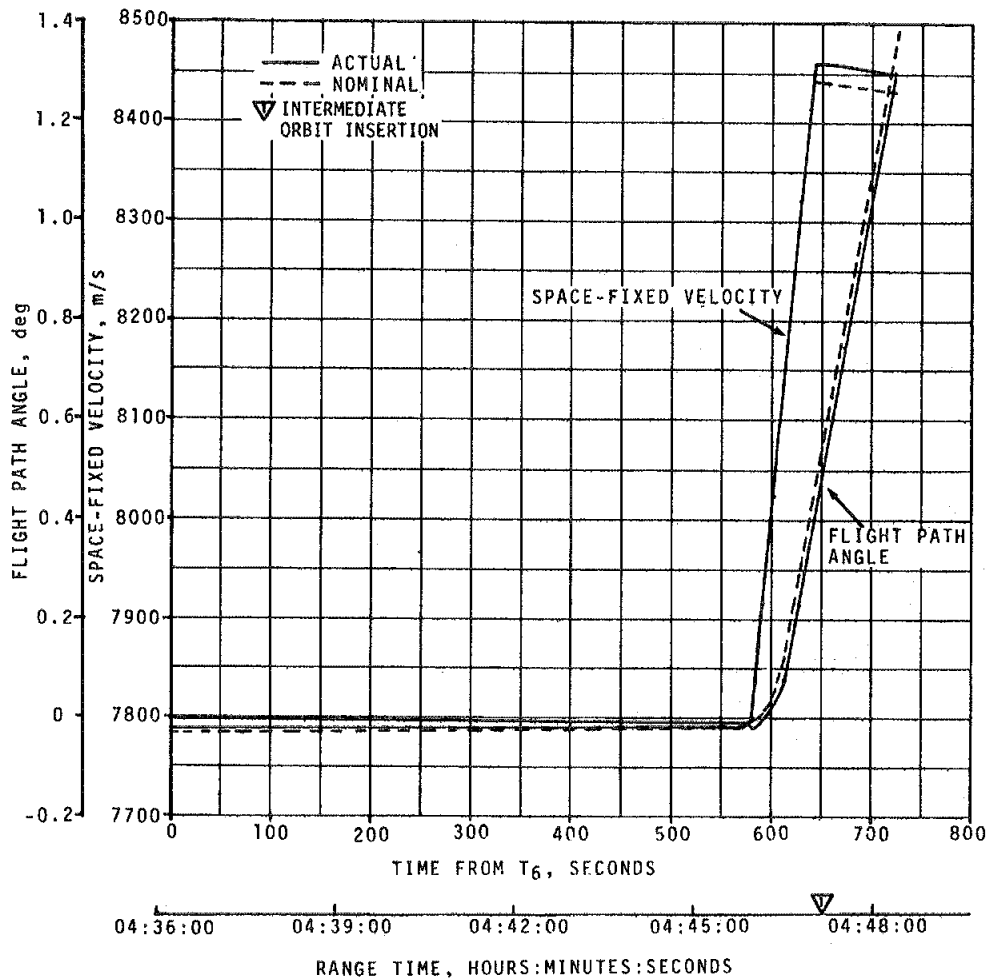


Figure 4-7. S-IVB Second Burn Phase Space-Fixed Velocity Comparison



the S-IVB second burn phase of flight, the space-fixed velocity and the total inertial acceleration were slightly greater than nominal, and the flight path angle was slightly less than nominal.

The trajectory parameters at S-IVB second cutoff are presented in Table 4-3.

#### 4.3.4 Intermediate Orbit Trajectory

The acceleration due to venting during the intermediate orbit is presented in Figure 4-9. The actual and nominal intermediate orbit insertion parameters are presented in Table 4-7.

#### 4.3.5 S-IVB Third Burn Trajectory

Comparisons between the actual and nominal total space-fixed velocity and flight path angle are shown in Figure 4-10. The actual and nominal total inertial acceleration comparisons are presented in Figure 4-11. These trajectory parameters were reasonably close to nominal until approximately 550 seconds into Time Base 8 (T<sub>8</sub>). Afterwards, the trajectory parameters were considerably lower than nominal.

The trajectory parameters at S-IVB third cutoff are presented in Table 4-3.

#### 4.3.6 Escape Orbit Trajectory

The escape orbit was hyperbolic with respect to the earth. The actual and nominal escape orbit injection conditions are compared in Table 4-8.

The solar orbit attained by the S-IVB/IU differed considerably from the predicted orbit as shown in Table 4-9. This difference was due to the abnormal performance of the S-IVB during its third burn. A planned LH<sub>2</sub> dump and LOX dump did not occur. The APS engines performed as shown in Figure 4-12, increasing the velocity by 9.7 m/s (31.8 ft/s). The APS engines were fired by ground command to increase the velocity.

Table 4-7. Intermediate Orbit Insertion Conditions

PARAMETER	ACTUAL	NOMINAL	ACT-NOM
Range Time, sec	17,227.60	17,222.34	5.26
Altitude, km (n mi)	200.88 (108.47)	201.57 (108.84)	-0.69 (-0.37)
Space-Fixed Velocity, m/s (ft/s)	8,459.30 (27,753.61)	8,440.63 (27,692.36)	18.67 (61.25)
Flight Path Angle, deg	0.498	0.539	-0.041
Heading Angle, deg	112.841	113.216	-0.375
Inclination, deg	32.302	32.490	-0.188
Descending Node, deg	41.657	41.271	0.386
Eccentricity	0.18070	0.17567	0.00503
Apogee*, km (n mi)	3,095.76 (1,671.58)	2,998.26 (1,618.93)	97.50 (52.65)
Perigee*, km (n mi)	195.85 (105.75)	196.24 (105.96)	-0.39 (-0.21)
Period, min	119.22	118.14	1.08
Geodetic Latitude, deg N	23.622	23.530	0.092
Longitude, deg E	-73.807	-73.545	-0.262

\* Based on a spherical earth of radius 6378.165 km  
(3443.934 n mi)

Table 4-8. Escape Orbit Injection Conditions

PARAMETER	ACTUAL	NOMINAL	ACT-NOM
Range Time, sec	22,291.32	22,285.33	5.99
Altitude, km (n mi)	2,281.56 (1,231.94)	2,175.51 (1,174.68)	106.05 (57.26)
Space-Fixed Velocity, m/s (ft/s)	9,637.73 (31,619.85)	11,157.93 (36,607.38)	-1,520.20 (-4,987.53)
Flight Path Angle, deg	-0.678	1.568	-2.246
Heading Angle, deg	56.555	56.811	-0.256
Eccentricity	1.0179	1.6711	-0.6532
$C_3$ , $m^2/s^2$ ( $ft^2/s^2$ )	824,712. (8,877,126.)	31,295,218. (336,858,921.)	-30,470,506. (-327,981,795.)
Inclination, deg	33.825	33.879	-0.054
Descending Node, deg	41.623	41.381	0.242

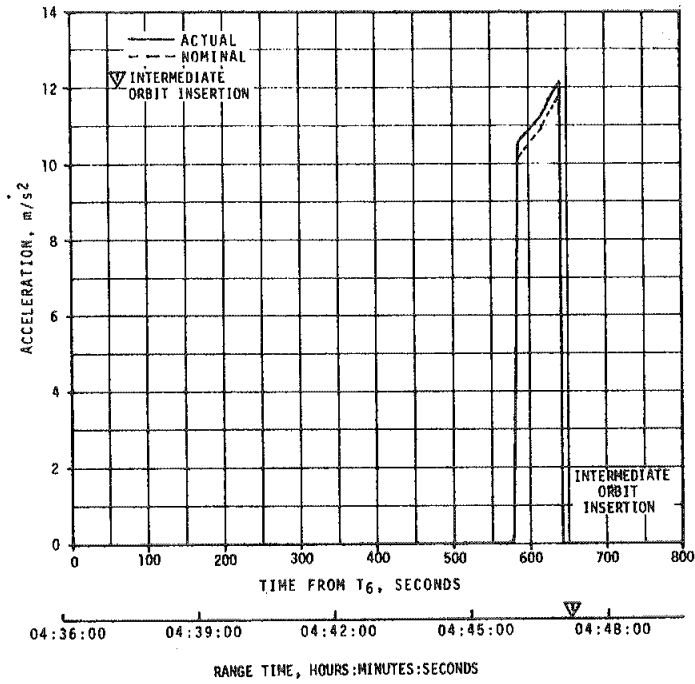


Figure 4-8. S-IVB Second Burn Phase Acceleration Comparison

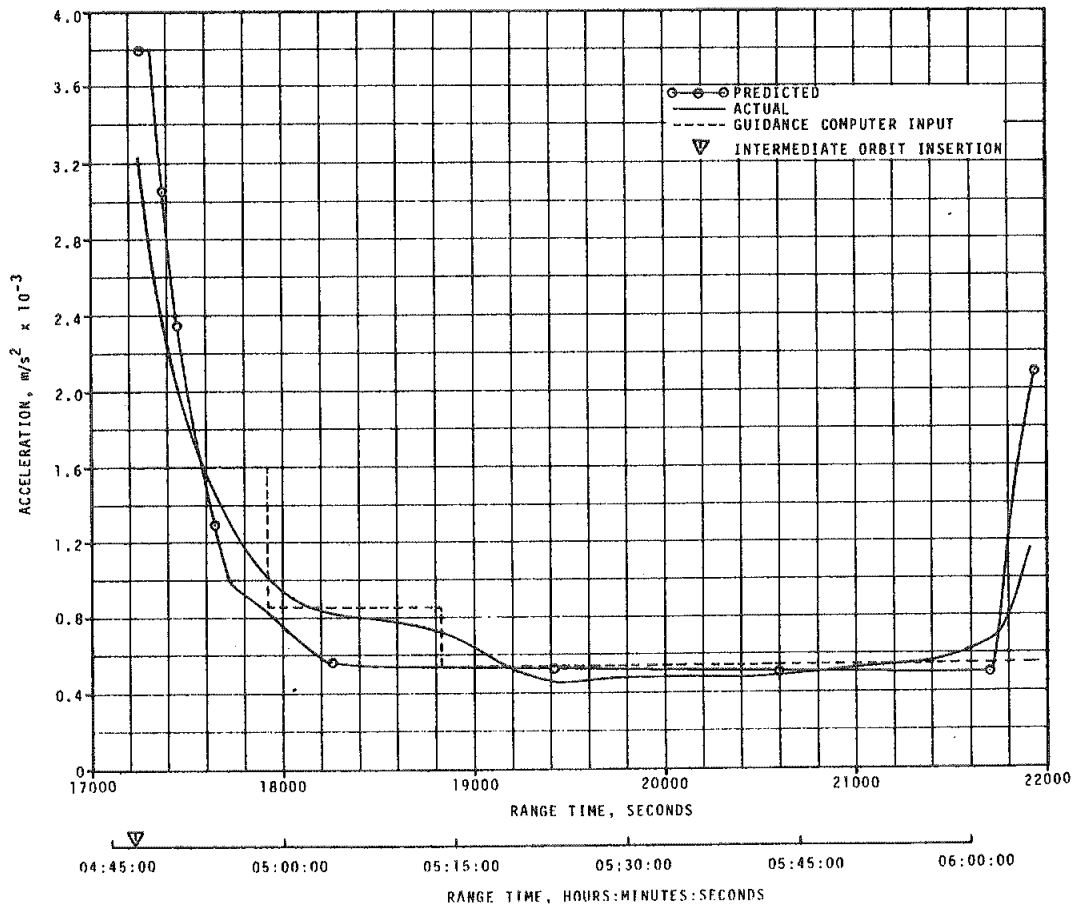


Figure 4-9. Acceleration Due to Venting - Intermediate Orbit

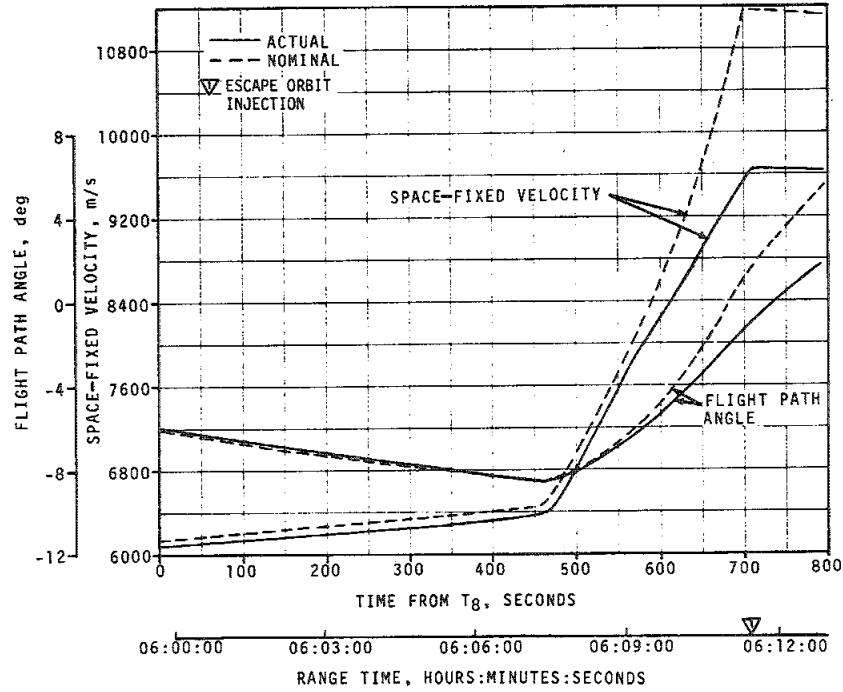


Figure 4-10. S-IVB Third Burn Phase Space-Fixed Velocity Comparison

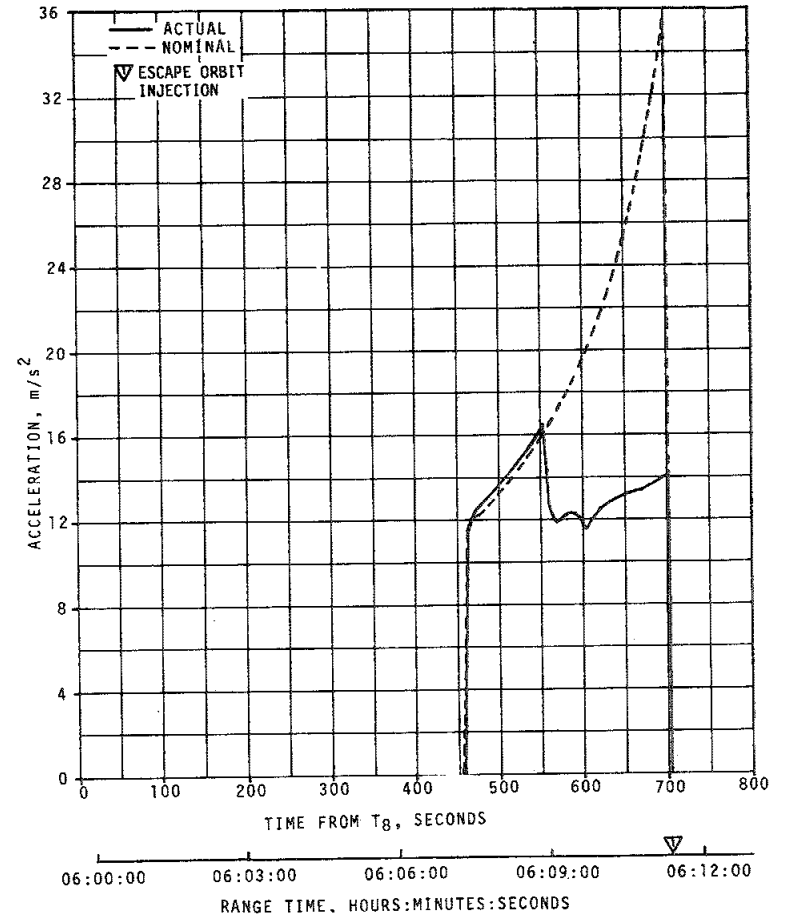


Figure 4-11. S-IVB Third Burn Phase Acceleration Comparison

Table 4-9. Comparison of Heliocentric Orbit Parameters

PARAMETER	ACTUAL	NOMINAL	ACT-NOM
Semimajor Axis, km (n mi)	138,620,150 (74,848,893)	113,074,150 (61,055,157)	25,546,000 (13,793,736)
Radius of Aphelion, km (n mi)	148,678,656 (80,280,052)	149,340,039 (80,637,170)	-661,383 (-357,118)
Radius of Perihelion, km (n mi)	128,561,640 (69,417,732)	76,808,263 (41,473,144)	51,753,377 (27,944,588)
Eccentricity	0.07256	0.32073	-0.24817
Inclination, deg	24.390	22.272	2.118
Period, days	325.8	240.0	85.8

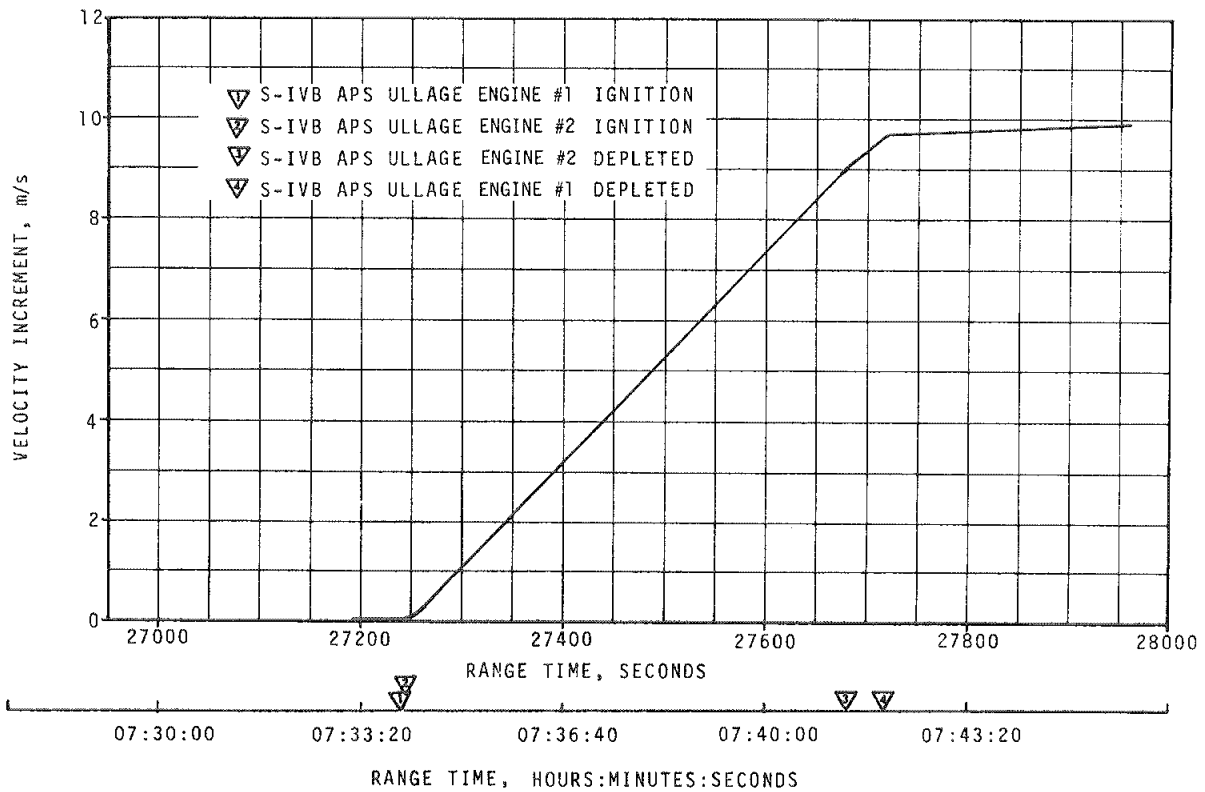


Figure 4-12. APS Velocity Increment

## SECTION 5

### S-IC PROPULSION

#### 5.1 SUMMARY

All S-IC propulsion systems performed satisfactorily. However, the combined thrust of the five F-1 engines was lower than predicted. At the 35 to 38 second time slice, average engine thrust reduced to standard conditions was 1.21 percent lower than predicted. Average reduced specific impulse was 0.174 percent lower than predicted, and reduced propellant consumption rate was 1.04 percent less than predicted. Engine No. 1 exhibited an unexpected increase in performance starting at 85 seconds. The most probable cause for this is a fuel pump head decay due to loss of lead from the front wear ring of the fuel pump.

Center Engine Cutoff (CECO) was initiated by the Instrument Unit (IU) as planned.

Outboard Engines Cutoff (OECO) was initiated by LOX low level sensors 2.8 seconds later than predicted but well within the 3 sigma limits of  $\pm 6.0$  seconds. The usable LOX residual at zero thrust was 2561 kilograms (5645 lbm) compared to the usable zero predicted, and the usable fuel residual was 7276 kilograms (16,040 lbm) compared to the usable 2585 kilograms (5700 lbm) predicted.

#### 5.2 S-IC IGNITION TRANSIENT PERFORMANCE

The fuel pump inlet preignition pressure and temperature were  $32.1 \text{ N/cm}^2$  (46.5 psia) and  $266.9^\circ\text{K}$  ( $20.8^\circ\text{F}$ ), respectively. These fuel pump inlet conditions were within the F-1 engine model specification limits (start box requirements) as shown in Figure 5-1.

The LOX pump inlet preignition pressure and temperature were  $55.3 \text{ N/cm}^2$  (80.2 psia) and  $96.1^\circ\text{K}$  ( $-286.7^\circ\text{F}$ ), respectively. The LOX pump inlet conditions were also within the F-1 engine model specification limits as shown in Figure 5-1.

Engine start-up sequence was nominal. A 1-2-2 start was planned and attained. Engine position starting order was 5, 3-1, 2-4. Two engines are considered to start together if their combustion chamber pressures reach  $68.9 \text{ N/cm}^2$  (100 psig) in a 100-millisecond time period. Figure 5-2

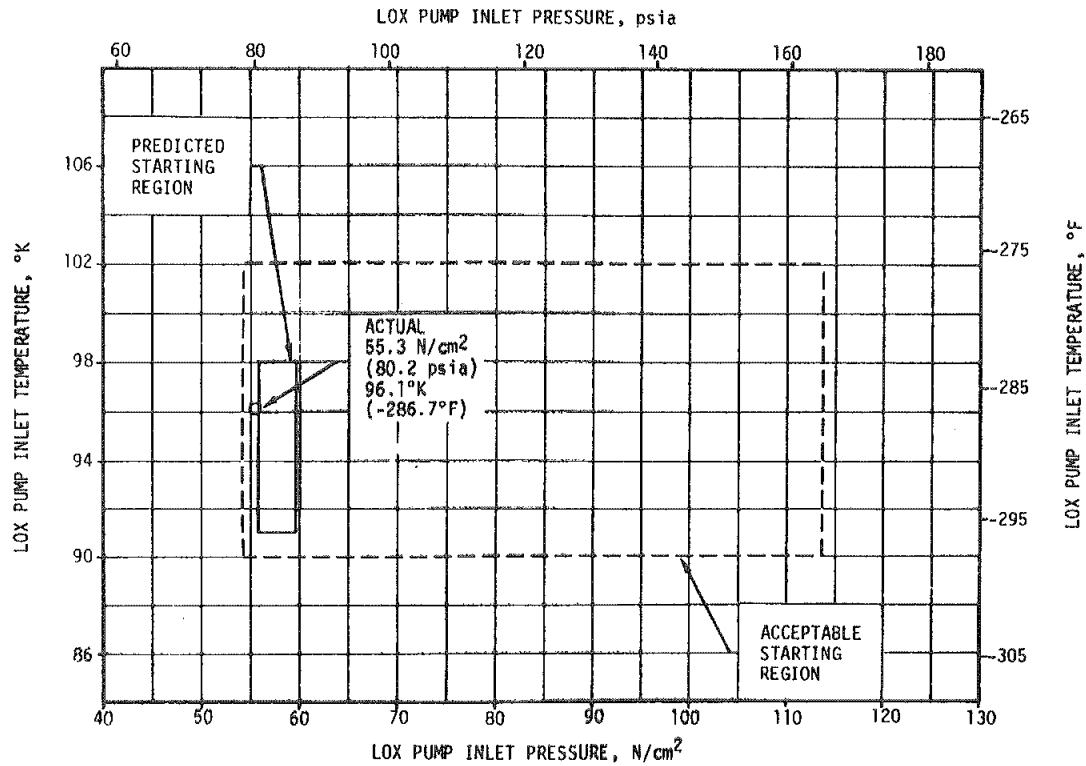
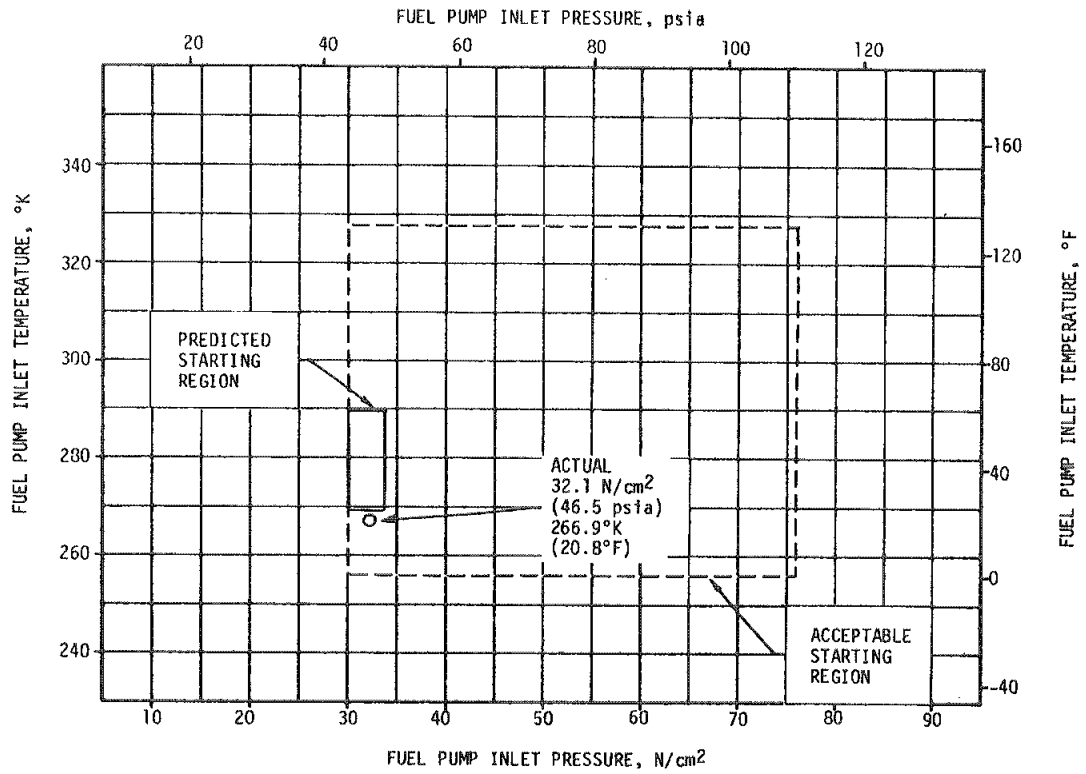


Figure 5-1. S-IC Start Box Requirements

shows the thrust buildup of each engine indicative of the successful 1-2-2 start. The shift in thrust buildup near the 4,900,000 Newtons (1,100,000 lbf) thrust level on the outboard engines is caused primarily by ingestion of GOX and helium during startup from the LOX pre valves (used as helium filled accumulators for POGO suppression). The thrust shift is absent on the center engine for which the POGO suppression system was not used. Engine No. 3 shows a spike of approximately 270,000 Newtons (60,000 lbf) at the 1,330,000 Newtons (300,000 lbf) level. This spike is the result of inertial surge during buildup and caused no problems and has been seen on previous flights.

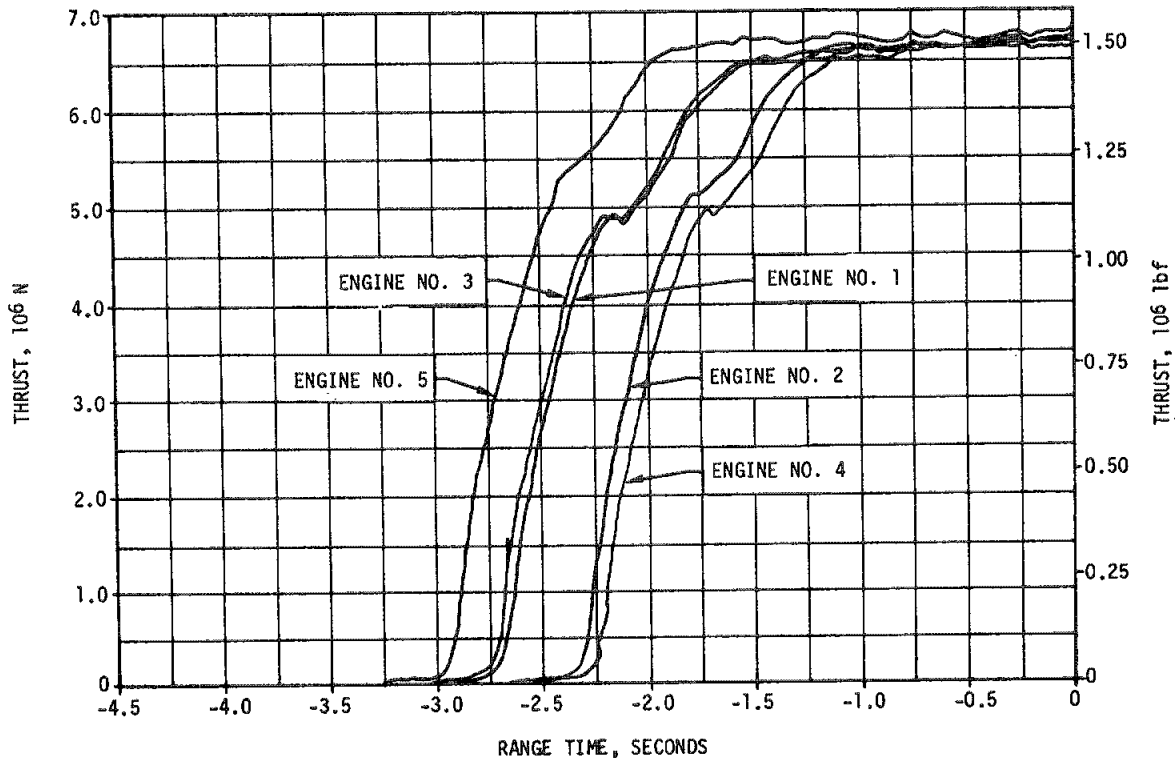


Figure 5-2. S-IC Engine Buildup Transient

The best estimate of propellants consumed between ignition and hold-down arms release was 38,770 kilograms (85,470 lbm). The predicted consumption was 39,150 kilograms (86,311 lbm). The best estimate for liftoff propellant loads was 1,466,931 kilograms (3,234,030 lbm) for LOX and 641,099 kilograms (1,413,381 lbm) for fuel.

### 5.3 S-IC MAIN STAGE PERFORMANCE

S-IC stage propulsion performance as determined by reconstruction was satisfactory. Sea level performance parameters and the nominal predictions



are shown in Figure 5-3. All stage flight performance parameters were within the predicted 3 sigma limits but the stage thrust was lower than predicted as evidenced by low velocity and altitude at the end of S-IC burn (see paragraph 4.1). Stage flight thrust at CECO was approximately 934,080 Newtons (210,000 lbf) or 2.29 percent lower than predicted. Preliminary analysis indicates the low thrust was due mostly to:

- a. Lower than predicted engine sea level performance.
- b. Higher fuel density than used in the prediction.

Stage thrust reduced to standard conditions at 36.5 seconds was 413,685 Newtons (93,000 lbf) (1.21 percent) lower than predicted. This was primarily due to:

<u>CAUSE</u>	<u>EFFECT ON STAGE THRUST</u>
a. Use of erroneous tag values in the prediction due to an error in measuring specific gravity and combustion pressures at the Mississippi Test Facility (MTF).	-177,920 Newtons (-40,000 lbf)
b. Thrust bias between Saturn V flights and respective acceptance firings.	-200,160 Newtons (-45,000 lbf)

Individual engine parameters reduced to standard sea level conditions at a 35 to 38 second time slice are shown in Table 5-1. Individual engine deviations from predicted thrust ranged from 1.49 percent lower (engine No. 4) to 1.05 percent lower (engine No. 3). Individual engine deviations from predicted specific impulse ranged from 0.225 percent lower (engine No. 4) to 0.150 percent lower (engines No. 2 and 3).

At approximately 85 seconds, engine No. 1 exhibited an unexpected increase in performance. The increase is evident in engine combustion chamber pressure, Gas Generator (GG) combustion chamber pressure, LOX discharge pressure, turbine manifold temperature and turbopump speed. This performance increase caused no problems on AS-504, but is under investigation. Presently, the best "fit" of data (according to the engine contractor) is obtained by a small decrease in fuel pump developed head from 80 to 120 seconds. The most probable cause of the fuel pump head decay is loss of lead from the front wear ring of the fuel pump. The wear ring provides a dynamic seal between the fuel impeller front shroud and fuel pump inlet assembly, therefore loss of this seal results in a decrease in fuel pump efficiency and a loss in developed head. The wear ring consists of a 0.053 centimeter (0.021 in.) thick, 2.29 centimeters (0.90 in.) wide, lead plating onto a brass forging. Loss of lead due to an inadequate bond has occurred during Research and Development (R&D) engine and

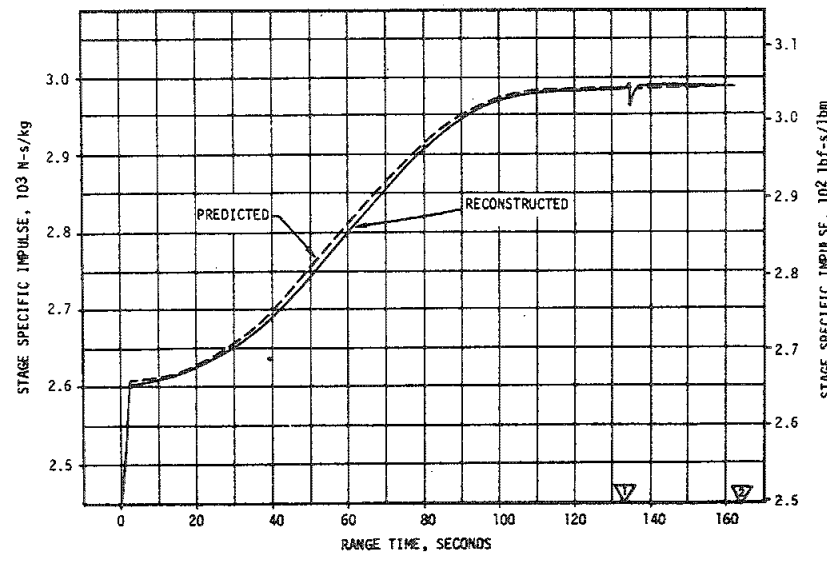
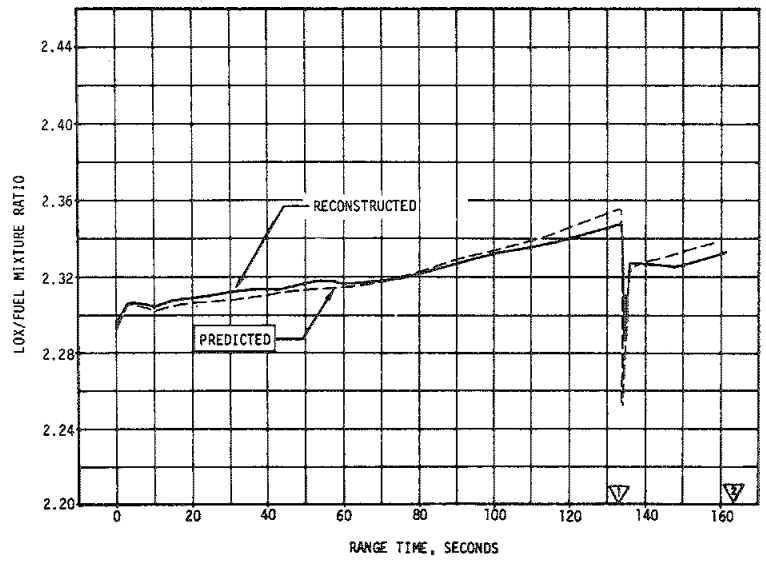
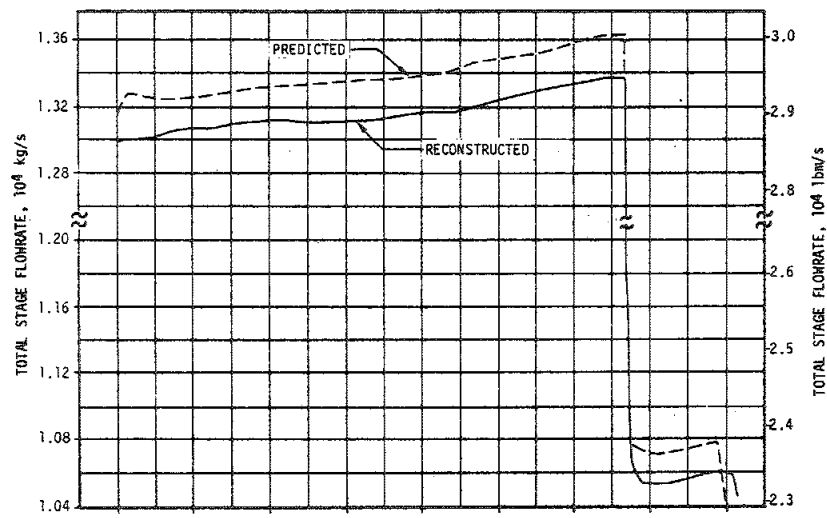
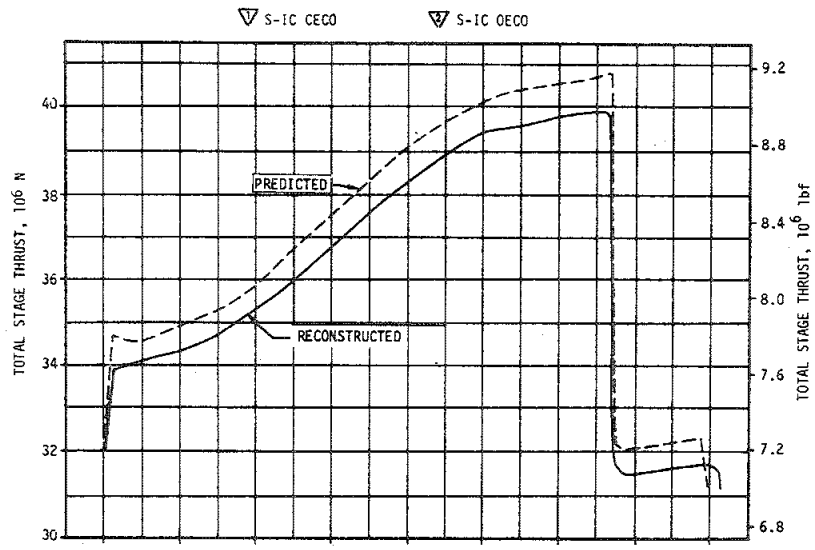


Figure 5-3. S-1C Steady State Operation

Table 5-1. S-IC Engine Performance Deviations

PARAMETER	ENGINE	PREDICTED	RECONSTRUCTED	DEVIATION PERCENT	AVERAGE DEVIATION PERCENT
Thrust $10^3$ N ( $10^3$ lbf)	1	6809 (1531)	6730 (1513)	-1.18	-1.21
	2	6782 (1525)	6703 (1507)	-1.18	
	3	6807 (1530)	6735 (1514)	-1.05	
	4	6856 (1541)	6752 (1518)	-1.49	
	5	6859 (1542)	6779 (1524)	-1.17	
Specific Impulse N-s/kg (lbf-s/lbm)	1	2596 (264.7)	2592 (264.3)	-0.151	-0.174
	2	2611 (266.2)	2607 (265.8)	-0.150	
	3	2607 (265.8)	2603 (265.4)	-0.150	
	4	2610 (266.1)	2604 (265.5)	-0.225	
	5	2611 (266.2)	2606 (265.7)	-0.188	
Total Flowrate kg/s (lbm/s)	1	2623 (5783)	2598 (5727)	-0.968	-1.04
	2	2598 (5727)	2573 (5672)	-0.960	
	3	2612 (5757)	2587 (5703)	-0.940	
	4	2627 (5791)	2592 (5715)	-1.312	
	5	2628 (5794)	2602 (5736)	-1.001	
Mixture Ratio LOX/Fuel	1	2.2864	2.2812	-0.227	-0.210
	2	2.2561	2.2519	-0.186	
	3	2.2704	2.2661	-0.189	
	4	2.2639	2.2590	-0.216	
	5	2.2906	2.2853	-0.231	

NOTE: Analysis was reduced to standard sea level and pump inlet conditions at 35 to 38 seconds.

initial Qual II turbopump component testing. During R&D testing, this lead loss has resulted in losses of from 12.2 to 58 meters (40 to 190 ft) of fuel pump developed head. Theoretical analyses have determined that a complete loss of the noted wear ring lead could result in a 29 to 71.6 meters (95 to 235 ft) developed head loss. Air-rig tests (fuel pump) conducted with a front wear ring clearance simulating complete loss of wear ring lead indicated a head loss of 67.1 meters (220 ft).

As a result of wear ring lead loss, a double inspection process was incorporated. These inspections required a "bake" wherein the wear ring was exposed to an elevated temperature which would aggravate any bonding deficiencies, followed by an ultrasonic inspection to identify areas of inadequate bonding of the lead to the brass forging. Of the S-IC-504 stage engines, No.'s 1, 2 and 5 did not incorporate the double inspection wear rings. All F-1 engines in AS-505 and subsequent vehicles have wear rings which were inspected by the double inspection process; therefore, a wear ring lead loss should not occur on subsequent vehicles.

#### 5.4 S-IC ENGINE SHUTDOWN TRANSIENT PERFORMANCE

CECO was initiated from a signal from the IU at 134.34 seconds as planned. Cutoff signal to the outboard engines was initiated by LOX low level sensors and occurred 2.8 seconds later than the predicted time of 160 seconds.

Most of the OECO deviation can be attributed to a combination of higher than predicted fuel density and lower than expected engine tag performance. Figure 5-4 shows the relative contribution of each influencing parameter to the cutoff deviation.

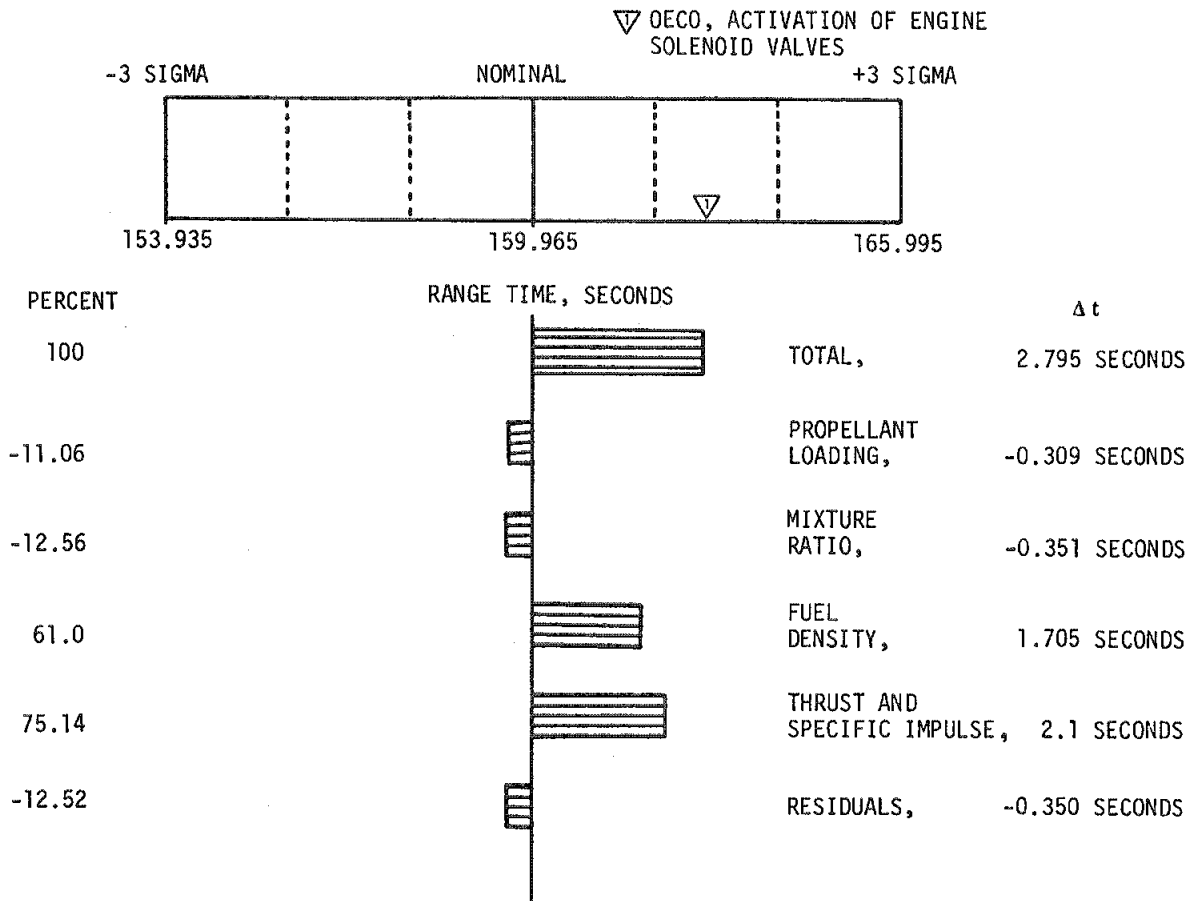


Figure 5-4. S-IC Outboard Engine Cutoff Deviations

Thrust decay of the F-1 engines is shown in Figure 5-5. The decay transient was nominal for engines incorporating the "Optimized Engine Shutdown" (Rocketdyne ECP 444). This ECP was effective for S-IC-504 and subsequent S-IC stages. The "bulge" in engine No. 3 decay curve starting at 5,900,000 Newtons (1,300,000 lbf) thrust is believed to be erroneous transducer response.

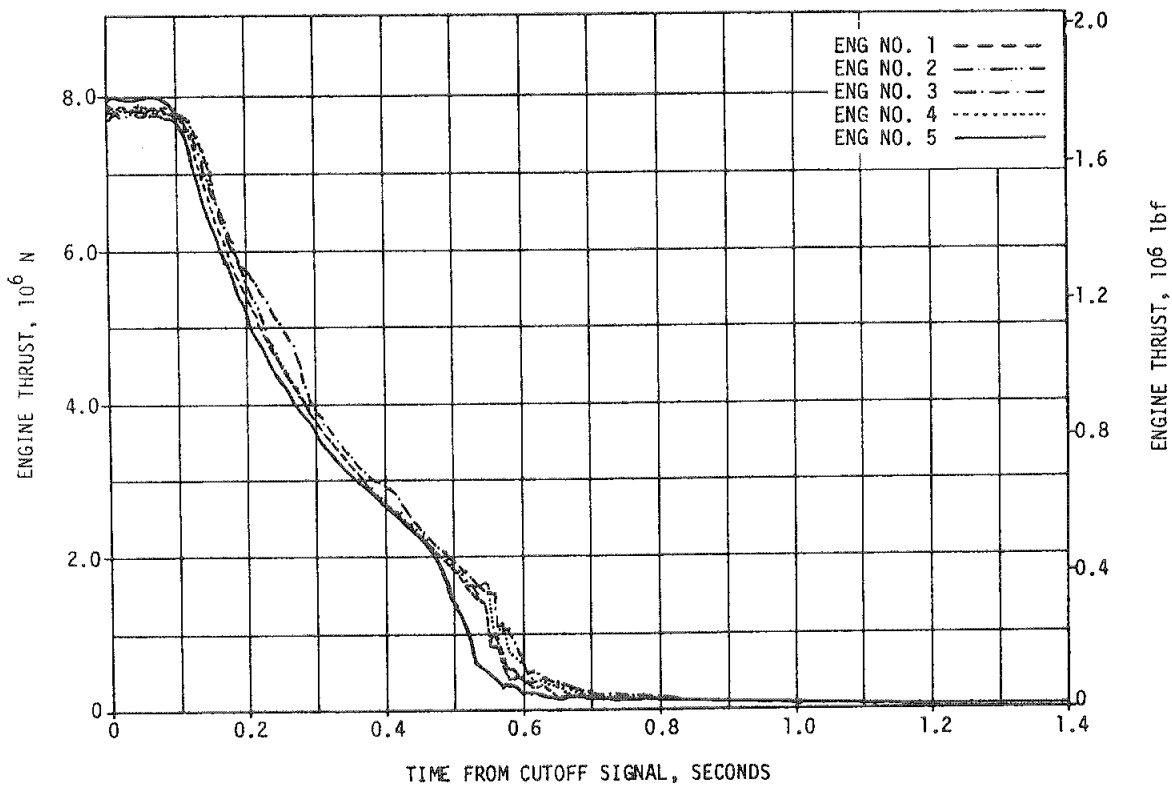


Figure 5-5. S-IC Engine Shutdown Transient Performance

The total stage impulse from OECO to separation was 10,636,814 N-s (2,391,251 lbf-s) which is greater than the predicted cutoff impulse of 10,188,402 N-s (2,290,444 lbf-s), but was within the 3 sigma limits.

#### 5.5 S-IC STAGE PROPELLANT MANAGEMENT

Minimum residuals are obtained by attempting to load the mixture ratio expected to be consumed by the engines plus the predicted unusable residuals. Also, a small additional amount of usable fuel (fuel bias) was loaded to minimize maximum residuals. An analysis of the usable residuals experienced during a flight is a good measure of the performance of the passive Propellant Utilization (PU) system. PU deviations were larger than usual because of stacked tolerances, resulting in a consumed mixture ratio shift of +1.83 sigma. This was within expected limits.

The LOX residual, at zero thrust, of 2561 kilograms (5645 lbm) was probably due mostly to early "breakthrough" of the LOX flow at the top of the suction duct. An early "breakthrough" could trip the cutoff sensors before the true liquid level reached the sensor. A good prediction of the "breakthrough" is difficult especially since only one other flight (AS-501) had a LOX cutoff and could be used for predicting

Table 5-2. S-IC Stage Propellant Mass History

EVENT	PREDICTED		LEVEL SENSOR DATA		RECONSTRUCTED	
	LOX	FUEL	LOX	FUEL	LOX	FUEL
Ignition Command	kg (1bm) 1,499,717 (3,306,308)	646,202 (1,424,631)	1,497,405 (3,301,214)	649,398 (1,431,678)	1,497,401 (3,301,203)	649,399 (1,431,678)
Holddown Arm Release	kg (1bm) 1,469,082 (3,238,770)	637,687 (1,405,858)	1,468,100 (3,236,606)	640,635 (1,412,358)	1,466,931 (3,234,030)	641,099 (1,413,381)
CECO	kg (1bm) 212,398 (468,257)	97,595 (215,161)	233,212 (514,144)	109,625 (241,681)	231,367 (510,077)	109,908 (242,304)
OECO	kg (1bm) 17,744 (39,118)	14,315 (31,560)	20,516 (45,230)	19,228 (42,390)	20,516 (45,230)	19,228 (42,390)
Separation	kg (1bm) 15,557 (34,297)	13,220 (29,146)	- -	- -	18,539 (40,870)	18,278 (40,297)
Zero Thrust	kg (1bm) 15,329 (33,795)	13,072 (28,819)	- -	- -	17,890 (39,440)	17,811 (39,266)

NOTE: Predicted and reconstructed values do not include pressurization gas so they will compare with level sensor data.

the AS-504 LOX "breakthrough". The higher than predicted fuel residual at zero thrust was due mostly to propellant loading error and higher consumed Mixture Ratio (MR) than expected for the actual flight fuel density. (A summary of the propellants remaining at major event times is presented in Table 5-2.)

## 5.6 S-IC PRESSURIZATION SYSTEMS

### 5.6.1 S-IC Fuel Pressurization System

The fuel tank pressurization system maintained the required ullage pressure in the fuel tank during the flight. Helium Flow Control Valves (HFCV's) No. 1 through No. 4 opened as programmed and the fifth flow control valve cycled five times between 6.5 and 45.5 seconds. HFCV No. 5 is not scheduled or expected to cycle anytime during the flight and should not be needed. It is only planned as a backup for additional pressurization flow if the flows from the other four valves are below required minimum.

The low flow prepressurization system was commanded on at -97 seconds and performed satisfactorily. High flow prepressurization was accomplished by the onboard pressurization system as planned. HFCV No. 1 was commanded on at -2.739 seconds. Ullage pressure decreased unexpectedly until HFCV No. 5 was cycled on by the stage pressure switch at 6.5 seconds. HFCV No. 5 cycled on four additional times (at approximately 15, 25, 35, and 43 seconds). HFCV's No. 2, 3 and 4 opened as planned at 50.2, 96.0 and 133.0 seconds, respectively. The fuel tank ullage pressure was below the predicted minimum

at approximately -1 second to 55 seconds as can be seen in Figure 5-6, but the fuel Net Positive Suction Pressure (NPSP) requirement was maintained throughout flight as seen in Figure 5-7. Helium bottle pressure, as shown in Figure 5-8, generally stayed within expected limits.

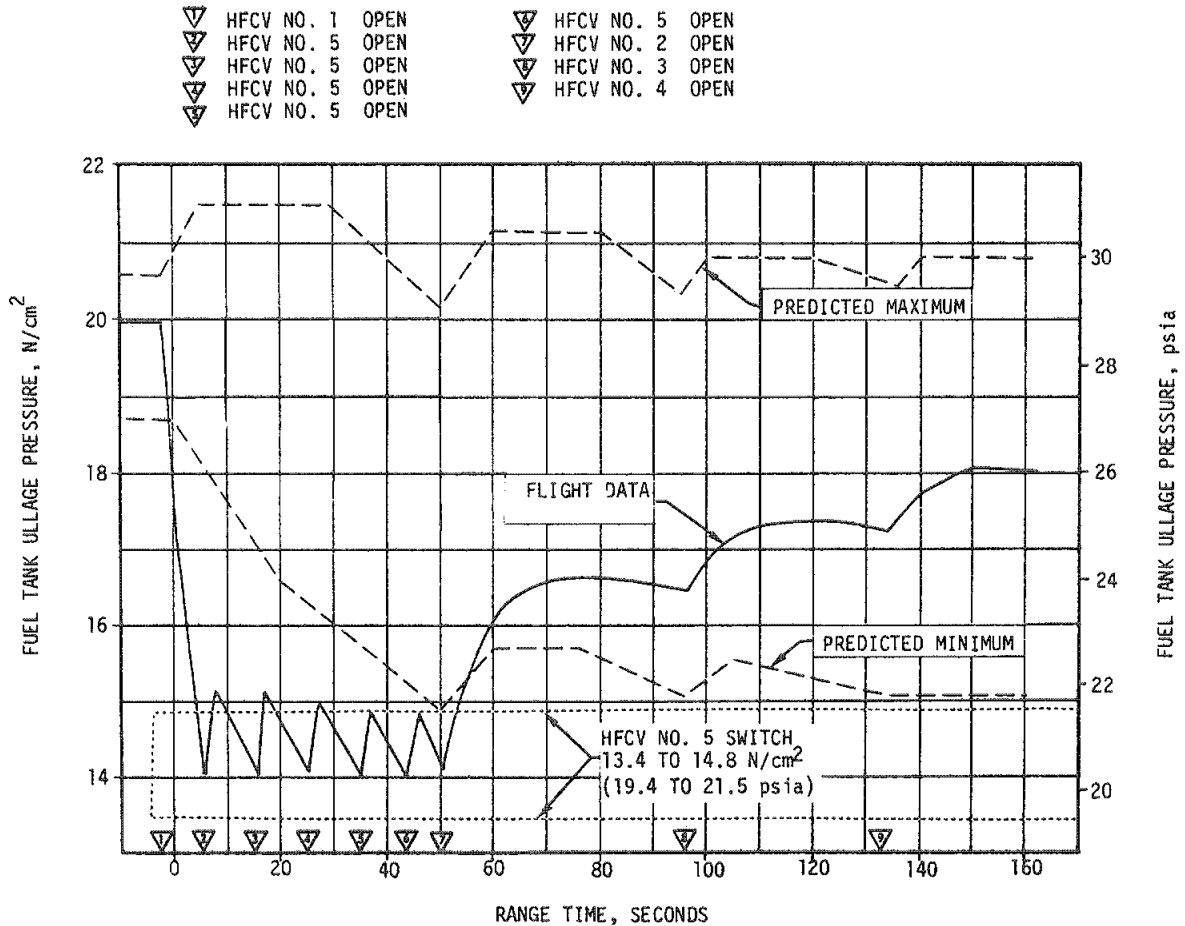


Figure 5-6. S-IC Fuel Ullage Pressure

Analyses indicate that the most probable cause of the low ullage pressure was that the smaller HFCV No. 2 orifice was installed in HFCV No. 1 and the No. 1 orifice was installed in HFCV No. 2. The five HFCV's were replaced after stage acceptance firing (TBC ECP 0358).

The heat exchangers performed as expected.

#### 5.6.2 S-IC LOX Pressurization System

The LOX pressurization system performed satisfactorily, and all performance requirements were met. The ground prepressurization system maintained ullage pressure within acceptable limits until launch commit. The onboard pressurization system subsequently maintained ullage pressure

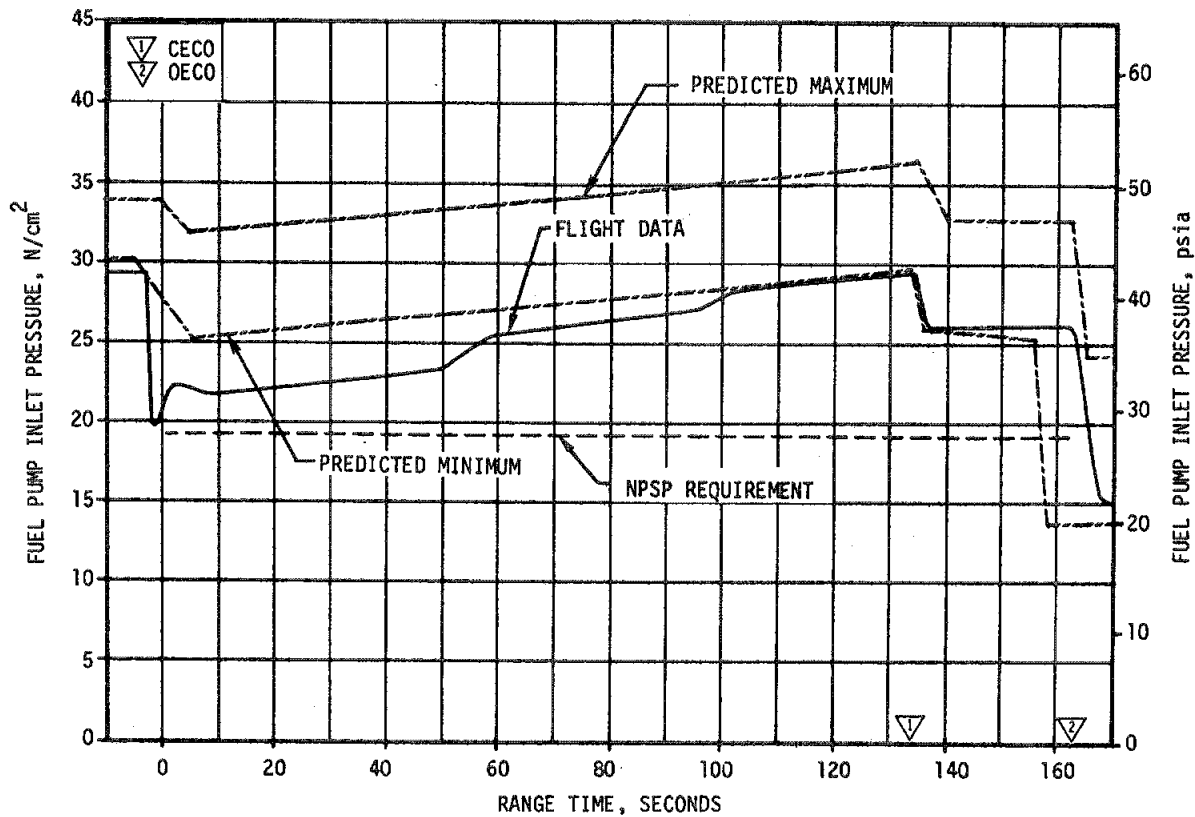


Figure 5-7. S-IC Fuel Pump Inlet Pressure, Engine No. 2

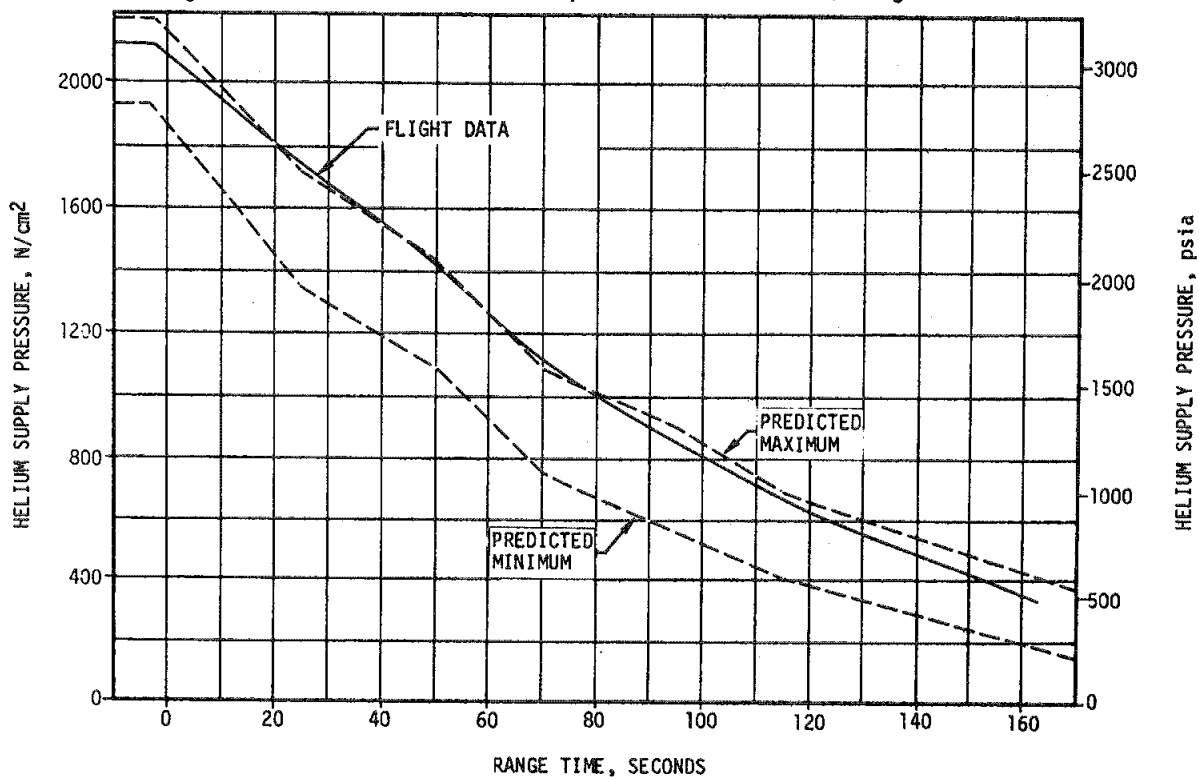


Figure 5-8. S-IC Helium Bottle Pressure For Fuel Pressurization



within the GOX Flow Control Valve (GFCV) band during the flight. The heat exchangers performed as expected.

The prepressurization system was initiated by opening of the ground supply valve at -71.93 seconds. The ullage pressure increased until it entered the switch band zone which terminated the flow at -57.16 seconds. The ullage pressure increased approximately  $0.52 \text{ N/cm}^2$  ( $0.75 \text{ psia}$ ) above the prepressurization switch setting to  $18.75 \text{ N/cm}^2$  ( $27.25 \text{ psia}$ ). This overshoot was within expected limits, and was less than that for AS-501, 502 and 503 even though the ullage volume was smaller for this vehicle. This was accomplished by reducing the initial prepressurization flowrate from approximately  $1.8 \text{ kg/s}$  ( $4.0 \text{ lbm/s}$ ) to  $0.45 \text{ kg/s}$  ( $1.0 \text{ lbm/s}$ ).

The LOX tank ullage pressure history is shown in Figure 5-9. During flight, the ullage pressure was maintained within required limits by the GFCV and followed the anticipated trend.

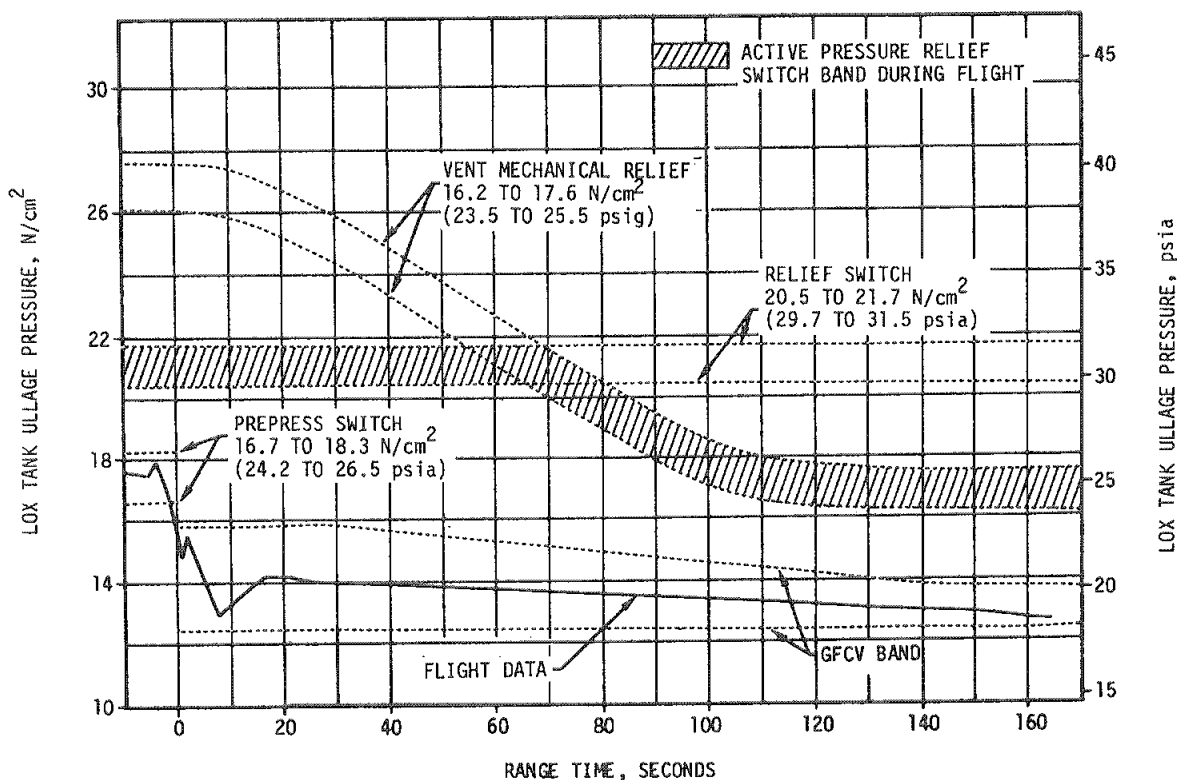


Figure 5-9. S-IC LOX Tank Ullage Pressure

The maximum GOX flowrate was  $23.85 \text{ kg/s}$  ( $52.6 \text{ lbm/s}$ ). After CECO, the GOX flow requirements for the remaining four engines increased until OECO.

The LOX pump inlet pressure met the NPSP requirements as shown in Figure 5-10. This figure is for engine No. 2, but is typical of the four outboard engines. Engine No. 5 LOX suction line pressure decayed unexpectedly after CECO. This pressure is shown in Figure 5-11 along

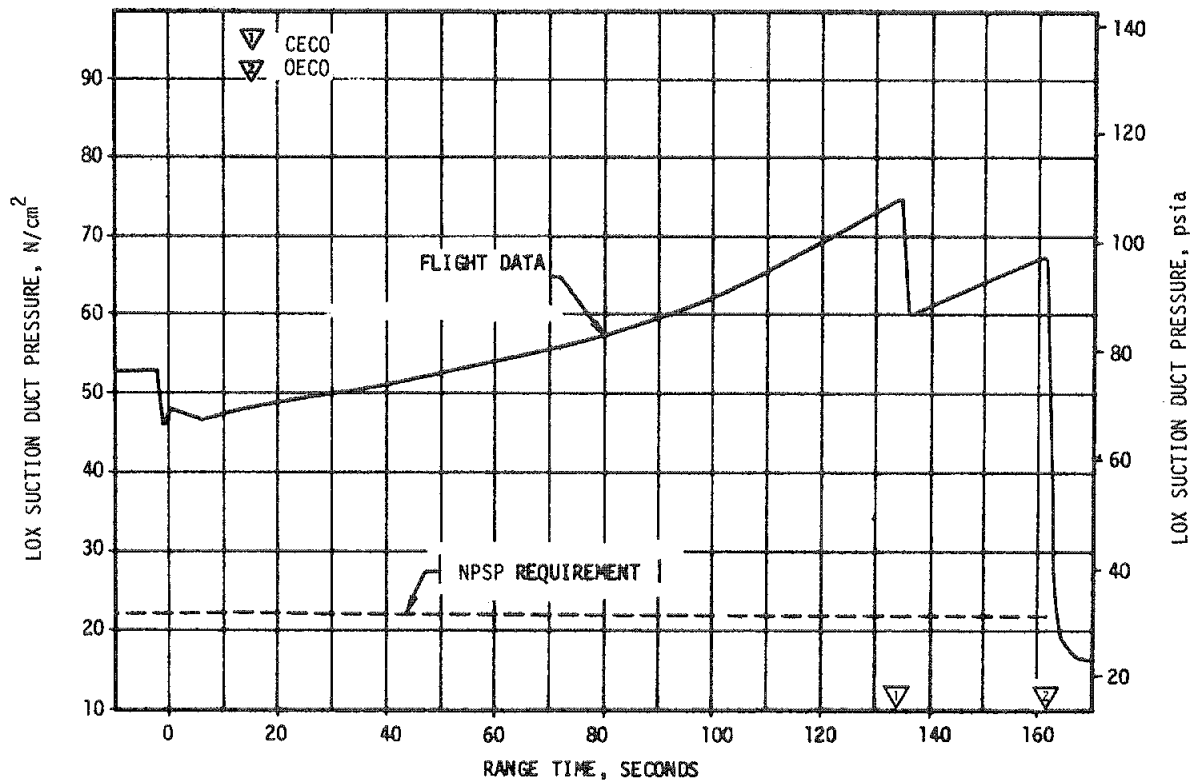


Figure 5-10. S-IC LOX Suction Duct Pressure, Engine No. 2

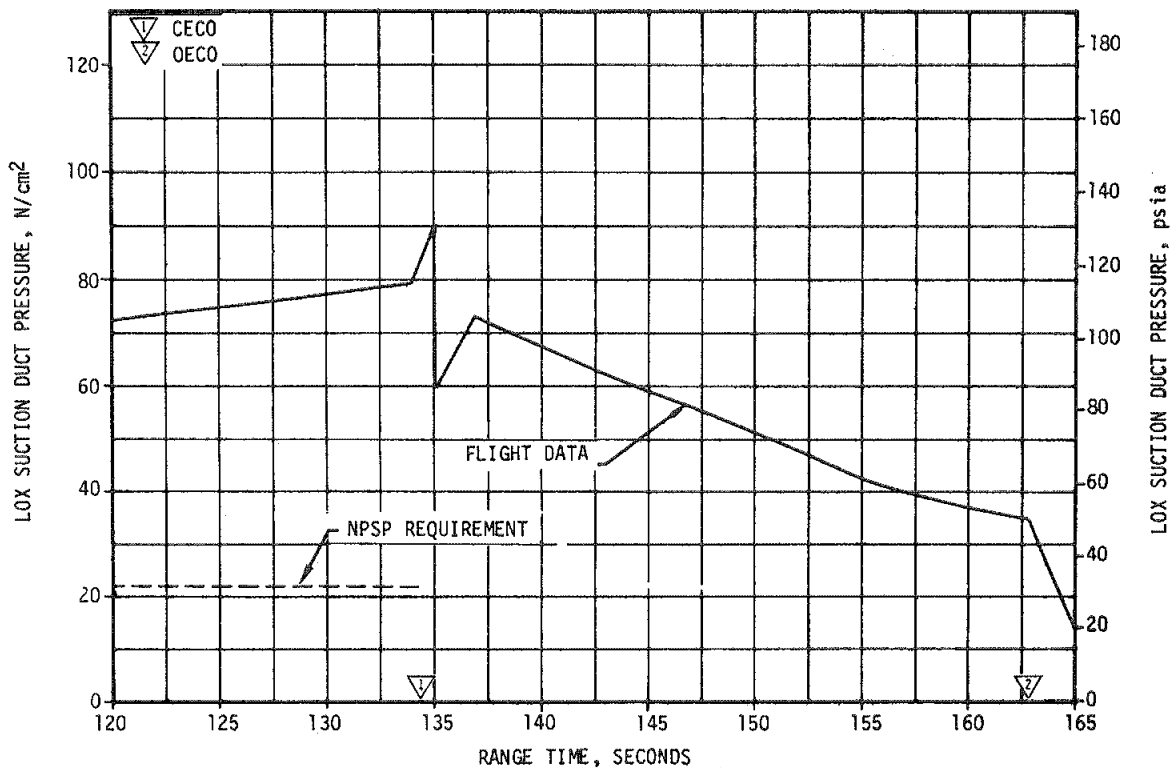


Figure 5-11. S-IC LOX Suction Duct Pressure, Engine No. 5

with pump NPSP requirements. No pressure decay at this time was predicted, but did occur on both AS-503 and AS-504. The decay rates on AS-503 and AS-504 were almost identical as shown in Figure 5-12. Analysis indicates that the most probable cause of this decay is a LOX leak, although the possibility of a natural phenomenon in the Pressure Volume Compensator (PVC) duct causing the pressure decay cannot be eliminated at this time. Investigation of these pressure decays is continuing.

#### 5.7 S-IC PNEUMATIC CONTROL PRESSURE SYSTEM

The pneumatic control pressure system functioned satisfactorily throughout the S-IC flight.

Sphere pressure was 2199 N/cm<sup>2</sup> (3190 psia) at liftoff and remained steady until CECO when it decreased to 2123 N/cm<sup>2</sup> (3080 psia). The decrease was due to center engine prevalve actuation. There was a further decrease to 1848 N/cm<sup>2</sup> (2680 psia) after OECO. This is shown in Figure 5-13. Pressure downstream of the regulator initially was 524 N/cm<sup>2</sup> (760 psia) and decreased to 517 N/cm<sup>2</sup> (750 psia) at 160 seconds. Regulator performance was within limits of 527 ±34 N/cm<sup>2</sup> (750 ±50 psig). There were two slight dips in outlet pressure at center engine and outboard engine cutoff.

The engine prevalues were closed after engine cutoff as required. Engine No. 5 prevalues closed at approximately 136 seconds. The prevalues for the other four engines closed at approximately 164 seconds.

#### 5.8 S-IC PURGE SYSTEMS

Performance of the S-IC purge systems was satisfactory during S-IC flight.

The turbopump LOX seal storage sphere pressure was within its limits of 1903 to 2275 N/cm<sup>2</sup> (2760 to 3300 psig) until ignition and 2275 to 689 N/cm<sup>2</sup> (3300 to 1000 psig) from liftoff to cutoff. Regulator outlet pressure remained within the 59 ±7 N/cm<sup>2</sup> (85 ±10 psig) limits. Turbopump LOX seal purge pressure at the engine interface was within the required limits of 69 N/cm<sup>2</sup> (100 psig) maximum to 21 N/cm<sup>2</sup> (30 psig) minimum. The radiation calorimeter purge operated satisfactorily throughout flight.

The LOX dome and GG LOX injector purge system met all requirements.

#### 5.9 POGO SUPPRESSION SYSTEM

The POGO suppression system performed satisfactorily prior to and during S-IC flight. The system was initially turned on approximately 24 minutes prior to launch to be sure the prevalues would fill with helium. Redline measurements indicated that the four outboard lines filled as scheduled. The pressure measurements downstream of the solenoid valves indicated

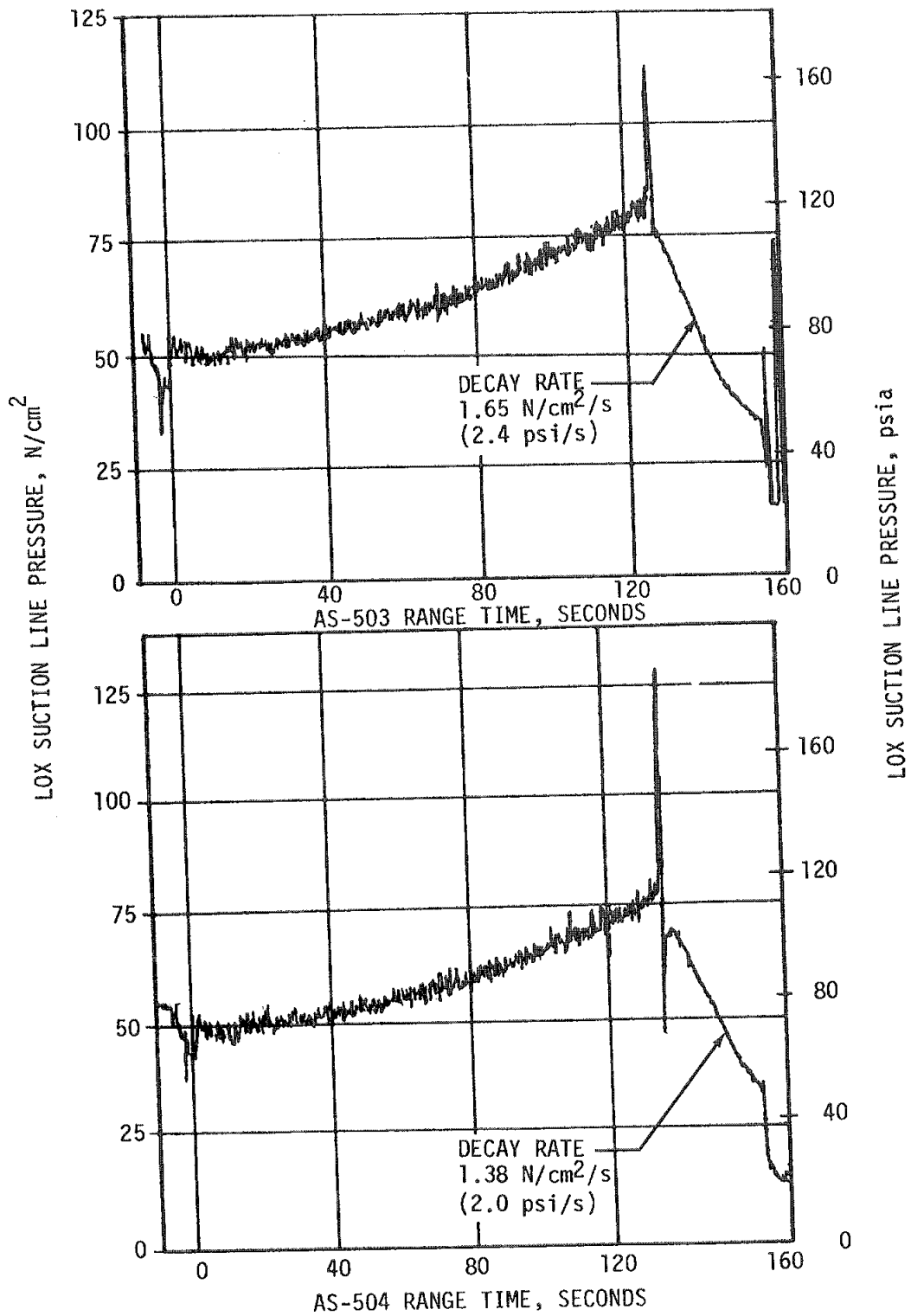


Figure 5-12. S-IC Center Engine LOX Suction Line Pressure

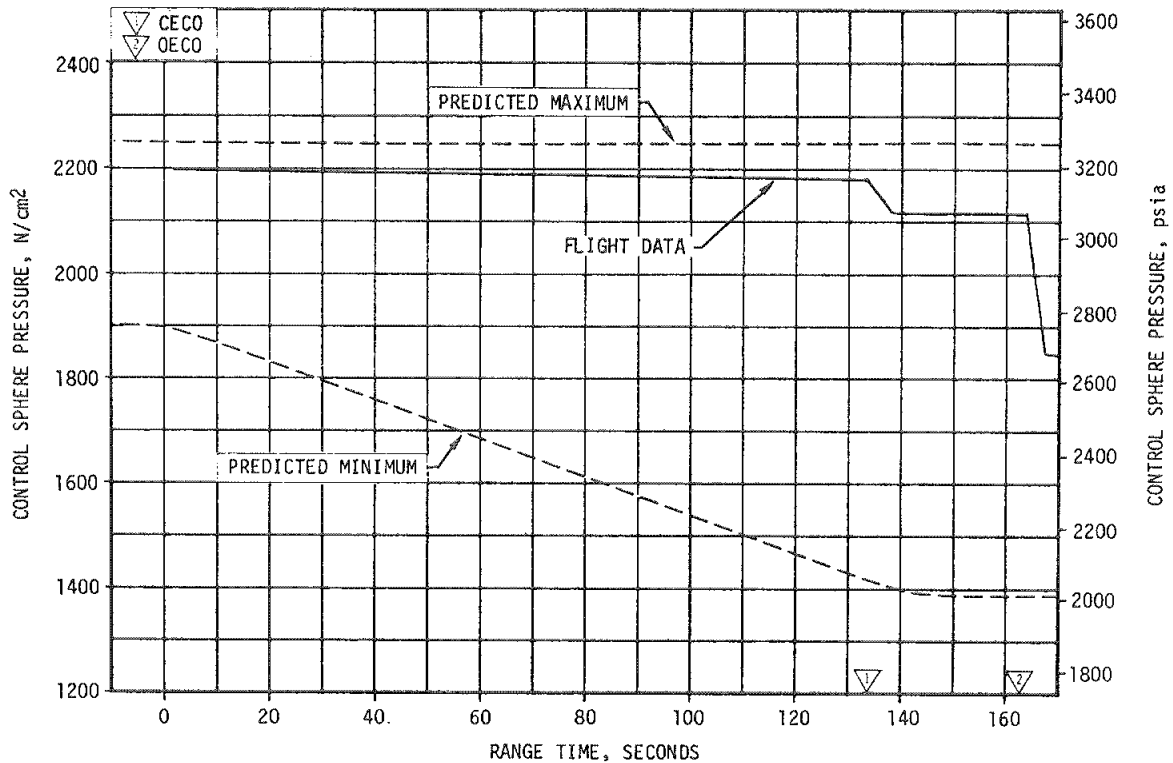


Figure 5-13. S-IC Control Sphere Pressure

that flow was properly established in the system. Eleven minutes prior to launch, the system was turned on again and flow was established. The temperature measurements did not change since the system still contained helium from the earlier initiation. The four resistance thermometers performed as expected during flight. In the outboard lines, the three upper measurements went cold momentarily at liftoff indicating that the LOX level shifted on the probes. The probes remained warm throughout flight, indicating helium in the prevalues. Figure 5-14 shows a plot of liquid level in the prevalue. At cutoff, the increased pressure forced LOX into the prevalues. The fourth resistance thermometer, at the tip of the valve cavity, was cold throughout flight as expected.

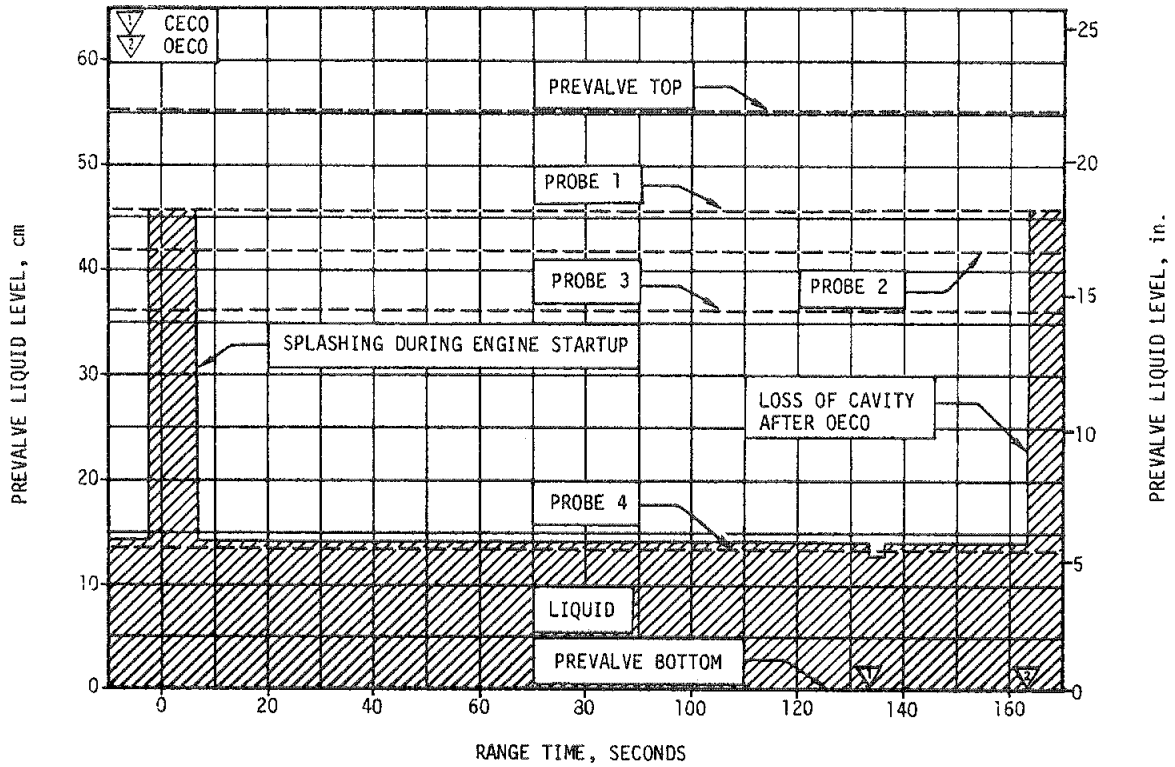


Figure 5-14. S-IC Prevalve Liquid Level, Typical Outboard Engine

SECTION 6  
S-II PROPULSION

6.1 SUMMARY

The S-II propulsion system performed satisfactorily during the entire flight. This was the first flight with uprated J-2 engines of 1,023,091 Newtons (230,000 lbf) nominal thrust installed. Total stage thrust, as determined by computer analysis of telemetered propulsion measurements at 61 seconds after Engine Start Command (ESC) was 0.20 percent below prediction. Total engine propellant flowrate (excluding pressurization flow) was 0.44 percent below and average specific impulse 0.25 percent above predictions at this time slice. Average Engine Mixture Ratio (EMR) was 0.33 percent above predicted. As sensed by the engines, ESC occurred at 164.17 seconds and Engine Cutoff (ECO) at 536.22 seconds with a burn time of 372.05 seconds, 2.27 seconds longer than predicted.

Low frequency performance oscillations were experienced by the center engine near the end of S-II burn. These oscillations were similar to, but appeared to be somewhat more severe than those occurring on the AS-503. Corrective action being planned for AS-505 is to cut off the center engine before the oscillations are expected.

The propellant management system met all performance requirements. The system differed from AS-503 in that control of the engine Propellant Utilization (PU) valves was closed-loop as was AS-501 and AS-502. All future S-II flights are presently scheduled to utilize open-loop control. The PU valve step from the high to low EMR position began at 440 seconds, well within the predicted range of  $429 \pm 20$  seconds. Cutoff was initiated by the LOX low level cutoff sensors located in the bottom of the LOX tank sump. A 1.5-second delay was incorporated for AS-504 between initiation of cutoff by these sensors and transmission of the command to the engines. Residual propellants remaining in the tanks at ECO signal were 2071 kilograms (4565 lbm) compared to a prediction of 2060 kilograms (4540 lbm).

The performance of the LOX and LH<sub>2</sub> tank pressurization systems was satisfactory. Ullage pressure in both tanks was more than adequate to meet engine inlet Net Positive Suction Pressure (NPSP) requirements throughout mainstage. Unlike all previous flights, the LOX ullage pressure did not drop below the regulator band after the step to low EMR.

This was prevented by opening the LOX tank ullage pressure regulator full open at 262.8 seconds (ESC + 98.6 seconds).

## 6.2 S-II CHILLDOWN AND BUILDUP TRANSIENT PERFORMANCE

The prelaunch servicing operations satisfactorily accomplished the engine conditioning requirements. Thrust chamber temperatures were within predicted limits both at launch and engine start as shown in Figure 6-1. Chamber temperatures increased during S-IC boost at rates

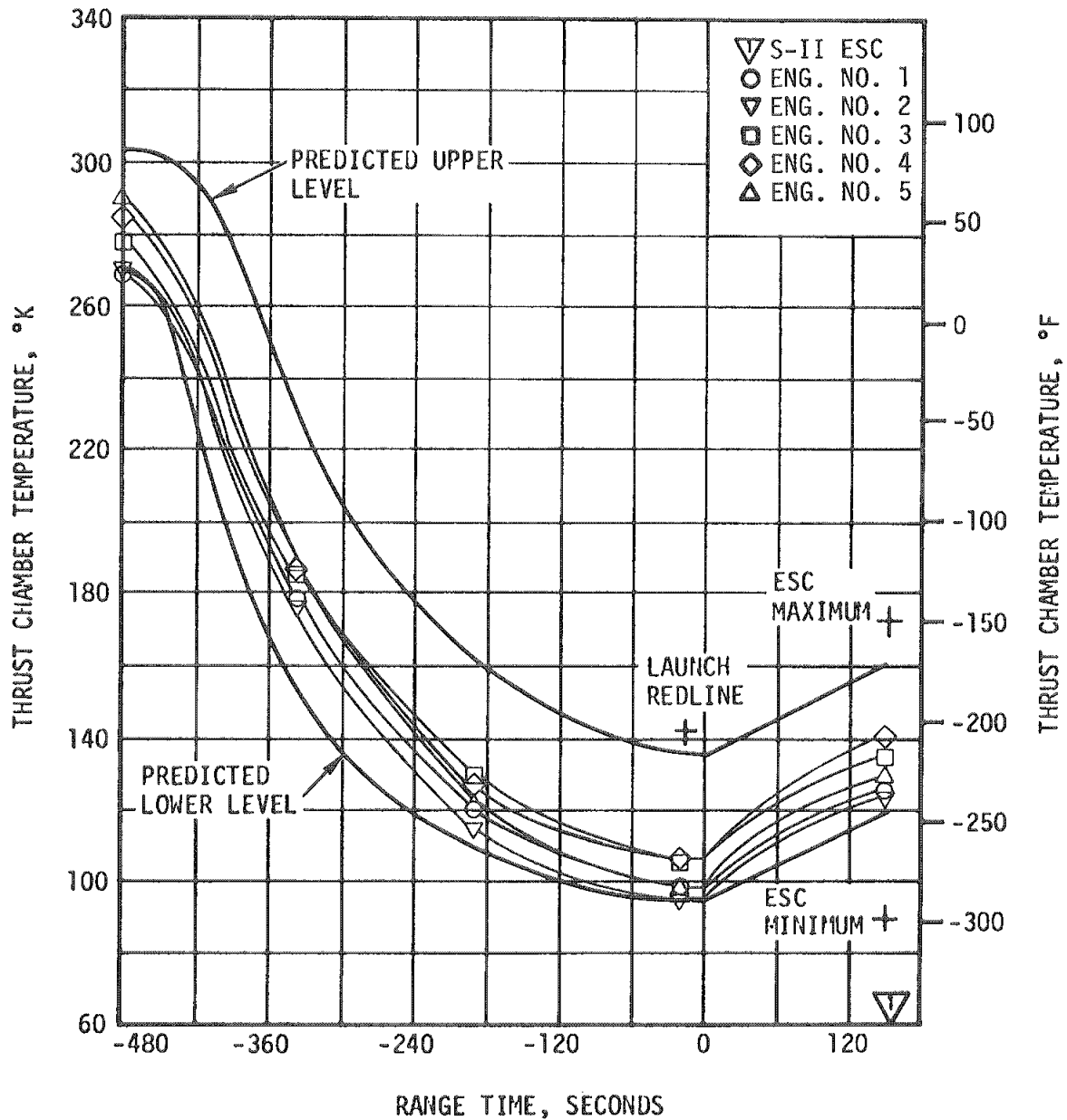


Figure 6-1. S-II Thrust Chamber Jacket Temperature



of from 10.4 to 12.6°K/min (18.7 to 22.7°F/min), which agrees closely with those experienced on previous flights. The general level of thrust chamber jacket temperature for AS-504 was slightly colder than for AS-503. Engine No. 2 approached the lower limit of the prediction band at -19 seconds, reaching 94.3°K (-290°F). This lower jacket temperature is attributed to the close proximity of engine No. 2 with the S-IC LOX vent line within the boattail. No impact on future stages is indicated by this condition since there is no lower temperature limit at liftoff, and the minimum engine start requirement is 88.7°K (-300°F). No change will be made to the present prediction band for AS-505.

Both temperature and pressure conditions of the J-2 engine start tanks were within the required prelaunch and engine start boxes as shown in Figure 6-2. Start tank conditions at -33 seconds were 107 to 113.1°K (-267 to -256°F) and 862 to 876 N/cm<sup>2</sup> (1250 to 1270 psia). At S-II ESC this band increased to 110.9 to 118.1°K (-260 to -247°F) and 889 to 917 N/cm<sup>2</sup> (1290 to 1330 psia). Heatup and self-pressurization rates during the S-IC boost interval were 0.83 to 1.21°K (1.5 to 2.2°F) and 10 to 14.3 N/cm<sup>2</sup> (14.5 to 20.8 psi), respectively. These values are in general agreement with AS-503 results.

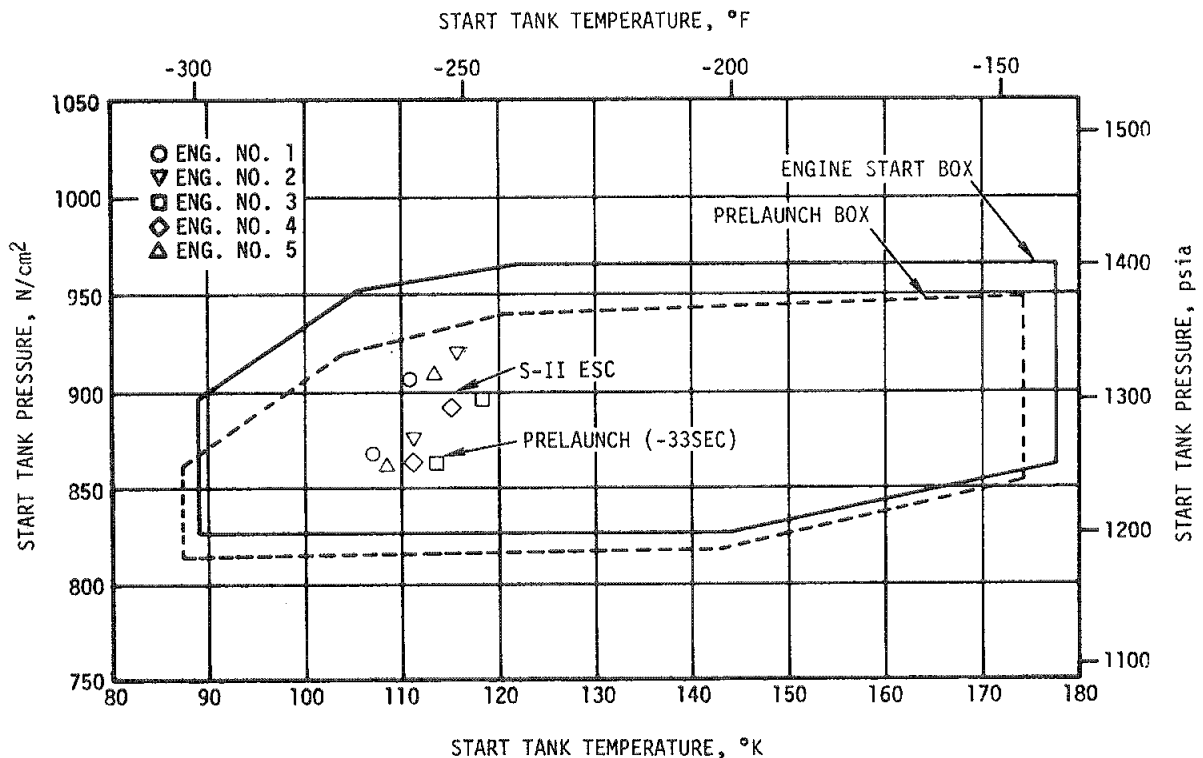


Figure 6-2. S-II Engine Start Tank Performance

All engine helium tank pressures were within the redline limit of 1931 to 2379 N/cm<sup>2</sup> (2800 to 3450 psia) established for prelaunch pressurization. The pressurization regulator in the Ground Support Equipment (GSE) pneumatic servicing unit was reset to a nominal pressure of 2068 N/cm<sup>2</sup> (3000 psia) in order to preclude exceeding the engine helium tank pressure requirement of 2379 N/cm<sup>2</sup> (3450 psia) at ESC. This requirement had been violated by one engine on the AS-503 flight with the subject regulator set 138 N/cm<sup>2</sup> (200 psi) higher.

The LOX and LH<sub>2</sub> recirculation systems used to chill the feed ducts, turbo-pumps, and other engine components performed satisfactorily. Engine pump inlet temperatures and pressures at engine start were well within the requirements as shown in Figure 6-3.

The LOX recirculation system performance was satisfactory throughout S-IC boost. At ESC the engine pump inlet pressures were slightly higher than predicted while the pump inlet temperatures were slightly colder than predicted. These pump inlet conditions, however, are an asset with respect to engine start requirements. The AS-504 Countdown Demonstration Test (CDDT) data evaluation led to the revision to the LOX pump discharge temperature redline limit. The redline limit was revised from 98.7°K to 99.8°K (-282.0 to -280°F) maximum at -22 seconds. Performance of the LOX recirculation system was similar to that of AS-503. At ESC, the LOX pump discharge temperatures were 7.7°K to 8.6°K (13.9°F to 15.4°F) subcooled, well below the 1.7°K (3.0°F) subcooling requirement.

The LH<sub>2</sub> recirculation system performance was satisfactory throughout S-IC boost. The LH<sub>2</sub> engine pump inlet temperatures and pressures agreed well with predictions and reflect the effects of lower vacuum levels in reducing heat leaks in the vacuum-jacketed lines.

ESC was received at 164.17 seconds, and the Start Tank Discharge Valve (STDV) solenoid activation signal occurred 1.0 second later. The thrust buildup envelope including each J-2 engine is shown in Figure 6-4. All engines performed within the required thrust buildup envelope. Engine thrust levels were between 880,748 and 925,230 Newtons (198,000 and 208,000 lbf) prior to "PU Activate" command at 169.7 seconds.

### 6.3 S-II MAIN STAGE PERFORMANCE

Two analytical techniques were used to evaluate the stage propulsion system performance. The primary method, propulsion reconstruction analysis, used telemetered engine and stage data to calculate longitudinal thrust, specific impulse, and stage mass flowrate. The second method used was trajectory simulation which adjusted the propulsion reconstruction data using a differential correction procedure. This six-degree-of-freedom trajectory simulation determined adjustments to thrust and mass flow histories to yield a simulated trajectory which closely matched the observed trajectory.

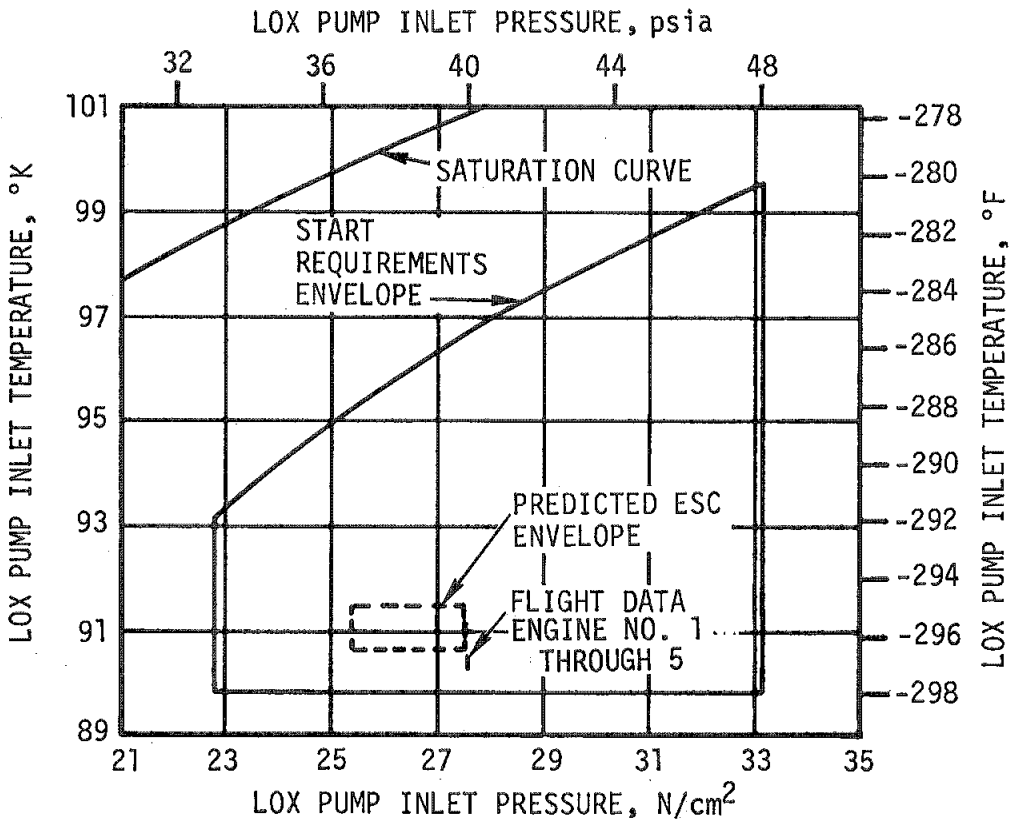
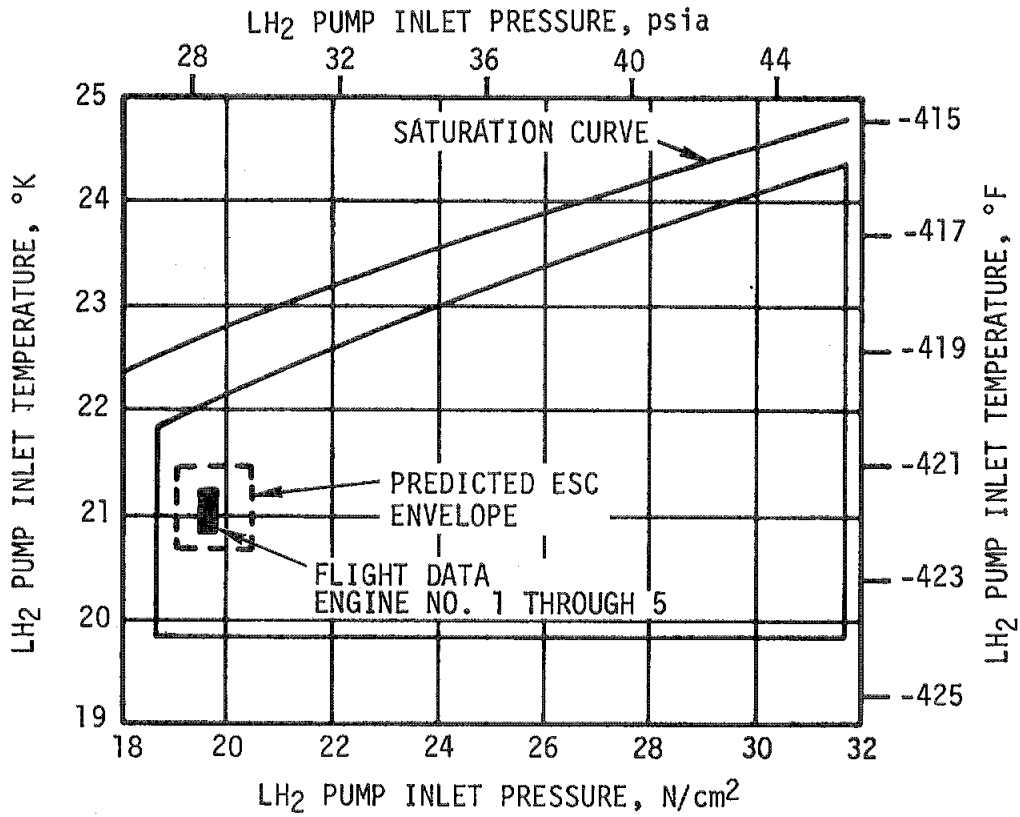


Figure 6-3. S-II Engine Pump Inlet Start Requirements

- ▽ 1 S-II ESC
- ▽ 2 S-II ENG STDV OPEN COMMAND
- ▽ 3 S-II MAINSTAGE

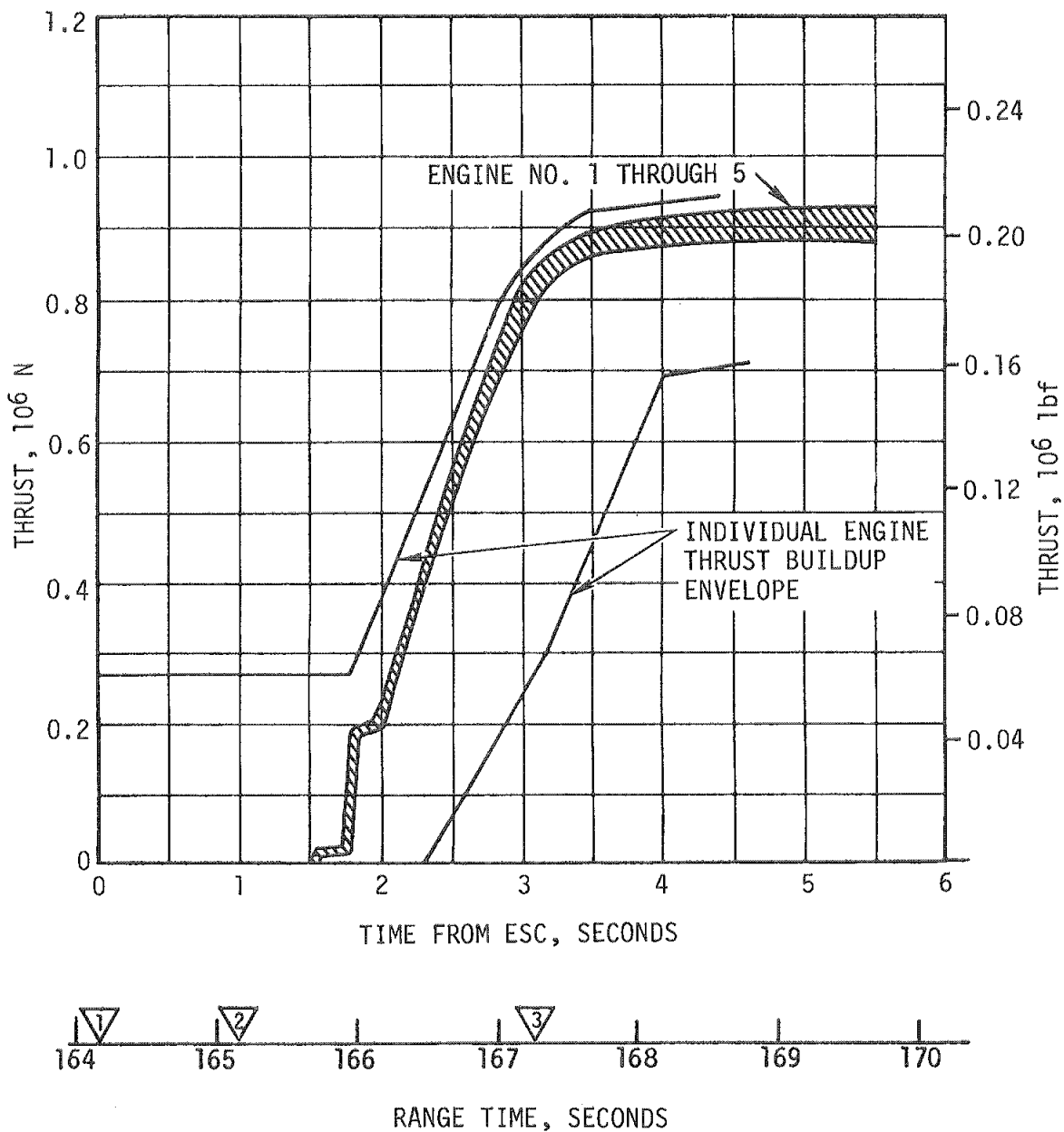


Figure 6-4. S-II Engine Thrust Buildup

Stage performance during the high EMR portion of the flight was very close to predicted as shown in Figure 6-5. At a time slice of ESC +61 seconds, total vehicle thrust was 5,140,414 Newtons (1,155,611 lbf), which is only 10,017 Newtons (2552 lbf) or 0.20 percent below the official preflight prediction. Average engine specific impulse was 4162.9 N-s/kg (424.5 lbf-s/lbm) or 0.25 percent above the predicted level. Propellant flowrate to the engines (excluding pressurization flow) was 1234.9 kg/s (2722.4 lbm/s) which was 0.44 percent below prediction, and the average EMR was 5.54 or 0.33 percent above preflight prediction.

The propellant utilization system was operated in the closed-loop control mode. Engine thrust chamber pressures began reaction to the PU control valve travel at approximately 288 seconds after ESC. This action reduced total vehicle thrust to 4,181,053 Newtons (939,938 lbf) at ESC + 330 seconds. Thus a change in total vehicle thrust of 959,361 Newtons (215,673 lbf) is indicated between high (5.54) and low (4.61) EMR operation. Additional minor thrust reductions occurred during the last 35 seconds of S-II operation due to a performance decrease on the center engine (associated with the oscillation period), and further movement of the PU control valves. At ESC + 365 seconds total stage thrust was down to 4,161,698 Newtons (935,587 lbf) at an EMR of 4.61.

As in previous flights, the disagreement between predicted and actual performance increases at the lower mixture ratio levels. Vehicle thrust and propellant flowrate at ESC + 320 seconds were below the predicted performance by 127,886 Newtons (28,750 lbf) and 37 kg/s (81.5 lbm/s), respectively.

Individual J-2 engine data are presented in Table 6-1 for ESC + 61-second time point. With the exception of engine No. 4, very good correlation between prediction and flight is indicated by the small magnitude of the deviations. Flight data reconstruction procedures were directed toward matching the engine and stage acceptance specific impulse values while maintaining the engine flow and pump data as a baseline.

The large disagreement on engine thrust and flow rate for engine No. 4 (J2070) stems from decisions made following stage acceptance testing at Mississippi Test Facility (MTF). During static firing, this engine operated 27,401 Newtons (6160 lbf) below its demonstrated performance in engine acceptance testing. This performance shift was attributed to the Gas Generator (GG) LOX bootstrap line resistance fluctuation phenomenon. A complete inspection was performed of the GG LOX injector, bootstrap line, bleed valve, control valve, orifice, and high pressure duct. No contamination, unusual restriction, or out-of-configuration conditions were detected. The engine contractor reported only two previous cases of bootstrap line resistance change of this magnitude. In both cases the problem did not recur upon subsequent operation. Therefore, it was

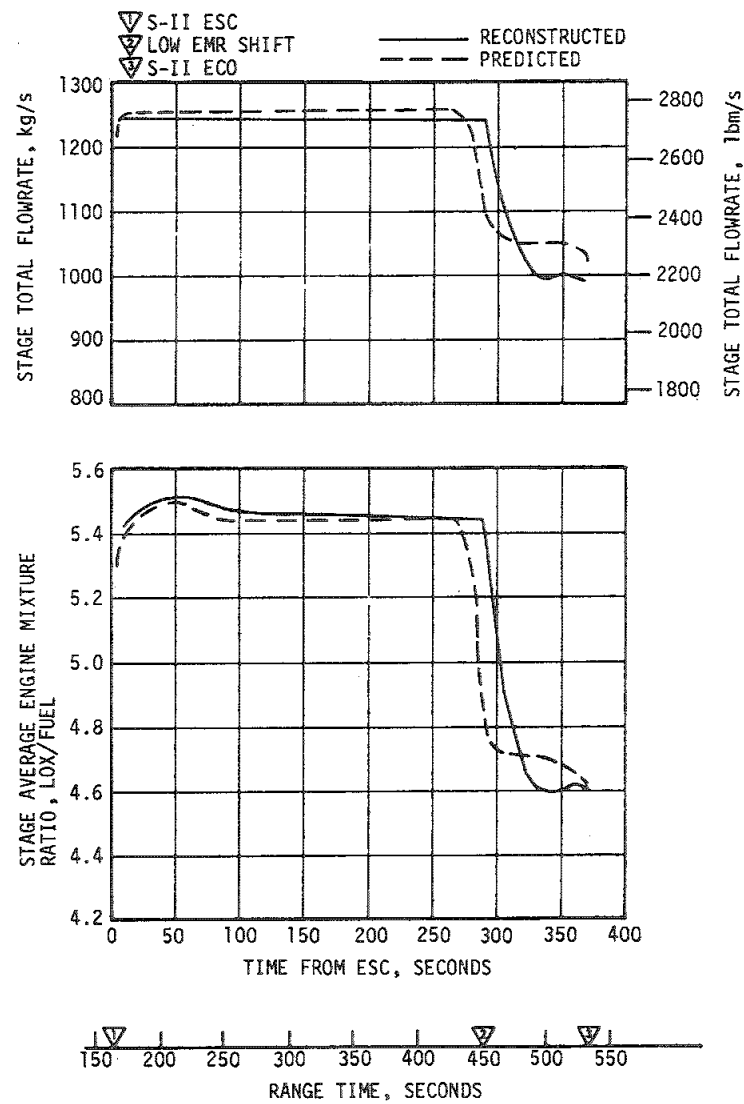
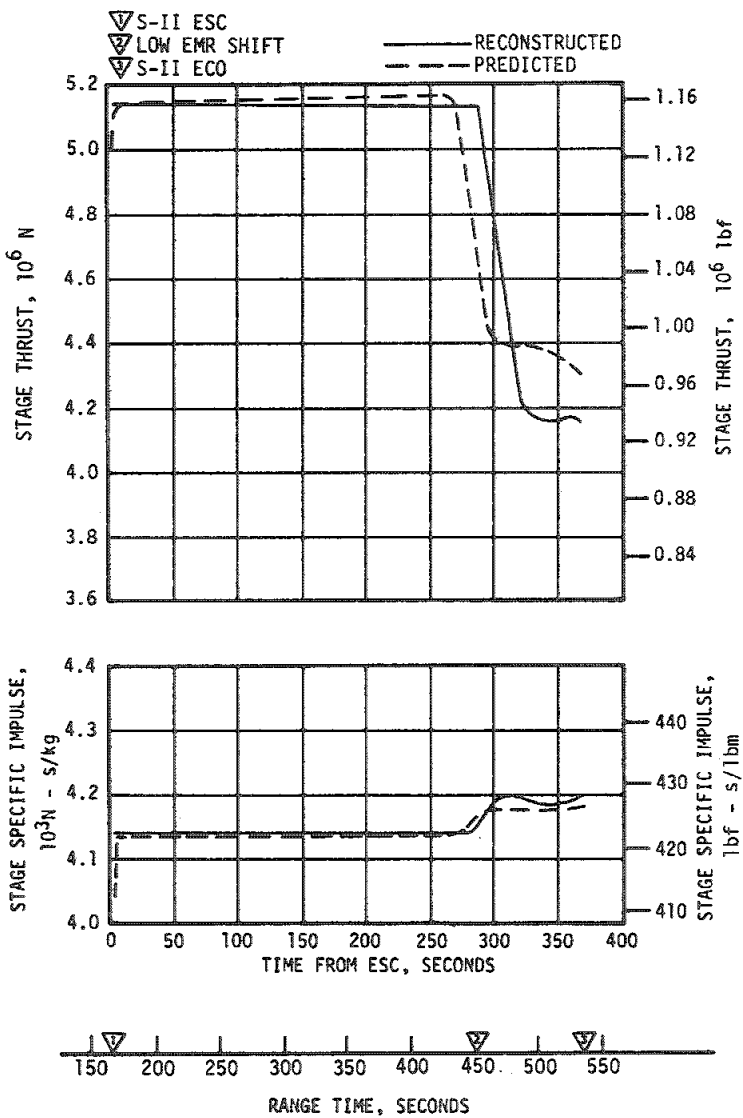


Figure 6-5. S-II Steady State Operation

Table 6-1. S-II Engine Performance Deviations (ESC +61 Seconds)

PARAMETER	ENGINE	PREDICTED	RECONSTRUCTION ANALYSIS	PERCENT DEVIATION FROM PREDICTED	AVERAGE PERCENT DEVIATION FROM PREDICTED
Thrust Newtons (lbf)	1	1,028,656 (231,251)	1,032,125 (232,031)	0.34	-0.20
	2	1,029,234 (231,381)	1,030,920 (231,760)	0.16	
	3	1,020,213 (229,353)	1,020,369 (229,388)	0.02	
	4	1,025,947 (230,642)	1,004,755 (225,878)	-2.07	
	5	1,046,382 (235,236)	1,052,245 (236,554)	0.56	
Specific Impulse N-s/kg (lbf-s/lbm)	1	4147.2 (422.9)	4167.8 (425.0)	0.50	0.25
	2	4164.9 (424.7)	4153.1 (423.5)	-0.28	
	3	4136.4 (421.8)	4153.1 (423.5)	0.40	
	4	4159.0 (424.1)	4166.8 (424.9)	0.19	
	5	4155.0 (423.7)	4173.7 (425.6)	0.45	
Flowrate kg/s (lbm/sec)	1	248.0 (546.8)	247.6 (545.93)	-0.16	-0.44
	2	247.1 (544.8)	248.3 (547.31)	0.46	
	3	246.7 (543.8)	245.7 (541.71)	-0.38	
	4	246.7 (543.8)	241.2 (531.65)	-2.23	
	5	251.8 (555.1)	252.1 (555.80)	0.13	
Mixture Ratio LOX/Fuel	1	5.54	5.57	0.54	0.33
	2	5.46	5.50	0.73	
	3	5.49	5.49	0.00	
	4	5.55	5.52	-0.54	
	5	5.57	5.62	0.90	

assumed that the performance of this engine (J2070) would return to the level exhibited during engine acceptance tests. Flight prediction was made based upon this assumption. Actual operation of engine No. 4 during the AS-504 flight, however, was very similar to the static firing level as measured during stage acceptance.

Data presented in Table 6-1 is actual flight data and has not been adjusted to standard J-2 engine conditions. Considering data that has been adjusted to standard conditions through use of a computer program, very little change from the stage acceptance test is indicated. Engine No. 3 (J2069) is 2224 Newtons (500 lbf) lower in thrust. All engines are within 9.8 N-s/kg (1 lbf-s/lbm) on engine specific impulse level. These magnitudes were maintained throughout the S-II flight and are considered normal run-to-run variations.

The postflight data analysis indicates that the AS-504 Augmented Spark Igniter (ASI) system performed satisfactorily. Redesigned fuel and LOX ASI line configurations were first incorporated on the J-2 engines of AS-503. The ASI supply line and thrust chamber temperatures were normal, and over-all engine vibration levels were generally as expected.

Predicted average performance characteristics of the stage propulsion system are compared in Table 6-2 with data obtained from the propulsion reconstruction and the trajectory simulation analyses. Results of the trajectory simulation analysis indicate that the total average thrust

Table 6-2. S-II Flight Reconstruction Comparison with Simulation Trajectory Match Results

PARAMETERS	UNITS	PREDICTED			RECONSTRUCTION ANALYSIS			PERCENT DEVIATION FROM PREDICTED		
		HIGH MIXTURE RATIO	LOW MIXTURE RATIO	TOTAL FLIGHT AVERAGE	HIGH MIXTURE RATIO	LOW MIXTURE RATIO	TOTAL FLIGHT AVERAGE	HIGH MIXTURE RATIO	LOW MIXTURE RATIO	TOTAL FLIGHT AVERAGE
Average Longitudinal Stage Thrust	N (lbf)	5,159,546 (1,159,912)	4,370,565 (982,542)	4,939,225 (1,110,382)	5,136,233 (1,154,671)	4,162,121 (935,682)	4,932,415 (1,108,851)	-0.45	-4.77	-0.14
Average Vehicle Mass Loss Rate	kg/s (lbfm/s)	1241.7 (2737.4)	1039.5 (2291.7)	1186.1 (2614.8)	1232.9 (2718.0)	988.8 (2180.0)	1180.7 (2603.1)	-0.71	-4.87	-0.45
Average Stage Longitudinal Specific Impulse	N-s/kg (lbf-s/lbfm)	4155.1 (423.7)	4204.1 (428.7)	4164.9 (424.7)	4165.9 (424.8)	4209.0 (429.2)	4177.6 (426.0)	0.26	0.12	0.31
PARAMETERS	UNITS	SIMULATION TRAJECTORY MATCH			PERCENT DEVIATION FROM PREDICTED					
		HIGH MIXTURE RATIO	LOW MIXTURE RATIO	TOTAL FLIGHT AVERAGE	HIGH MIXTURE RATIO	LOW MIXTURE RATIO	TOTAL FLIGHT AVERAGE			
Average Longitudinal Stage Thrust	N (lbf)	5,132,380 (1,153,805)	4,177,779 (939,202)	4,928,354 (1,107,938)	-0.53	-4.41	-0.22			
Average Vehicle Mass Loss Rate	kg/s (lbfm/s)	1237.9 (2729.2)	993.7 (2190.8)	1185.3 (2613.2)	-0.30	-4.40	-0.06			
Average Stage Longitudinal Specific Impulse	N-s/kg (lbf-s/lbfm)	4146.3 (422.8)	4204.1 (428.7)	4158.0 (424.0)	-0.21	0.	-0.16			

and mass flowrate were 0.22 percent and 0.06 percent, respectively, below predicted values. Deviations of the simulated trajectory from the postflight observed trajectory were very small. Maximum variation in velocity and acceleration were 1.6 m/s (5.4 ft/s) and 0.21 m/s<sup>2</sup> (0.69 ft/s<sup>2</sup>).

The observed trajectory data indicate that vehicle velocity at the end of S-II stage burn was 81.7 m/s (268 ft/s) less than the predicted. The three major factors contributing to this velocity loss were a greater than predicted vehicle mass, initial trajectory conditions at S-II ignition and low S-II propulsion performance. The vehicle mass was heavier than predicted due to excess S-IVB stage propellants and an additional amount of GOX on the S-II stage as a result of the LOX step pressurization sequence. The trajectory simulation showed that assumed deviations between actual and predicted propulsion performance during the S-II burn contributed approximately 12.2 to 15.2 m/s (40 to 50 ft/s) to the velocity variation. However, propulsion reconstruction analysis showed only 3 to 5 m/s (10 to 16.5 ft/s) to be due to differences in predicted and actual propulsion performance. In any case, the velocity loss is well within the 3-sigma propulsion tolerance of 22.8 m/s (75 ft/s).

Low frequency oscillations (16-19 hertz) occurred in the engine parameters during the latter portion of powered flight and damped out shortly before cutoff. These oscillations were similar to, but appeared to be somewhat more severe than those observed on AS-503. Initial oscillation in the engine parameters occurred intermittently over several short time



intervals in the center engine LOX pump inlet pressure beginning at 482 seconds (refer to paragraph 6.6.2). These short periods of oscillation were also detected in the center engine crossbeam (at center engine thrust pad) and LOX sump accelerometers at 482 and 487 seconds, respectively. Continuous oscillation buildup at these locations began at approximately 497 seconds and damped out at approximately 531 seconds.

Center engine thrust chamber pressure oscillations began at approximately 500 seconds, peaked at 506 seconds (predominant frequency 16.9 hertz), and damped out at 531 seconds. The peak-to-peak amplitude of chamber pressure oscillations at 506 seconds was about 55.2 N/cm<sup>2</sup> (80 psi), as compared to 41.4 to 48.3 N/cm<sup>2</sup> (60 to 70 psi) maximum peak-to-peak oscillations observed in the center engine chamber pressure on AS-503. During the oscillation period, small amplitude oscillations (16 to 19 hertz) were also evident in the outboard engines chamber pressure measurement. The amplitudes and frequencies of the center engine chamber pressure oscillations are shown in the Vehicle Dynamic Characteristics, Section 9, Figure 9-5.

The LOX NPSP was maintained at a high level during the latter portion of flight by a LOX tank step pressurization sequence. A comparison of LOX NPSP for all S-II flight stages is shown in Figure 6-6. Higher NPSP, as

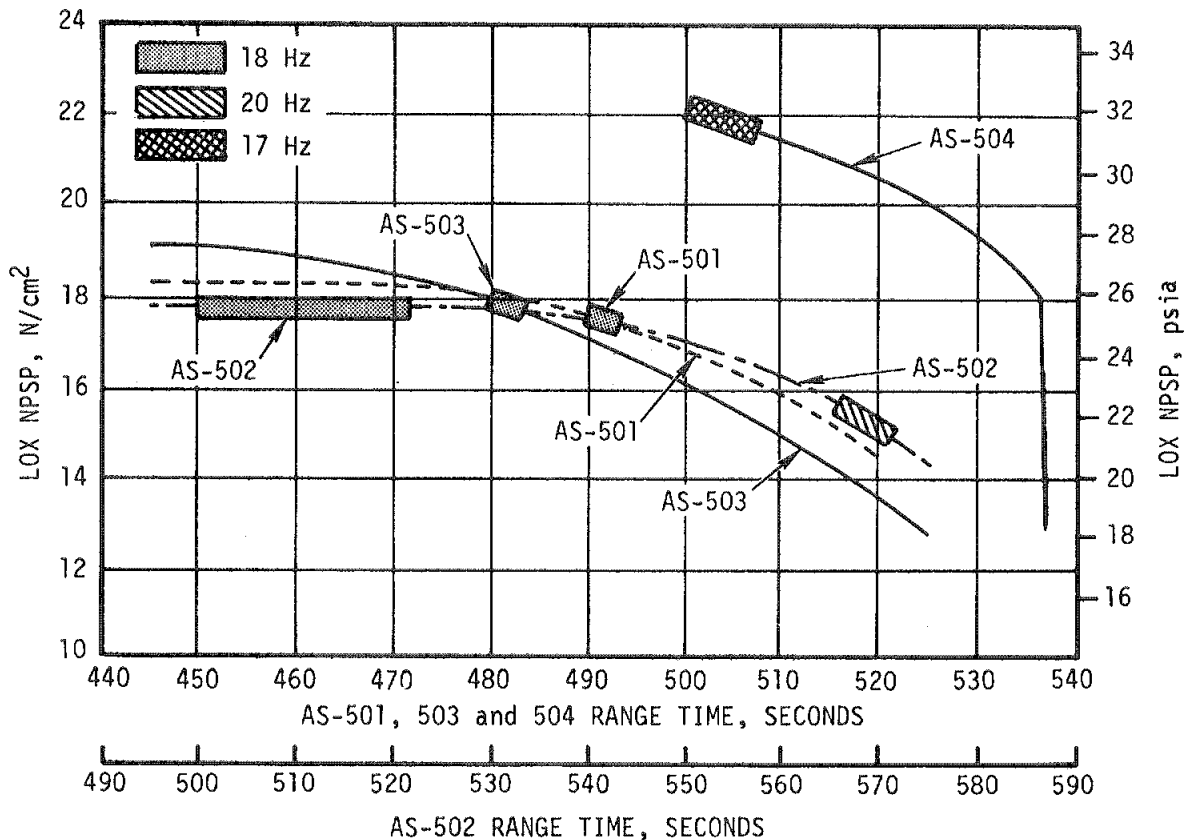


Figure 6-6. S-II LOX NPSP History

provided on AS-504, apparently is not a factor in eliminating the low frequency oscillations. Cause of the low frequency oscillations has not yet been conclusively identified. The problem appears to be associated with inflight LOX liquid levels. Figure 6-7 shows the LOX level history for all S-II flight stages. The LOX tank levels for AS-503 and AS-504 are near the same vehicle station at the onset of oscillation.

Corrective action being planned for AS-505 consists of shutting the center engine off at 299 seconds after Time Base 3 ( $T_3$ ) (NASA Change Order 1643). This time is approximately 40 seconds before the oscillation problem occurred on AS-504.

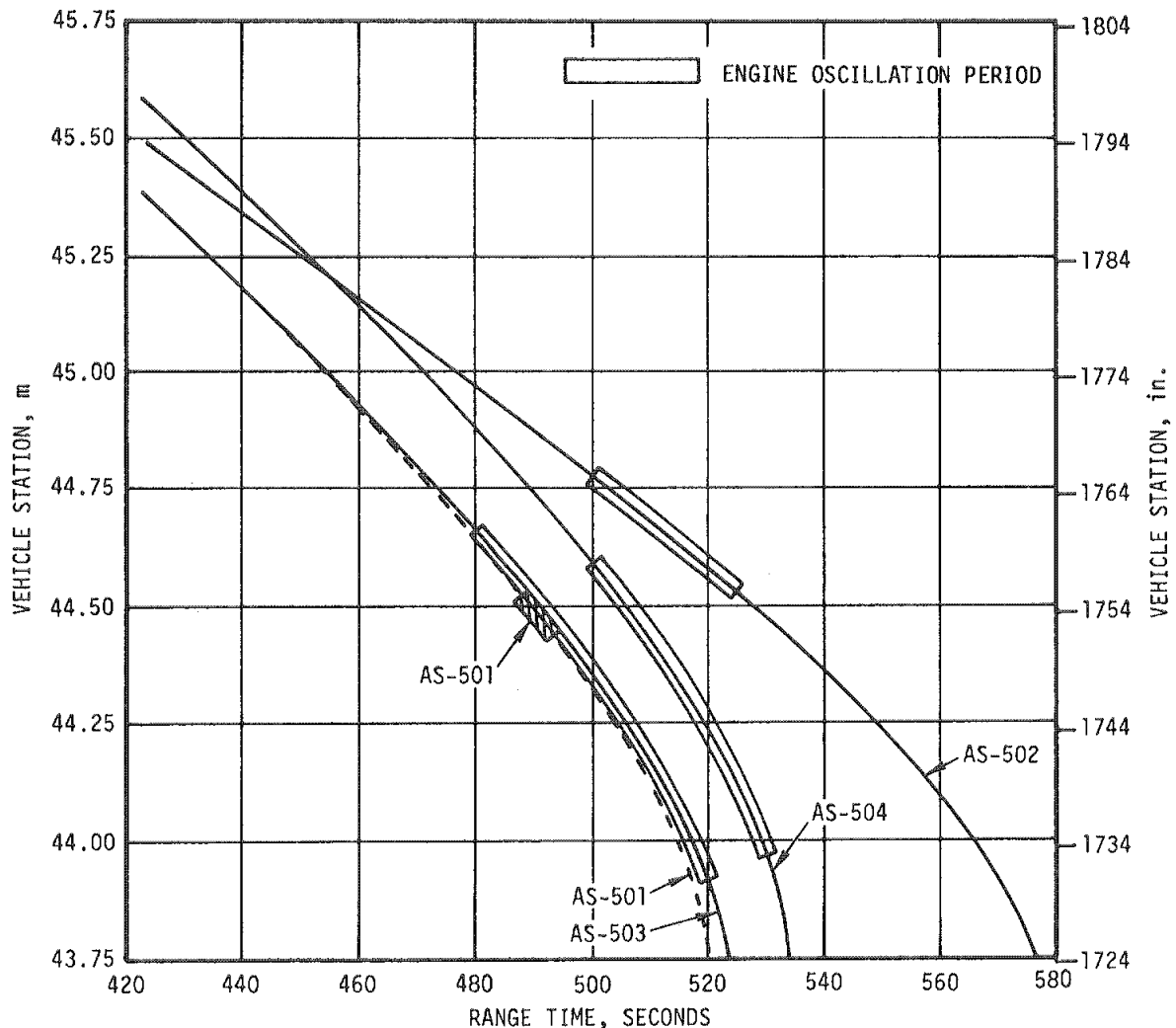


Figure 6-7. S-II Inflight LOX Level History

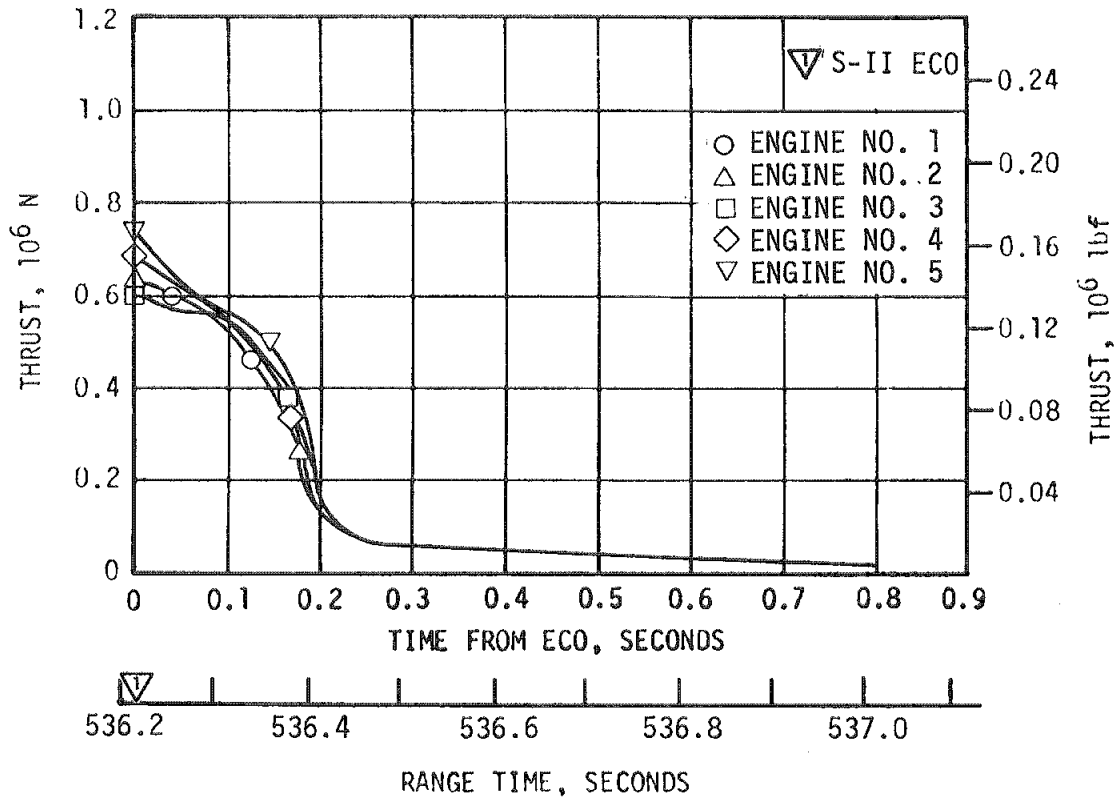


Figure 6-8. S-II Engine Shutdown Transient

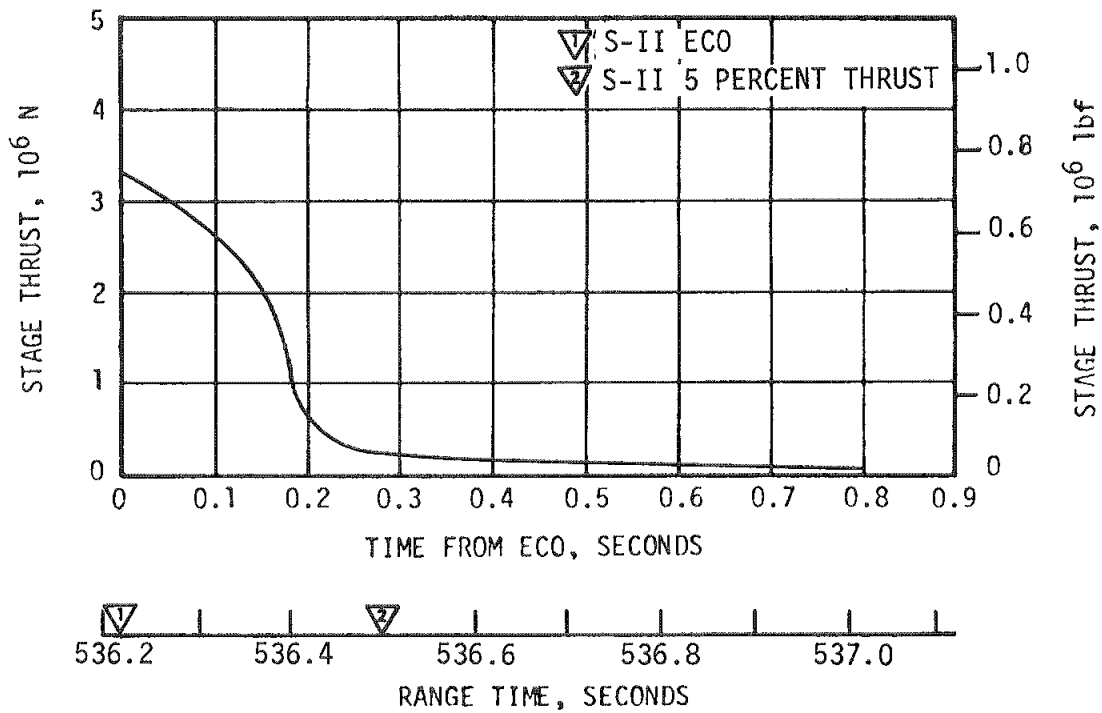


Figure 6-9. S-II Stage Thrust Decay

#### 6.4 S-II SHUTDOWN TRANSIENT PERFORMANCE

Engine shutdown sequence was initiated by the stage LOX low level sensors. This flight was the first to utilize a delay timer which resulted in a 1.5 second delay of ECO after the low level sensor dry indication. At the time of ECO (536.22 seconds) all engines were operating at low mixture ratio.

As in the static testing of the Battleship and S-II-501 stages, the 1.5 second timer resulted in engine performance decay prior to receipt of cutoff signal. Total vehicle thrust, one second before cutoff was approximately 4,161,698 Newtons (935,587 lbf) with a specific impulse of 4195.3 N-s/kg (427.8 lbf-s/lbm). Total vehicle thrust was down to 3,247,202 Newtons (730,000 lbf) at cutoff. Again repeating static test experience, the center engine was first to show effects of LOX depletion. The greatest decrease in performance occurred in engine No. 3.

All engines were cut off by the stage propellant low level sensors system. No engine mainstage pressure switch dropout cutoffs were received. The lowest thrust chamber pressure at the time of cutoff was on engine No. 3 and was  $317 \text{ N/cm}^2$  (460 psia).

Individual engine and stage thrust decay profiles are shown in Figures 6-8 and 6-9, respectively. Due to the performance decay prior to cutoff, the postcutoff decay transient was considerably shortened. The time of 5 percent vehicle thrust occurred 0.28 seconds after ECO as compared to 0.41 seconds for the AS-501 flight. Vehicle cutoff impulse through the 5 percent stage thrust level was estimated to be 460,391 N-s (103,500 lbf-s). Guidance data indicates the total impulse from ECO to S-II/S-IVB separation at 537.2 seconds to be 535,121 N-s (120,300 lbf-s) compared to a predicted value of 840,269 N-s (188,900 lbf-s) for this time period.

#### 6.5 S-II STAGE PROPELLANT MANAGEMENT

The propellant management system performed satisfactorily during the propellant loading operation and properly controlled propellant consumption during flight. The AS-504 stage employed a closed-loop PU system utilizing feedback signals from the tank mass sensing probes rather than fixed, open-loop commands from the Instrument Unit (IU). (Open-loop operation was used on AS-503 and is planned for use on AS-505 and subsequent vehicles).

The facility Propellant Tanking Control System (PTCS) together with the propellant management system successfully accomplished S-II loading and replenishment. During the prelaunch countdown all propellant management subsystems operated properly with no problems noted. Operation of the PU valves during the slew check was normal.

The only anomaly during CDDT was a suspected failure of the LOX overflow liquid level monitoring point sensor. The GSE "revert" interlock for this sensor was removed for the countdown since LOX liquid level could be monitored through the use of other point sensors.

During the AS-503 prelaunch autosequence, the LH<sub>2</sub> fill valve closure command was sent late. Along with a relatively slow fill valve closure time, the closed position was not attained until -34 seconds, just four seconds prior to "ready-for-launch" interlock. Consequently, for AS-504, the fill valve commands were issued at start of autosequence to eliminate this marginal condition. The LH<sub>2</sub> fill valve again closed slower during AS-504 launch (and CDDT) than during stage acceptance testing at MTF. The closing time during launch countdown was 22.1 seconds (23.04 seconds for AS-504 CDDT). This total closing time exceeds the MTF cryogenic acceptance test value of 20 seconds maximum; however, there is no cryogenic closing time requirement at Kennedy Space Center (KSC). A review of the closing time data from both CDDT and launch verifies that there is nothing wrong with the valve itself. It is believed that the differences in closing times from earlier launches and MTF acceptance testing is due to differences in actuation gas temperatures.

The "PU Activate" command was received 5.5 seconds after ESC causing the PU valves to move from the nominal engine start position of 5.0 EMR to the high EMR position, providing a nominal EMR of 5.5 for the first phase of S-II Programmed Mixture Ratio (PMR). The closed-loop PU valve step began at 440 seconds versus the originally planned time of  $429 \pm 20$  seconds. This later than predicted PU valve step was primarily due to errors in predicted engine flows. Actual shift of EMR began at 452.5 seconds. The engines reached an average low EMR of 4.61 at 491 seconds. The PU control system responded as expected during flight and no instabilities were noted. Figure 6-10 gives a comparison of actual versus predicted PU valve position for AS-504 flight. The closed-loop PU error at ECO was approximately -20.9 kilograms (-46 lbm) LH<sub>2</sub> versus a 3-sigma tolerance of  $\pm 665$  kilograms (1465 lbm).

The engine shutdown sequence was initiated by the LOX low level sensors and after a 1.5 second timer delay, ECO occurred at 536.22 seconds. The Launch Vehicle Digital Computer (LVDC) sensed ECO and started T<sub>4</sub> at 536.25 seconds. Burn time was 2.27 seconds longer than expected. Based on point level sensor data, propellant residuals (mass in tanks and sumps) at ECO were 665 kilograms (1466 lbm) LOX, and 1406 kilograms (3099 lbm) LH<sub>2</sub> versus the predicted of 644 kilograms (1420 lbm) LOX, and 1416 kilograms (3120 lbm) LH<sub>2</sub>. Table 6-3 presents a comparison of propellant masses as measured by the PU probes, engine flowmeters and point level sensors. The propellant mass measured by the point level sensors matches more closely the trajectory results.

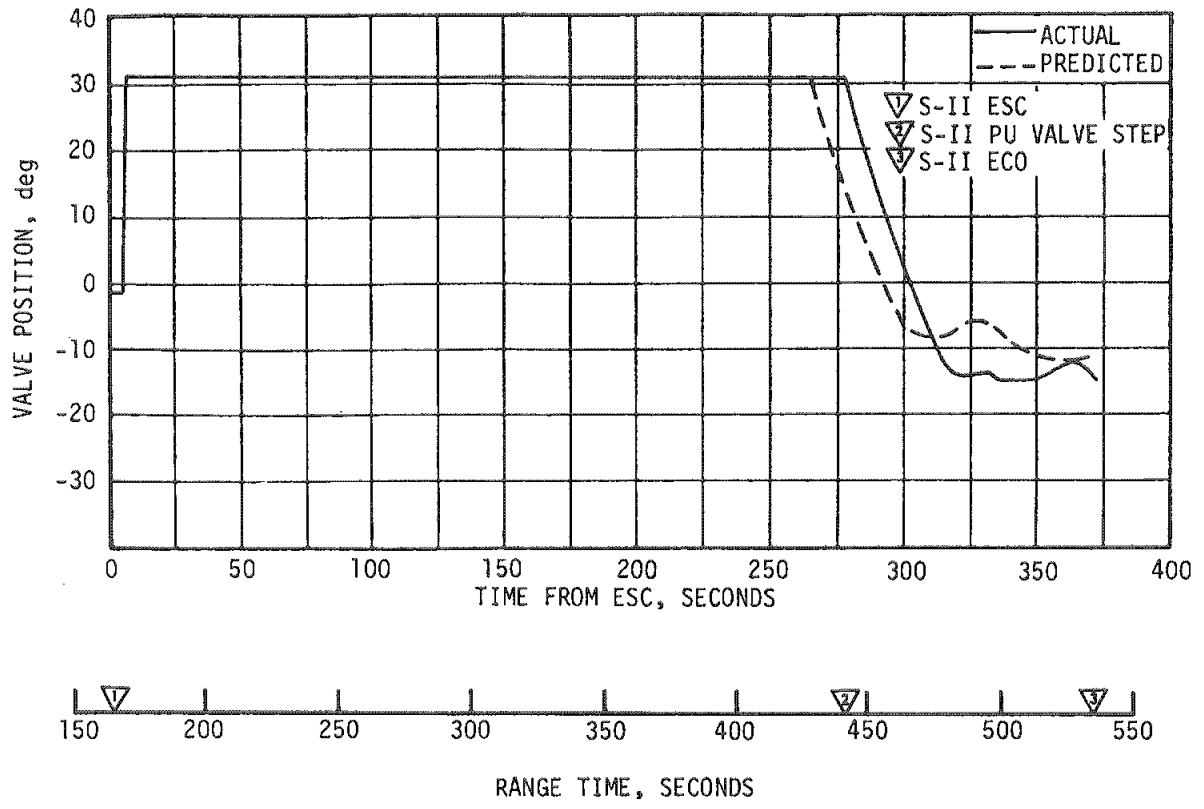


Figure 6-10. S-II PU Valve Position

## 6.6 S-II PRESSURIZATION SYSTEMS

The pressurization system function is to provide the necessary positive pressure on the J-2 engines propellant pumps and to increase the structural capability of the tanks. Prior to launch, the LOX and LH<sub>2</sub> tanks are prepressurized by ground source gaseous helium. During powered flight, the LOX tank is pressurized by GOX from the LOX heat exchangers. The LH<sub>2</sub> tank is pressurized by GH<sub>2</sub> bleed from the thrust chamber hydrogen injector manifold.

### 6.6.1 S-II Fuel Pressurization System

The LH<sub>2</sub> tank vent valves were closed at -94.7 seconds range time and the ullage was pressurized to 24.1 N/cm<sup>2</sup> (35.0 psia) in approximately 25 seconds. The ullage pressure decayed to 21.4 N/cm<sup>2</sup> (31 psia) at 76.9 seconds when the first vent cycle began. One vent cycle occurred on the No. 2 vent valve during the S-IC boost phase. The No. 1 vent valve did not open. Vent valve No. 2 reseal occurred at 97.9 seconds at a pressure

Table 6-3. S-II Propellant Mass History

EVENT RANGE TIME	UNITS	PREDICTED		POINT SENSOR ANALYSIS (BEST ESTIMATE)		PU SYSTEM ANALYSIS		ENGINE FLOWMETER INTEGRATION	
		LOX	LH2	LOX	LH2	LOX	LH2	LOX	LH2
Ground Ignition	kg (lbm)	371,452 (818,911)	71,668 (158,000)	371,891 (819,879)	71,854 (158,412)	371,430 (818,862)	71,585 (157,818)	370,795 (817,462)	71,379 (157,363)
S-II Ignition 165.17 sec	kg (lbm)	371,452 (818,911)	71,659 (157,981)	371,891 (819,879)	71,854 (158,412)	371,179 (818,309)	71,683 (158,033)	370,795 (817,462)	71,379 (157,363)
S-II PU Valve Step 440 sec	kg (lbm)	95,474 (210,485)	20,950 (46,187)	85,199 (187,832)	19,122 (42,156)	86,427 (190,539)	19,149 (42,217)	84,986 (187,361)	18,403 (40,572)
S-II ECO 536.22 sec	kg (lbm)	644 (1420)	1416 (3120)	665 (1466)	1406 (3099)	1016 (2240)	1390 (3064)	665 (1466)	1406 (3099)
S-II Residual After Thrust Decay	kg (lbm)	486 (1071)	1350 (2977)	550 (1213)	1344 (2963)	901 (1987)	1328 (2928)	550 (1213)	1344 (2963)

NOTE: Propellant mass in tanks and sump only. Propellant trapped external to tanks and LOX sump is not included

of 19.8 N/cm<sup>2</sup> (28.7 psia). The differential pressure across the vent valve at this time was 19.4 N/cm<sup>2</sup> (28.2 psid). LH<sub>2</sub> ullage pressure decreased to 19.3 N/cm<sup>2</sup> (28 psia) at S-II ESC. The differential pressure across the vent valve at this time was also 19.3 N/cm<sup>2</sup> (28 psid). Figure 6-11 presents the actual fuel tank ullage pressure for AS-504 compared to predicted values from prepressurization until ECO. During S-II boost the LH<sub>2</sub> tank vent valves were in the low pressure vent mode controlling ullage pressure between 19 to 20.3 N/cm<sup>2</sup> (27.5 to 29.5 psid) referenced to the vent valve sense line, and 1.3 seconds prior to ESC the LH<sub>2</sub> tank vent valves were switched to the high pressure vent mode, limiting the maximum ullage pressure to 22.8 N/cm<sup>2</sup> (33 psid).

LH<sub>2</sub> tank ullage pressure was maintained within the regulator range of 19.7 to 20.7 N/cm<sup>2</sup> (28.5 to 30 psia) during S-II boost until the LH<sub>2</sub> tank pressure regulator was stepped open at 462.8 seconds range time. Ullage pressure increased to 21.6 N/cm<sup>2</sup> (31.4 psia). The LH<sub>2</sub> vent valves started venting at 485 seconds and continued venting throughout the remainder of the S-II flight closing at 537.7 seconds.

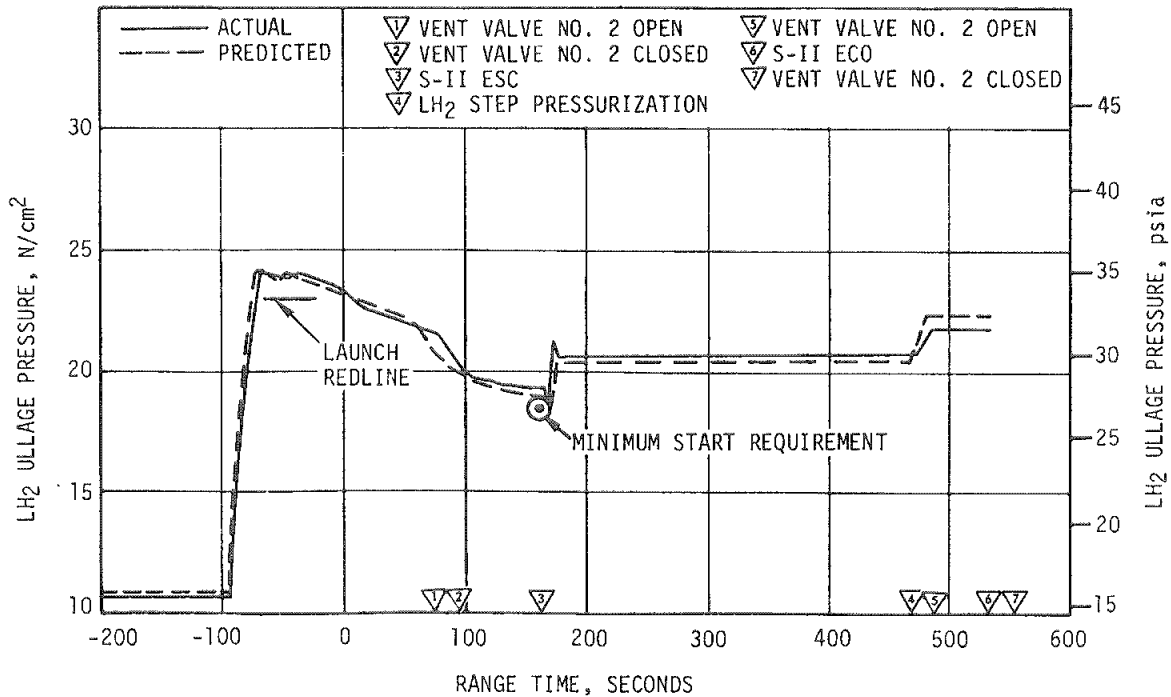


Figure 6-11. S-II Fuel Tank Ullage Pressure

Figure 6-12 shows LH<sub>2</sub> inlet total pressure, temperature and NPSP compared to prediction. The NPSP supplied exceeded the NPSP required throughout the S-II boost phase of the flight, and parameters were close to predicted values.

The LH<sub>2</sub> inlet pressures of engines No. 1 and 5 during the low frequency oscillation period are shown in Figures 6-13 and 6-14, respectively. Center engine LH<sub>2</sub> pump inlet pressure began oscillating at approximately 503 seconds, peaked at 507 seconds (frequency 16.7 hertz), and damped out at about 522 seconds. Engine No. 1 LH<sub>2</sub> pump inlet pressure shows only slight evidence of oscillation.

#### 6.6.2 S-II LOX Pressurization System

After a two-minute cold helium chilldown flow through the LOX tank, the vent valves were closed at -185.4 seconds and the LOX tank ullage was prepressurized to 26.9 N/cm<sup>2</sup> (39 psia) in approximately 50 seconds. One makeup pressure cycle was required after which the pressure remained approximately constant at 26.9 N/cm<sup>2</sup> (39 psia) until engine start. Figure 6-15 presents the LOX tank ullage pressure for AS-504 as compared to predicted from prepressurization until ECO.



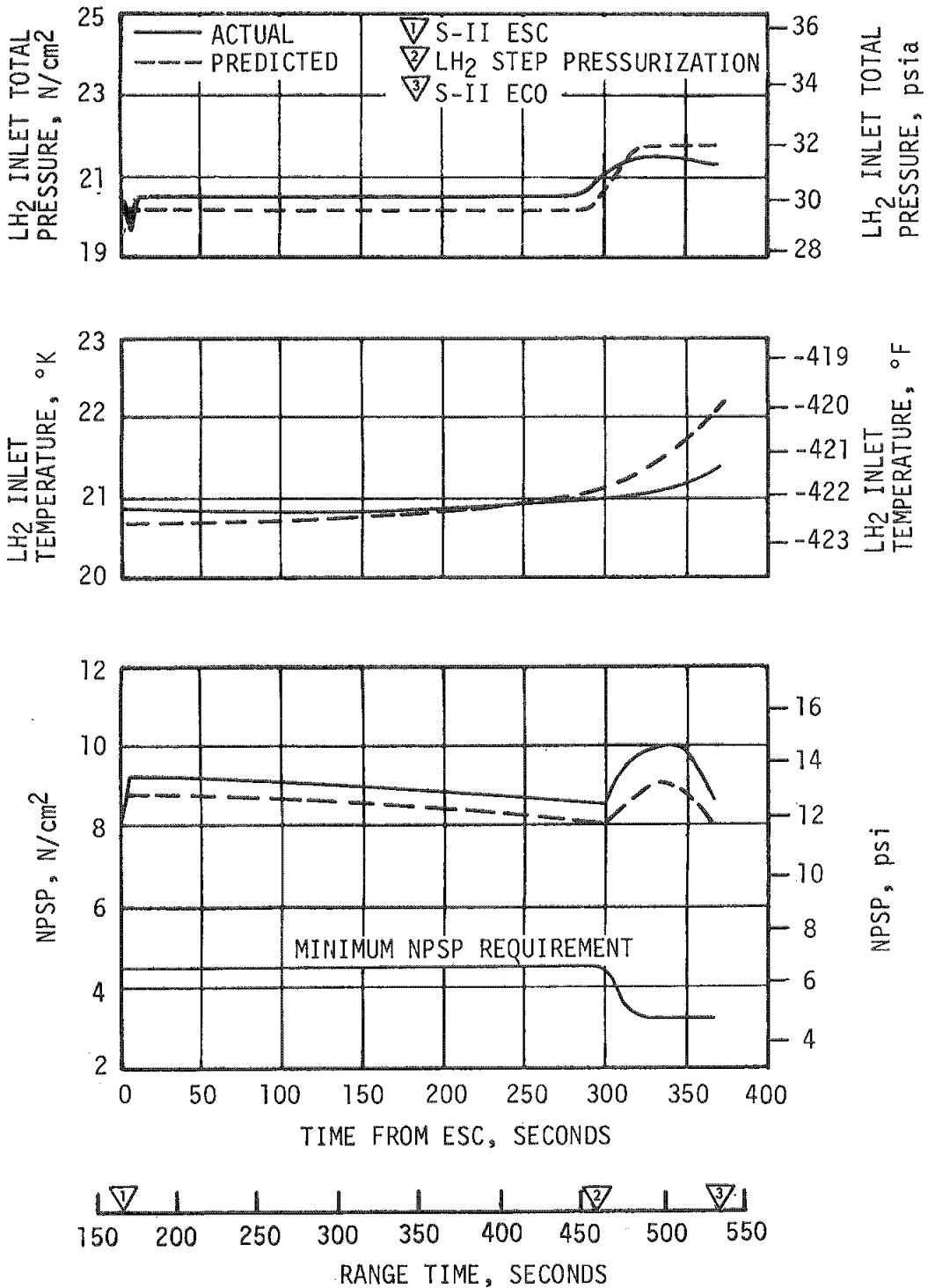


Figure 6-12. S-II Fuel Pump Inlet Conditions

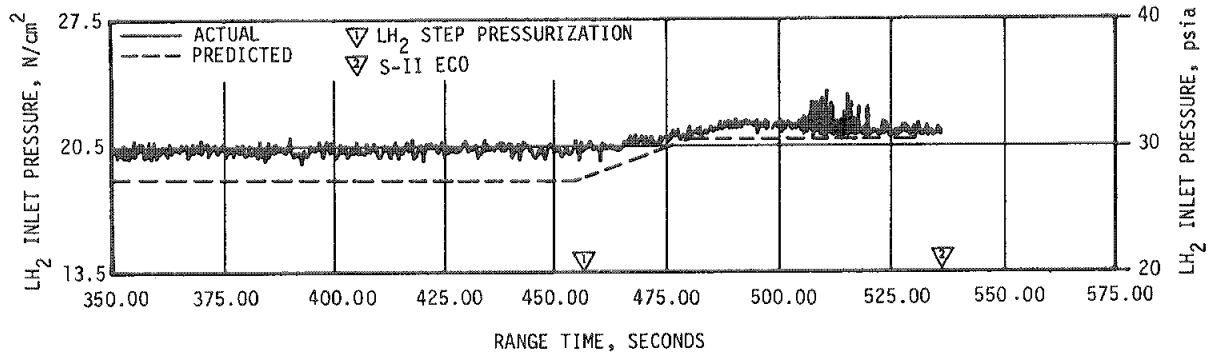


Figure 6-13. S-II Engine No. 1 LH2 Inlet Pressure

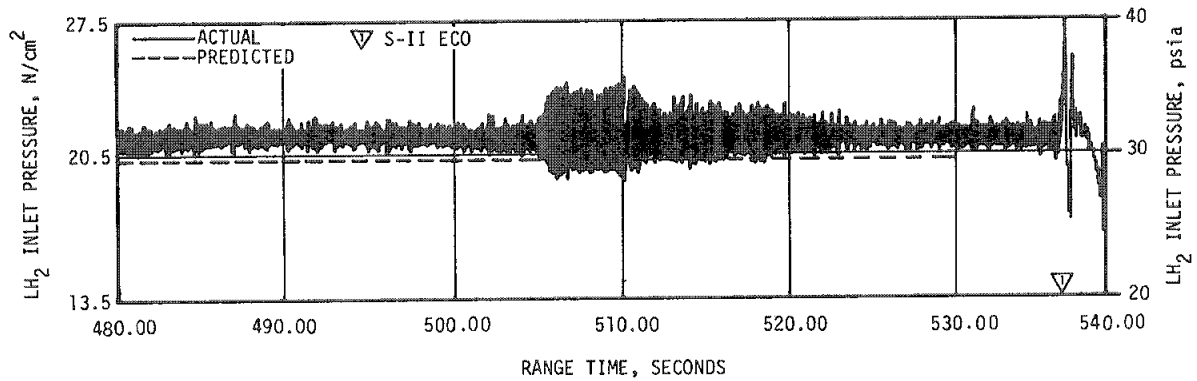


Figure 6-14. S-II Engine No. 5 LH2 Inlet Pressure

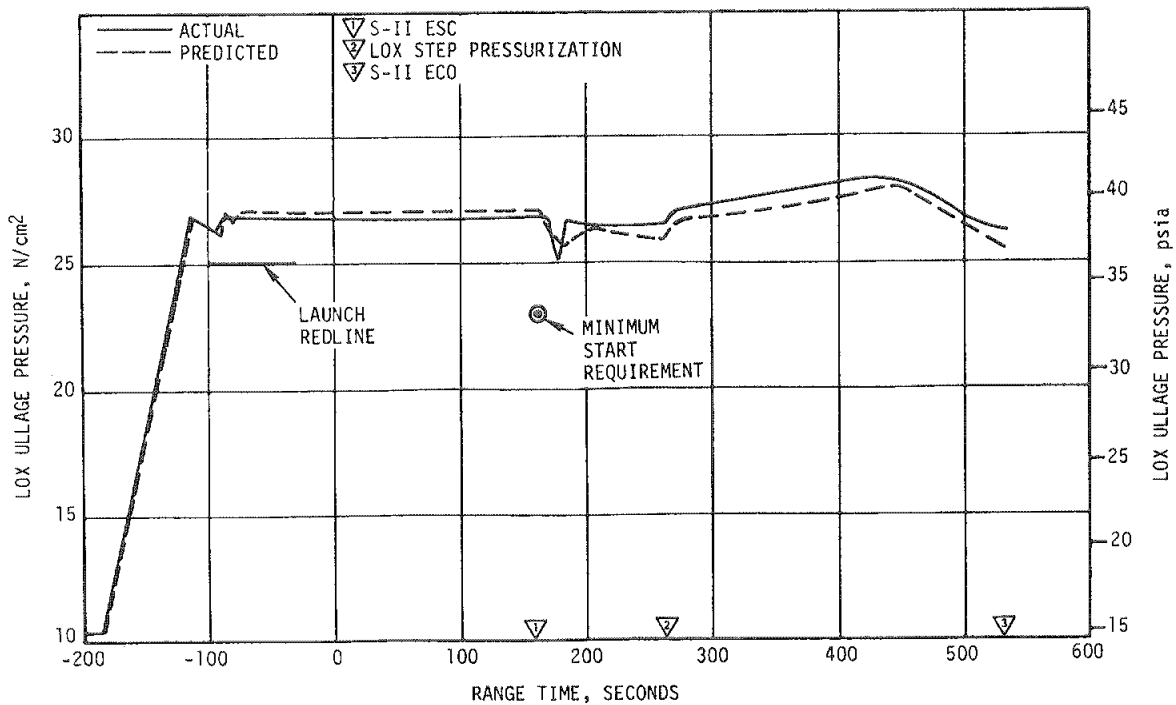


Figure 6-15. S-II LOX Tank Ullage Pressure

With the exception of the characteristic pressure slump associated with the engine start, the ullage pressure remained within the regulator range of 24.8 to 25.9 N/cm<sup>2</sup> (36 to 37.5 psia) during burn until the LOX regulator step open command was initiated. The LOX tank regulator stepped full open at 262.8 seconds. Tank pressure rose to 28.5 N/cm<sup>2</sup> (41.4 psia) maximum. The vent valve cracking range of 27.6 to 29 N/cm<sup>2</sup> (40 to 42 psia) was reached but not exceeded. No venting of the LOX tank occurred. After EMR shift, the ullage pressure began a slight decay and reached 25.5 N/cm<sup>2</sup> (37 psia) at ECO.

Figure 6-16 shows LOX pump inlet total pressure, temperature and NPSP. The NPSP supplied exceeded NPSP requirements throughout the S-II boost phase of the flight. As shown in LOX inlet temperature, the total magnitude of LOX liquid stratification did not exceed the prediction as it did on AS-503. In addition, the abruptness of the temperature rise near cutoff indicates less liquid disturbance than experienced on AS-503.

The LOX inlet pressures of engines No. 1 and 5 during the low frequency oscillation period are shown in Figures 6-17 and 6-18, respectively. Center engine LOX pump inlet pressure oscillations reached peak amplitude at approximately 504 seconds (frequency 17.2 hertz), and damped out at about 531 seconds. The LOX inlet pressure rose approximately 0.69 N/cm<sup>2</sup> (1 psi) then decreased approximately 6.2 N/cm<sup>2</sup> (9 psi) after the oscillations started as compared to a relatively constant engine No. 1 inlet pressure. This phenomenon also occurred during the AS-503 flight. The oscillations in LOX inlet pressure of the outboard engines started at approximately 505 seconds. Oscillations are indicated by the engine No. 1 gimbal pad accelerometer at about the same time.

The engine contractor has performed J-2 engine pump tests with pressure oscillations induced. A drop in LOX inlet pressure similar to that shown in Figure 6-18 was also observed on these tests at a transducer tap location similar to that used on the S-II stage center engine feed line. Measurements made further upstream, however, showed the pressure oscillations without the shift in level, indicating that the problem is associated with tap location not actual line pressure deviation.

#### 6.7 S-II PNEUMATIC CONTROL PRESSURE SYSTEM

Performance of the pneumatic control pressure system was satisfactory. Figure 6-19 shows main receiver pressure and regulator outlet pressure of the system from before liftoff until ECO. The regulator outlet pressure was 483 N/cm<sup>2</sup> (700 psia) except during valve actuations. The main receiver pressure was well above the predicted minimum allowable limits.

Pressure decay in the main receiver from initial pressurization at -30 seconds to initial valve actuation at 162.3 seconds was negligible. Pressure decreased from 2110 N/cm<sup>2</sup> (3060 psia) to 2093 N/cm<sup>2</sup> (3035 psia) during

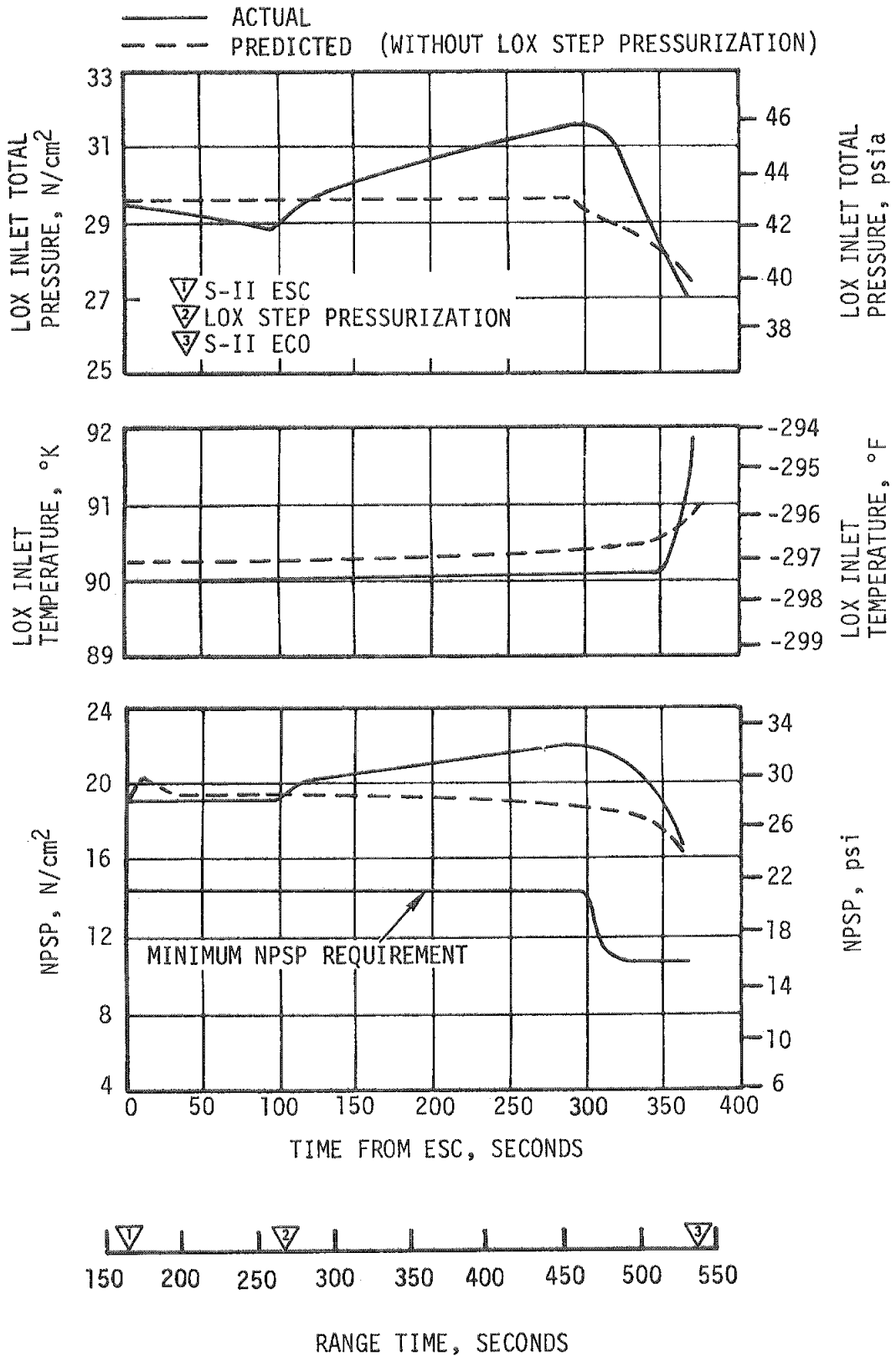


Figure 6-16. S-II LOX Pump Inlet Conditions

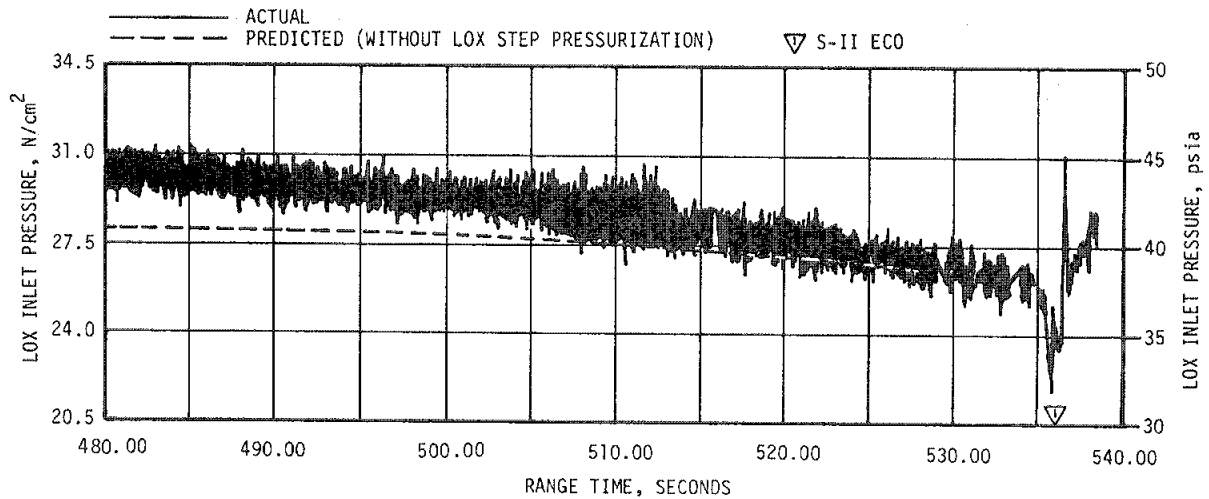


Figure 6-17. S-II Engine No. 1 LOX Inlet Pressure

this period. Receiver pressure decreased to 1999 N/cm<sup>2</sup> (2900 psia) after actuation of the recirculation system valves which were closed at 162.3 seconds. Pressure drop at engine cutoff was somewhat higher than seen previously on AS-503. This was expected since the new prevalues, used for the first time on AS-504, have a larger actuator volume than the original prevalues. System receiver pressure decay was less than on AS-503, which indicates the new valves have less piston leakage than those previously used.

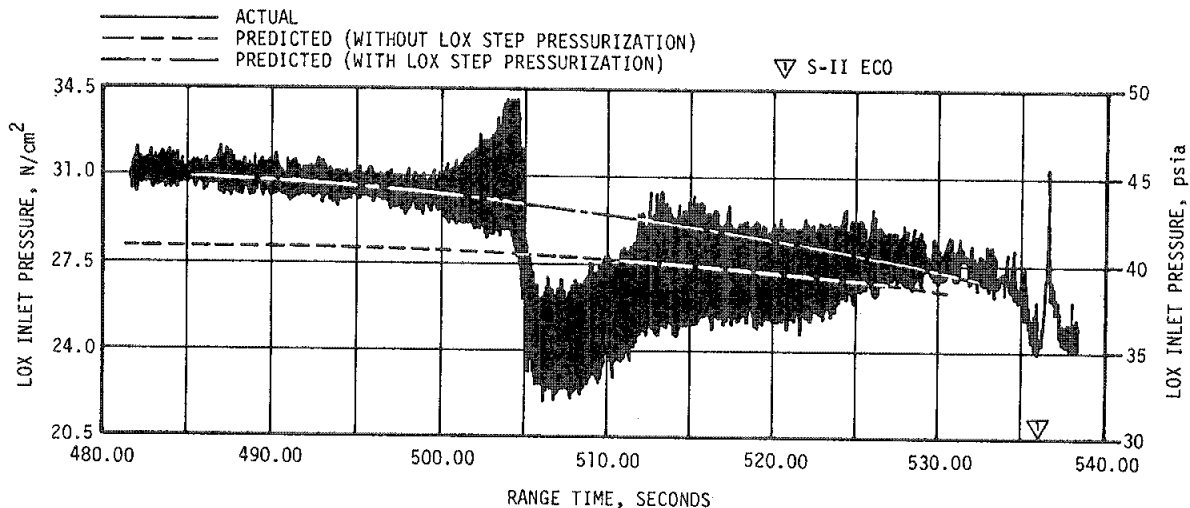


Figure 6-18. S-II Engine No. 5 LOX Inlet Pressure

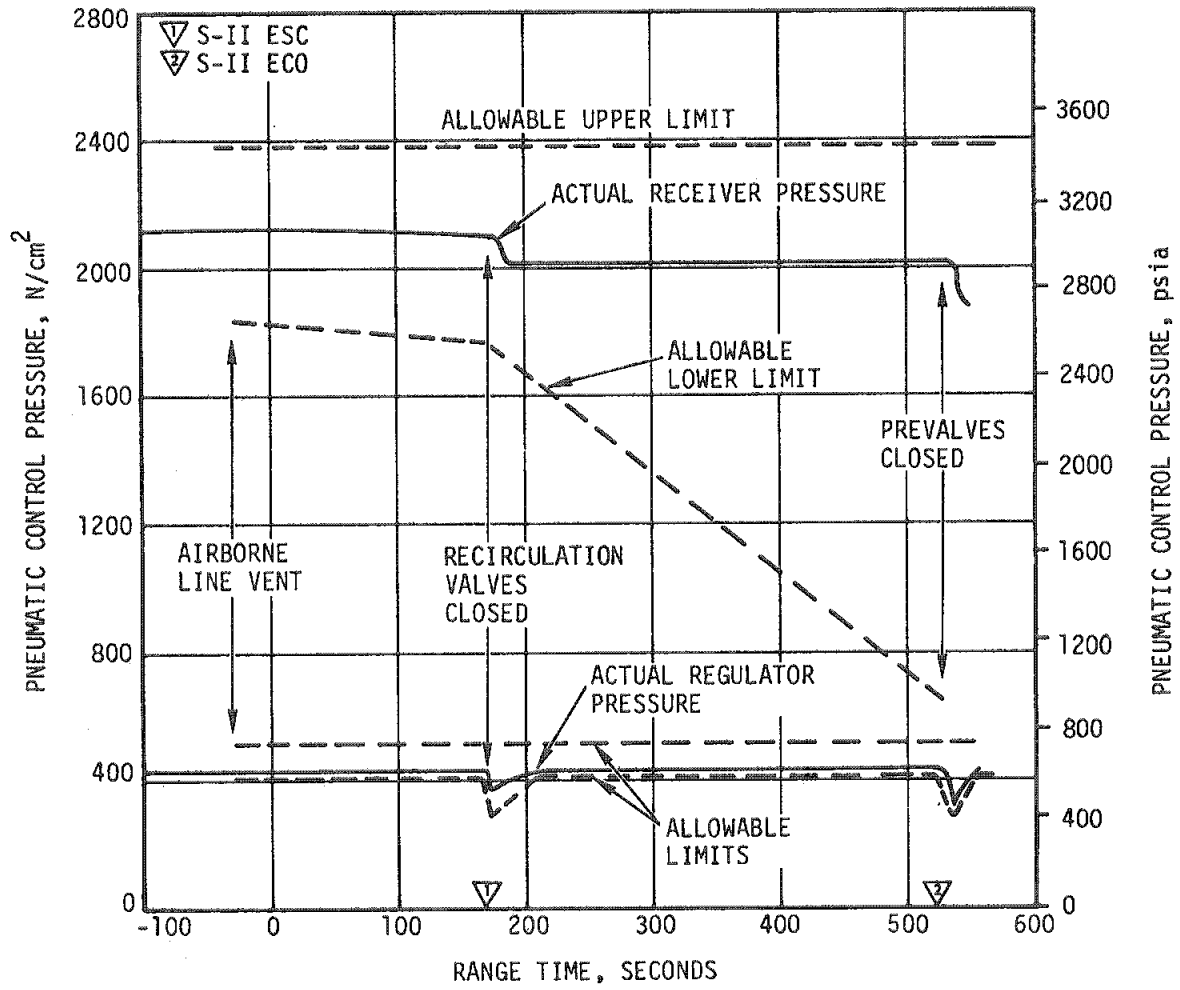


Figure 6-19. S-II Pneumatic Control Pressures

### 6.8 S-II HELIUM INJECTION SYSTEM

The inflight helium injection system supplements natural convection recirculation in the LOX recirculation lines. This system injects helium into the bottom of the return lines to decrease the return line fluid density thereby increasing the recirculation driving force.

The performance of the helium injection system was satisfactory. Requirements were met and parameters were in good agreement with predictions. The supply bottle was pressurized to 2137 N/cm<sup>2</sup> (3100 psia) prior to liftoff and by ESC was 545 N/cm<sup>2</sup> (790 psia). Helium injection system average total flowrate during supply bottle blowdown (-30 seconds to 1.3 seconds prior to ESC) was 1.93 SCMM (68 SCFM).

## SECTION 7

### S-IVB PROPULSION

#### 7.1 SUMMARY

The J-2 engine operated satisfactorily throughout the operational phase of first and second burns with normal engine shutdowns. Operation of the J-2 engine during third burn was anomalous, as a result of the experimental nature of the preplanned "out-of-specification" engine restart. As a result of the third burn anomaly, the planned propellant dump through the engine was not successful.

The engine performance during first burn, as determined from standard altitude reconstruction analysis, deviated from the predicted Start Tank Discharge Valve (STDV) + 60-second time slice by +0.764 percent for thrust and -0.117 percent for specific impulse. The first burn duration was 123.84 seconds from STDV open command. This time was 10.27 seconds longer than predicted due to the performance of the lower stages and to S-IVB total weight variation.

The Continuous Vent System (CVS) adequately regulated LH<sub>2</sub> tank ullage pressure between 13.1 and 13.5 N/cm<sup>2</sup> (19.0 and 19.6 psia) during parking orbit, and the Oxygen/Hydrogen (O<sub>2</sub>/H<sub>2</sub>) burner satisfactorily achieved LH<sub>2</sub> tank repressurization for restart. Repressurization of the LOX tank was not required.

The engine first restart conditions were within limits. The restart at full open Propellant Utilization (PU) valve position was successful and there were no indications of overtemperature conditions in the Gas Generator (GG). S-IVB second burntime was 62.06 seconds from STDV open command and cutoff was by timer. The engine performance during second burn, as determined from the standard altitude reconstruction analysis, although well within specifications, deviated from the predicted STDV + 60-second time slice by -0.587 percent for thrust and -0.182 percent for specific impulse.

The CVS regulated the LH<sub>2</sub> tank ullage pressure between 13.1 and 13.5 N/cm<sup>2</sup> (19.0 and 19.6 psia) during intermediate coast. The O<sub>2</sub>/H<sub>2</sub> burner was successfully restarted before third burn. The LH<sub>2</sub> tank was satisfactorily repressurized for third burn by the ambient repressurization system. Repressurization of the LOX tank was not required.

Engine conditions for the second restart were unusual as a result of the extended fuel lead experiment. This was a planned experiment to evaluate the mission rule concerning failure of both LOX and LH<sub>2</sub> chilldown systems.

The restart at full open PU valve position was successful. However, the chamber pressure did indicate abnormal conditions during the start transient. Mainstage performance was not as predicted due to various anomalies which occurred during the burn. Third burn had a timed cutoff which occurred as expected at STDV +242.06 seconds.

Subsequent to third burn, the start bottle was safed satisfactorily. However, propellant dump did not occur as planned due to the third burn anomaly. The stage propellant tanks were satisfactorily safed by latching open the vent valves. The stage ambient and cold helium spheres were adequately safed as planned.

The stage pneumatic control system performed adequately during the mission. During the early stages of launch countdown the regulator discharge pressure was high and was controlled by the backup system. Prior to liftoff, control was resumed by the regulator. Subsequently, the regulator pressure was high during boost and coast phase, however, there were no adverse effects on system components or functioning.

The Auxiliary Propulsion System (APS) pressurization system developed a helium leak in Module No. 2 at 4 hours and 25 minutes which ceased at 7 hours. However, the ullage pressures in the APS were acceptable throughout the mission.

## 7.2 S-IVB CHILLDOWN AND BUILDUP TRANSIENT PERFORMANCE FOR FIRST BURN

The propellant recirculation systems performed satisfactorily, meeting start box requirements for fuel and LOX as shown in Figure 7-1.

The main fuel injector temperature (alternate for thrust chamber jacket temperature) at launch was well below the maximum allowable redline limit of 188.9°K (-120°F). At S-IVB first burn Engine Start Command (ESC), the temperature was 200°K (-100°F), which is within the requirement of  $211 \pm 27.5^\circ\text{K}$  ( $-79.9 \pm 49.5^\circ\text{F}$ ) as shown in Figure 7-2. The chilldown and loading of the engine Gaseous Hydrogen (GH<sub>2</sub>) start sphere and pneumatic control sphere prior to liftoff was satisfactory. Figure 7-3 shows the start tank performance for first burn. At first ESC the start tank conditions were within the required S-IVB region of  $896.3 \pm 68.9 \text{ N/cm}^2$  and  $133.2 \pm 44.4^\circ\text{K}$  ( $1300 \pm 100 \text{ psia}$  and  $-220 \pm 80^\circ\text{F}$ ) for initial start. The discharge was completed and the refill initiated at first burn ESC +3.95 seconds. The refill was satisfactory and in good agreement with the acceptance test.

As a result of the J-2 engine control helium sphere's pneumatic connection with the stage LOX and LH<sub>2</sub> ambient helium repressurization spheres, there was a replenishing of the engine control sphere in flight. The



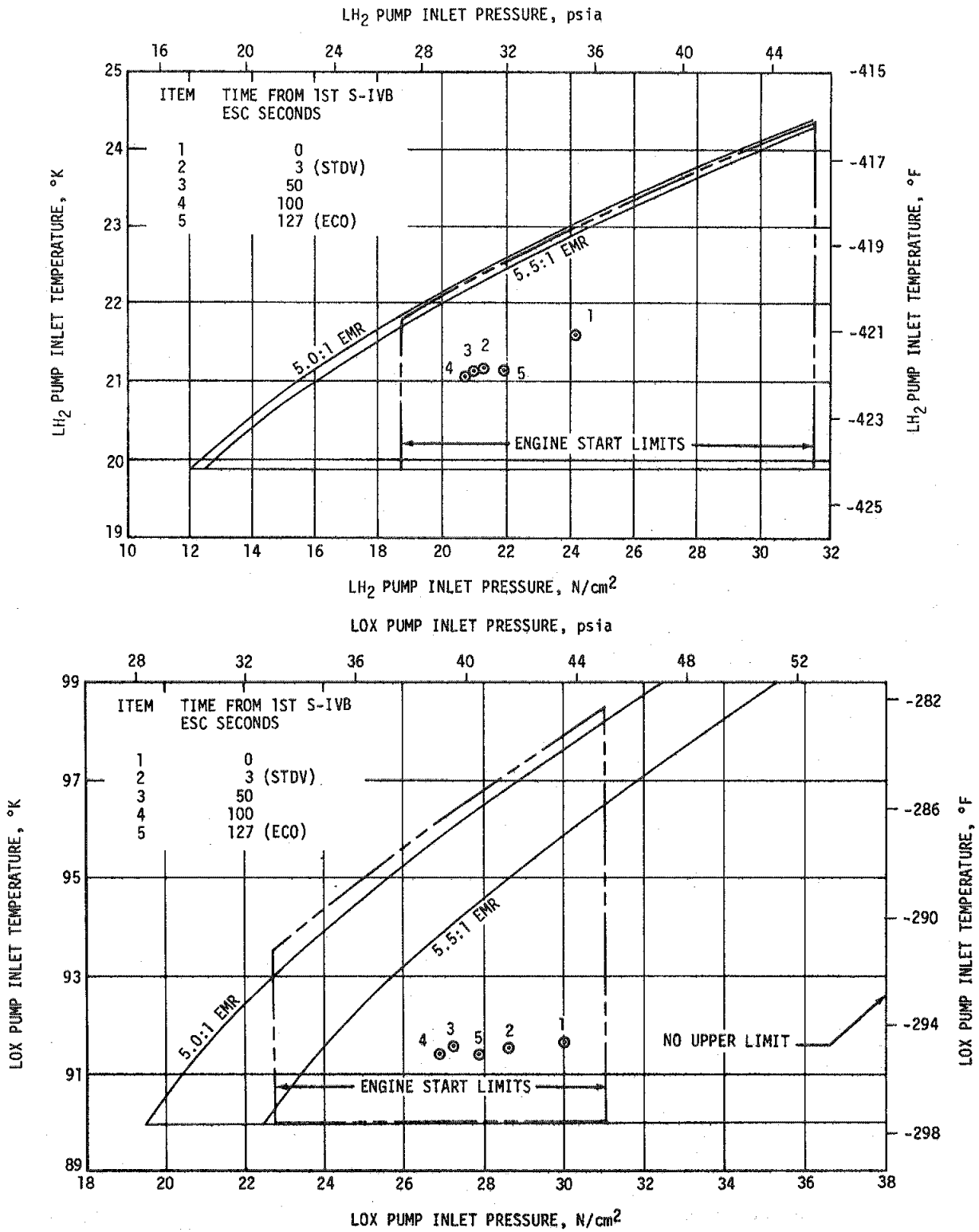


Figure 7-1. S-IVB Start Box and Run Requirements - First Burn

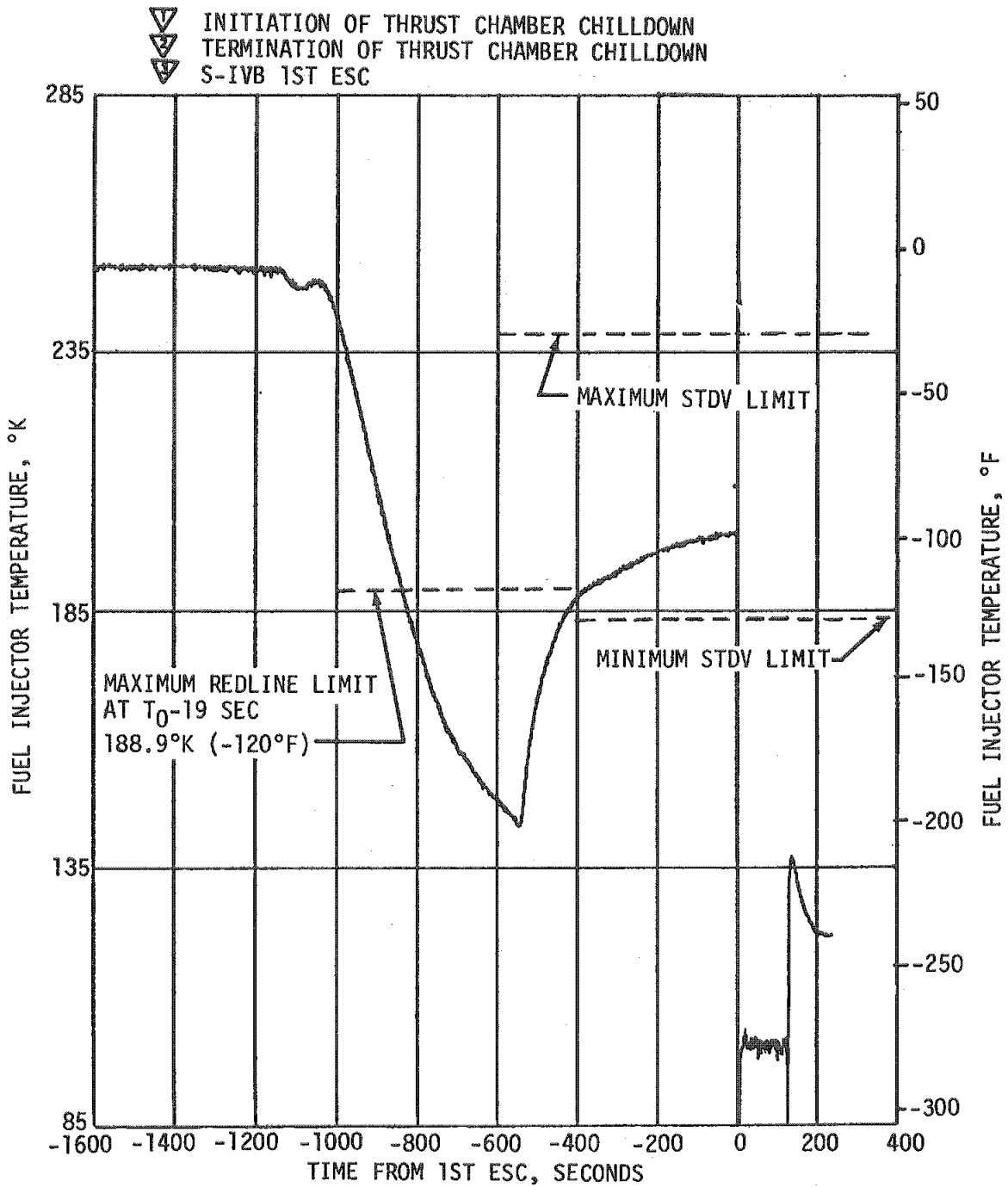


Figure 7-2. S-IVB Fuel Injector Temperature - First Burn

engine control bottle pressure and start sphere temperature at liftoff were  $2205 \text{ N/cm}^2$  ( $3200 \text{ psia}$ ) and  $152^\circ\text{K}$  ( $-186^\circ\text{F}$ ), respectively. LOX and LH<sub>2</sub> system chilldowns, which were continuous from before liftoff until just prior to S-IVB first burn ESC, were satisfactory. At ESC the LOX pump inlet temperature was  $91.7^\circ\text{K}$  ( $-294.8^\circ\text{F}$ ) and the LH<sub>2</sub> pump inlet temperature was  $21.6^\circ\text{K}$  ( $-421^\circ\text{F}$ ).

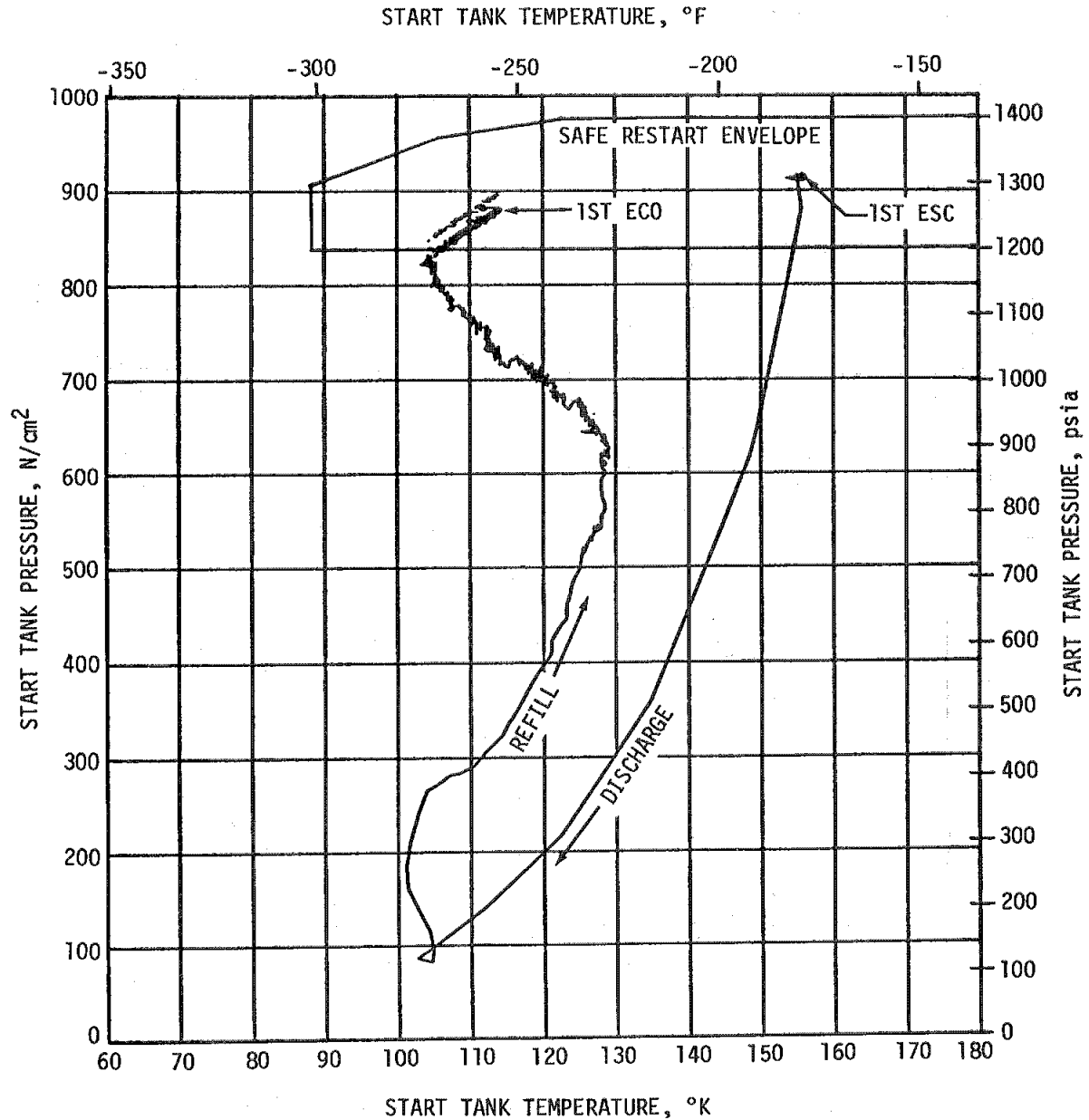


Figure 7-3. S-IVB Start Tank Performance - First Burn

The first burn start transient was satisfactory. The thrust buildup was satisfactory and well within the limits set by the engine manufacturer as shown in Figure 7-4.

Table 7-1 shows the major sequence of events during the buildup transient. The PU valve was in proper null position prior to first start. The total impulse from STDV to STDV +2.5 seconds was 1,087,545 N-s (244,490 lbf-s) for first start. This was greater than the value of 1,018,029 N-s (228,862 lbf-s) obtained during the same interval for the acceptance test.

First burn fuel lead generally followed the predicted pattern and resulted in satisfactory conditions as indicated by the thrust chamber temperatures and the associated fuel injector temperatures.

### 7.3 S-IVB MAIN STAGE PERFORMANCE FOR FIRST BURN

Two analytical techniques were employed in evaluating S-IVB stage propulsion system performance. The primary method, propulsion reconstruction analysis, utilized telemetered engine and stage data to compute longitudinal thrust, specific impulse, and stage mass flowrate. In the second method, flight simulation, a five-degree-of-freedom trajectory simulation was utilized to fit propulsion reconstruction analysis results to the trajectory. Using a differential correction procedure, this simulation determined adjustments to the reconstruction analysis of thrust and mass flow histories to yield a simulated trajectory which closely matched the observed postflight trajectory.

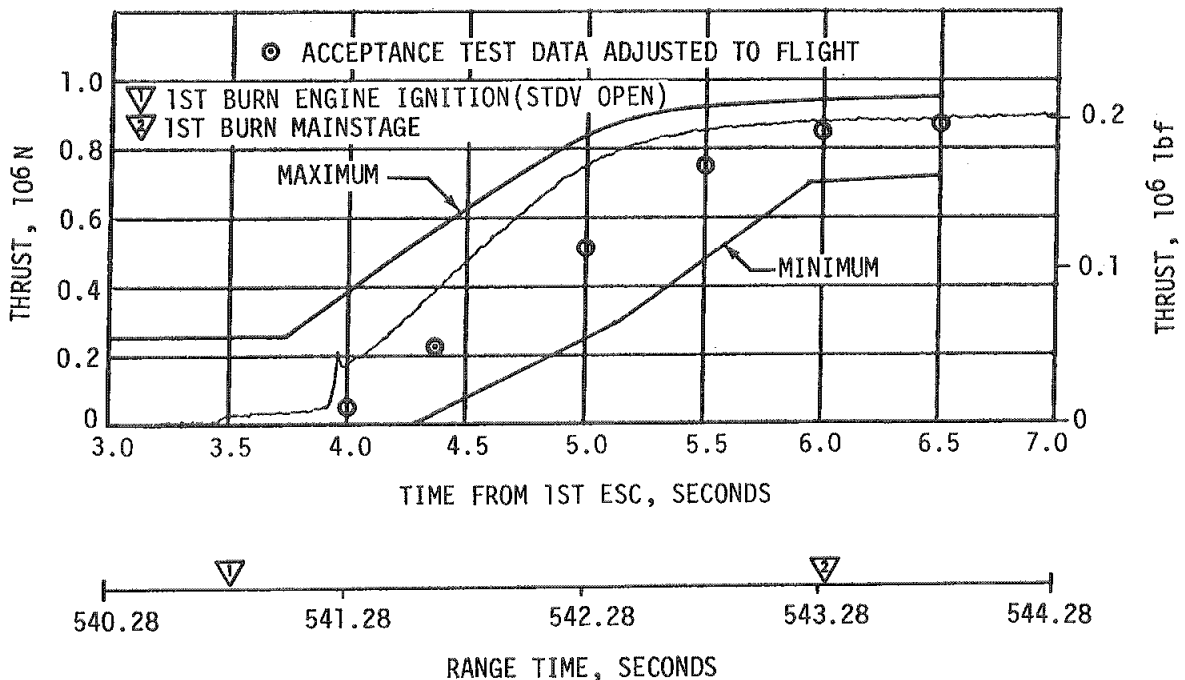


Figure 7-4. S-IVB Buildup Transient - First Burn

Table 7-1. S-IVB Engine Start Sequence Events - First Burn

EVENT	TIME OF EVENT IN RANGE TIME (SECONDS)	
	PREDICTED	ACTUAL
S-IVB Engine Start Indication	532.2	537.28
S-IVB STDV Open Indication	535.16	540.82
S-IVB Thrust OK Signal-Switch 1 (on)	537.86	541.97
S-IVB Thrust OK Signal-Switch 2 (on)	537.86	542.01
S-IVB Engine Cutoff at the J-2 Engine	648.73	664.66
S-IVB Thrust OK Signal Dropout Switch 1 (off)	651.34	664.68
S-IVB Thrust OK Signal Dropout Switch 2 (off)	651.34	664.92

The propulsion reconstruction analysis showed that the stage performance during mainstage operation was satisfactory. A comparison of predicted and actual performance of thrust, total flowrate, specific impulse, and mixture ratio versus time is shown in Figure 7-5. Table 7-2 shows the specific impulse, flowrates and mixture ratio deviations from the predicted STDV + 60-second time slice. This time slice performance is the standardized altitude performance which is comparable to engine acceptance tests. The 60-second time slice performance disagreed with the predicted by 0.764 percent in thrust. Specific impulse performance for first burn disagreed with predicted by -0.117 percent.

The overall propulsion reconstruction of longitudinal thrust differed from the predicted by 0.509 percent. Longitudinal specific impulse for first burn was 0.28 percent less than predicted.

The flight simulation analysis showed an increase of 0.012 percent, compared to the prediction, in specific impulse. Other comparisons are shown in Table 7-3.

The S-IVB burn time was 10.27 seconds longer than predicted. Table 7-4 shows that the primary contributors to the long burn time were deviations in the preconditions of flight.

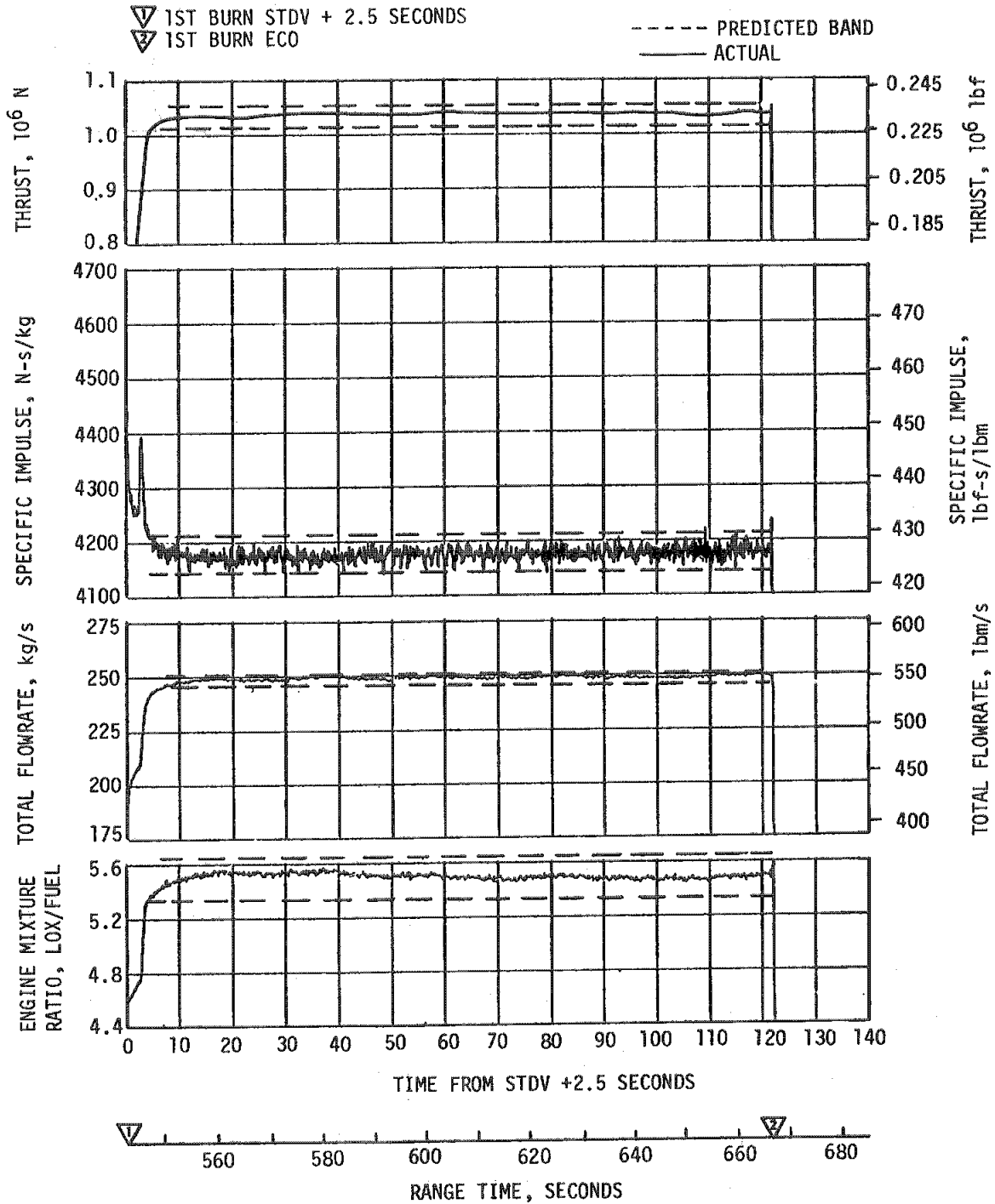


Figure 7-5. S-IVB Steady State Performance - First Burn

Table 7-2. S-IVB Steady State Performance - First Burn  
(STDV +60-Second Time Slice at Standard Altitude Conditions)

PARAMETER	PREDICTED	RECONSTRUCTION	FLIGHT DEVIATION	PERCENT DEVIATION FROM PREDICTED
Thrust N (lbf)	1,025,782 (230,605)	1,033,615 (232,366)	7833 (1761)	0.764
Specific Impulse N-s/kg (lbf-s/lbm)	4178.6 (426.1)	4173.7 (425.60)	-4.9 (-0.5)	-0.117
LOX Flowrate (kg/s (lbm/s)	207.35 (457.14)	209.45 (461.76)	2.10 (4.62)	1.01
Fuel Flowrate kg/s (lbm/s)	38.12 (84.03)	38.17 (84.15)	0.05 (0.12)	0.143
Engine Mixture Ratio LOX/Fuel	5.440	5.487	0.047	0.864

#### 7.4 S-IVB SHUTDOWN TRANSIENT PERFORMANCE FOR FIRST BURN

S-IVB Engine Cutoff (ECO) was initiated at STDV +123.84 seconds by a guidance velocity cutoff command which was 15.9 seconds later than predicted for first burn. The ECO transient was satisfactory and agreed closely with the acceptance test and predictions as shown by Figure 7-6. The predicted total cutoff impulse to zero percent of rated thrust was 217,749 N-s (48,952 lbf-s) as compared to actual values of 221,326 N-s (49,756 lbf-s) from engine data and 229,284 N-s (51,545 lbf-s) from guidance data. Cutoff occurred with the PU valve in the 5.5 position.

#### 7.5 S-IVB PARKING COAST PHASE CONDITIONING

The CVS maintained the fuel tank ullage pressure between 13.1 and 13.5 N/cm<sup>2</sup> (19.0 and 19.6 psia). CVS thrust and acceleration levels are shown in Figure 7-7. Continuous venting was initiated at 723.8 seconds. Regulation continued, with the expected operation of the main poppet periodically opening, cycling, and reseating. Continuous venting was terminated at 16,619.4 seconds.

Table 7-3. Comparison of S-IVB Stage Flight Reconstruction Data  
With Performance Simulation Results - First Burn

PARAMETERS	UNITS	PREDICTED	FLIGHT RECONSTRUCTION	PERCENT DEV FROM PRED
		FIRST BURN FLIGHT AVERAGE	FIRST BURN FLIGHT AVERAGE	FIRST BURN FLIGHT AVERAGE
Longitudinal Vehicle Thrust	N (lbf)	1,026,093 (230,675)	1,031,315 (231,849)	0.509
Vehicle Mass Loss Rate	kg/s (lbf/s)	245.96 (542.25)	247.91 (546.54)	0.791
Longitudinal Vehicle Specific Impulse	N-s/kg (lbf-s/lbf)	4171.7 (425.4)	4160.1 (424.21)	-0.280
PARAMETERS	UNITS	FLIGHT SIMULATION	PERCENT DEV FROM PRED	
		FIRST BURN FLIGHT AVERAGE	FIRST BURN FLIGHT AVERAGE	
Longitudinal Vehicle Thrust	N (lbf)	1,033,949 (232,441)	0.766	
Vehicle Mass Loss Rate	kg/s (lbf/s)	247.87 (546.46)	0.776	
Longitudinal Vehicle Specific Impulse	N-s/kg (lbf-s/lbf)	4,172.24 (425.45)	0.012	



Table 7-4. S-IVB Burn Time Deviations

CONTRIBUTOR	BURN TIME (SECONDS)
Performance of Lower Stages	9.81
Vehicle Mass at S-II/S-IVB Separation	1.81
S-IVB Engine Performance	-0.31
Uncertainties in Performance	<u>-1.04</u>
Total	10.27

Calculations based on estimated temperatures indicate that the mass vented was approximately 1456 kilograms (3209 lbm) and that the boiloff mass was approximately 1519 kilograms (3346 lbm).

#### 7.6 S-IVB CHILLDOWN AND RESTART FOR SECOND BURN

The O<sub>2</sub>/H<sub>2</sub> burner system was used on AS-504 for repressurization during first restart preparations and for ullage settling prior to second restart. The ambient helium repressurization system was retained as a backup system and as the repressurization source for third burn. The O<sub>2</sub>/H<sub>2</sub> burner, mounted on the aft thrust structure, heats cold helium used for repressurizing the propellant tanks.

Repressurization was satisfactorily accomplished by the O<sub>2</sub>/H<sub>2</sub> burner. Burner Start Command (BSC) was initiated at 16,618.5 seconds. LOX tank ullage pressure at BSC was approximately 29.0 N/cm<sup>2</sup> (42.1 psia); therefore, repressurization of the LOX tank was not required. The LH<sub>2</sub> repressurization control valves were opened at BSC +7.0 seconds. The fuel tank was repressurized from 13.1 to 20.9 N/cm<sup>2</sup> (19.1 to 30.1 psia) in 180.4 seconds which yields a ramp rate of 2.52 N/cm<sup>2</sup>/min (3.66 psi/min) as shown in Figure 7-8. Figure 7-9 shows the performance of the O<sub>2</sub>/H<sub>2</sub> burner pressurant coil. There were 11.1 kilograms (24.5 lbm) of cold helium used from the cold helium spheres during repressurization. The burner continued to operate for a total of 460 seconds providing nominal propellant settling forces. Thrust and burner chamber conditions are presented in Figure 7-10. The performance of the AS-504 O<sub>2</sub>/H<sub>2</sub> burner during first restart preparations was nominal in all respects.

The S-IVB stage provided adequate conditioning of propellants to the J-2 engine for the first restart. The engine start sphere was recharged properly and maintained sufficient pressure during coast. The engine

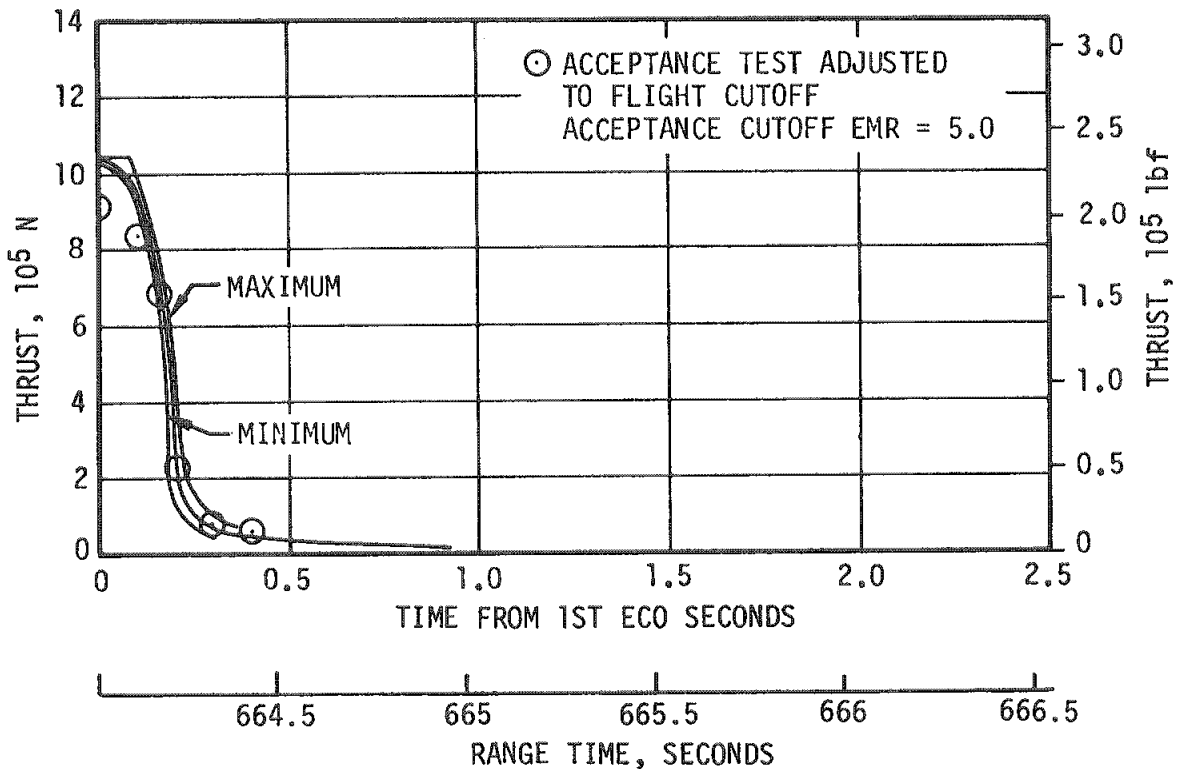


Figure 7-6. S-IVB Shutdown Transient Performance - First Burn

control sphere gas usage was as predicted during the first burn; the ambient helium spheres recharged the control sphere to a nominal level, adequate for a proper restart.

Table 7-5, showing the major events during the start transient, indicates that all events occurred as required and performance was as predicted.

The propellant recirculation chilldown systems performed satisfactorily and met STDV requirements for fuel and LOX as shown in Figure 7-11. Second burn fuel lead generally followed the predicted pattern and resulted in satisfactory conditions as indicated by the thrust chamber temperatures and the associated fuel injector temperatures shown in Figure 7-12. The  $LH_2$  chilldown system performance for second burn progressed satisfactorily. However, the fuel pump inlet temperature did not reach a steady state level. The temperature was still decreasing when chilldown was terminated by pre valve opening.

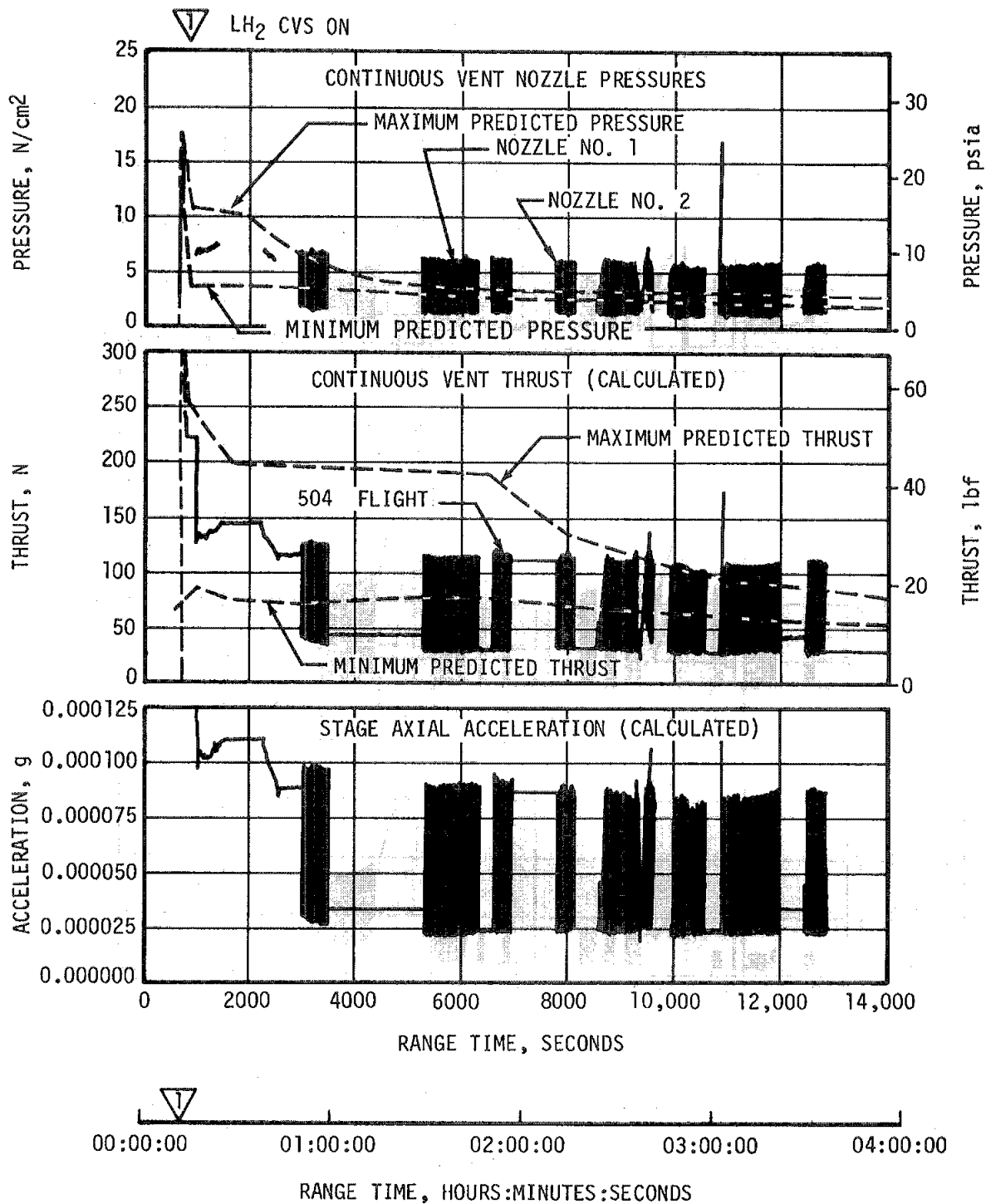


Figure 7-7. S-IVB CVS Performance (Sheet 1 of 3)

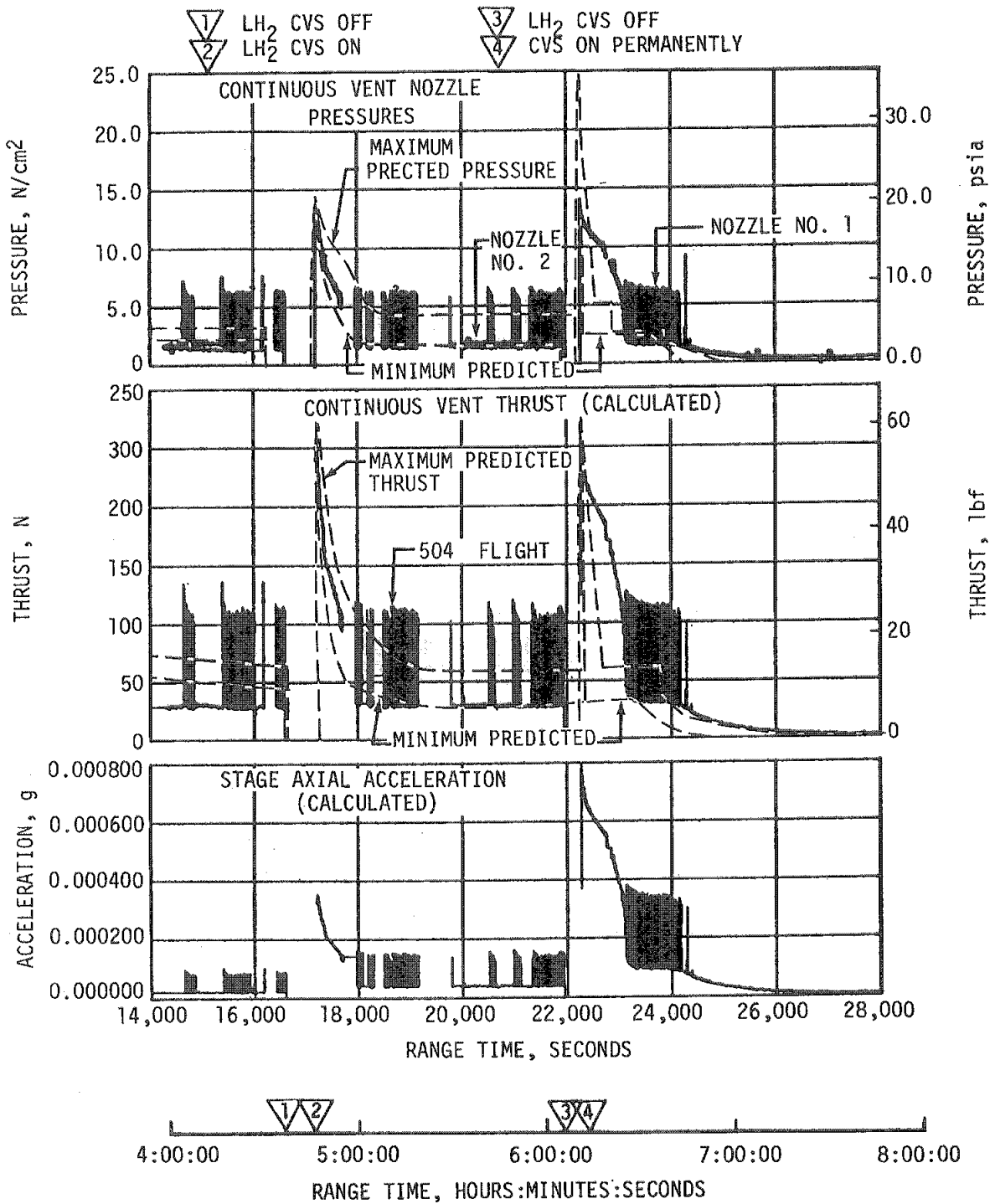


Figure 7-7. S-IVB CVS Performance (Sheet 2 of 3)

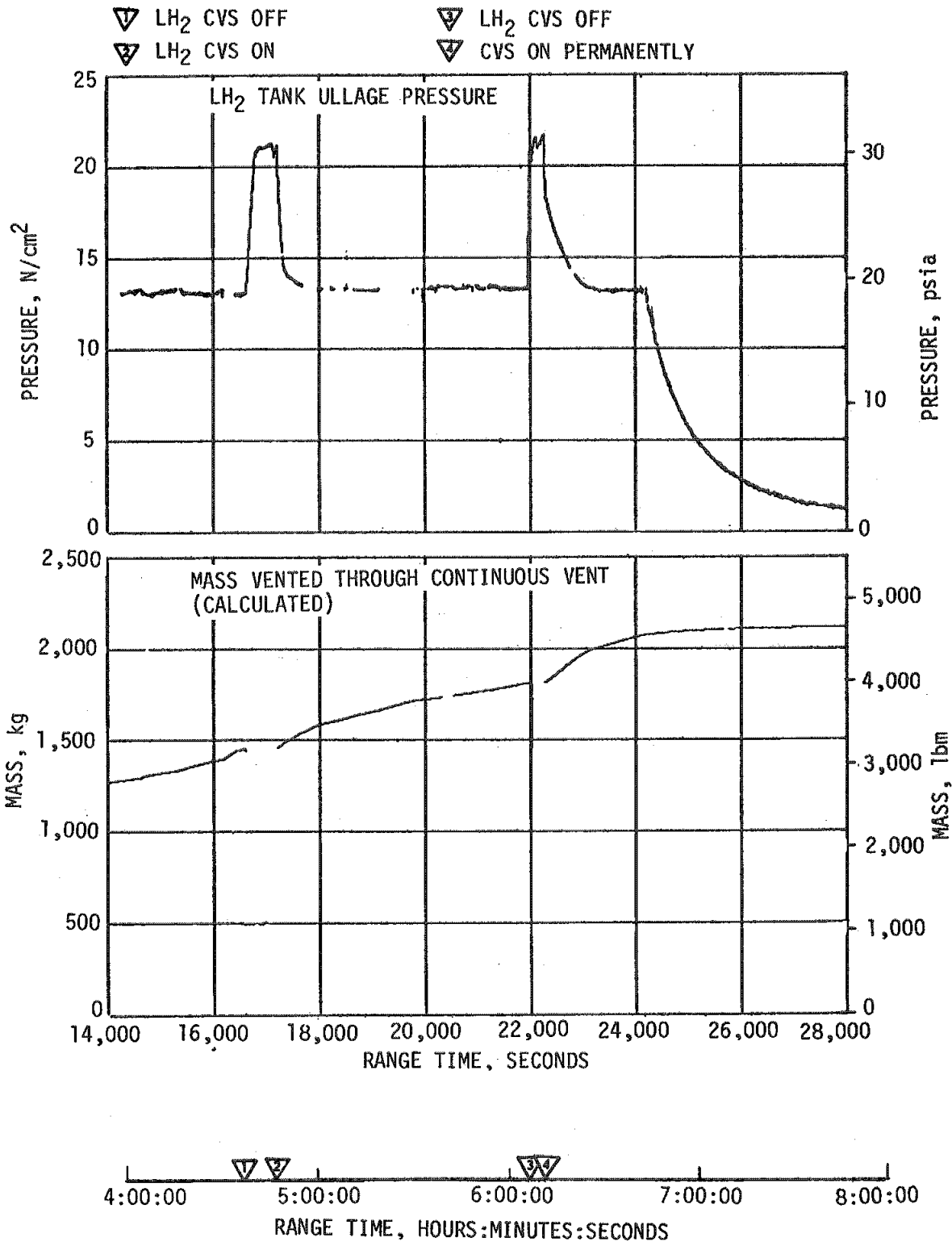


Figure 7-7. S-IVB CVS Performance (Sheet 3 of 3)

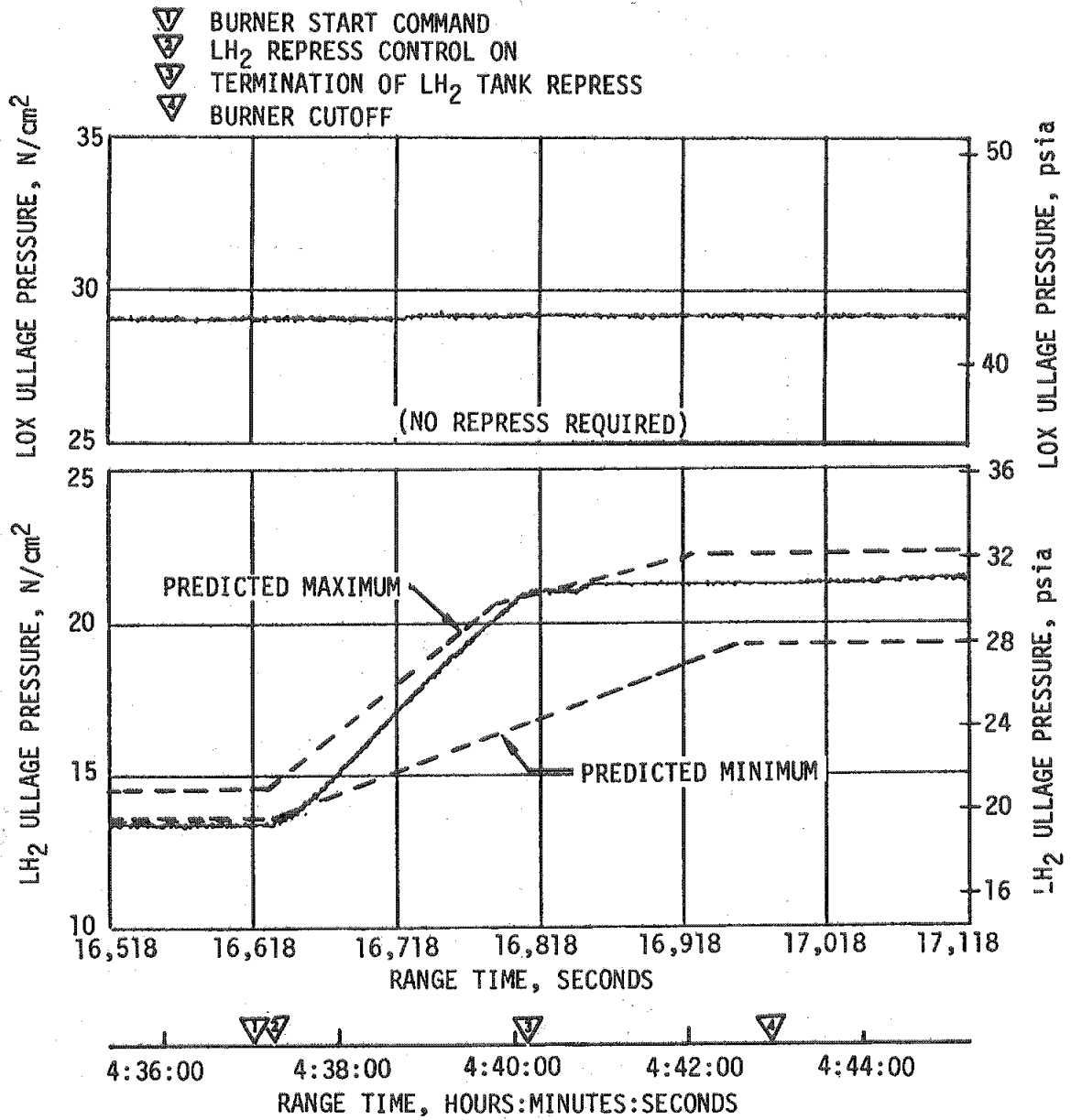


Figure 7-8. S-IVB Ullage Conditions During Repressurization Using O<sub>2</sub>/H<sub>2</sub> Burner - First Restart

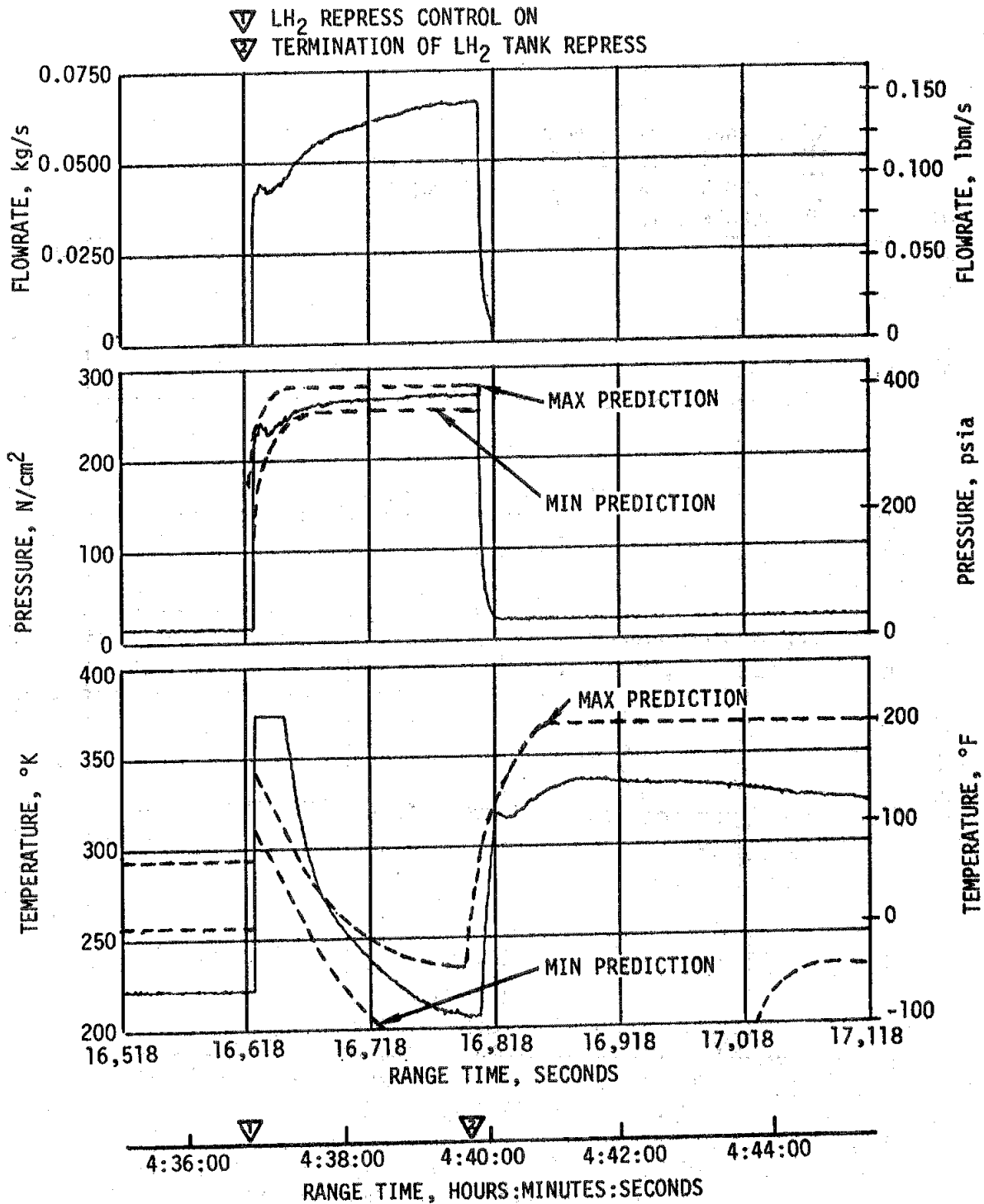


Figure 7-9. O<sub>2</sub>/H<sub>2</sub> Burner LH<sub>2</sub> Pressurant Coil Discharge Conditions - First Restart

- ▽ BURNER START COMMAND
- ▽ TERMINATION OF LH<sub>2</sub> TANK REPRESS
- ▽ BURNER CUTOFF

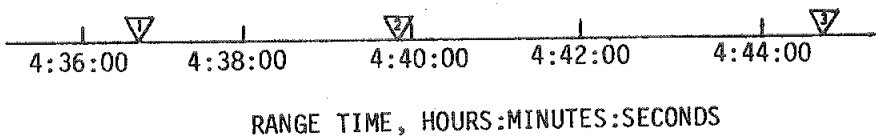
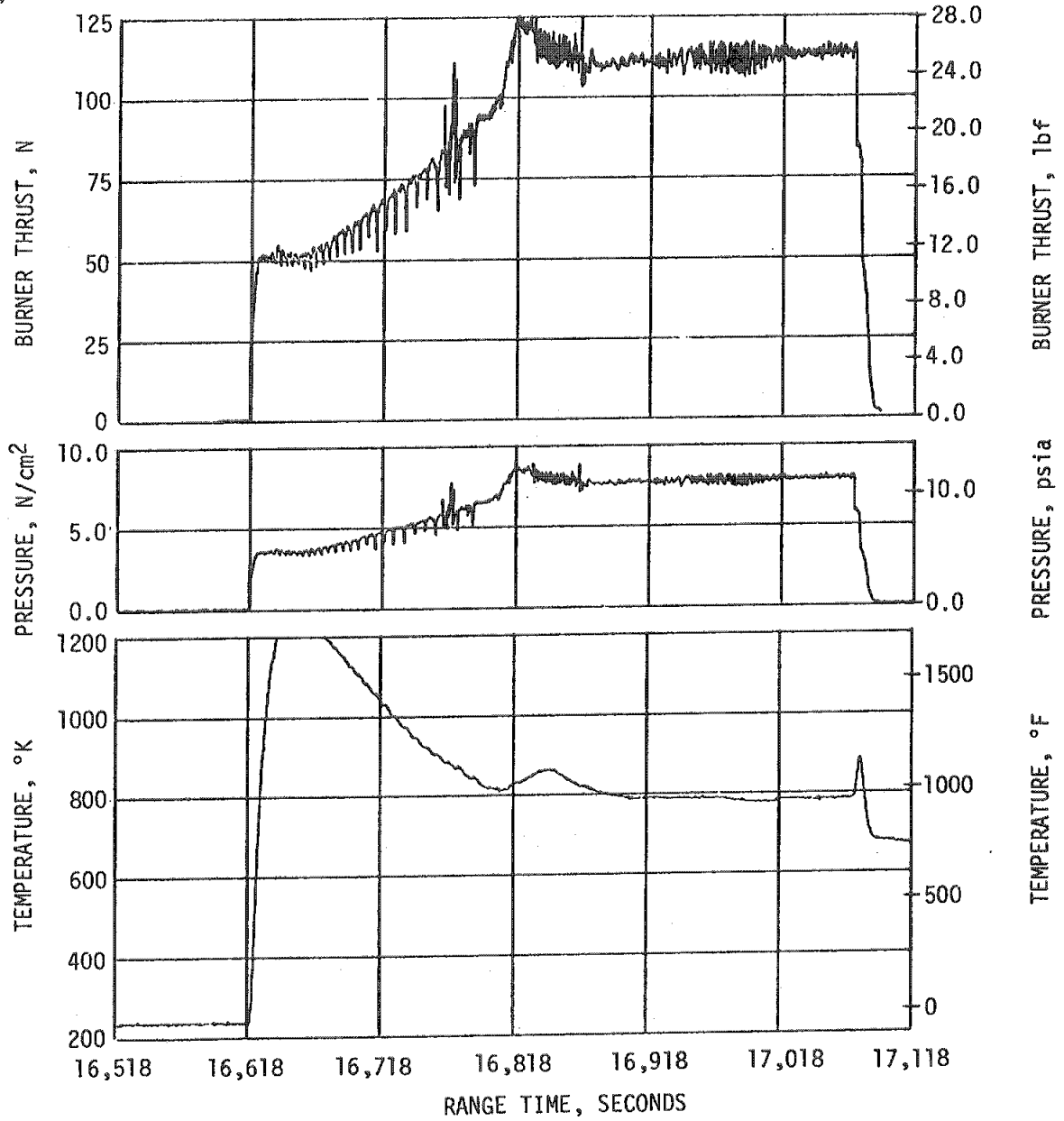


Figure 7-10. S-IVB O<sub>2</sub>/H<sub>2</sub> Burner Thrust and Thrust Chamber Conditions - First Restart



Table 7-5. S-IVB Engine Start Sequence Events - Second Burn

EVENT	TIME OF EVENT IN RANGE TIME (SECONDS)	
	PREDICTED	ACTUAL
S-IVB Engine Start Indication	17,141.94	17,147.20
S-IVB STDV Open Indication	17,149.74	17,155.54
S-IVB Thrust OK Signal-Switch 1 (on)	17,152.44	17,157.02
S-IVB Thrust OK Signal-Switch 2 (on)	17,152.44	17,157.06
S-IVB Engine Cutoff at the J-2 Engine	17,212.34	17,217.60
S-IVB Thrust OK Signal Dropout - Switch 1	17,211.64	17,217.85
S-IVB Thrust OK Signal Dropout - Switch 2	17,211.64	17,217.81

All previous stages had reached a pump inlet steady state condition when the prevalve opened. The higher than normal LH<sub>2</sub> pump inlet temperature due to the lack of a steady state inlet temperature resulted in the pump inlet conditions being outside of the start box at second ESC. At STDV the fuel pump inlet conditions were within the start box. LOX pump chilldown was completely satisfactory.

The second burn thrust buildup was satisfactory and within the limits set by the engine manufacturer as shown in Figure 7-13. This buildup was similar to the thrust buildup on AS-501, 502 and 503. The PU valve was in the proper full open (4.5 Engine Mixture Ratio [EMR]) position prior to the second start. The total impulse from STDV to STDV +2.5 seconds was 1,012,806 N-s (227,688 lbf-s). This was approximately the same as the value of 1,018,029 N-s (228,862 lbf-s) obtained during the same interval for the acceptance test.

The LOX pump inlet temperature was 91.6°K (-294.9°F). The start tank performed satisfactorily during the second burn blowdown and recharge sequence as shown in Figure 7-14.

#### 7.7 S-IVB MAIN STAGE PERFORMANCE FOR SECOND BURN

The propulsion reconstruction analysis showed that the stage performance during mainstage operation was satisfactory. A comparison of predicted and actual performance of thrust, total flowrate, specific impulse, and mixture ratio versus time is shown in Figure 7-15. Table 7-6 shows the specific impulse, flowrates, and mixture ratio deviations from the predicted STDV + 60-second time slice. This time slice performance is

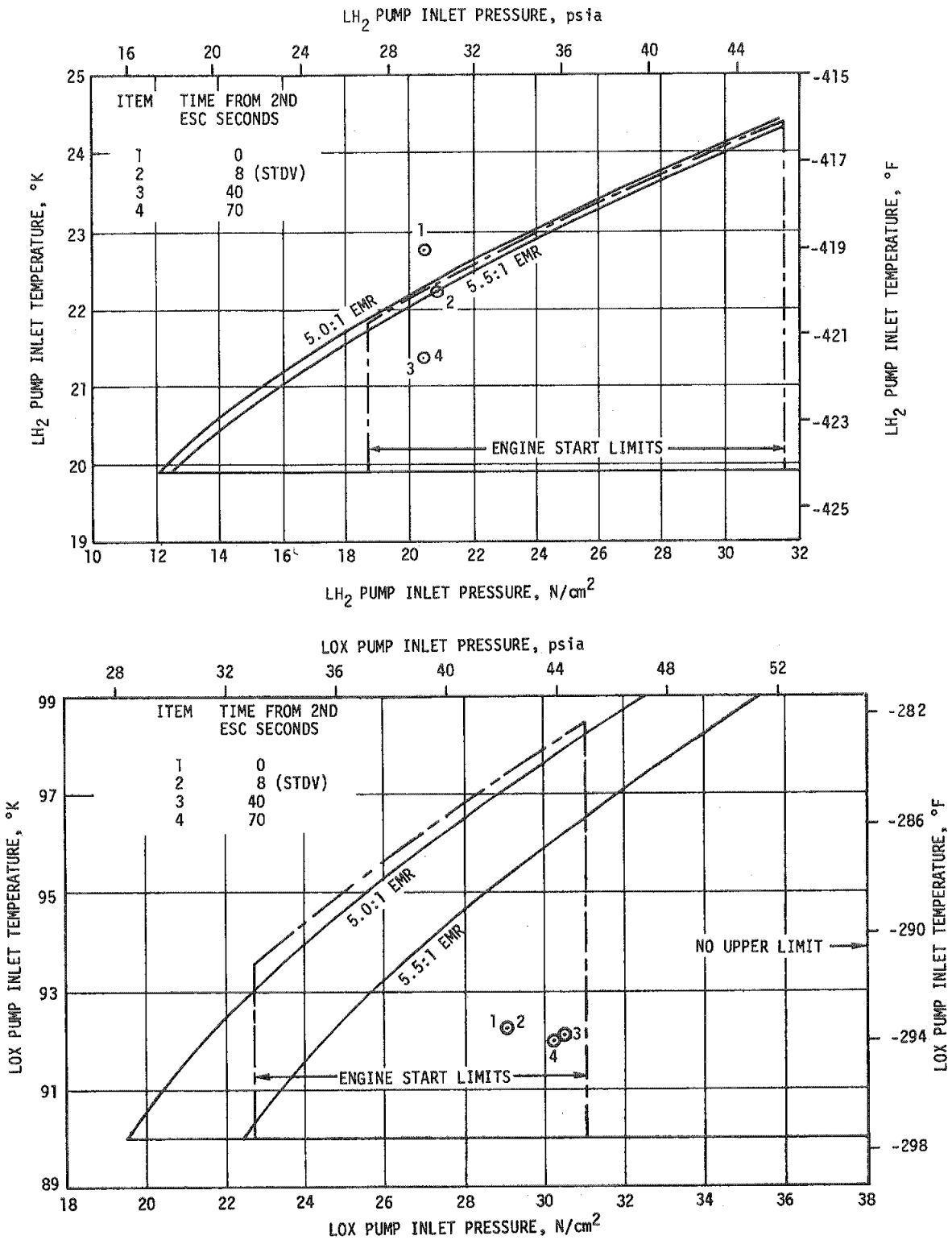


Figure 7-11. S-IVB Start Box and Run Requirements - Second Burn

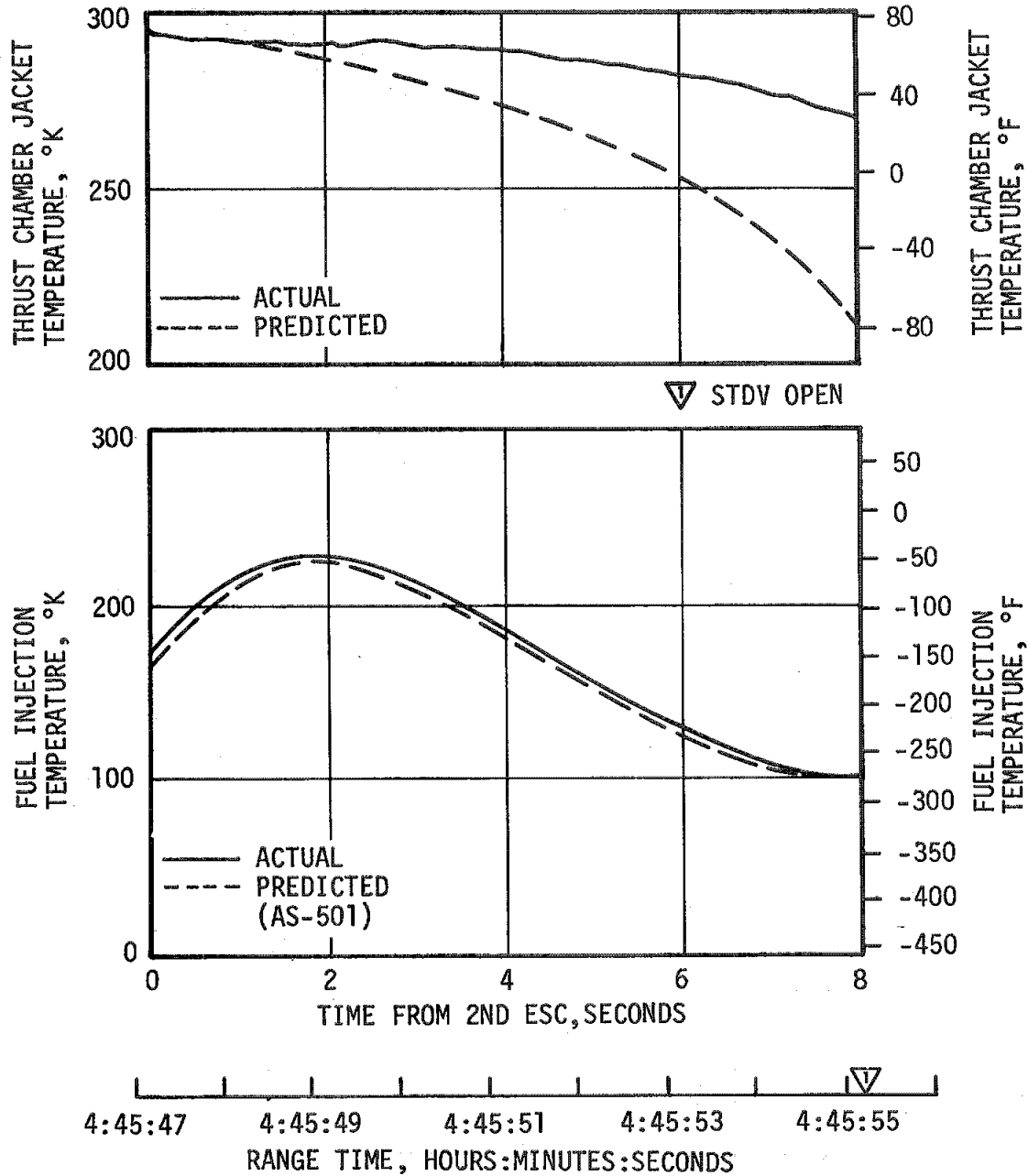


Figure 7-12. S-IVB Fuel Lead - Second Burn

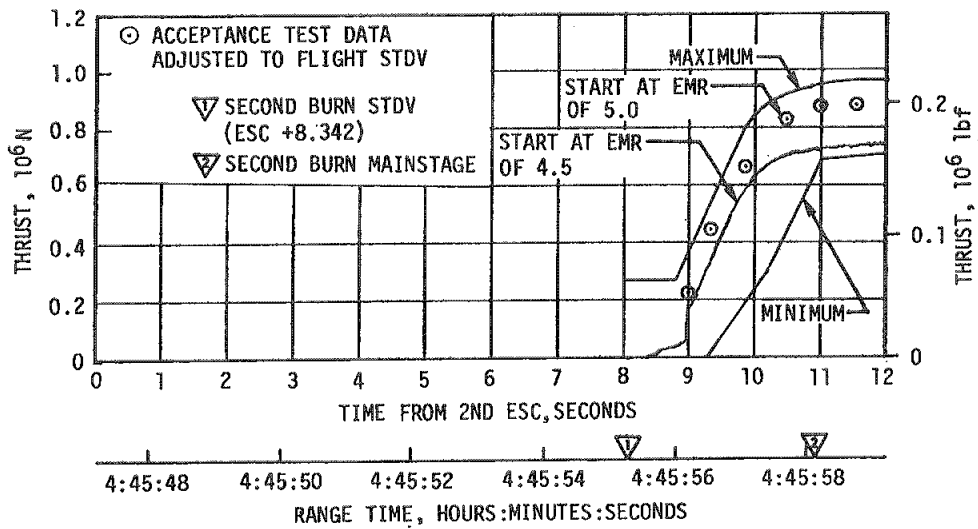


Figure 7-13. S-IVB Buildup Transients - Second Burn

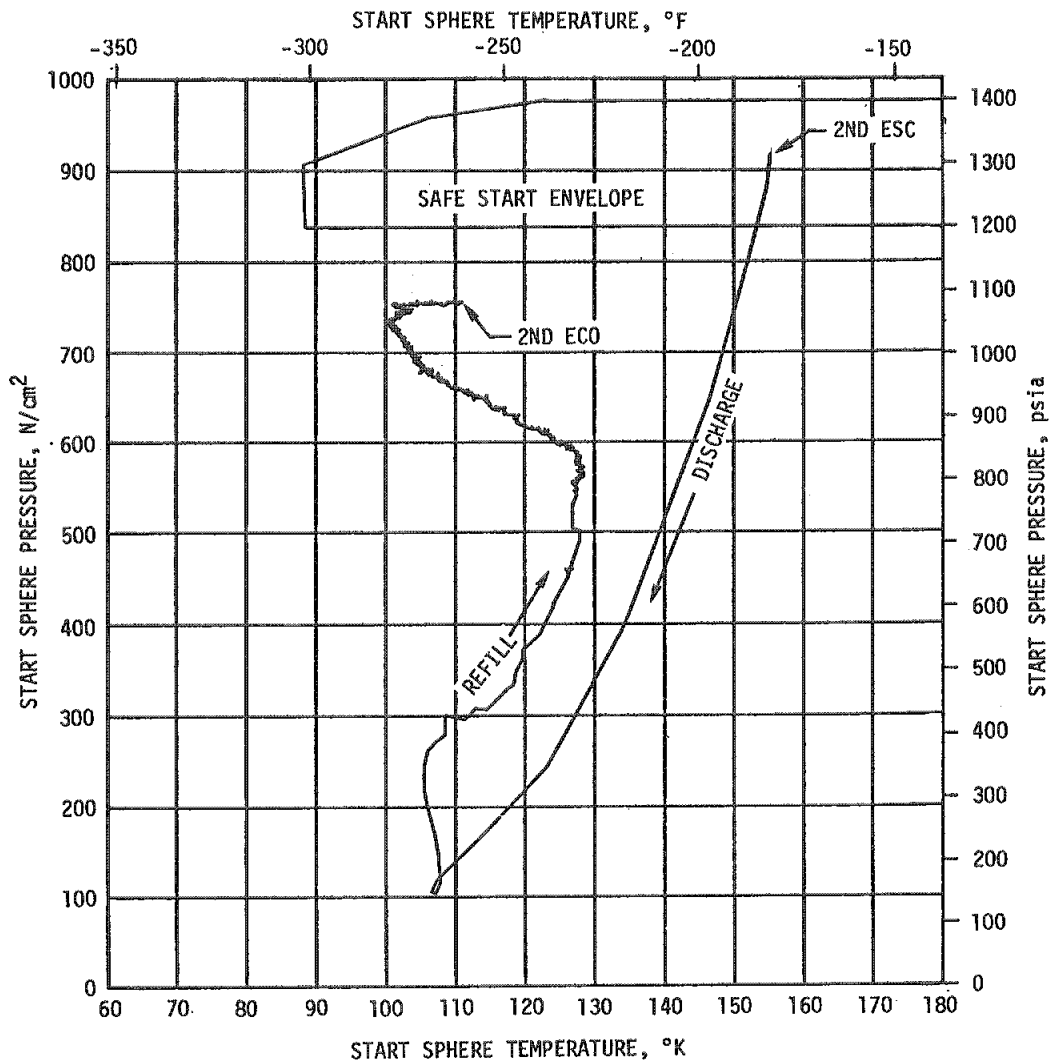


Figure 7-14. Start Tank Performance - Second Burn

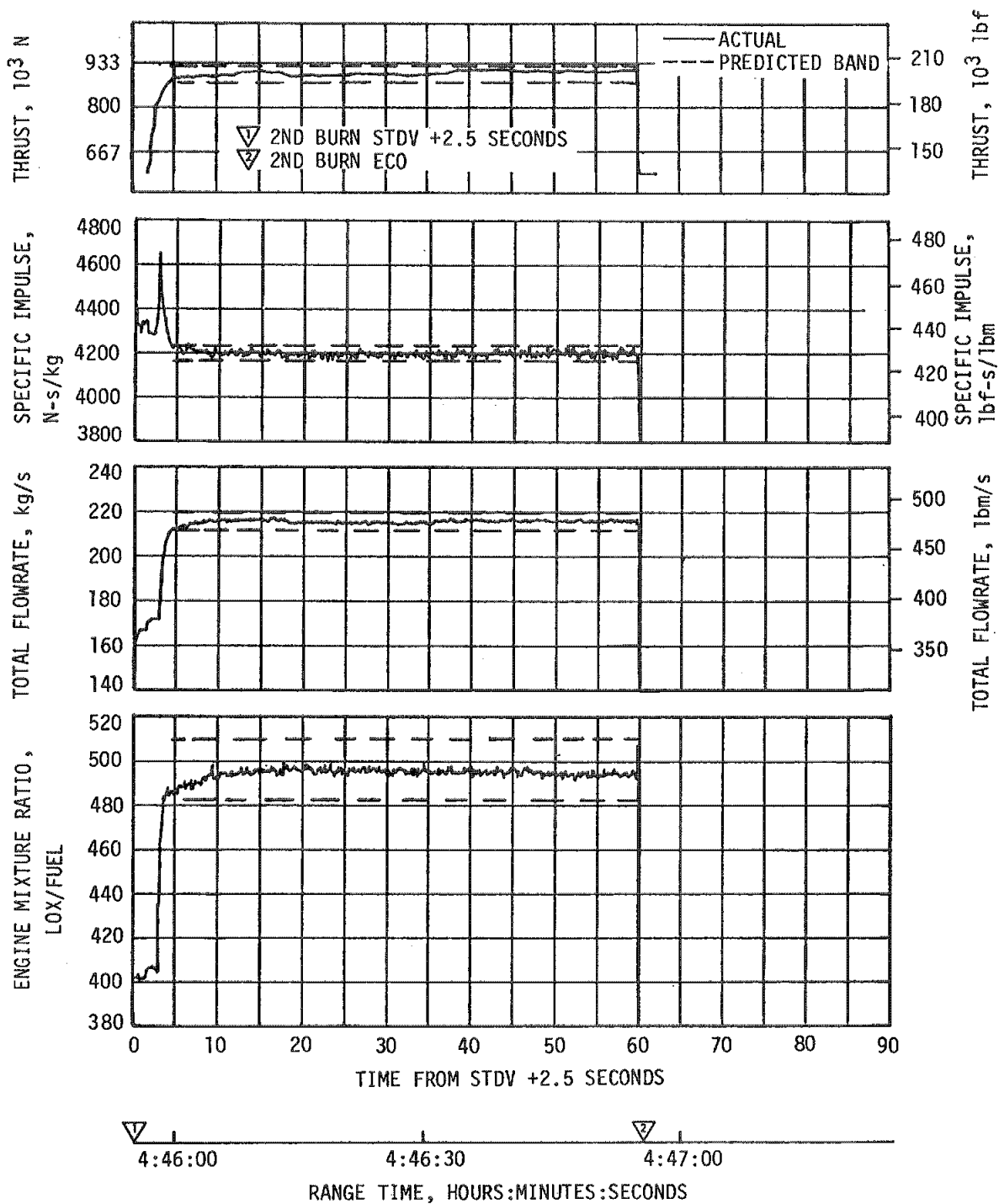


Figure 7-15. S-IVB Steady State Performance - Second Burn

Table 7-6. S-IVB Steady State Performance - Second Burn  
(STDV +60-Second Time Slice at Standard Altitude Conditions)

PARAMETER	PREDICTED	2ND BURN RECONSTRUCTION	FLIGHT DEVIATION	PERCENT DEVIATION FROM PREDICTED
Thrust N (lbf)	910,866 (204,771)	905,515 (203,568)	-5351 (-1203)	-0.587
Specific Impulse N-s/kg (lbf-s/lbm)	4207.8 (429.08)	4200.2 (428.3)	-7.60 (-0.78)	-0.182
LOX Flowrate kg/s (lbm/s)	179.77 (396.32)	179.07 (394.78)	-0.70 (-1.54)	-0.388
Fuel Flowrate kg/s (lbm/s)	36.70 (80.91)	36.51 (80.49)	-0.19 (-0.42)	-0.52
Engine Mixture Ratio LOX/Fuel	4.898	4.905	0.007	0.143

standardized altitude performance which is comparable to engine acceptance tests. The 60-second time slice performance disagreed with the predicted by -0.587 percent in thrust. Specific impulse performance for second burn disagreed with predicted by -0.182 percent.

The overall propulsion reconstruction of longitudinal thrust was less than predicted by 0.567 percent. Longitudinal specific impulse for second burn was less than predicted by 0.49 percent.

The flight simulation analysis showed a decrease of 0.568 percent compared to the prediction in specific impulse. Other comparisons are shown in Table 7-7.

During the burn the engine experienced shifts of 6672 Newtons (1500 lbf) of thrust due to  $3.93 \text{ N/cm}^2$  (5.7 psia) shifts in GG chamber pressure. These shifts, also experienced on AS-503, are attributed to changes in the GG system flowrate resistance on the LOX side and are not considered abnormal.

Table 7-7. Comparison of S-IVB Stage Flight Reconstruction Data  
With Performance Simulation Results - Second Burn

PARAMETERS	UNITS	PREDICTED	FLIGHT RECONSTRUCTION	PERCENT DEV FROM PRED
		SECOND BURN FLIGHT AVERAGE	SECOND BURN FLIGHT AVERAGE	SECOND BURN FLIGHT AVERAGE
Longitudinal Vehicle Thrust	N (lbf)	898,002 (201,879)	892,896 (200,731)	-0.567
Vehicle Mass Loss Rate	kg/s (lbf/s)	213.21 (470.04)	213.04 (469.68)	-0.076
Longitudinal Vehicle Specific Impulse	N-s/kg (lbf-s/lbf)	4211.8 (429.49)	4191.2 (427.38)	-0.490
PARAMETERS	UNITS	FLIGHT SIMULATION	PERCENT DEV FROM PRED	
		SECOND BURN FLIGHT AVERAGE	SECOND BURN FLIGHT AVERAGE	
Longitudinal Vehicle Thrust	N (lbf)	900,453 (202,421)	0.268	
Vehicle Mass Loss Rate	kg/s (lbf/s)	215.14 (474.31)	0.908	
Longitudinal Vehicle Specific Impulse	N-s/kg (lbf-s/lbf)	4,187.93 (427.05)	-0.568	

The helium control system for the J-2 engine performed satisfactorily during mainstage operation. There was little pressure decay during the burn due to the connection with the stage repressurization system. Helium usage was estimated from flowrates during the burn and approximately 0.076 kilogram (0.168 lbm) was consumed.

At second burn ESC, the start bottle pressure was 904.2 N/cm<sup>2</sup> (1311.5 psia). The blowdown performance was satisfactory. Due to the short duration of second burn the start bottle pressure at the end of second burn was 736.4 N/cm<sup>2</sup> (1068 psia). However, during the second burn coast of 80 minutes, the start bottle pressure reached the required start box requirements of 827.4 N/cm<sup>2</sup> (1200 psia).

#### 7.8 S-IVB SHUTDOWN TRANSIENT PERFORMANCE FOR SECOND BURN

S-IVB ECO was initiated at STDV +62.06 seconds by a timed cutoff command. Second burn time was 0.54 second shorter than predicted. The transient was satisfactory and agreed closely with the acceptance test and predictions. The predicted total cutoff impulse to zero percent of rated thrust was 195,802 N-s (44,018 lbf-s) as compared to an actual value of 191,440 N-s (43,118 lbf-s). Cutoff occurred with the PU valve in the null position. The thrust during second cutoff is shown in Figure 7-16.

#### 7.9 S-IVB INTERMEDIATE ORBIT COAST PHASE CONDITIONING

The fuel tank CVS was opened for the second coast at 17,218 seconds. The fuel tank ullage pressure decayed normally and was regulated between 13.1 and 13.5 N/cm<sup>2</sup> (19.0 and 19.6 psia) as seen in Figure 7-7. GH<sub>2</sub> (358.2 kilograms [788.9 lbm]) was vented through the propulsive vent system before it was closed at 21,965 seconds during this coast period, and 372.6 kilograms (820.7 lbm) of GH<sub>2</sub> were boiled off.

#### 7.10 S-IVB ENGINE CHILLDOWN AND BUILDUP TRANSIENT PERFORMANCE FOR THIRD BURN

The ambient repressurization system was utilized to repressurize the fuel tank for third burn as shown in Figure 7-17. The LH<sub>2</sub> tank was pressurized from 13.4 to 20.8 N/cm<sup>2</sup> (19.4 to 30.2 psia). Approximately 13.1 kilograms (28.9 lbm) of helium were added to the LH<sub>2</sub> tank during repressurization.

The O<sub>2</sub>/H<sub>2</sub> burner was successfully ignited prior to third burn to demonstrate a restart capability and to provide an acceleration for propellant settling. Repressurization of the propellant tanks using the burner was not attempted.

The burner was ignited at 21,827.6 seconds and burned satisfactorily for 134.4 seconds. Cutoff was commanded at 21,962.0 seconds. Thrust level, chamber temperature and pressure during this period are presented in Figure 7-18.



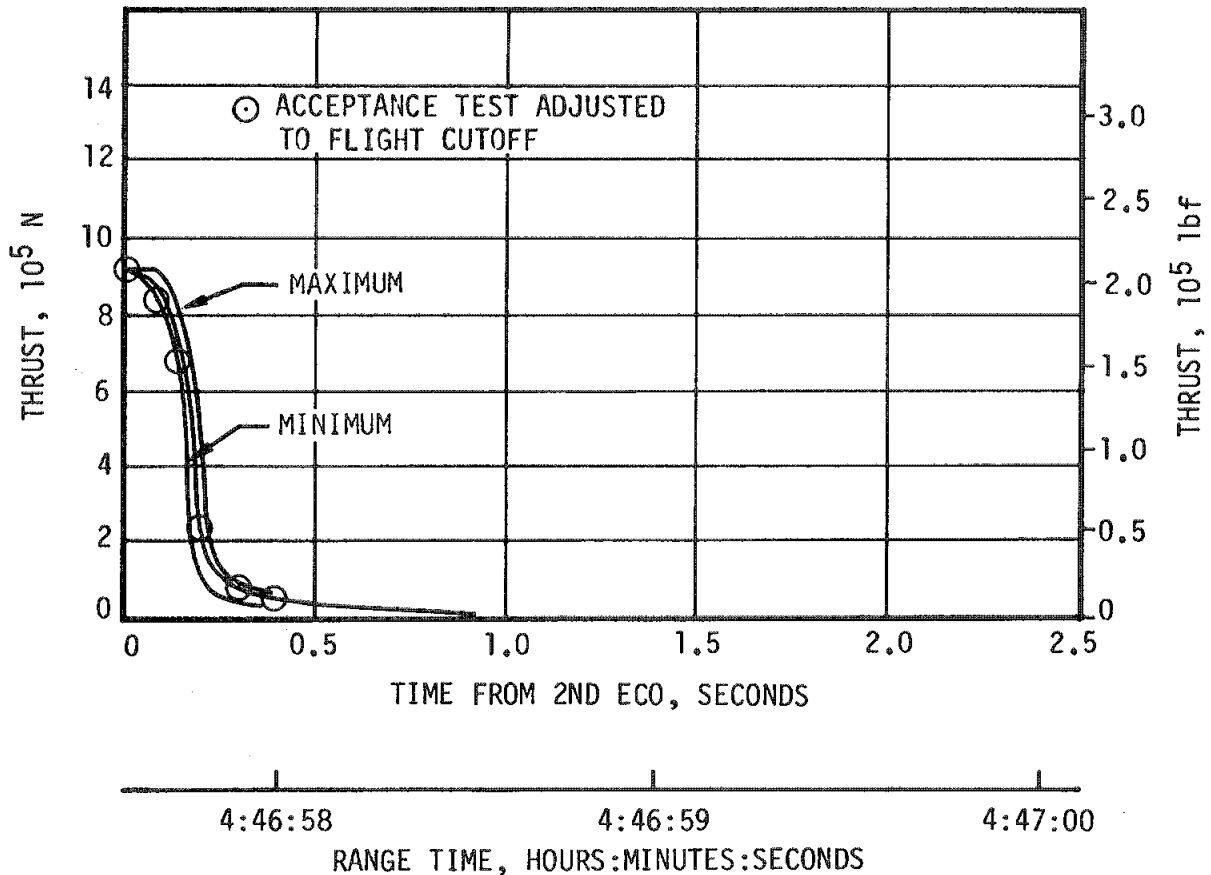


Figure 7-16. S-IVB Shutdown Transient Performance - Second Burn

The engine start sphere was recharged properly and maintained sufficient pressure during coast for the second restart. The engine control sphere gas usage was as predicted during the second burn; the ambient helium spheres recharged the control sphere to a nominal level, adequate for the second restart.

The purpose of third burn was to demonstrate restart capability after an 80 minute coast and to demonstrate the mission rule related to a failure of both chilldown systems. Normally the engine requires LOX and LH<sub>2</sub> chilldown to condition the pumps prior to ESC. To simulate a chilldown system failure, after the chillpumps were spun up, the chilldown shutoff valves were closed. An attempt was then made to restart the J-2 engine under the simulated failure condition. A ground command initiated a 51.9-second fuel lead to condition the thrust chamber and fuel pump inlet. At STDV, the resulting fuel pump inlet conditions were well within the start and run boxes, indicating adequate conditioning of the

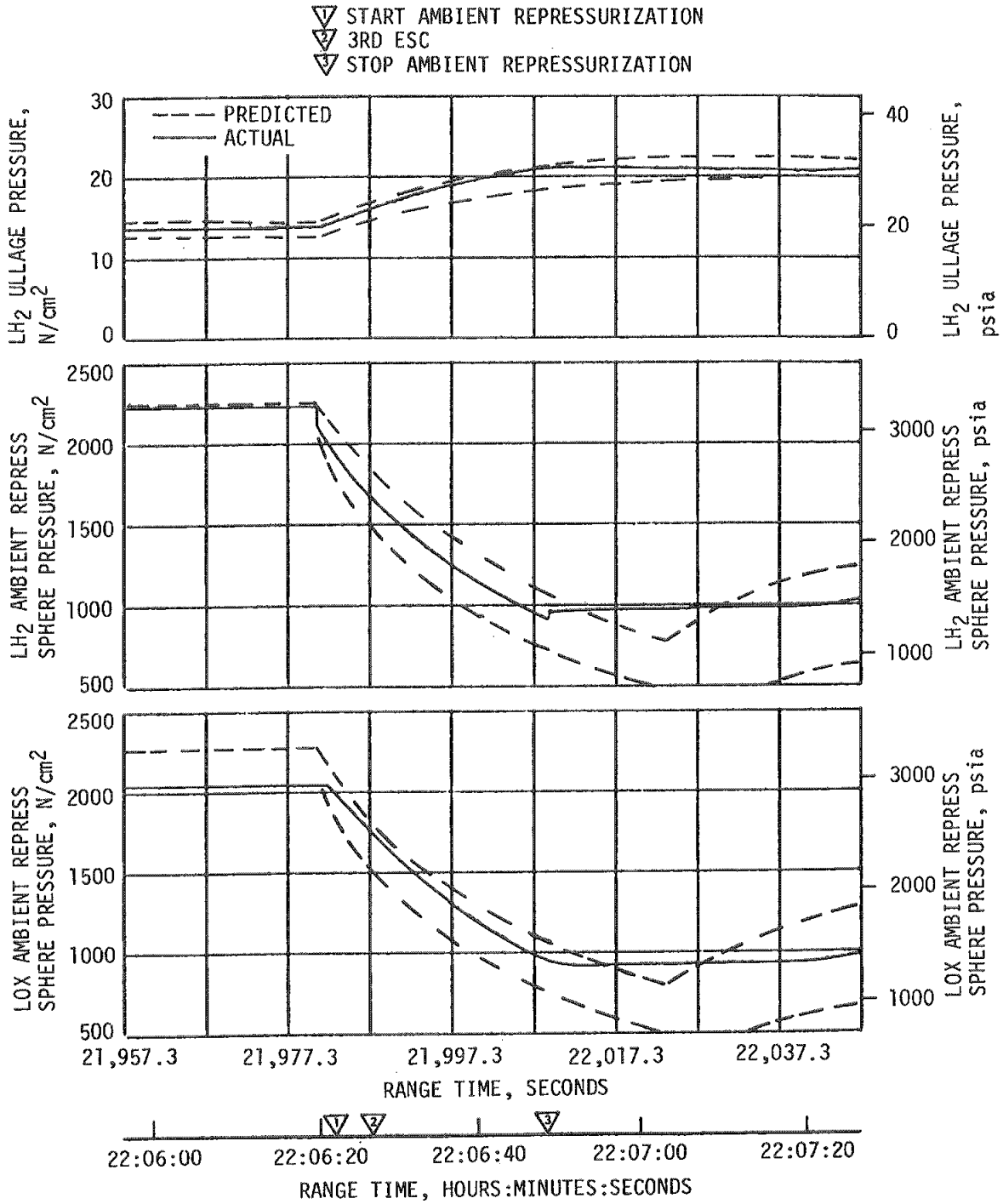


Figure 7-17. LH<sub>2</sub> and LOX Ambient Repressurization Sphere Pressures and LH<sub>2</sub> Ullage Pressure

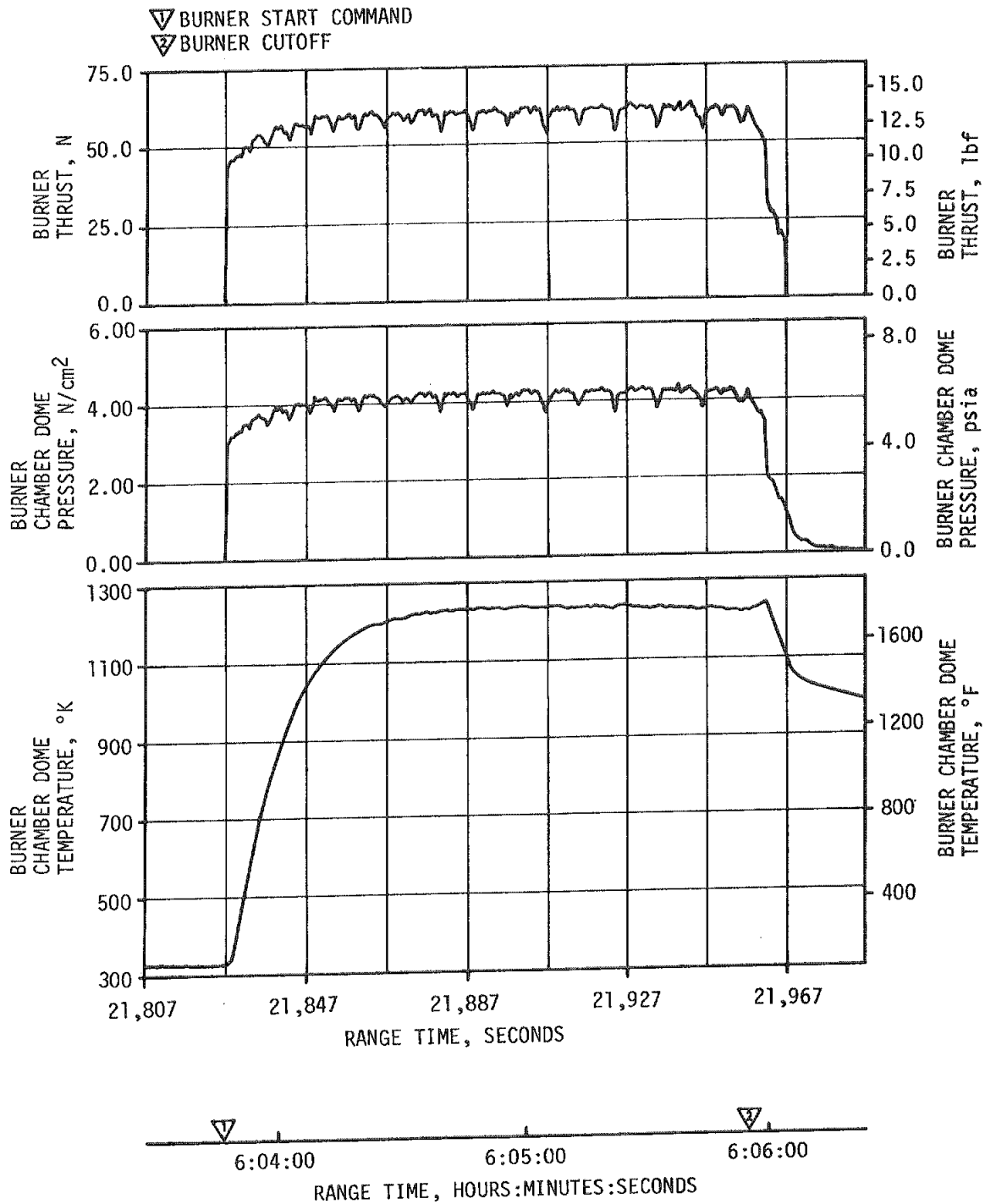


Figure 7-18. S-IVB O<sub>2</sub>/H<sub>2</sub> Burner Thrust and Thrust Chamber Conditions - Second Burn

fuel pump inlet. The LH<sub>2</sub> pump inlet temperature at STDV was 21.8°K (-420.4°F). Due to the absence of chilldown, the LOX pump inlet temperature was offscale high at STDV. The LOX pump inlet temperature was 116.5°K (-250°F) at STDV compared to an expected temperature of 91.5°K (-295°F). The LOX pump inlet conditions were outside the start box and this condition is related to the abnormal performance seen on third burn. The LOX and LH<sub>2</sub> pump inlet conditions are shown in Figure 7-19. The start tank performed satisfactorily during the third burn blowdown and recharge sequence, as shown in Figure 7-20.

The effect of the third burn fuel lead is shown in Figure 7-21 which presents thrust chamber temperature and fuel injector temperature. The abnormal propellant quality and the cold hardware conditions at STDV could have been the source of the abnormal start condition which persisted throughout third burn. Early engine injector development testing by the engine manufacturer indicated that thrust chamber pressure oscillations could occur as a result of excessive chilling of thrust chamber and injector.

The fuel injector temperature indicated that a saturated liquid or a low quality two phase condition may have existed approximately 35 seconds before STDV. At STDV the fuel flow was 6.3 kg/s (14 lbm/s) which was within 0.5 kg/s (1.1 lbm/s) of the predicted flowrate.

The third burn start transient was abnormal as shown in Figure 7-22. The thrust buildup was within the limits set by the engine manufacturer, but somewhat erratic as evidenced by Figure 7-23. A comparison of second and third burn chamber pressure during the start transient is shown in Figure 7-23. The higher Main Oxidizer Valve (MOV) plateau during the start transient, and the higher than normal injector temperatures correlate with the engine manufacturer combustion instability tests. Table 7-8 shows the major sequence of events during the buildup transients. The PU valve was in proper full open position prior to third start. The start impulse over the interval from STDV to STDV +2.5 seconds was 974,841 N-s (219,153 lbf-s). This value was lower than the 1,018,029 N-s (228,862 lbf-s) impulse obtained during the corresponding interval of the acceptance test.

#### 7.11 S-IVB MAIN STAGE PERFORMANCE FOR THIRD BURN

The propulsion reconstruction analysis showed that the stage performance during mainstage operation was not as expected. A comparison of predicted and actual performance of thrust, total flowrate, specific impulse, and mixture ratio versus time is shown in Figure 7-24. Table 7-9 shows the specific impulse, flow rates, and mixture ratio deviations from the predicted at the 60-second time slice.

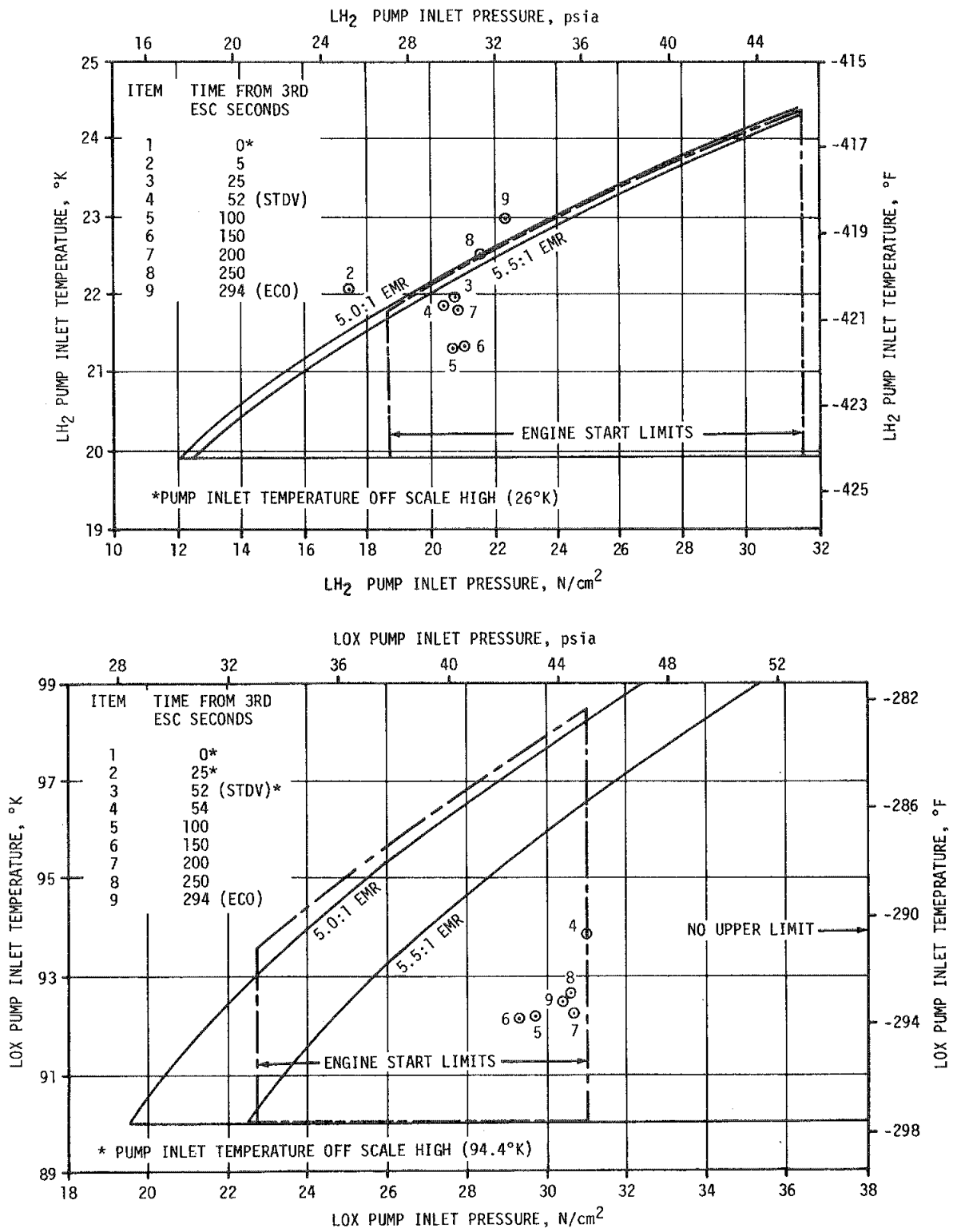


Figure 7-19. S-IVB Start Box and Run Requirements - Third Burn

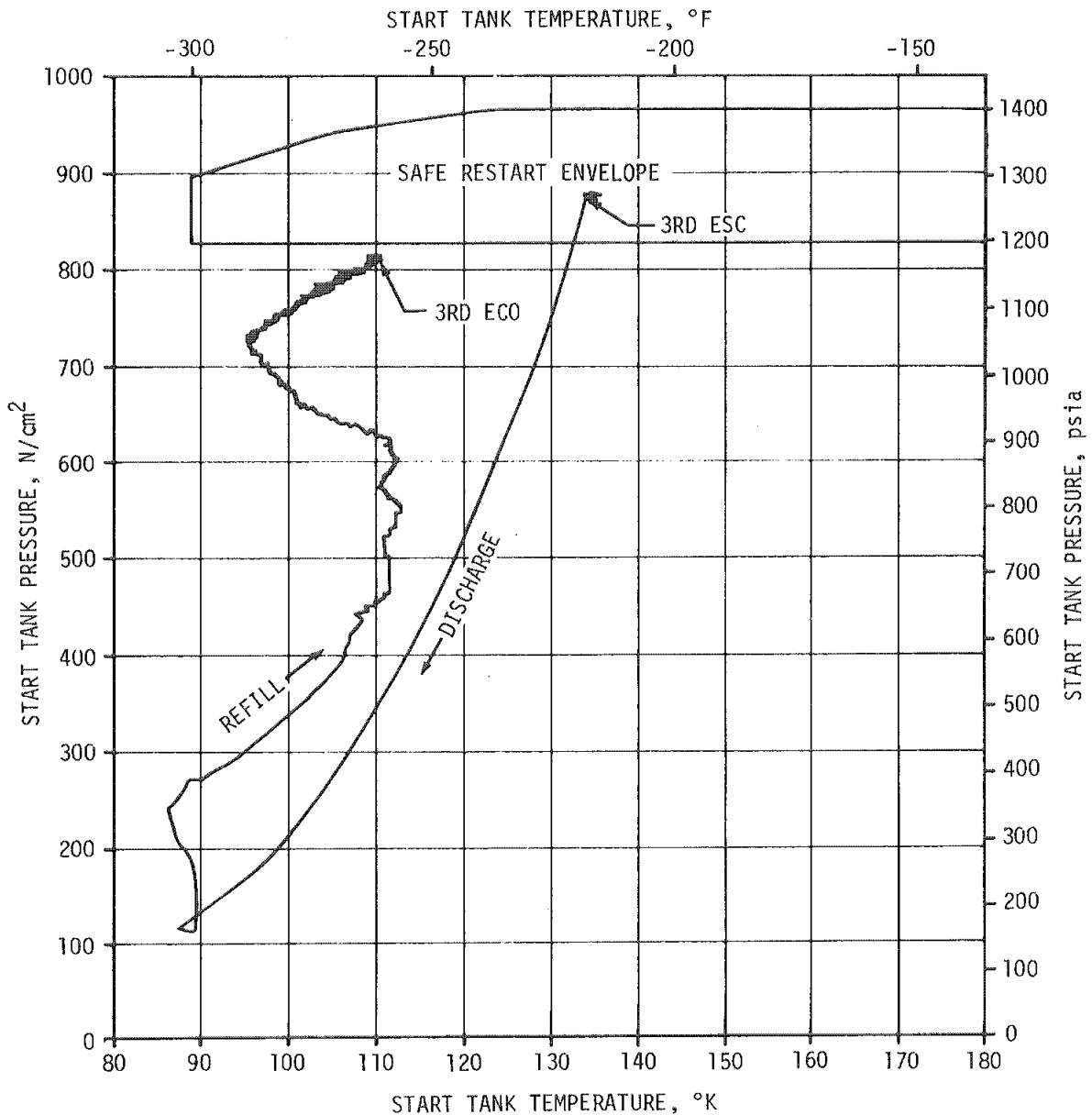


Figure 7-20. S-IVB Start Tank Performance - Third Burn

The 60-second time slice performance for third burn shows thrust was 2.57 percent lower than predicted and specific impulse 2.31 percent lower than predicted. This reduced level of performance, which lasted until STDV +99 seconds, is attributed to the presence of thrust chamber pressure oscillations which began during the start transient. Table 7-10 is a comparison of third burn results and engine manufacturer instability tests. Figure 7-25 provides a flow diagram of the anomalies which occurred during third burn.

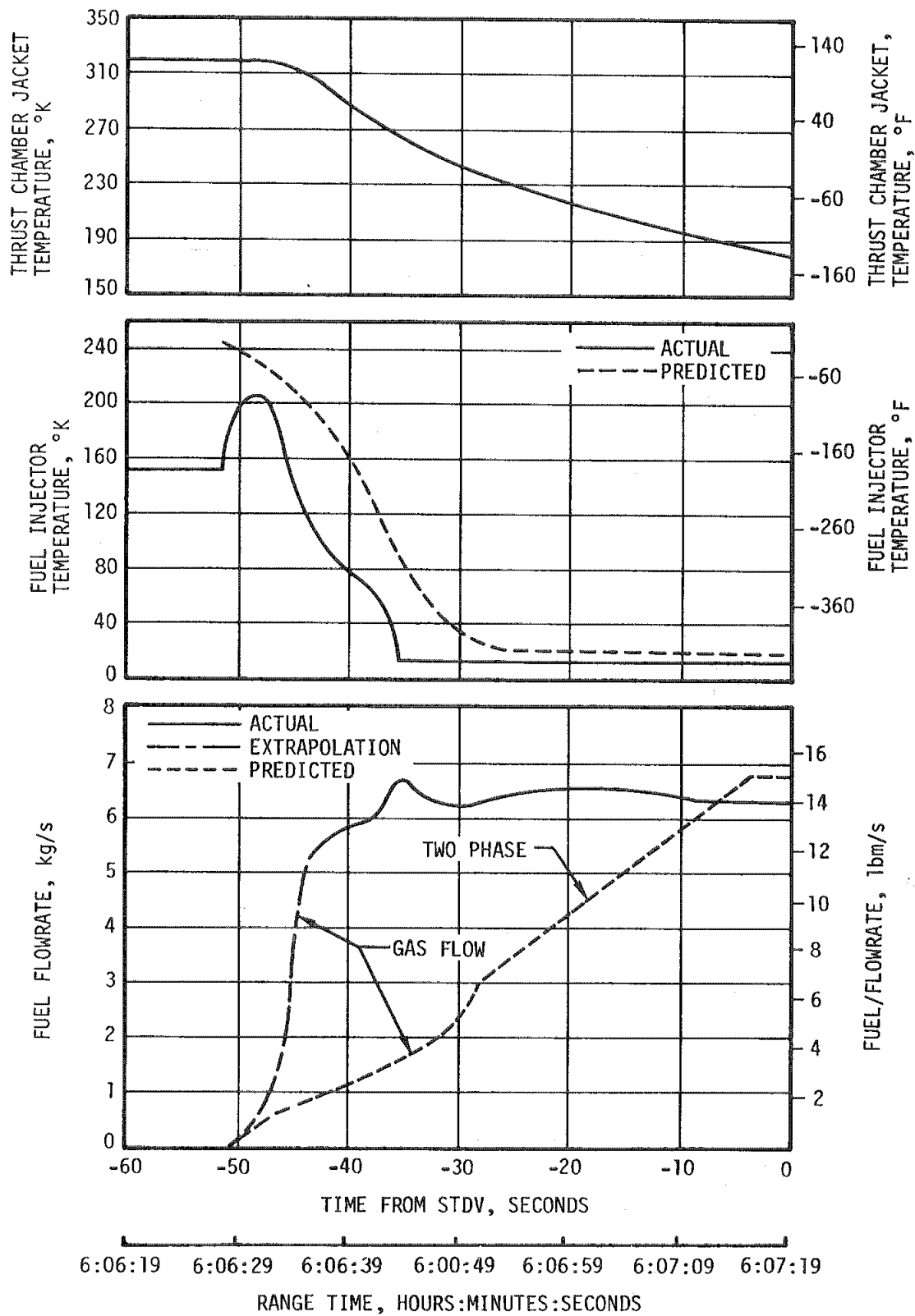


Figure 7-21. Effects of Extended S-IVB LH<sub>2</sub> Lead - Third Burn

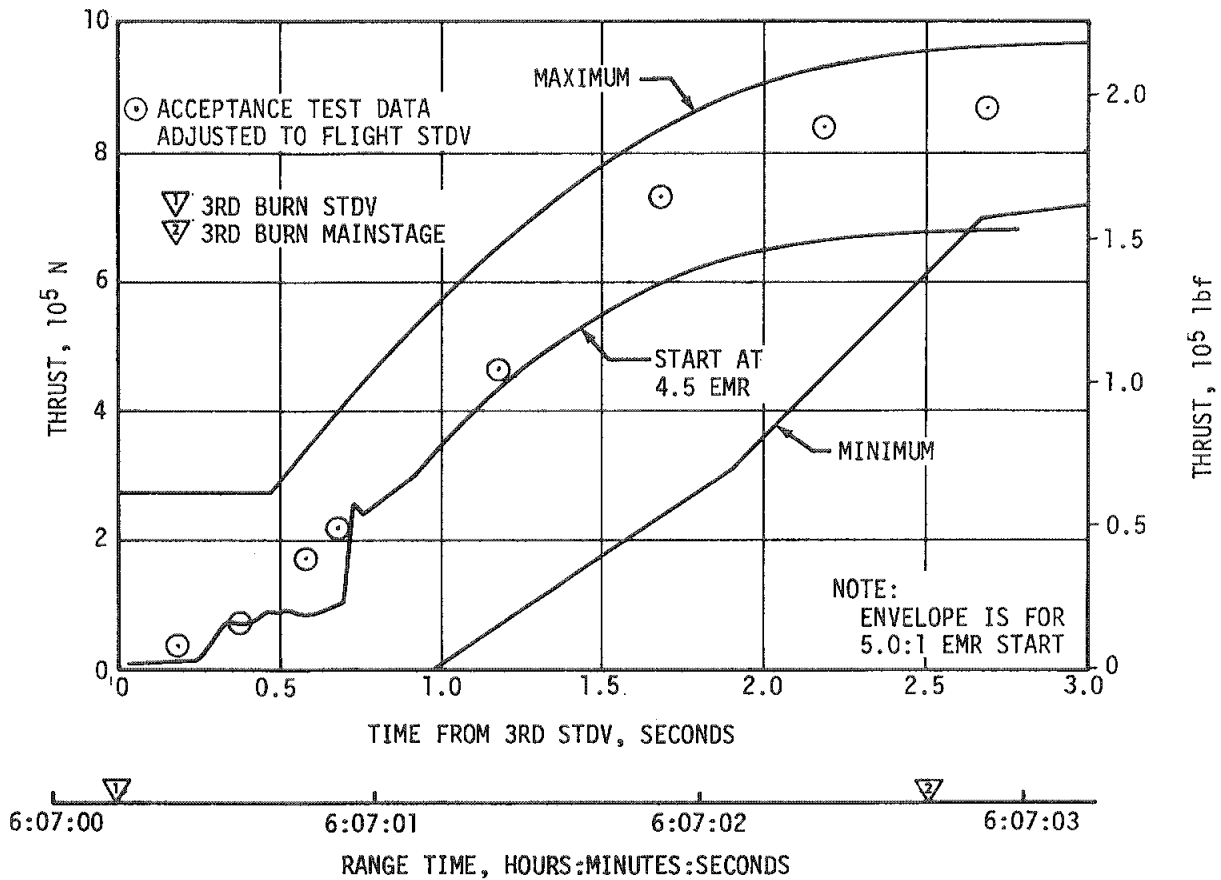


Figure 7-22. S-IVB Buildup Transient - Third Burn

Figure 7-26 presents a sequence of events during third burn. At approximately ESC +0.62 seconds a  $69 \text{ N/cm}^2$  (100 psid) spike was noted in the gas generator chamber pressure as shown in Figure 7-27. Due to slow response time the magnitude of the pressure spikes cannot be measured by flight instrumentation, however, correlation with a close-coupled transducer during the J-2 engine gas generator development testing indicated the actual pressure may be as high as  $3447.5 \text{ N/cm}^2$  (5000 psid). This



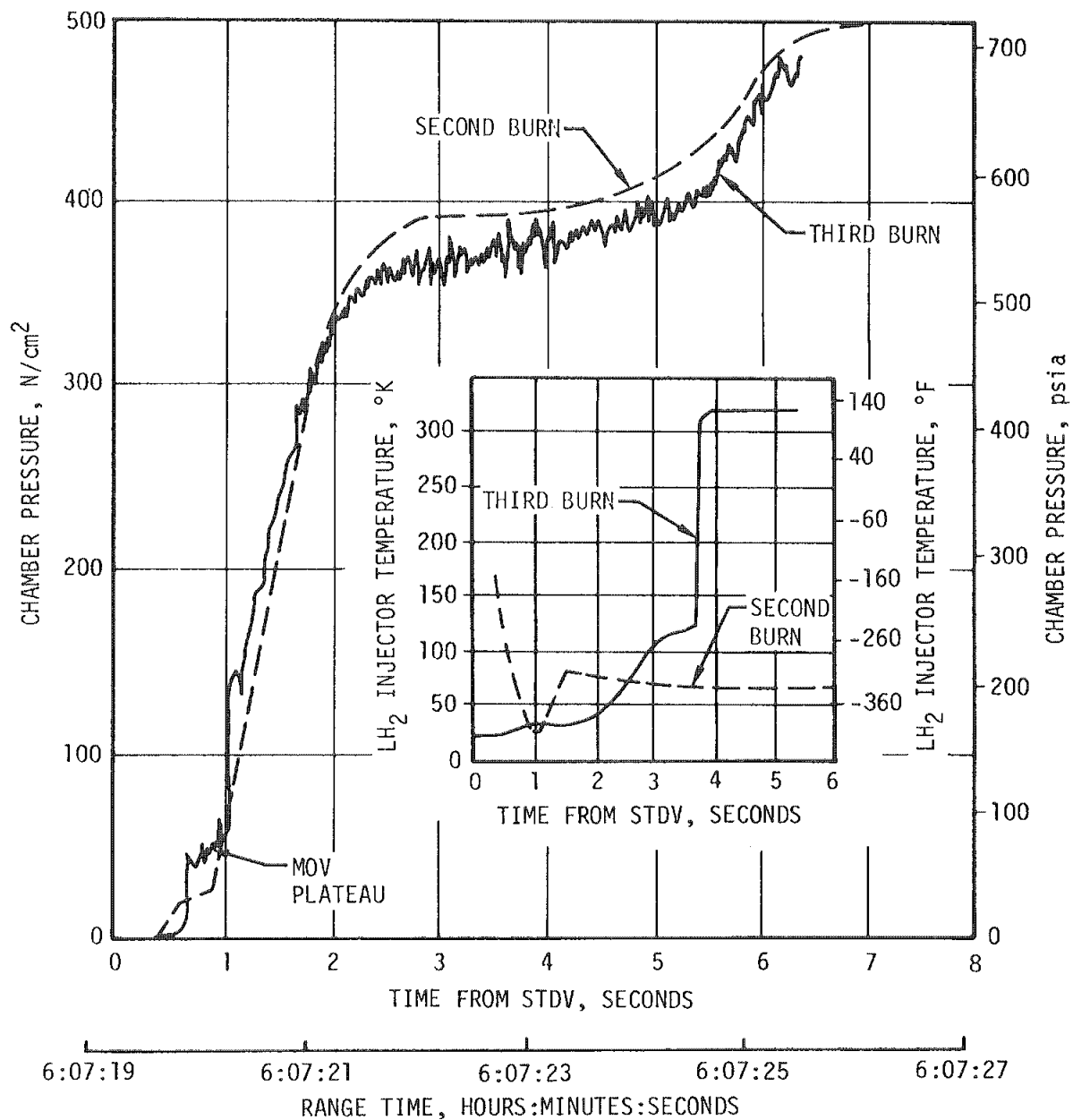


Figure 7-23. S-IVB Transient Chamber Pressure and LH<sub>2</sub> Injector Temperature - Third Burn

Table 7-8. S-IVB Engine Start Sequence Events - Third Burn

EVENT	TIME OF EVENT IN RANGE TIME (SECONDS)	
	PREDICTED	ACTUAL
S-IVB Engine Start Indication	22,024.92	22,030.93
S-IVB STDV Open Indication	22,032.79	22,039.260
S-IVB Thrust OK Signal-Switch 1 (on)	Not available	22,040.702
S-IVB Thrust OK Signal Switch 2 (on)	Not available	22,040.785
S-IVB Engine Cutoff at the J-2 Engine	22,275.33	22,281.32
S-IVB Thrust OK Signal Dropout Switch 1 (off)	Not available	22,281.509

pressure could "blow out" the gas generator spark plugs or severely damage the combustor. It is speculated at this time that the erratic behavior of the engine area ambient and thrust chamber jacket temperature measurements shown in Figure 7-28 were caused by hot gases escaping from the gas generator.

At STDV +50 seconds the engine pneumatic regulator pressure dropped as shown in Figure 7-29. At this time it is believed that the high vibration levels which accompany thrust chamber pressure oscillations caused the helium control solenoid valve to fail closed. Control bottle pressure did not decay after the loss of regulator pressure, as shown by Figure 7-30. Helium usage was estimated from flow rates to be approximately 0.953 kilograms (2.1 lbm) consumed during the burn; this value includes helium consumed during the extended fuel lead.

After engine pneumatic regulator pressure was lost, the accumulator pressure decayed to a level insufficient to keep the ASI LOX valve, GG valve, and LOX and fuel bleed valves fully open. The GG valve left the open position at 93 seconds after STDV as shown in Figure 7-31. The LOX bleed valve opened 6 seconds later, thus by-passing LOX flow back to the LOX tank and resulting in an engine chamber pressure decrease at STDV +99 seconds of 138 N/cm<sup>2</sup> (200 psid). An average LOX flowrate of 21.3 kg/s (47 lbm/s) was returning through the bleed valve to the LOX tank. At STDV +142 seconds the LH<sub>2</sub> bleed valve opened resulting in an additional

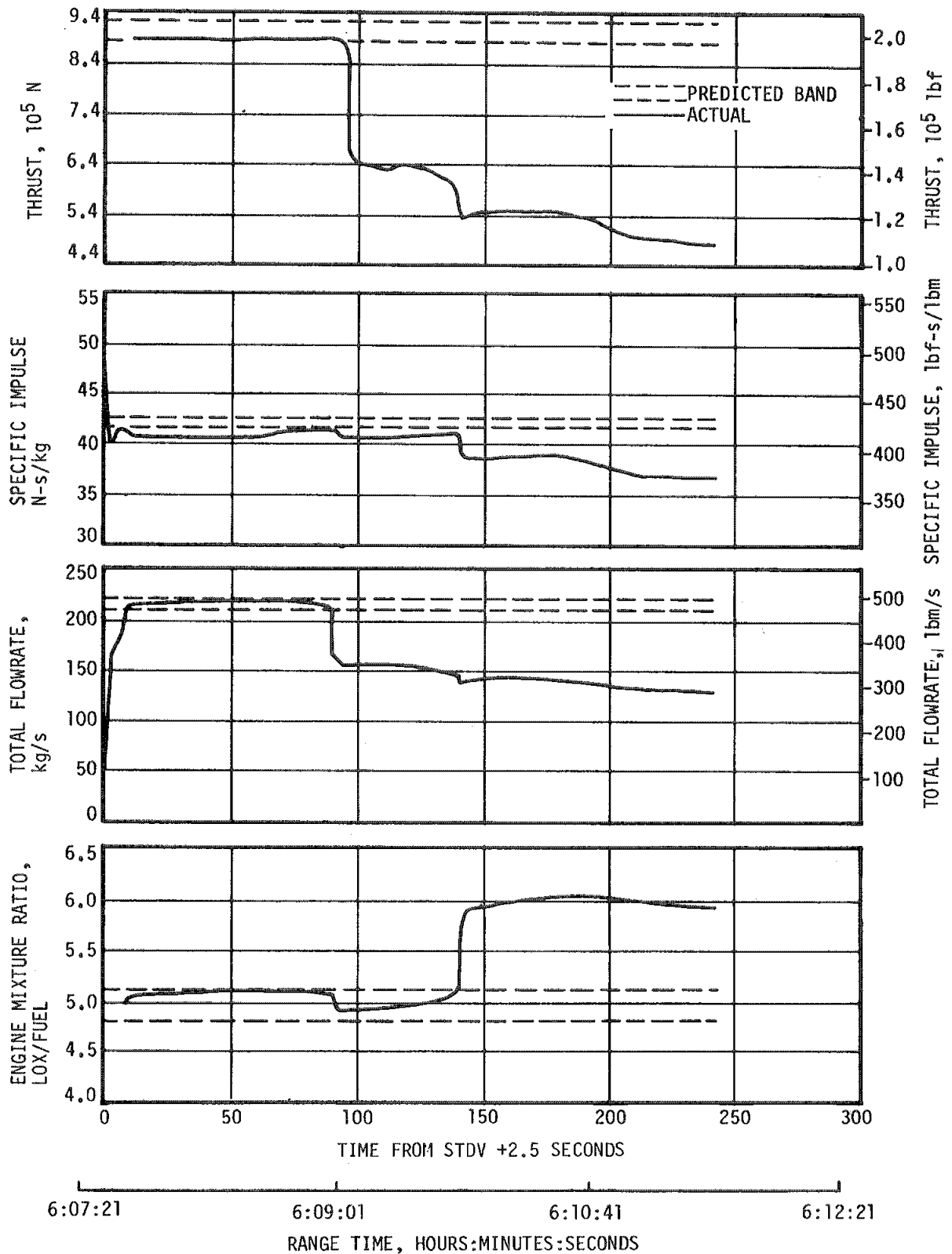


Figure 7-24. S-IVB Steady State Performance - Third Burn

Table 7-9. S-IVB Steady State Performance - Third Burn  
(STDV +60-Second Time Slice At Standard Altitude Conditions)

PARAMETER	FLIGHT** PREDICTED	ACTUAL	FLIGHT DEVIATION	PERCENT DEVIATION FROM PREDICTED
Thrust N* (lbf)	910,866 (204,771)	887,491 (199,516)	-23,375 (-5,255)	-2.57
Specific Impulse N-s/kg (lbf-s/lbm)	4207.8 (429.1)	4110.9 (419.2)	-96.9 (-9.9)	-2.31
LOX Flowrate kg/s (lbm/s)	179.77 (396.32)	180.21 (397.30)	+0.24 (+0.98)	0.25
Fuel Flowrate kg/s (lbm/s)	36.70 (80.91)	35.69 (78.68)	-1.01 (-2.23)	-2.76
Engine Mixture Ratio LOX/Fuel	4.898	(5.049)	0.151	0.31
* Based on chamber pressure ** Same as predicted for second burn				

34.48 N/cm<sup>2</sup> (50 psid) decrease in chamber pressure. During the remainder of mainstage the reduction in performance is due to the powered down condition of the GG. The erratic behavior of the MOV and Main Fuel Valve (MFV) position indication during burn can be attributed to the vibration levels present during third burn. MOV and MFV discrettes indicate that the valves were fully open throughout third burn.

Table 7-11 shows a comparison of the S-IVB stage flight reconstruction data with simulation and predicted data for third burn.

#### 7.12 S-IVB SHUTDOWN TRANSIENT PERFORMANCE FOR THIRD BURN

S-IVB ECO was initiated at STDV +242.06 seconds by a timed cutoff. The ECO transient was unusual due to the drop in performance during mainstage which resulted in a very low chamber pressure at cutoff as shown in Figure 7-32. Because of the low closing pressure required by the MOV and MFV there was sufficient accumulator pressure to close these valves at cutoff. The cutoff transient total impulse was 194,467 N-s (43,718 lbf-s) predicted as compared to 208,581 N-s (46,891 lbf-s) from actual engine data.

Table 7-10. S-IVB Third Burn Performance Comparison

PARAMETER	STDV + 60-SECOND DATA SLICE			ENGINE MFGR. 5-SECOND STABILITY TEST		
	SECOND BURN	THIRD BURN	DIFFERENCE	UNSTABLE	STABLE	DIFFERENCE
Chamber Pressure N/cm <sup>2</sup> (psia)	483.2 (700.8)	470.8 (682.9)	-12.4 (-17.9)	490.8 (711.8)	506.2 (734.2)	-15.4 (-22.4)
EMR	4.91	5.05	0.14	5.39	5.25	0.14
LOX Flowrate kg/s (lbm/s)	179.1 (394.8)	180.4 (397.7)	1.3 ( 2.9)	192.6 (424.7)	191.6 (422.4)	1.0 ( 2.3)
Fuel Flowrate kg/s (lbm/s)	36.5 (80.5)	35.7 (78.7)	-0.8 (-1.8)	35.7 (78.7)	36.5 (80.5)	-0.8 (-1.8)
LOX Pump Speed	7806	8021	115	8313	8261	52
Fuel Pump Speed	25,707	25,646	-61	25,903	25,887	16
Fuel Turb. Inlet Temp °K (°F)	870 (1106)	857 (1083)	-13 (-23)	933 (1219)	948 (1247)	-15 (-28)

### 7.13 S-IVB STAGE PROPELLANT MANAGEMENT

ON AS-504 the PU system was operated in the open-loop mode, which means the LOX flowrate is not controlled to insure simultaneous depletion of propellants. The PU system successfully accomplished the requirements associated with propellant loading.

A comparison of propellant mass values at the time of critical flight events determined from different analyses, is presented in Table 7-12. The best estimate full load propellant masses as presented in Section 21 are also shown in this table for comparison and are seen to be 0.41 percent greater than predicted for LOX and 0.46 percent greater than predicted for LH<sub>2</sub>. These deviations are within the required loading accuracy.

During first burn the PU valve was positioned at null for start, then shifted to the 5.5 EMR position for mainstage, and remained there, as programmed during first burn. The PU valve was commanded to the 4.5 EMR position 119.80 seconds prior to second burn start command, and remained there for 132.81 seconds. At Time Base 6 (T<sub>6</sub>) +582.96 seconds the valve was commanded to the null position (approximately 5.0 EMR) and remained there throughout the remainder of the second burn operation. For the second restart the valve was again positioned at the 4.5 EMR position for start and shifted to null (approximately 5.0 EMR) at T<sub>8</sub> +462.95 seconds where it remained for the duration of the third burn. The actual times are within 50 milliseconds of predicted.

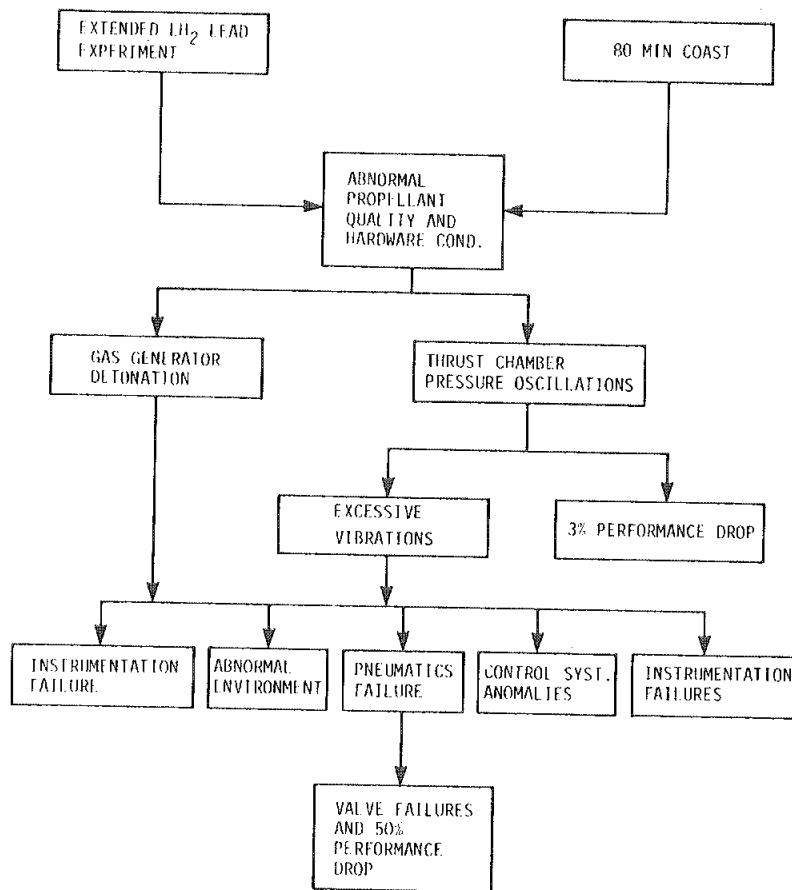


Figure 7-25. Flow Diagram, Summary of S-IVB Third Burn Anomalies

## 7.14 S-IVB PRESSURIZATION SYSTEM

### 7.14.1 S-IVB Fuel Pressurization System

The LH<sub>2</sub> tank prepressurization command was received at -97 seconds. The pressurized signal was received 17 seconds later. At the termination of prepressurization, the ullage pressure was at relief conditions, approximately 21.8 N/cm<sup>2</sup> (31.6 psia). The pressure decreased slightly and was at 21.4 N/cm<sup>2</sup> (31.1 psia) at liftoff, as shown in Figure 7-33.

A small ullage pressure collapse occurred during the first 20 seconds of boost, and the pressure then returned to the relief level at 60 seconds due to self-pressurization. Another ullage collapse occurred from 505 to 515 seconds, dropping pressure from 21.6 to 21.3 N/cm<sup>2</sup> (31.3 to 30.9 psia). This was caused by the LH<sub>2</sub> surface agitation induced by the S-II center engine vibration period. The pressure recovered to 21.6 N/cm<sup>2</sup> (31.4 psia) at ESC.

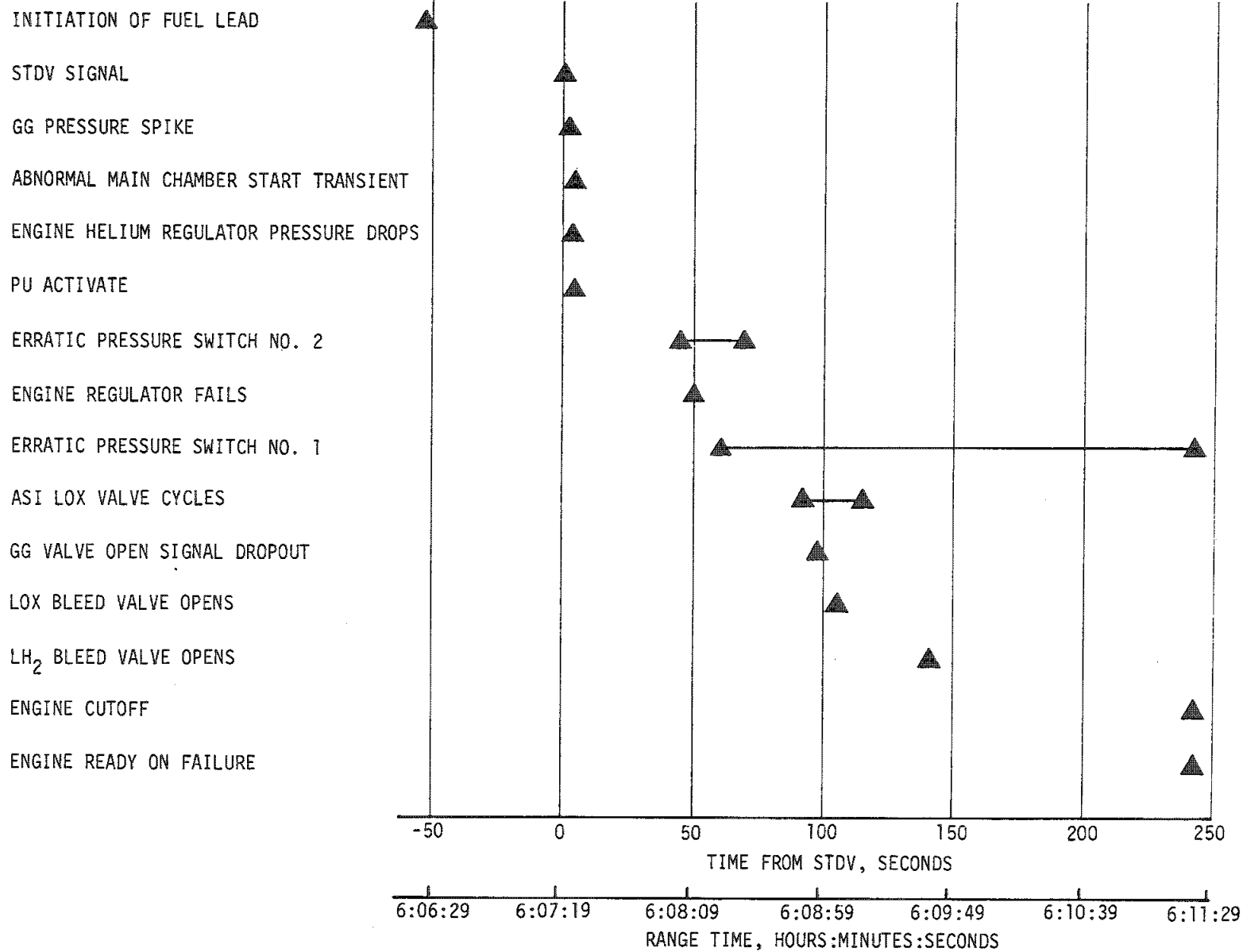


Figure 7-26. S-IVB Third Burn Sequence of Events

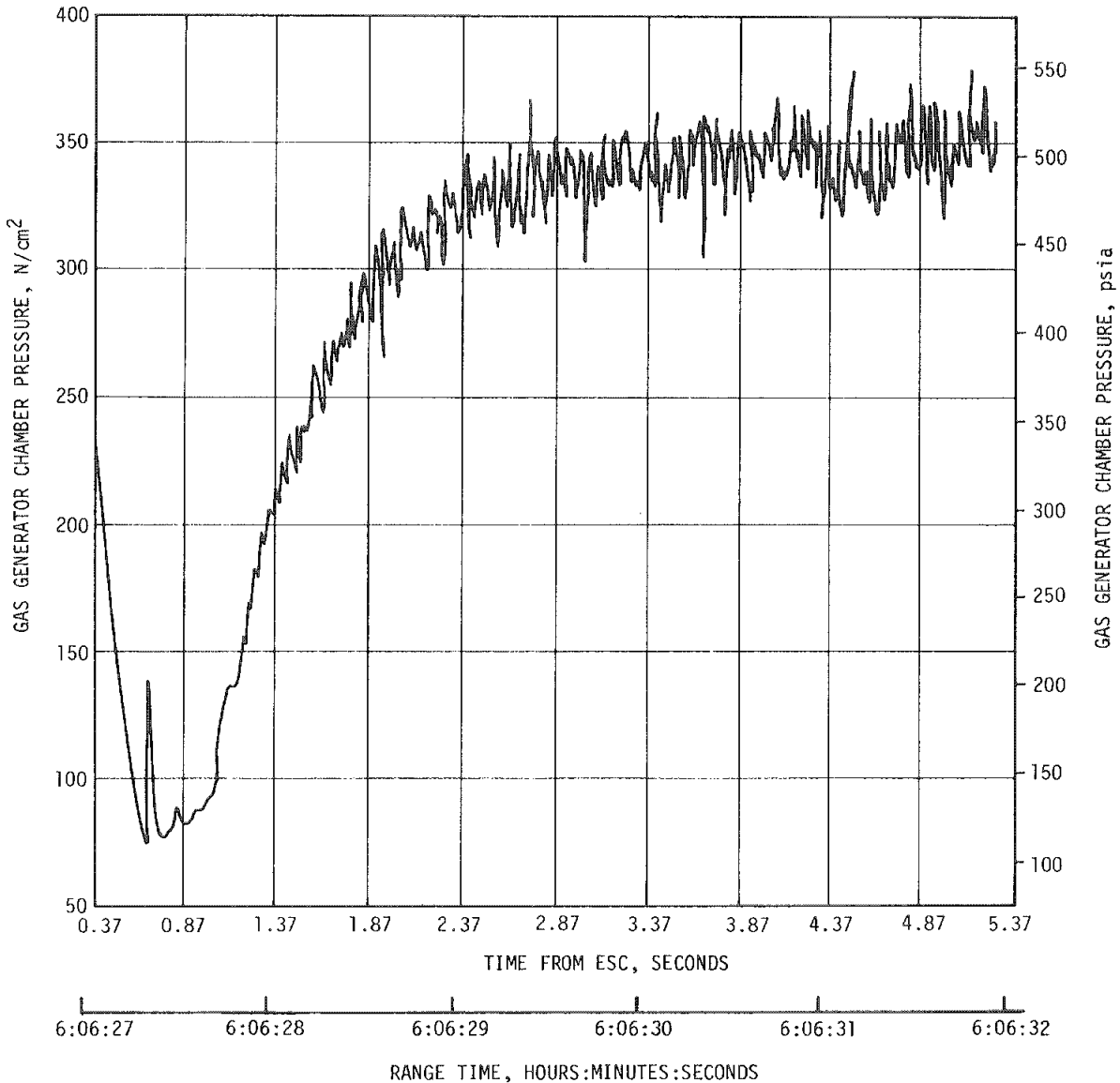


Figure 7-27. S-IVB Gas Generator Chamber Pressure - Third Burn Start Transient

During first burn, the average pressurization flowrate was approximately 0.35 kg/s (0.76 lbm/s) providing a total consumption of 42.3 kilograms (93.2 lbm). The ullage pressure was at the relief level throughout the burn as predicted.

During  $\text{O}_2/\text{H}_2$  burner repressurization for second burn, the  $\text{LH}_2$  tank was pressurized from 13.1 to 20.7  $\text{N/cm}^2$  (19.1 to 30.1 psia). The  $\text{LH}_2$  ullage



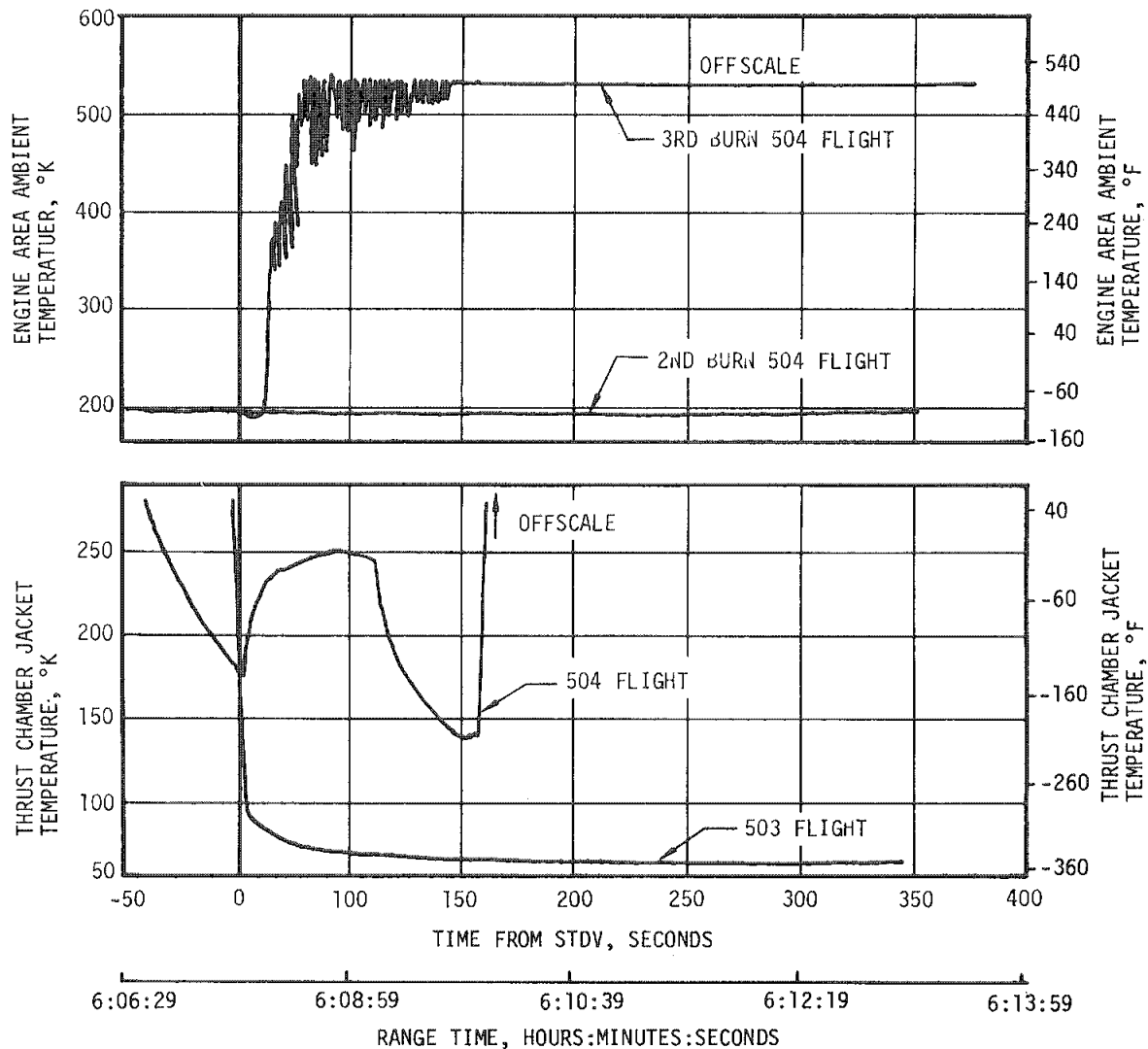


Figure 7-28. S-IVB Thrust Chamber Jacket and Engine Area Ambient Temperatures - Third Burn

pressure was 20.8 N/cm<sup>2</sup> (30.2 psia) at second burn ESC as shown in Figure 7-34. Approximately 11.1 kilograms (24.5 lbm) of helium were used in the repressurization operation. This provided a total of 95.3 kilograms (43.3 lbm) during second burn.

The ambient repressurization system was utilized to repressurize the fuel tank for third burn. Approximately 13.1 kilograms (28.9 lbm) of helium were added to the LH<sub>2</sub> tank during repressurization. Following the termination of repressurization at third STDV -32 seconds, the ullage pressure

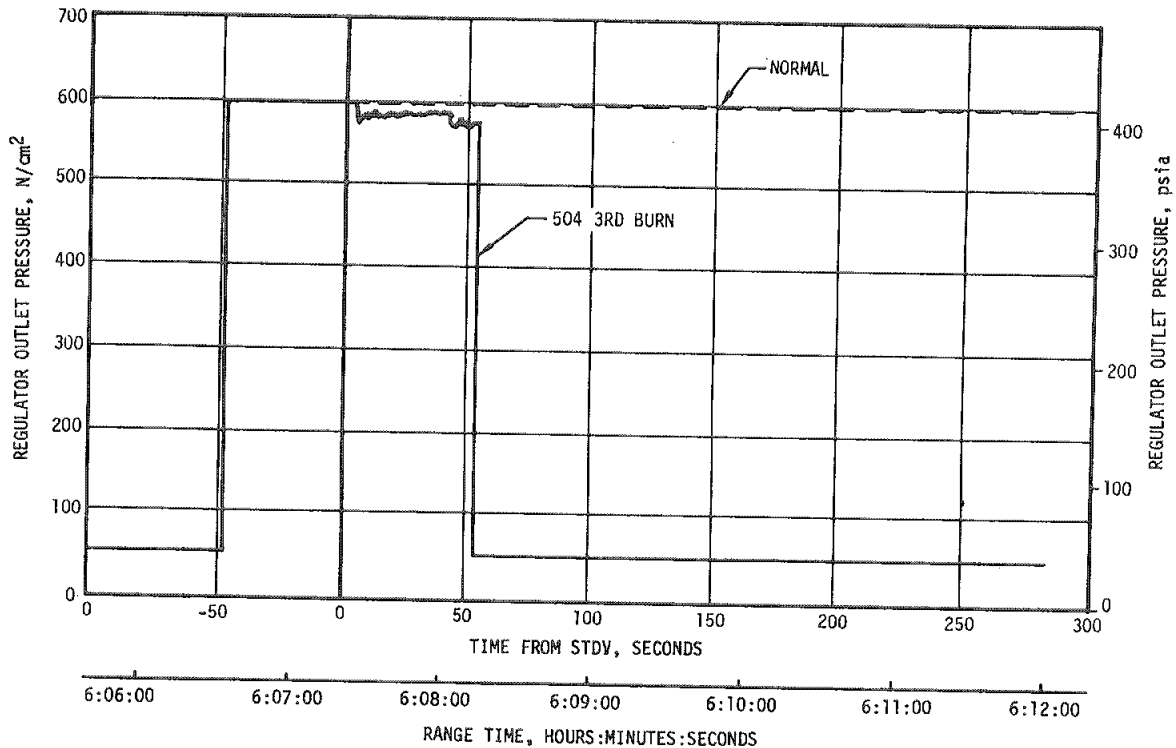


Figure 7-29. S-IVB Engine Regulator Outlet Pressure

decreased slightly to 20.4  $N/cm^2$  (29.6 psia) at third STDV as a result of ullage volume increase during fuel lead. The fuel pressurization system operated normally during third burn considering the changing engine performance. The total mass of  $GH_2$  added to the fuel tank was 54.8 kilograms (120.6 lbm).

The ullage pressure decrease and subsequent stabilization after the LOX bleed valve opened was the result of a new equilibrium condition being achieved after the shift in engine performance. After the  $LH_2$  bleed valve came open at STDV +142 seconds, these factors again changed, and in addition, return flow through the bleed valve was being added to the  $LH_2$  tank. The cumulative effect of all those factors caused the ullage pressure rise noted at that time.

Figures 7-35, 7-36, and 7-37 summarize the fuel pump inlet conditions for first, second, and third burns, respectively.

The  $LH_2$  pump inlet Net Positive Suction Pressure (NPSP) was calculated from the pump interface temperature and local pressure. These values indicated that the NPSP at first burn ESC was 10.5  $N/cm^2$  (15.2 psia).

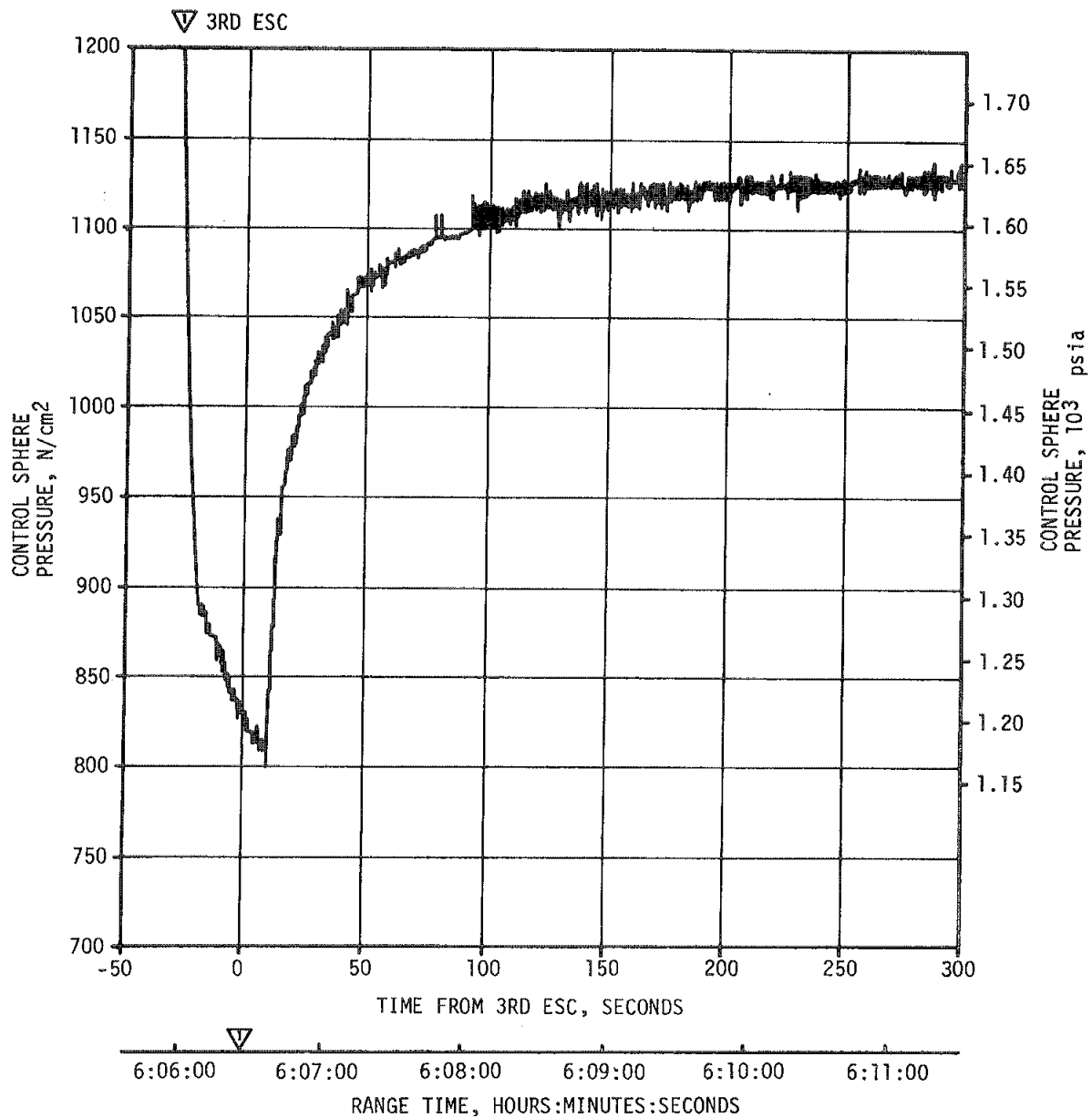


Figure 7-30. S-IVB Control Sphere Pressure - Third Burn

At the minimum point, the NPSP was  $3.7 \text{ N/cm}^2$  ( $5.4 \text{ psi}$ ) above that required. Throughout the burn NPSP was in satisfactory agreement with predicted.

The NPSP at second burn ESC was  $0.7 \text{ N/cm}^2$ . The failure of second burn fuel pump NPSP to meet minimum requirements at ESC is due to the pump inlet temperature not reaching a steady state level as discussed previously. This caused the temperature to be higher than normally seen

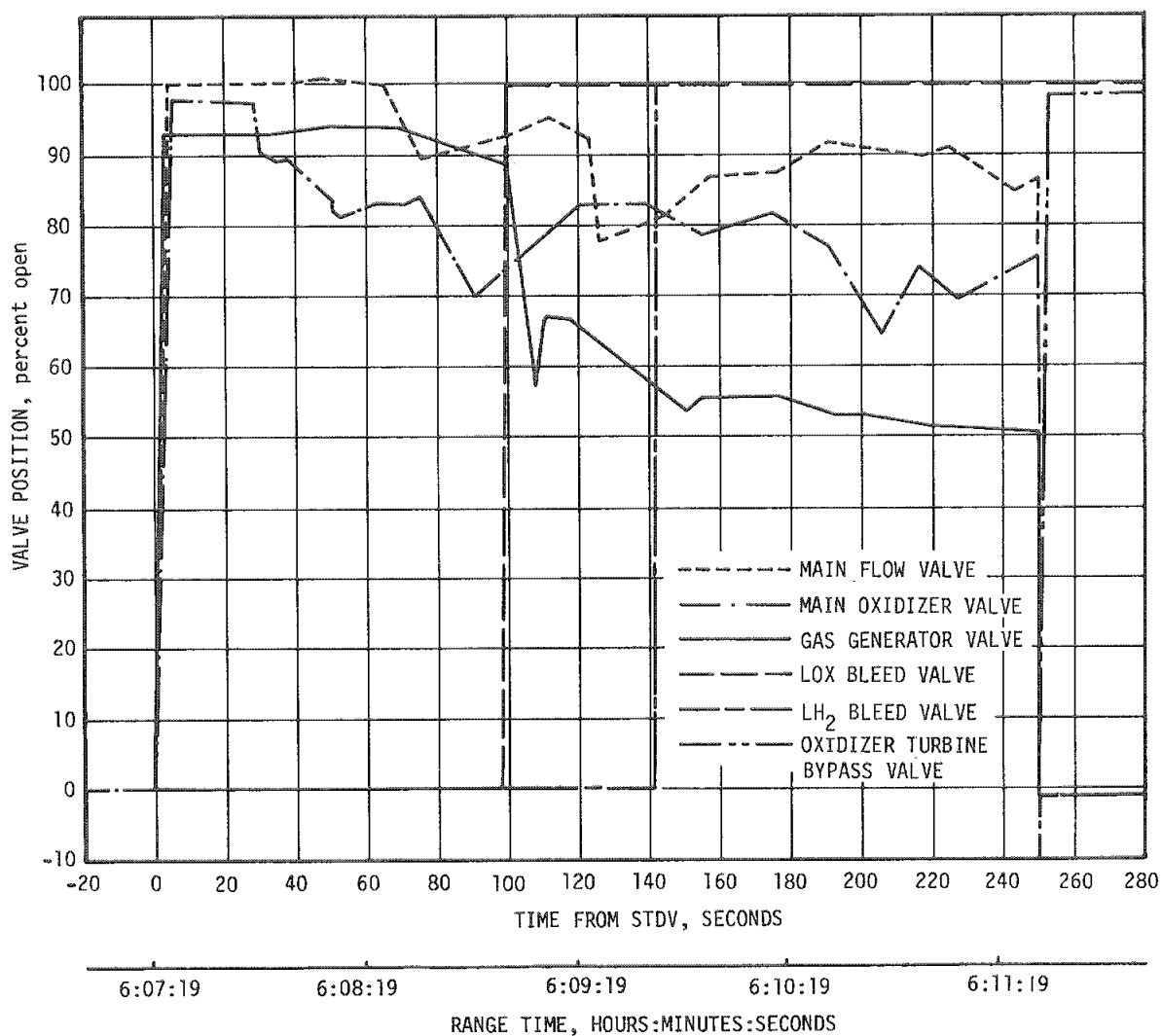


Figure 7-31. S-IVB Engine Valve Position - Third Burn

at the end of restart chilldown, raising the saturation at the pump inlet. At STDV, the NPSP was  $3.5 \text{ N/cm}^2$  (5.1 psia) which was  $0.4 \text{ N/cm}^2$  (0.6 psi) above start requirements.

The NPSP at third burn STDV was  $4.6 \text{ N/cm}^2$  (6.7 psia) which was  $1.5 \text{ N/cm}^2$  (2.2 psi) above the required. At STDV +142 seconds, the LH<sub>2</sub> bleed valve opened, allowing a portion of the J-2 engine fuel flow to be diverted back to the fuel tank. The high energy level of the returning

Table 7-11. Comparison of S-IVB Stage Flight Reconstruction Data With Performance Simulation Results - Third Burn

PARAMETERS	UNITS	PREDICTED	FLIGHT RECON- STRUCTION	PERCENT DEV. FROM PRED.	FLIGHT SIMULATION	PERCENT DEV. FROM PRED.
		THIRD BURN FLIGHT AVERAGE	THIRD BURN FLIGHT AVERAGE	THIRD BURN FLIGHT AVERAGE	THIRD BURN FLIGHT AVERAGE	THIRD BURN FLIGHT AVERAGE
*Longitudinal Vehicle Thrust	N (lbf)	908,100 (204,149)	686,116 (154,245)	-24.4	689,996 (155,125)	-24.0
Vehicle Mass Loss Rate	kg/s (lbf/s)	215.64 (475.4)	171.1 (377.3)	-20.6	169.2 (373.1)	-21.5
Longitudinal Vehicle Specific Impulse	N-s/kg (lbf-s/lbf)	4,212.0 (429.5)	4,008.7 (408.8)	-4.8	4062.6 (414.3)	-3.5

\*Based on chamber pressure

flow caused the LH<sub>2</sub> bulk temperature to rise. The resulting continual increase in pump inlet temperature reduced the available NPSP at the fuel pump interface. At STDV +196.4 seconds the rising pump inlet temperature caused the NPSP to fall below run requirements; the NPSP then remained below run requirements for the duration of third burn. Normally, the violation of NPSP run requirements would create a high probability of cavitation at the pump inlet, leading to possible pump damage. However, under the lower performance level due to the LOX and LH<sub>2</sub> bleed valves coming open, the probability of cavitation was significantly reduced.

#### 7.14.2 S-IVB LOX Pressurization System

LOX tank prepressurization was initiated at -167 seconds and increased the LOX tank ullage pressure from ambient to 28.1 N/cm<sup>2</sup> (40.8 psia) within 22 seconds as shown in Figure 7-38. Three makeup cycles were required to maintain the LOX tank ullage pressure before the ullage temperature stabilized.

During boost there was a relatively high rate of ullage pressure decay caused by an acceleration effect and temperature collapse. Makeup cycles were inhibited until 495 seconds. At that time, the LOX tank pressure switch was enabled, thus initiating a makeup cycle which increased the ullage pressure from 26.2 to 28.2 N/cm<sup>2</sup> (38.0 to 41.0 psia). The LOX tank ullage pressure was 28.1 N/cm<sup>2</sup> (40.8 psia) at ESC.

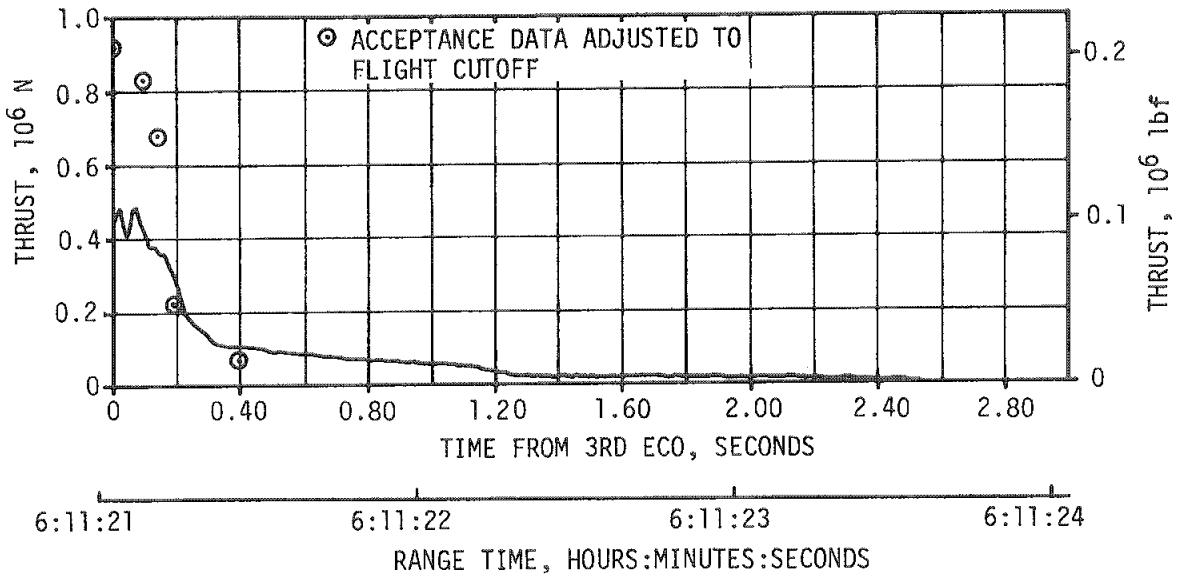


Figure 7-32. S-IVB Shutdown Transient Performance - Third Burn

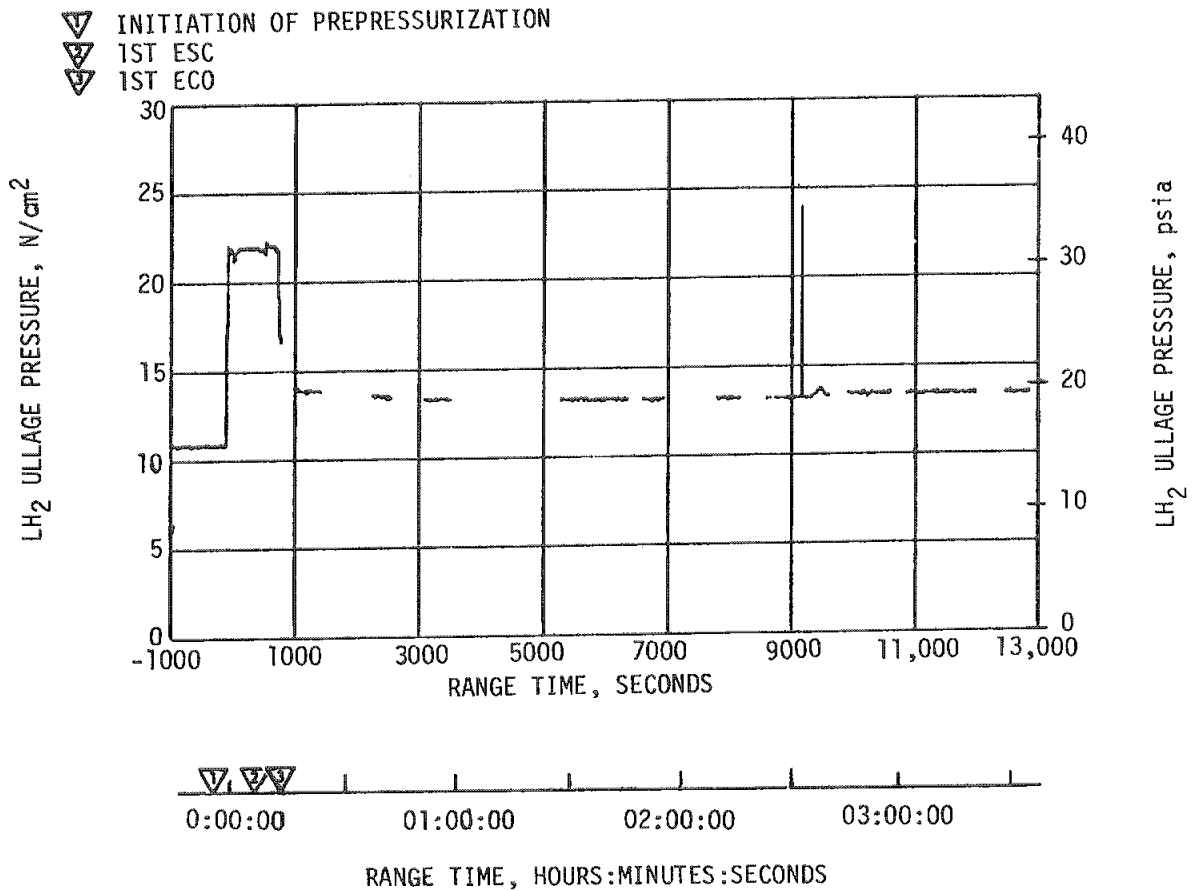


Figure 7-33. S-IVB LH<sub>2</sub> Ullage Pressure - First Burn and Parking Orbit

Table 7-12. S-IVB Stage Propellant Mass History

EVENT		PREDICTED		PU INDICATED (CORRECTED)		PU VOLUMETRIC		FLOW INTEGRAL		BEST ESTIMATE	
		LOX	LH <sub>2</sub>	LOX	LH <sub>2</sub>	LOX	LH <sub>2</sub>	LOX	LH <sub>2</sub>	LOX	LH <sub>2</sub>
S-IC Liftoff	kg (1bm)	85,686 (188,906)	19,737 (43,513)	85,823 (189,204)	19,742 (43,522)	86,028 (189,659)	19,871 (43,807)	86,137 (189,900)	19,761 (43,565)	86,040 (189,686)	19,826 (43,709)
First Ignition (ESC)	kg (1bm)	85,686 (188,906)	19,737 (43,513)	85,771 (189,089)	19,717 (43,467)	86,026 (189,654)	19,871 (43,807)	86,137 (189,900)	19,761 (43,565)	86,040 (189,686)	19,826 (43,709)
First Cutoff (ECO)	kg (1bm)	62,480 (137,744)	15,425 (34,000)	60,445 (133,257)	14,910 (32,870)	60,614 (133,632)	15,030 (33,135)	60,433 (133,232)	15,013 (33,098)	60,519 (133,421)	14,968 (32,999)
Second Ignition (ESC)	kg (1bm)	62,233 (137,202)	13,669 (30,135)	60,294 (132,923)	13,293 (29,305)	60,447 (133,263)	13,320 (29,516)	60,288 (132,913)	13,387 (29,513)	60,322 (132,988)	13,321 (29,369)
Second Cutoff (ECO)	kg (1bm)	51,471 (113,474)	11,434 (25,208)	49,141 (108,930)	11,033 (29,323)	49,575 (109,295)	11,131 (24,540)	49,558 (109,257)	11,139 (24,558)	49,577 (109,298)	11,102 (24,476)
Third Ignition (ESC)	kg (1bm)	51,367 (113,245)	11,064 (24,391)	49,339 (108,772)	10,675 (23,534)	49,494 (109,117)	10,736 (23,669)	49,444 (109,005)	10,904 (24,040)	49,408 (108,927)	10,668 (23,520)
Third Cutoff (ECO)	kg (1bm)	8538 (18,824)	2195 (4840)	15,367 (33,877)	4060 (8950)	15,473 (34,112)	4045 (8917)	15,473 (34,112)	4045 (8917)	15,445 (34,051)	4060 (8951)

During parking orbit, at 9241 seconds, the maneuver to transposition and docking attitude caused a rise in LOX ullage pressure from 26.8 to 29.4 N/cm<sup>2</sup> (38.9 to 42.7 psia). This was greater than the 1.2 N/cm<sup>2</sup> (1.8 psi) predicted increase, as shown in Figure 7-38, possibly due to greater than expected ullage heating.

Repressurization of the LOX tank prior to second burn was not required. The tank ullage pressure was 29.1 N/cm<sup>2</sup> (42.3 psia) at second ESC, satisfying the engine start requirements as shown in Figure 7-39. Pressurization system performance during second burn was satisfactory. There were no over-control cycles as compared to one predicted.

Repressurization of the LOX tank prior to third burn was not required. During third burn the system responded to engine performance changes which affected the otherwise normal operation. When the engine LOX bleed valve opened at STDV +99 seconds, LOX was returned to the LOX tank through the return line. This resulted in lower than normal net usage of LOX and also added heat to the LOX bulk. Since the pressurizing helium flow continued at a slightly increased rate, LOX ullage pressure increased rapidly and reached relief pressure within 50 seconds. Five Non Propulsive Vent (NPV) cycles occurred before ECO.

Heat exchanger performance was satisfactory up to third burn but at that time deviated somewhat from normal because of engine anomalies. Heat exchanger outlet temperature decreased in response to LOX bleed valve opening and then increased again after the LH<sub>2</sub> bleed valve opened at STDV +142 seconds. These temperature changes occurred in response to turbine exhaust gases in the heat exchanger which vary with turbine power level and mixture ratio changes caused by the opening of the bleed valves.

The LOX NPSP was 18.4 N/cm<sup>2</sup> (26.7 psi) at first burn STDV. This was 2.7 N/cm<sup>2</sup> (3.9 psi) above the required NPSP at that time. The LOX pump static pressure during first burn followed the cyclic trends of the LOX tank ullage pressure.

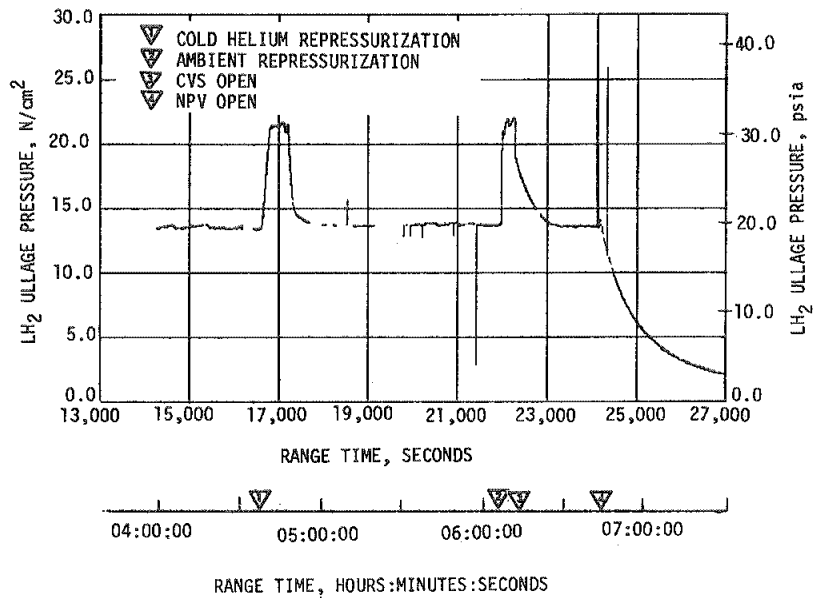


Figure 7-34. S-IVB Ullage Pressure - Second and Third Burn

The NPSP calculated at the engine interface was 16.8 N/cm<sup>2</sup> (24.4 psia) at second burn STDV. At all times during second burn, NPSP was above the required level. Figures 7-40, 7-41, and 7-42 summarize the LOX pump conditions for first burn, second burn, and third burn respectively.

At third burn STDV +99 seconds the LOX bleed valve opened and allowed high energy LOX to return to the LOX tank. This resulted in a gradual increase in the LOX bulk and LOX pump inlet temperatures, and caused a small reduction in NPSP. However, the NPSP remained well above the required level at all times.

The cold helium supply was adequate to meet all flight requirements. At liftoff the cold helium spheres contained 172 kilograms (379 lbm). During the 123.8-second first burn 19.1 kilograms (42 lbm) of cold helium were consumed. During a 180.4-second O<sub>2</sub>/H<sub>2</sub> burner repressurization of the LH<sub>2</sub> tank, 11.1 kilograms (24.5 lbm) of cold helium were consumed. During a 62.06-second second burn, 8.8 kilograms (19.3 lbm) of cold helium were consumed. During a 242-second third burn, 42.3 kilograms (93.1 lbm) of cold helium were consumed. At third burn ECO the cold helium spheres contained 90.8 kilograms (200 lbm) of cold helium.

#### 7.15 S-IVB PNEUMATIC CONTROL PRESSURE SYSTEM

The stage pneumatic control and purge system performed adequately during all phases of the mission. During the early stages of the countdown at



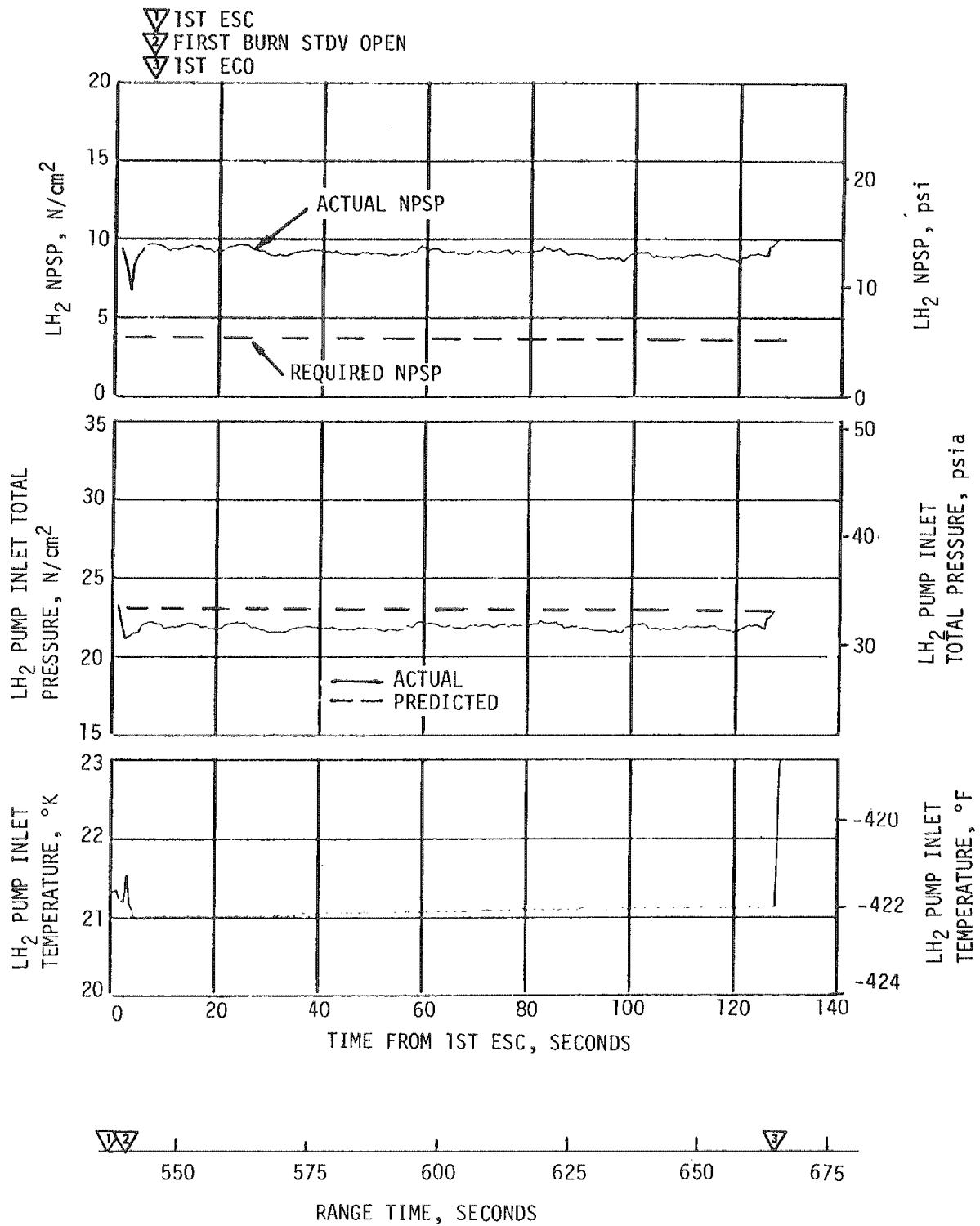
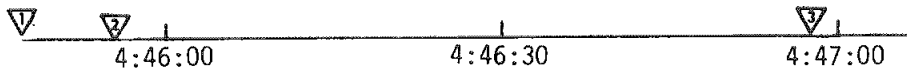
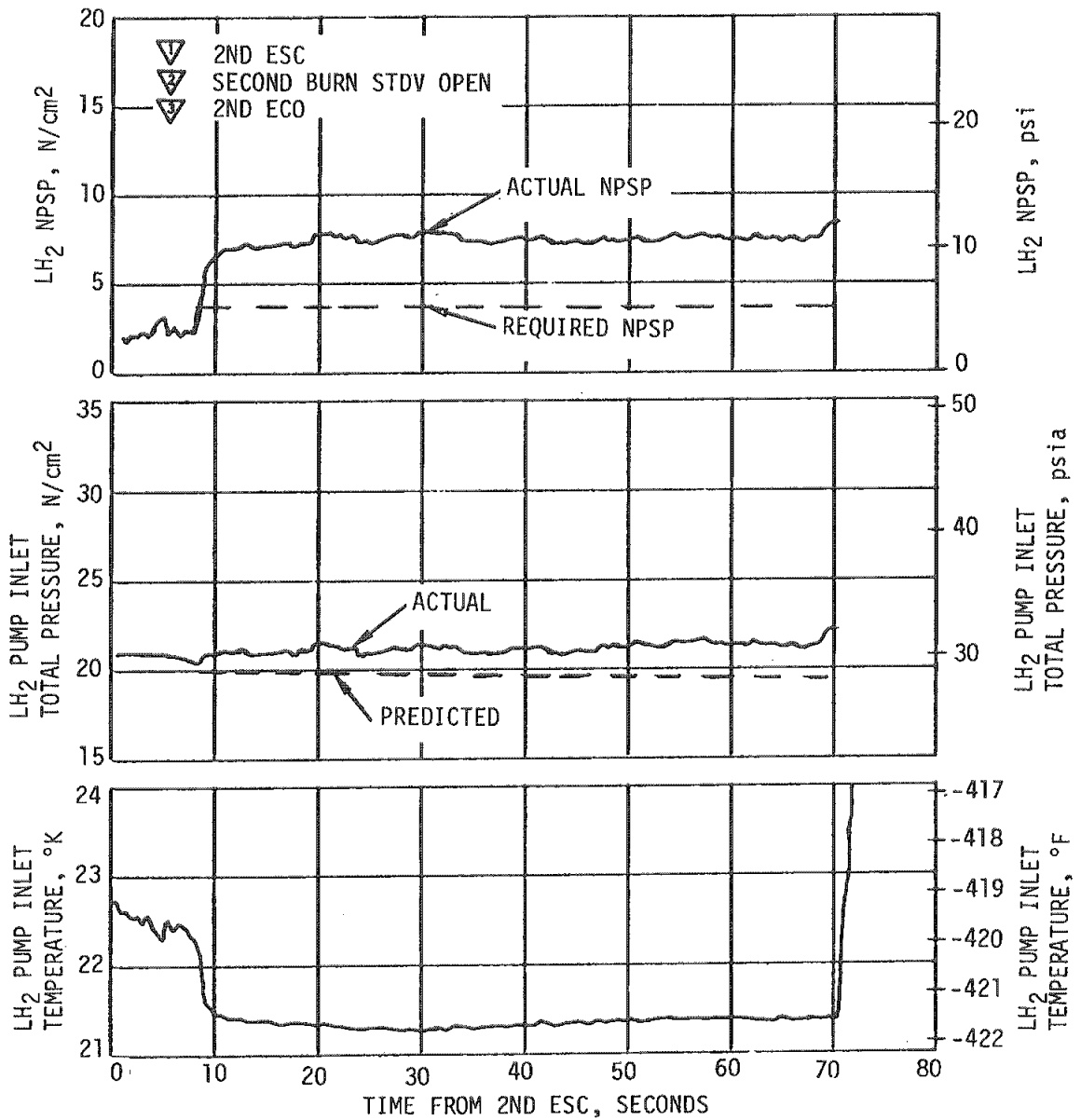


Figure 7-35. S-IVB Fuel Pump Inlet Conditions - First Burn



RANGE TIME, HOURS:MINUTES:SECONDS

Figure 7-36. S-IVB Fuel Pump Inlet Conditions - Second Burn

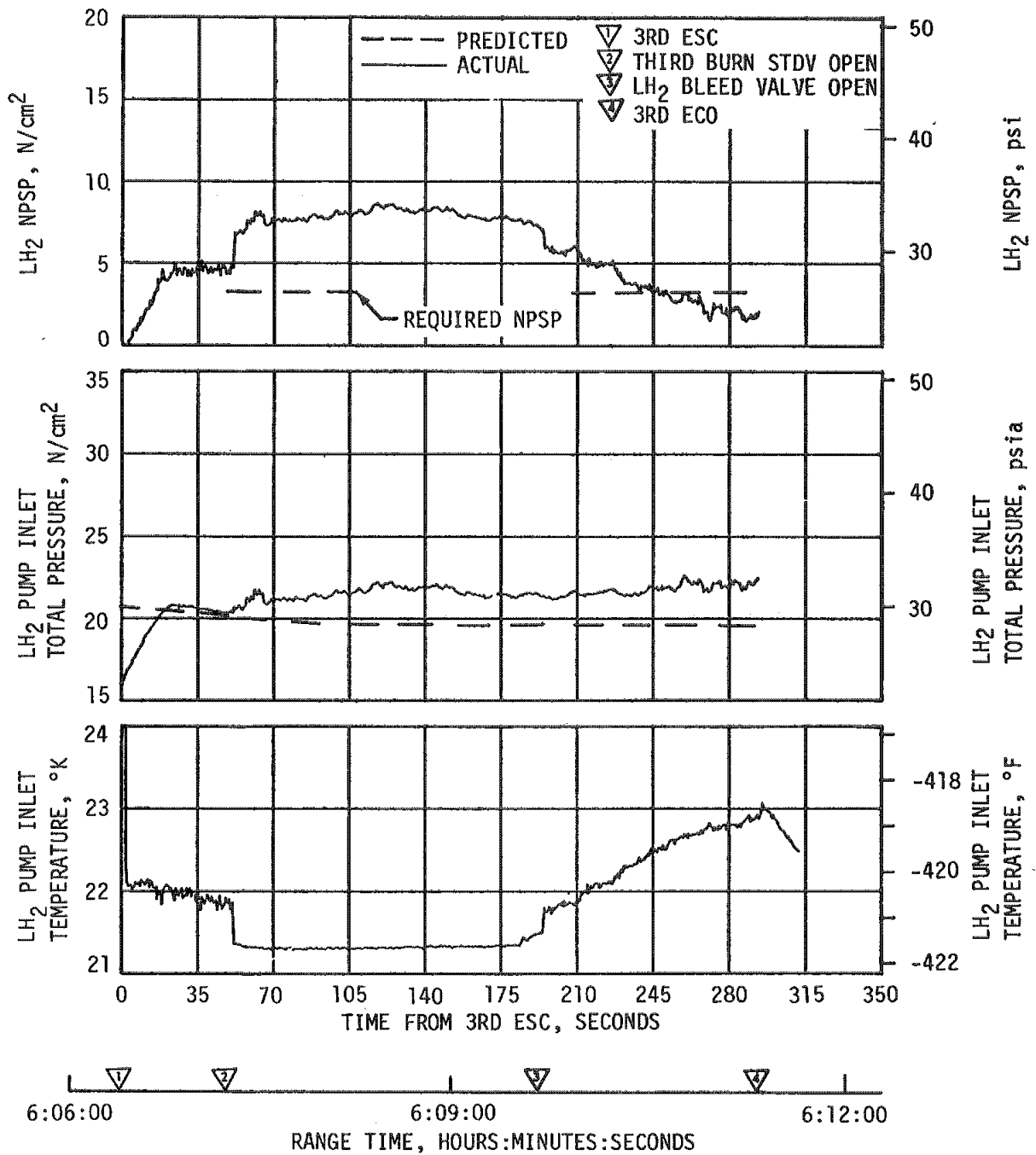


Figure 7-37. S-IVB Fuel Pump Inlet Conditions - Third Burn

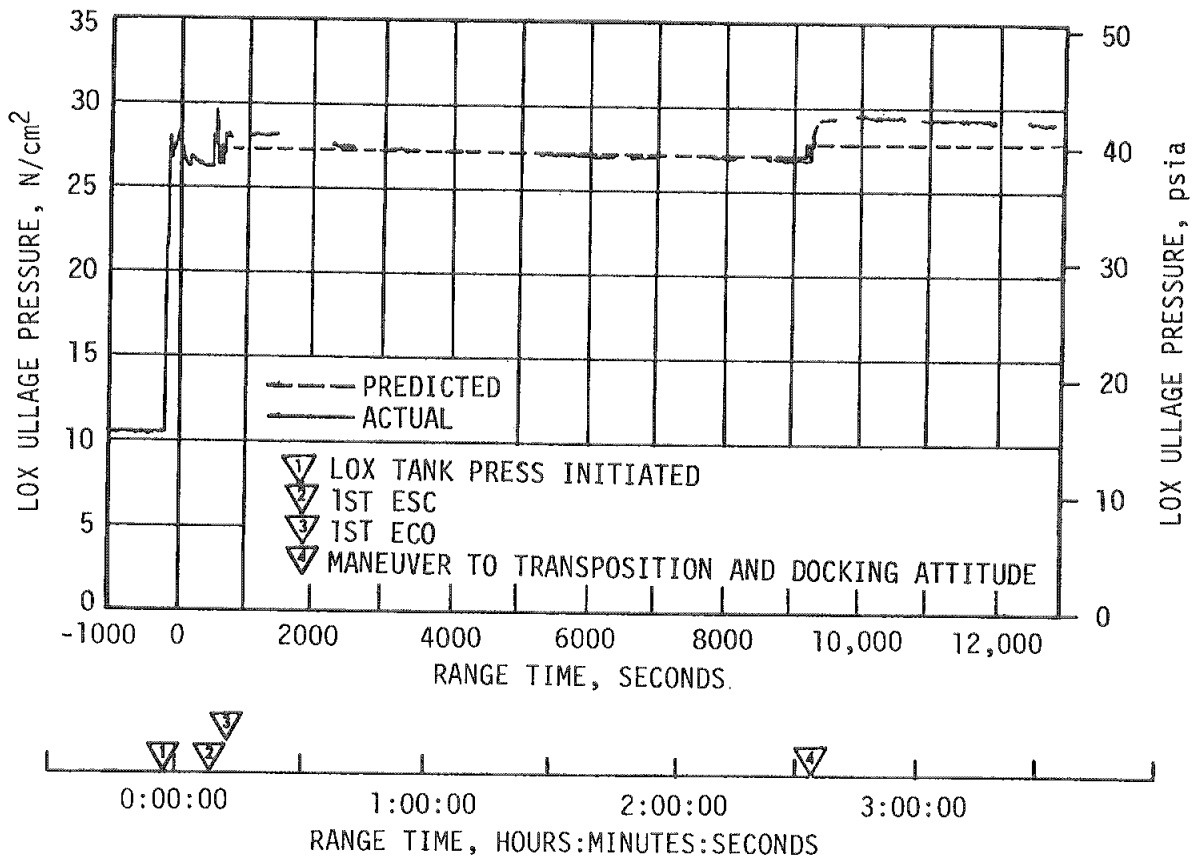


Figure 7-38. S-IVB LOX Tank Ullage Pressure - First Burn And Parking Orbit

approximately -3:07:00, the regulator discharge pressure was high 420.6 to 427.5  $N/cm^2$  (610 to 620 psia). As a result, the module outlet pressure was controlled by the backup system, a pressure switch and shutoff valve in the pneumatic power control module. Specified redlines precluded liftoff with the pressure above 427.9  $N/cm^2$  (585 psia), or with the regulator malfunctioning; however, re-evaluation of the situation resulted in raising the redline limit to 434.4  $N/cm^2$  (630 psia), and defining backup operation as acceptable for launch.

Prior to liftoff, pressure control was resumed by the primary system regulator. The regulator was regulating high during boost and higher

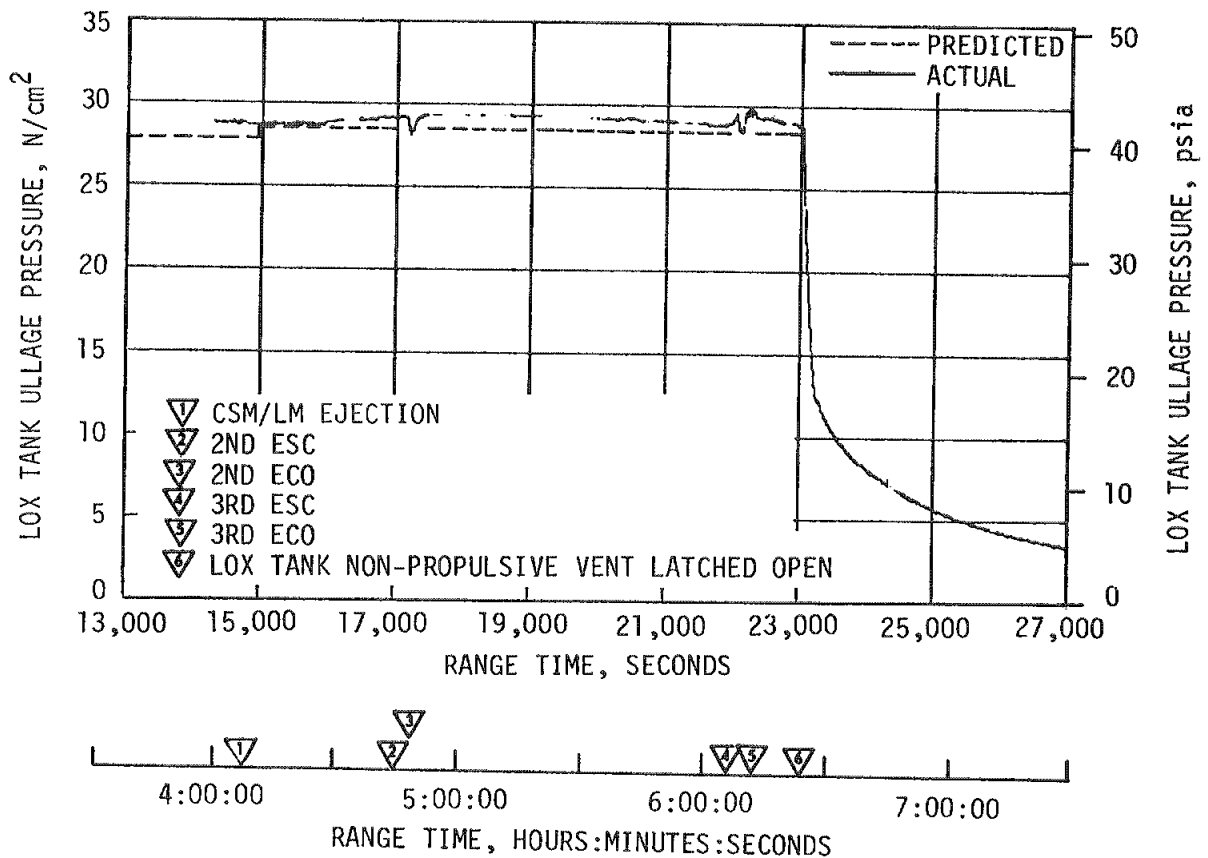


Figure 7-39. S-IVB LOX Tank Ullage Pressure - Second Burn, Intermediate Coast and Third Burn

than normal during the majority of coast. The higher regulator outlet pressure had no adverse effect on component or system functioning. Pneumatic control bottle temperature and pressure, and regulator outlet pressure are shown in Figure 7-43. Bottle masses at pertinent times are shown in Table 7-13. During third burn preparation, shortly after CVS closure, the pneumatic control system went into backup mode. This backup regulation lasted approximately 205 seconds. During this time interval the regulator discharge pressure dropped from 427  $N/cm^2$  (620 psia) to

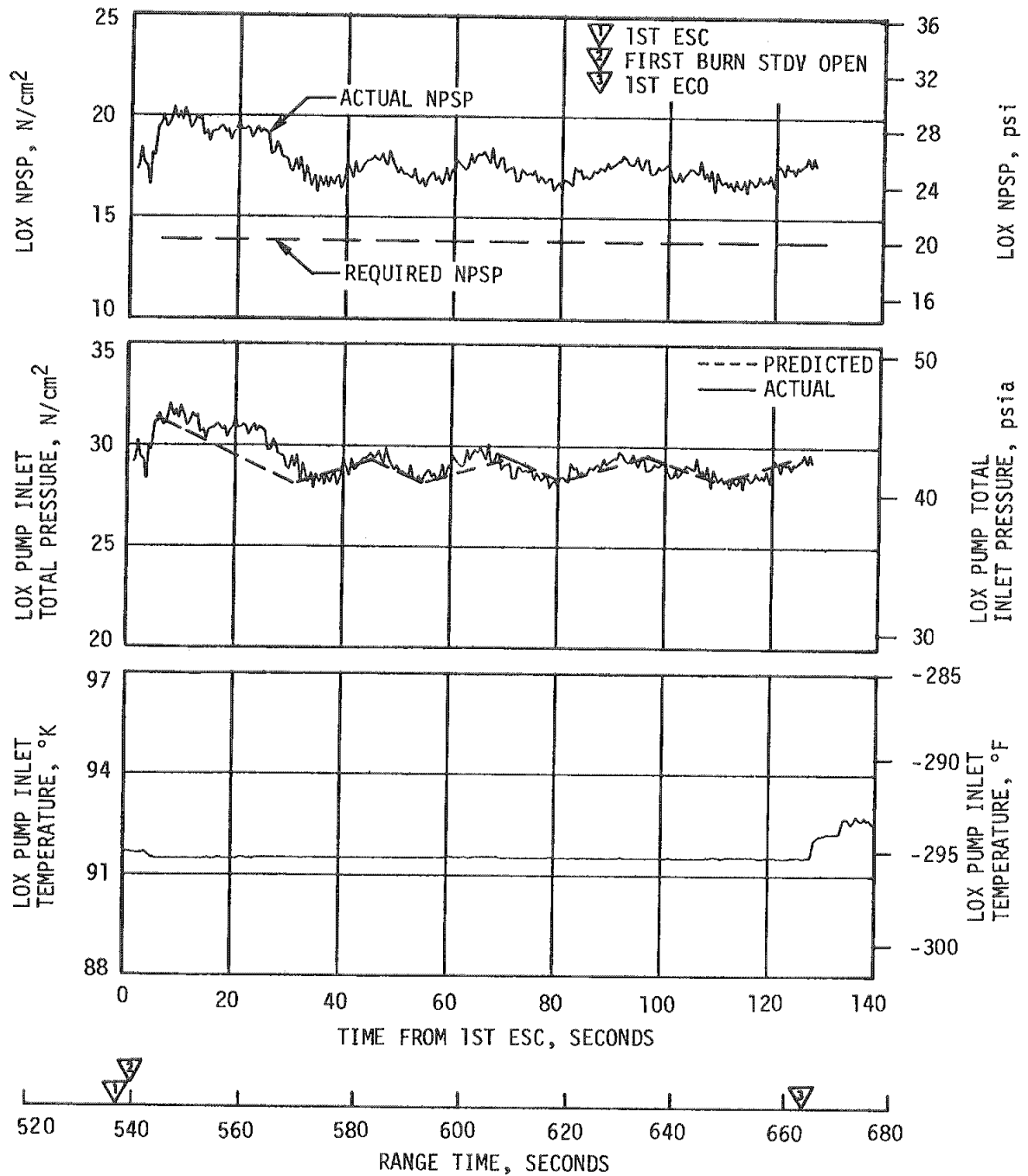


Figure 7-40. S-IVB LOX Pump Inlet Conditions - First Burn

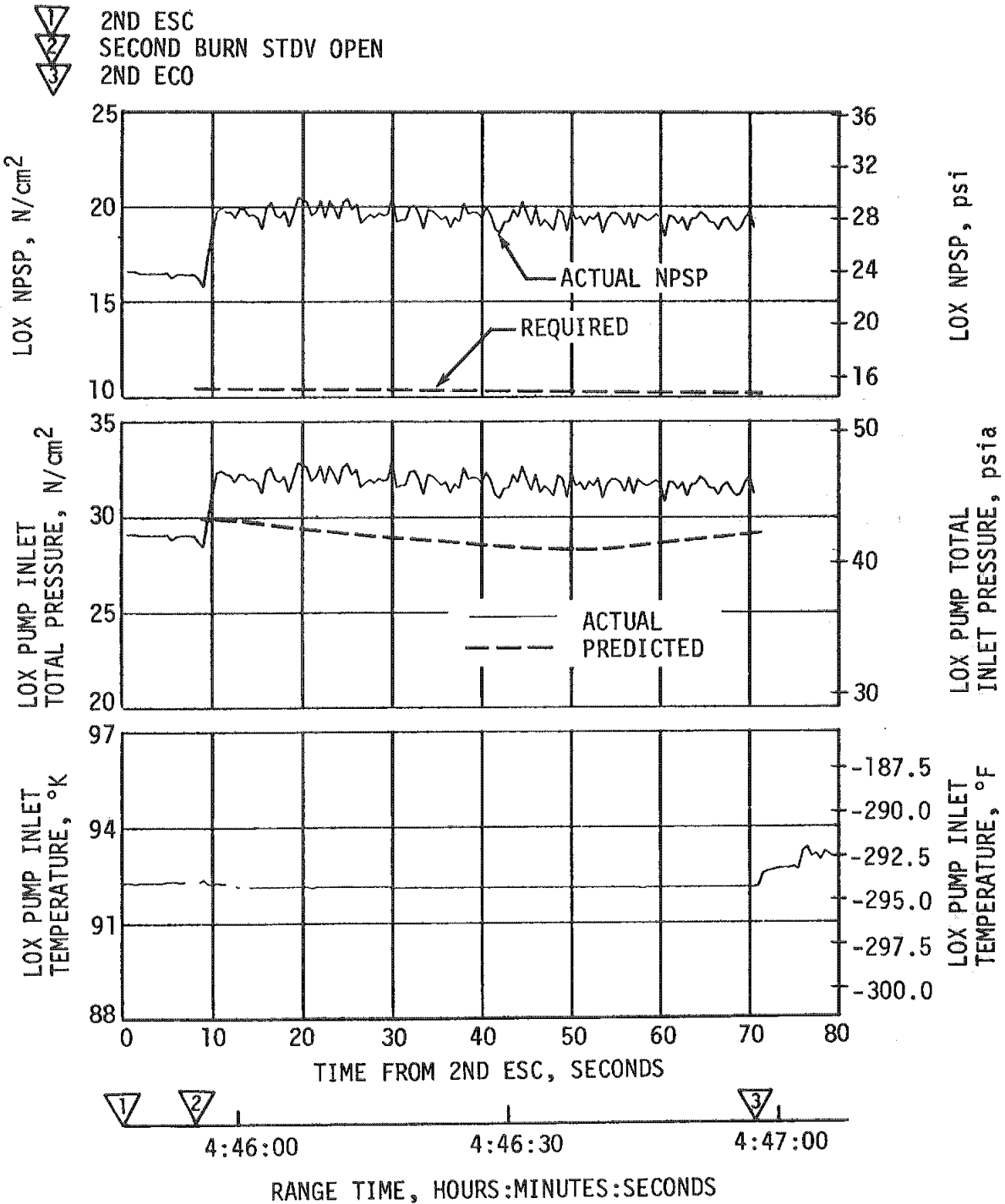


Figure 7-41. S-IVB LOX Pump Inlet Conditions - Second Burn

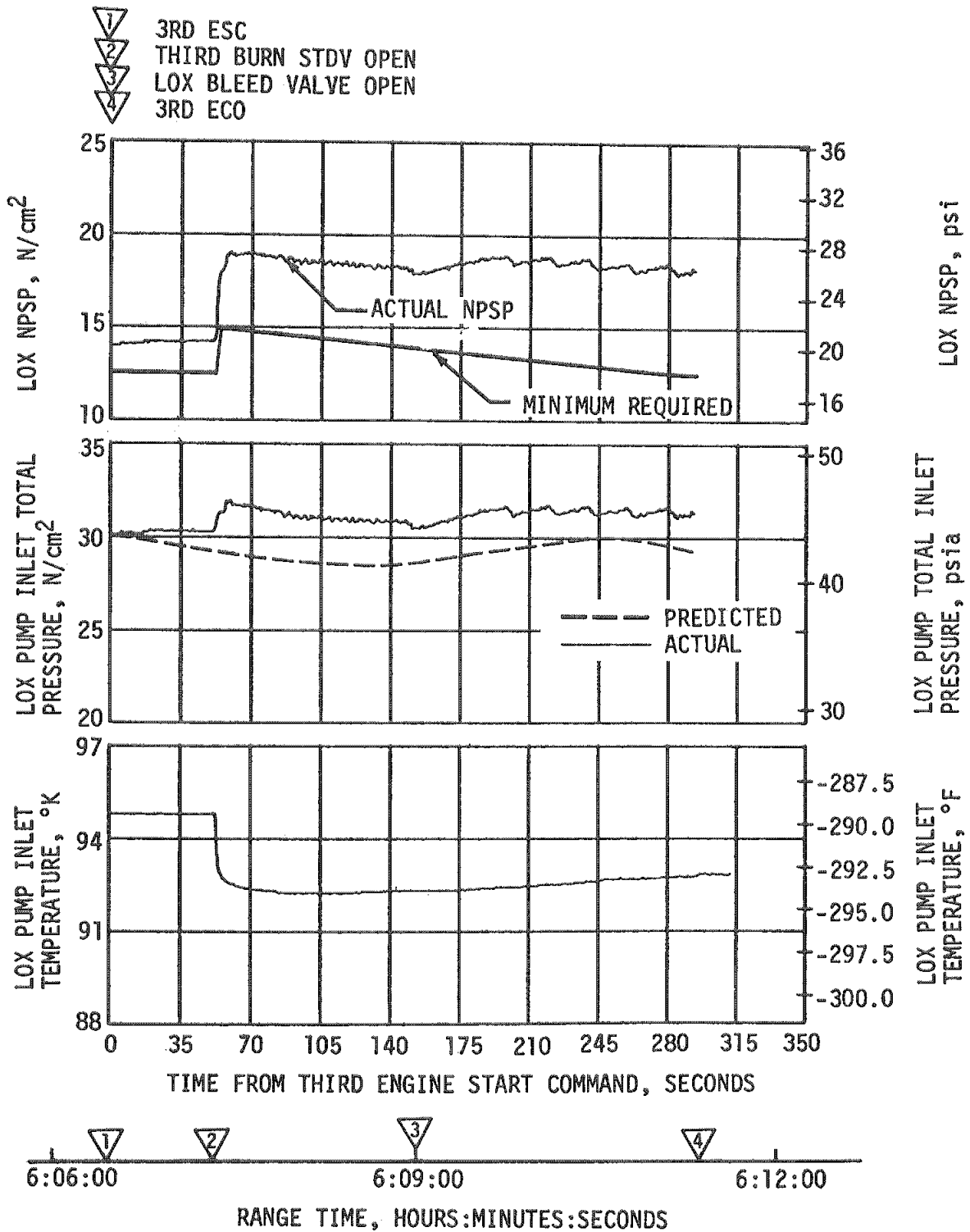


Figure 7-42. S-IVB LOX Pump Inlet Conditions - Third Burn





PREVALVES OPEN  
ENGINE PUMP PURGE OFF

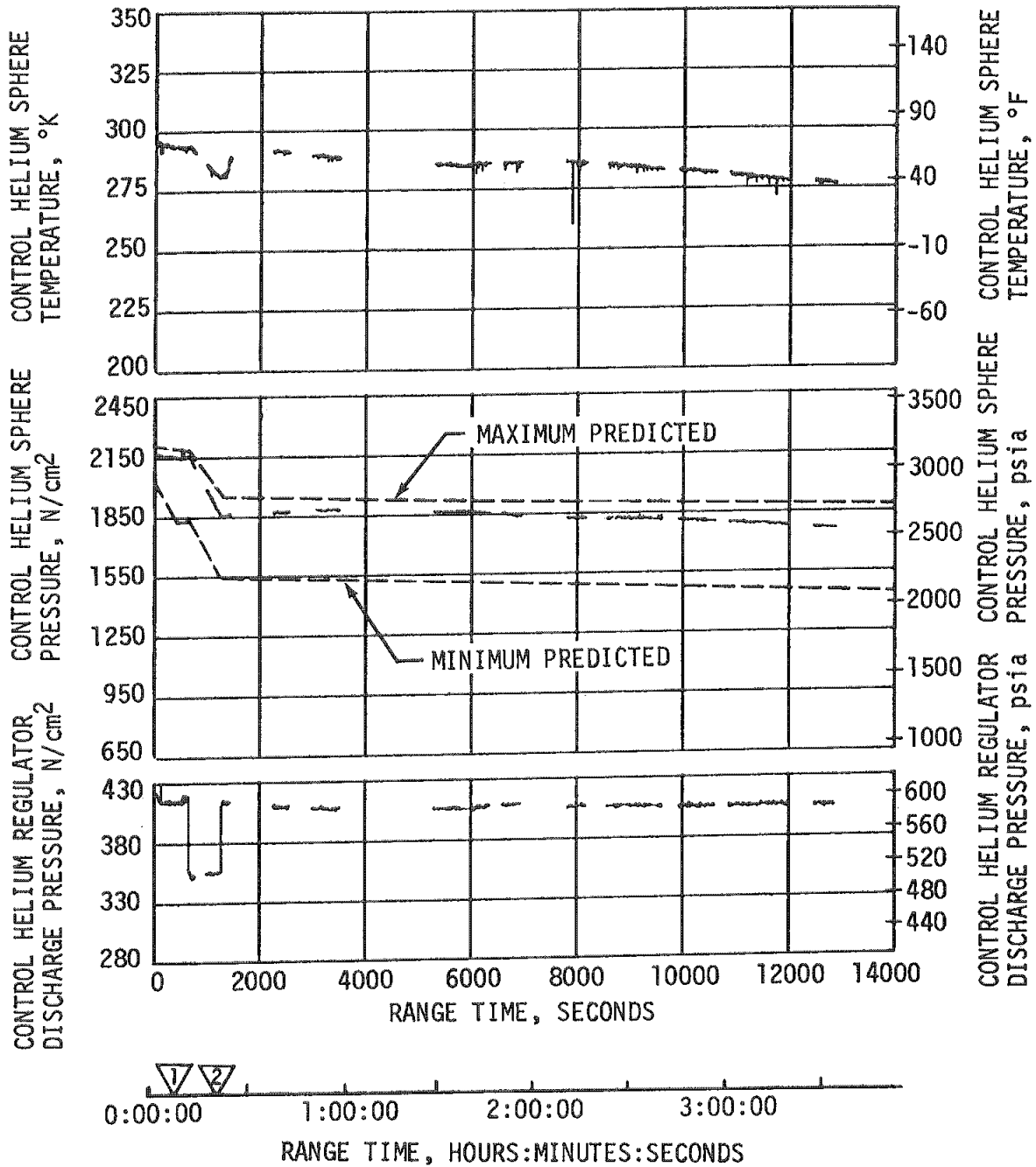


Figure 7-43. S-IVB Pneumatic Control Performance  
(Sheet 1 of 2)

- ▽ LOX AND LH<sub>2</sub> VENT VALVES BOOST CLOSED, O<sub>2</sub>/H<sub>2</sub> BURNER PROPELLANT VALVES OPEN AND CONTINUOUS VENT SYSTEM CLOSE
- ▽ PREVALVES CLOSED
- ▽ ENGINE PUMP PURGE ON AND LH<sub>2</sub> TANK CVS VALVE OPEN
- ▽ LOX AND LH<sub>2</sub> VENT BOOST CLOSED
- ▽ PREVALVES OPEN O<sub>2</sub>/H<sub>2</sub> BURNER FUEL VALVE CLOSED, BURNER LOX VALVE CLOSED, LH<sub>2</sub> TANK CVS VALVE CLOSED
- ▽ ENGINE PUMP PURGE ON
- ▽ LH<sub>2</sub> TANK LATCHING VALVE OPEN

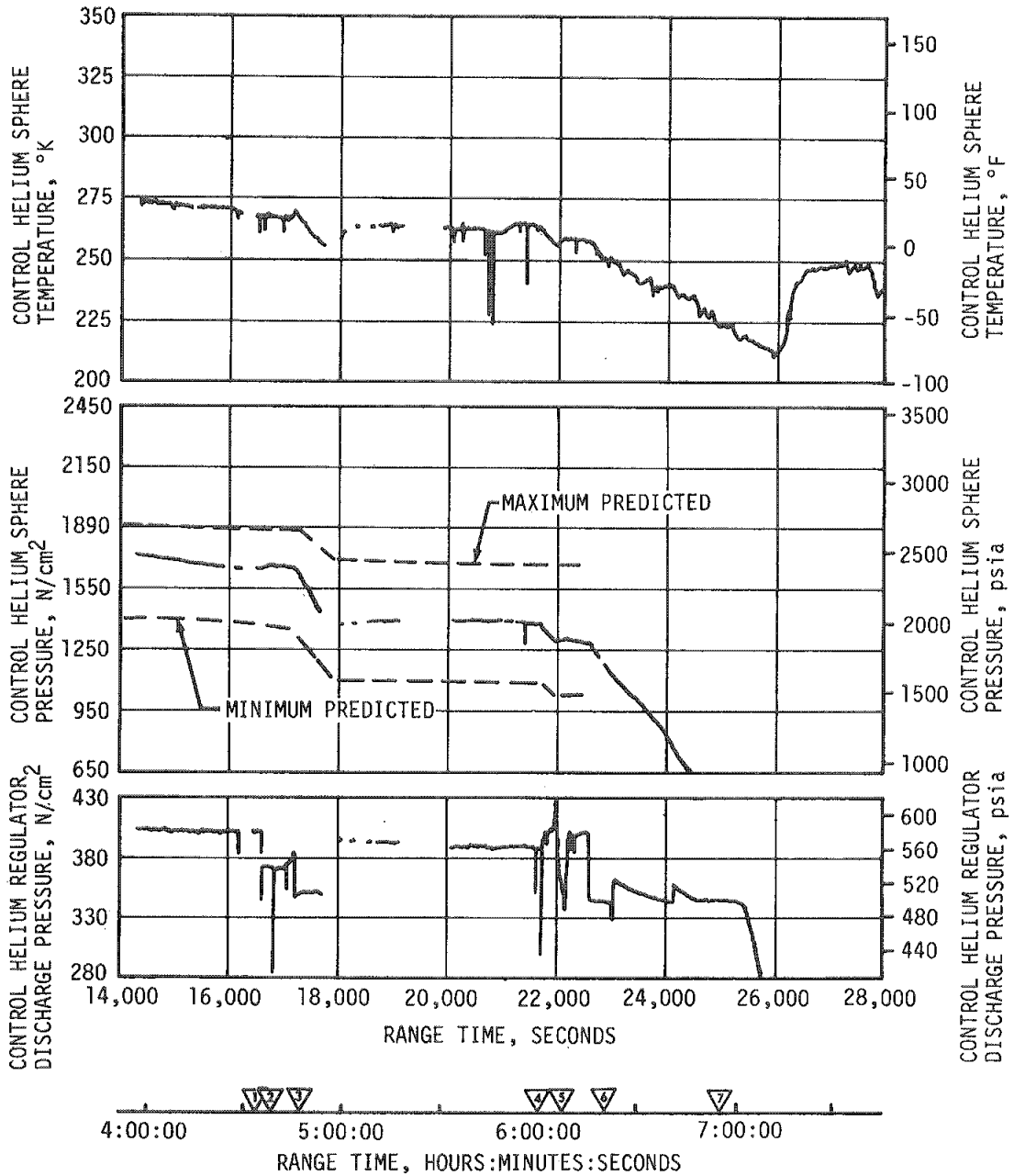


Figure 7-43. S-IVB Pneumatic Control Performance  
(Sheet 2 of 2)

Table 7-13. S-IVB Pneumatic Helium Bottle Mass

TIME	BOTTLE MASS	
	kg	lbm
Liftoff	4.00	8.81
First Burn ESC	4.00	8.81
First Burn ECO	3.99	8.79
Second Burn ESC	3.43	7.56
Second Burn ECO	3.42	7.54
Third Burn ESC	2.87	6.33
Third Burn ECO	2.84	6.26

331 N/cm<sup>2</sup> (480 psia). The regulator resumed normal regulation for the duration of the mission after the dropout of the backup system's shutoff valve. Possible causes of this regulator problem were helium supply contamination or marginal mating between the regulator poppet and seat.

#### 7.16 S-IVB AUXILIARY PROPULSION SYSTEM

The APS pressurization systems demonstrated adequate performance throughout the flight and met control system demands as required until APS propellant depletion. Module No. 2 developed a helium leak at approximately 4 hours 25 minutes. The leak ceased at approximately 7 hours. The average leak rate was 3851 SCCM (235 SCIM). The probable cause of this problem was leakage of one or more Teflon seals in the helium high pressure system upstream of the regulator. The Module No. 1 regulator outlet pressure was maintained at 137 N/cm<sup>2</sup> (199 psia). Module No. 2 regulator outlet pressure was 131 to 134 N/cm<sup>2</sup> (190 to 195 psia) which was below the 135 ± 2 N/cm<sup>2</sup> (196 ± 3 psia) regulation band. This is within instrumentation accuracy and other system pressures verify proper regulation. The APS ullage pressures in the tanks were acceptable, ranging from 129 to 132 N/cm<sup>2</sup> (188 to 192 psia). The APS helium bottle masses during flight are presented in Table 7-14.

The oxidizer and fuel supply systems performed as expected during the flight. The propellant temperatures measured in the propellant control module were as expected. The maximum temperature recorded was 323°K (121 °F). The bulk temperatures of the propellants in the bladder ranged from 302 to 308°K (88 to 95°F).

Table 7-14. S-IVB APS Helium Bottle Mass

EVENT	BOTTLE MASS			
	kg		lbm	
	MODULE 1	MODULE 2	MODULE 1	MODULE 2
Liftoff	0.462	0.462	1.018	1.018
First Burn ESC	0.462	0.462	1.018	1.018
First Burn ECO	0.462	0.461	1.018	1.016
End First Ullage Burn	0.441	0.441	0.972	0.973
Separation	0.414	0.416	0.913	0.917
Start Second Ullage Burn	0.402	0.400	0.885	0.877
Second Burn ESC	0.386	0.381	0.851	0.840
Second Burn ECO	0.385	0.377	0.848	0.831
End Third Ullage Burn	0.383	0.373	0.843	0.822
Start Fourth Ullage Burn	0.375	0.370	0.826	0.815
Third Burn ESC	0.360	0.352	0.793	0.775
Third Burn ECO	0.341	0.329	0.751	0.724
Start of Ullage Depletion Burn	0.341	0.329	0.751	0.724
End Ullage Depletion Burn (7:41:40)	0.233	0.217	0.514	0.478

The propellants in Module No. 2 (at position III) were depleted first as shown in Figure 7-44. The fuel was depleted at 27,671 seconds, resulting in a burntime of 425 seconds, while the oxidizer was depleted at 27,782 seconds. The fuel was also depleted first in Module No. 1 (at position I) at 27,713 seconds resulting in a burntime of 468.4 seconds, as shown in Figure 7-45. The oxidizer was depleted at 27,850 seconds. Fuel was depleted first in both modules because the propellants were loaded for a

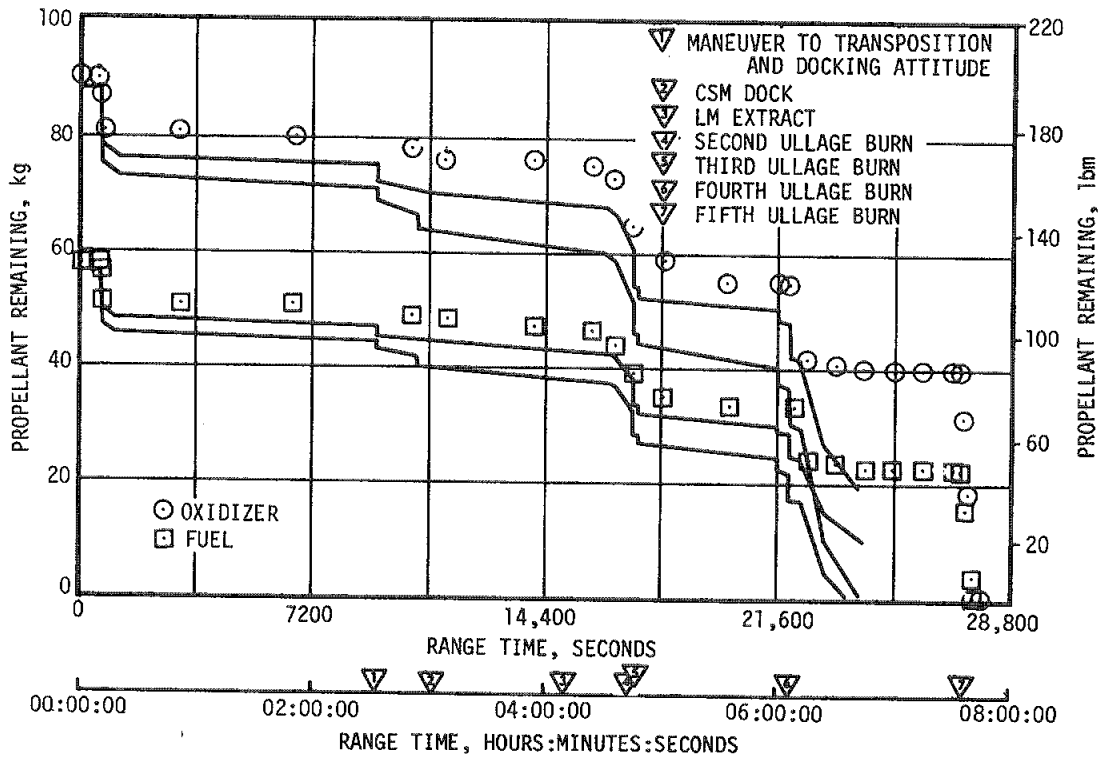


Figure 7-44. S-IVB APS Propellant Remaining Versus Mission Time - Module No. 2

1.65 to 1.0 EMR while the attitude control engines normally operate at a 1.60 EMR during minimum impulse bit pulsing. Also the oxidizer was not off-loaded to account for the last ullage burn to propellant depletion at the ullage engine EMR of 1.27 to 1.0. The fuel load for the flight was maximum. Table 7-15 presents the APS oxidizer and fuel consumption at significant events during the flight.

The attitude control engine chamber pressures normally ranged from 62 to 68 N/cm<sup>2</sup> (90 to 98 psia) until loss of data. The ullage engine chamber pressures were normal at 64 to 69 N/cm<sup>2</sup> (93 to 100 psia) during their burns, including the burn to propellant depletion.

## 7.17 S-IVB ORBITAL SAFING OPERATION

### 7.17.1 Fuel Tank Safing

Due to the loss of pneumatic control of the engine valves, the LH<sub>2</sub> dump through the engine could not be accomplished. The CVS and NPV were opened as programmed at third ECO +0.6 seconds and third ECO +1868

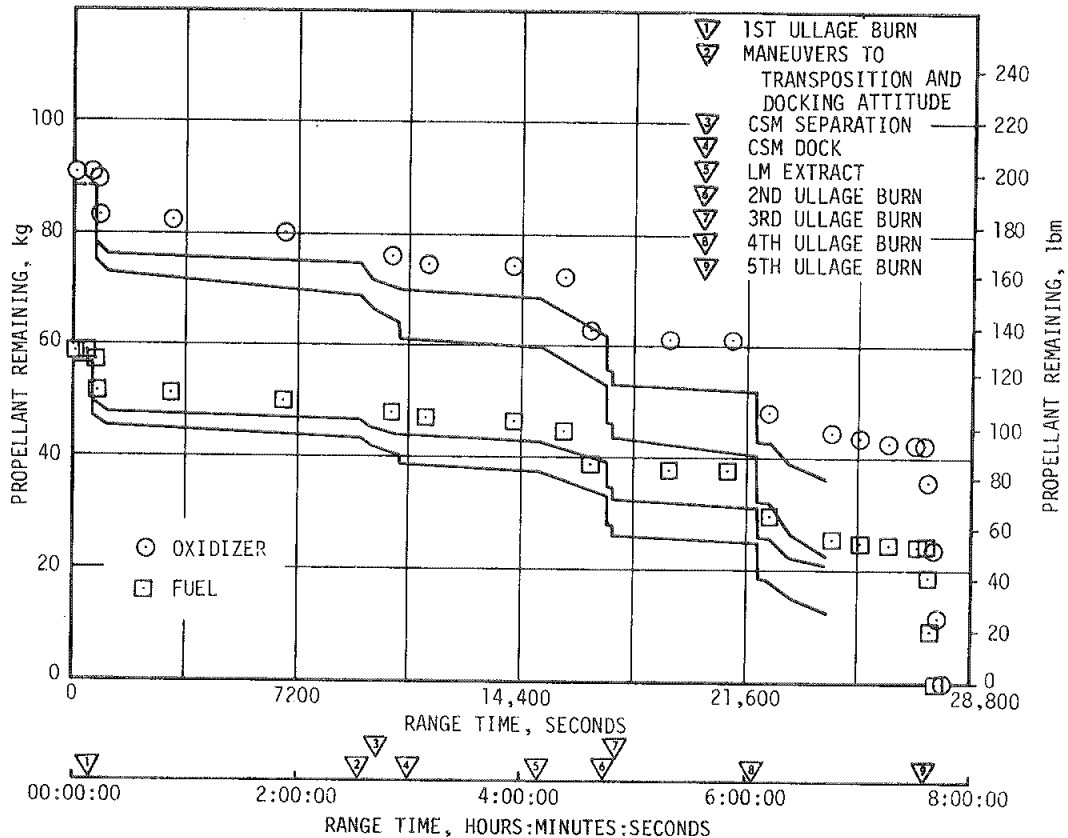


Figure 7-45. S-IVB APS Propellant Remaining Versus Mission Time - Module No. 1

seconds, respectively. The LH<sub>2</sub> residual mass at third engine cutoff was 4060 kilograms (8951 lbm) and the LH<sub>2</sub> ullage pressure was 21.8 N/cm<sup>2</sup> (31.6 psia). The ullage pressure is shown out to 28,000 seconds in Figure 7-7. The ullage pressure subsequently decreased to approximately 0.76 N/cm<sup>2</sup> (1.1 psia) at 40,800 seconds. The residual mass at this time was approximately 2906 kilograms (6400 lbm). At approximately 44,000 seconds, the ullage pressure started to rise. The ullage pressure, NPV pressure and CVS pressure indicated that flow through the CVS and NPV was restricted due to solidification of hydrogen in the vent line. The ullage pressure was 2.5 N/cm<sup>2</sup> (3.7 psia) at 47,400 seconds (end of data) and was still increasing very slowly.

#### 7.17.2 LOX Tank Dump and Safing

There was no LOX dump due to the loss of engine pneumatic control during third burn. The LOX tank was satisfactorily safed by utilizing the LOX

Table 7-15. S-IVB APS Propellant Consumption

TIME PERIOD	MODULE NO. 1		MODULE NO. 2	
	OXIDIZER kg (lbm)	FUEL kg (lbm)	OXIDIZER kg (lbm)	FUEL kg (lbm)
Initial Load	91.0 (200.6)	57.9 (127.6)	91.0 (200.6)	58.1 (128.2)
First J-2 Burn (Roll Control)	0.5 (1.0)	0.3 (0.4)	0.4 (0.9)	0.3 (0.6)
J-2 ECO to End of First APS Ullage Burn	7.2 (16.1)	5.7 (12.4)	6.7 (15.4)	5.3 (11.6)
End of 1st Ullage Burn to S-IVB/LM/CSM Separation	9.4 (20.6)	5.9 (13.0)	8.9 (18.8)	5.4 (12.0)
From Separation to Start of 2nd Ullage Burn	4.8 (10.5)	2.9 (6.5)	6.5 (14.5)	4.1 (9.0)
Start of 2nd Ullage Burn to 2nd ESC	5.0 (11.1)	4.0 (8.7)	5.5 (12.0)	4.3 (9.6)
Second J-2 Burn (Roll Control)	0.4 (0.8)	0.2 (0.4)	1.3 (2.8)	0.8 (1.6)
J-2 ECO to End of 3rd APS Ullage Burn	1.0 (2.2)	0.7 (1.7)	1.5 (3.4)	1.1 (2.2)
End of 3rd Ullage to Start of 4th Ullage Burn	2.6 (5.9)	1.7 (3.8)	0.9 (1.9)	0.7 (1.4)
Start of 4th Ullage Burn to 3rd ESC	4.9 (10.6)	3.8 (8.4)	5.9 (13.1)	4.6 (10.2)
Third J-2 Burn (Roll Control)	7.0 (15.4)	4.4 (9.8)	8.3 (18.2)	5.2 (11.6)
Third Burn ECO to Ullage Depletion Burn	5.4 (11.8)	3.3 (7.1)	4.6 (10.3)	2.9 (6.3)
Ullage Depletion Burn	42.0 (92.7)	24.5 (54.0)	39.4 (86.7)	22.6 (49.7)

NPV system. The ullage pressure was 28.9 N/cm<sup>2</sup> (41.9 psia) when the LOX NPV valve was latched open at 23,042 seconds. The ullage pressure decayed to 1.7 N/cm<sup>2</sup> (2.5 psia) in 7000 seconds. At 47,000 seconds, the ullage pressure had decreased to 0.3 N/cm<sup>2</sup> (0.5 psia).

### 7.17.3 Cold Helium Dump

Cold helium was dumped through the O<sub>2</sub>/H<sub>2</sub> burner heating coils and into the LH<sub>2</sub> tank, and overboard through the fuel tank vents. This was used to avoid the possibility of freezing the LOX tank vent system.

The first dump was initiated at 22,284.5 seconds and programmed to continue for 1872 seconds as shown in Figure 7-46. During this period, the pressure decayed normally from 414 to 34.5 N/cm<sup>2</sup> (600 to 50 psia). Approximately 79 kilograms (174 lbm) of helium were dumped overboard during this period, leaving a residual of 10.4 kilograms (23 lbm). During the second dump beginning at 24,356 seconds and lasting 1728 seconds, an additional 1.8 kilogram (4 lbm) were dumped.

### 7.17.4 Ambient Helium Dump

The ambient helium in the LOX and LH<sub>2</sub> repress spheres was dumped, via the fuel tank. The 200-second dump started at 24,156.5 seconds. The pressure decayed from 1170 to 75 N/cm<sup>2</sup> (1698 to 109 psia). Shortly after the blowdown the bottle mass was 2.95 kilograms (6.51 lbm). During dump 18.4 kilograms (40.6 lbm) was dumped through the fuel tank and vented through the fuel tank vents. The ambient helium repressurization bottles pressure for dump is shown in Figure 7-47.

### 7.17.5 Stage Pneumatic Control Sphere Safing

The stage pneumatic control sphere was safed by initiating the J-2 engine pump purge and dumping helium through the turbopump seal vent. The safing period of 3520 seconds satisfactorily reduced the potential energy in the spheres. Initial and final sphere conditions are listed in Table 7-16. Stage pneumatic dump is presented in Figure 7-43.

### 7.17.6 Engine Start Tank Safing

The engine start tank was safed during a 60-second period at 22,340 seconds. Safing was accomplished by opening the sphere vent valve. Pressure was decreased from 817 to 60 N/cm<sup>2</sup> (1180 to 87 psia) with 1.92 kilogram (4.33 lbm) of hydrogen being vented as shown in Figure 7-48.

### 7.17.7 Engine Control Sphere Safing

The engine control sphere was not safed by the onboard sequence program due to the third burn anomaly. The control bottle pressure did not respond to any of the commands subsequent to third burn as shown by Figure 7-49. However, by the time data was lost, the engine control bottle pressure had been reduced to 69 N/cm<sup>2</sup> (100 psia) due to helium leakage.



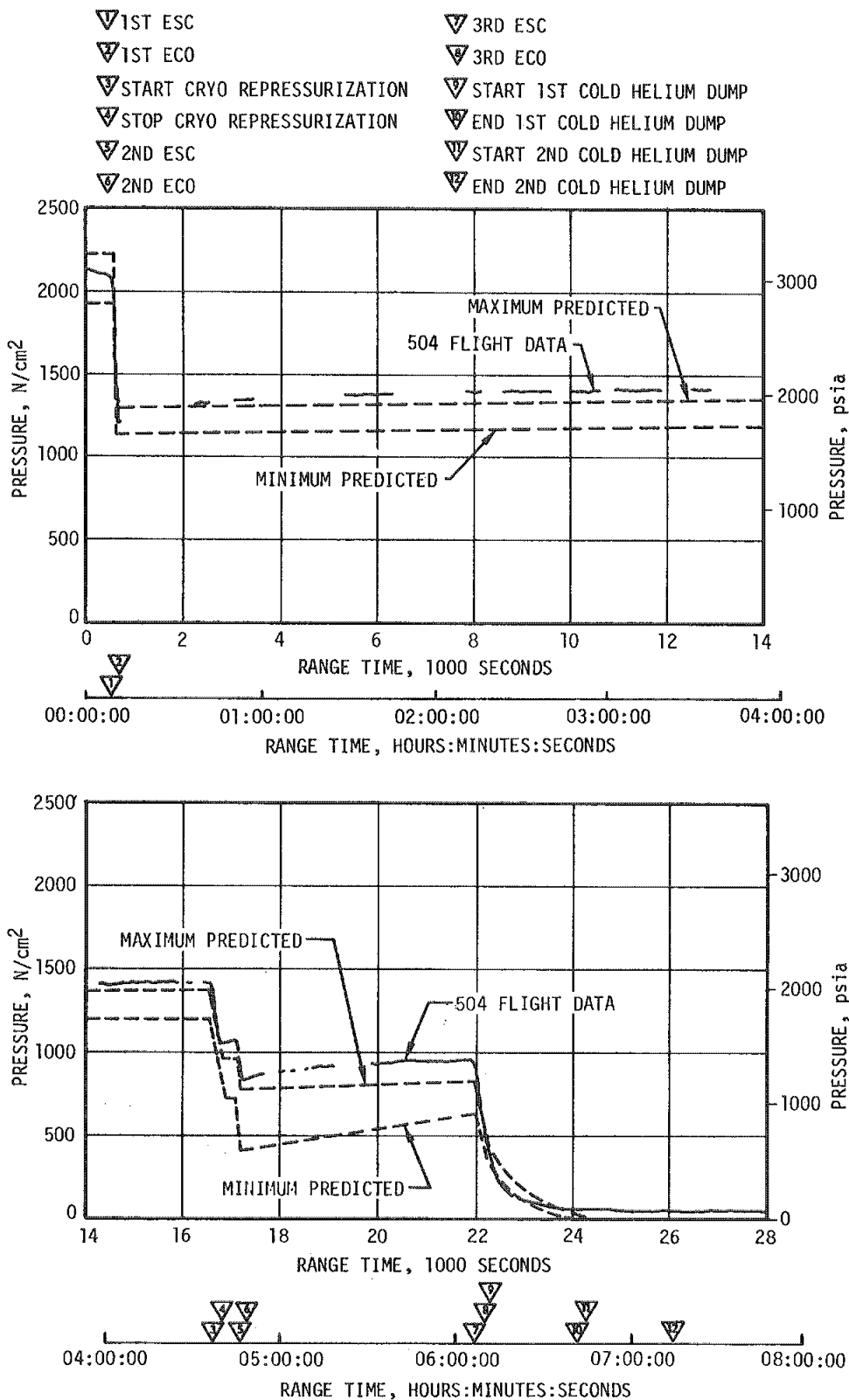


Figure 7-46. S-IVB Cold Helium Supply History

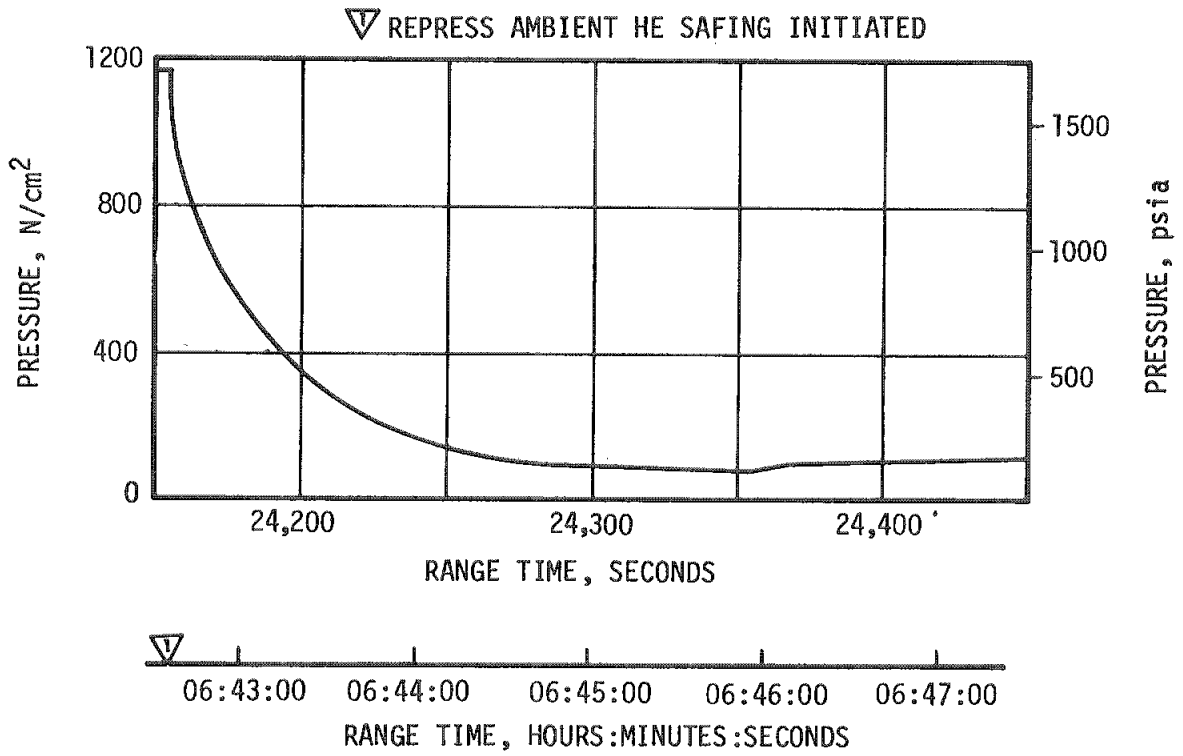


Figure 7-47. S-IVB Ambient Helium Repressurization Spheres Safing

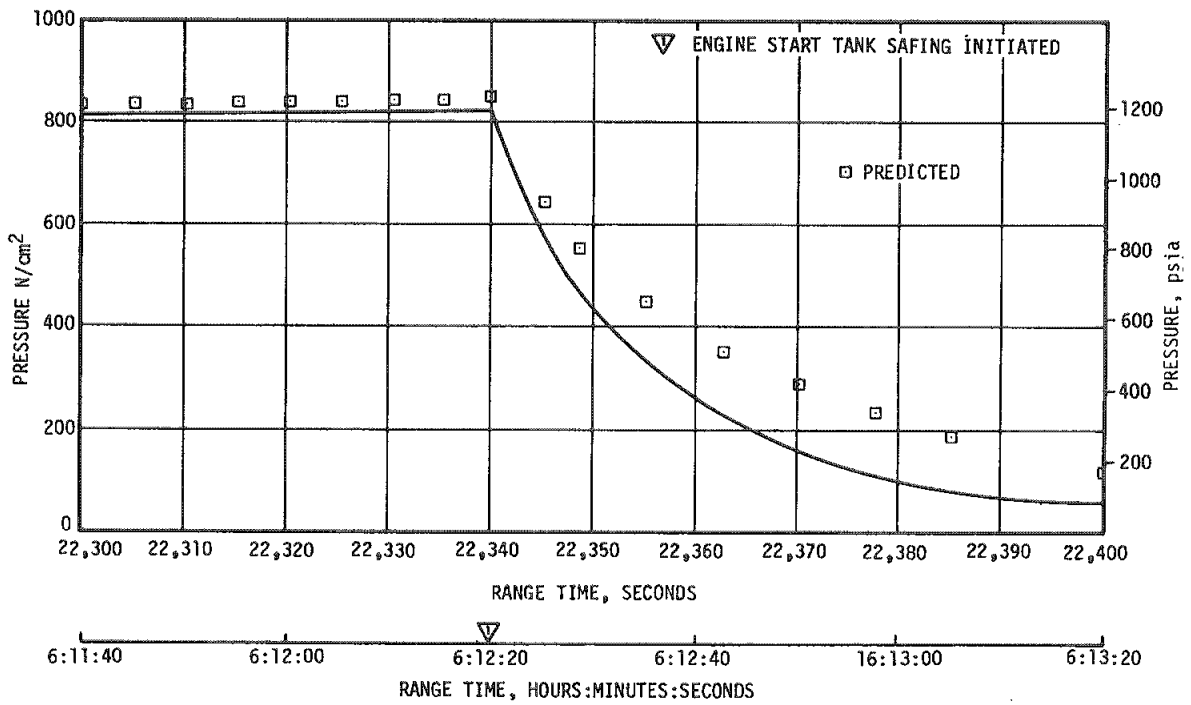


Figure 7-48. S-IVB Start Tank Safing

Table 7-16. S-IVB Pneumatic Safing Conditions

PARAMETER	INITIAL CONDITIONS	FINAL CONDITIONS
Press N/cm <sup>2</sup> (psia)	1158 (1680)	241 (350)
Temp °K (°F)	258 (465)	215 (387)
Mass kg (lbm)	2.76 (6.07)	0.69 (1.52)

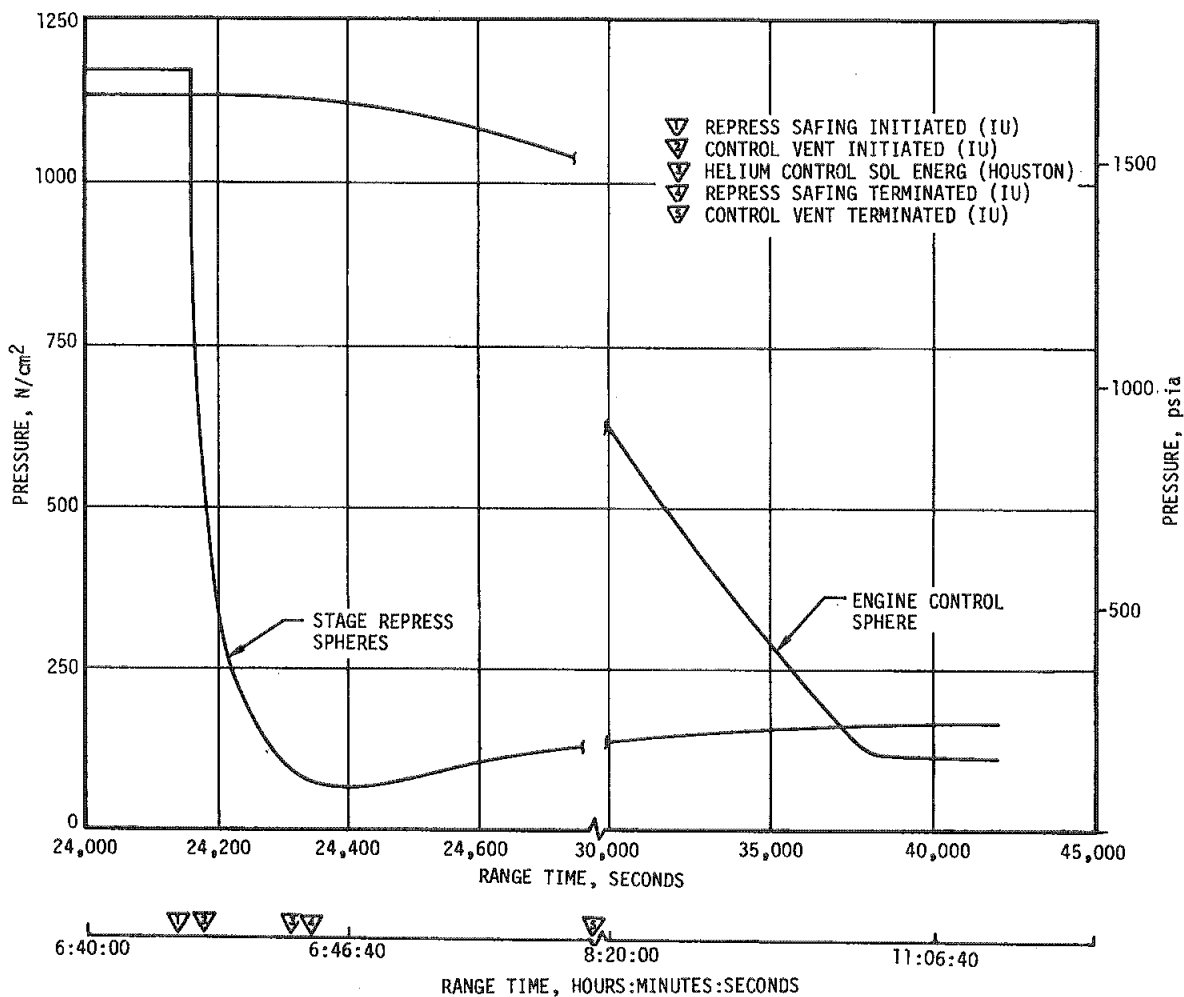


Figure 7-49. S-IVB Pneumatic Safing History

## SECTION 8

### HYDRAULIC SYSTEMS

#### 8.1 SUMMARY

The hydraulic systems performed satisfactorily for the S-IC, S-II and first two burns of the S-IVB stages. Except for the third burn of the S-IVB stage all parameters were within the specification limits and there were no deviations or anomalies. During the third burn the yaw actuator experienced abnormal oscillations at 0.65 hertz with a 3 degree peak-to-peak amplitude.

#### 8.2 S-IC HYDRAULIC SYSTEM

Analysis indicates that all actuators performed as commanded during the flight, with a maximum actuator deflection equivalent to 2.05 degrees engine gimbal angle at approximately 78 seconds. All of the hydraulic supply pressures and temperatures were within the operating limits.

#### 8.3 S-II HYDRAULIC SYSTEM

Reservoir fluid volumes, temperatures and accumulator pressures (indicative of system supply pressures) were within predicted ranges. Temperature rise rates were close to the predicted rate.

Throughout the flight all servoactuators responded to commands with good precision. The maximum difference between actuator command and position was 0.1 degree. Oscillations were present at the actuators starting at 503 to 505 seconds and continued for 20 to 25 seconds. The frequencies of the oscillations for the eight actuators varied between 16.5 and 18 hertz. Peak-to-peak amplitudes varied from 8900 to 34,600 Newtons (2000 to 7800 lbf). These oscillations are considered to be in response to engine performance oscillations occurring at this time and are not the result of actuator commands.

#### 8.4 S-IVB HYDRAULIC SYSTEM

All hydraulic systems performed within predicted limits during the first and second burns. However, along with the other S-IVB anomalies reported during third burn, the hydraulic system exhibited abnormal behavior.

Immediately after start of third burn the yaw actuator commenced to limit cycle at an approximate maximum amplitude of 3 degrees peak-to-peak with a frequency of 0.65 hertz as shown in Figure 8-1. This oscillatory motion continued for the first 100 seconds of third burn. Cycling ceased soon after engine thrust degradation occurred during the burn.

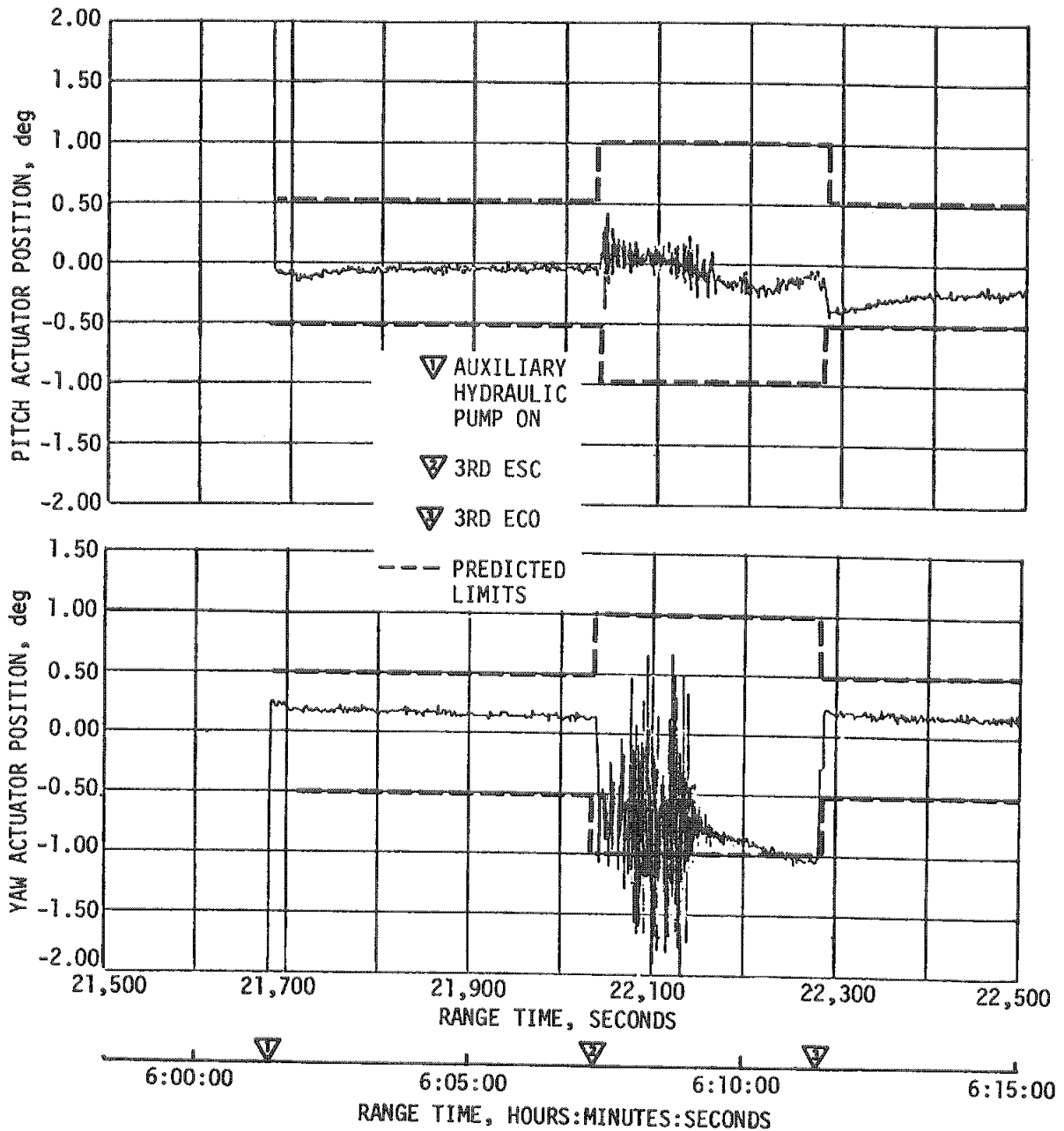


Figure 8-1. S-IVB Hydraulic System Actuator Positions - Third Burn

Hydraulic system pressure and temperature measurements indicated normal levels during the burn as shown in Figures 8-2 through 8-4. Low amplitude pressure oscillations were present during the actuator cyclic activity which is normal for the resultant flow demand.

The response of the pitch and yaw actuators at third burn engine start appeared normal. At 22,046.4 seconds, the yaw actuator response appeared irregular. Later in the burn the command signals to the pitch and yaw hydraulic servos started to cycle at a frequency of approximately 0.65 hertz. Nonlinearities continued to appear during the rest of the burn at the higher thrust level but to a lesser extent in the pitch plane. After thrust cutback, the control system oscillations dampened out. During the period of high oscillations the pitch actuator maximum excursion was 0.5 degree (peak-to-peak) with a maximum apparent amplitude gain of 1.10. The pitch actuator appeared to lag the signal to a greater extent when in the extend direction. The opposite was true of the yaw actuator. The amplitude of the yaw oscillations approached 3 degrees (peak-to-peak) with a maximum apparent amplitude gain of 1.31. Figures 8-5 and 8-6 show actuator signal and position activity over a short period of time showing their response in greater detail. Throughout the high activity, the yaw actuator position cycled about a bias which was the same as that observed towards the end of burn when no dynamic activity was noted. The signal bias was approximately 0.3 degree less during the high activity.

The pitch actuator motion led the yaw actuator by approximately 61 degrees during the period of high thrust, indicating engine motion was following an elliptical path.

The static gains of the actuators were normal prior to third burn and after the engine thrust had cut back and the oscillations had dampened out. This indicates that the mechanical feedback networks within the actuators were operating properly except possibly during the period of high oscillations.

At 22,200 seconds the pitch actuator response appeared noisy and produced an offset. At engine cutoff the offset was -0.34 degree. Actuator position drifted back toward null over an extended period of time. It is currently felt that abnormal actuator behavior (both pitch and yaw) was due to an abnormal actuator environment.

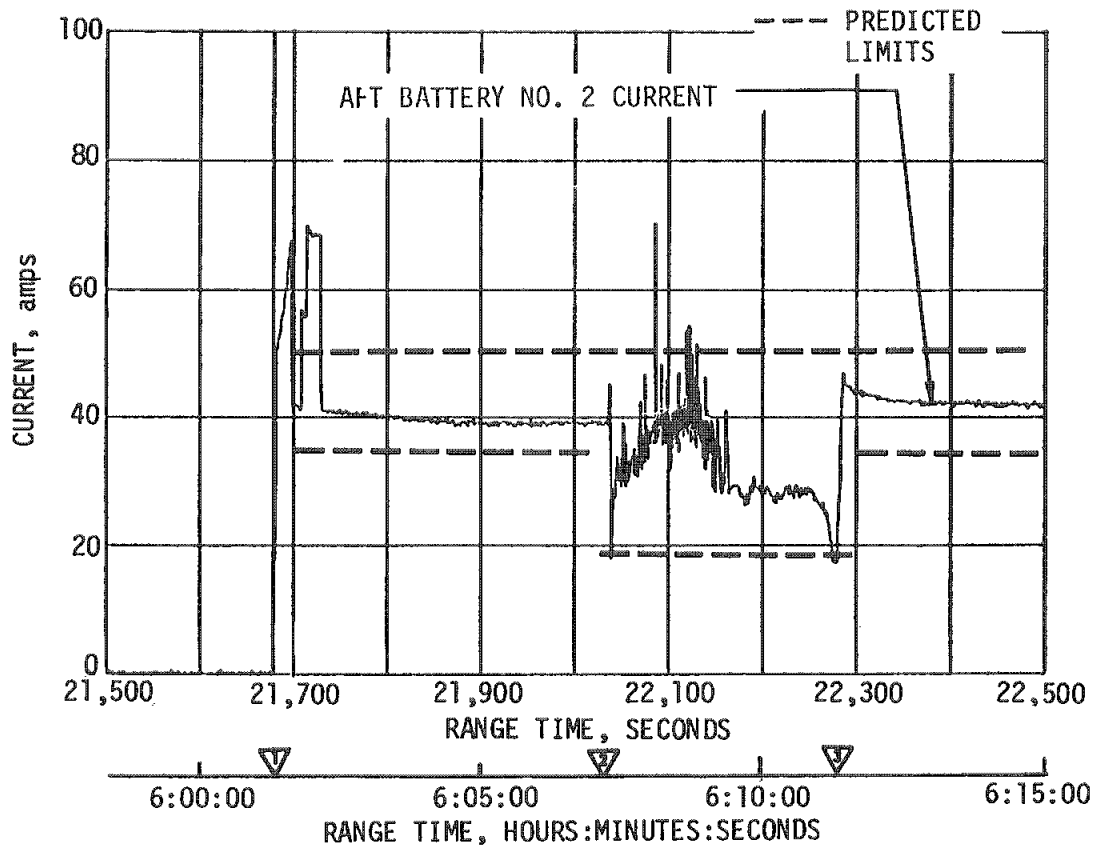
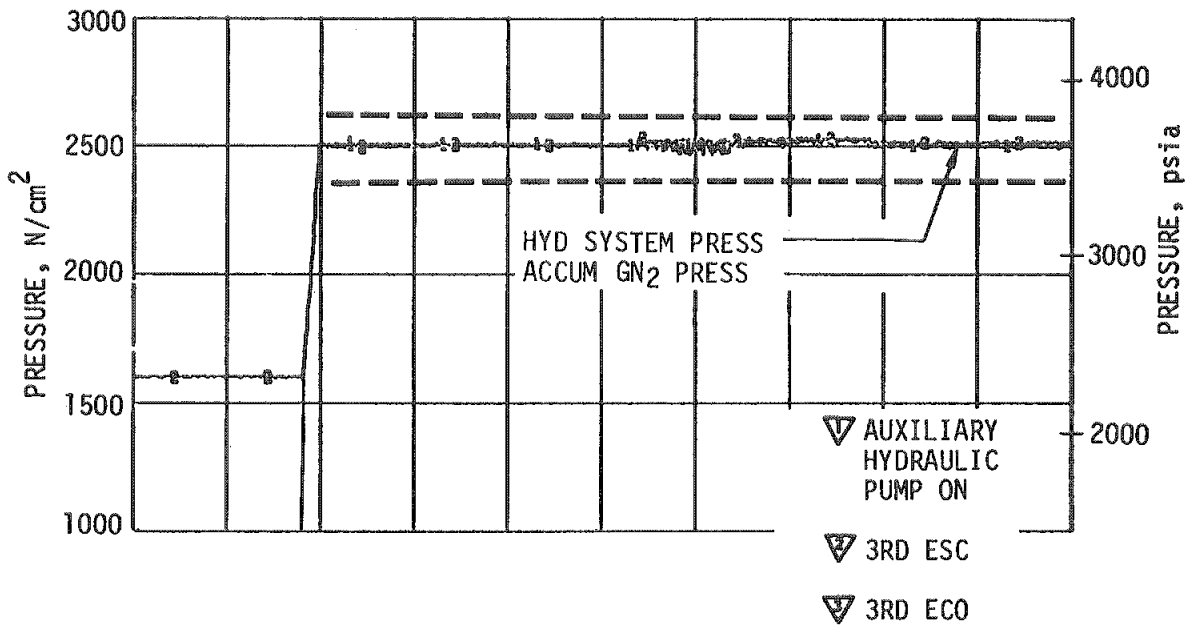


Figure 8-2. S-IVB Hydraulic System Actuator Performance - Third Burn

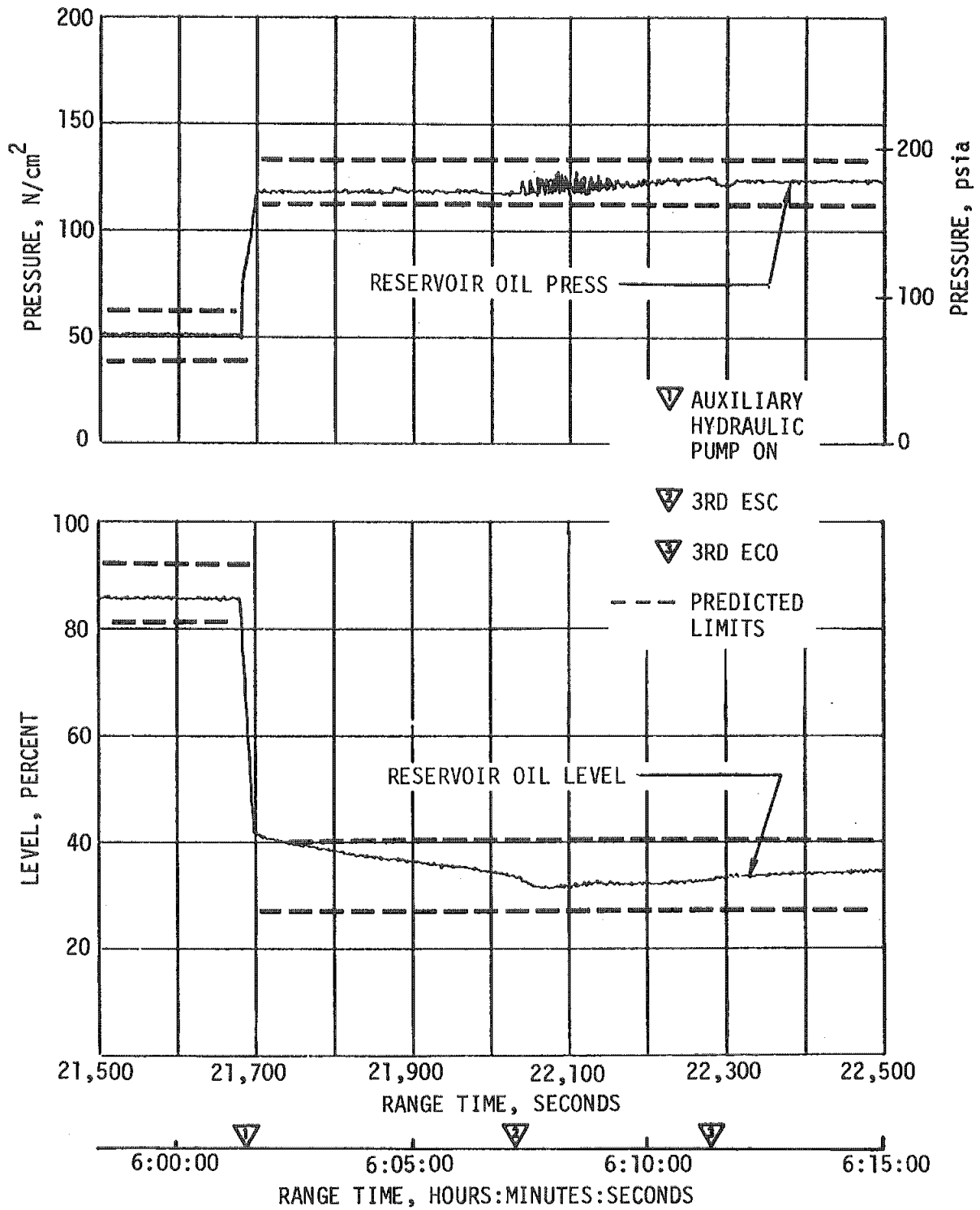


Figure 8-3. S-IVB Hydraulic Reservoir Performance - Third Burn



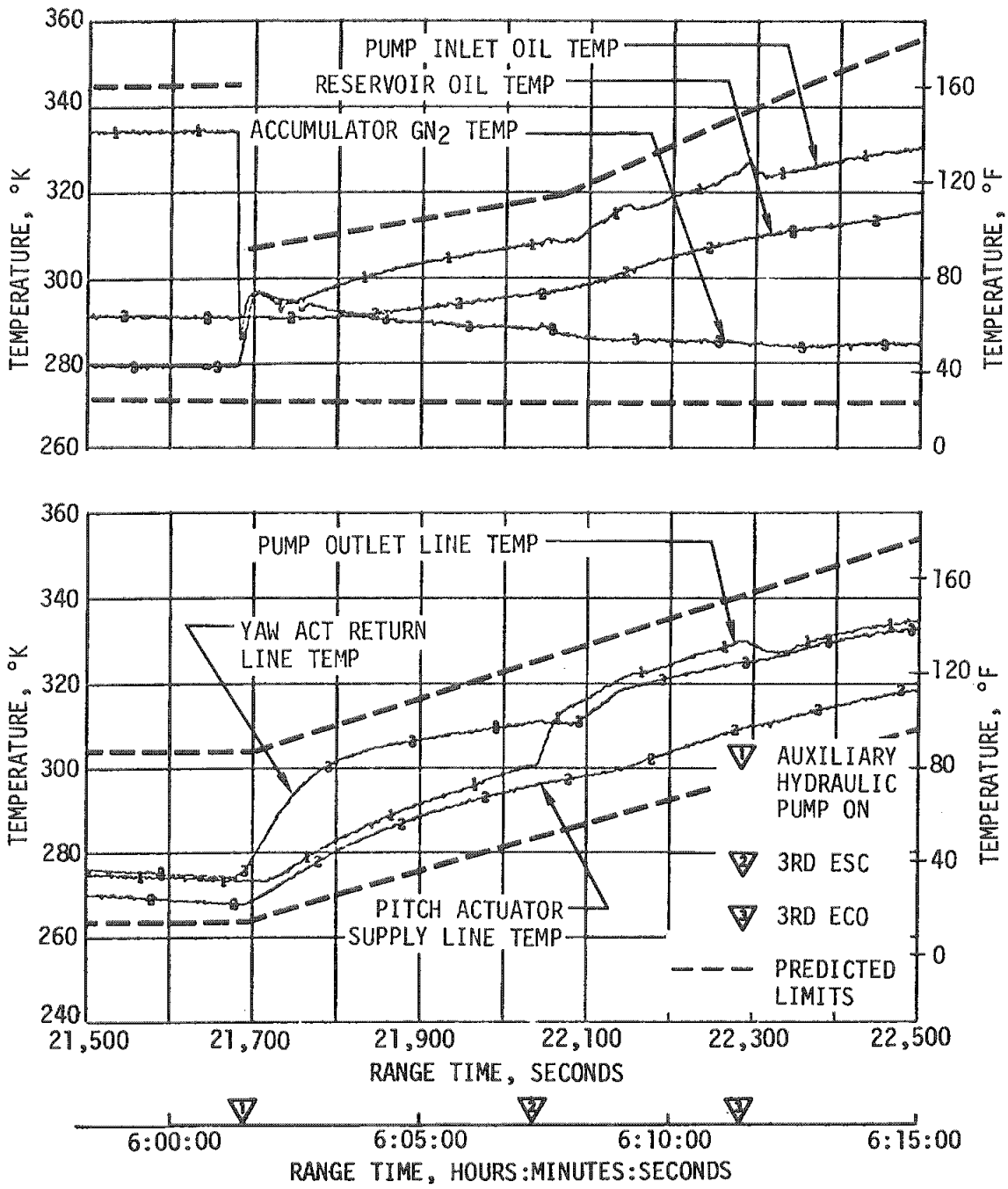


Figure 8-4. S-IVB Hydraulic System Temperature - Third Burn

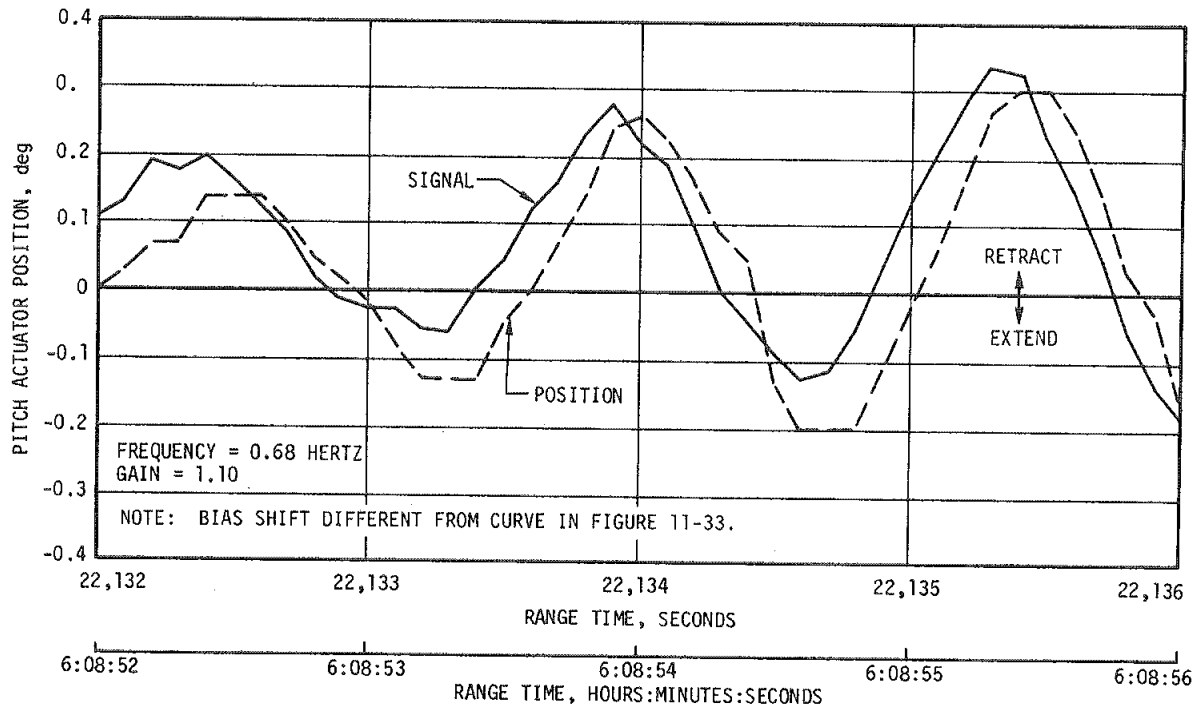


Figure 8-5. S-IVB Pitch Actuator Signal and Position - Third Burn

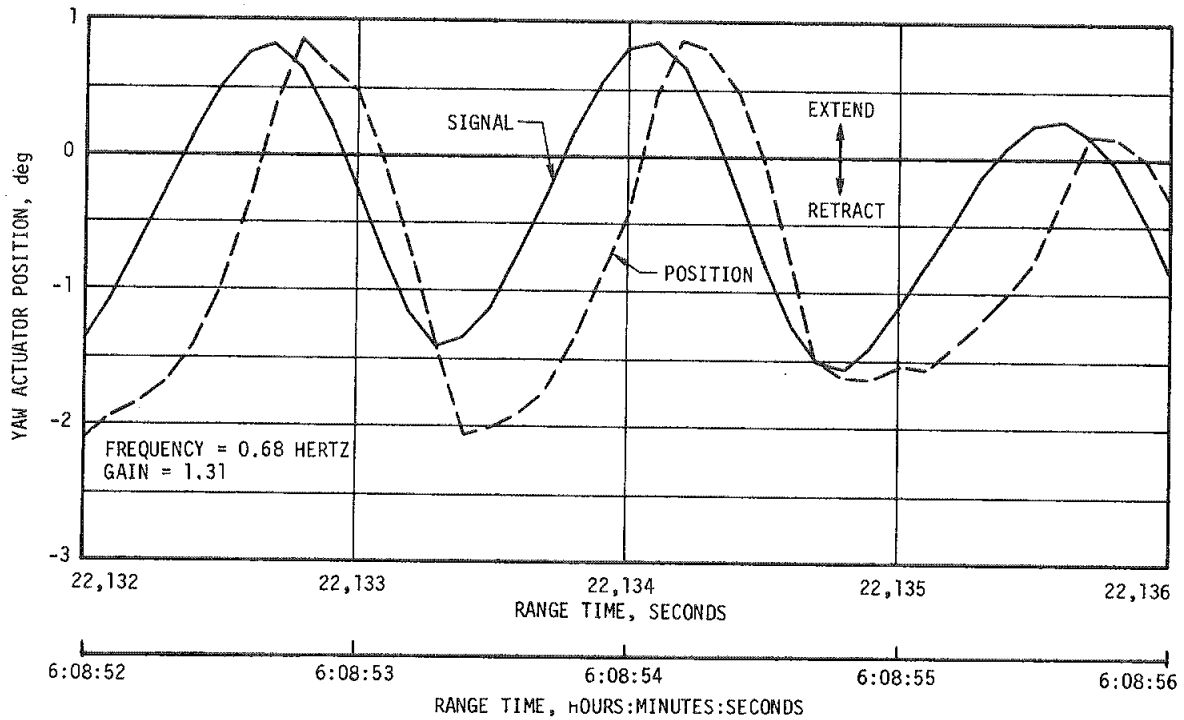


Figure 8-6. S-IVB Yaw Actuator Signal and Position - Third Burn.

## SECTION 9

### STRUCTURES

#### 9.1 SUMMARY

The structural loads and dynamic environment experienced by the AS-504 launch vehicle were well within the vehicle structural capability. The high altitude winds for this flight were the highest measured during any previous Saturn launch; however, due to a wind bias trajectory, the structural loads for AS-504 were well below the limit design values.

The maximum bending moment condition,  $9.7 \times 10^6$  N-m ( $86 \times 10^6$  lbf-in.), was experienced at 79.4 seconds. The maximum longitudinal loads on the S-IC thrust structure, fuel tank, and intertank were experienced at 134.3 seconds, Center Engine Cutoff (CECO). The maximum longitudinal loads on the AS-504 vehicle structure above the intertank occurred at 162.8 seconds, Outboard Engine Cutoff (OECO), at the maximum longitudinal acceleration of 3.85 g.

Vehicle dynamic characteristics generally followed the trends established by preflight analyses. There was no evidence of an unstable coupled thrust-structure-feed system oscillation (POGO) during S-IC powered flight. A 5.2 hertz longitudinal oscillation was excited by the S-IC CECO transient and damped slowly, indicating that the structural damping may be lower than expected.

The low frequency (16 to 19 hertz) oscillation anomaly observed on AS-503 also occurred on AS-504 near the end of S-II stage burn. The oscillations reached a maximum level of approximately  $\pm 12.0$  g at the center of the S-II thrust structure crossbeam.

S-IC stage vibrations were generally as expected. The heat shield vibration measurements agreed closely with the AS-503 data, verifying the higher than expected levels measured on AS-503. S-II stage vibrations were, in general, within the envelopes established by previous flights.

#### 9.2 TOTAL VEHICLE STRUCTURES EVALUATION

##### 9.2.1 Longitudinal Loads

The longitudinal loads which existed at the time of maximum aerodynamic loading (maximum bending moment), at CECO and at OECO are shown in

Figure 9-1. These loads were as expected with the maximum longitudinal loads on the S-IC thrust structure, fuel tank, and intertank occurring at 134.3 seconds (CECO) at a longitudinal acceleration of 3.6 g, and on all AS-504 vehicle structure above the intertank the maximum longitudinal loads occurred at 162.8 seconds (OECO) at an acceleration of 3.85 g.

Figure 9-2 shows longitudinal dynamic response time histories at the S-IC center engine gimbal block, at the instrument unit, and at the command module during S-IC OECO. The dynamic response at OECO was slightly more severe than that experienced on previous flights, but not sufficiently high to pose a threat to structural integrity.

### 9.2.2 Bending Moments

The lateral loads experienced during thrust buildup and release were much lower than design because of the favorable winds experienced during launch. The wind speed at launch was low, 6.9 m/s (13.5 knots) at the 18.3 meter (60 ft) level. The comparable launch vehicle and spacecraft peak redline wind is 18.9 m/s (36.8 knots) and 14.4 m/s (28 knots), respectively.

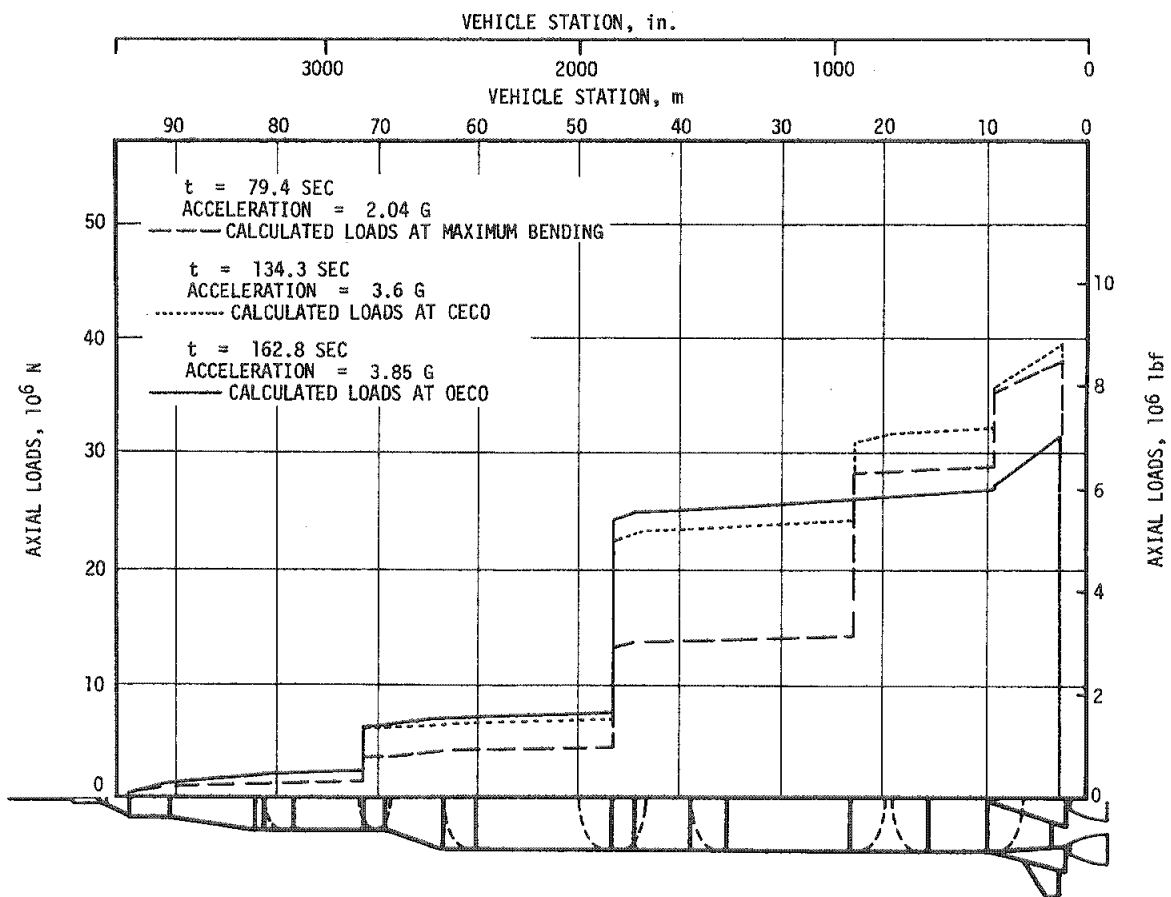


Figure 9-1. Longitudinal Loads at Maximum Bending Moment, Center Engine Cutoff, and Outboard Engine Cutoff

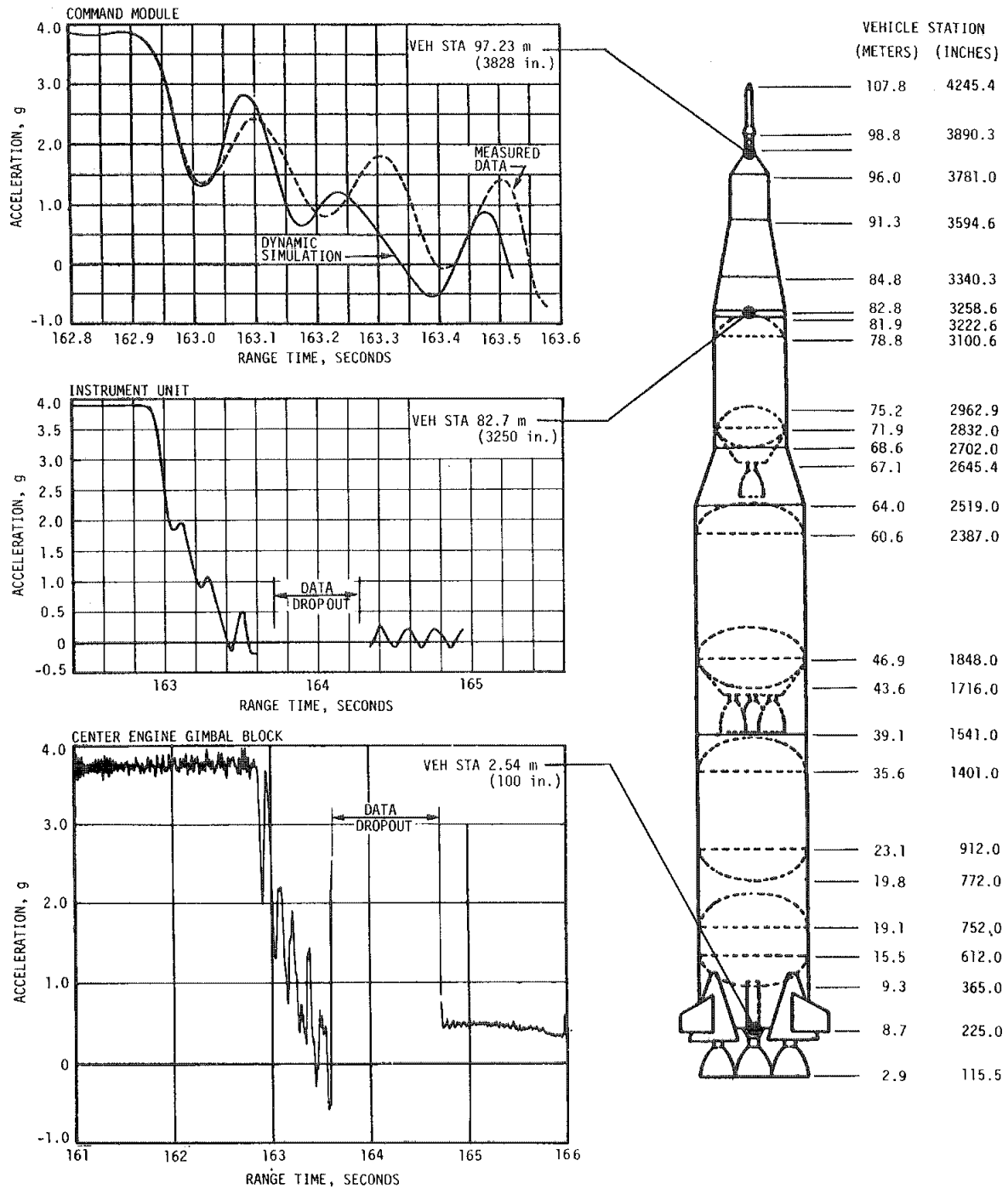


Figure 9-2. Longitudinal Structural Dynamic Response Due to Outboard Engine Cutoff

The high altitude winds which existed during the maximum aerodynamic loading phase of flight were approximately twice the magnitude of those encountered during the AS-503 flight, and the highest measured during any previous Saturn I or Saturn V launch. However, due to a wind bias trajectory the maximum bending moment of  $9.7 \times 10^6$  N-m ( $86 \times 10^6$  lbf-in), experienced at 79.4 seconds, was less than 40 percent of the design criteria. The calculated bending moment diagram shown in Figure 9-3 is based on loads computations using measured inflight parameters such as thrust, gimbal angle, dynamic pressure, angle-of-attack, and modal accelerations.

### 9.2.3 Vehicle Dynamic Characteristics

9.2.3.1 Longitudinal Dynamic Characteristics. Throughout the S-IC boost phase of AS-504 flight the predicted first longitudinal mode frequencies were present, as shown in Figure 9-4. Modal amplitude versus range time is also shown. The measured frequencies, determined by spectral analysis using 5-second time slices, agree well with the analytical predictions.

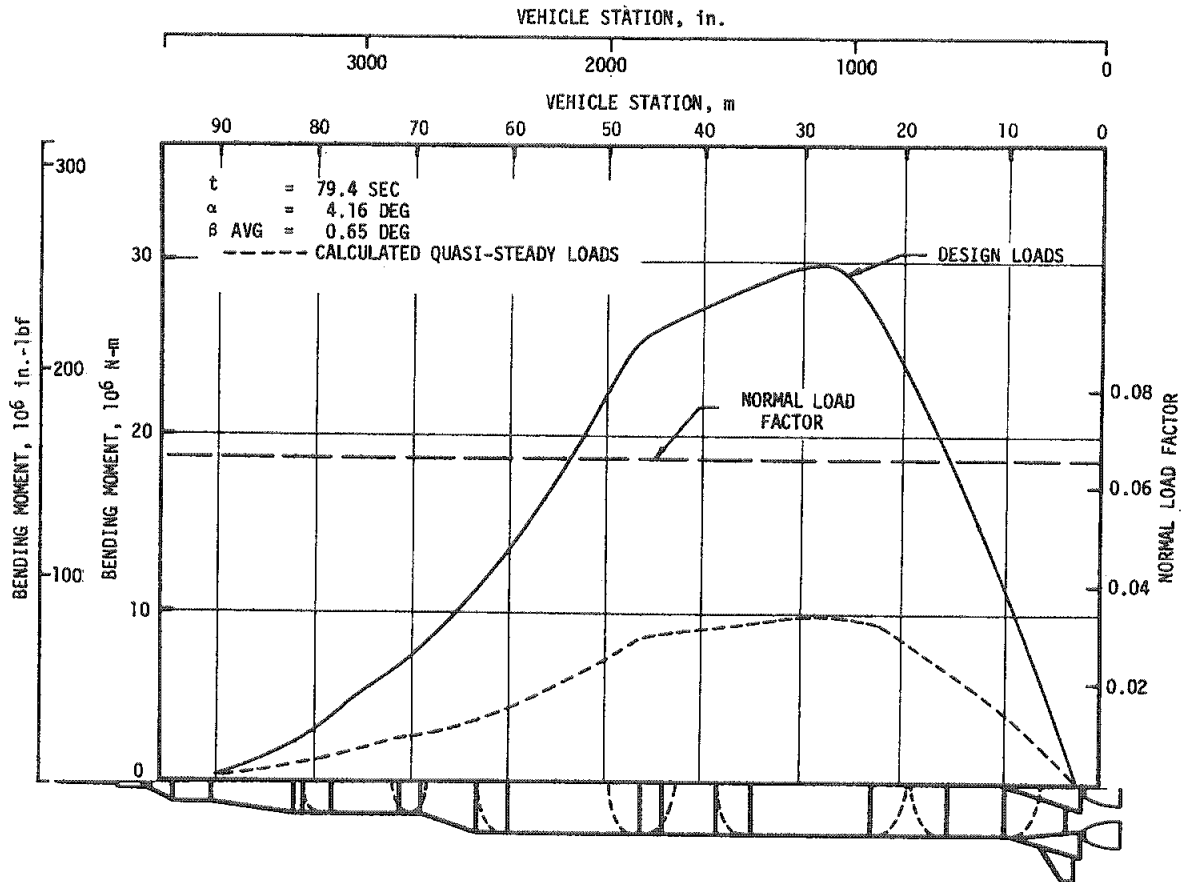


Figure 9-3. Maximum Bending Moment Near Max Q

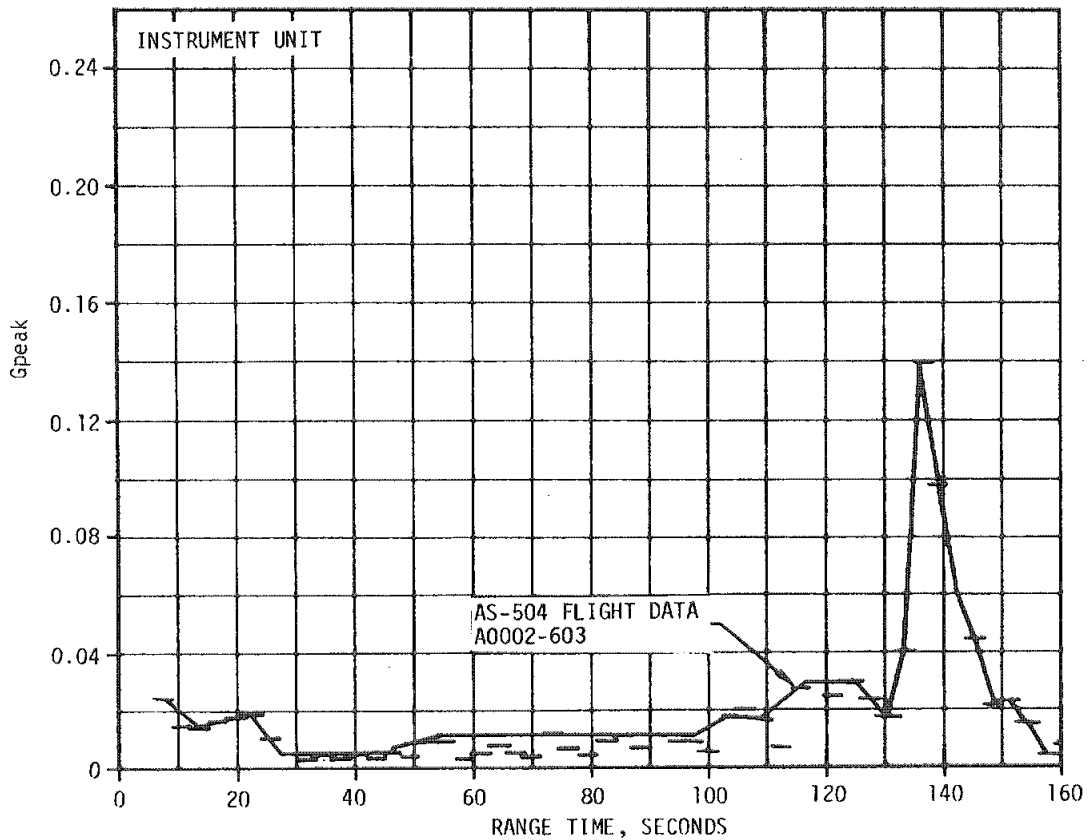
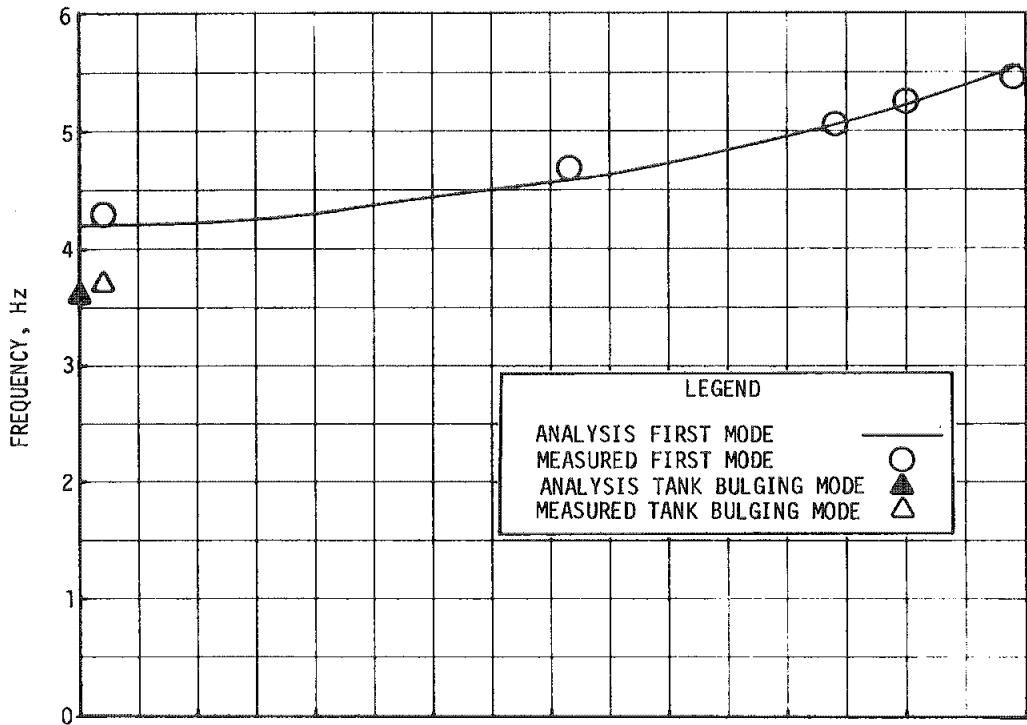


Figure 9-4. First Longitudinal Modal Frequencies and Amplitudes During S-IC Powered Flight

The most significant structural responses during S-IC burn were observed after CECO, and after OECO. CECO excited the first structural mode frequency (5.2 hertz) of the AS-504 vehicle. The maximum command module amplitude in this mode was 0.35 Gpeak at 135 seconds. Except for the POGO oscillations on AS-502, this amplitude was larger than any measured on previous flights. The decay of this CECO transient was slower than would be expected, requiring about 13 seconds to damp. The slow decay is attributed to low structural damping (about 0.5 percent critical damping).

The S-IC OECO also excited the first longitudinal mode with a maximum command module amplitude of -0.8 Gpeak occurring at 163.6 seconds. This transient resulted in rough S-IC/S-II separation dynamics and is discussed in greater detail in Section 12.

9.2.3.2 POGO Evaluation. The S-IC CECO and OECO thrust decay transients excited the first longitudinal mode which damped slowly. There was no evidence of POGO associated with these transients. Since the CECO transient produced a fairly strong response, had there been POGO instability it would have diverged at that time.

Longitudinal acceleration data show the first longitudinal mode exists at low amplitudes throughout S-IC flight. Because of the apparent low damping, it is believed that there are enough random excitation forces to keep this mode oscillating at a perceivable level throughout S-IC flight.

The lack of any significant inlet pressure buildup in the engine is further indication of freedom from POGO, thus the helium accumulator fix is believed to be working as expected.

During S-II powered flight, the same anomaly (18 hertz oscillations) occurred late in flight time that was evident on AS-503. Figure 9-5 shows the frequency and amplitude trends with time of the structural and propulsion measurements required for POGO evaluation. The oscillations reached a maximum level of approximately  $\pm 12.0$  g at the center of the S-II thrust structure crossbeam. This anomaly is discussed in greater detail in Section 6.

Test programs and analyses are proceeding on an expedited basis, yet this 18 hertz anomaly has not been resolved. A recommendation has been made and implemented to cut off the center engine of the S-II stage after 299 seconds of burn. This is the most positive method to avoid the problem without major impact and within the technical understanding of the anomaly.

There was no significant structural response or indication of POGO during S-IVB powered flight.



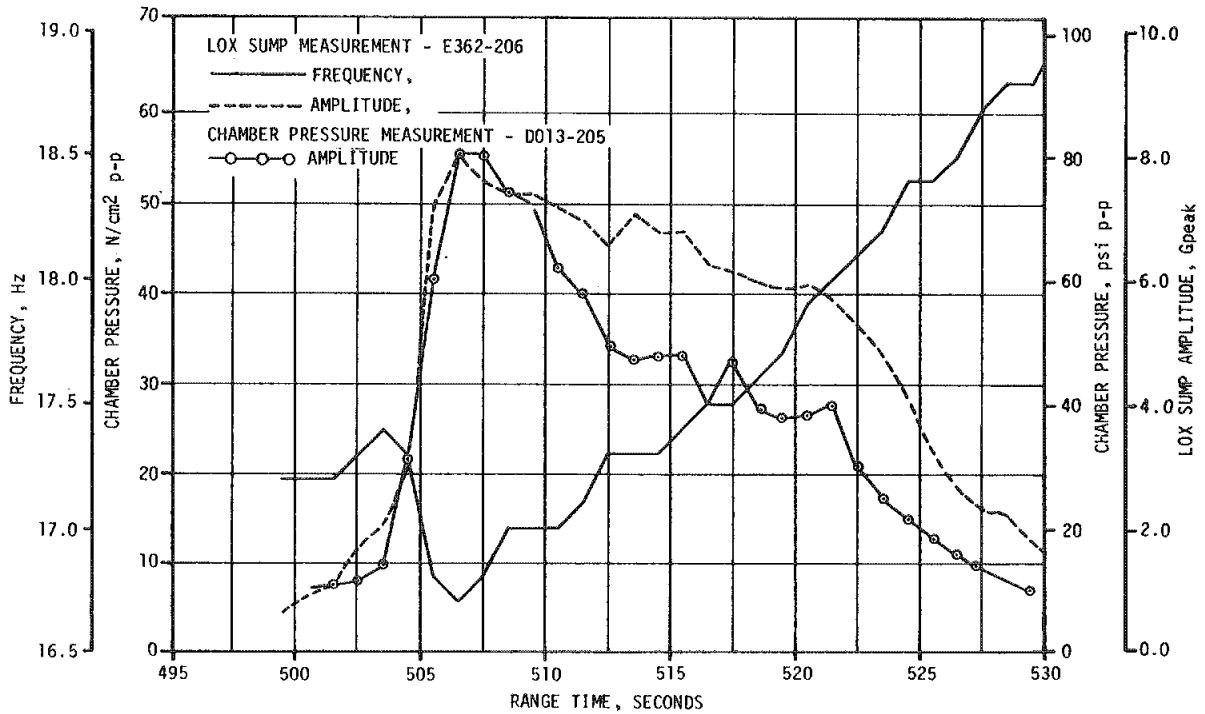
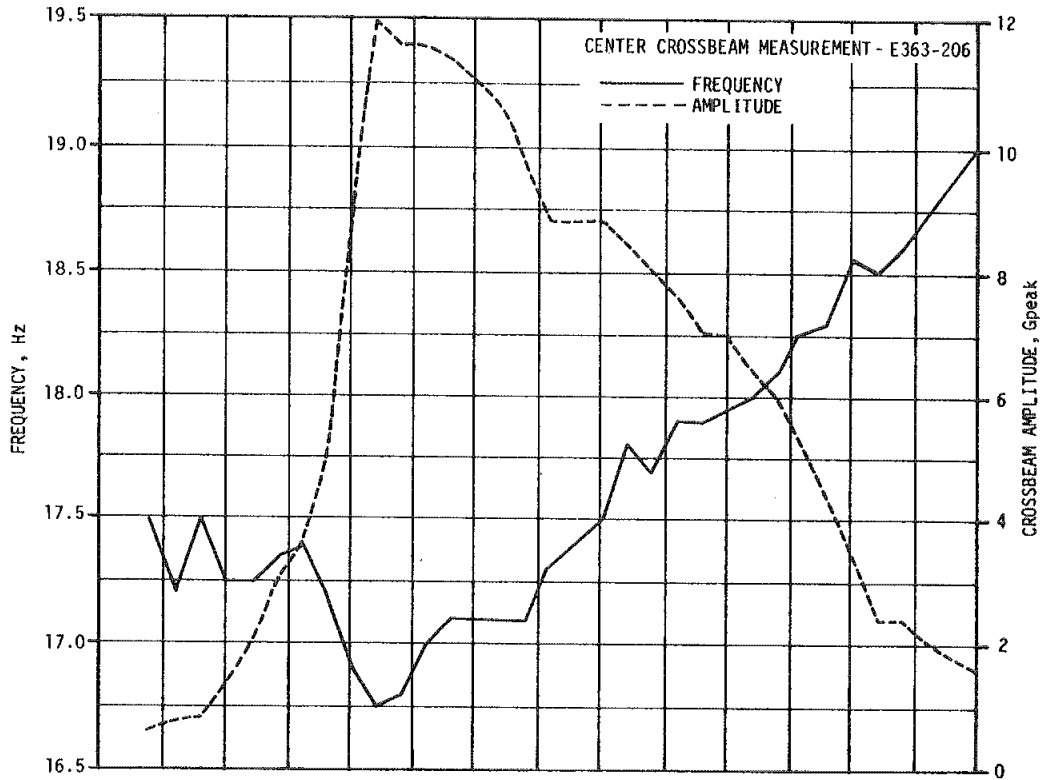


Figure 9-5. S-II Stage Response/Frequency Characteristics

9.2.3.3 Lateral Dynamic Characteristics. Oscillations in the first four modes were detectable throughout S-IC powered flight. Spectral analyses were performed to determine modal frequencies using 5-second time slices. The frequencies of these oscillations agreed well with the analytical predictions, as shown in Figure 9-6.

### 9.3 VIBRATION EVALUATION

#### 9.3.1 S-IC Stage and Engine Evaluation

Structure, engine, and component vibration measurements taken on the S-IC stage are summarized in Table 9-1 and Figures 9-7 through 9-9. A total of 44 single sideband vibration measurements were recorded of which 31 yielded valid data throughout flight. Measurement locations are shown in Figure 9-10.

9.3.1.1 S-IC Stage Structure. Stage structure vibration data exhibited composite RMS levels and spectra shapes within the data envelopes of previous flights. The forward skirt structure RMS levels lagged those measured on previous flights because the Max Q region occurred later in flight for AS-504.

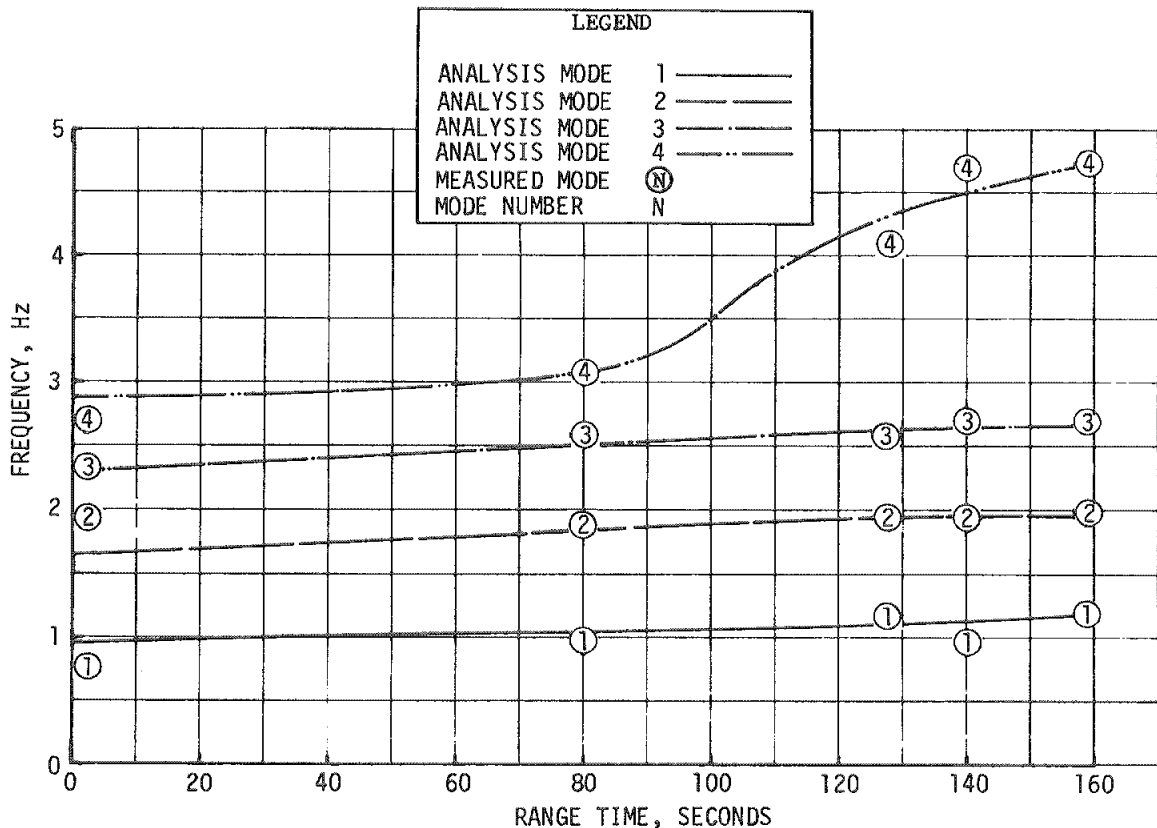


Figure 9-6. AS-504 Lateral Analysis/Measured Modal Frequency Correlation

Table 9-1. S-IC Stage Vibration Summary

MEASUREMENT	MAXIMUM GRMS		OVERALL GRMS LIMIT	REMARKS
	PREVIOUS FLIGHT DATA	AS-504		
<b>STRUCTURE</b>				
Thrust Structure				
E023-115	14.7 at 0	12.5 at -1	22	
E024-115	11.2 at 0	7.5 at -1	25	
E053-115	6.9 at 149.5	5.8 at 155	17	
E054-115	3.7 at 150	2.6 at 155	17	
E079-115	3.3 at 148	2.6 at 158	17	
E080-115	4.2 at 148	2.9 at 158	17	
Intertank Structure				
E020-118	7.7 at 2	4.5 at 6	27	
E021-118	9.1 at 4	6.3 at -1	27	
Forward Skirt Structure				
E046-120	Invalid	3.6 at 94	30	Located near command destruct vibration isolated panel
E047-120	6.1 at 3.9	5.4 at 2.5	30	
<b>ENGINE</b>				
Combustion Chamber				
E036-101	8.8 at 20.5		49	AS-504 data were questionable
E036-102	9.7 at 0		49	
E036-103	8.3 at 53		49	
E036-104	8.4 at 106.8		49	
E036-105	8.2 at 130.5		49	
Turbopump				
E037-101	41.5 at 20.0		41	AS-504 data were questionable
E038-101	39.0 at 1.0		41	
E039-101	26.5 at 125.0	18.8 at 130.0	41	AS-504 data contained spikes at all analysis times Partial Failure
E040-101	12.5 at 132.5	17.3 at 123.8	41	
E041-101	19.7 at 152.0	20.9 at 158.0	41	
E041-102	17.5 at 144.5	17.2 at 14.4	41	
E042-102	9.6 at 86	Totally Invalid	41	
E042-103	9.3 at 132.0	10.9 at 148.1	41	These measurements are considered total failures, however, some maximum GRMS levels could be observed.
E042-104	11.2 at 79.0	9.9 at 69.3	41	
E042-105	8.5 at 96.5	10.7 at 26.6	41	
<b>COMPONENTS</b>				
Engine Actuators				
E030-101	9.4 at 111	4.1 at 161	30	
E030-102	5.0 at 123	4.4 at 127	30	
E031-101	6.2 at 136	6.7 at 118	30	
E031-102	7.8 at 107	5.8 at 36	30	
E032-101	15.1 at 111	13.8 at 124	30	
E032-102	14.0 at 89	11.2 at 115	30	
E033-101	8.8 at 100	8.5 at 118	30	
E033-102	7.0 at 127	5.6 at 109	30	
E034-101	5.0 at -1.0	5.3 at 124	30	
E034-102	5.5 at 135	4.1 at 127	30	
E035-101	15.0 at 68	9.8 at 88	30	
E035-102	10.5 at 127	7.1 at 109	30	
Heat Shield Panels				
E105-106	76.6 at -1	72.6 at 0	33	
E106-106	62.6 at -1	70.8 at 0	33	
E107-106	68.0 at -1	74.4 at 0	33	
Propellant Delivery System				
E025-118	2.7 at 132	1.3 at 5.5	9	
E026-118	2.4 at 4.6	3.1 at 118	9	
E027-115	10.4 at -0.5	7.7 at 112	22	
E028-115	9.7 at 4.6	11.3 at 118	22	

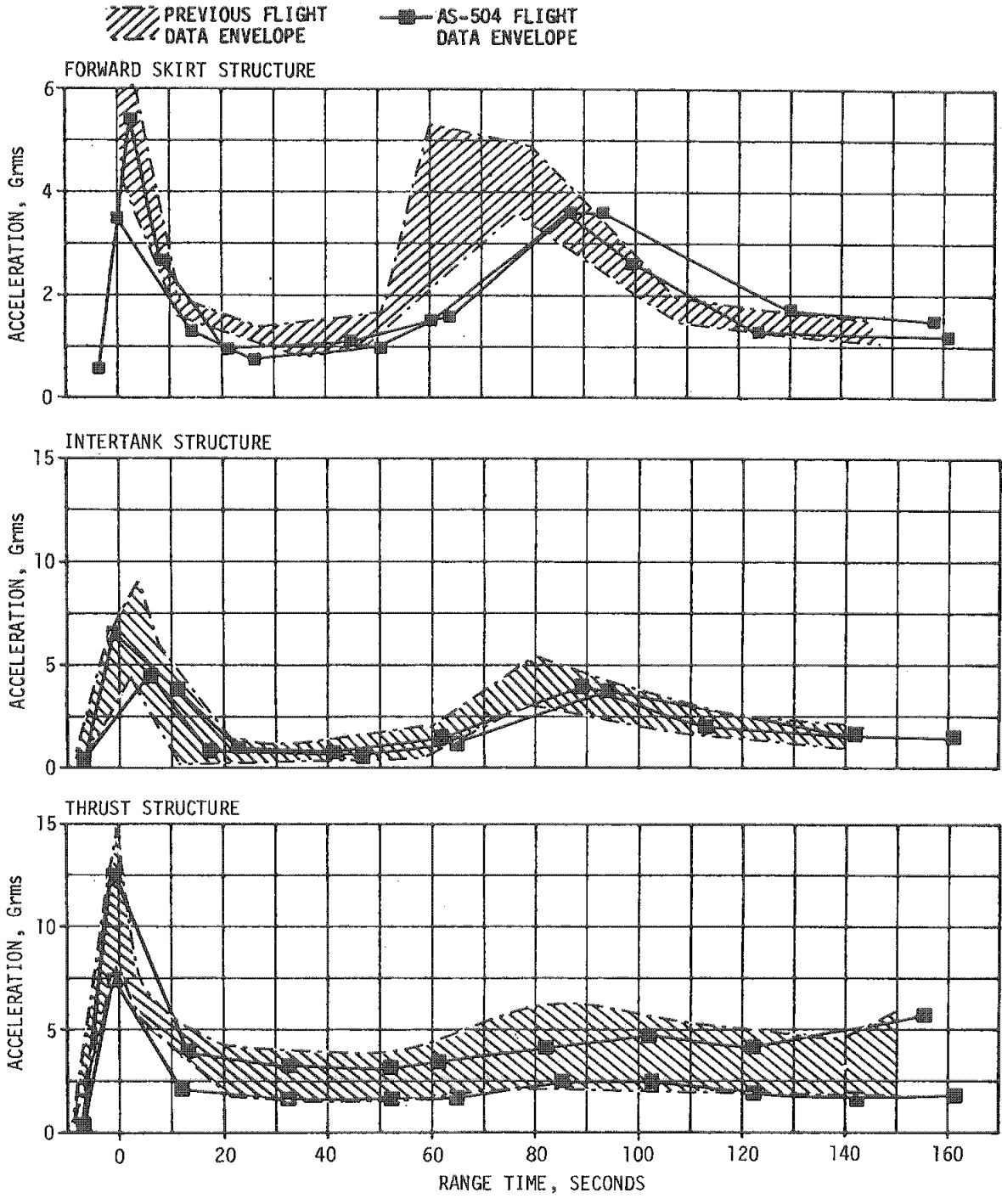


Figure 9-7. S-IC Stage Structure Vibration Envelopes

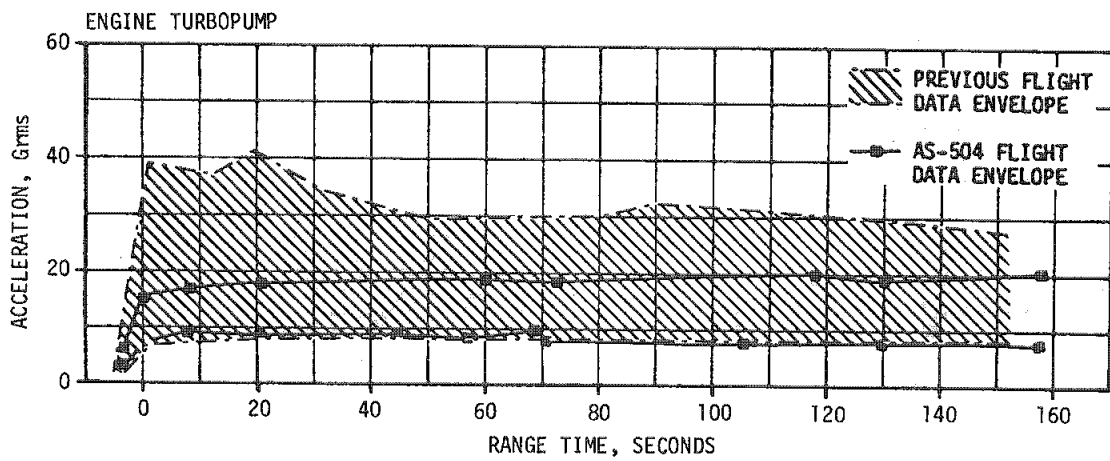


Figure 9-8. S-IC Stage Engine Turbopump Vibration Envelope

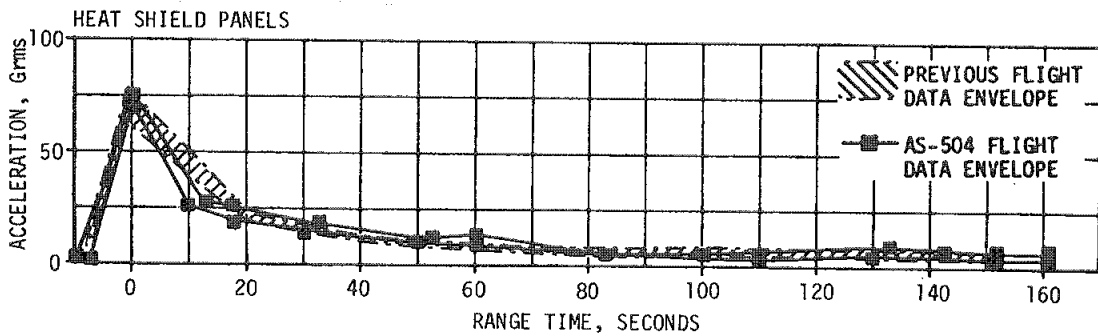
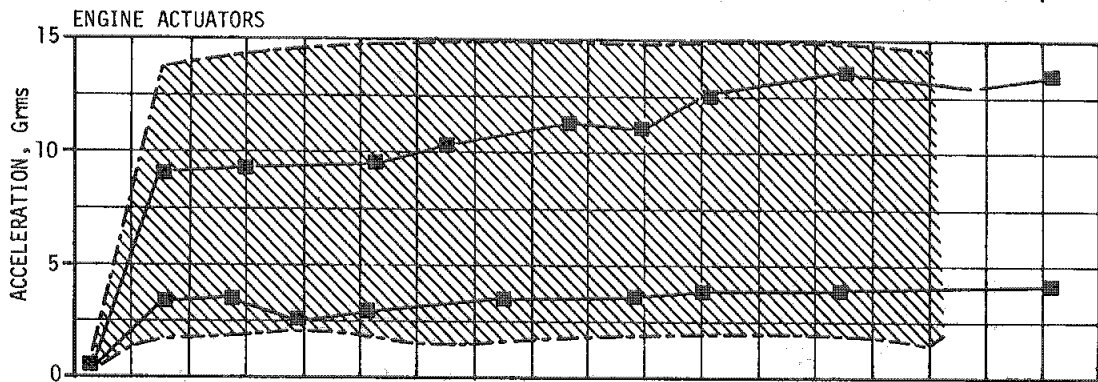
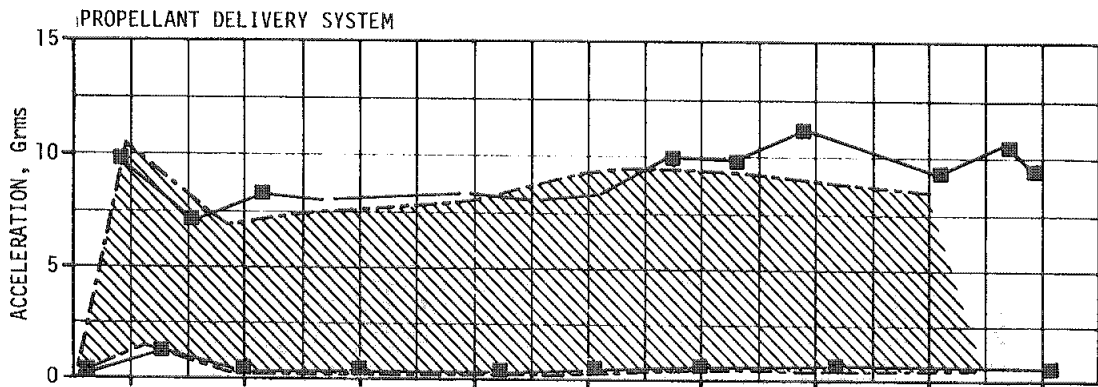


Figure 9-9. S-IC Stage Components Vibration Envelopes

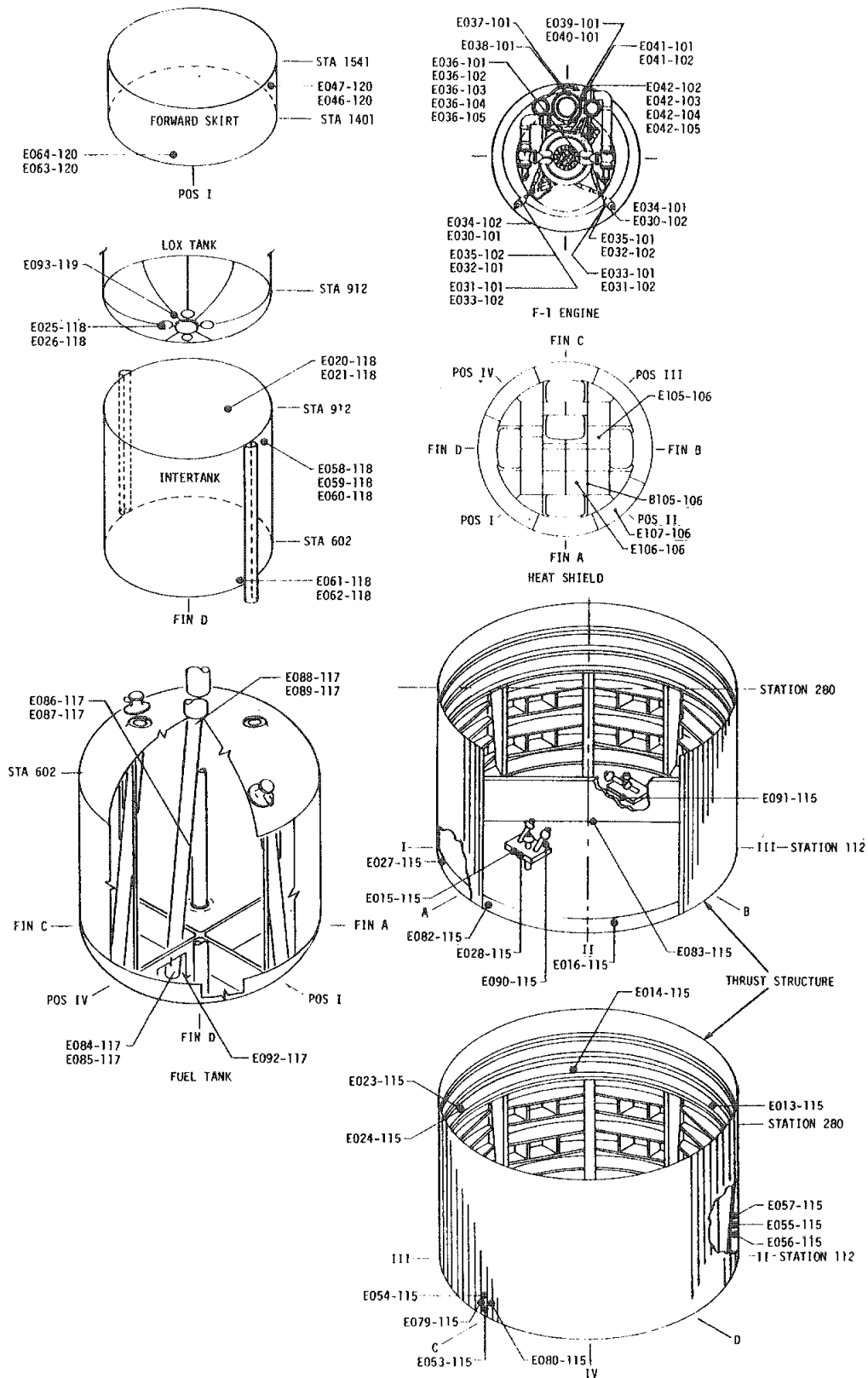


Figure 9-10. S-IC Vibration Measurement Locations

9.3.1.2 F-1 Engines. The F-1 engine combustion chamber measurements exhibited composite RMS levels that were 60 to 70 percent of expected and are considered invalid. Generally, the valid turbopump measurements compared closely with past flight data in both overall levels and spectra shapes. The upper limit of the previous flight data envelope for the turbopump was established by two AS-503 measurements which were abnormally high.

9.3.1.3 S-IC Components. All S-IC component vibration measurements were valid and the levels measured were generally similar to those on previous flights. Four actuator measurements exhibited levels a little lower than expected; however, the data appear valid. The heat shield vibration measurements agreed closely with the previous data and; therefore, verified the high vibration levels measured at liftoff on AS-503.

### 9.3.2 S-II Stage and Engine Evaluation

Comparisons of Grms values for AS-501, AS-502, AS-503 and AS-504 are shown in Table 9-2 and Figures 9-11 through 9-13. The variations between the four flights are considered normal.

9.3.2.1 S-II Stage Structure. In general, the S-II stage structure vibration levels were within the envelopes established by previous flights. The engine No. 1 beam lateral vibration and thrust cone longerons normal and longitudinal vibration levels were below the envelopes established by previous flights.

9.3.2.2 S-II Stage J-2 Engines. The AS-504 vibration levels were lower than the AS-503 engine measurements, recorded prior to S-II engine start, and throughout the flight for the LOX pumps. These lower levels verify the existence of suspected high level noise on AS-503 engine measurements.

9.3.2.3 S-II Stage Components. The much higher levels shown for the container 206 normal response appear to be valid data. Comparison of this data with qualification test levels shows that this container has been tested at higher levels.

Table 9-2. S-II Stage Maximum Overall Vibration Levels

ZONE	STATIC FIRING		FLIGHT				
	VEHICLE	MAXIMUM GRMS RANGE	VEHICLE	MAXIMUM GRMS RANGE			
				LIFTOFF	TRANSONIC	MAX Q	MAINSTAGE
Forward Skirt Containers	S-II-1,-2,-3	0.7 to 2.5	AS-501,2,3 AS-504	0.7 to 9.1	0.7 to 3.7	1.1 to 5.3	0.0 to 0.9
	S-II-4	1.2 to 3.1		1.9 to 8.4	1.4 to 5.2	1.7 to 5.0	0.3 to 0.6
Forward Skirt Stringers	S-II-1,-2,-3	1.6 to 4.8	AS-501,2,3 AS-504	1.2 to 13.1	1.0 to 11.3	1.7 to 9.2	0.3 to 1.3
	S-II-4	2.3 to 5.0		1.9 to 9.0	1.9 to 8.1	3.5 to 7.8	0.4 to 1.0
Aft Skirt	S-II-1,-2,-3	10.1 to 31.7	AS-501,2,3 AS-504	5.3 to 17.3	3.6 to 8.3	5.4 to 12.1	0.4 to 2.2
	S-II-4	9.8 to 19.6		16.6	7.3	10.9	1.8
Interstage	S-II-1,-2,-3	Interstage not installed	AS-501,2,3 AS-504	3.1 to 16.0	2.0 to 6.5	2.6 to 7.2	1.1 to 3.6
	S-II-4			6.9 to 18.3	2.8 to 4.7	4.0 to 7.3	0.7 to 1.1
Thrust Cone Containers	S-II-1,-2,-3	2.2 to 15.8	AS-501,2,3 AS-504	0.3 to 7.0	0.4 to 2.6	0.3 to 2.2	0.3 to 3.8
	S-II-4	5.6 to 11.8		0.5 to 7.5	0.2 to 2.0	0.4 to 2.8	0.3 to 3.1
Thrust Cone Longerons	S-II-1,-2,-3	4.1 to 12.3	AS-501,2,3 AS-504	0.2 to 5.1	0.6 to 2.0	0.7 to 2.7	1.0 to 7.2
	S-II-4	5.3 to 10.1		0.4 to 1.9	0.1 to 0.8	0.3 to 1.7	0.5 to 3.5
Engine Beam	S-II-1,-2,-3	5.4 to 15.3	AS-501,2,3 AS-504	0.5 to 1.5	0.3 to 0.9	0.4 to 1.0	5.3 to 13.9
	S-II-4	3.1 to 14.9		0.7	0.2	0.2	3.1
Engine Combustion Domes	S-II-1,-2,-3	Invalid data	AS-503 AS-504	2.2 to 7.1	5.5 to 9.9	2.1 to 7.7	7.0 to 9.6
	S-II-4			0.0 to 2.5	0.0 to 2.0	0.0 to 3.9	2.8 to 10.1
LOX Pumps	S-II-1,-2,-3	Invalid data	AS-503 AS-504	Not Evaluated		0.0 to 1.7	3.5 to 4.5
	S-II-4			0.0 to 1.9	0.0 to 1.4		2.8 to 9.2
LH2 Pumps	S-II-1,-2,-3	Invalid data	AS-503 AS-504	Not Evaluated		1.5 to 3.7	9.2 to 13.3
	S-II-4			3.0 to 7.3	0.0 to 2.2		8.8 to 19.9
LOX Sump Prevalves	S-II-1,-2,-3	Instrumentation not installed	AS-503 AS-504	0.7 to 0.8	0.5	0.5	0.5 to 0.7
	S-II-4				Invalid Data		
LH2 Prevalves	S-II-1,-2,-3	Instrumentation not installed	AS-503 AS-504	0.8 to 1.0	0.8	0.8 to 1.1	0.9 to 1.2
	S-II-4			1.8 to 3.2	0.2 to 0.4	0.3 to 0.8	0.3 to 1.4

NOTE: Values listed for AS-501, -502, -503 are based on PSD's. Values listed for AS-504 are based on GRMS histories.



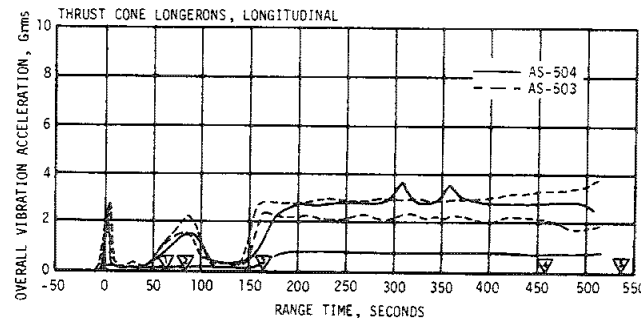
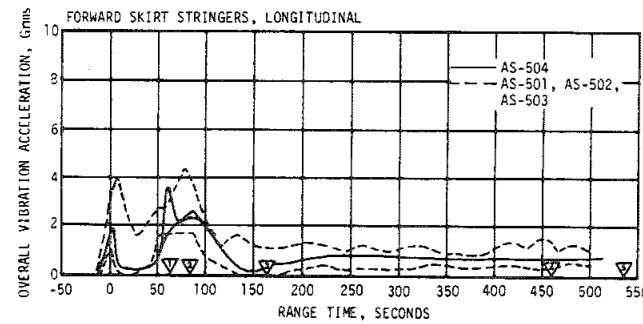
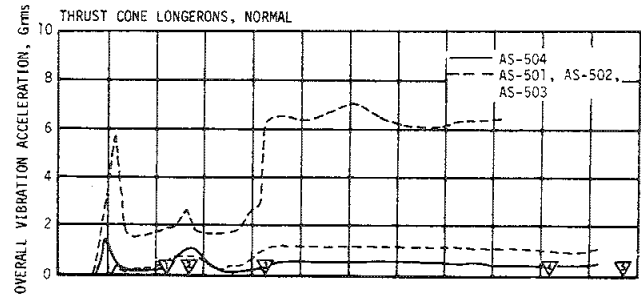
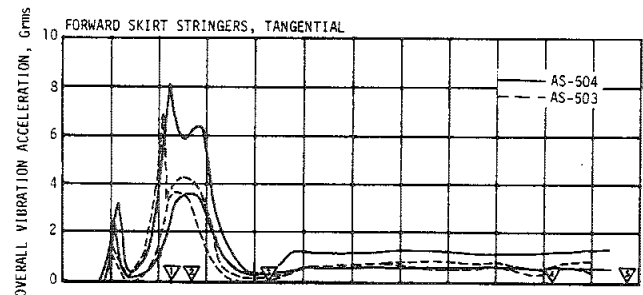
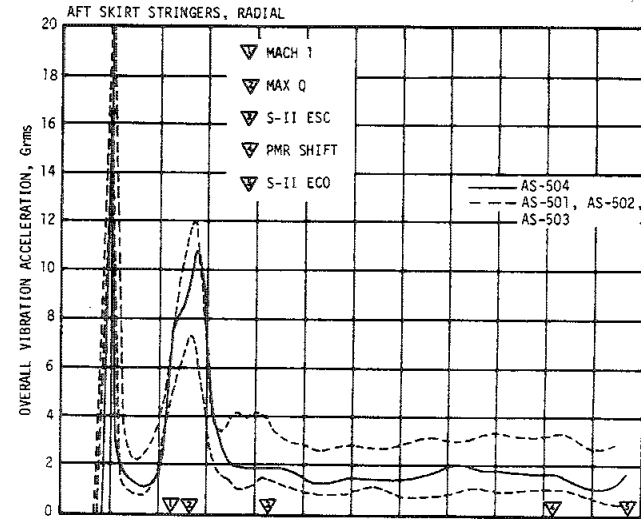
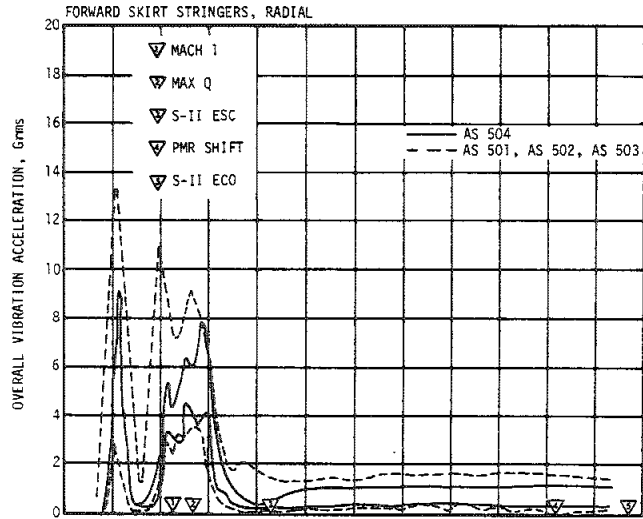


Figure 9-11. S-II Stage Structure Vibration Envelopes (Sheet 1 of 2)

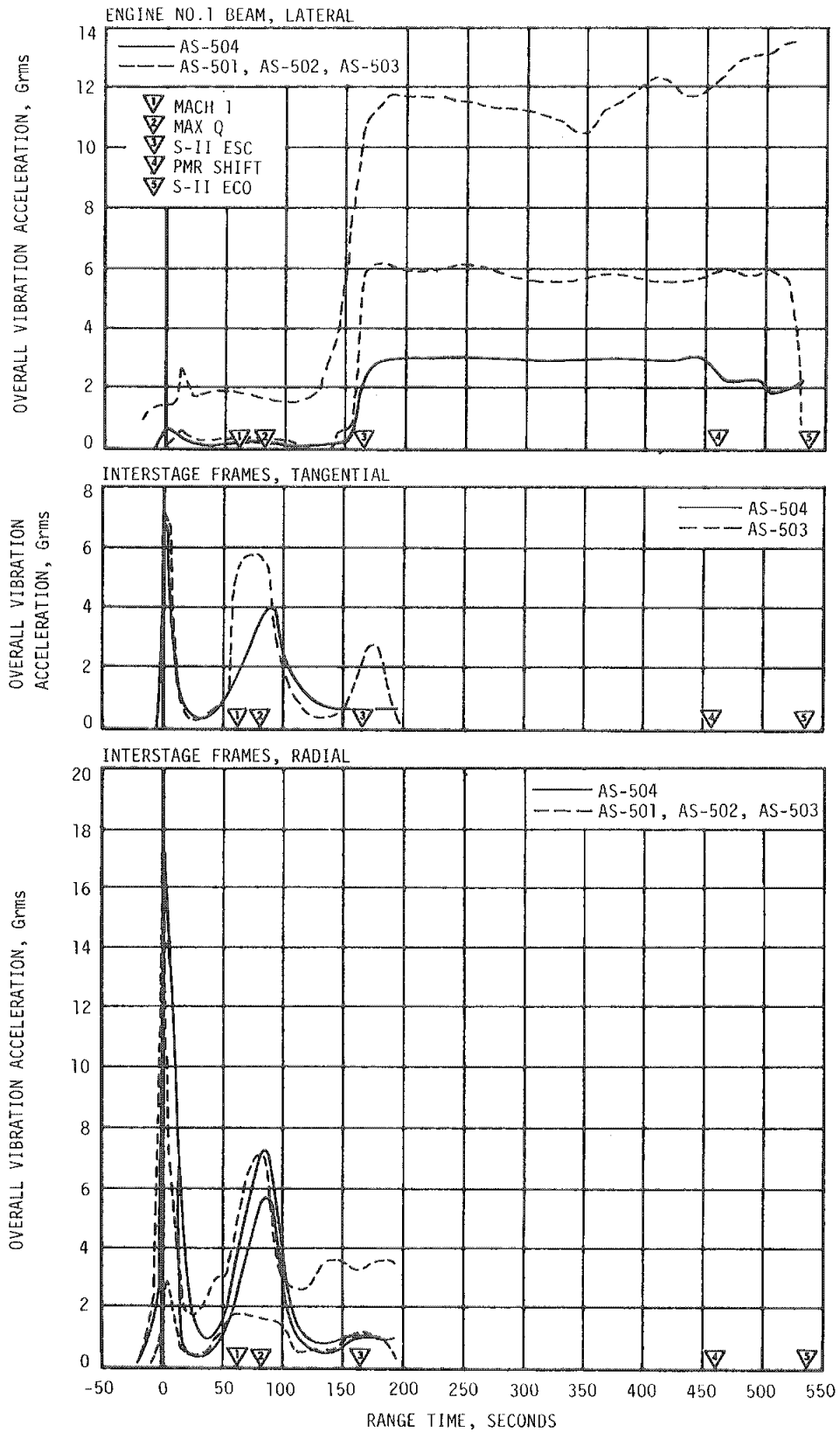


Figure 9-11. S-II Stage Structure Vibration Envelopes (Sheet 2 of 2)

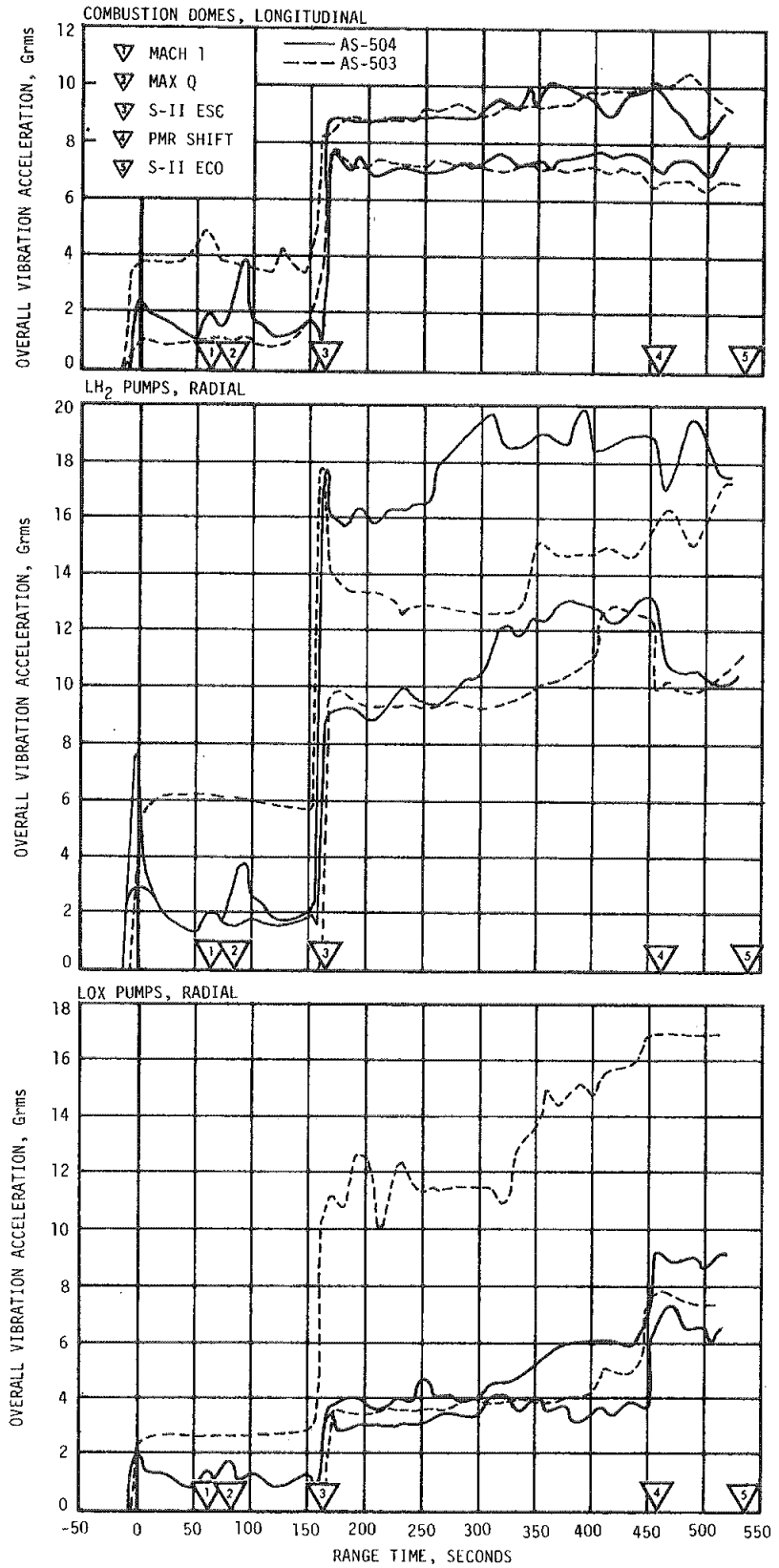


Figure 9-12. S-II Stage Engine Vibration Envelopes

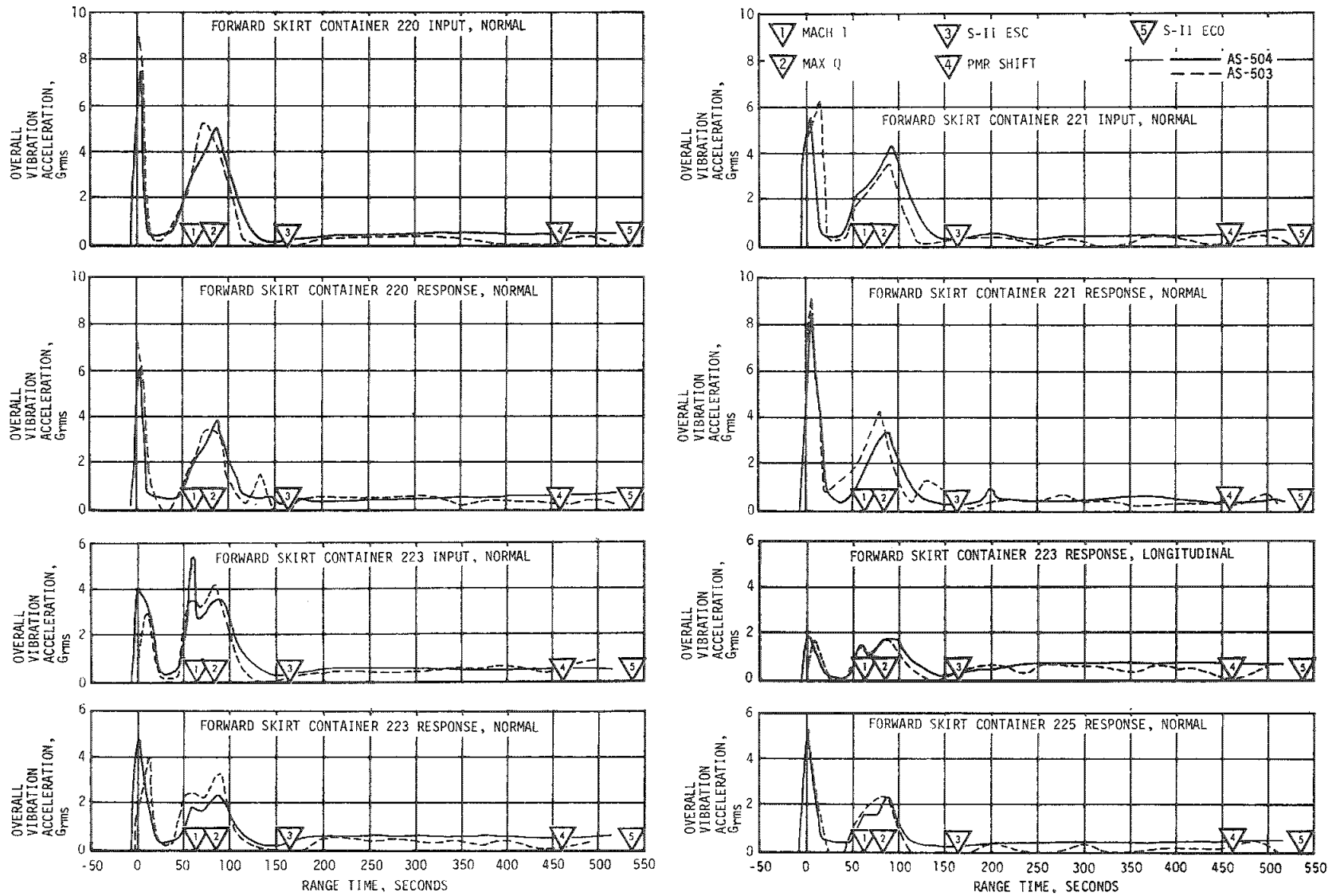


Figure 9-13. S-II Stage Component Vibration Envelopes (Sheet 1 of 2)

9-19/9-20

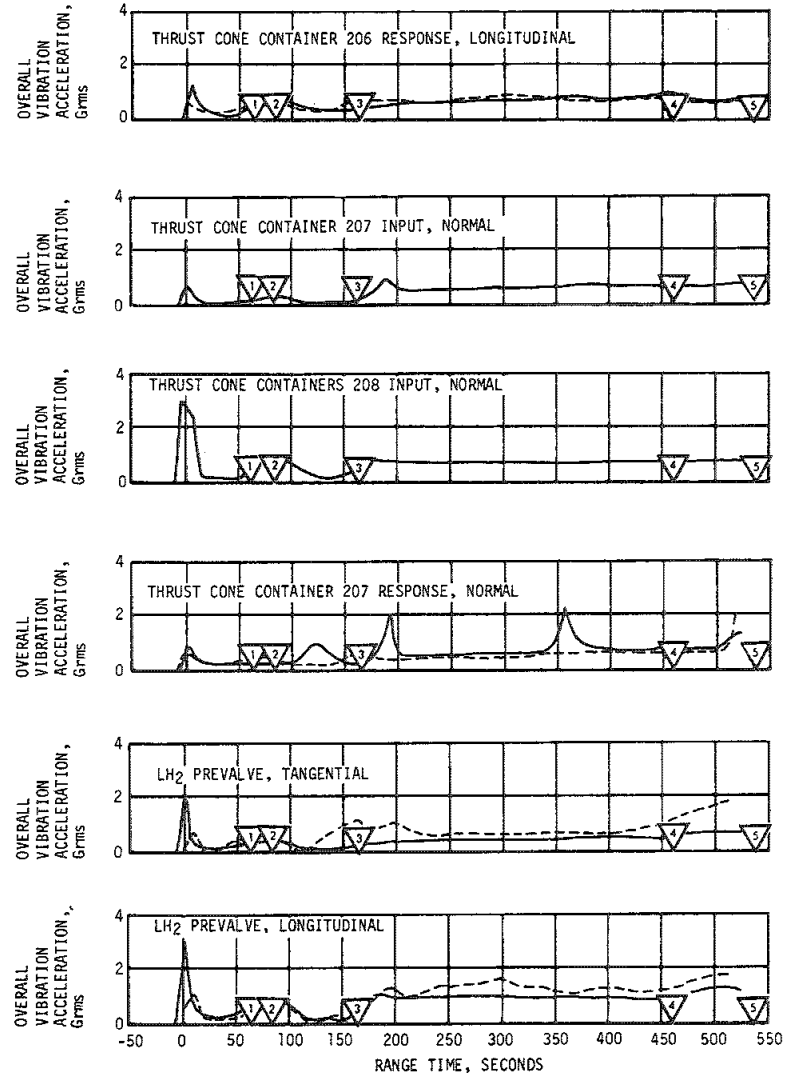
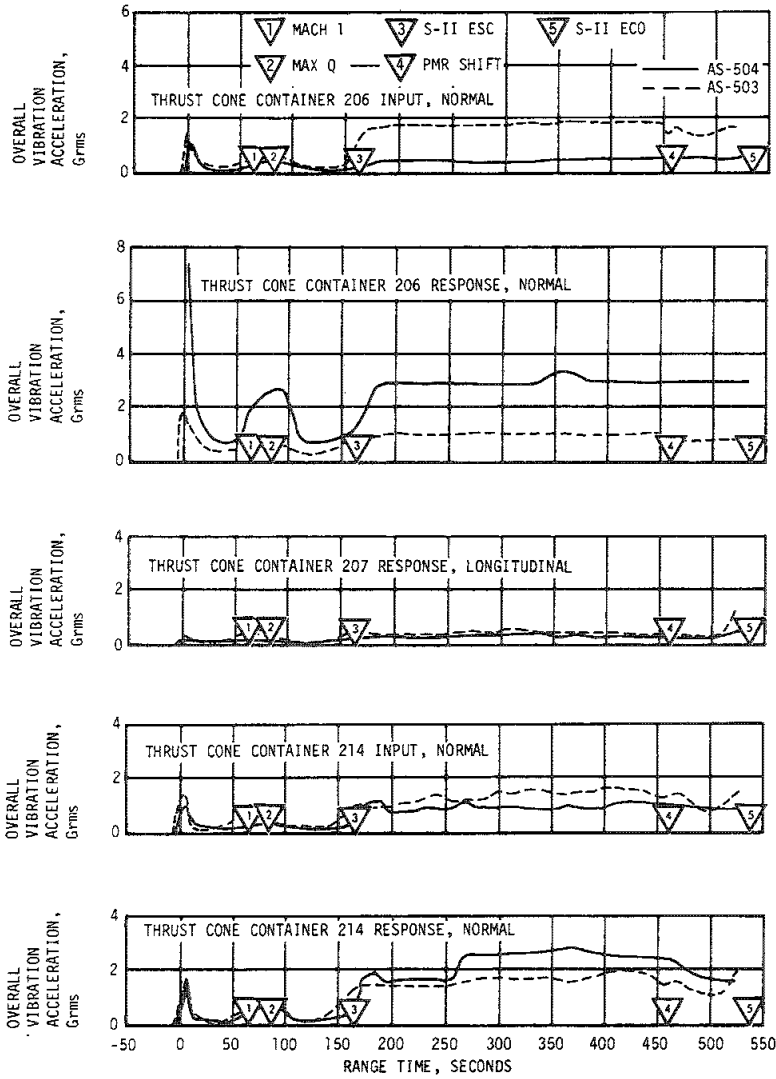


Figure 9-13. S-II Stage Component Vibration Envelopes (Sheet 2 of 2)

## SECTION 10

### GUIDANCE AND NAVIGATION

#### 10.1 SUMMARY

##### 10.1.1 Flight Program

The guidance and navigation system performed satisfactorily during all periods for which data are available. The boost navigation and guidance schemes were properly executed, and the desired parking orbit insertion parameters were achieved with good accuracy. The third burn of the S-IVB stage placed the S-IVB/IU in a heliocentric orbit. All target parameters were satisfactorily achieved and all orbital operations were nominal. System performance was unaffected by either the unexpected change in thrust level during S-IVB third burn, or the failure to dump residual propellants following the burn.

##### 10.1.2 Instrument Unit Components

The Launch Vehicle Digital Computer (LVDC), the Launch Vehicle Data Adapter (LVDA), and the ST-124M-3 inertial platform functioned satisfactorily. The platform temperature and pressure experienced minor deviations, but there was no apparent platform performance degradation. There was also a problem with the H60-603 telemetry during the period from S-II/S-IVB separation until CSM/S-IVB separation. Navigation and guidance functions were not affected.

#### 10.2 GUIDANCE AND NAVIGATION SYSTEM DESCRIPTION

##### 10.2.1 Flight Program Description

The flight program controls the LVDC from Guidance Reference Release (GRR) until the end of the mission. The program performs seven primary functions: navigation, guidance, event sequencing, attitude control, data management, ground command processing, and hardware evaluation.

10.2.1.1 Preflight Prepare-to-Launch Mode. At approximately -13 minutes, the LVDC is commanded into the Prepare-to-Launch (PTL) mode by the RCA-110A computer. This routine performs prelaunch functions and prepares the LVDC for the flight mode.

10.2.1.2 Boost Initialize. The flight program contains routines which initialize navigation quantities, and boost-to-parking orbit parameters. The program also computes coordinate transformation matrices.

10.2.1.3 Boost Routines. The boost routines perform navigation and guidance, event sequencing, and attitude control. Boost navigation includes the computations and logic necessary to determine vehicle state vectors during powered flight.

Boost guidance has two operating modes. These are pre-Iterative Guidance Mode (IGM), used from liftoff until shortly after Launch Escape Tower (LET) jettison during S-II stage operation, and IGM, used during the remainder of boost to parking orbit. Pre-IGM guidance is a series of preset commands which include a yaw maneuver for launcher clearance, a roll maneuver to obtain the desired flight azimuth, and a pitch tilt maneuver. IGM is a near optimum guidance scheme based on a flat earth optimum steering function for planar motion of a point-mass vehicle.

Event sequencing is accomplished by the switch selector on an interrupt basis.

Attitude control is accomplished in the minor loop section of the program on an interrupt basis. The boost minor loop processes platform gimbal angles and computes attitude commands to drive the gimbal angles to their desired values.

10.2.1.4 Orbital Routines. The orbital program includes two monitor routines. The first is the IU Hardware Evaluation Program (HEP), and the second is the Telemetry Executive Program (TEP). Navigation, guidance, event sequencing, attitude control, and ground command processing are initiated from either HEP or TEP. The HEP routine was reduced to an interruptible one-instruction loop because no hardware evaluation functions were defined.

Once the vehicle acquires a ground station, TEP is entered. This routine provides time sharing telemetry of compressed and real time data. In addition, various special data are telemetered on an interrupt basis. Data from the LVDA are telemetered automatically.

Orbital guidance controls the vehicle attitude during the earth parking orbit ( $T_5$ ) and after S-IVB second and third burn cutoffs ( $T_7$  and  $T_9$ ).

Orbital navigation includes the computations necessary to determine vehicle state vectors during coast periods. This is accomplished by integration of space-fixed accelerations. These accelerations are obtained by solving an approximate atmospheric drag equation, rotating prestored, body-fixed vent accelerations through the gimbal angles, and solving for gravitational accelerations.

Event sequencing in orbit is accomplished exactly as in the boost phase with the added capability to receive time base updates and special output sequence commands from ground stations.

Ground command processing is accomplished by the Command Decoder interrupt with the Digital Command System (DCS) routine.

10.2.1.5 Flight Program Differences. The significant changes to the AS-504 flight program were:

- a. S-II stage propellant utilization system operated closed loop.
- b. Fixed attitude and fixed duration for S-IVB stage out-of-orbit burns.
- c. Logic to provide three boost phases.

#### 10.2.2 Instrument Unit System Description

The LVDC is a high-reliability general purpose random-access digital computer which contains the logic circuits, memory, and timing system required to perform mathematical operations necessary for navigation, guidance, and vehicle flight sequencing. The LVDC is also used for prelaunch and orbital checkout.

The LVDA is the input/output device for the LVDC. These two components operate in conjunction to carry out the flight program. This program performs the following functions:

- a. Processes the inputs from the platform.
- b. Performs navigation calculations.
- c. Provides first stage tilt program.
- d. Calculates IGM steering commands.
- e. Resolves steering commands into the vehicle system for attitude error commands.
- f. Issues cutoff and sequencing signals.

The ST-124M-3 inertial platform assembly has a three-gimbal configuration, with gas bearing gyros and pendulous integrating gyro accelerometers mounted on the stable element, which provides an inertial space-fixed coordinate reference frame for attitude control and navigation measurements. Gimbal angles are measured by resolvers. Inertial velocity is obtained from measurements of the angular rotation of the accelerometer measuring head.

### 10.3 GUIDANCE COMPARISONS

The postflight guidance hardware error analysis is based on comparisons of the ST-124M-3 platform measured velocities with the observed post-flight trajectory established from external tracking data. Figure 10-1 presents the comparisons of the platform measured velocities with



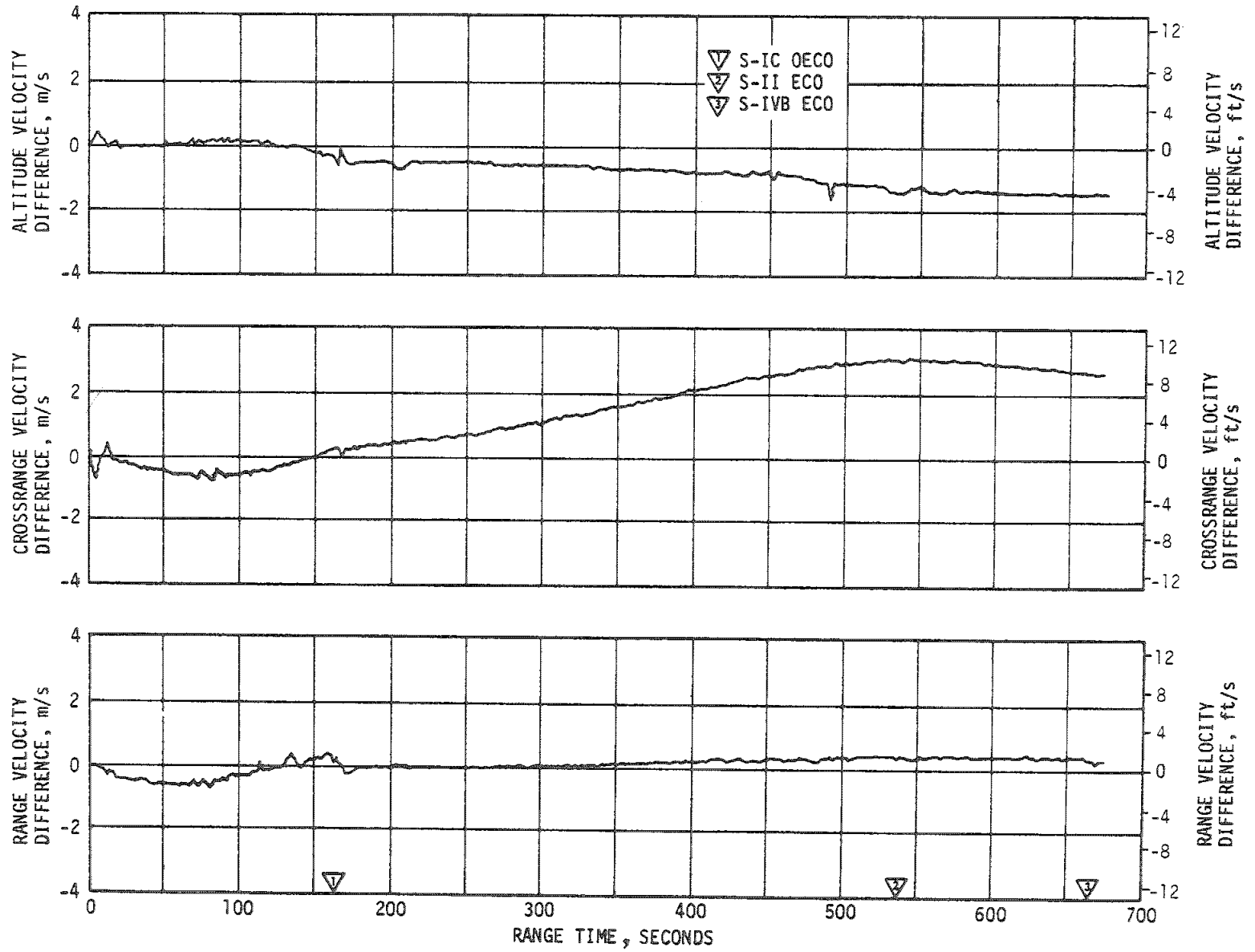


Figure 10-1. Tracking and ST-124M-3 Platform Velocity Comparison (Trajectory Minus Guidance)

corresponding values from the final postflight trajectory. A positive difference indicates trajectory data greater than the platform measurement. The differences shown during S-IC stage burn probably reflect more trajectory error than guidance. However, the differences are within the accuracies of the data compared.

The crossrange velocity difference built up to about 3.0 m/s (9.84 ft/s) by S-II ECO, and then gradually reduced to 2.66 m/s (8.73 ft/s) by S-IVB first cutoff. Altitude and range velocity differences at S-IVB first cutoff were -1.42 m/s (-4.66 ft/s) and 0.31 m/s (1.02 ft/s), respectively. The differences were within the accuracy of the data compared and/or the 3 sigma hardware errors.

The velocity differences are shown through parking orbit insertion only. Due to limited external tracking during the S-IVB second and third burns, the C-band radar data were constrained to platform velocity changes in establishing the postflight trajectory. The telemetered platform velocities are set to zero during orbit, and accumulated during S-IVB second and third burns. Since these velocity changes were used to establish the trajectory, comparisons show no buildup in differences during the burn times.

Velocities measured by the ST-124M-3 platform system at significant flight event times are shown in Table 10-1, along with corresponding values computed from the final Postflight Observed Trajectory and the Preflight Operational Trajectory. The differences between the telemetered velocities and postflight trajectory values reflect some combination of small guidance hardware errors and tracking errors. The differences between the LVDC and predicted trajectory values reflect off nominal flight conditions and vehicle performance.

Comparisons of navigation (in the PACSS 13 coordinate system) positions, velocities, and flight path angle at significant flight event times are shown in Table 10-2. For the boost to parking orbit portion of flight, the guidance LVDC and observed trajectory parameters are in relatively good agreement. At parking orbit insertion, the velocity component differences were -1.73 m/s (5.68 ft/s), 2.46 m/s (8.07 ft/s), and 0.12 m/s (0.39 ft/s) for altitude, crossrange, and range velocities, respectively. The difference in total velocity was 0.86 m/s (2.82 ft/s). These differences are well within the accuracy of the 3 sigma hardware errors and/or the trajectory data.

The AS-504 vehicle was approximately 2.89 kilometers (1.56 n mi) lower in altitude and 29.33 m/s (96.23 ft/s) lower in total velocity than nominal at S-IC OECO. The burn time between T<sub>2</sub> and T<sub>3</sub> was about 2.76 seconds longer than nominal. At S-II ECO the geocentric radius and total velocity were about 2.339 kilometers (1.26 n mi) and 81.70 m/s (268.04 ft/s), respectively, lower than nominal. These deviations required about 10.3 seconds longer burn time during the S-IVB first burn. At S-IVB first cutoff the radius was 36 meters (118 ft) greater and the total velocity was 0.87 m/s (2.86 ft/s) less than nominal.

Table 10-1. Inertial Platform Velocity Comparisons

EVENT	DATA SOURCE	VELOCITY m/s (ft/s)**		
		ALTITUDE ( $\dot{X}_m$ )	CROSSRANGE ( $\dot{Y}_m$ )	RANGE ( $\dot{Z}_m$ )
S-IC CECO 134.34 sec	Guidance	2191.97 (7191.50)	3.63 (11.91)	1405.45 (4611.05)
	Postflight Trajectory	2192.09 (7191.90)	3.37 (11.05)	1405.50 (4611.22)
	Preflight Trajectory	2251.17 (7385.72)	-1.50 (-4.92)	1468.85 (4819.06)
S-IC OECO 162.76 sec	Guidance	2563.44 (8410.23)	-0.97 (-3.18)	2249.18 (7379.20)
	Postflight Trajectory	2563.00 (8408.79)	-0.71 (-2.33)	2249.28 (7379.53)
	Preflight Trajectory	2596.71 (8519.39)	-3.27 (-10.73)	2257.40 (7406.17)
S-II ECO 536.22 sec	Guidance	3448.46 (11,313.84)	-3.95 (-12.96)	6778.73 (22,239.93)
	Postflight Trajectory	3447.07 (11,309.28)	-0.94 (-3.08)	6779.16 (22,241.34)
	Preflight Trajectory	3327.70 (10,917.65)	-0.49 (-1.61)	6843.92 (22,453.80)
S-IVB First Cutoff 664.66 sec	Guidance	3176.26 (10,420.80)	3.00 (9.84)	7596.83 (24,923.98)
	Postflight Trajectory	3174.84 (10,416.14)	5.66 (18.57)	7597.14 (24,925.00)
	Preflight Trajectory	3107.35 (10,194.72)	2.17 (7.12)	7587.14 (24,892.19)
Parking Orbit Insertion 674.65 sec	Guidance	3175.65 (10,418.80)	3.00 (9.84)	7598.80 (24,930.45)
	Postflight Trajectory	3174.23 (10,414.14)	5.69 (18.67)	7599.08 (24,931.36)
	Preflight Trajectory	3106.67 (10,192.49)	2.17 (7.12)	7589.06 (24,898.49)
** PACSS 12 Coordinate System				

Table 10-1. Inertial Platform Velocity Comparisons (Continued)

EVENT	DATA SOURCE	VELOCITY m/s (ft/s)**		
		ALTITUDE ( $\dot{X}_m$ )	CROSSRANGE ( $\dot{Y}_m$ )	RANGE ( $\dot{Z}_m$ )
S-IVB Second Cutoff* 17,217.60 sec	Guidance	-610.75 (-2003.77)	-54.75 (-179.62)	274.05 (899.11)
	Postflight Trajectory	-610.84 (-2004.07)	-54.78 (-179.72)	273.94 (898.75)
	Preflight Trajectory	NA	NA	NA
Intermediate Orbit Insertion* 17,227.60 sec	Guidance	-613.60 (-2013.12)	-55.00 (-180.45)	275.35 (903.38)
	Postflight Trajectory	-613.70 (-2013.45)	-55.05 (-180.61)	275.25 (903.05)
	Preflight Trajectory	NA	NA	NA
S-IVB Third Cutoff * 22,281.32 sec	Guidance	2878.70 (9444.55)	-197.20 (-646.98)	1379.85 (4527.07)
	Postflight Trajectory	2878.70 (9444.55)	-197.20 (-646.98)	1379.85 (4527.07)
	Preflight Trajectory	NA	NA	NA
Escape Orbit Injection * 22,291.32 sec	Guidance	2885.10 (9465.55)	-197.85 (-649.11)	1382.95 (4537.24)
	Postflight Trajectory	2885.10 (9465.55)	-197.85 (-649.11)	1382.95 (4537.24)
	Preflight Trajectory	NA	NA	NA
<p>* Values represent velocity change during respective time base.  ** PACSS 12 Coordinate System  NA - Not Available</p>				

Table 10-2. Guidance Comparisons

EVENT	DATA SOURCE	POSITIONS * meters (ft)				VELOCITIES * m/s (ft/s)				FLIGHT PATH ANGLE (deg)
		X <sub>s</sub>	Y <sub>s</sub>	Z <sub>s</sub>	R	$\dot{X}_s$	$\dot{Y}_s$	$\dot{Z}_s$	V <sub>s</sub>	
S-IC CECO 134.34 sec	Guidance	6,413,917 (21,043,035)	36,159 (118,631)	99,435 (326,230)	6,414,790 (21,045,899)	712.06 (2336.15)	125.65 (412.24)	1786.12 (5859.97)	1926.93 (6321.95)	22.5951
	Postflight Trajectory	6,413,976 (21,043,229)	36,116 (118,491)	99,508 (326,471)	6,414,850 (21,046,095)	712.31 (2336.98)	125.40 (411.42)	1788.52 (5867.85)	1929.23 (6329.49)	22.5766
	Preflight Trajectory	6,417,490 (21,054,759)	36,002 (118,118)	101,411 (332,713)	6,418,393 (21,057,719)	770.13 (2526.66)	121.04 (397.12)	1851.27 (6073.72)	2008.72 (6590.28)	23.4681
S-IC OECO 162.76 sec	Guidance	6,435,545 (21,113,993)	39,657 (130,108)	161,636 (530,302)	6,437,696 (21,121,050)	808.15 (2651.41)	119.80 (393.04)	2624.26 (8609.78)	2748.49 (9017.36)	18.5527
	Postflight Trajectory	6,435,530 (21,113,944)	39,603 (129,931)	161,523 (529,932)	6,437,679 (21,120,993)	807.26 (2648.49)	120.06 (393.88)	2623.36 (8606.83)	2747.38 (9013.72)	18.5394
	Preflight Trajectory	6,438,505 (21,123,704)	39,083 (128,225)	158,543 (520,154)	6,440,576 (21,130,498)	866.59 (2843.14)	118.56 (388.98)	2635.36 (8646.18)	2776.71 (9109.95)	19.6098
S-II ECO 536.22 sec	Guidance	6,313,328 (20,713,018)	77,966 (255,794)	1,776,820 (5,829,462)	6,559,061 (21,519,229)	-1771.34 (-5811.48)	89.28 (292.91)	6703.33 (21,992.55)	6933.99 (22,749.31)	0.9254
	Postflight Trajectory	6,313,089 (20,712,233)	78,535 (257,661)	1,776,783 (5,829,340)	6,558,827 (21,518,462)	-1772.68 (-5815.88)	92.22 (302.55)	6704.46 (21,996.27)	6935.28 (22,754.17)	0.9177
	Preflight Trajectory	6,315,786 (20,721,083)	77,823 (255,324)	1,776,726 (5,829,153)	6,561,400 (21,526,902)	-1846.43 (-6057.83)	93.17 (305.68)	6769.25 (22,208.81)	7017.17 (23,022.20)	0.4638
S-IVB First Cutoff 664.66 sec	Guidance	5,998,574 (19,680,361)	88,974 (291,909)	2,662,208 (8,734,278)	6,563,393 (21,533,442)	-3161.25 (-10,371.56)	82.71 (271.36)	7120.20 (23,360.24)	7790.86 (25,560.56)	-0.00002
	Postflight Trajectory	5,998,068 (19,678,700)	89,907 (294,971)	2,662,436 (8,735,027)	6,563,038 (21,532,277)	-3162.94 (-10,377.11)	85.19 (279.49)	7120.55 (23,361.39)	7791.90 (25,563.98)	-0.0066
	Preflight Trajectory	6,028,479 (19,778,475)	88,189 (289,334)	2,593,707 (8,509,536)	6,563,357 (21,533,322)	-3080.19 (-10,105.60)	83.93 (275.37)	7155.81 (23,477.06)	7791.03 (25,561.13)	-0.0016
Parking Orbit Insertion 674.65 sec	Guidance	5,966,531 (19,575,233)	89,796 (294,606)	2,733,239 (8,967,319)	6,563,394 (21,533,445)	-3246.19 (-10,650.23)	81.61 (267.75)	7084.04 (23,241.60)	7792.81 (25,566.96)	0.0014
	Postflight Trajectory	5,966,007 (19,573,513)	90,752 (297,744)	2,733,468 (8,968,070)	6,563,026 (21,532,239)	-3247.92 (-10,655.90)	84.07 (275.82)	7084.16 (23,241.99)	7793.67 (25,569.78)	-0.0058
	Preflight Trajectory	5,997,246 (19,676,004)	89,023 (292,069)	2,665,098 (8,743,761)	6,563,356 (21,533,319)	-3165.68 (-10,386.09)	82.82 (271.72)	7120.63 (23,361.65)	7793.06 (25,567.78)	-0.0009

\* PACSS 13 Coordinate System

Table 10-2. Guidance Comparisons (Continued)

EVENT	DATA SOURCE	POSITIONS * meters (ft)				VELOCITIES* m/s (ft/s)				FLIGHT PATH ANGLE (deg)
		X <sub>s</sub>	Y <sub>s</sub>	Z <sub>s</sub>	R	$\dot{X}_s$	$\dot{Y}_s$	$\dot{Z}_s$	V <sub>s</sub>	γ
S-IVB Second Cutoff 17,217.60 sec	Guidance	2,394,204 (7,855,000)	169,576 (556,352)	6,128,168 (20,105,538)	6,581,444 (21,592,664)	-7851.76 (-25,760.37)	14.56 (47.77)	3124.85 (10,252.13)	8450.74 (27,725.52)	0.3640
	Postflight Trajectory	2,357,836 (7,735,682)	171,502 (562,669)	6,135,270 (20,128,839)	6,574,979 (21,571,452)	-7872.56 (-25,828.62)	13.84 (45.42)	3085.88 (10,124.28)	8455.77 (27,742.04)	0.3843
	Preflight Trajectory	2,332,352 (7,652,073)	171,191 (561,649)	6,145,717 (20,163,113)	6,575,637 (21,573,613)	-7866.90 (-25,810.05)	54.19 (177.77)	3051.59 (10,011.79)	8438.20 (27,684.38)	0.4287
Intermediate Orbit Insertion 17,227.60 sec	Guidance	2,315,497 (7,596,775)	169,708 (556,785)	6,158,996 (20,206,680)	6,582,064 (21,594,698)	-7887.58 (-25,877.89)	12.04 (39.50)	3040.19 (9974.38)	8453.21 (27,733.63)	0.4766
	Postflight Trajectory	2,278,942 (7,475,844)	171,754 (563,497)	6,165,709 (20,228,703)	6,575,640 (21,573,621)	-7908.96 (-25,948.05)	11.40 (37.39)	3001.32 (9846.86)	8459.30 (27,753.62)	0.4977
	Preflight Trajectory	2,253,493 (7,393,350)	171,720 (563,386)	6,175,813 (20,261,855)	6,576,351 (21,575,954)	-7901.99 (-25,925.18)	51.80 (169.95)	2966.49 (9732.56)	8440.63 (27,692.35)	0.5391
S-IVB Third Cutoff 22,281.32 sec	Guidance	5,179,326 (16,992,539)	-168,481 (-527,759)	-6,942,380 (-22,776,837)	8,663,166 (28,422,461)	7612.26 (24,974.61)	-46.11 (-151.28)	5901.21 (19,360.93)	9631.88 (31,600.66)	-1.0534
	Postflight Trajectory	5,210,165 (17,093,717)	-169,392 (-555,749)	-6,917,030 (-22,693,669)	8,661,398 (28,416,661)	7587.17 (24,892.29)	-42.95 (-140.92)	5927.80 (19,448.16)	9628.38 (31,589.17)	-1.0066
	Preflight Trajectory	5,497,750 (18,037,237)	-190,638 (-625,452)	-6,546,262 (-21,477,238)	8,550,739 (28,053,607)	8672.82 (28,454.13)	-51.19 (-167.94)	7007.47 (22,990.38)	11,150.11 (36,581.74)	1.0926
Escape Orbit Injection 22,291.32 sec	Guidance	5,255,355 (17,241,978)	-168,947 (-554,288)	6,833,116 (-22,582,401)	8,661,673 (28,417,562)	7586.69 (24,890.72)	-45.74 (-150.07)	5946.79 (19,510.47)	9639.72 (31,626.38)	-0.7233
	Postflight Trajectory	5,285,357 (17,340,410)	-169,885 (-557,366)	-6,857,386 (-22,497,986)	8,659,538 (28,410,559)	7562.68 (24,811.94)	-42.28 (-138.72)	5974.10 (19,600.06)	9637.73 (31,619.85)	-0.6783
	Preflight Trajectory	5,584,380 (18,321,458)	-191,150 (-627,131)	-6,475,935 (-21,246,507)	8,553,337 (28,062,131)	8645.52 (28,364.56)	-50.61 (-166.05)	7053.50 (23,141.39)	11,157.93 (36,607.37)	1.5680
*PACSS 13 Coordinate System										

At S-IVB second cutoff, the respective radius and total velocity differences (trajectory minus LVDC) were -6.465 kilometers (-3.49 n mi) and 5.03 m/s (16.5 ft/s) for the postflight trajectory, and -5.807 kilometers (-3.14 n mi) and -12.53 m/s (-41.11 ft/s) for the preflight trajectory.

At S-IVB third cutoff, the respective radius and total velocity differences were -1.768 kilometers (-0.955 n mi) and -3.50 m/s (-11.48 ft/s) for the postflight trajectory, and -112.427 kilometers (-60.166 n mi) and 1518.23 m/s (4981.07 ft/s) for the preflight trajectory. The comparisons with the postflight trajectory are relatively good. However, due to excessive thrust variations during the third burn this particular burn was considerably off nominal. Since both second and third burn cutoffs were time cutoffs, the velocity and radius variations were due more to performance variations than to guidance. In general, the guidance system performed as programmed.

#### 10.4 NAVIGATION AND GUIDANCE SCHEME EVALUATION

##### 10.4.1 Flight Program Performance

The flight program performed all boost and orbital navigation functions properly. Accelerations were computed correctly throughout all of boost, and no unreasonable accelerometer readings were indicated by the reasonableness tests or zero change tests.

The tower avoidance maneuver was executed properly. The maneuver to remove the roll bias and the start of the time tilt pitch guidance were both initiated at 13.3 seconds. The roll bias was removed at 33.0 seconds. Tilt arrest occurred at 158.0 seconds. The program detected OECO at 162.8 seconds.

IGM is separated into three phases which are:

- a. The first phase, beginning approximately 40 seconds into the S-II stage burn and ending at the propellant Mixture Ratio (MR) shift.
- b. The second phase, from MR shift until shortly before S-II stage cutoff.
- c. The third phase, beginning about 10 seconds after S-IVB first ignition and ending a few seconds before cutoff.

Three phases are required due to the changes in thrust and vehicle mass loss rate that occur at MR shift and again at S-II/S-IVB staging. During periods of changing thrust and propellant flow rates artificial tau modes or ramp functions are used to modify the time-to-go equations.

During the periods just prior to stage cutoff, attitude freeze or chi freeze modes are used. These modes prevent the control system from introducing vehicle rotations during staging, or during thrust decay and buildup periods.

Chi bars are the steering angles required to null out the velocity deficiencies in the predicted remaining burn time. These angles are biased to enforce terminal position requirements. Prior to orbital insertion, a chi bar steering mode is used. This mode enforces only terminal velocity requirements without regard to position.

The active-guidance phases start and stop times are given in Table 10-3. Included in this table are the start and stop times for the artificial tau phases and chi freezes. There were 10.48 and -0.52 degree changes in commanded pitch and yaw, respectively, when IGM computations were initiated during S-II stage burn.

The Steering Misalignment Correction (SMC) (a correction factor for thrust misalignments, etc.) was initiated at 223.2 seconds. The orbital insertion conditions after S-IVB first burn are given in Table 10-4.

The orbital guidance routine was entered at the start of T<sub>5</sub>. The program commanded the vehicle to local horizontal 20 seconds into the time base. All following commands were proper, including the inertial attitude freezes for S-IVB second and third burns. A heliocentric orbit was achieved by the S-IVB third burn. Performance during IGM flight is shown in Figure 10-2.

#### 10.4.2 Attitude Error Computations

The minor loop performed as expected during flight. No unreasonable gimbal angles were detected.

#### 10.4.3 Program Sequencing

All programmed events occurred properly. Bit 1 in mode code word 26 that indicates the S-IVB stage engine-on command for third burn was set by ground command approximately 60 seconds early. Since program implementation is to change the state of the bit when the engine-on command is issued, this bit was set back to zero when the engine-on command was issued on time by the flight program.

### 10.5 GUIDANCE SYSTEM COMPONENT EVALUATION

#### 10.5.1 LVDC Performance

The LVDC performed as predicted for the AS-504 mission. No valid error monitor words and no self-test error data have been observed that indicate any deviation from correct operation.

#### 10.5.2 LVDA Performance

The LVDA performance was nominal. No valid error monitor words and no self-test error data indicating deviations from correct performance were observed.



Table 10-3. Start and Stop Times for IGM Guidance Commands

EVENT	IGM PHASES (sec)		ARTIFICIAL TAU* (sec)		TERMINAL GUIDANCE (CHI BAR STEERING) (sec)		ATTITUDE FREEZE (CHI FREEZE) (sec)	
	START	STOP	START	STOP	START	STOP	START	STOP
First Phase IGM	204.6	461.5						
Second Phase IGM	461.5	527.1	461.5	492.7			527.1	551.0
Third Phase IGM	551.0	657.8	551.0	552.9	631.4	657.8	657.8	664.8

\* Times to nearest computation cycle.

Table 10-4. Parking Orbit Insertion Parameters

PARAMETER*	PREDICTED	POSTFLIGHT TRAJECTORY	TRAJECTORY MINUS PREDICTED	LVDC	LVDC MINUS PREDICTED
Inertial Velocity m/s ft/s	7793.06 (25,567.78)	7793.67 (25,569.78)	0.61 (2.00)	7792.84 (25,567.06)	-0.22 (-0.72)
Altitude km (n mi)	191.36 (103.33)	191.04 (103.15)	-0.32 (-0.18)	191.41 (103.35)	0.05 (0.02)
Flight Path Angle deg	-0.0009	-0.0058	-0.0049	0.0014	0.0023
Descending Node deg	42.570	42.538	-0.032	42.570	0.000
Inclination deg	32.561	32.552	-0.009	32.561	0.000
Apogee Alt km (n mi)	185.31 (100.06)	186.57 (100.74)	1.26 (0.68)	191.77 (103.55)	6.46 (3.49)
Perigee Alt km (n mi)	185.10 (99.95)	184.61 (99.68)	-0.49 (-0.27)	190.82 (103.03)	5.72 (3.08)
Eccentricity	0.000016	0.000149	0.000133	0.000075	0.000059
Period Minutes	88.20	88.20	0.00	88.19	-0.01

\* Actual time 674.66  
Predicted time 658.72

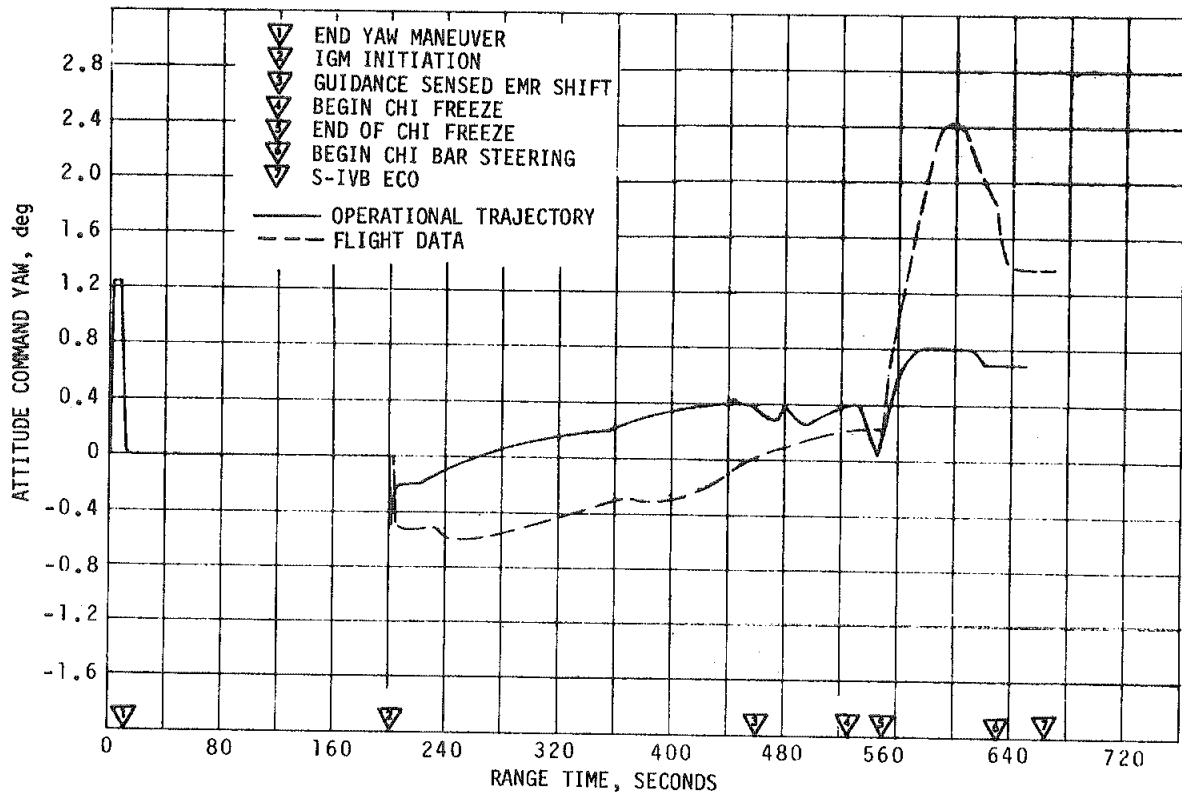
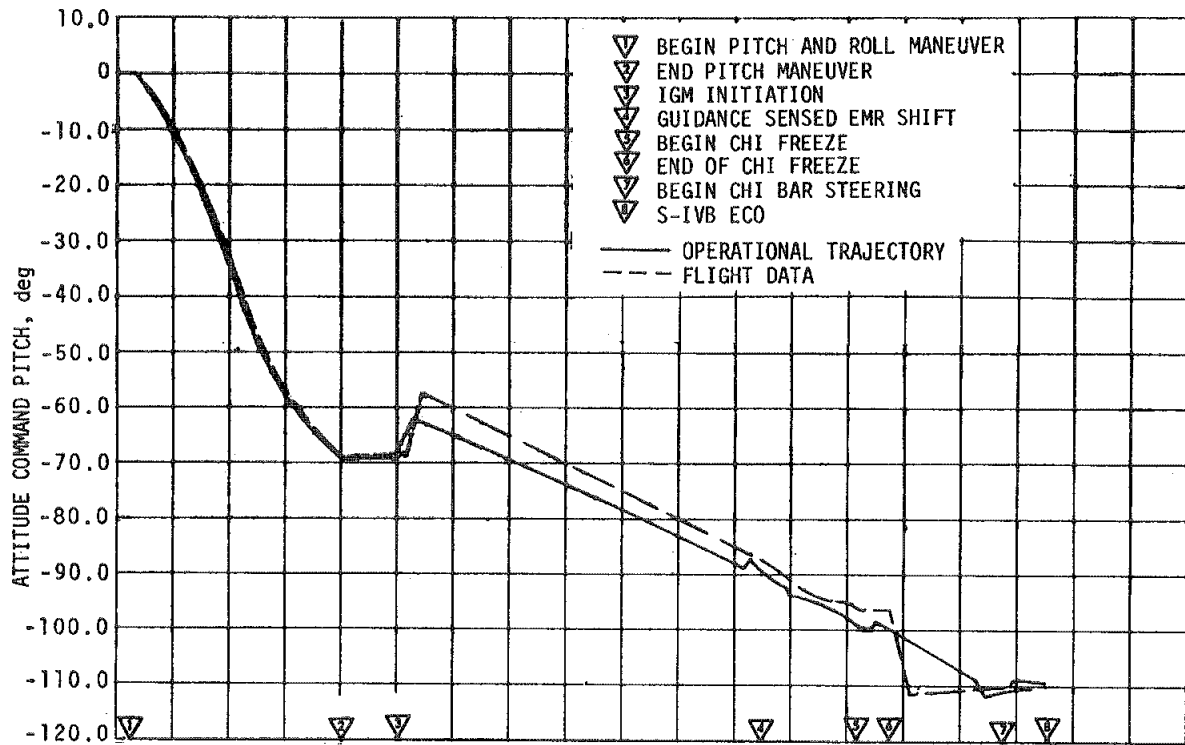


Figure 10-2. Attitude Commands During Active Guidance Period

### 10.5.3 Ladder Outputs

The ladder networks and converter amplifiers performed satisfactorily. No data have been observed that indicate an out-of-tolerance condition between channel A and the reference channel converter-amplifiers.

### 10.5.4 Telemetry Outputs

Analysis of the available LVDA telemetry buffer and flight control computer attitude error plots indicated symmetry between the buffer outputs and the ladder outputs. The available LVDC power supply plots indicated satisfactory power supply performance.

H60-603 telemetry data included an incorrect identifier bit during the period from S-II/S-IVB separation until CSM/SLA separation. Analysis of telemetry data indicates the cause of the anomaly was within either the RT4 logic chain in the LVDA (serial No. P22), or the RT4 input circuitry in the 410K multiplexer (see paragraph 19.3.4).

A detailed evaluation of the LVDA logic chain, and a review of applicable failure history have been completed. If the deviation cause is within the LVDA, the most probable mechanism is a particle short in a flatpack transistor. This is not the only mechanism which could have been involved, but a review of the history indicates it as the most probable.

This is considered an isolated failure and the only corrective action recommended is a real-time data handling procedural change for contingency planning.

### 10.5.5 Discrete Outputs

No valid discrete output register words (tags 043 and 052) were observed to indicate guidance or simultaneous memory failure.

### 10.5.6 Switch Selector Functions

Switch selector data indicate that the LVDA switch selector functions were performed satisfactorily. No error monitor words were observed that indicate disagreement in the Triple Modular Redundant (TMR) switch selector register positions or in the switch selector feedback circuits. No mode code 24 words or switch selector feedback words were observed that indicated a switch selector feedback was in error. In addition, no indications were observed to suggest that the B channel input gates to the switch selector register positions were selected.

### 10.5.7 ST-124M-3 Inertial Platform Performance

The inertial platform system performed as designed. The inertial gimbal temperature fell below specifications, and the gas bearing differential pressure and platform internal ambient pressure exceeded specifications;

however, there are no indications of degraded inertial platform performance as a result of these deviations. These deviations are discussed in paragraph 18.4.

The accelerometer servo loops functioned as designed and maintained the accelerometer float within the measuring head stops ( $\pm 6$  degrees) throughout the flight. The accelerometer encoder outputs indicated that the accelerometers accurately measured the vehicle acceleration.

The X, Y, and Z gyro servo loops for the stable element functioned as designed. The operational limits of the servo loops were not reached at any time during the mission.

SECTION 11  
CONTROL SYSTEM

11.1 SUMMARY

The AS-504 Flight Control Computer (FCC), Thrust Vector Control (TVC), and Auxiliary Propulsion System (APS) satisfied all requirements for vehicle attitude control through the intermediate orbit. Bending and slosh dynamics were adequately stabilized. The preprogrammed S-IC boost phase yaw, roll, and pitch maneuvers were properly executed. The S-IC outboard engine radial cant was accomplished as planned.

The peak winds observed during the flight exceeded the 95 percentile wind envelopes and were the highest observed on a Saturn flight. However, less than 10 percent of the available engine deflection was utilized by the response of the control system to disturbances. The maximum engine deflection was caused by a wind shear at about 85 seconds.

S-IC/S-II first and second plane separations were accomplished with no significant attitude deviations. At Iterative Guidance Mode (IGM) initiation, pitch-up transients occurred that were similar to those seen on AS-501 and AS-502. FCC switch points 3 and 4 produced transient excursions in yaw due to the steady-state yaw error of 0.2 degree. S-II/S-IVB separation occurred as expected and without producing any significant attitude deviations.

During first and second S-IVB burns, satisfactory control was maintained over the vehicle. During the Command and Service Module (CSM) separation from the S-IVB/Instrument Unit (IU) and during the Transposition, Docking, and Ejection (TD&E), the control system maintained a fixed inertial attitude to provide a stable docking platform.

During the S-IVB third burn the control system experienced high amplitude oscillations in the yaw plane for the first 100 seconds of burn. These oscillations were also evident in the pitch and roll planes but reached a peak of  $\pm 2.5$  deg/s in yaw at about 22,135 seconds. LOX and LH<sub>2</sub> sloshing was coupled to the control oscillations. After the performance shift, these oscillations damped out, and pitch and yaw attitude control was near nominal. However, a large roll torque had been developing and it peaked at 386 N-m (285 lbf-ft). During the first burn the maximum roll torque was 7.9 N-m (5.8 lbf-ft). At the performance shift the torque changed from bidirectional to unidirectional (counterclockwise).

APS control was as expected, except for the large demands placed upon the system by the control oscillations. The APS propellants were depleted by an ullage burn after third burn.

## 11.2 CONTROL SYSTEM DESCRIPTION

The control system on AS-504 was essentially the same as that on AS-503. The flight program and the FCC were updated to provide the logic for S-IVB third burn. The flight program was also modified to provide for CSM/Lunar Module (LM) separation after S-IVB first burn.

## 11.3 S-IC CONTROL SYSTEM EVALUATION

The AS-504 control system performed satisfactorily during S-IC powered flight. Less than 10 percent of available engine deflection was used; although the actual flight wind magnitude was at times greater than the 95 percentile wind.

As expected from this large wind some control variables did exceed the preflight predicted 95 percentile wind envelopes; however, all dynamics were well within vehicle capability. In the region of high dynamic pressures, the maximum angles-of-attack were -3.3 degrees in pitch and 2.8 degrees in yaw. The maximum average pitch engine deflection was 0.4 degree and was caused by a wind shear. The maximum average yaw engine deflection was 0.5 degree due to a wind shear. Absence of any divergent bending or slosh frequencies in vehicle motion indicates that bending and slosh dynamics were adequately stabilized.

Vehicle attitude errors required to trim out the effects of thrust unbalance, thrust misalignment, and control system misalignments were well within predicted envelopes. Vehicle dynamics prior to S-IC/S-II first plane separation were well within staging requirements.

### 11.3.1 Liftoff Clearances

The vehicle cleared the mobile launcher structure well within the available clearance envelopes. Reduction of the camera data showing liftoff motion was not performed for the AS-504 flight, but simulations with flight data show that less than 20 percent of the available clearance was used. The ground wind was from the southeast with a magnitude of 6.9 m/sec (13.5 knots) at the 18.3 meters (60 ft) level. The bottom of the launch vehicle cleared the top of the tower with a separation distance of 13.5 meters (44.3 ft). Because the AS-504 vehicle was heavier than previous Saturn V vehicles the time to clear the top of the tower was 0.6 second greater.

Table 11-1 shows the predicted and measured misalignments, soft release forces, winds, and the thrust to weight ratio.

Table 11-1. AS-504 Misalignment Summary

PARAMETER	PREFLIGHT PREDICTED			LAUNCH		
	PITCH	YAW	ROLL	PITCH	YAW	ROLL
Thrust Misalignment, deg*	+0.34	+0.34	+0.34	-0.14	-0.3	-0.05
Center Engine Cant, deg	-	-	-	0.0	-0.17	-
Servo Amp Offset, deg/eng	+0.1	+0.1	+0.1	-	-	-
Vehicle Stacking and Pad Misalignment, deg	+0.29	+0.29	0.0	0.089	-0.07	0.0
Peak Soft Release Force per Rod, N (lbf)	316,000 (71,000)			**		
Wind	95 Percentile Envelope			6.9 m/s (13.5 knots) at 18.3 meters (60 ft)		
Thrust to Weight Ratio	1.206			1.186		
<p>* Thrust misalignment of 0.34 degree encompasses the center engine cant. A positive polarity was used to determine minimum fin tip/umbilical tower clearance. A negative polarity was used to determine vehicle/GSE clearances.</p> <p>** No data available to update predicted value.</p>						

### 11.3.2 S-IC Flight Dynamics

Table 11-2 lists maximum control parameters during S-IC burn. Pitch, yaw and roll time histories are shown in Figures 11-1, 11-2 and 11-3. Dynamics in the region between liftoff and 40 seconds result primarily from guidance commands. Maximum yaw and roll dynamics occurring in this region were: maximum yaw rate, -0.6 deg/s at 12.4 seconds; maximum yaw error, 1.1 degrees at 11.1 seconds; and maximum yaw engine deflection, 0.4 degree at 11.1 seconds. The maximum roll rate was 1.3 degrees per second at 15.3 seconds and the maximum roll error was -0.9 degree at 14.6 seconds.

- ▽ BEGIN TOWER CLEARANCE YAW MANEUVER
- ▽ END YAW MANEUVER
- ▽ BEGIN PITCH AND ROLL MANEUVER
- ▽ S-IC RADIAL ENGINE CANT
- ▽ END ROLL MANEUVER
- ▽ MACH 1
- ▽ MAX Q
- ▽ CECO
- ▽ TILT ARREST
- ▽ OEEO

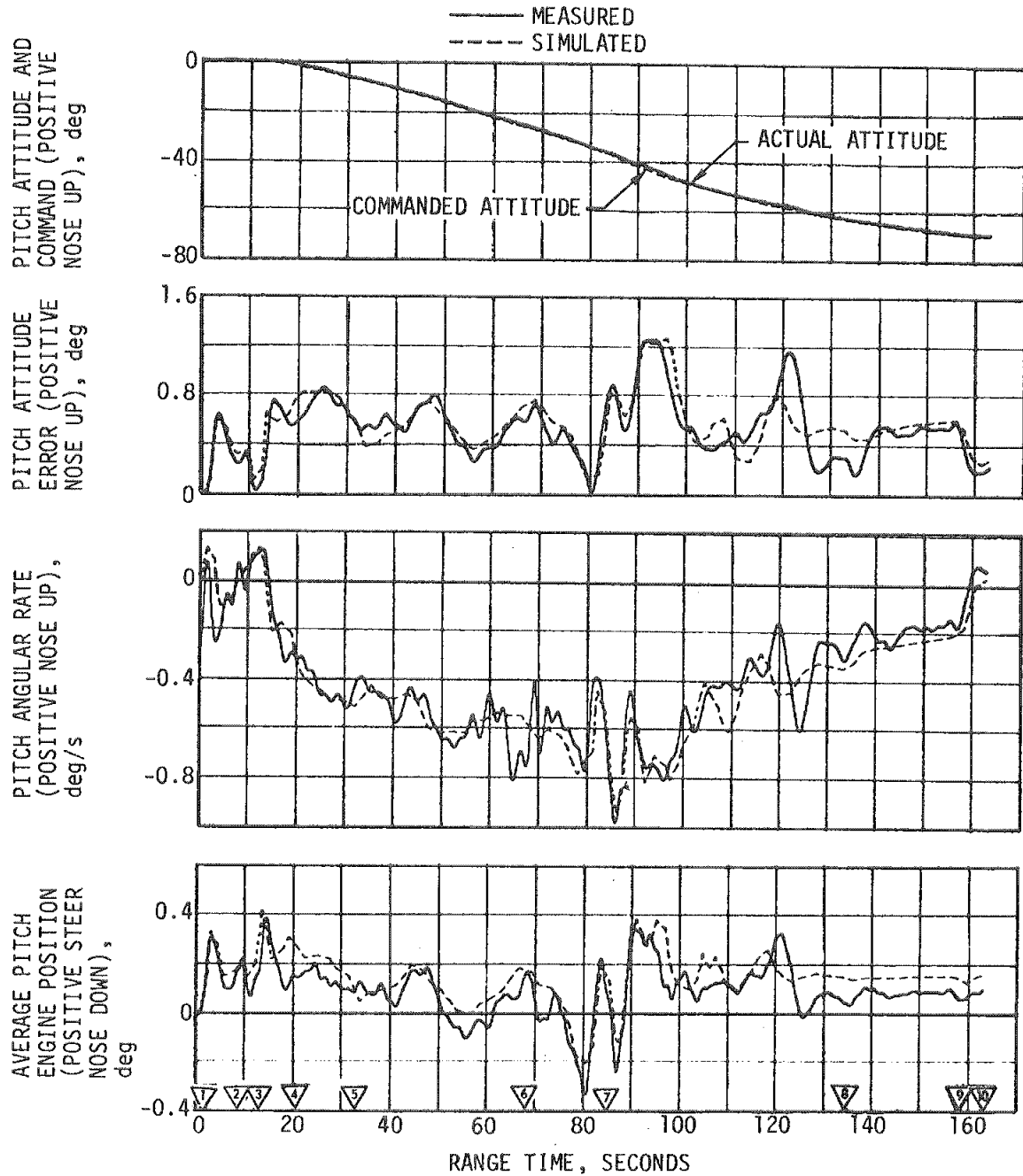


Figure 11-1. Pitch Plane Dynamics During S-IC Burn



- ▽ BEGIN TOWER CLEARANCE YAW MANEUVER
- ▽ END YAW MANEUVER
- ▽ BEGIN PITCH AND ROLL MANEUVER
- ▽ S-IC RADIAL ENGINE CANT
- ▽ END ROLL MANEUVER
- ▽ MACH 1
- ▽ MAX Q
- ▽ CECO
- ▽ TILT ARREST
- ▽ OECC

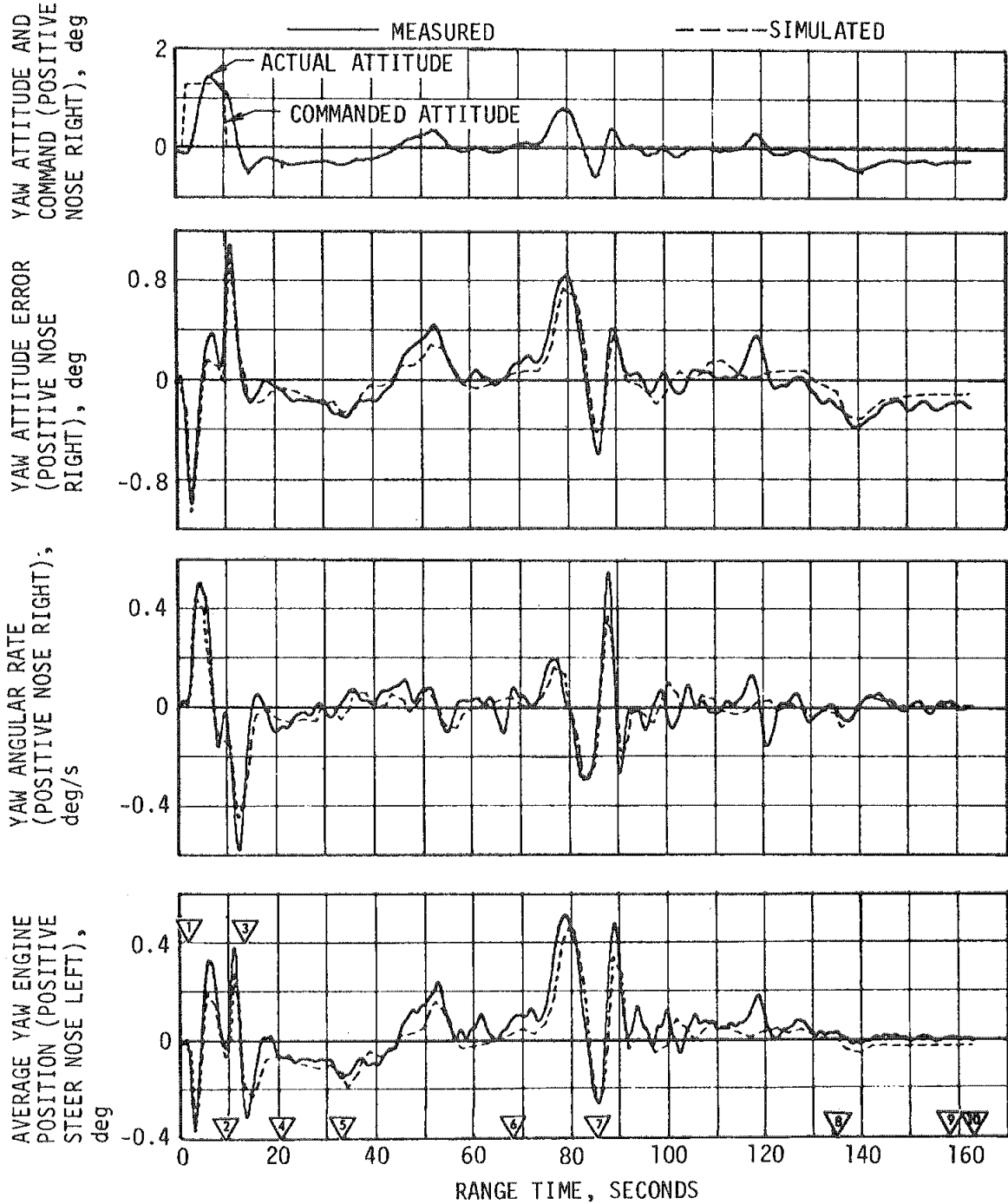


Figure 11-2. Yaw Plane Dynamics During S-IC Burn

- 1 BEGIN TOWER CLEARANCE YAW MANEUVER
- 2 END YAW MANEUVER
- 3 BEGIN PITCH AND ROLL MANEUVER
- 4 S-IC RADIAL ENGINE CANT
- 5 END ROLL MANEUVER
- 6 MACH 1
- 7 MAX Q
- 8 CECO
- 9 TILT ARREST
- 10 OECO

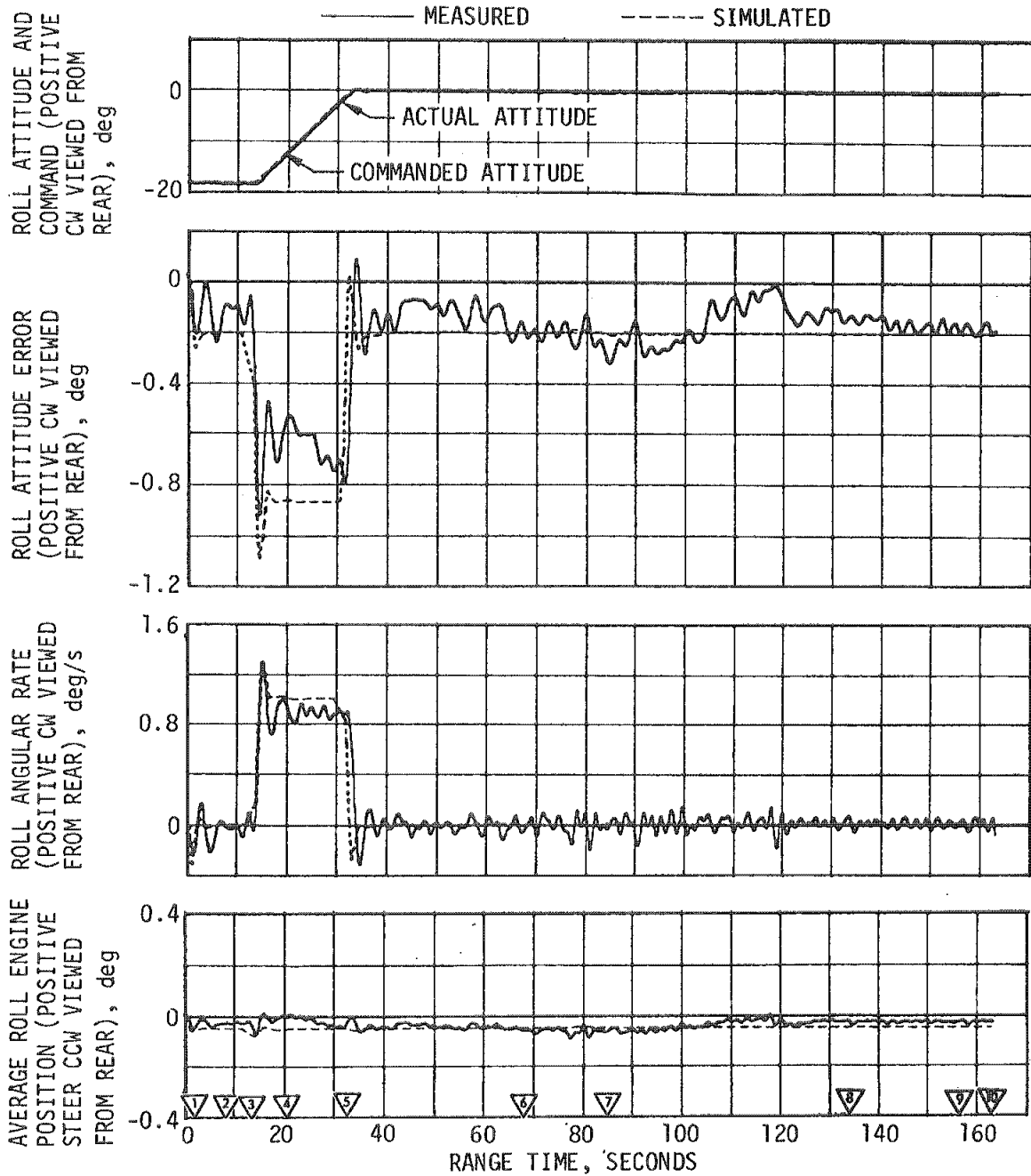


Figure 11-3. Roll Plane Dynamics During S-IC Burn

Table 11-2. Maximum Control Parameters During S-IC Boost Flight

PARAMETERS	UNITS	PITCH PLANE		YAW PLANE		ROLL PLANE	
		MAGNITUDE	RANGE TIME (sec)	MAGNITUDE	RANGE TIME (sec)	MAGNITUDE	RANGE TIME (sec)
Attitude Error	deg	1.3	91.8	1.1	11.1	-0.9	14.6
Rate	deg/s	-1.0	85.9	-0.6	12.4	1.3	15.3
Average Gimbal Angle	deg	0.4	14.5	0.5	78.8	-0.1	77.2
Angle-of-Attack	deg	-3.7	55.2	2.8	77.5	-	-
Angle-of-Attack Dynamic Pressure Product	deg-N/cm <sup>2</sup> (deg-lbf/in <sup>2</sup> )	9.9 (14.4)	79.4	8.53 (12.4)	77.5	-	-
Normal Acceleration *	m/s <sup>2</sup> (ft/s <sup>2</sup> )	-0.439 (-1.33)	92.8	0.425 (1.39)	79.4	-	-

\* Subsequent to the yaw maneuver

In the region between 40 and 110 seconds maximum dynamics were caused by the pitch tilt program, wind magnitude, and wind shears. The peak angle-of-attack in pitch was -3.7 degrees at 55.2 seconds and the peak yaw angle-of-attack was 2.8 degrees at 77.5 seconds. Peak engine deflection in pitch was 0.4 degree at 90.1 seconds. The maximum pitch rate was -1.0 deg/s at 85.9 seconds and resulted from the combined effects of pitch guidance and winds. Maximum pitch error was 1.3 degrees at 91.8 seconds. Significant dynamics due to wind shears occurred in pitch and yaw between 80 and 90 seconds. Normal acceleration during S-IC flight is shown in Figure 11-4. Subsequent to the yaw maneuver the maximum normal acceleration is less than 0.05 g in pitch and yaw. The pitch and yaw plane wind velocities and angles of attack are shown in Figure 11-5. The winds are shown both as determined from balloon and rocket measurements and as derived from the vehicle Q-ball. The wind used to bias the trajectory is also shown for comparison. The control gain switches had the predicted effect on flight dynamics.

Dynamics from 110 seconds to S-IC/S-II separation were caused by high altitude winds, separated air flow, center engine shutdown, and tilt arrest. The prominent pitch attitude error of 1.2 degrees and yaw attitude error of 0.4 degree at 120 seconds is caused by the loss of fin stabilizing action due to separated air flow coupled with a wind shear. The transient at Center Engine Cutoff (CECO) indicates that the center engine cant was -0.17 degree in yaw and zero in pitch. At Outboard Engine Cutoff (OECO) the vehicle had attitude errors as follows: pitch 0.2 degree;

- ▽ 1 BEGIN TOWER CLEARANCE YAW MANEUVER
- ▽ 2 END YAW MANEUVER
- ▽ 3 BEGIN PITCH AND ROLL MANEUVER
- ▽ 4 S-IC RADIAL ENGINE CANT
- ▽ 5 END ROLL MANEUVER
- ▽ 6 MACH 1
- ▽ 7 MAX Q
- ▽ 8 CECO
- ▽ 9 TILT ARREST

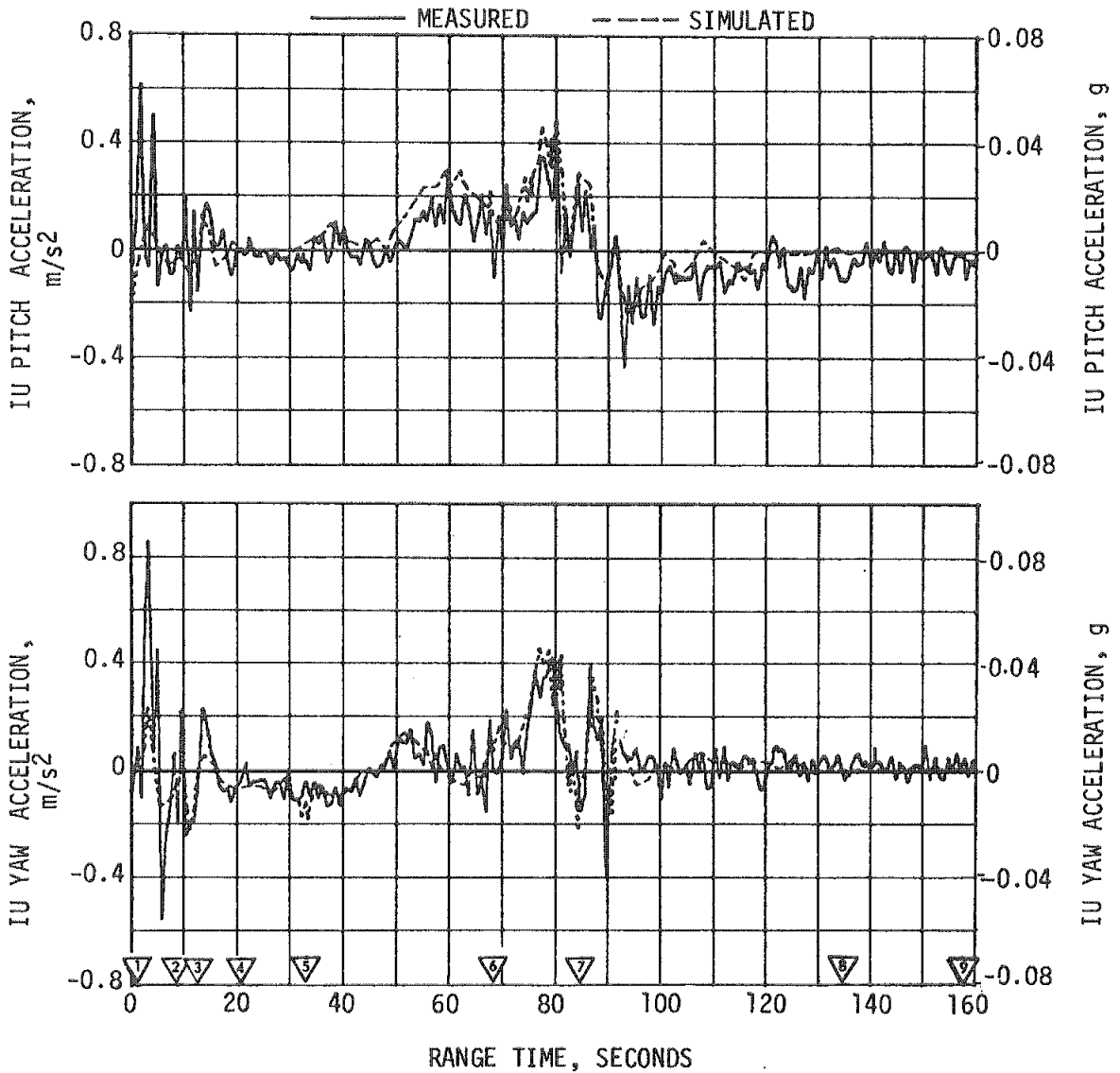


Figure 11-4. Normal Acceleration During S-IC Burn

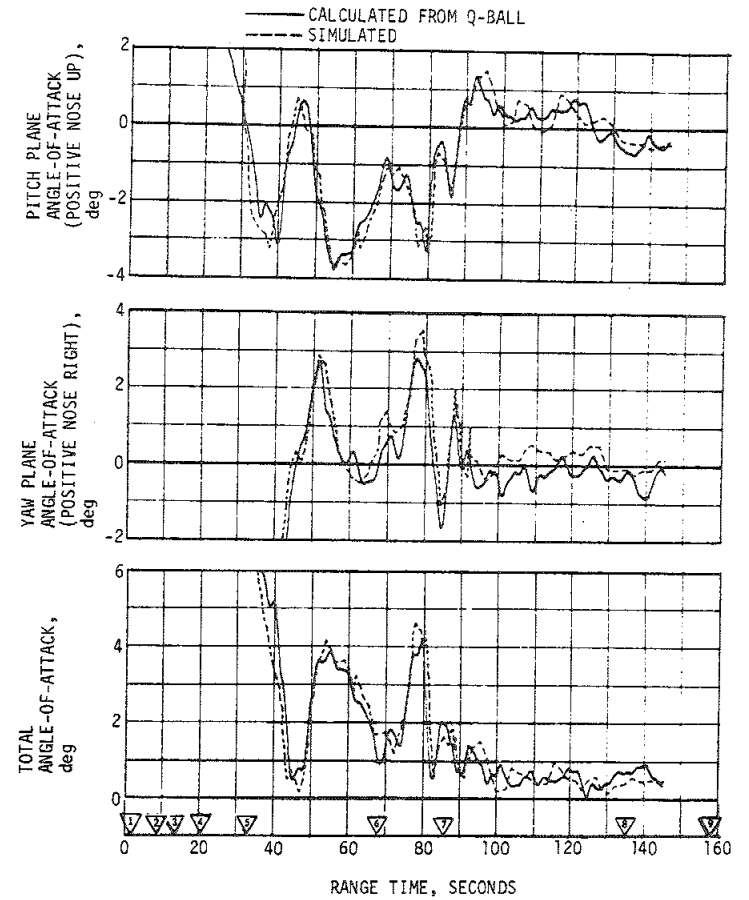
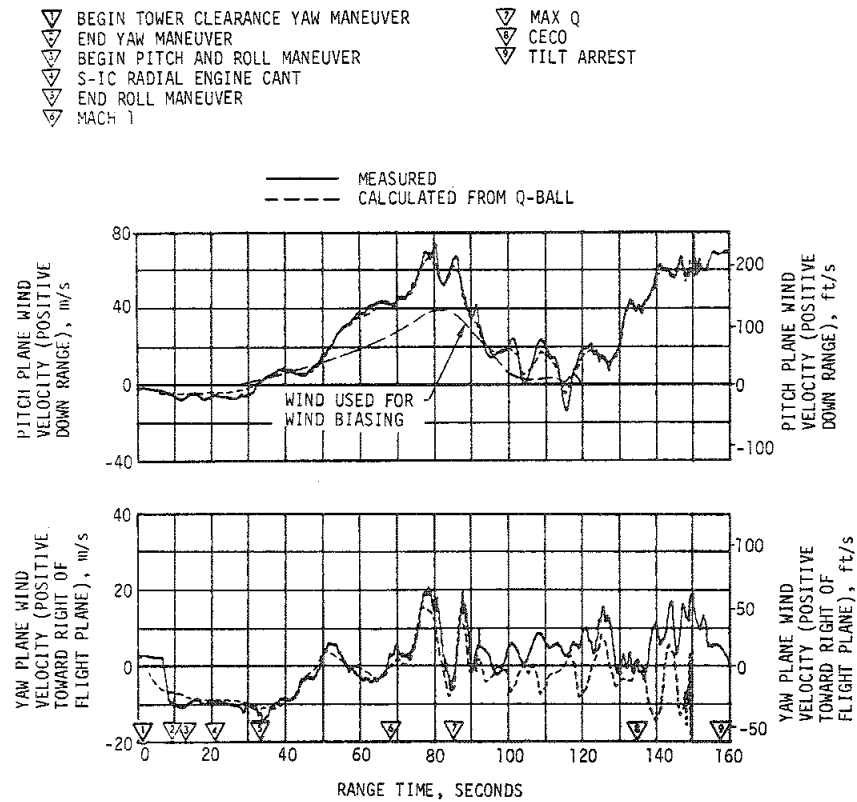


Figure 11-5. Pitch and Yaw Plane Wind Velocity and Free Stream Angles-of-Attack During S-IC Burn

yaw -0.2 degree; and roll -0.2 degree. These errors are required to trim out the effects of thrust unbalance, offset center of gravity, thrust misalignment, and control system biases. The maximum equivalent thrust misalignments were -0.14 degree in pitch, -0.03 degree in yaw, and -0.05 degree in roll.

Engine response to slosh is shown in Figure 11-6. The figure was derived by passing measured engine deflection time histories through band-pass filters, retaining only slosh frequencies. The small engine motion at slosh frequencies other than at the time of known disturbances indicates that slosh was adequately stabilized. The engine response to slosh was approximately 0.1 degree peak-to-peak. The maximum slosh amplitude in the S-IC fuel tank was -0.3 meter (-12 inches) in pitch at 81 seconds and 0.27 meter (10.5 inches) in yaw at 85 seconds. The maximum slosh amplitude in the S-IC LOX tank was 0.28 meter (11 inches) in pitch at 80 seconds and 0.33 meter (13 inches) in yaw at 77.5 seconds.

#### 11.4 S-II CONTROL SYSTEM EVALUATION

The S-II stage attitude control system performance was satisfactory. Analysis of the magnitude of modal components in the engine deflection revealed that vehicle structural bending and propellant sloshing had negligible effect on control system performance. The maximum values of control parameters occurred in response to S-IC/S-II separation disturbances and non-uniform J-2 engine thrust buildups. Attitude rates for pitch, yaw, and roll were 0.2, -0.1 and -0.9 deg/s, respectively, at S-IC/S-II separation. The response at other times was also within expectations.

##### 11.4.1 Attitude Control Dynamics and Stability

Between the events of S-IC OEEO and initiation of IGM, the attitude commands were held constant. Significant events occurring during that interval were S-IC/S-II separation, S-II stage J-2 engine start, second plane separation, and Launch Escape Tower (LET) jettison. The attitude control dynamics throughout this interval indicated stable operation as shown in Figures 11-7, 11-8 and 11-9. Steady state attitudes were achieved within 20 seconds from S-IC/S-II separation. The maximum control excursions occurred in the roll axis following S-IC/S-II separation when -0.9 deg/s rate and -0.9 degree attitude error occurred, as shown in Table 11-3.

At IGM initiation the FCC received thrust vector control commands to pitch the vehicle up as shown in Figure 11-7. During IGM, the vehicle pitched down at a constant commanded rate of approximately -0.1 deg/s. During the transient interval following initiation of IGM guidance, the engines deflected 1.0 degree in pitch as a result of a pitch-up command of 1 deg/s.

- ▽ 1 BEGIN TOWER CLEARANCE YAW MANEUVER
- ▽ 2 END YAW MANEUVER
- ▽ 3 BEGIN PITCH AND ROLL MANEUVER
- ▽ 4 S-IC RADIAL ENGINE CANT
- ▽ 5 END ROLL MANEUVER
- ▽ 6 MACH 1
- ▽ 7 MAX Q
- ▽ 8 CECO
- ▽ 9 TILT ARREST

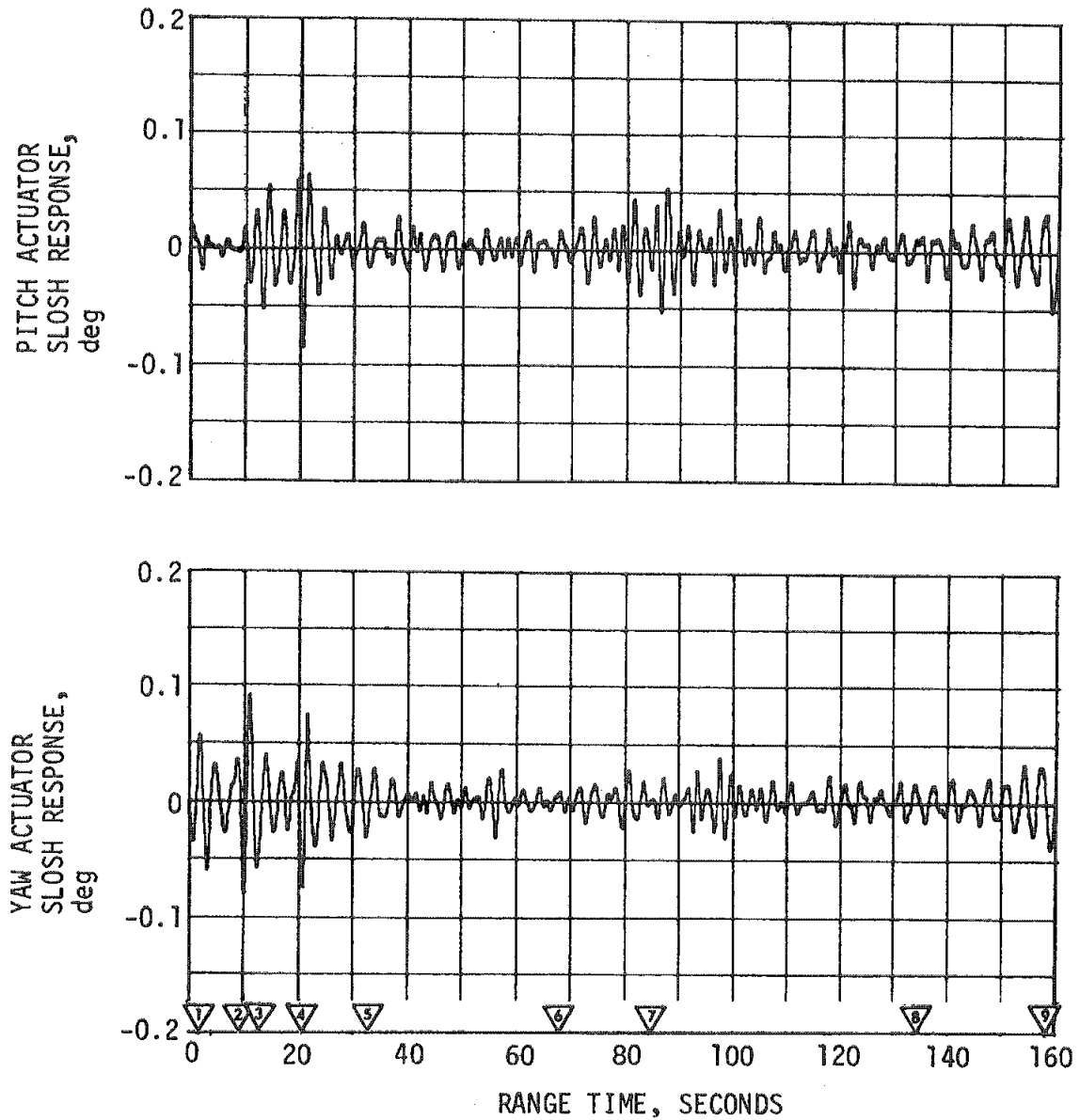


Figure 11-6. S-IC Engine Deflection Response to Propellant Slosh

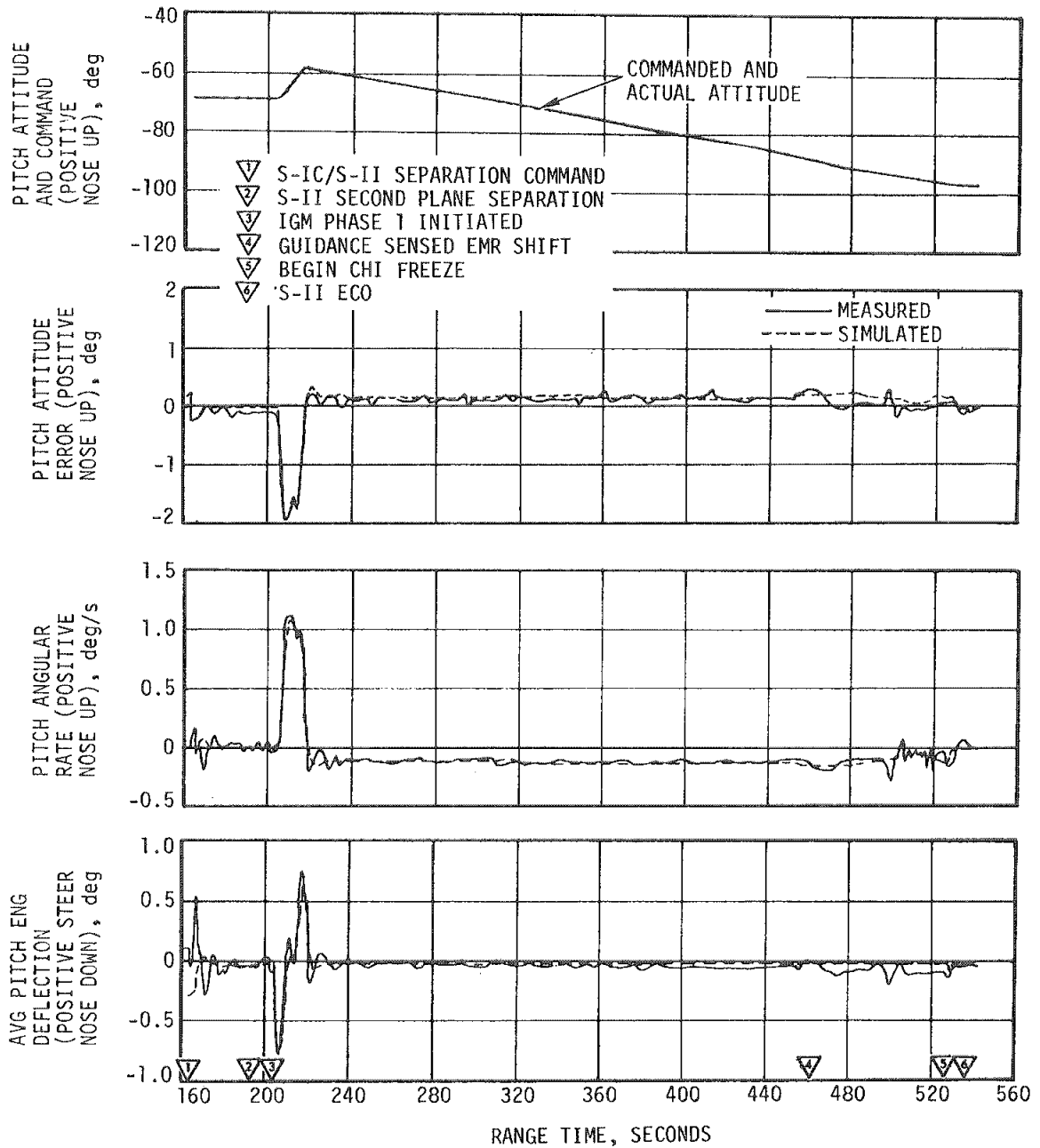


Figure 11-7. Pitch Plane Dynamics During S-II Burn



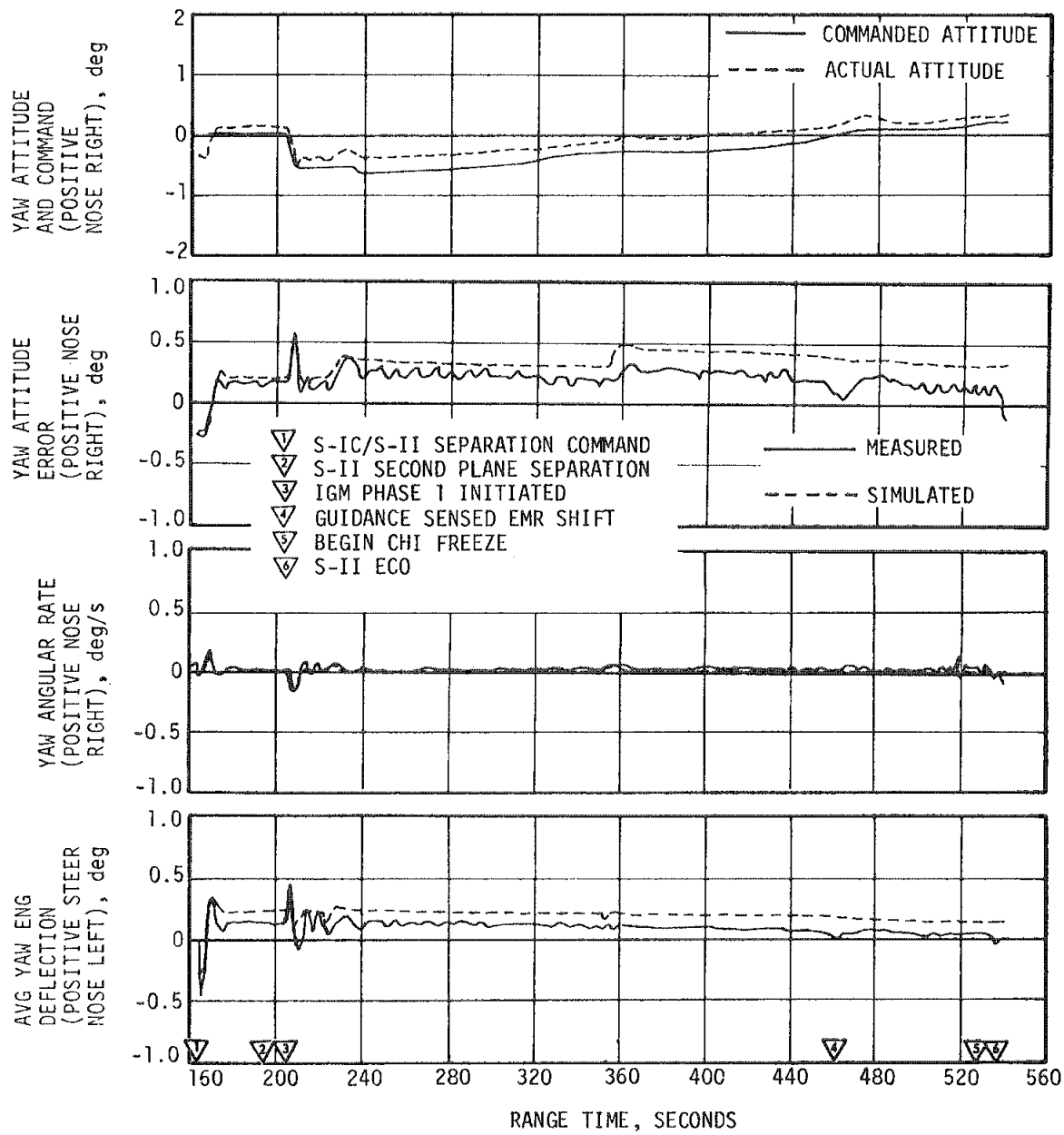


Figure 11-8. Yaw Plane Dynamics During S-II Burn

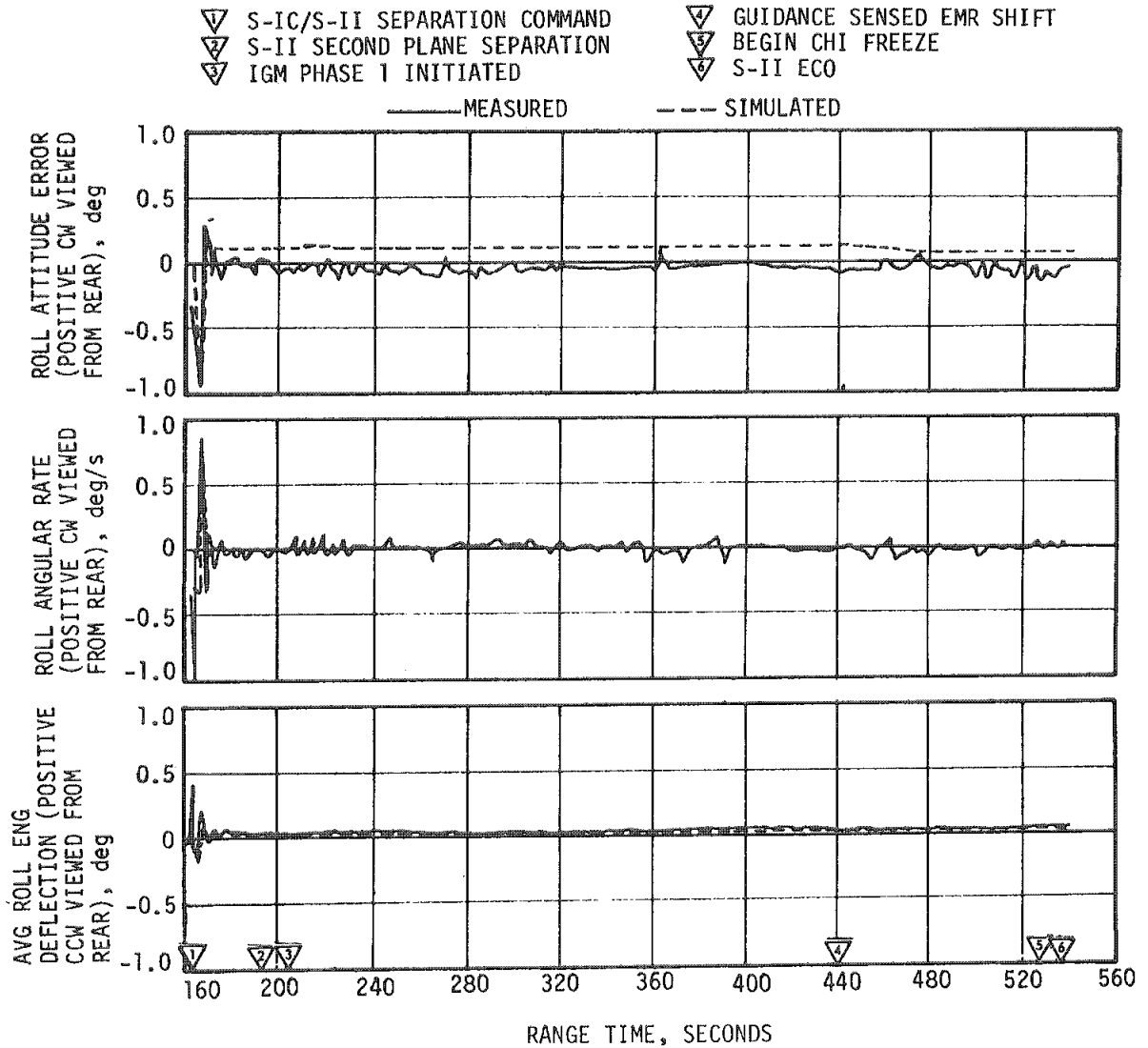


Figure 11-9. Roll Plane Dynamics During S-II Burn

Table 11-3. Maximum Control Parameters During S-II Boost Flight

PARAMETER	S-IC/S-II SEPARATION	FIRST PHASE IGM INITIATE	FIRST ARTIFICIAL TAU INITIATE	S-II CUTOFF
Pitch Plane				
Attitude Error, deg	0.2	-2.0	0.3	-0.1
Rate, deg/s	0.2	1.1	-0.2	0.2
Average Gimbal Angle, deg	0.6	-0.9	-0.1	-0.1
Slosh Component of Average Gimbal Angle, deg p-p	0.06	0.04	0.03	-
Yaw Plane				
Attitude Error, deg	-0.3	0.6	0.2	-0.4
Rate, deg/s	0.2	-0.2	0.1	-0.1
Average Gimbal Angle, deg	-0.5	0.4	0.1	0.0
Slosh Component of Average Gimbal Angle, deg p-p	0.02	0.02	0.02	-
Roll Plane				
Attitude Error, deg	-0.9	-0.1	-0.1	-0.1
Rate, deg/s	-0.9	0.1	-0.1	0.0
Average Gimbal Angle, deg	0.4	0.0	0.0	0.0

These transient magnitudes are similar to those experienced at IGM initiation of flights AS-501 and AS-502.

A steady-state yaw attitude error of approximately 0.2 degree occurred following S-II engine start. Consequently, flight control gain switching points 3 and 4 produced transient yaw excursions. These transients were approximately 0.2 deg/s maximum in yaw body rate and 0.2 deg/s maximum in engine yaw deflection at switch point No. 3 and approximately 0.05 deg/s yaw body rate and 0.05 degree engine yaw deflection at switch point No. 4. The effects of initiating phase 2 IGM and associated tau mode were most apparent in the pitch axis when a -0.2 deg/s pitch rate occurred. At S-II stage engine cutoff the attitude errors were -0.4 degree in yaw and roll and attitude rates were 0.2 deg/s in pitch, -0.1 deg/s in yaw and 0.0 deg/s in roll.

Simulated data are shown for comparison in Figures 11-7, 11-8 and 11-9. Differences between this set and actual flight data are attributed largely to uncertainties in J-2 engine thrust buildup or to engine and thrust misalignments.

#### 11.4.2 Liquid Propellant Dynamics and Their Effects on Flight Control

Estimates of liquid propellant dynamics were extracted from the capacitance probe propellant level 10 samples per second measurements. The slosh data show that the propellant slosh modes were excited primarily at start of S-II boost and at initiation of IGM, as expected. The slosh oscillations were stable and decayed throughout S-II boost. The LOX slosh mode oscillations were more sustained than LH<sub>2</sub> slosh. Slosh perturbations of significant magnitudes were not observed at Engine Mixture Ratio (EMR) shift when steering commands were present.

A damping ratio of 0.02 is estimated for the LH<sub>2</sub> slosh mode. Maximum LH<sub>2</sub> slosh amplitude at the probe was 4 centimeters (1.6 in.) and occurred at approximately 170 seconds. The S-II stage slosh frequencies agreed with those of previous flights. The LH<sub>2</sub> slosh occurred near the calculated uncoupled natural frequency. The LOX slosh frequency varied between 0.5 and 1.0 hertz during most of the S-II boost period of flight. During the time span (starting at 505 seconds) when low frequency oscillations were excited in the vehicle, propellant oscillations were indicated between 0.5 to 0.8 hertz for LOX and 0.2 to 0.4 hertz for LH<sub>2</sub> based on 10 samples per second data.

The presence of periodic sloshing modes in the engine deflections were analyzed using bandpass filtering as shown in Figure 11-10. The maximum deflections were less than 0.06 and 0.02 degree peak-to-peak in pitch and yaw, respectively.

#### 11.5 S-IVB CONTROL SYSTEM EVALUATION

The S-IVB TVC provided satisfactory pitch and yaw control during first and second burns. The APS provided satisfactory roll control during first and second burns.

During S-IVB first burn, control system transients were experienced at S-II/S-IVB separation, guidance initiation, chi bar guidance mode initiation, chi freeze, and J-2 engine cutoff. During second burn, control system transients occurred at engine start and engine cutoff. These transients were expected and were well within the capabilities of the control system.

During third burn high amplitude yaw oscillations occurred during the first 100 seconds of burn. These oscillations were also evident in

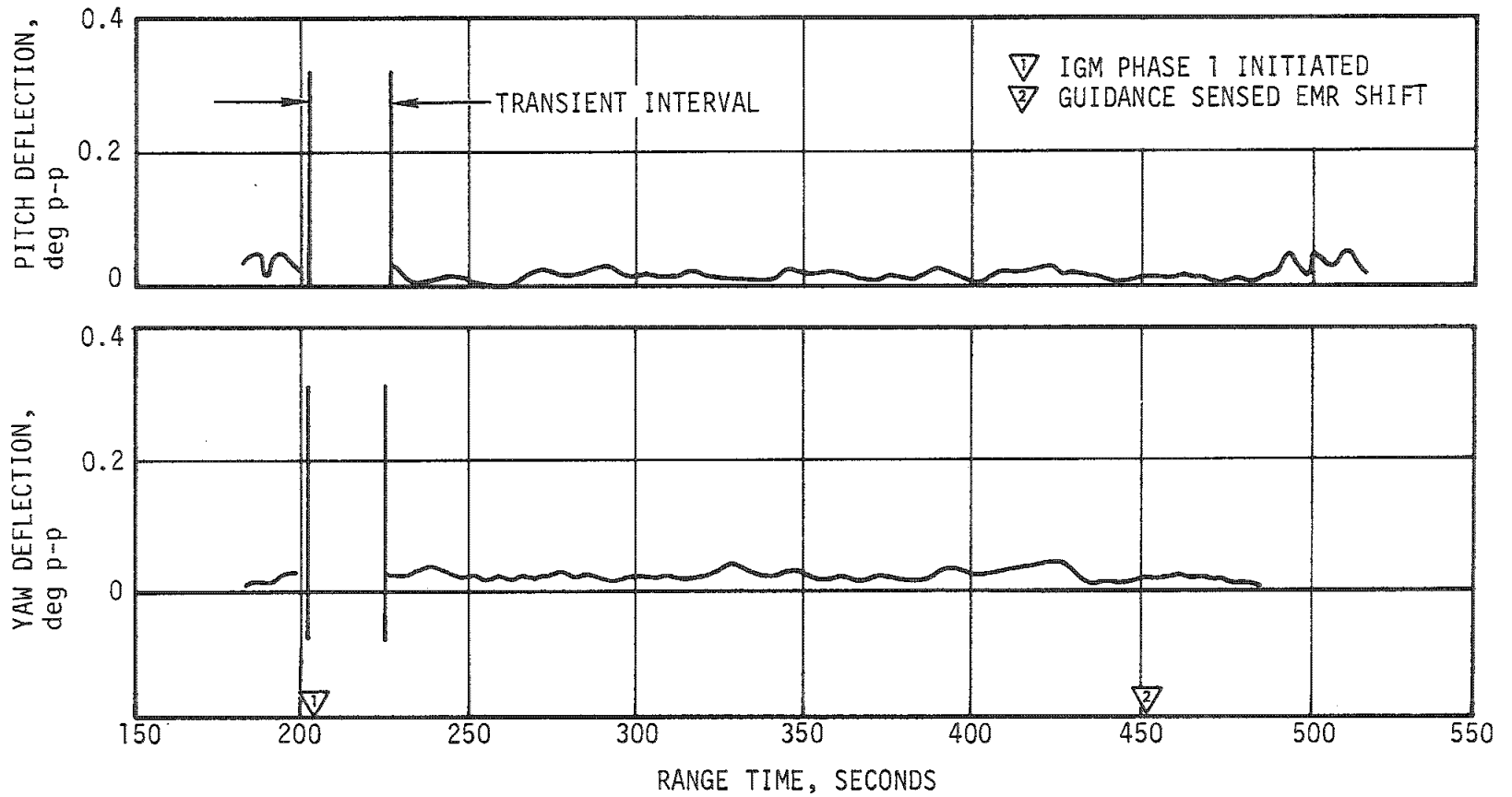


Figure 11-10. S-II Engine Deflection Response to Propellant Slosh

the pitch and roll planes, but to a much smaller degree. After 145 seconds of third burn an unexpectedly large roll torque developed.

#### 11.5.1 Control System Evaluation During First Burn

The S-IVB first burn attitude control system response to guidance commands for pitch, yaw and roll is presented in Figures 11-11, 11-12 and 11-13, respectively. Maximum attitude errors and rates occurred at ignition and guidance initiation. A summary of the first burn maximum values of critical flight control parameters is presented in Table 11-4.

The pitch and yaw effective thrust vector misalignments during first burn were -0.3 and 0.48 degree, respectively.

As experienced on previous flights, a steady-state roll torque of 7.9 N-m (5.8 lbf-ft), counterclockwise looking forward, required roll APS firings during first burn. This roll torque agrees with the roll torque of 8.5 N-m (6.3 lbf-ft) experienced on AS-503.

The Propellant Utilization (PU) sensors indicated only LOX sloshing occurred during first burn. The propellant slosh amplitudes and frequencies were comparable to those experienced on previous flights and did not have an appreciable effect on the control system.

#### 11.5.2 Control System Evaluation During Parking Orbit

The S-IVB/IU was controlled as expected during orbit. Significant events during parking orbit were the spacecraft separation, TD&E maneuver, and the maneuver to the local horizontal prior to second burn. The attitude control response during the maneuver to TD&E attitude is shown in Figures 11-14, 11-15, and 11-16 for pitch, yaw and roll, respectively. Figures 11-17, 11-18, and 11-19 show the pitch, yaw and roll attitudes during CSM/LM docking, and Figures 11-20, 11-21 and 11-22 show the same during LM ejection from the S-IVB. The S-IVB/IU was successfully stabilized for the docking with the LM.

Prior to second burn the inhibit was removed by ground command allowing the vehicle to maneuver to the local horizontal. The control system response for pitch, yaw and roll is presented in Figures 11-23, 11-24 and 11-25, respectively.

#### 11.5.3 Control System Evaluation During Second Burn

The S-IVB second burn attitude control system response to guidance commands for pitch, yaw and roll is presented in Figures 11-26, 11-27 and 11-28, respectively. The effect of LOX propellant sloshing is very pronounced on the pitch attitude, attitude error, angular rate, and

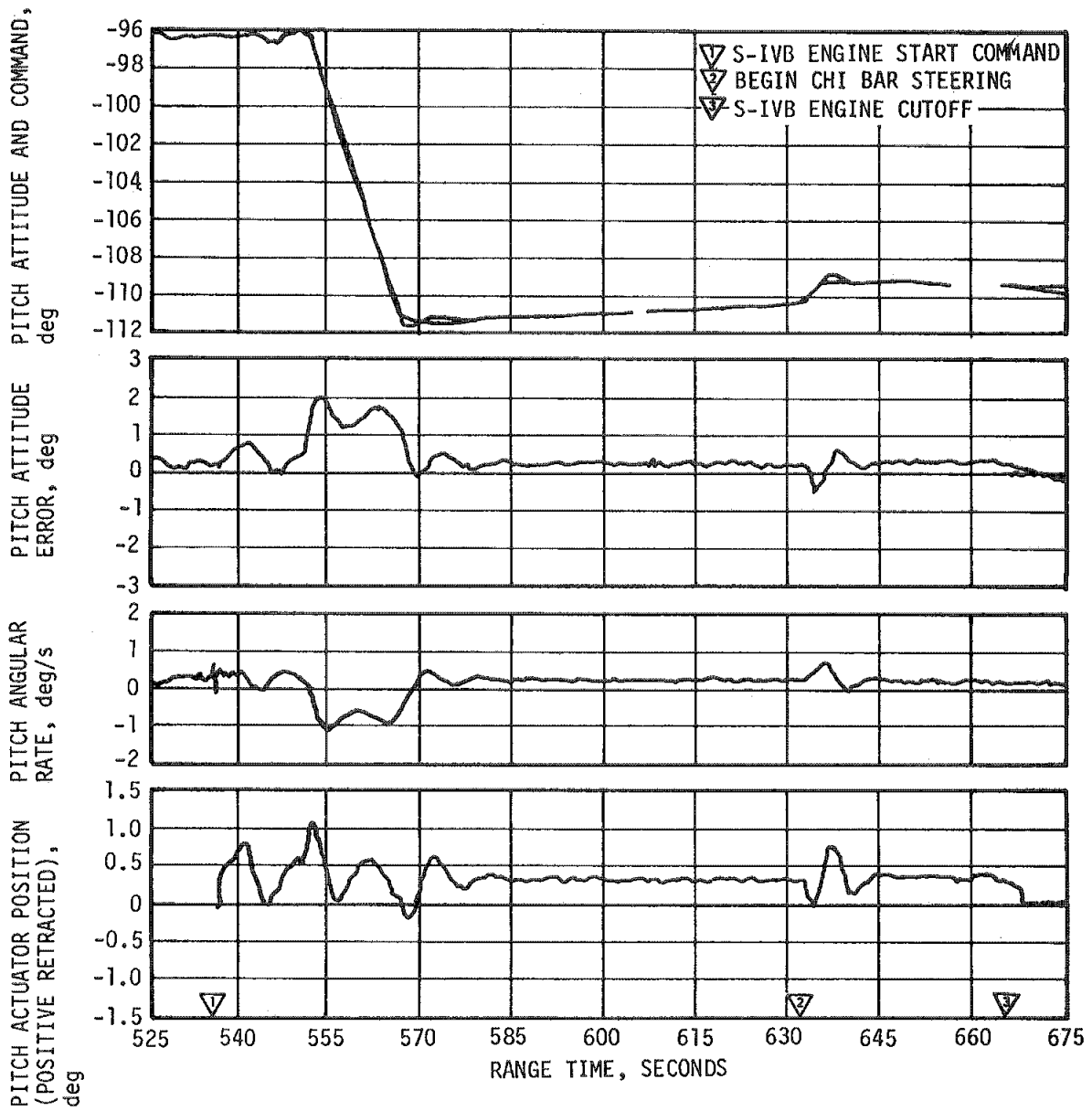


Figure 11-11. Pitch Attitude Control During S-IVB First Burn

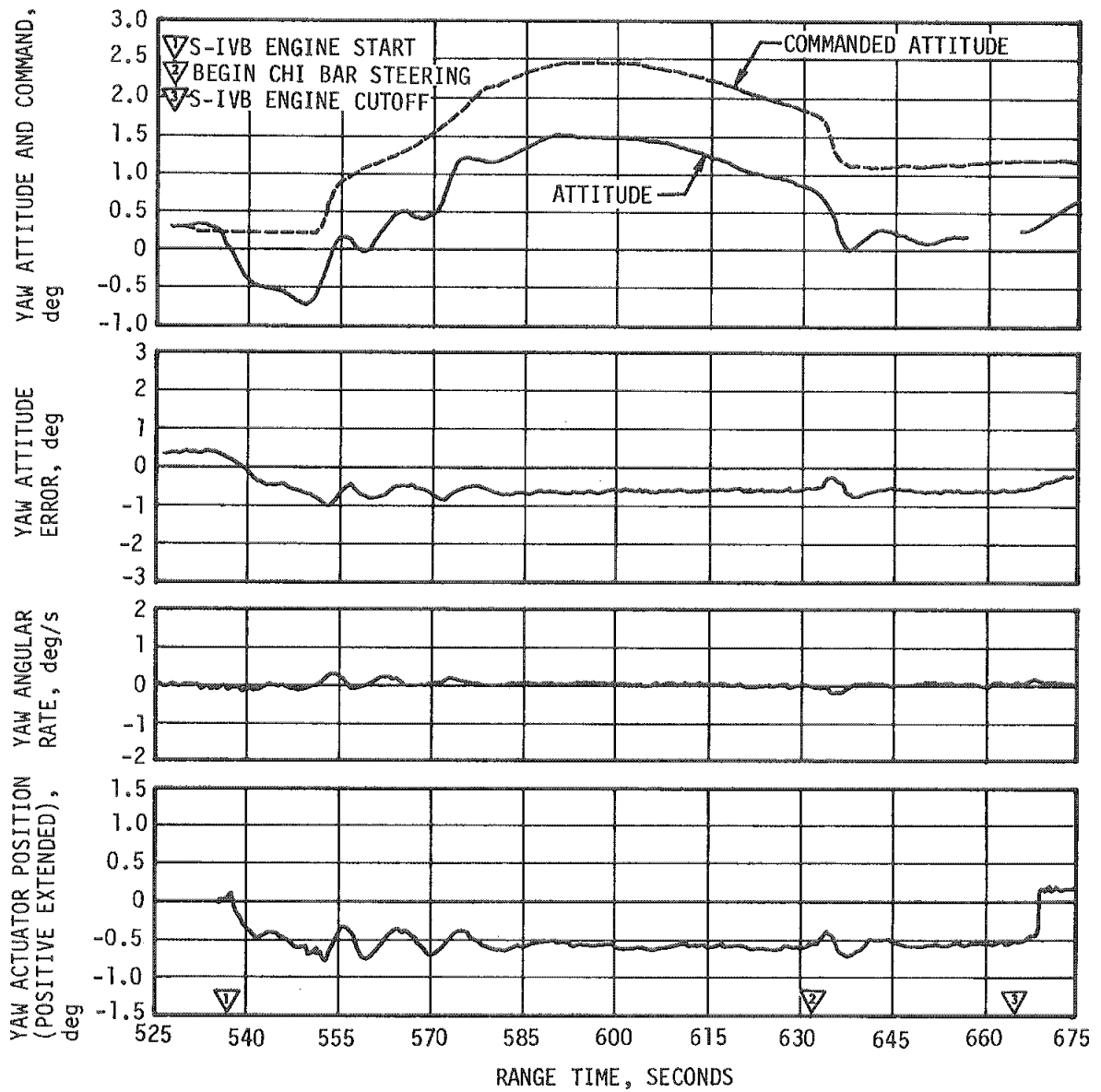


Figure 11-12. Yaw Attitude Control During S-IVB First Burn



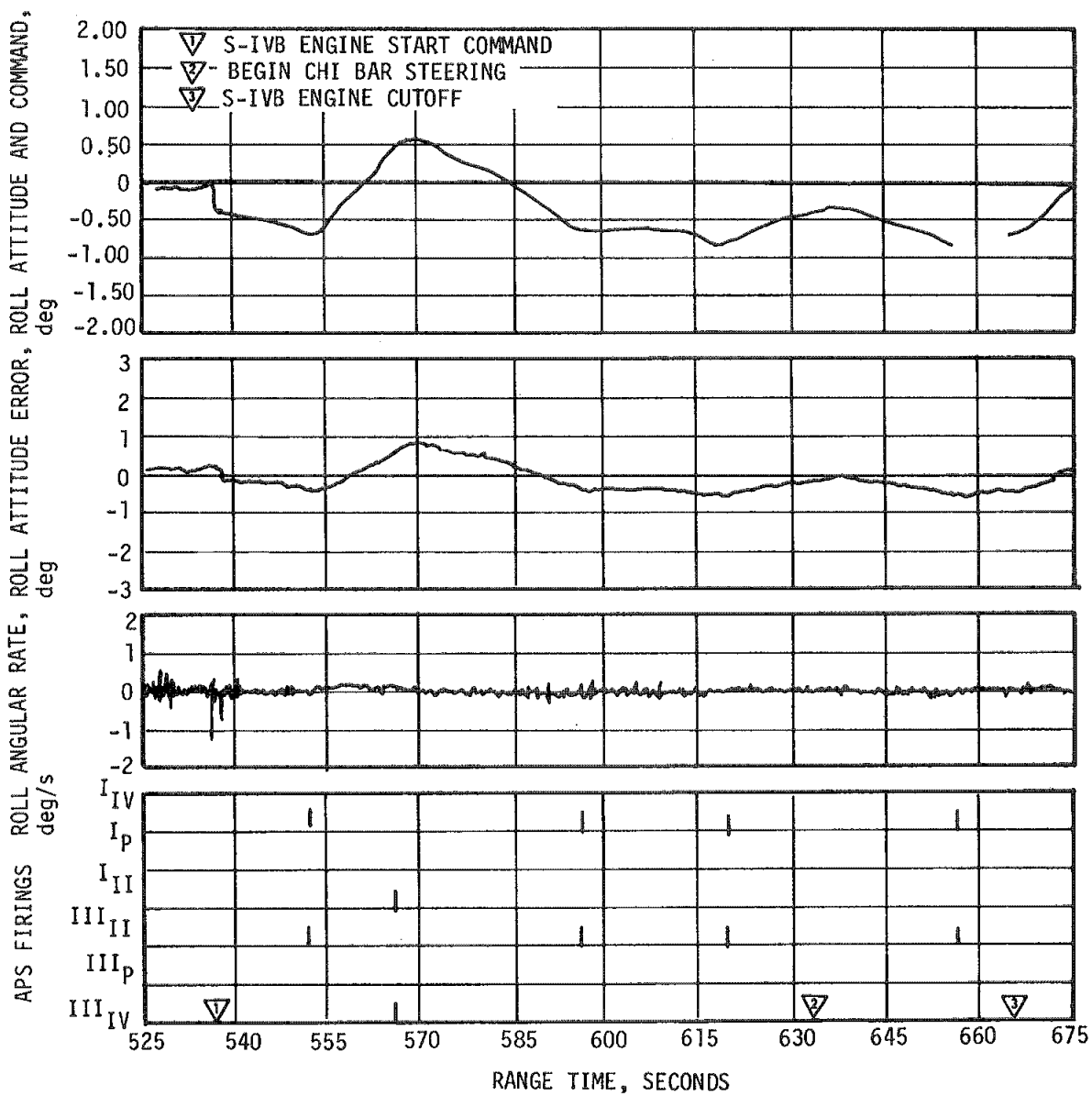


Figure 11-13. Roll Attitude Control During S-IVB First Burn

▽ MANEUVER TO SEPARATION ATTITUDE

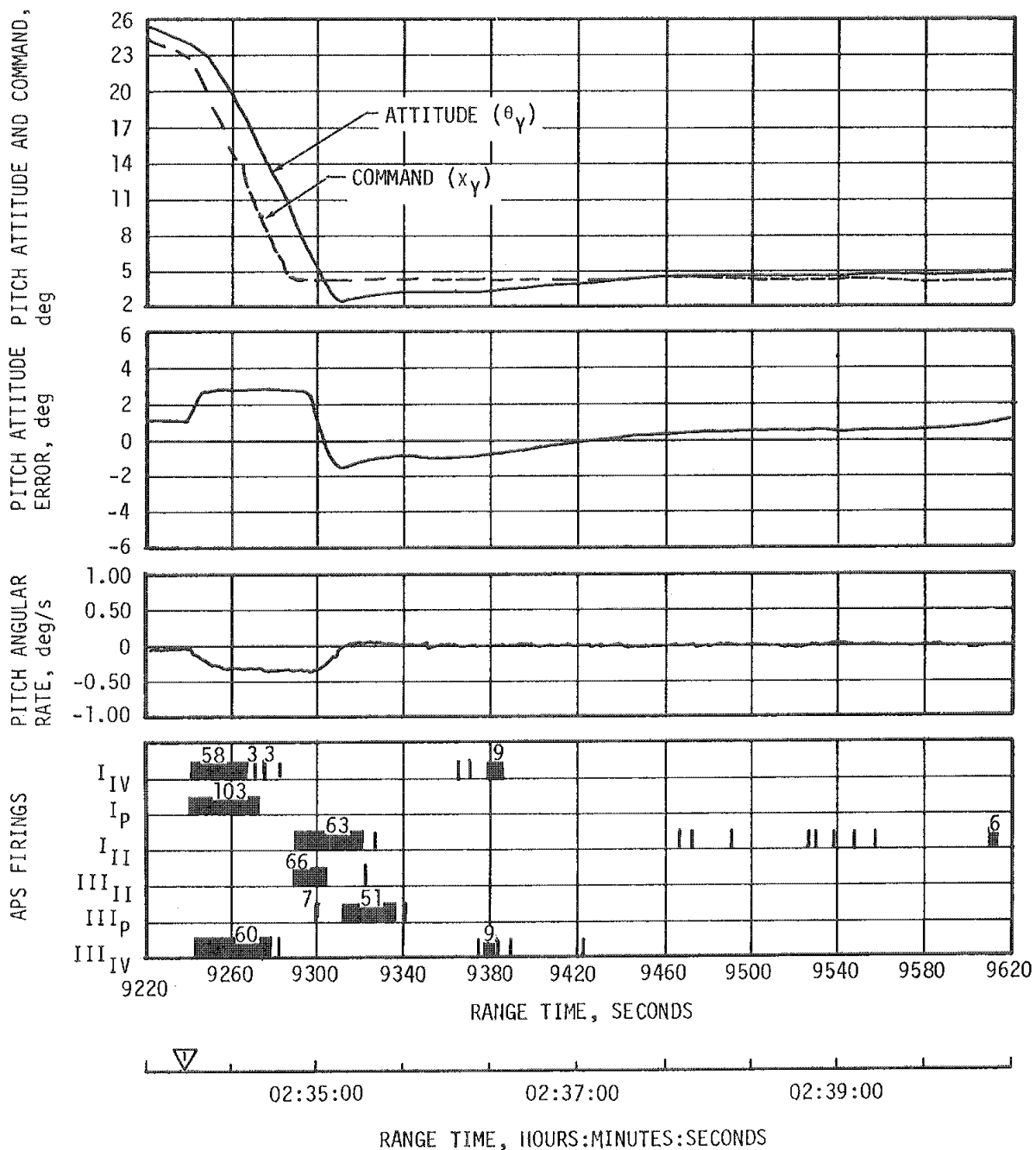


Figure 11-14. Pitch Attitude Control During Maneuver to TD&E Attitude

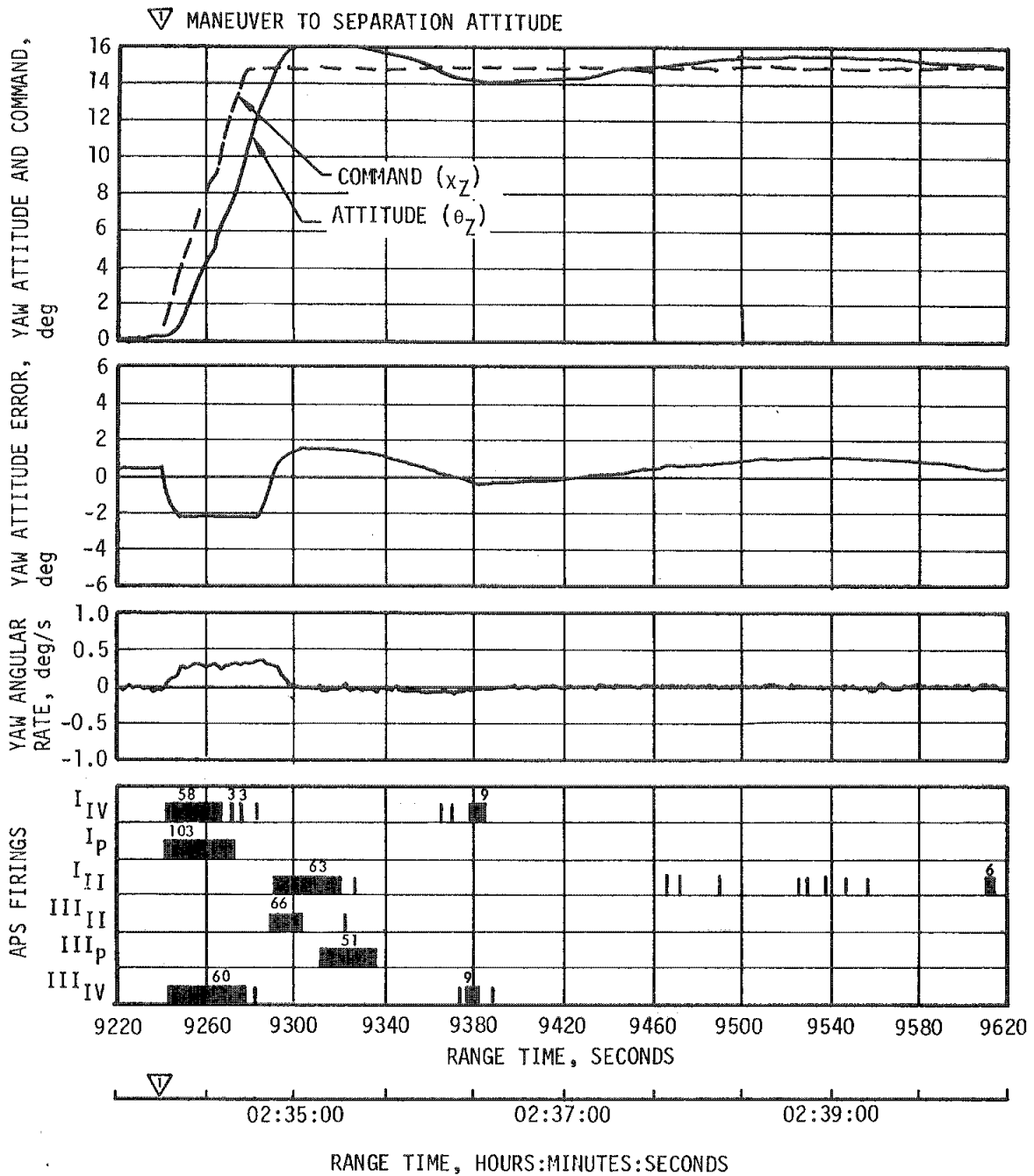


Figure 11-15. Yaw Attitude Control During Maneuver to TD&E Attitude

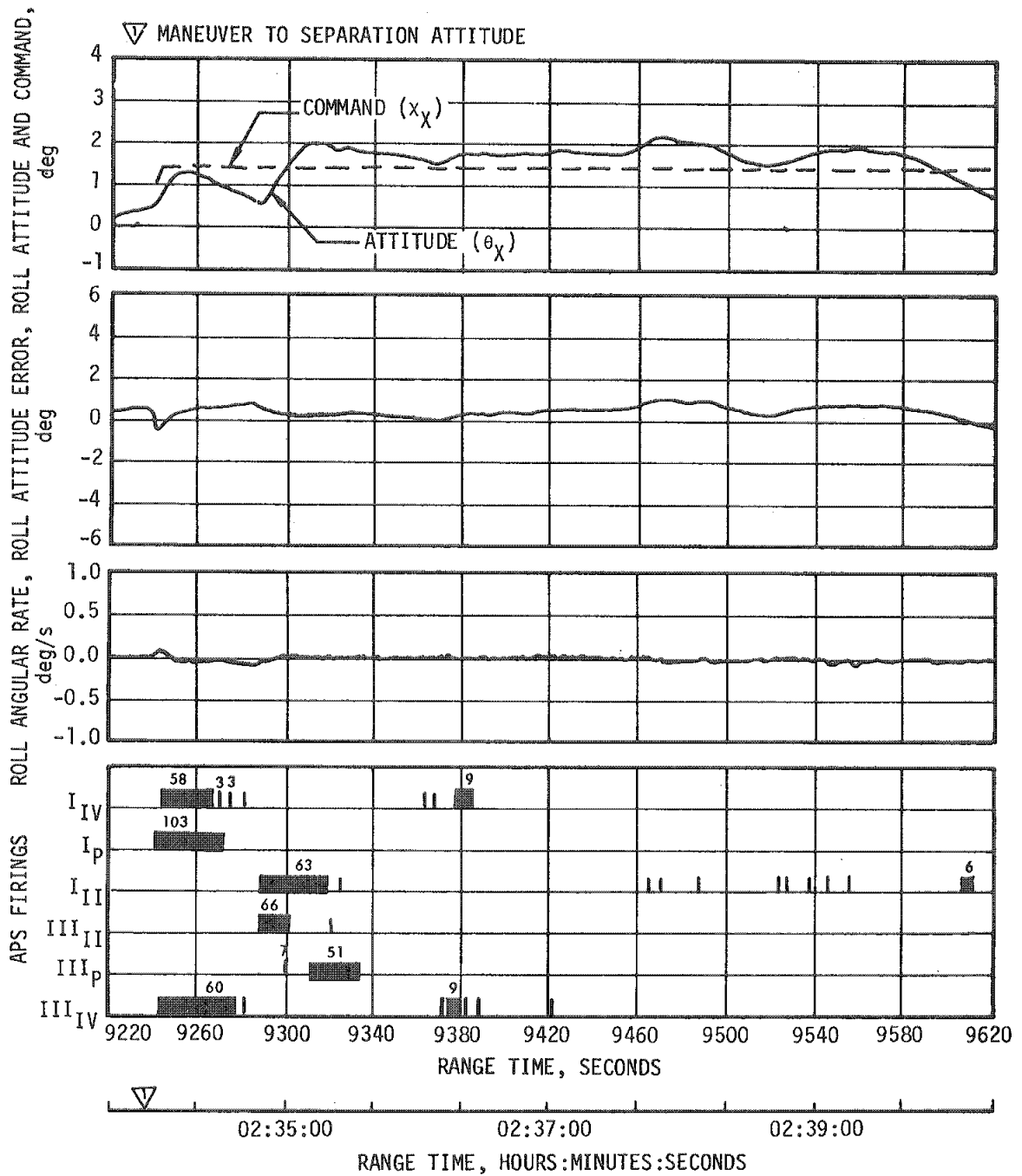


Figure 11-16. Roll Attitude Control During Maneuver to TD&E Attitude

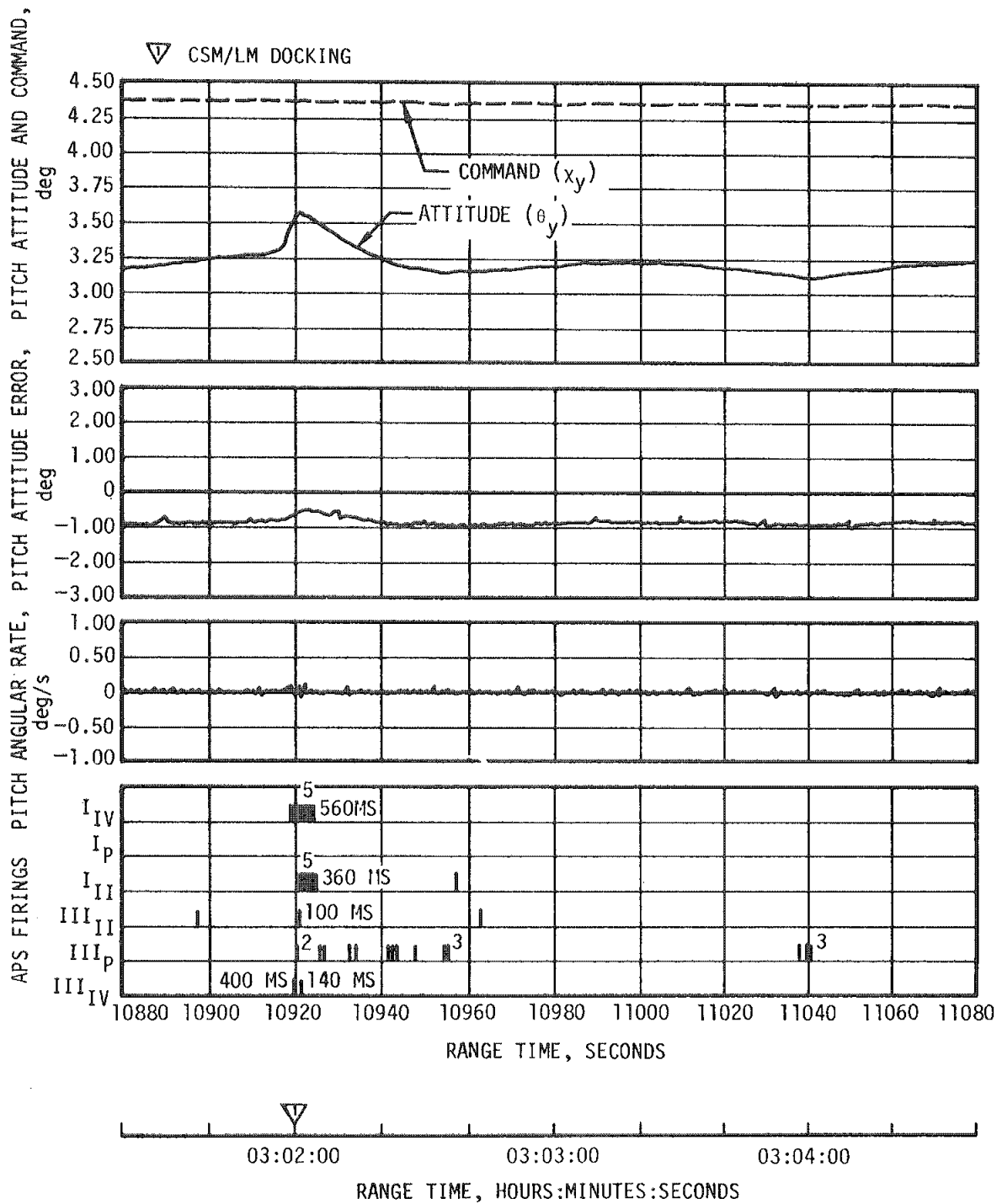


Figure 11-17. Pitch Attitude Control During Hard Dock

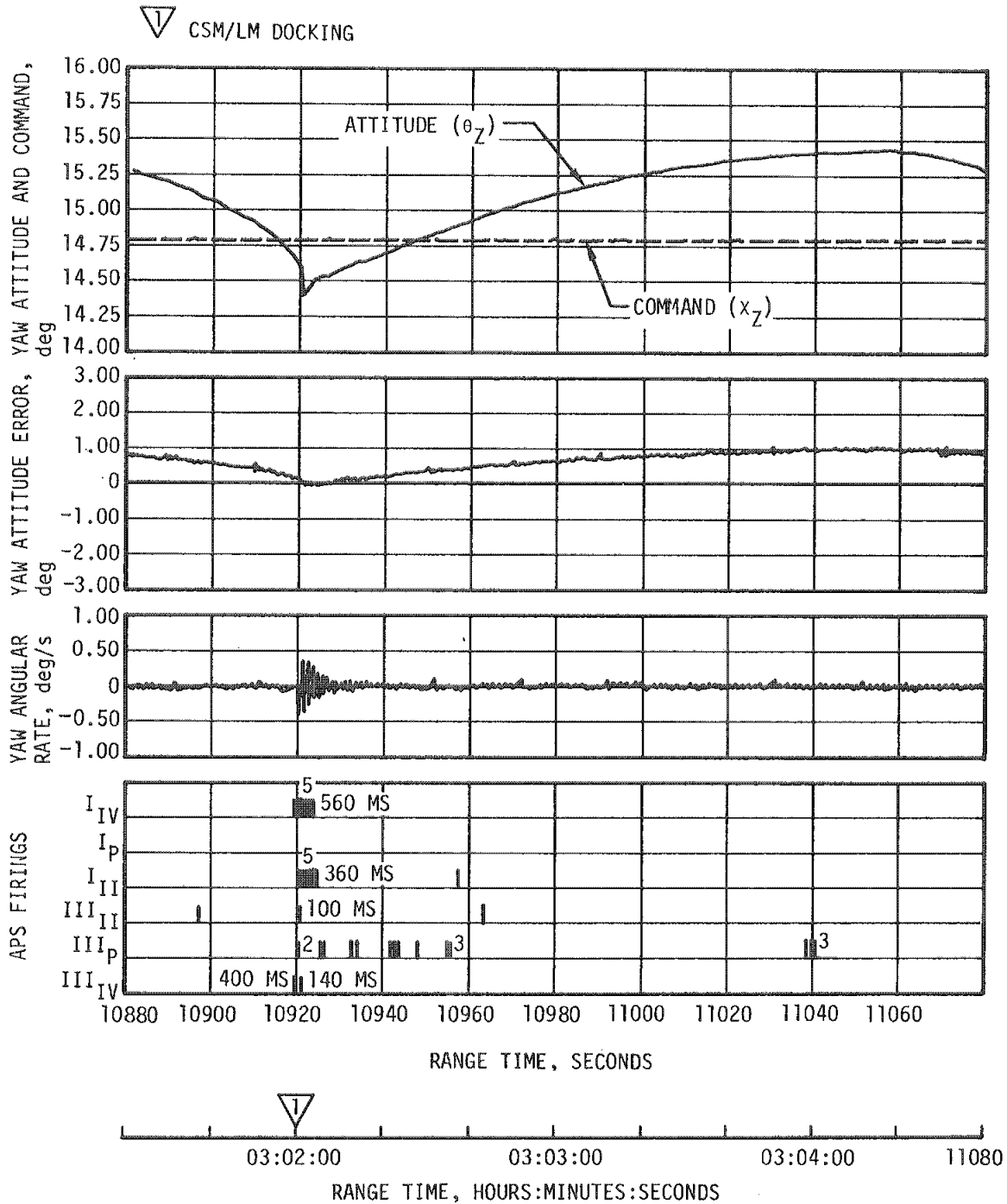


Figure 11-18. Yaw Attitude Control During Hard Dock

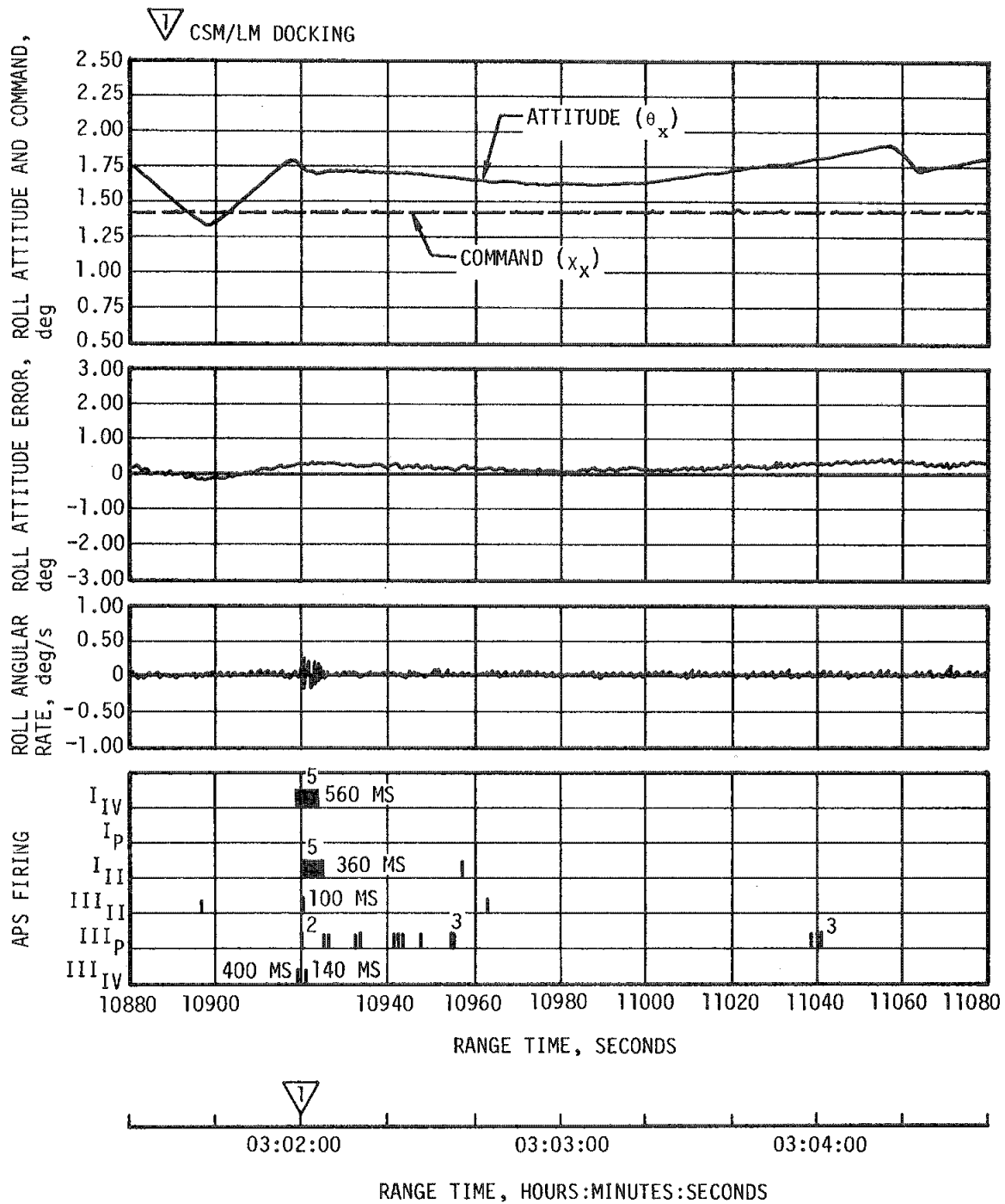


Figure 11-19. Roll Attitude Control During Hard Dock

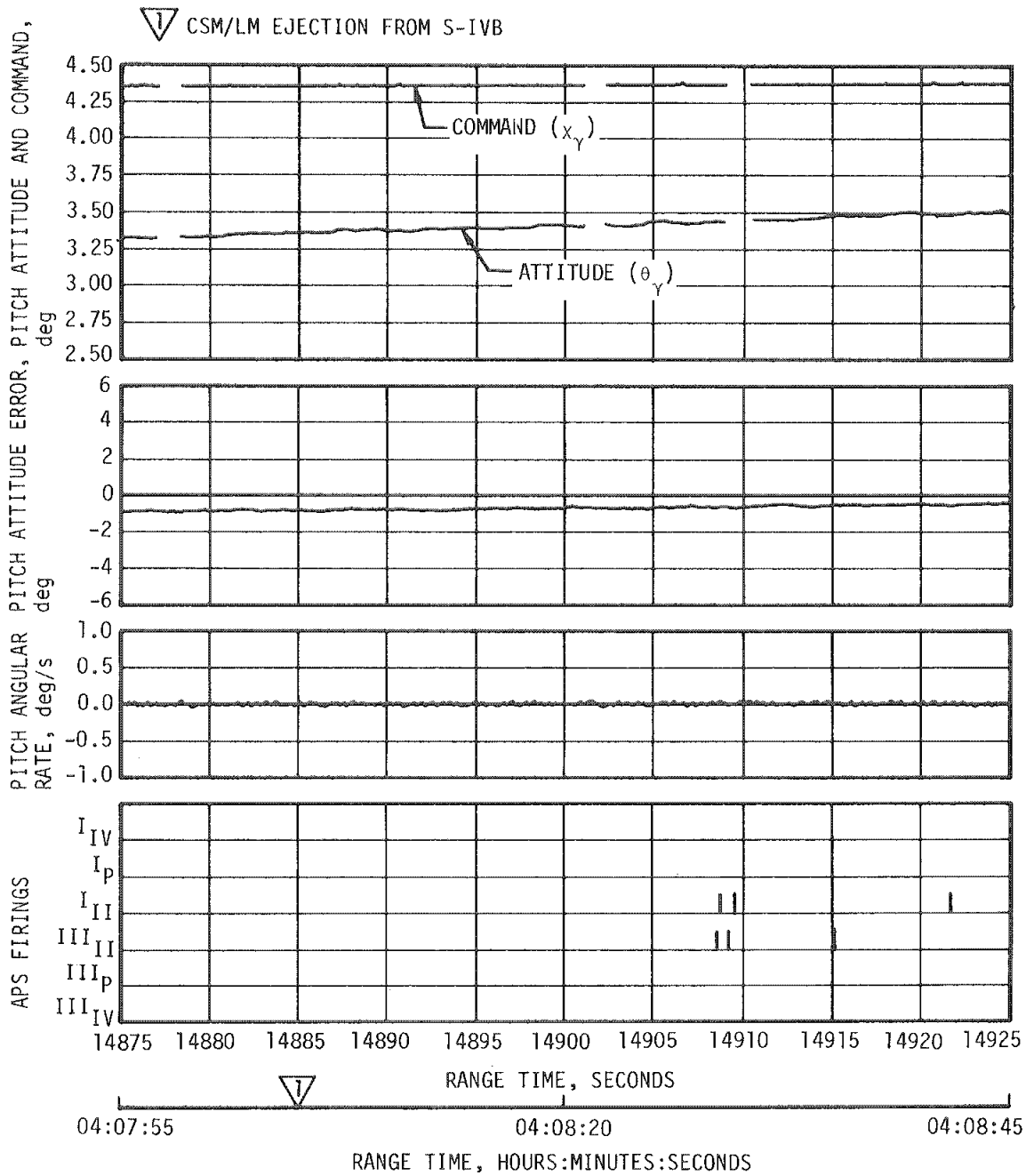


Figure 11-20. Pitch Attitude Control During LM Ejection



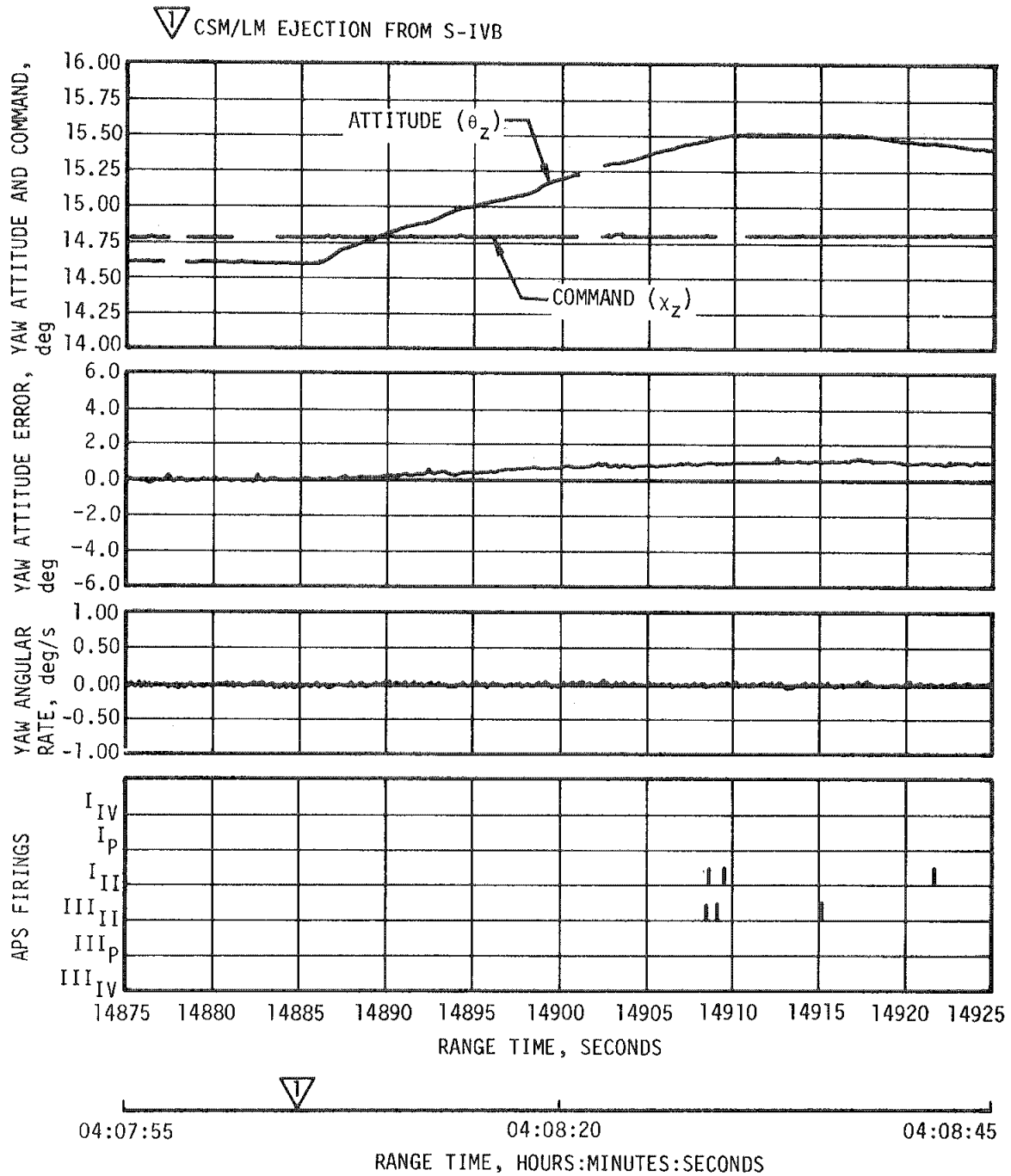


Figure 11-21. Yaw Attitude Control During LM Ejection

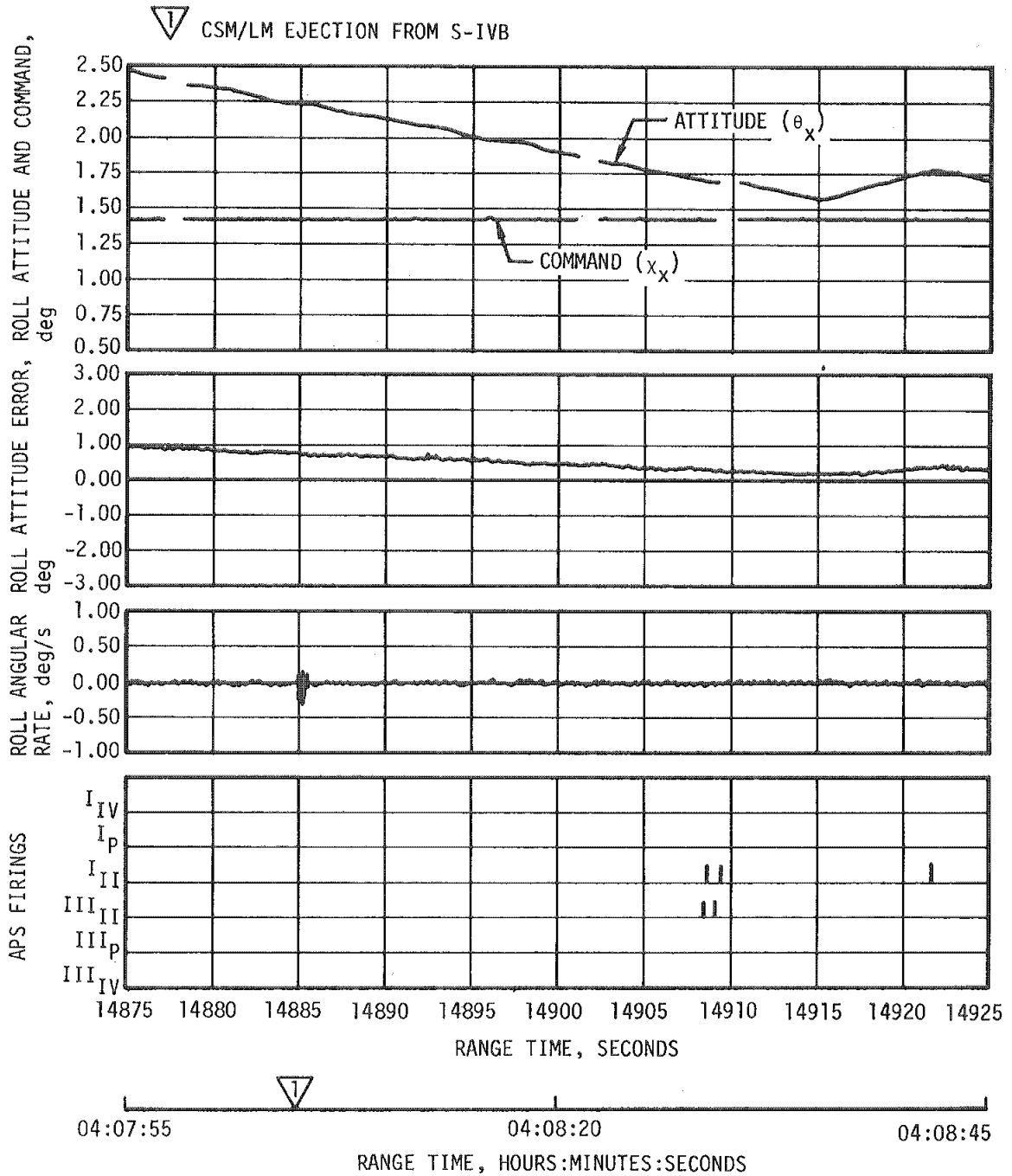


Figure 11-22. Roll Attitude Control During LM Ejection

4

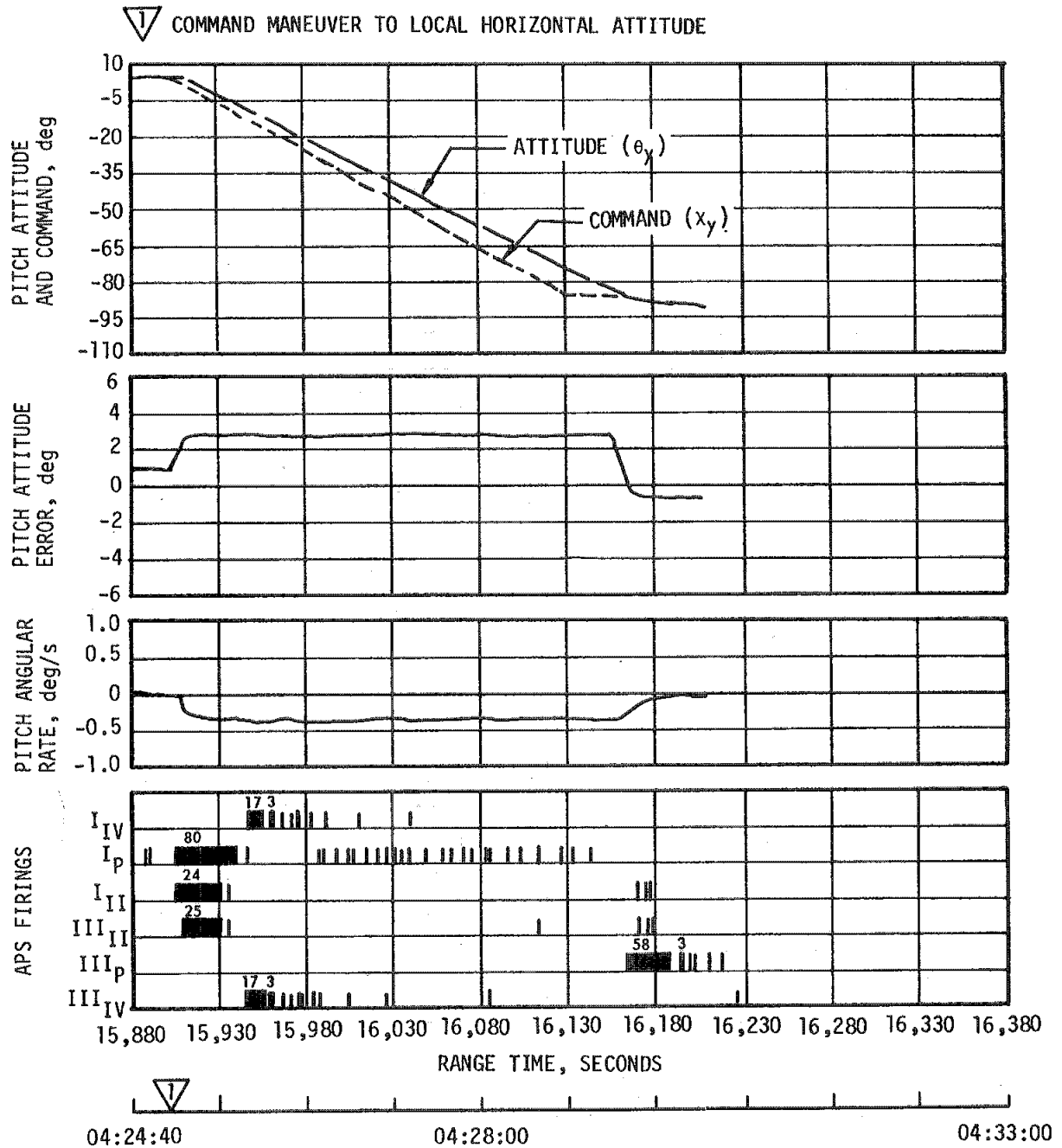


Figure 11-23. Pitch Attitude Control During Alignment of S-IVB to Local Horizontal Prior to Second Burn

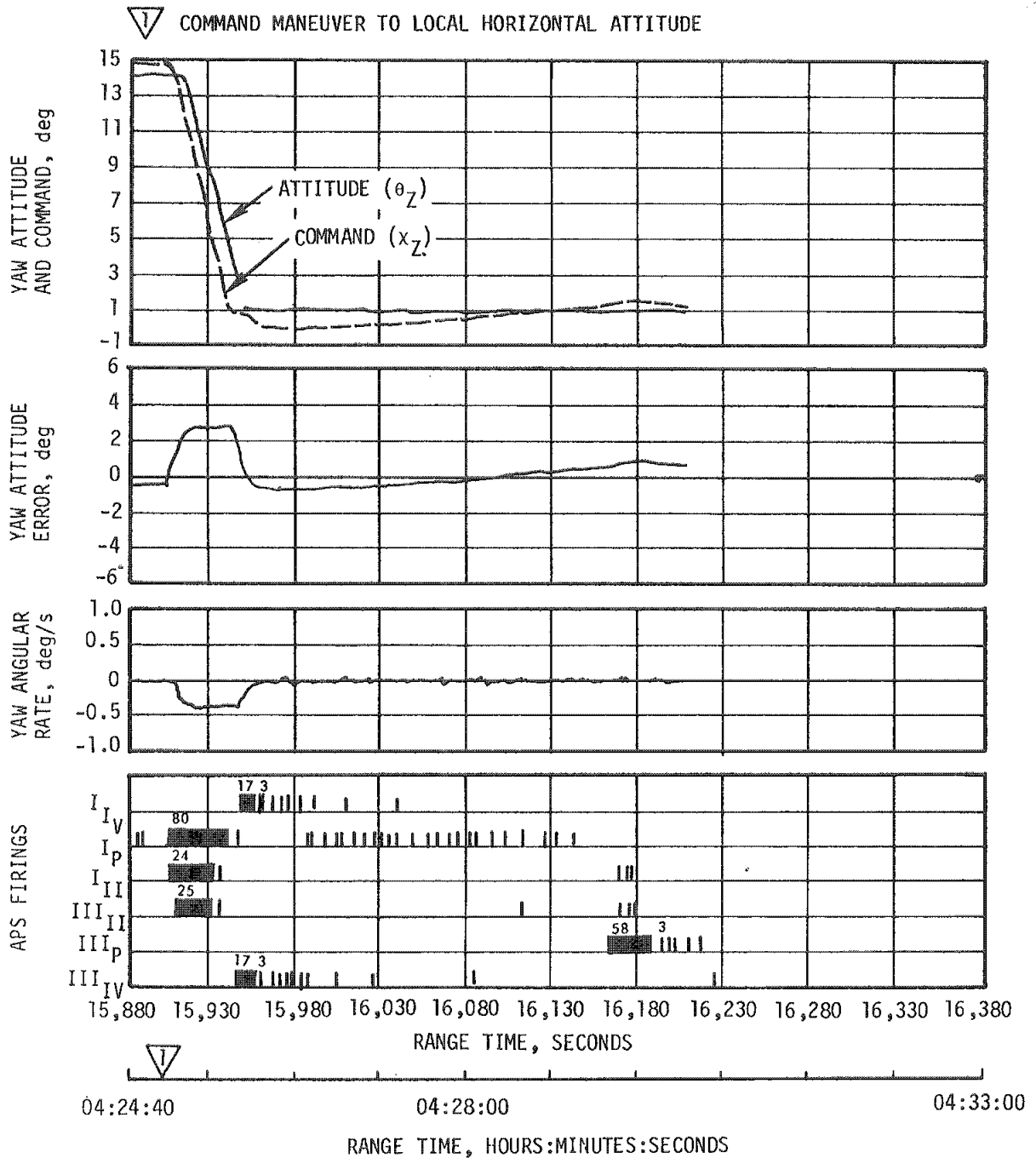


Figure 11-24. Yaw Attitude Control During Alignment of S-IVB to Local Horizontal Prior to Second Burn

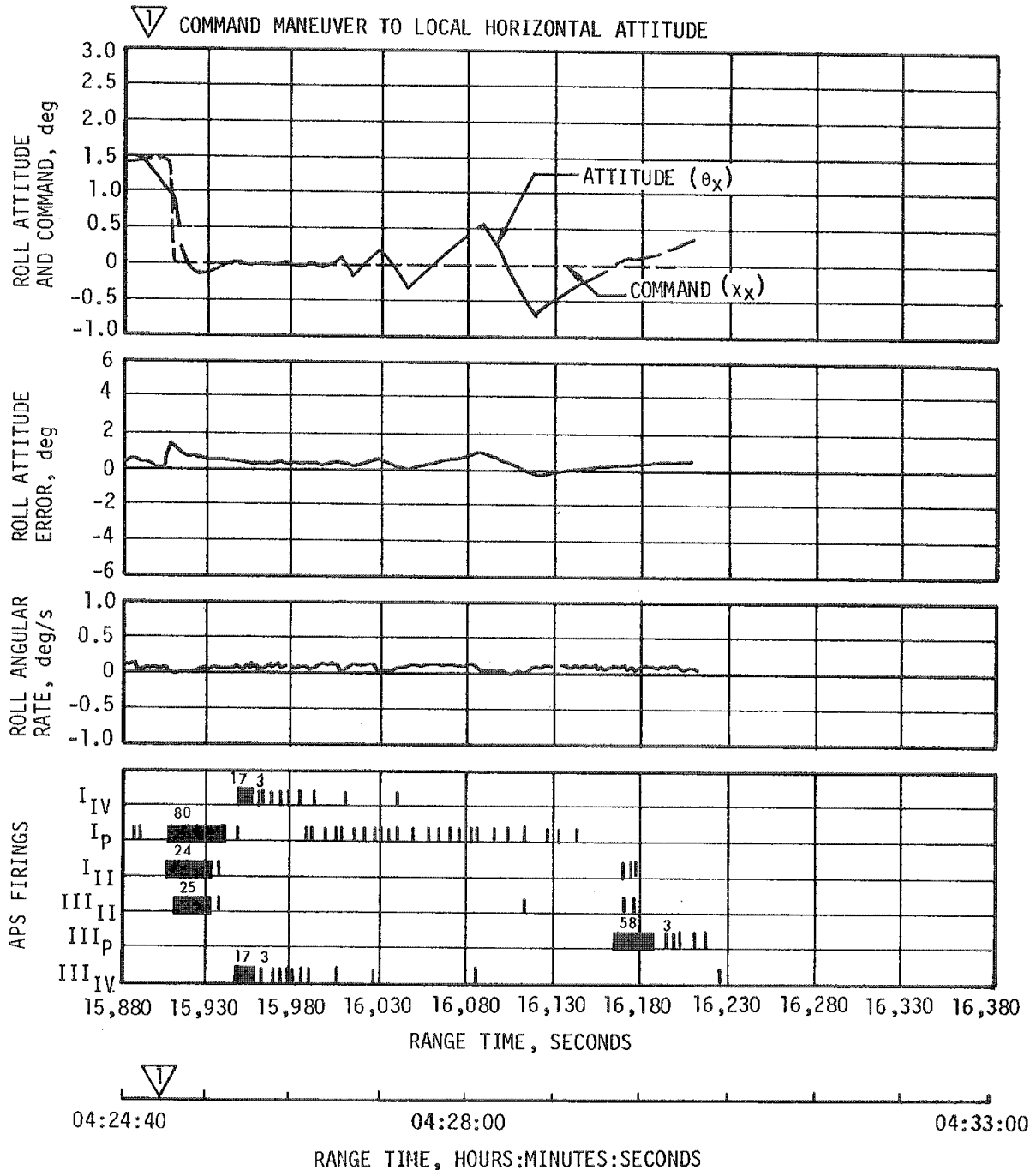


Figure 11-25. Roll Attitude Control During Alignment of S-IVB to Local Horizontal Prior to Second Burn

▽ S-IVB 2ND ESC  
 ▽ 2 S-IVB 2ND ECO

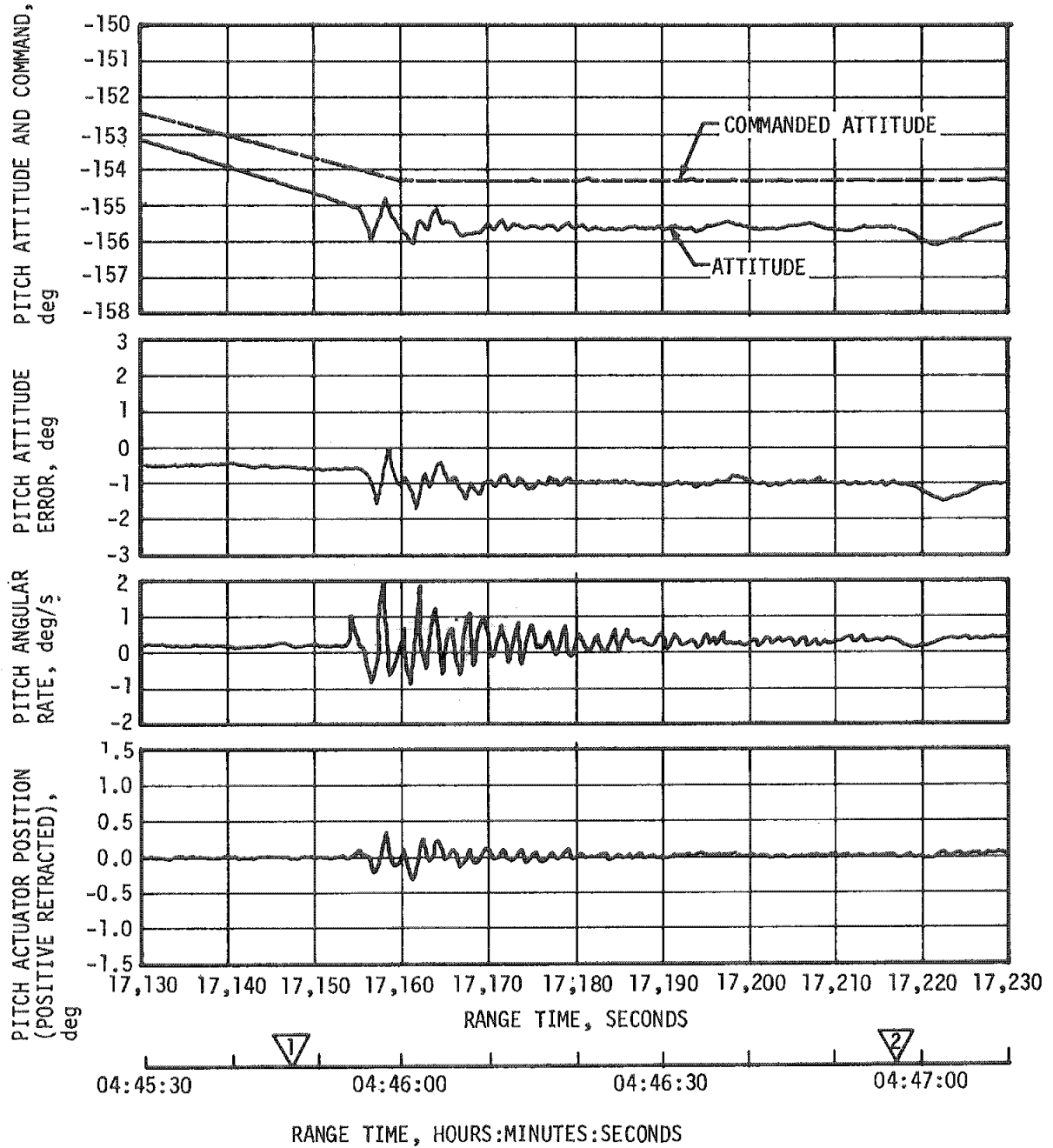


Figure 11-26. Pitch Attitude Control During S-IVB Second Burn

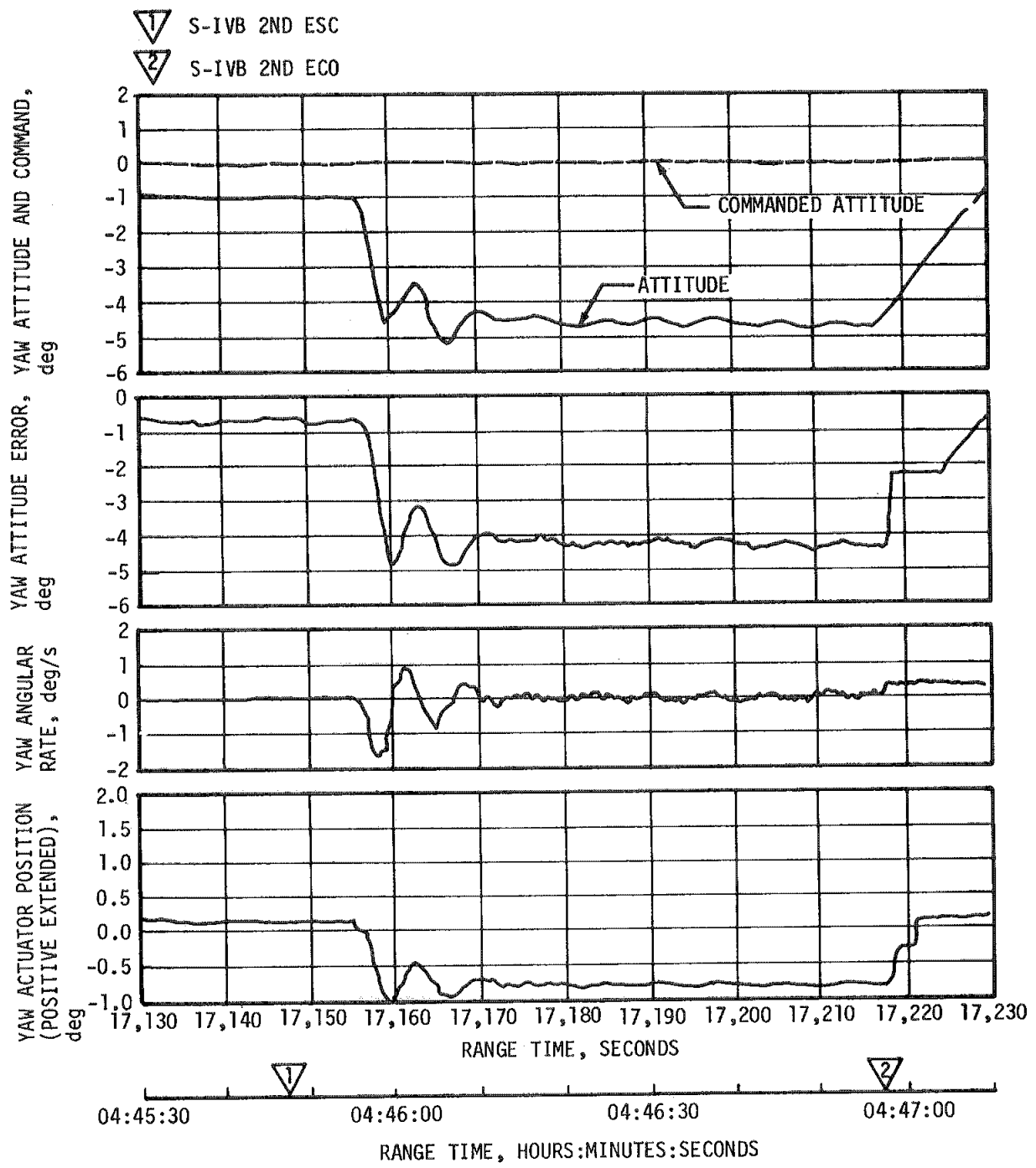


Figure 11-27. Yaw Attitude Control During S-IVB Second Burn

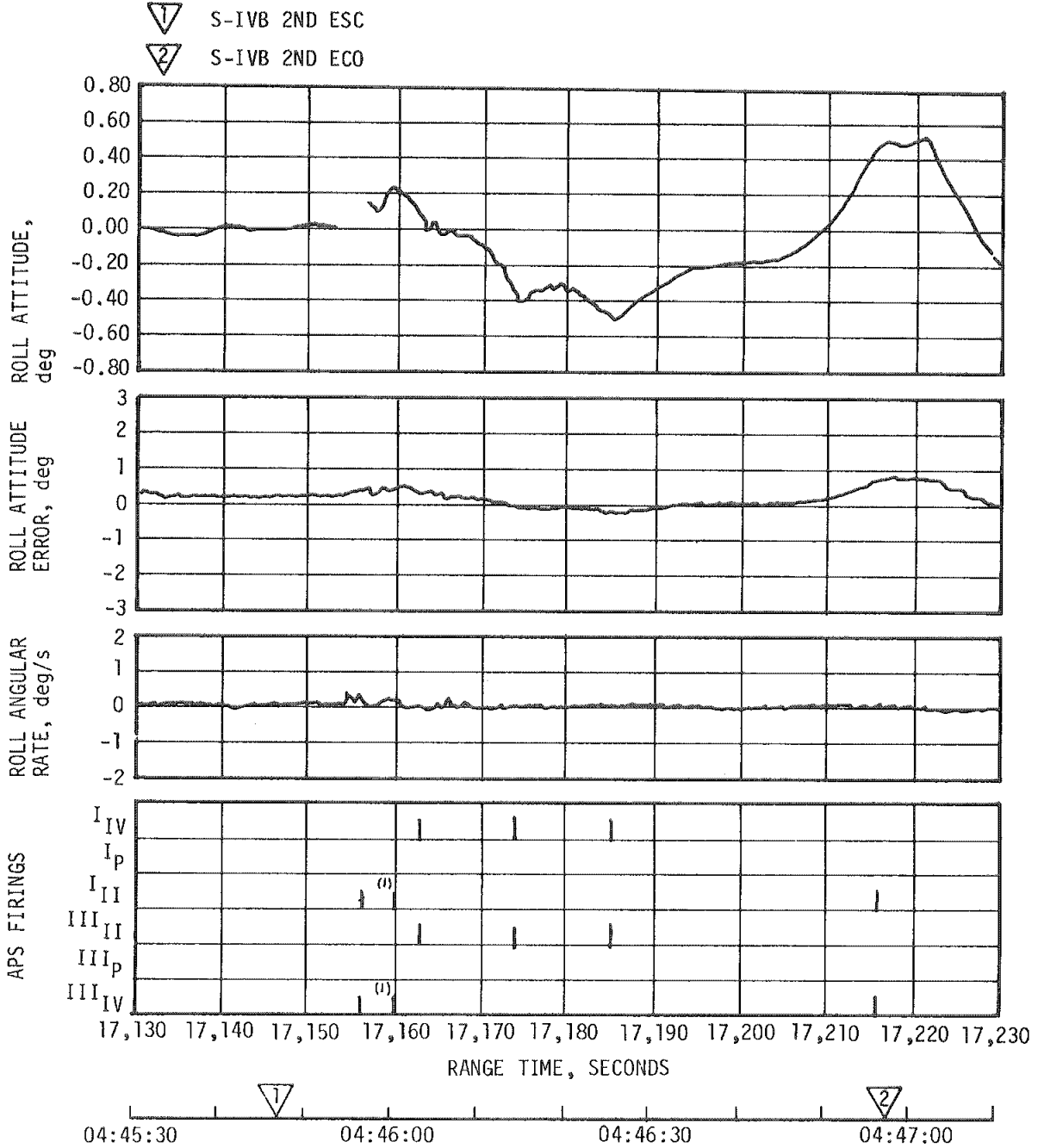


Figure 11-28. Roll Attitude Control During S-IVB Second Burn



Table 11-4. Maximum Control Parameters During First Burn

PARAMETER	IGNITION AND GUID. INITIATION	CHI BAR	CHI FREEZE	S-IVB CUTOFF
Pitch Attitude Error, deg	+2.1	+0.5	+0.3	+0.3
Yaw Attitude Error, deg	-1.1	-0.8	-0.6	-0.7
Roll Attitude Error, deg	+0.9	0	-0.5	-0.3
Pitch Rate, deg/s	-1.2	+0.5	+0.3	0
Yaw Rate, deg/s	+0.3	-0.2	0	0
Roll Rate, deg/s	+0.1	0	0	0
Pitch Actuator Position, deg	+1.1	+0.8	+0.3	+0.3
Yaw Actuator Position, deg	-0.8	-0.8	-0.6	-0.5

Note: Attitude rates and actuator positions reflect measured values with estimated biases removed; however, biases were not removed from the data shown in Figures 11-11, 11-12, and 11-13.

actuator position as seen in Figure 11-26. The LOX slosh was well damped and was within the capabilities of the control system. The maximum attitude errors and rates occurred at S-IVB ignition. A summary of the second burn maximum values of critical flight control parameters is presented in Table 11-5.

The pitch and yaw effective thrust vector misalignments during second burn were -0.26 and 0.45 degree, respectively. The steady-state roll torque was negligible during the short (62 sec) second burn.

#### 11.5.4 Control System Evaluation During Intermediate Orbit

The attitude control of the S-IVB/IU was as expected during the intermediate orbit. The vehicle correctly maneuvered to the local horizontal following S-IVB second burn and maintained this attitude until the attitude freeze for third burn.

#### 11.5.5 Control System Evaluation During Third Burn

Evaluation of the AS-504 mission up to third burn ignition indicates normal control system operation. During third burn, however, abnormal control system performance was observed in three areas:

- a. High amplitude oscillations occurred in the yaw plane during the first 100 seconds of burn.

Table 11-5. Maximum Control Parameters During Second Burn

PARAMETER	IGNITION	S-IVB CUTOFF
Pitch Attitude Error, deg	-1.7	-1.6
Yaw Attitude Error, deg	-4.9	-4.5
Roll Attitude Error, deg	+0.6	+0.8
Pitch Rate, deg/s	+1.8	+0.2
Yaw Rate, deg/s	-1.6	+0.3
Roll Rate, deg/s	+0.4	0
Pitch Actuator Position, deg	+0.4	-0.1
Yaw Actuator Position, deg	-1.2	-0.9

Note: Attitude rates and actuator positions reflect measured values with estimated biases removed; however, biases were not removed from the data in Figures 11-26, 11-27 and 11-28.

- b. The pitch actuator was biased from the null position after the end of third burn by 0.3 degree.
- c. Roll control system firings indicate the presence of abnormally high roll torques during the latter 150 seconds of burn.

The S-IVB third burn attitude control system response to guidance commands for pitch, yaw, and roll is presented in Figures 11-29, 11-30 and 11-31, respectively. The maximum control system values are tabulated in Table 11-6.

The third burn control system oscillations occurred shortly after thrust buildup and continued until the thrust chamber pressure decreased at approximately 22,138 seconds. Although the oscillation occurred in pitch, yaw, and roll, the oscillations were predominately in the yaw plane. The oscillations of 0.6 to 0.7 hertz indicated a maximum attitude excursion of 3 degrees peak-to-peak (p-p), maximum rate excursion of 5 deg/s (p-p), and a maximum actuator oscillation of 2.6 degrees (p-p).

The average level of attitude error was erratic and in a direction which is less negative than expected assuming nominal third burn center of gravity offsets, and a thrust misalignment consistent with second burn. After the chamber pressure decreased the attitude error stabilized at the expected third burn value. The average actuator position was as

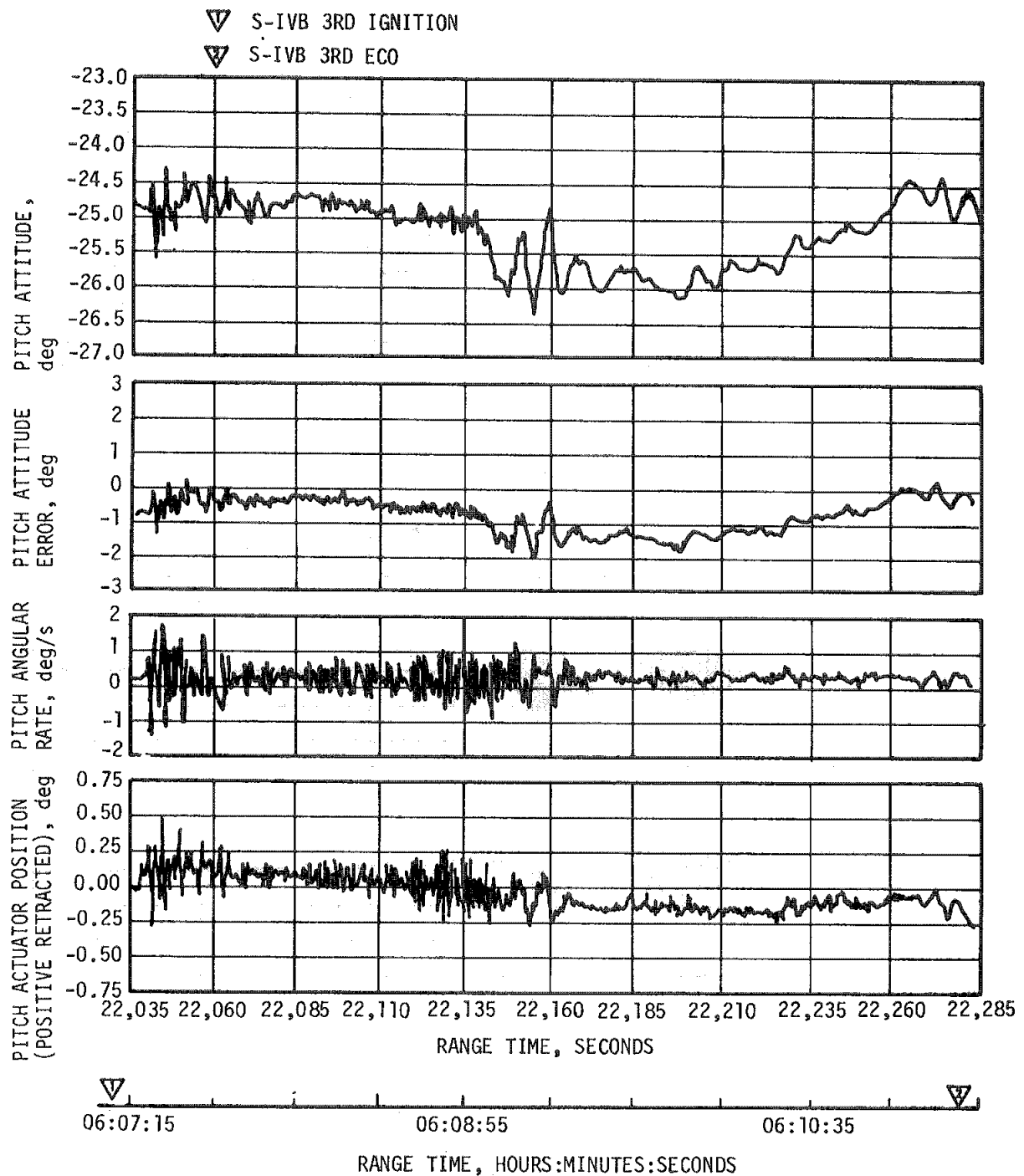


Figure 11-29. Pitch Attitude Control During S-IVB Third Burn

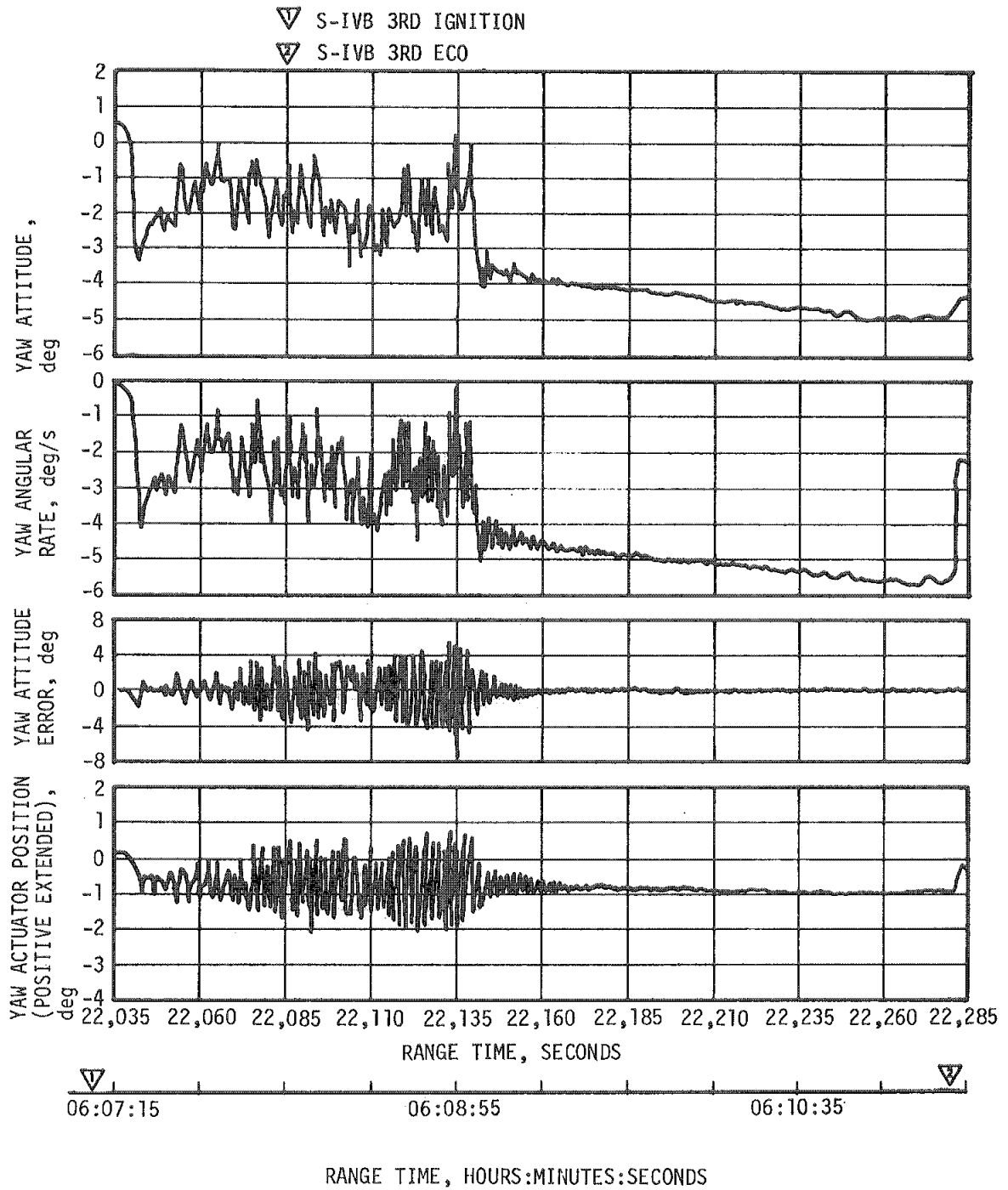
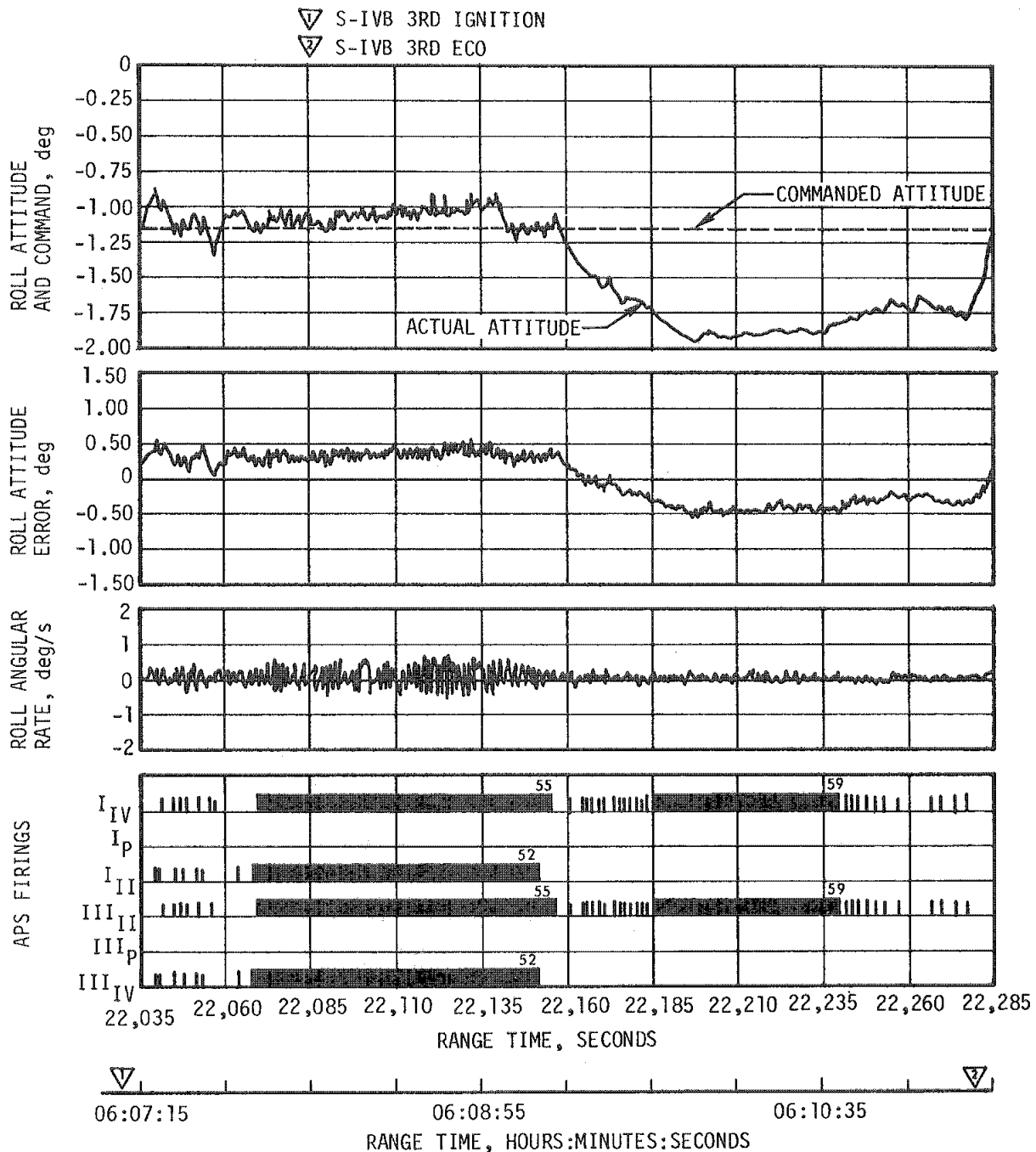


Figure 11-30. Yaw Attitude Control During S-IVB Third Burn



\*INDICATES MORE THAN MINIMUM PULSES

Figure 11-31. Roll Attitude Control During S-IVB Third Burn

Table 11-6. Maximum Control Parameters During S-IVB Third Burn

PARAMETER	IGNITION	S-IVB CUTOFF
Pitch Attitude Error, deg	-1.4	0
Yaw Attitude Error, deg	-4.2	-5.7
Roll Attitude Error, deg	+0.5	-0.3
Pitch Rate, deg/s	-1.4	+0.3
Yaw Rate, deg/s	-2.0	0
Roll Rate, deg/s	+0.3	0
Pitch Actuator Position, deg	+0.5	-0.2
Yaw Actuator Position, deg	-1.2	-1.0

Note: Attitude rates and actuator positions reflect measured values with estimated biases removed; however, biases were not removed from the data shown in Figures 11-29, 11-30 and 11-31.

expected during the entire burn and thus, is inconsistent with the attitude error. The average value of actuator command current is also inconsistent with the actuator position. During the oscillatory period the actuator position was greater than commanded in the retract direction, resulting in a bias that represents an actuator gain increase. The increased gain coupled with the large phase lag (40 to 50 degrees at 0.6 hertz) between commanded and actual actuator position resulted in the yaw response seen during third burn. Normal phase lag in both directions is 25 degrees. Possible sources of phase lag are abnormal actuator loads from engine side loads or abnormal actuator environment (temperature or vibrations).

The pitch plane oscillations (maximum of 1.0 degree p-p in attitude error) were at a much lower amplitude than the yaw oscillations. Before thrust chamber pressure decrease, the pitch phase lag was less than the yaw lag and occurred in the opposite direction (the pitch lag occurred in the extend direction whereas the yaw lag was in the retract). It is currently felt that the pitch oscillations are the result of coupling with the yaw dynamics.

Figures 11-32 and 11-33 show the calculated and measured pitch and yaw actuator positions at the beginning of S-IVB third burn and at the end of the peak yaw oscillations. The calculated engine position was obtained by scaling the measured actuator current or command and passing

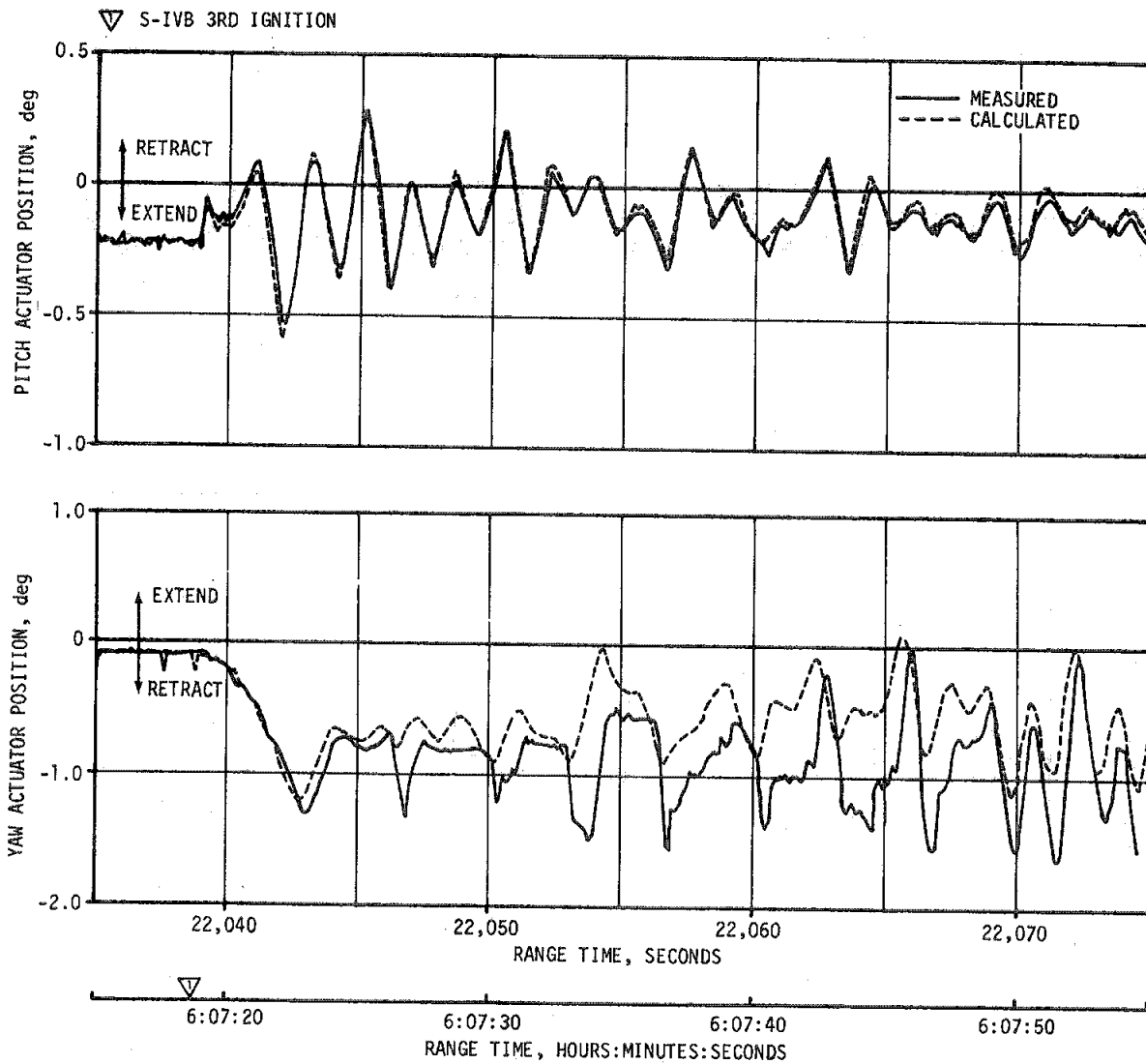


Figure 11-32. Measured and Calculated Engine Positions at Start of S-IVB Third Burn Prior to Oscillation Buildup

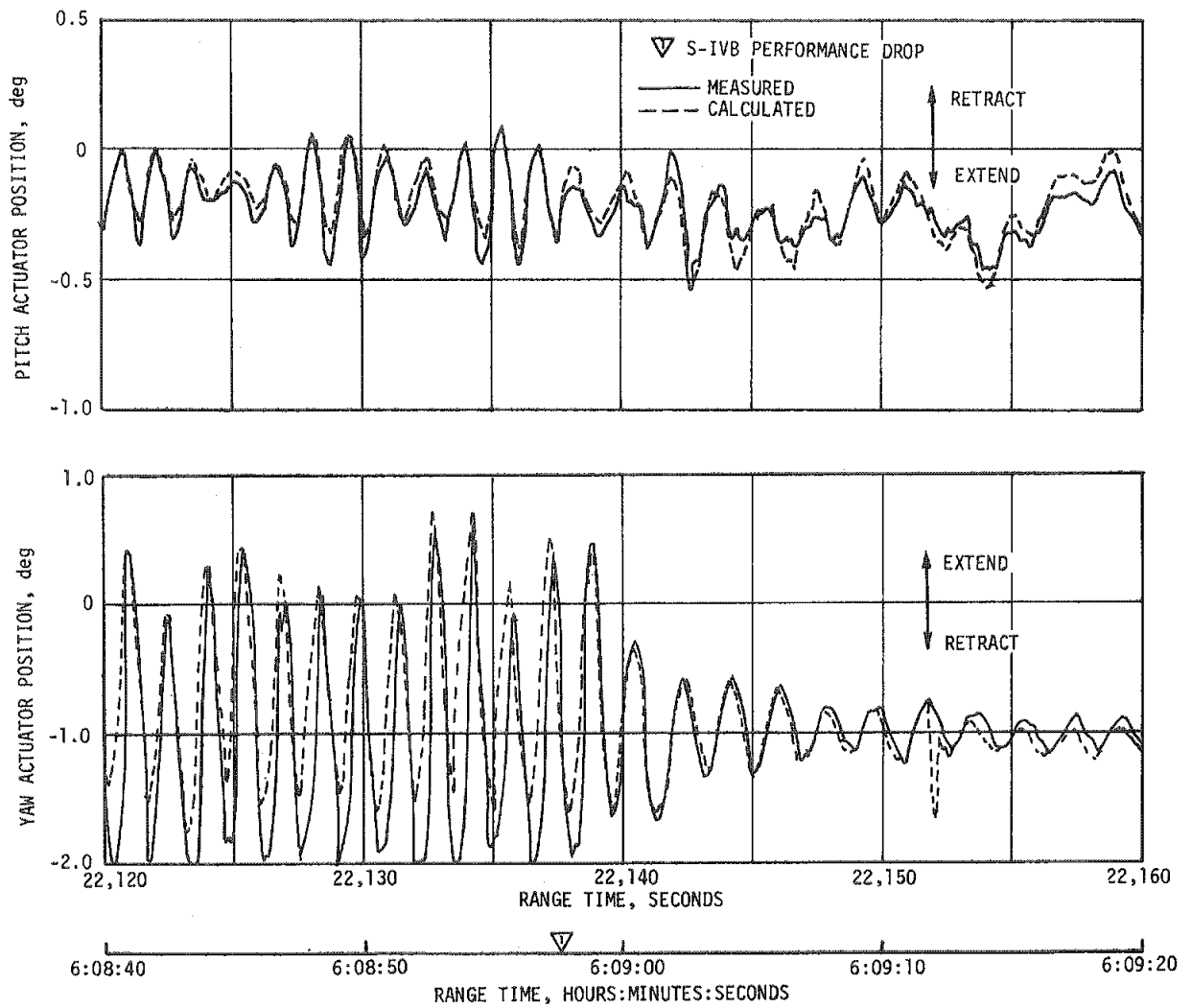


Figure 11-33. Measured and Calculated Engine Positions at End of S-IVB Third Burn Oscillation Period



it through a linear actuator model to obtain the proper phase and attenuation characteristics. The measured attitude errors and rates were summed in a linear model of the control system to verify that the control system was operating properly. These calculated commands gave excellent agreement with the observed commands (measured actuator currents).

Figure 11-32 indicates that the pitch actuator position is following the command as expected at the beginning of the burn, but that the yaw actuator has a pronounced lag and behaves in a highly non-linear fashion. Figure 11-33 shows that during the peak oscillatory period, both actuators are lagging the predicted position and indicate a slight gain over the command. Following the thrust cutback at 22,138 seconds, the actuators appear to behave in a linear fashion again and exhibit the proper phase and gain relationships with the commands. Analysis of the accelerometer data from the IU (pitch, yaw, and longitudinal) verifies that the actuator position measurements are valid and that the waveforms are not due to a faulty measurement. The apparent longitudinal oscillation seen in the IU longitudinal accelerometer is due to the measurement being offset from the center of gravity and sensing a component of angular acceleration.

Flight data indicated that a bias in the magnetic amplifier resulted in a small positive actuator position at the beginning of the burn which was balanced by the negative thrust misalignment observed in first and second burns. Figures 11-32 and 11-33 show the bias removed to agree with the attitude error signals telemetered in the LVDC guidance data. The amplifier offset, however, is within the specification and is not considered a deviation. It only becomes apparent due to the expanded scales shown in the plots which show 3 percent of the full range of the actuator movement.

After approximately 160 seconds of S-IVB burn the pitch attitude error began to move in a positive direction. This drift in attitude error can be attributed to an actuator bias of 0.3 degree which was present after cutoff. After cutoff the actuator position slowly drifted toward zero. The source of the pitch bias is unknown; however, the trend of the actuator after cutoff is indicative of the presence of an abnormal environment during burn.

During the first 100 seconds of S-IVB third burn, the roll plane dynamics oscillated at 0.6 hertz due to the pitch and yaw oscillations. Following the thrust decrease, abnormally high roll torques were experienced. Following the LH<sub>2</sub> bleed opening, the roll torque reached a maximum of 386 N-m (285 lbf-ft). A time history plot of the roll torque is shown in Figure 11-34. The largest roll torque previously experienced was 54 N-m (40 lbf-ft).

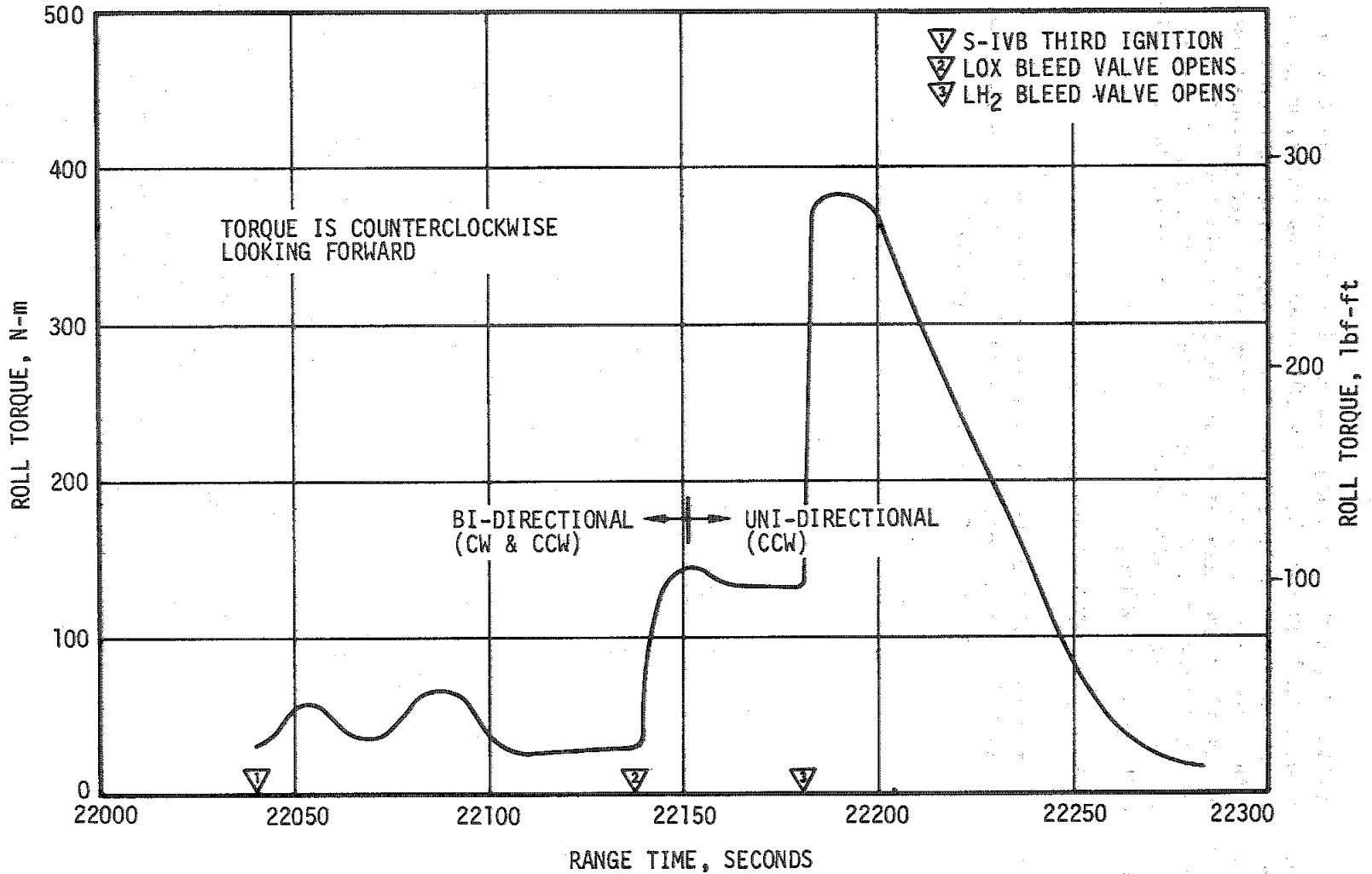


Figure 11-34. S-IVB Roll Torque - Third Burn

LOX and LH<sub>2</sub> slosh frequencies and amplitudes at the probe during third burn are presented in Figure 11-35. The LOX slosh does not damp out as in second burn but appears to have coupled with and driven the control system until the first thrust decrease. After the thrust decrease the control system oscillations decreased but the LOX continued to slosh at 0.6 hertz. The LOX slosh height was approximately twice the amplitude seen on AS-503 and increased with burn time. LH<sub>2</sub> sloshing during third burn was driven by LOX sloshing.

#### 11.6 INSTRUMENT UNIT CONTROL COMPONENTS EVALUATION

The overall performance of the control system was as expected. The problem associated with the telemetering of the real time guidance data had no effect on the on-board guidance and control systems.

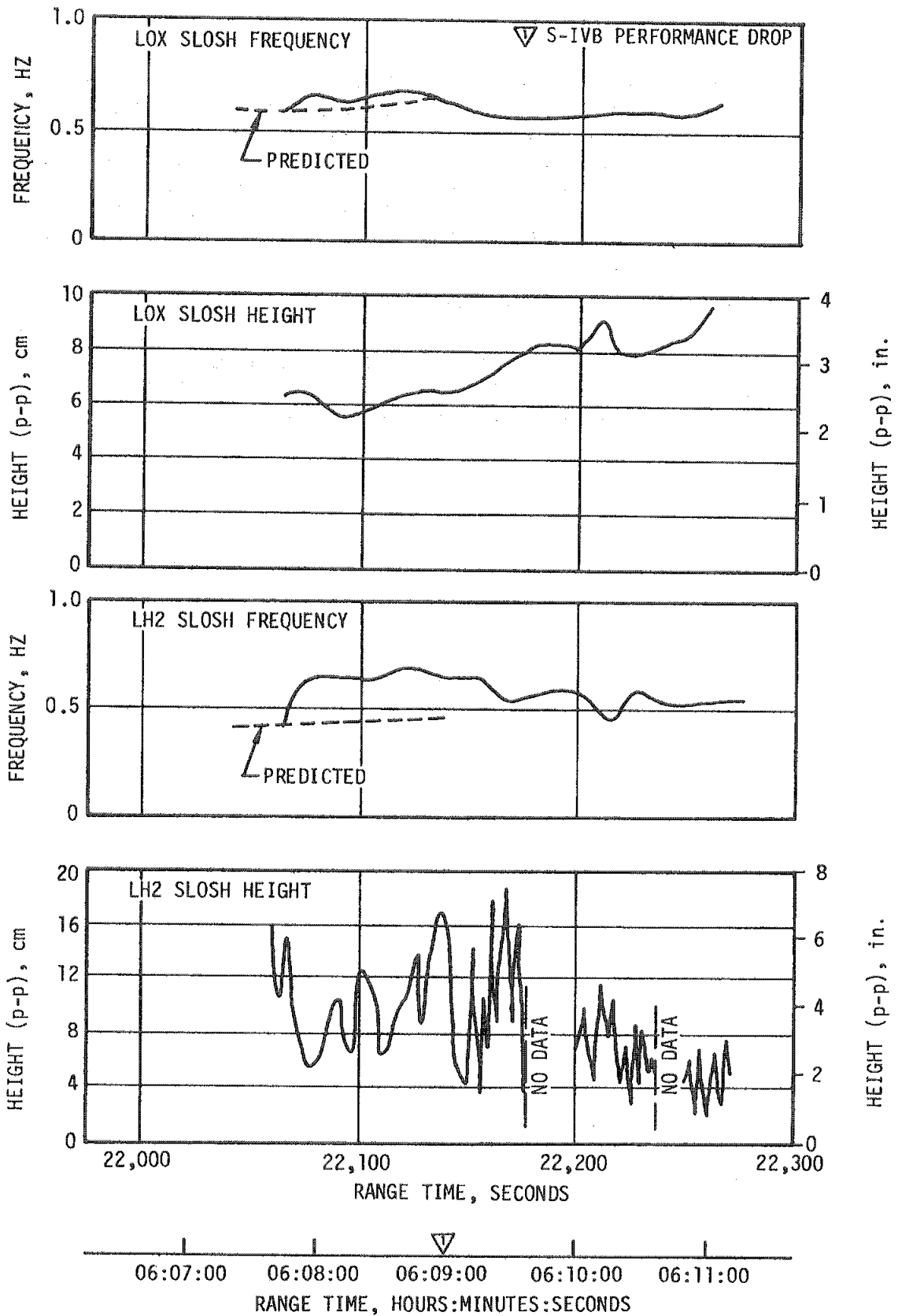


Figure 11-35. S-IVB Slosh Frequencies and Heights During Third Burn

## SECTION 12

### SEPARATION

#### 12.1 SUMMARY

The AS-504 retro motor performance was satisfactory. The clearances during first plane separation were adequate. The S-II ullage motors performed as expected and maintained propellant seating.

During the S-IC/S-II first plane separation, the Command Module (CM) longitudinal accelerometer recorded an oscillating acceleration reaching  $-0.8$  g. The Instrument Unit (IU) accelerometer showed oscillations of the same frequency, 5.2 hertz, but of about half the amplitude. The astronauts reported indications of a steady-state deceleration, but the longitudinal measurements do not support this. The separation subsystem performed nominally and did not contribute to these oscillations. They were apparently a result of the dynamics of the Saturn V vehicle.

Second plane separation was satisfactory. There was no instrumented coverage of the event for reducing the actual interstage motion.

The S-II retro motors and S-IVB ullage motors performed as expected, providing for satisfactory S-II/S-IVB staging. There was no chamber pressure data for these motors on this flight.

Command and Service Module (CSM) separation from the launch vehicle occurred as predicted during parking orbit. Transposition, Docking, and Ejection (TD&E) occurred with adequate attitude control of the launch vehicle. The presence of the Lunar Module (LM) on this flight did not create any difficulties.

#### 12.2 S-IC/S-II SEPARATION EVALUATION

##### 12.2.1 S-IC Retro Motor Performance

AS-504 S-IC retro motor performance was satisfactory. Performance of the retro motors located at Fin A, Position I and Fin C, Position IV could not be analyzed since the chamber pressure measurements for these motors were not recorded on the airborne tape recorder. However, telemetry data for these motors were sufficient to indicate that the motors fired.

Telemetry data again indicated high chamber pressure values, which have been determined from previous flights to be erroneous because of the instrumentation used. AS-504 S-IC pressure data was adjusted to correct for the instrumentation inaccuracy. This was accomplished by biasing the pressure values using a characteristic velocity to match the total integrated flowrates to known propellant weights. The average pressures were slightly higher when compared to the nominal Thiokol model specification of  $1114 \text{ N/cm}^2$  (1616 psia) for a  $288^\circ\text{K}$  ( $60^\circ\text{F}$ ) grain temperature.

With the exception of the apparently high chamber pressures, AS-504 S-IC retro motors performed normally and provided a successful S-IC/S-II stage separation.

#### 12.2.2 S-II Ullage Motor Performance

The S-II ullage motors performed as predicted, within the required limits. Chamber pressure data again indicated that motor web burn-through occurred as predicted. Propellant seating was maintained as required.

#### 12.2.3 S-IC/S-II Stage Separation

The AS-504 Apollo 9 astronauts reported that a rough S-IC/S-II stage separation was experienced in that they were thrown forward out of their seats and had to reach for the instrument panel or grasp their armrest for support. Electrical cables were also observed rising from the floor of the spacecraft indicating steady-state "negative g".

All data that has been reviewed for the AS-504 flight indicate that the S-IC/S-II separation sequence was nominal, and that all separation transients measured were comparable to previous flights and within the levels predicted in earlier analyses. Predicted and reconstructed dynamic pressures at separation were  $0.0348 \text{ N/cm}^2$  ( $7.3 \text{ lbf/ft}^2$ ) and  $0.053 \text{ N/cm}^2$  ( $11.1 \text{ lbf/ft}^2$ ), respectively. Table 12-1 presents the significant separation event times for the AS-504 flight and shows good correlation with the predicted event times and those event times measured on the AS-503 flight.

All available longitudinal accelerometer measurements for the AS-504 flight gave no indication of any steady-state "negative g" condition during S-IC/S-II separation. Figure 12-1 shows that during separation the CM was experiencing approximately 5.2 hertz longitudinal oscillation about a mean slightly above the zero g level. This accelerometer data shows a maximum peak amplitude of  $-0.8 \text{ g}$  at 163.6 seconds with damping of the oscillations beginning at approximately that time. It should be noted that the CM negative acceleration peak occurred at a later time than the peak LM response measured, indicating that the

Table 12-1. S-IC/S-II Separation Event Comparison  
AS-503 Versus AS-504

PARAMETER	SOURCE AND SAMPLE PERIOD		TIME OF OCCURRENCE RANGE TIME, SEC		TIME FROM OEEO SEC		PRED SEC
			AS-503	AS-504	AS-503	AS-504	AS-504
S-IC Stop Solenoid Signal (OEEO)	KXXX	0.008 sec	153.793	162.776	0	0	0
S-IC Engine Thrust Decay Reaches 90 Percent	DXXX	0.008 to 0.010 sec	153.927	162.902	0.134	0.126	0.110
S-II Ullage Motor Thrust Buildup Begins (Average)	DXXX	0.010 sec	154.345	163.332	0.552	0.556	0.630
S-IC Separation Command 1	K001-115	0.008 sec	154.472	163.451	0.679	0.675	0.7
S-IC Separation EBW Fire Signal	Ca1c	(To1 ± 0.002 sec)	154.476	163.455	0.683	0.679	0.721
S-IC Retro Motor EBW Fire Signal	Ca1c	(To1 ± 0.002 sec)	154.480	163.459	0.687	0.683	0.725
S-IC Retro Motor Thrust Buildup Begins (Average)	DXXX	0.008 to 0.010 sec	154.495	163.468	0.702	0.692	0.735

maximum LM response was not related to the CM negative longitudinal acceleration transient. Also shown in Figure 12-1 are the CM pitch and yaw measurements which indicate some coupling effect with the longitudinal acceleration and contribute to the total response to the cutoff transient.

The IU low range longitudinal responses measured on the AS-503 and AS-504 flights are presented in Figure 12-2. These curves show low amplitude oscillations about a mean above the zero g level and also indicate that no steady-state "negative g" condition existed during separation. Comparison of the AS-504 IU acceleration curve with the CM responses in Figure 12-1 shows a gain factor of about 2 over the IU responses.

Figure 12-3 shows that the measured dynamic responses for AS-503 and AS-504 correlate closely with the dynamic responses simulated. These post-flight calculated dynamic loads were computed using the predicted mass characteristics of each vehicle and measured flight parameters recorded during flight. Figure 12-4 presents similar data for the AS-501 and AS-502 flights. The AS-501 CM accelerometer curve shows amplitudes of about the same magnitude as measured on the AS-504 flight.

The average F-1 Engine thrust decay curves for AS-501 through AS-504 are presented in Figure 12-5. Also individual engine thrust decay curves are presented for the last 20 percent of the thrust for the AS-503 and AS-504 vehicles. The steeper slope of AS-504 thrust decay apparently achieved a steady-state acceleration closer to the zero g limit at an earlier time than on AS-503. This may allow greater "negative g" to be experienced before damping. During the last portion of the decay, both curves are within the ± 3 sigma limits predicted for each flight.

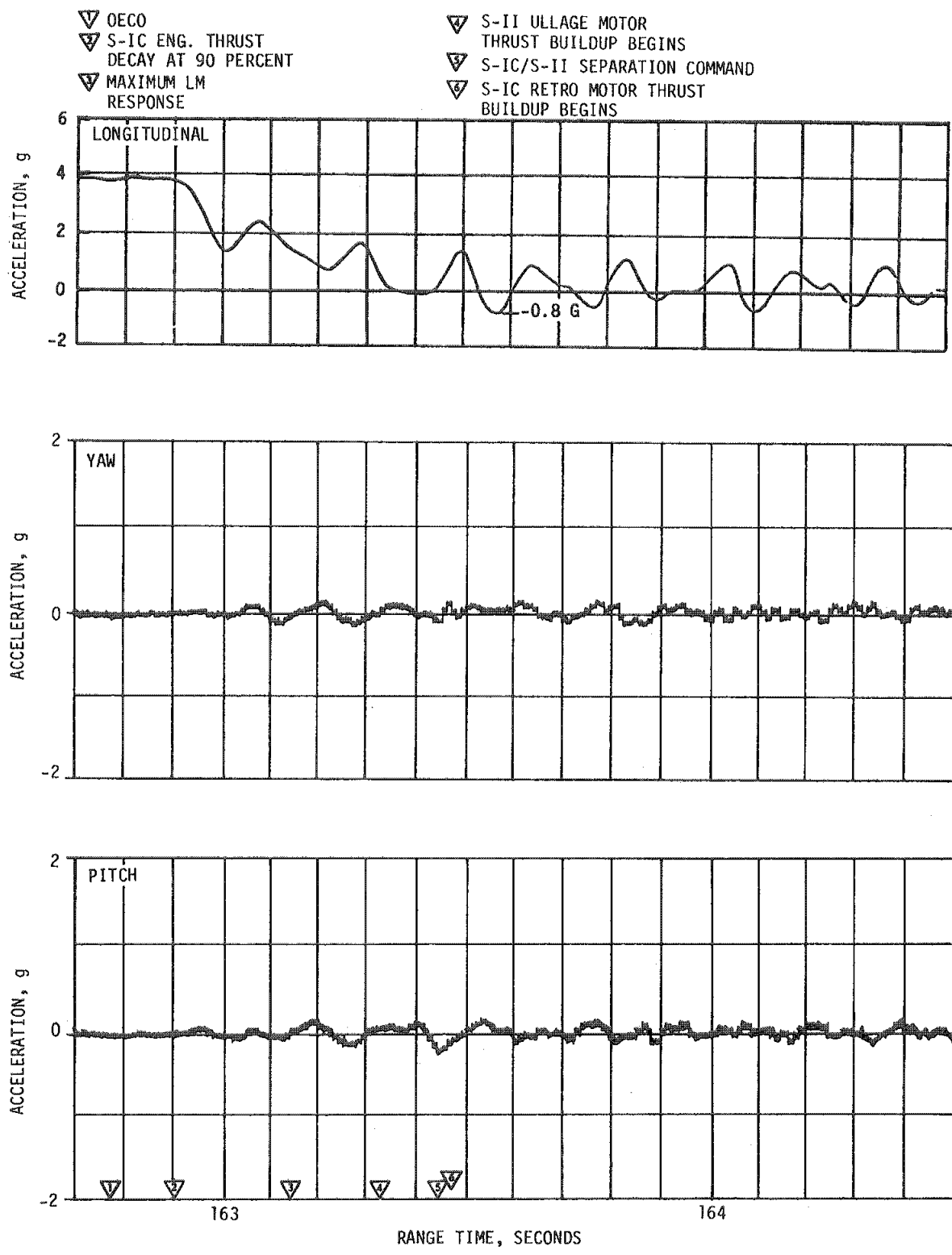


Figure 12-1. AS-504 Command Module Accelerations



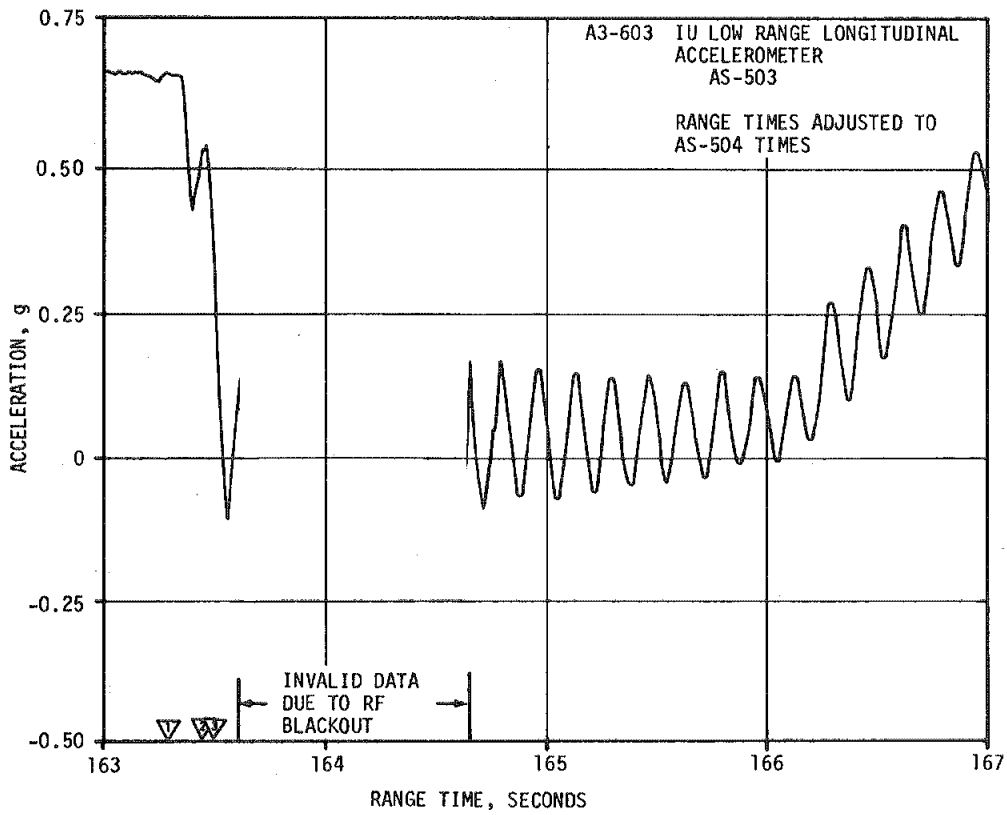
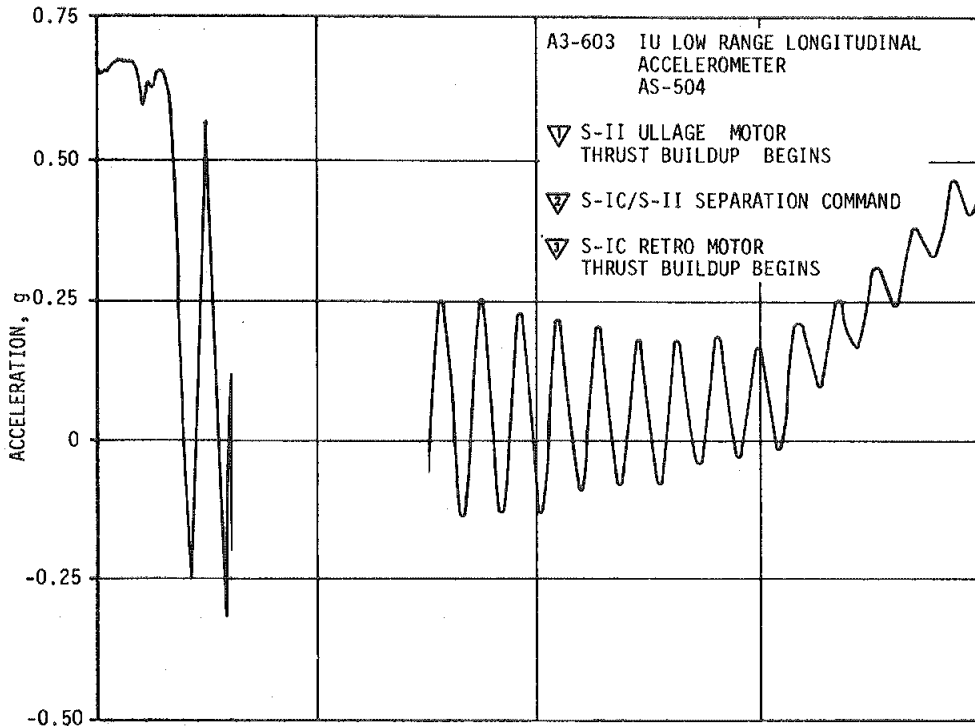


Figure 12-2. Instrument Unit Longitudinal Accelerometer

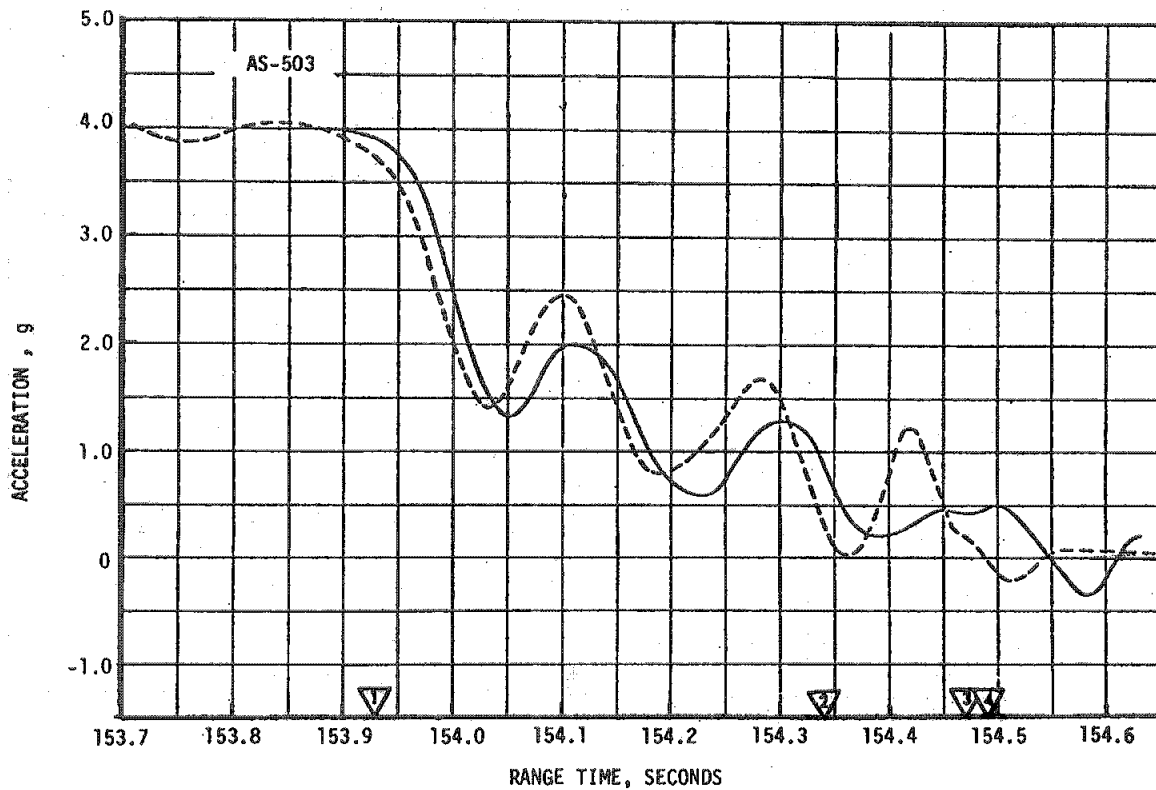
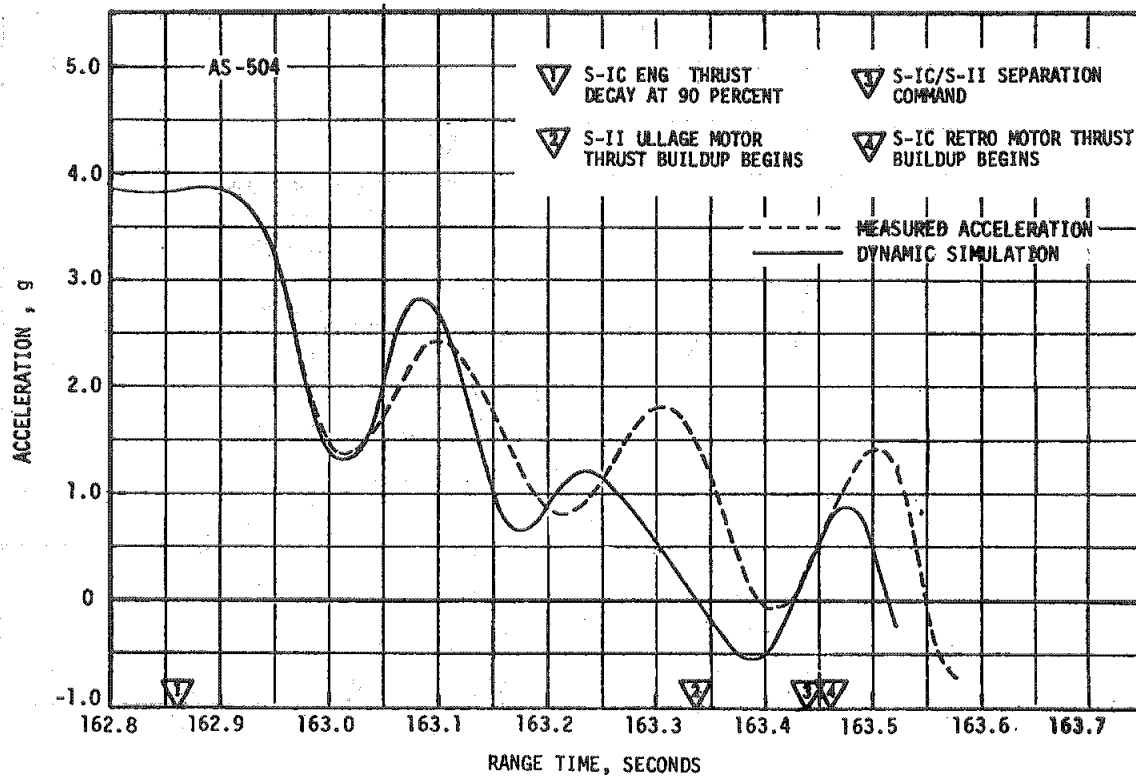


Figure 12-3. Longitudinal Acceleration at Command Module During S-IC Thrust Cutoff (AS-503 & AS-504)

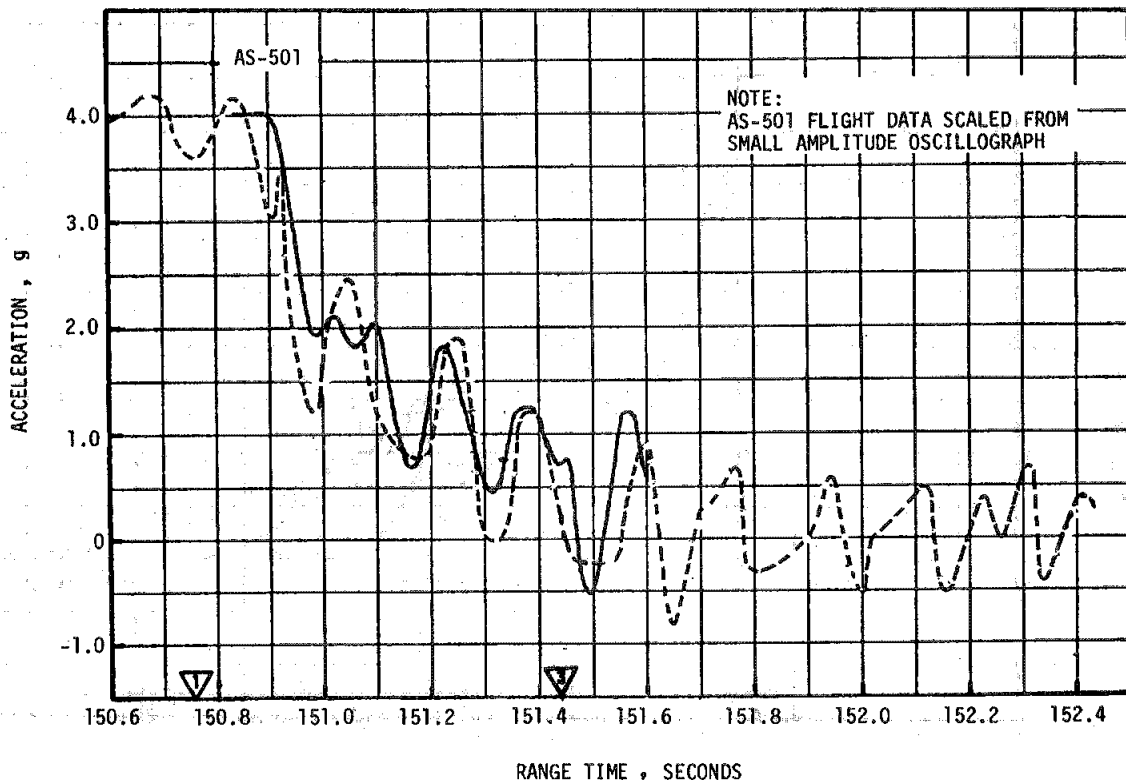
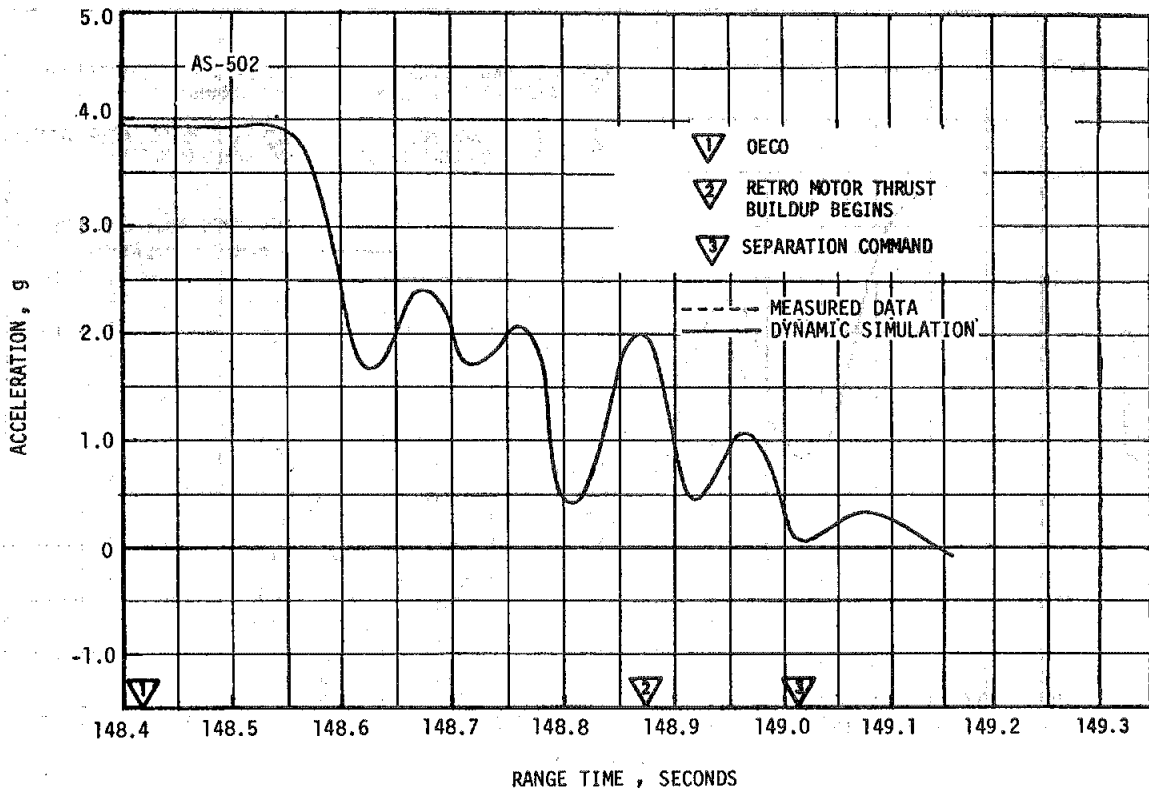


Figure 12-4. Longitudinal Acceleration at Command Module During S-IC/S-II Separation (AS-502 & AS-501)

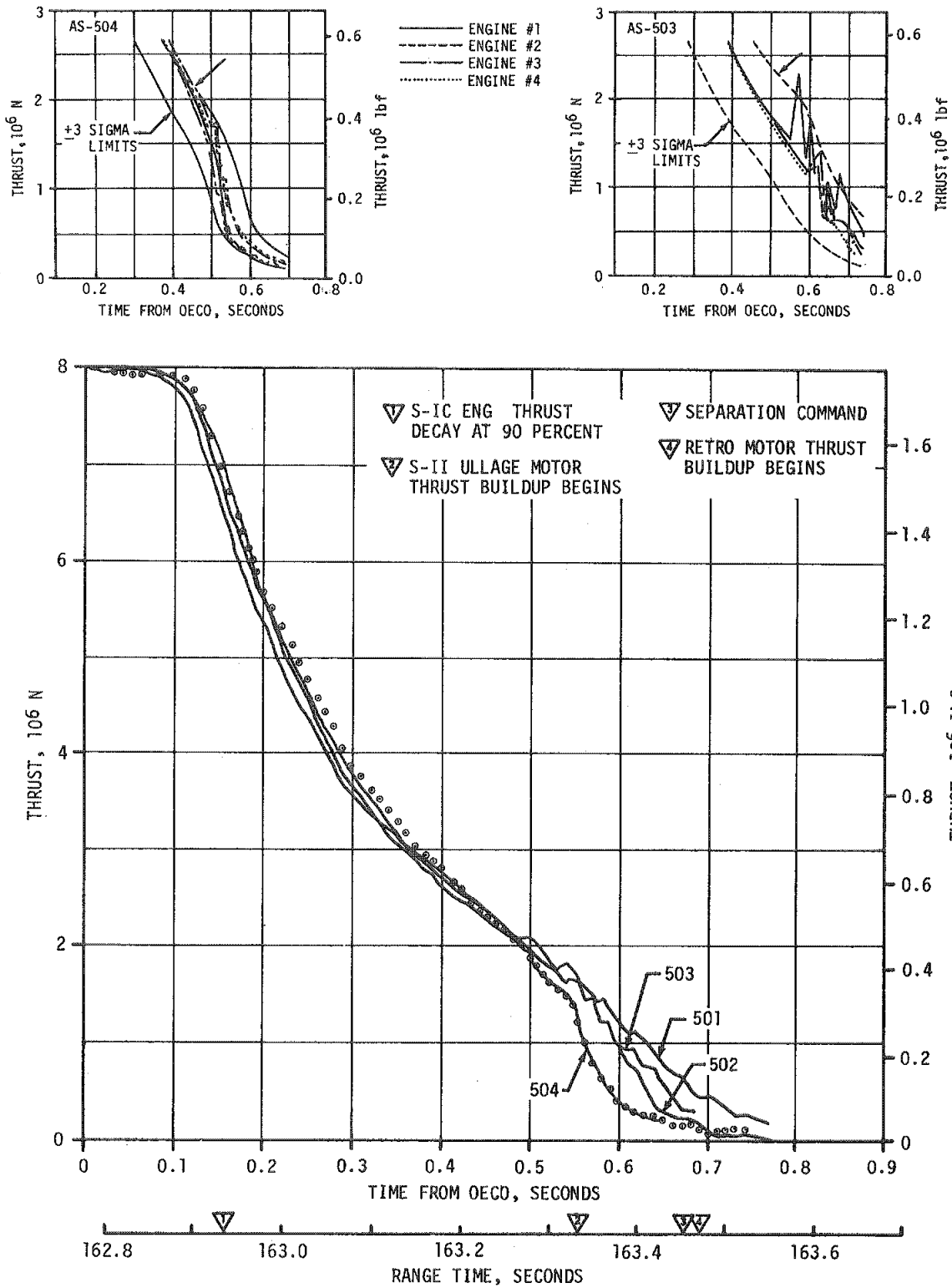


Figure 12-5. Average S-IC OECO Thrust Decay, AS-501 Through AS-504

Figure 12-6 presents a comparison of the AS-503 and AS-504 S-IC intertank longitudinal acceleration measurements which show the separation dynamics to be approximately the same for both vehicles and show no indication of retro fire before S-IC/S-II separation. If the retro motor thrust build-up did start before separation, the slope of the acceleration curve would be less, and if separation had not occurred by 100 percent retro thrust, then the vehicle would only attain approximately -0.4 g.

It appears that these separation transients are a dynamic characteristic of the Saturn V vehicle. Consequently, similar separation dynamics can be anticipated on future Saturn V flights.

### 12.3 S-II SECOND PLANE SEPARATION EVALUATION

S-II second plane separation was apparently nominal, as indicated by the lack of disturbance to the S-II during separation. The simulation calculation indicated a minimum clearance of 1.0 meter (39 in.), between the interstage and engine No. 2.

### 12.4 S-II/S-IVB SEPARATION EVALUATION

#### 12.4.1 S-II Retro Motor Performance

The four retro motors mounted on the S-II stage performed satisfactorily and separated the S-II stage from the S-IVB stage. No instrumentation existed to measure the chamber pressure of the retro motors.

#### 12.4.2 S-IVB Ullage Motor Performance

The ullage motors performed satisfactorily during S-II/S-IVB staging, maintaining propellant seating. They were then properly jettisoned, on command. No instrumentation existed to measure the chamber pressure of the ullage motors.

#### 12.4.3 S-II/S-IVB Separation Dynamics

The analysis of separation dynamics was done by comparing the data from the AS-504 flight to that of AS-503 and AS-501. Since the data compared very closely, detailed reconstruction was not performed to determine precisely the lateral clearance used and the separation completion time. From the comparative analysis performed it can be estimated that a detailed reconstruction would yield a separation completion time of approximately 1.0 second and a lateral clearance utilization of less than 12.7 centimeters (5 in.). The S-II stage showed a low tailoff thrust level and a light stage weight. The S-IVB angular rates were all small with pitch and yaw rates less than  $\pm 0.2$  deg/s. The S-II angular rates reached 1.5 and 2.2 deg/s in pitch and yaw, respectively, by the end of separation.

## 12.5 S-IVB/IU/LM/CSM SEPARATION EVALUATION

The separation of the CSM from the launch vehicle was as expected. The Spacecraft LM Adapter (SLA) panels separated satisfactorily from the launch vehicle. There were no large control disturbances due to the separation. The available CSM data were not of a high enough sample rate to provide useful analysis.

## 12.6 LUNAR MODULE EJECTION EVALUATION

The LM was satisfactorily ejected from the launch vehicle after the docking maneuver was completed. There were no significant control disturbances during the ejection. The available CSM data were not of high enough sample rate to provide useful analysis.

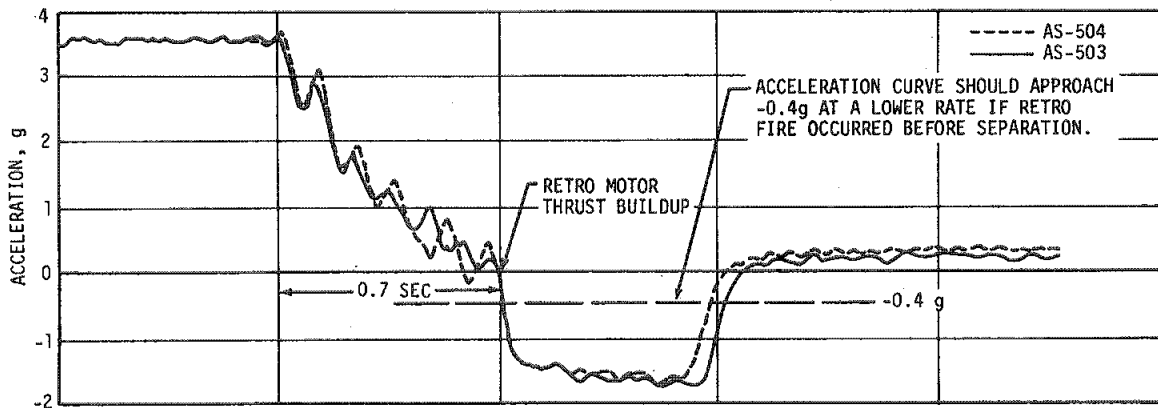


Figure 12-6. AS-504 and AS-503 S-IC Intertank - Longitudinal Acceleration

## SECTION 13

### ELECTRICAL NETWORKS

#### 13.1 SUMMARY

The launch vehicle electrical networks are comprised of independently battery-powered electrical systems for the four stages with inter-connecting cabling to satisfy stage-to-stage electrical interface requirements. Each stage electrical system distributes power to continuous users such as instrumentation and communications, and responds to commands initiated either by the stage or the Instrument Unit (IU) through the stage switch selector.

In general, all AS-504 launch vehicle electrical systems performed satisfactorily. The only deviation noted during the flight was the apparent failure of the S-IVB forward battery heater.

#### 13.2 S-IC STAGE ELECTRICAL SYSTEM

The S-IC stage electrical power is obtained from two 28-vdc batteries and is distributed to stage components through the power distribution system. Battery No. 1 (1D10) furnishes operational power and battery No. 2 (1D20) instrumentation power. Batteries No. 3, 4 and 5, which furnished power to the optical instrumentation system on AS-502 and AS-503 were deleted on AS-504 along with the optical system.

The electrical system performance during S-IC powered flight was excellent. Both battery voltages remained well within the design limits of 26.5 to 32 vdc and currents stayed below 39 percent of the 64 ampere limit for battery No. 1 and below 60 percent of the 125 ampere limit for battery No. 2, as shown in Figures 13-1 and 13-2, respectively. (See Section 2 for Event Times reference.)

Batteries No. 1 and No. 2 power consumptions were only slightly less than expected, as shown in Table 13-1. The batteries were not instrumented to measure temperatures.

Seven 5-vdc power supplies provide closely regulated voltages for stage instrumentation. These power supplies stayed within the required limits of  $5 \pm 0.05$  vdc during flight. No power supply voltage drops were experienced as on AS-502 flight. Recirculation inverter operation was nominal.

There were 18 switch selector functions programmed for the S-IC stage. All switch selector channels functioned correctly as commanded by the IU.

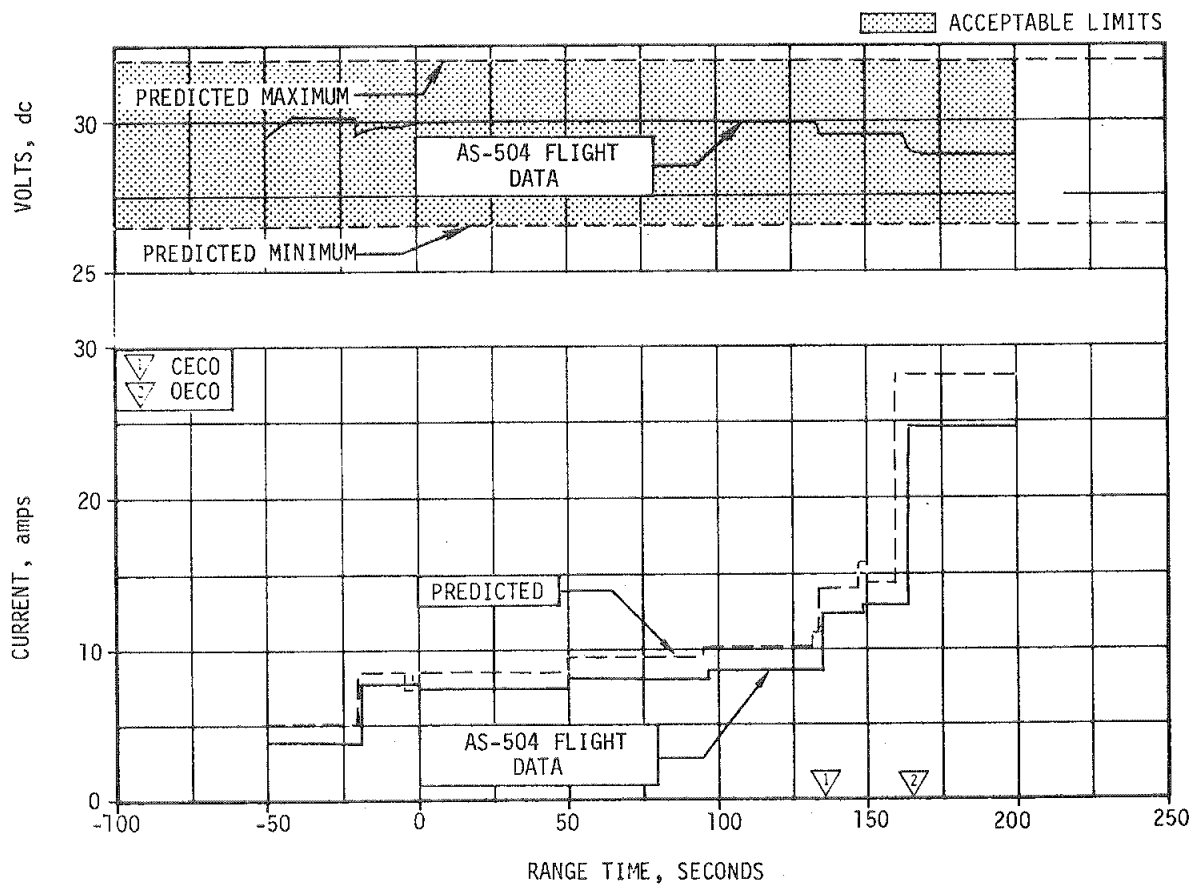


Figure 13-1. S-IC Stage Battery No. 1 Voltage and Current, Bus 1D10

The separation and retro motor Exploding Bridge Wire (EBW) were armed and triggered, as programmed. Charging times and voltages were within the requirements of 1.5 second for the maximum allowable charging time and  $4.2 \pm 0.4$  volts for the minimum allowable voltage level at the voltage monitor measurements.



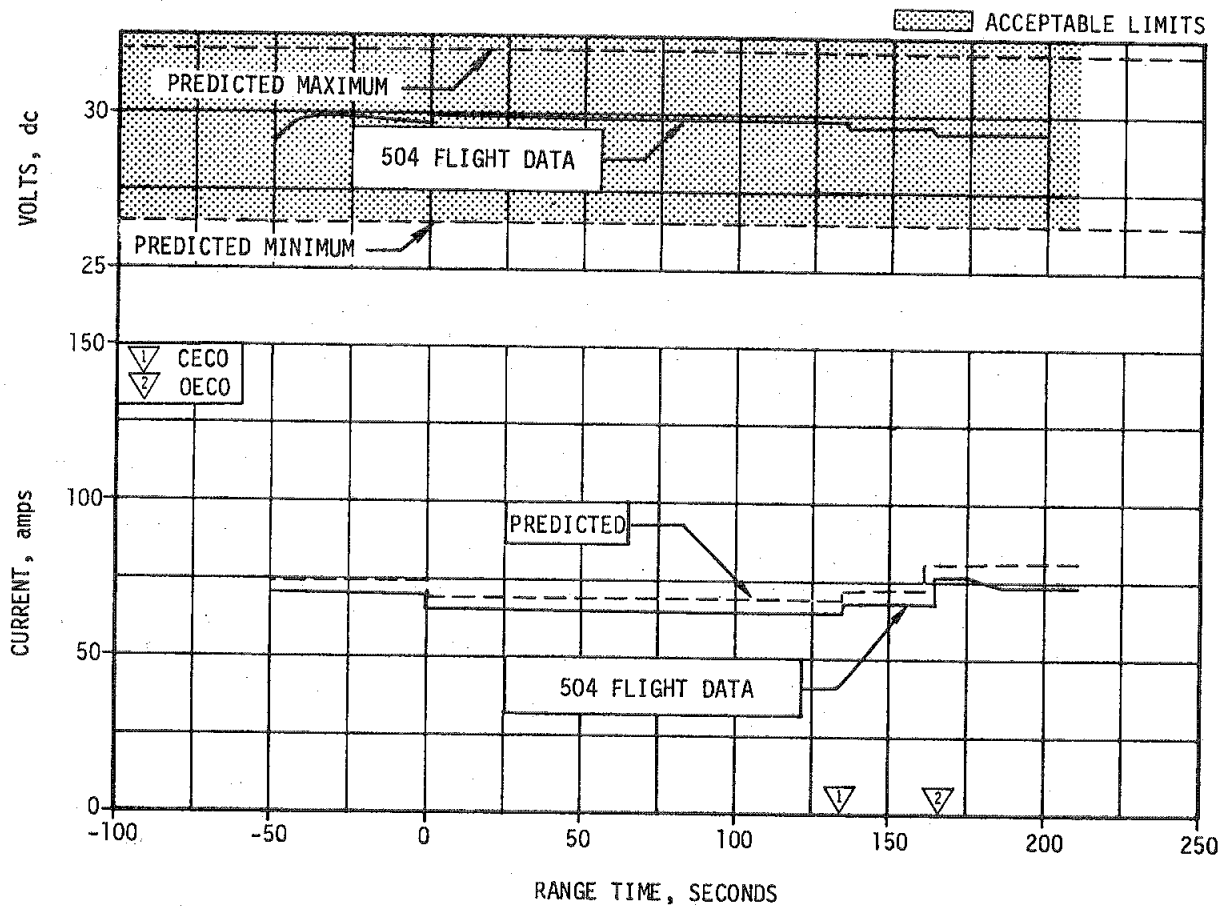


Figure 13-2. S-IC Stage Battery No. 2 Voltage and Current, Bus 1D20

Table 13-1. S-IC Stage Battery Power Consumption

BATTERY	BUS DESIGNATION	CAPACITY AMP-MIN	POWER CONSUMPTION AMP-MIN		PERCENT OF CAPACITY
			MAX EXPECTED	ACTUAL	
Operational No. 1	1D10	640	32.7	28.9	4.5
Instrumentation No. 2	1D20	1250	321.0	294.4	23.5

NOTE: Battery capacities are based on 10 minute discharge time.

### 13.3 S-II STAGE ELECTRICAL SYSTEM

The S-II stage electrical system utilizes four 28-vdc batteries, the output of which is distributed to stage components through the power distribution system. Two of these batteries are connected in series to furnish 56 vdc to the five LH2 recirculation pump inverters.

The electrical portion of the S-II separation system installed on the AS-504 vehicle differed from AS-503 in that the all engine cutoff relay circuitry, which is controlled by switch selector channel 18, was powered by both the main and instrumentation dc power buses, in contrast to AS-503 which was powered only by the main dc power bus. This dual bus capability would have permitted the AS-504 flight to switch to an alternate flight sequence time for Time Base 4, alternate (T4a) for early S-II/S-IVB staging, if the need arose due to the loss of the main battery.

The S-II electrical system performed satisfactorily during all phases of the AS-504 flight. Battery bus voltages remained well within specified limits throughout the flight, as shown in Figures 13-3 through 13-6. (See Section 2, Table 2-2 and Table 2-3 for Event Times reference.) Main bus current averaged 35 amperes during S-IC boost, and varied from 50 to 52.5 amperes during S-II boost. Instrumentation bus current varied from 54 to 57 amperes during S-IC and S-II boost. Recirculation bus current averaged 92 amperes during S-IC boost. Ignition bus current averaged 27.5 amperes during the S-II ignition sequence.

Battery power consumption in ampere-hours and as a percent of rated capacity, and battery temperatures, are shown in Table 13-2. Power consumptions and temperatures were very close to those seen on AS-503.

Five 5-vdc power supplies furnish closely regulated voltages for stage instrumentation. These power supplies provided proper measuring voltage to the telemetry and other instrumentation.

There was no evidence of intermittent operation of any of the temperature bridge power supplies, such as that experienced on AS-503 flight.

The five LH2 recirculation inverters which furnish power to the recirculation pumps operated properly during the J-2 engine chilldown period.

Performance of the EBW circuitry for the separation system was satisfactory. Firing units charge and discharge responses were within predicted time and voltage limits.

### 13.4 S-IVB STAGE ELECTRICAL SYSTEM

The S-IVB stage electrical system contains three 28-vdc batteries and one 56-vdc battery which supply the stage systems and components through the power distribution system.

- ▽ S-IC/S-II SEPARATION COMMAND
- ▽ S-II ENGINE IGNITION
- ▽ S-II ECO

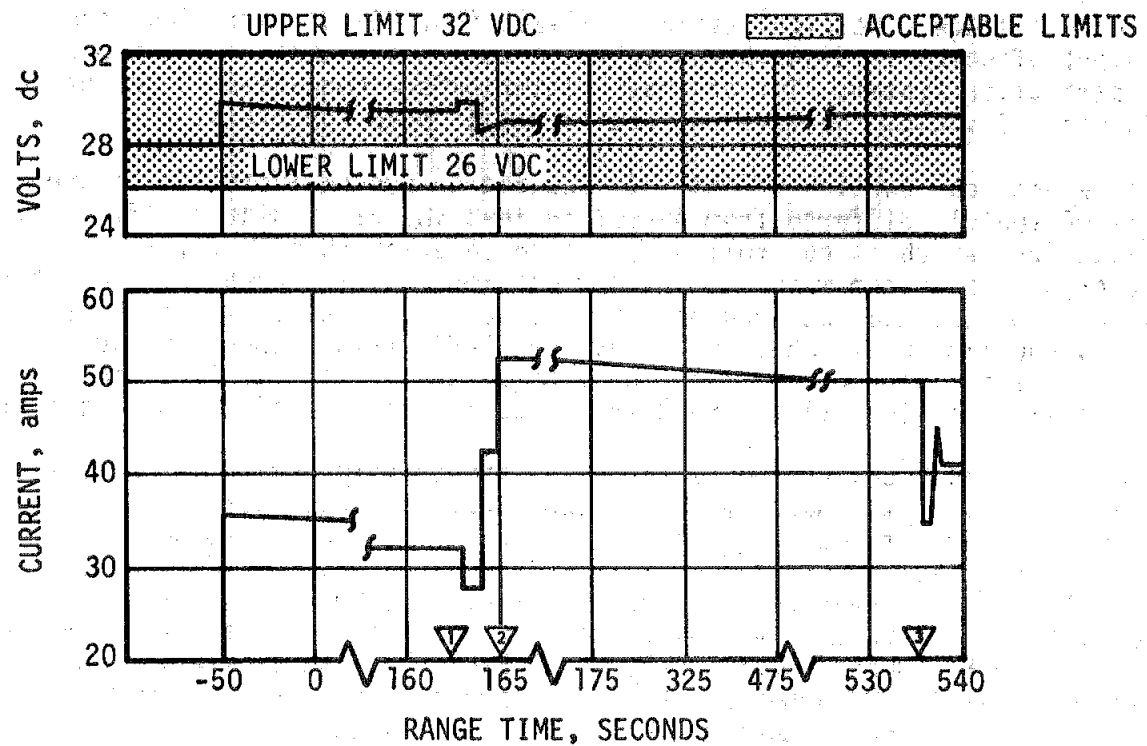


Figure 13-3. S-II Stage Main DC Bus Voltage and Current

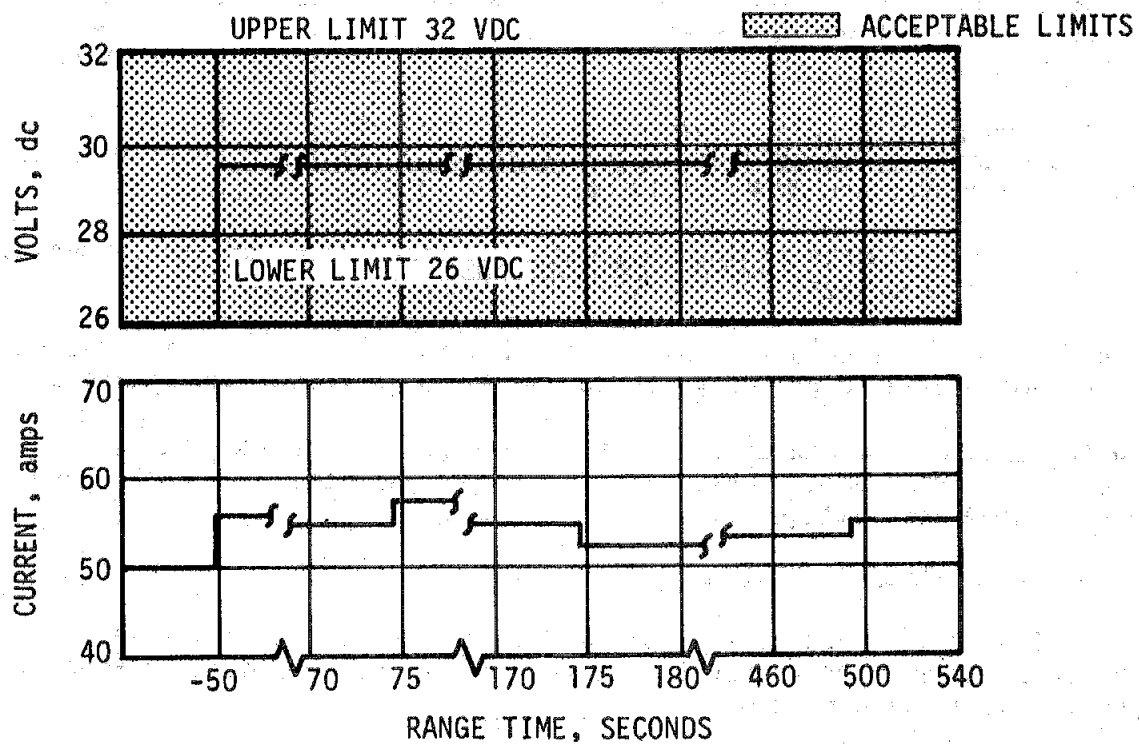


Figure 13-4. S-II Stage Instrumentation Bus Voltage and Current

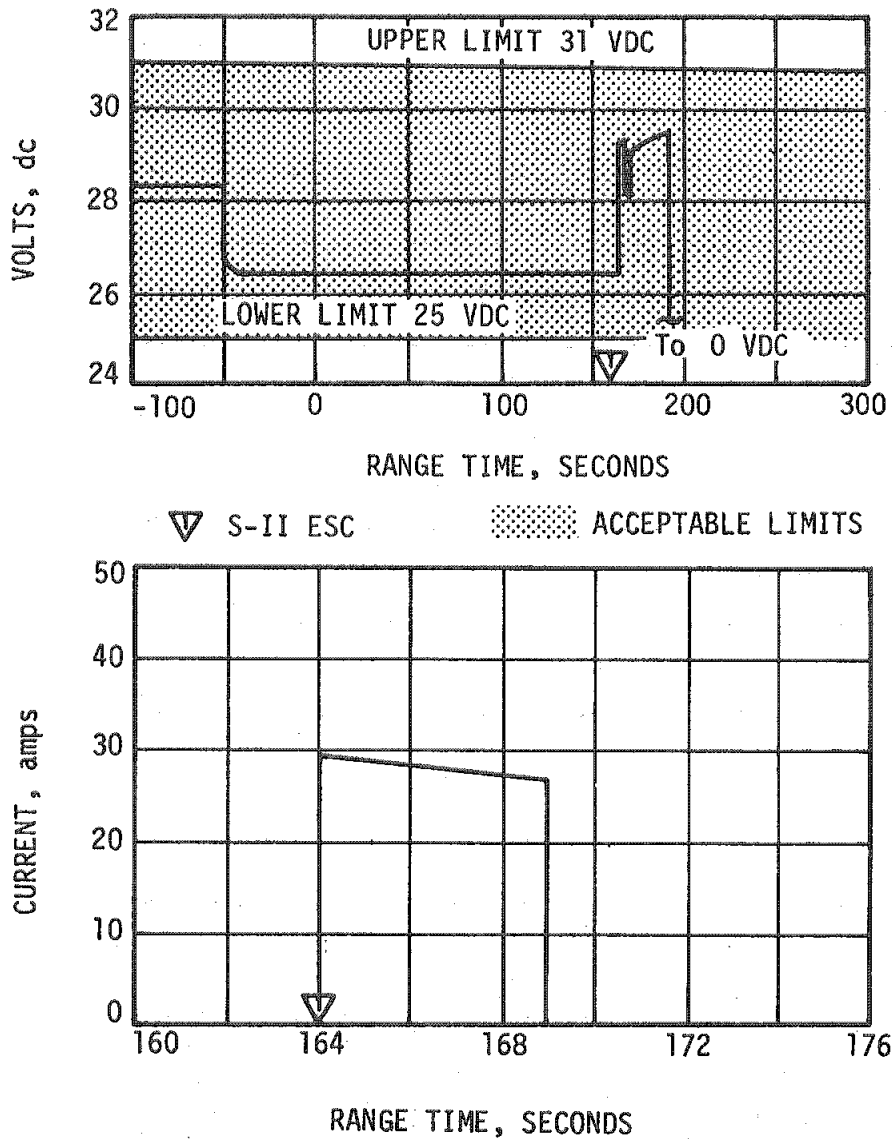


Figure 13-5. S-II Stage Ignition DC Bus Voltage and Current

The electrical system performed satisfactorily throughout all phases of flight and responded normally to IU commands. Battery voltages and currents stayed well within acceptable limits during boost and restart as shown in Figures 13-7 through 13-10. Battery temperatures remained below the 322°K (120°F) limit for the powered portion of the flight (does not apply after insertion into orbit). The highest temperature of 317°K (112°F) was reached on aft battery No. 2 during passivation after auxiliary hydraulic pump turn off as shown in Figure 13-10.

▽ S-II LH<sub>2</sub> RECIRC.  
PUMPS OFF      ACCEPTABLE LIMITS

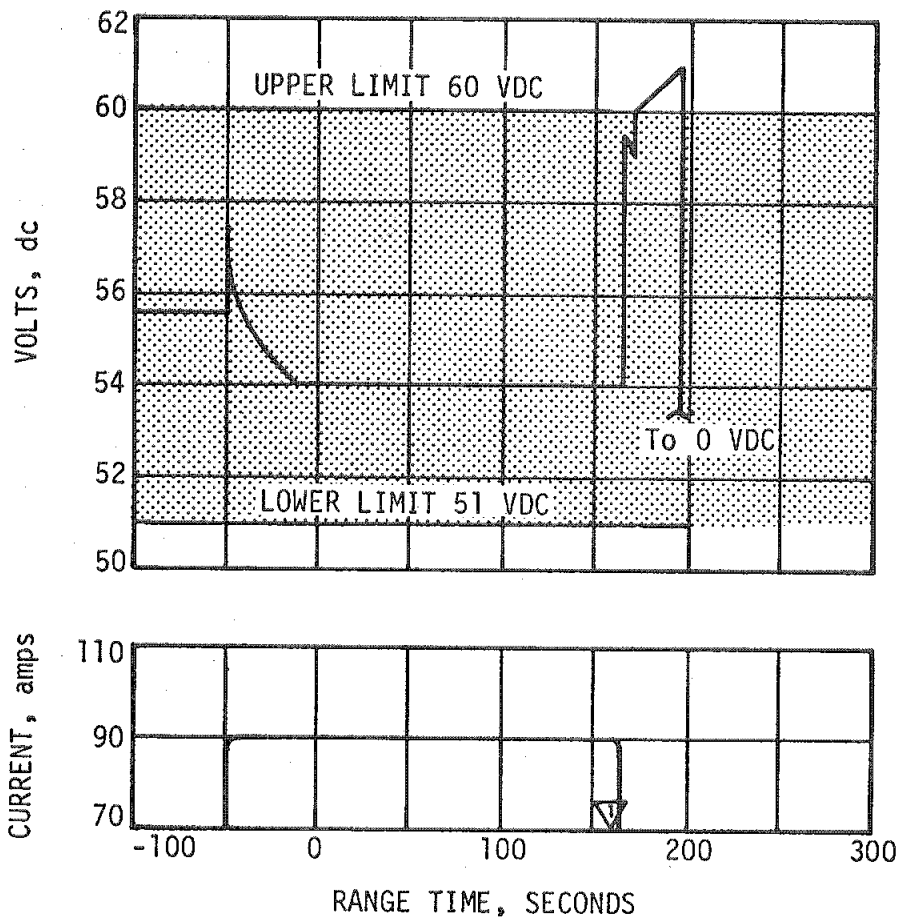
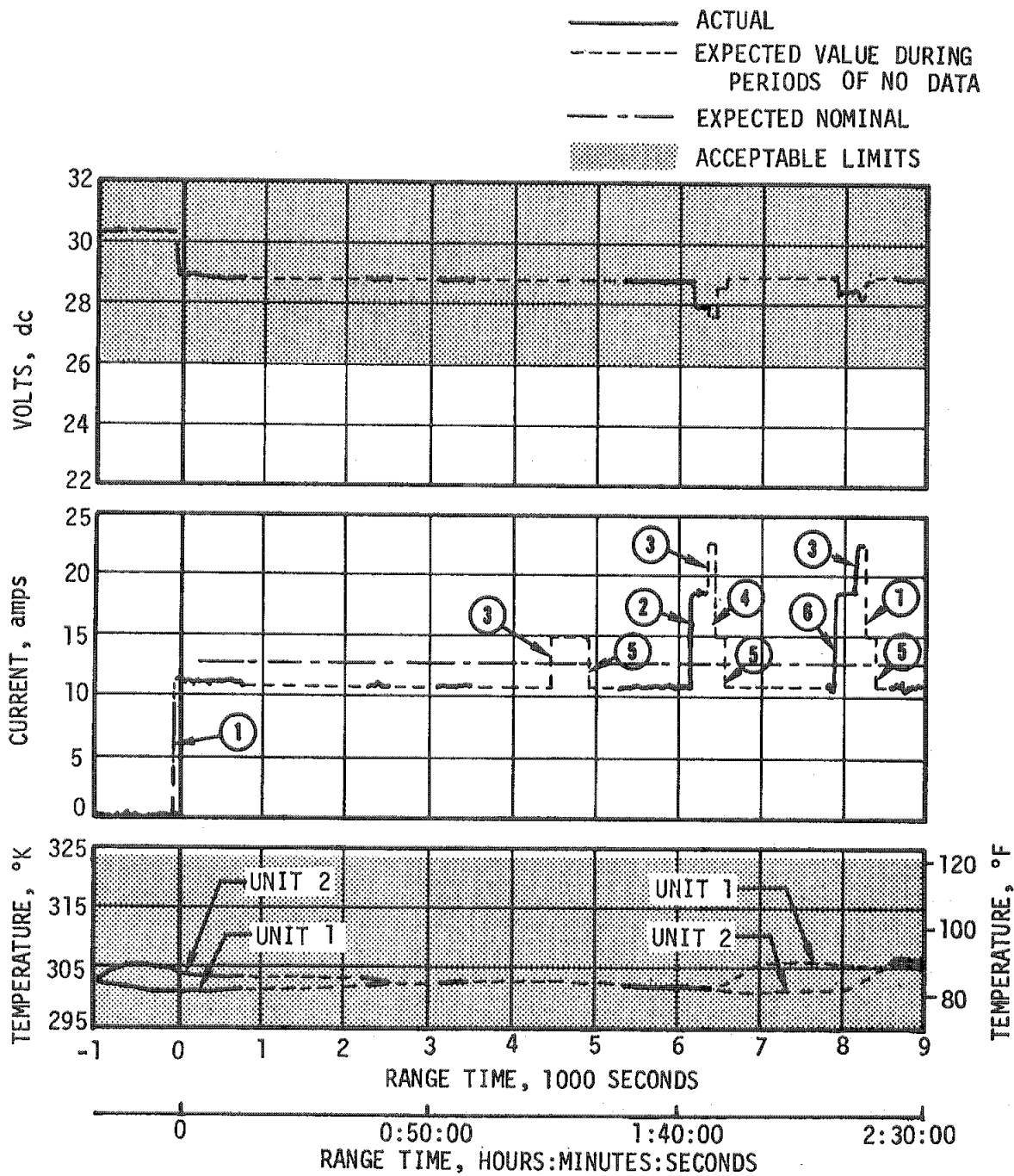


Figure 13-6. S-II Stage Recirculation DC Voltage and Current

Table 13-2. S-II Stage Battery Power Consumption

BATTERY	BUS DESIGNATION	CAPACITY (AMP-HR)	* POWER CONSUMPTION		TEMPERATURE	
			AMP-HR* (sec)	PERCENT OF CAPACITY	MAX	MIN
Main	2D11	35	7.51	21.4	308.2°K (95°F)	302.6°K (85°F)
Instrumentation	2D21	35	11.9	34.0	309.8°K (98°F)	302.6°K (85°F)
Recirculation No. 1	2D51	30	5.44	18.1	304.3°K (88°F)	301.2°K (82.5°F)
Recirculation No. 2	2D51 and 2D61	30	5.48	18.3	305.4°K (90°F)	302.6°K (85°F)

\*Power consumption calculated from -50 seconds.



- |                             |                             |
|-----------------------------|-----------------------------|
| ① TRANSFER TO INTERNAL      | ⑤ FWD BATT 2 HTR OFF        |
| ② FWD BATT 1 UNIT 1 HTR ON  | ⑥ FWD BATT 1 UNIT 2 HTR ON  |
| ③ FWD BATT 2 HTR ON         | ⑦ FWD BATT 1 UNIT 2 HTR OFF |
| ④ FWD BATT 1 UNIT 1 HTR OFF |                             |

Figure 13-7. S-IVB Stage Forward Battery No. 1 Voltage, Current and Temperature (Sheet 1 of 3)

- ① FWD BATT 2 HTR CYCLE
  - ② FWD BATT 1 UNIT 1 CYCLE
  - ③ FWD BATT 1 UNIT 2 CYCLE
- ACTUAL
  - - - - - EXPECTED VALUE DURING PERIODS OF NO DATA
  - · - · - · EXPECTED NOMINAL

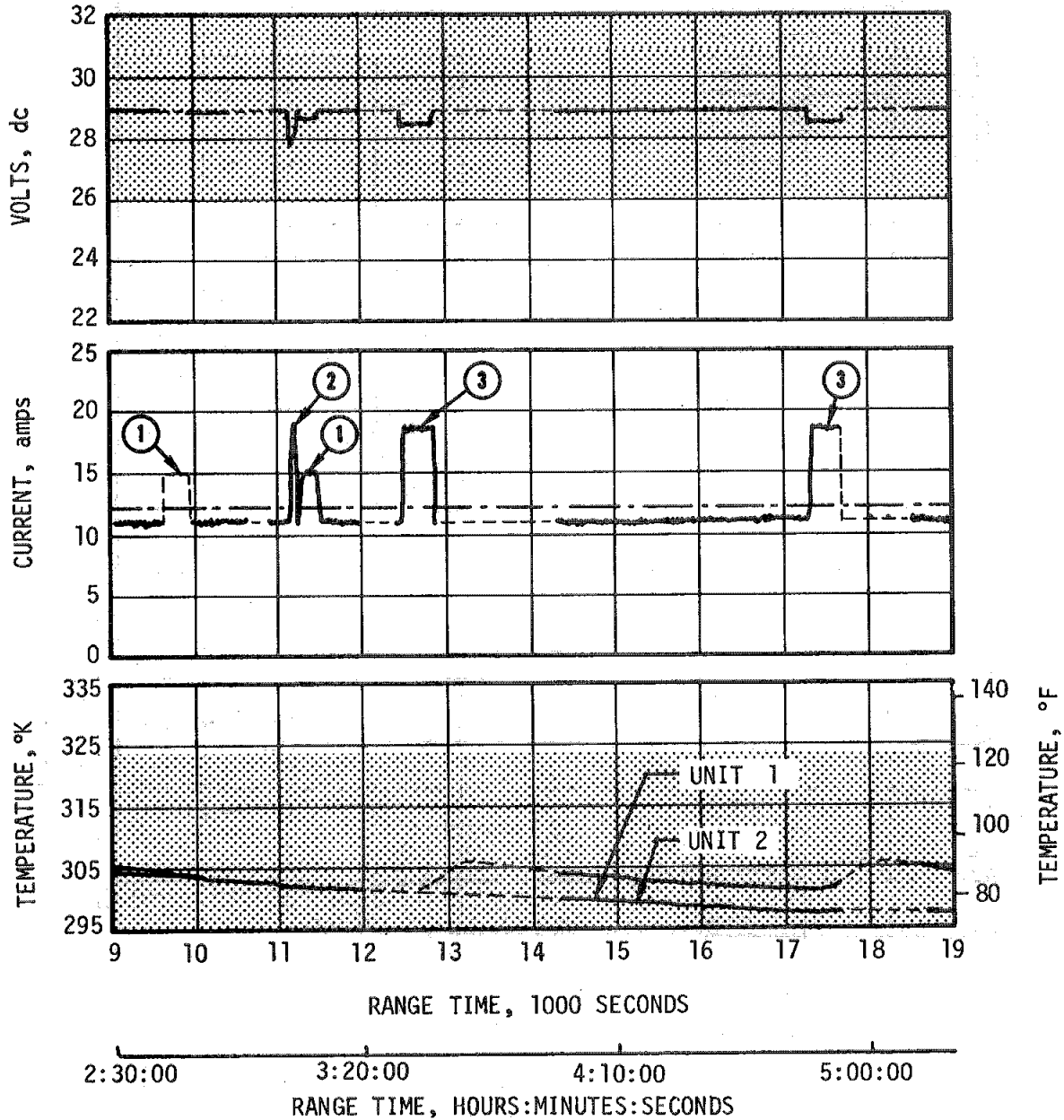


Figure 13-7. S-IVB Stage Forward Battery No. 1 Voltage, Current and Temperature (Sheet 2 of 3)

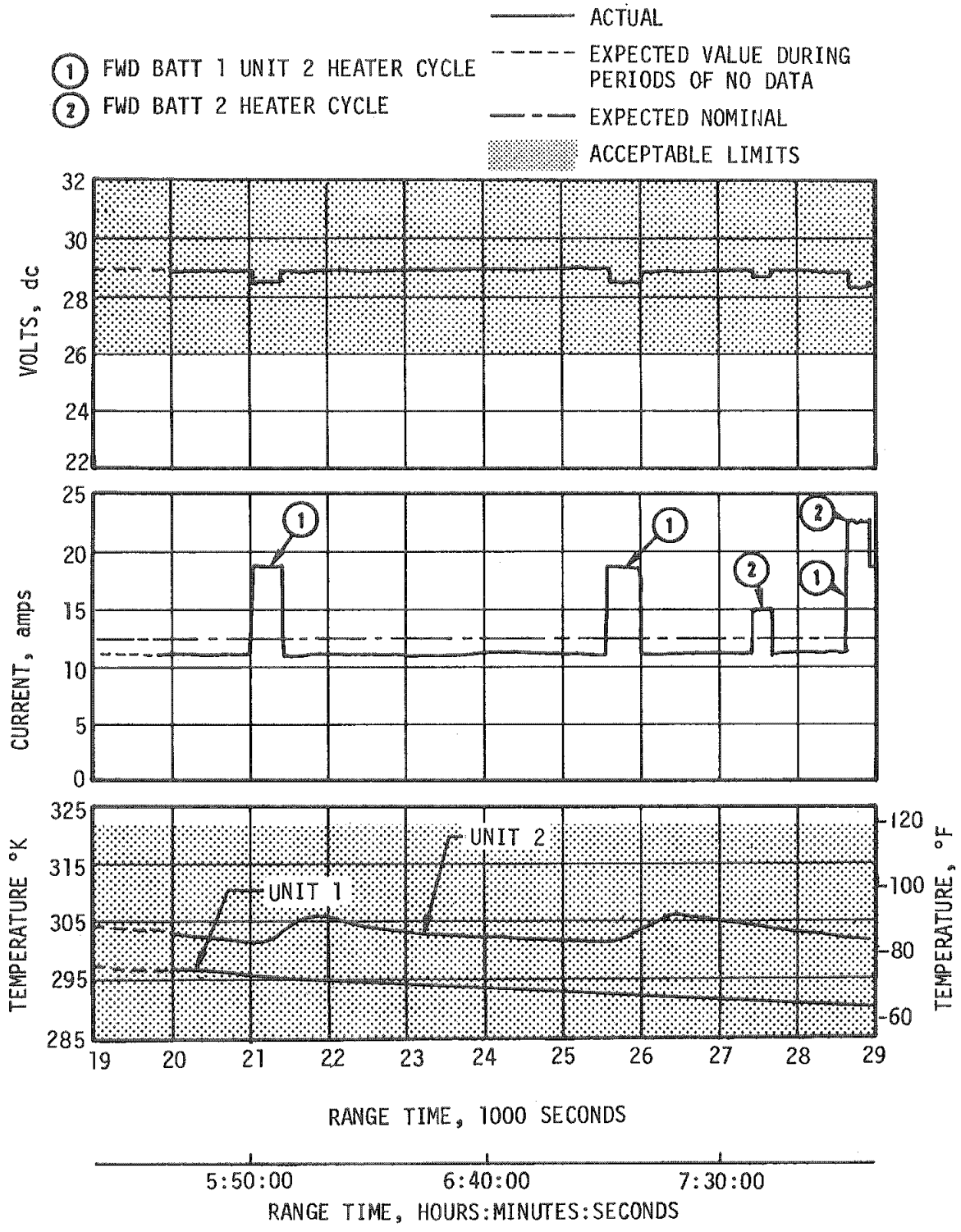


Figure 13-7. S-IVB Stage Forward Battery No. 1 Voltage, Current and Temperature (Sheet 3 of 3)



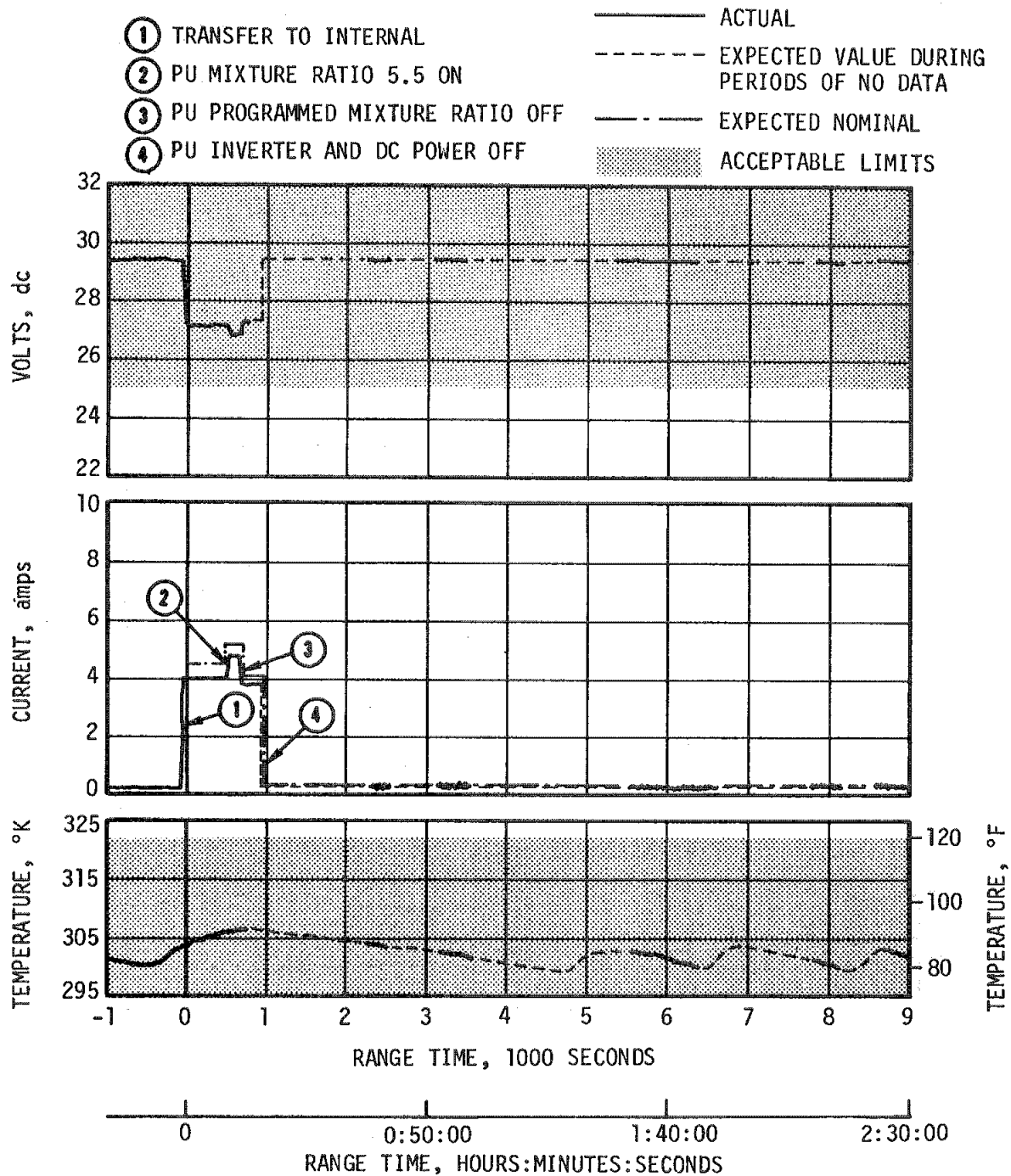


Figure 13-8. S-IVB Stage Forward Battery No. 2 Voltage, Current and Temperature (Sheet 1 of 3)

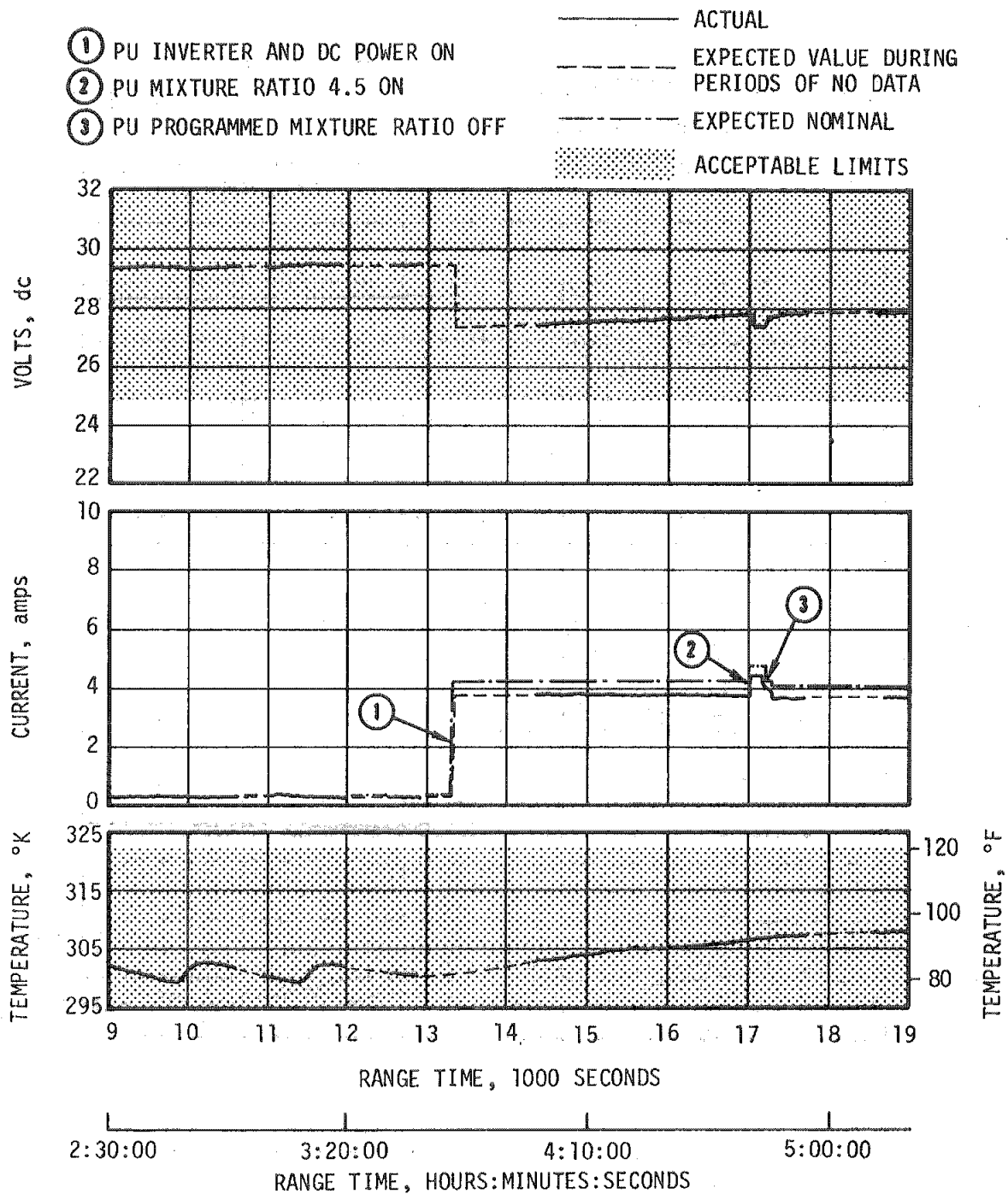


Figure 13-8. S-IVB Stage Forward Battery No. 2 Voltage, Current and Temperature (Sheet 2 of 3)

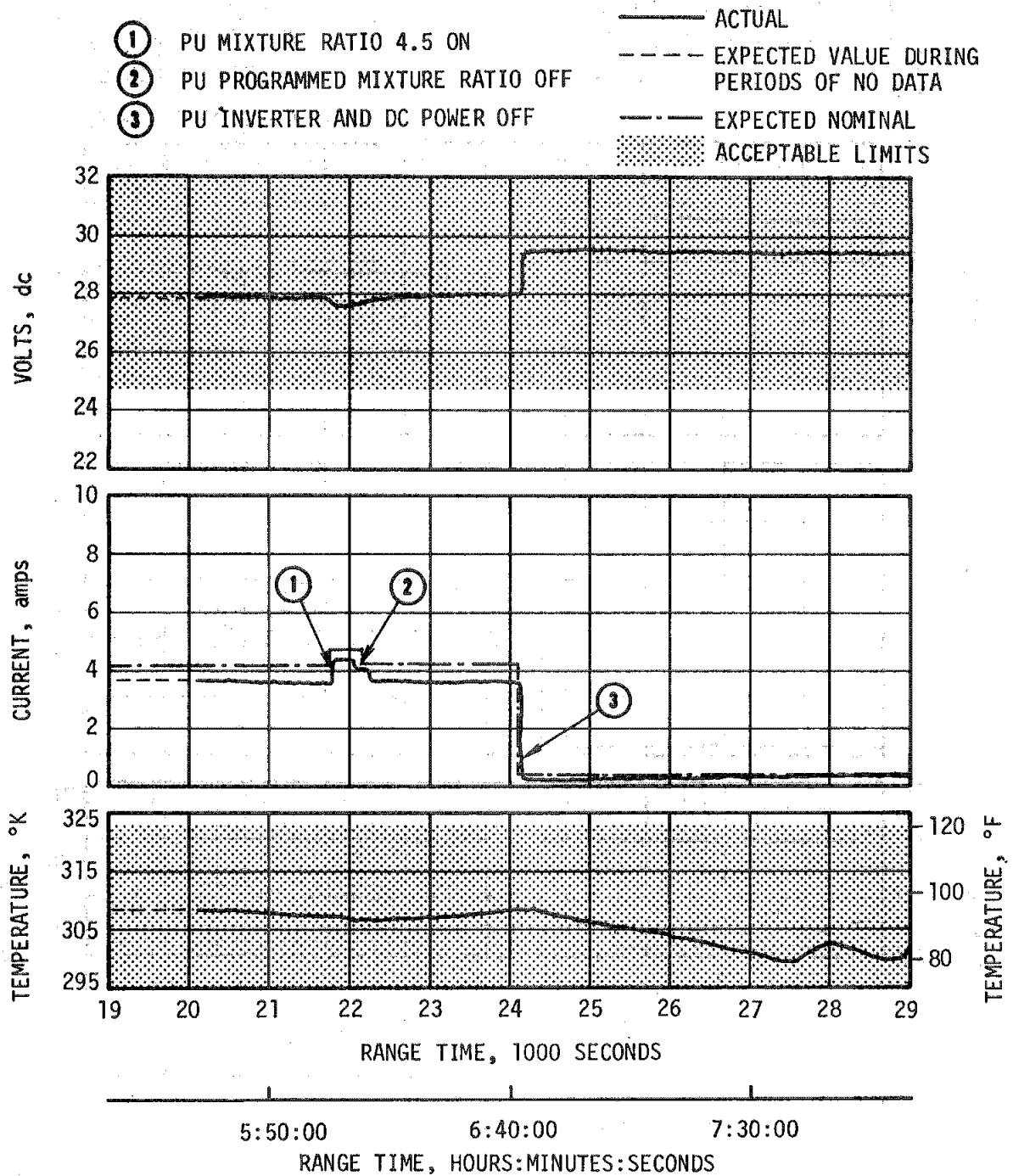
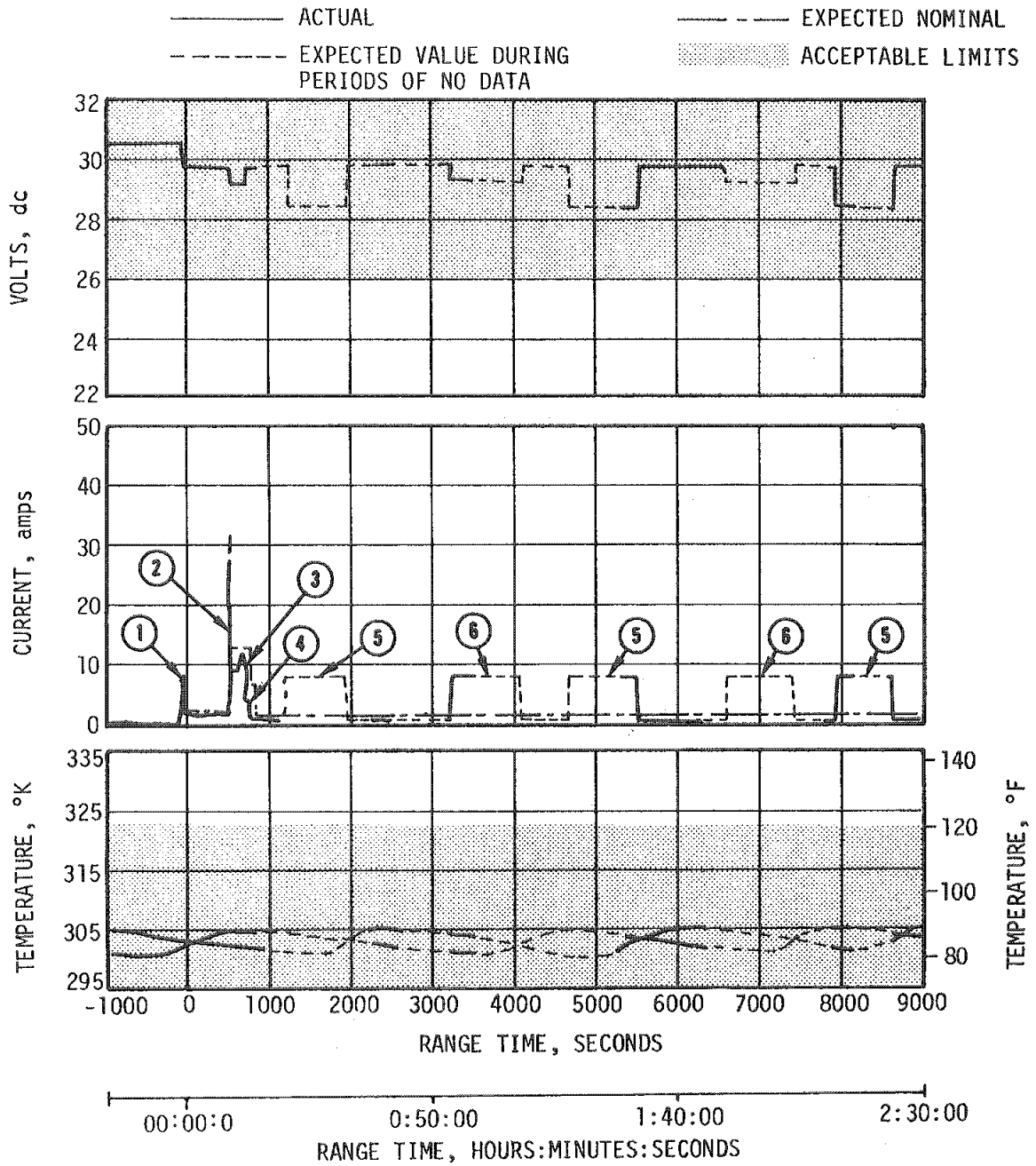
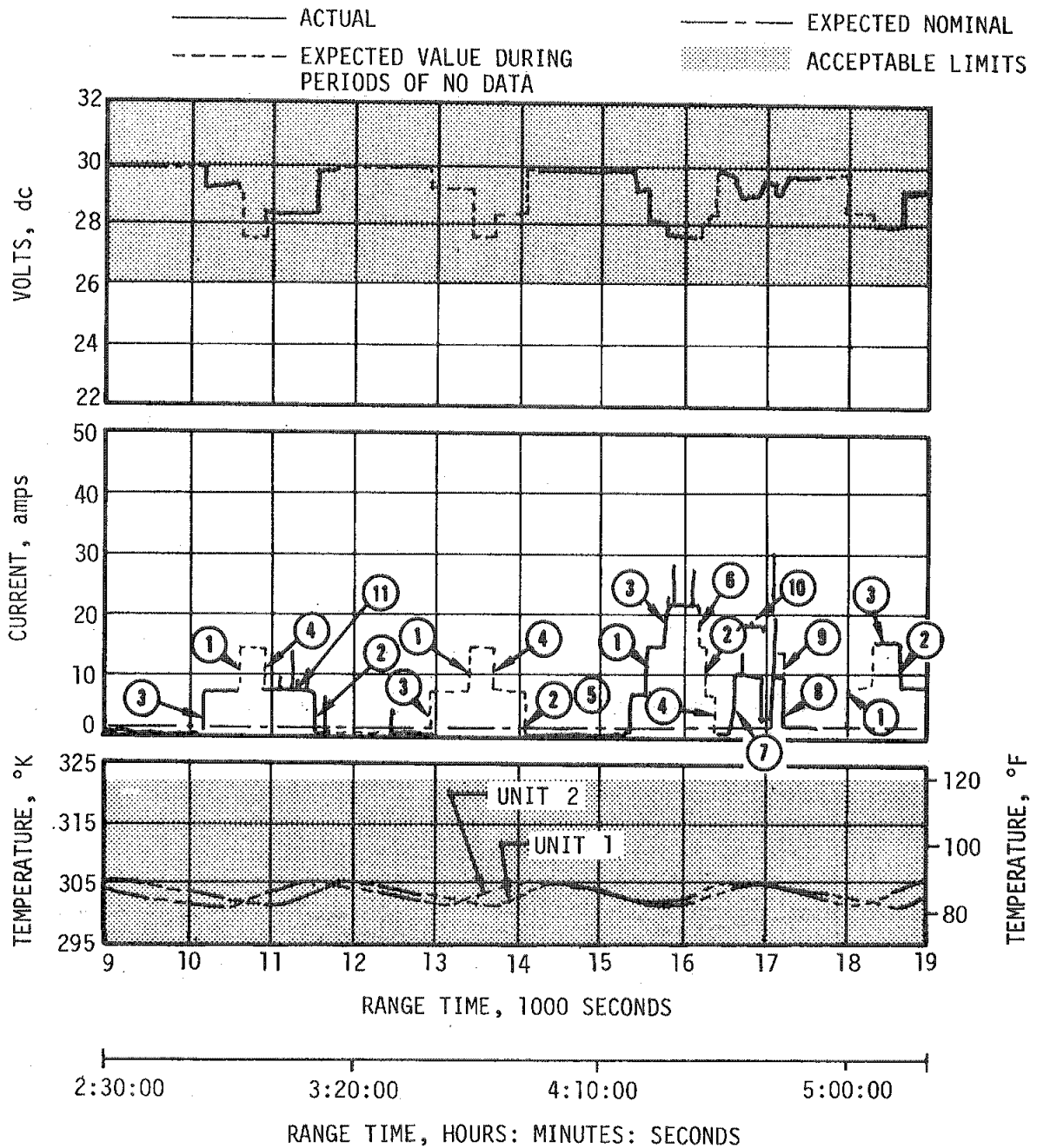


Figure 13-8. S-IVB Stage Forward Battery No. 2 Voltage, Current and Temperature (Sheet 3 of 3)



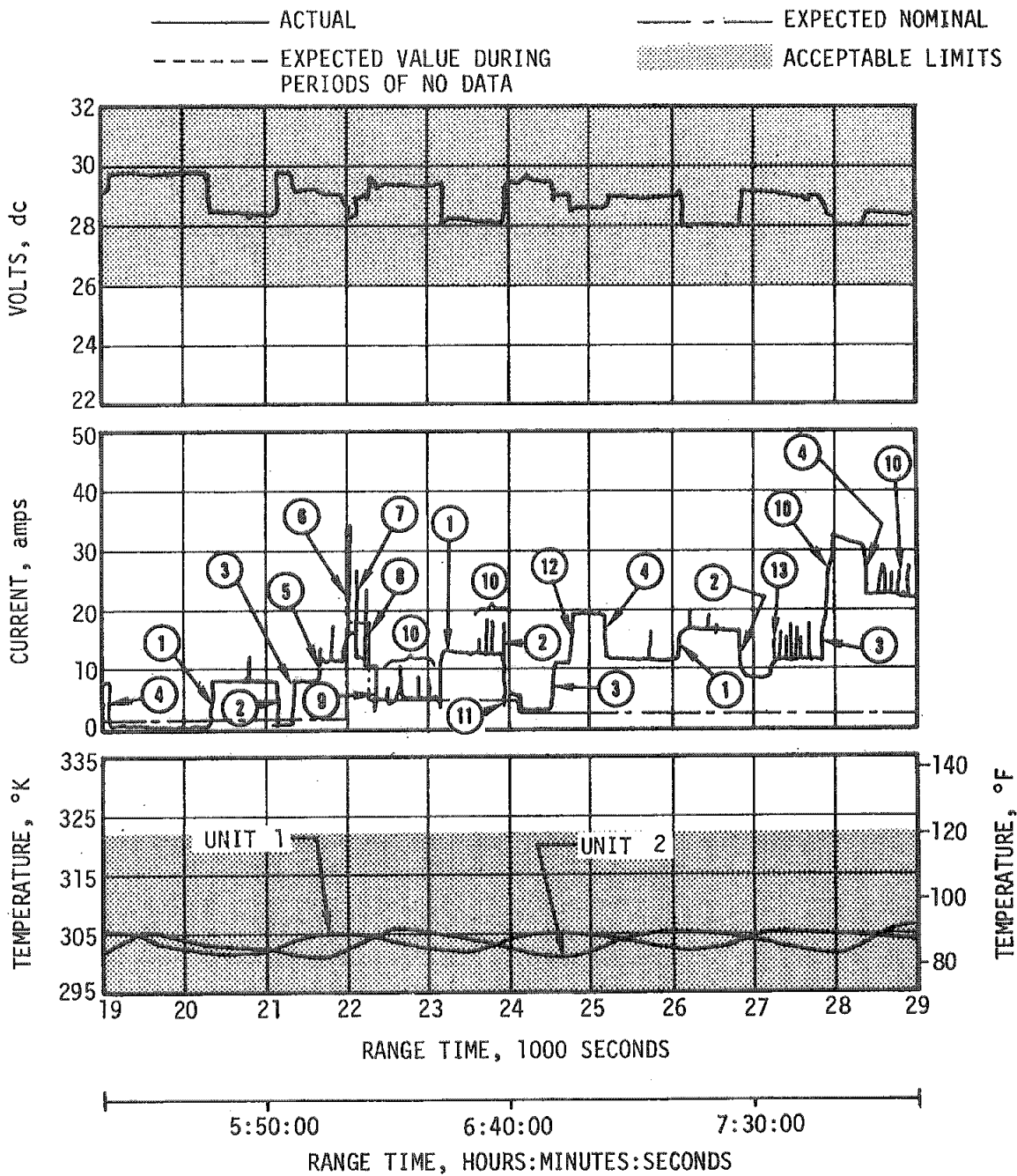
- |   |                               |
|---|-------------------------------|
| ① TRANSFER TO INTERNAL; AFT 1 UNIT 2 HEATER CYCLE | ④ ULLAGE ENGINE OFF           |
| ② ENGINE START; ULLAGE ENGINES ON                 | ⑤ AFT BATT 1 UNIT 1 HTR CYCLE |
| ③ ENGINE CUTOFF                                   | ⑥ AFT BATT 1 UNIT 2 HTR CYCLE |

Figure 13-9. S-IVB Stage Aft Battery No. 1 Voltage, Current and Temperature (Sheet 1 of 3)



- |                             |  |
|-----------------------------|--|
| ① AFT BATT 1 UNIT 1 HTR ON  | ⑦ ULLAGE ENGINES ON                    |
| ② AFT BATT 1 UNIT 1 HTR OFF | ⑧ ENGINE CUTOFF AND ULLAGE ENGINES OFF |
| ③ AFT BATT 1 UNIT 2 HTR ON  | ⑨ ENGINE START                         |
| ④ AFT BATT 1 UNIT 2 HTR OFF | ⑩ AFT BATT 2 UNIT 1 HTR CYCLE          |
| ⑤ AFT BATT 2 UNIT 2 HTR ON  | ⑪ APS (TYPICAL)                        |
| ⑥ AFT BATT 2 UNIT 2 HTR OFF |  |

Figure 13-9. S-IVB Stage Aft Battery No. 1 Voltage, Current and Temperature (Sheet 2 of 3)



- ① AFT BATT 1 UNIT 1 ON
- ② AFT BATT 1 UNIT 1 OFF
- ③ AFT BATT 1 UNIT 2 ON
- ④ AFT BATT 1 UNIT 2 OFF
- ⑤ S-IVB ULLAGE ENGINES ON
- ⑥ ENGINE START
- ⑦ S-IVB ULLAGE ENGINES OFF
- ⑧ AFT BATT 1 UNIT 2 HTR OFF
- ⑨ ENGINE CUTOFF
- ⑩ APS CYCLING
- ⑪ MAINSTAGE & HE CONTROL SOLENOID VLV CLOSE
- ⑫ ENGINE START ON
- ⑬ ULLAGE ENGINES 1 & 2 OFF

Figure 13-9. S-IVB Stage Aft Battery No. 1 Voltage, Current and Temperature (Sheet 3 of 3)

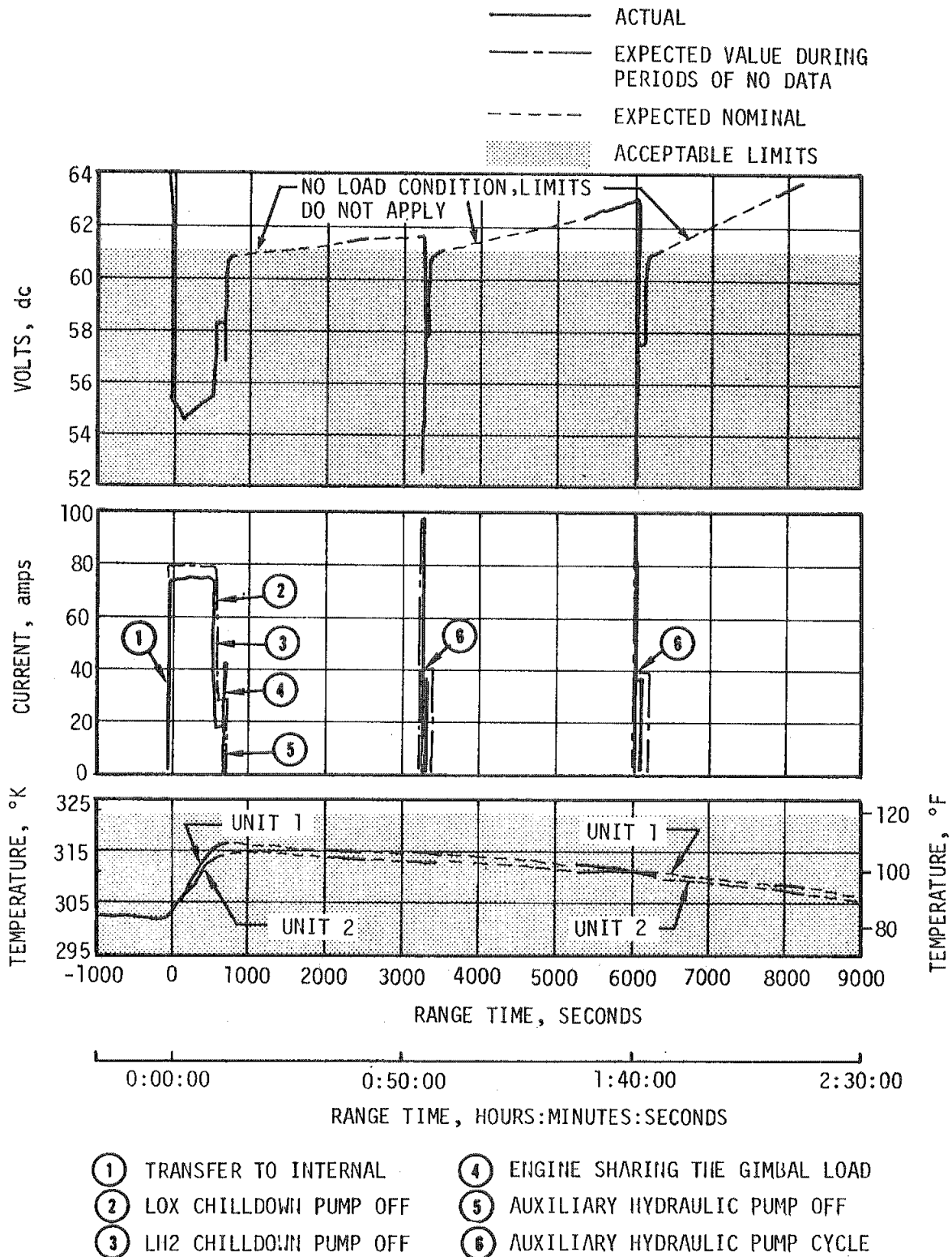
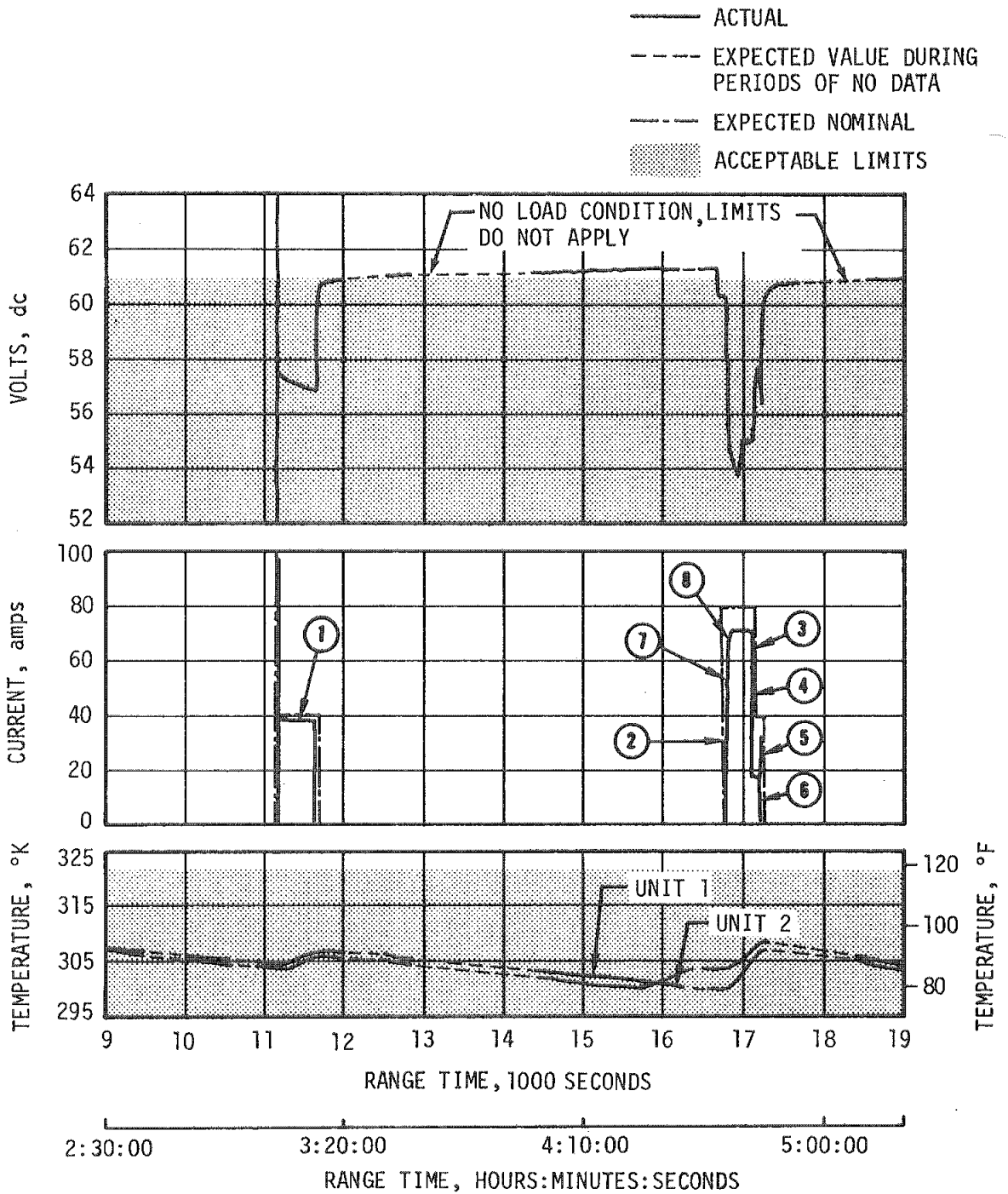


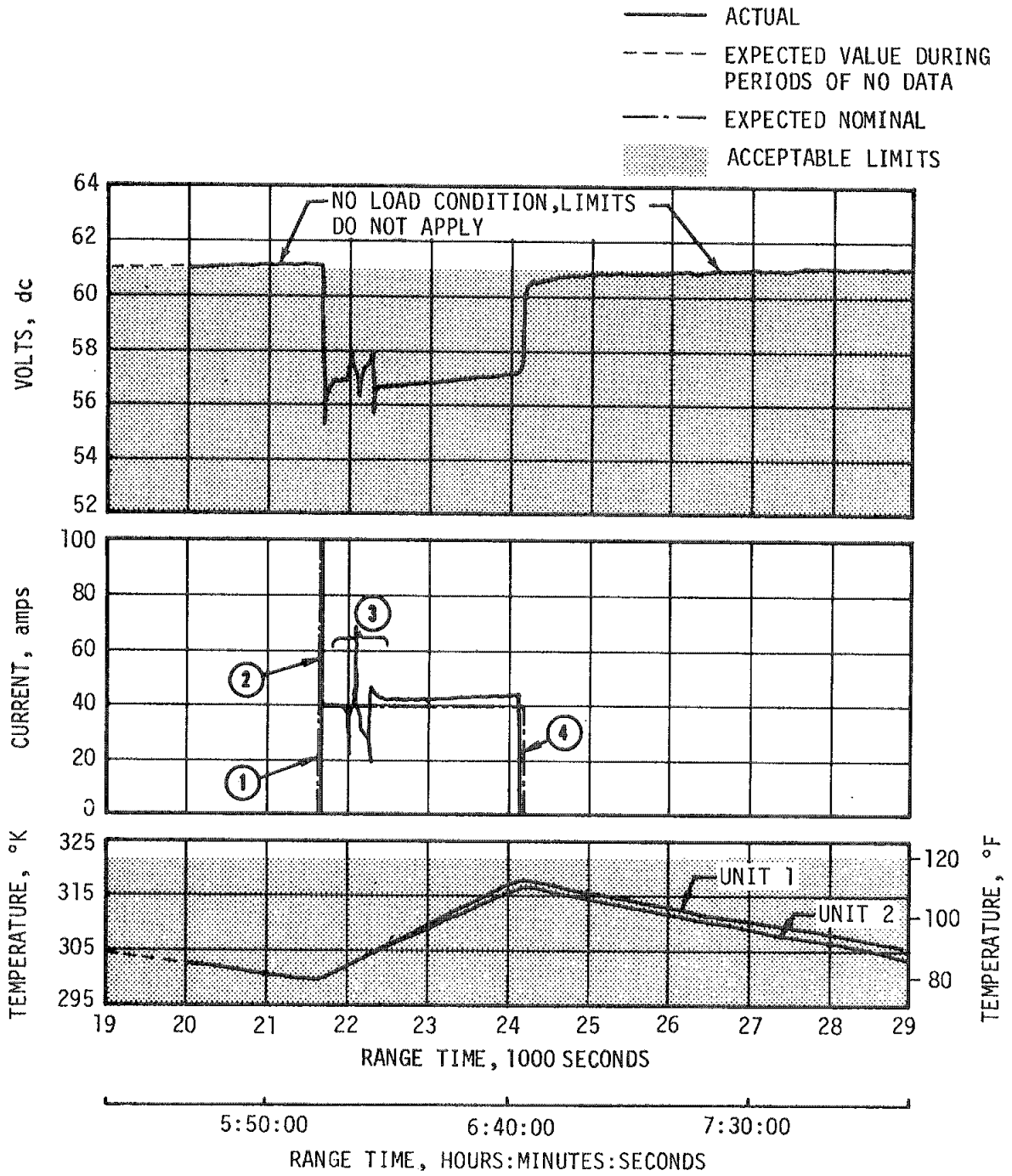
Figure 13-10. S-IVB Stage Aft Battery No. 2 Voltage, Current and Temperature (Sheet 1 of 3)



- |                                  |                                |
|----------------------------------|--------------------------------|
| ① AUXILIARY HYDRAULIC PUMP CYCLE | ④ LOX CHILLDOWN PUMP OFF       |
| ② AUXILIARY HYDRAULIC PUMP ON    | ⑤ ENGINE SHARING GIMBAL MODE   |
| ③ LH2 CHILLDOWN PUMP OFF         | ⑥ AUXILIARY HYDRAULIC PUMP OFF |

Figure 13-10. S-IVB Stage Aft Battery No. 2 Voltage, Current and Temperature (Sheet 2 of 3)





- ① AUXILIARY HYDRAULIC PUMP ON
- ② LH2 AND LOX CHILLDOWN PUMPS CYCLE
- ③ ENGINE SHARING GIMBAL LOAD
- ④ AUXILIARY HYDRAULIC PUMP OFF

Figure 13-10. S-IVB Stage Aft Battery No. 2 Voltage, Current and Temperature (Sheet 3 of 3)

Due to an apparent failure in the battery heater circuit, forward battery No. 1, unit 1, temperature dropped below 294°K (70°F) at 22,800 seconds (06:20:00). At this temperature the battery heater should have cycled on, but did not. By 29,000 seconds (08:03:20) battery temperature had dropped to 291°K (63°F) as shown in Figure 13-7, but the battery suffered no degradation in performance as verified by data through 47,400 seconds (13:10:00).

S-IVB stage battery power consumptions, in ampere-hours and as a percent of rated capacity, are given in Table 13-3. Battery parameters, except for the low temperature on forward battery No. 1, unit 1, were within specifications through 47,400 seconds (13:10:00).

Three 5-volt excitation modules provide closely regulated measuring voltage to instrumentation measurement transducers and signal conditioners. All three excitation modules stayed within required limits of  $5 \pm 0.030$  vdc. However, the aft 5-volt excitation module (M0025-404) voltage read at the lower limit of 4.97 as on AS-503 (on AS-503 it read out-of-limits due to the narrower limits of  $5 \pm 0.025$  volts). These limits were extended to  $5 \pm 0.030$  on AS-504. The condition was caused by the use of different grounds for the module and the multiplexer (M0069-404) reference voltage. The calibration curve used in data reduction for the affected module will be shifted approximately 20 millivolts for future flights to take care of the problem. Seven 20-vdc excitation modules provide signal conditioning power for event measurements (eleven such modules were used on AS-503). These modules performed satisfactorily.

Table 13-3. S-IVB Stage Battery Power Consumption

BATTERY	CAPACITY (AMP-HRS) <sup>1</sup>	POWER CONSUMPTION		PERCENT OF CAPACITY
		NOMINAL EXPECTED <sup>2</sup> (AMP-HRS)	ACTUAL <sup>3</sup> (AMP-HRS)	
Fwd No. 1	228	105.6	85.47	38
Fwd No. 2	25	17.0	12.89	52
Aft No. 1	228	63.0*	43.99	19
Aft No. 2	67	67.9	59.84	89

<sup>1</sup>Amp-hour ratings are specification values.

<sup>2</sup>Predicted nominal amp-hour usage based on a 7.5 hour flight.

<sup>3</sup>Actual usage for 8 hours based on available flight data.

\* Predicted maximum amp-hour usage based on a 7.5 hour flight.

The LOX and LH2 chilldown inverters performed satisfactorily and met their load requirements.

The switch selector functioned correctly and executed all IU commands through the sequencer at the proper times.

The Propellant Utilization (PU) system performed in a satisfactory manner throughout the flight. ECP 3008 was implemented for AS-504 and subsequent vehicles to minimize PU voltage and frequency positive level shifts which occurred on AS-503 during the PU hardover mode of operation. Positive level shifts of less than 0.08 percent were noted on AS-504.

All EBW firing units responded as predicted. The ullage motor ignition EBW firing units were charged at 494 seconds and fired at 537 seconds. The ullage motor jettison EBW firing units were charged at 546 seconds and fired at 549 seconds.

### 13.5 INSTRUMENT UNIT ELECTRICAL SYSTEM

The IU electrical system utilizes three 28-vdc batteries and a bus network to distribute power to the various IU components. AS-504 differed from AS-503 electrically, as follows:

- a. Four measuring racks were used on AS-504 (ten on AS-503).
- b. Three batteries were used on AS-504 (four on AS-503).
- c. One measuring distributor was used on AS-504 (two on AS-503).
- d. Flight Control Computer (FCC) power input was removed from the 6D41 bus.
- e. Command and Communications System (CCS) power input was switched from 6D11 bus to 6D41 bus.
- f. A spare connector on the control distributor was used for the vehicle Overall Test (OAT) switch selector monitoring.
- g. One Apollo interface cable was removed.
- h. IU network cables were reduced in number from 182 to 126.

Design minimum IU life is 24,480 seconds (06:48:00) and battery performance during this period was nominal as shown in Figures 13-11 through 13-13. Actual battery life exceeded this time considerably. Battery 6D30 output was dropping off with the battery still providing power after 45,720 seconds (12:42:00). The CCS was still operating after 47,880 seconds (13:18:00) using battery 6D40 power. Battery voltages, currents and temperatures remained within predictions until power began to fall off due to battery depletion. Battery 6D40 registered the highest temperature of approximately 328°K (130°F) at 45,720 seconds (12:42:00) at which point current output had dropped off to 23 amperes from a nominal output of over 30 amperes.

Battery power consumption in ampere-hours and as a percent of rated capacity remained well within design limits, as shown in Table 13-4.

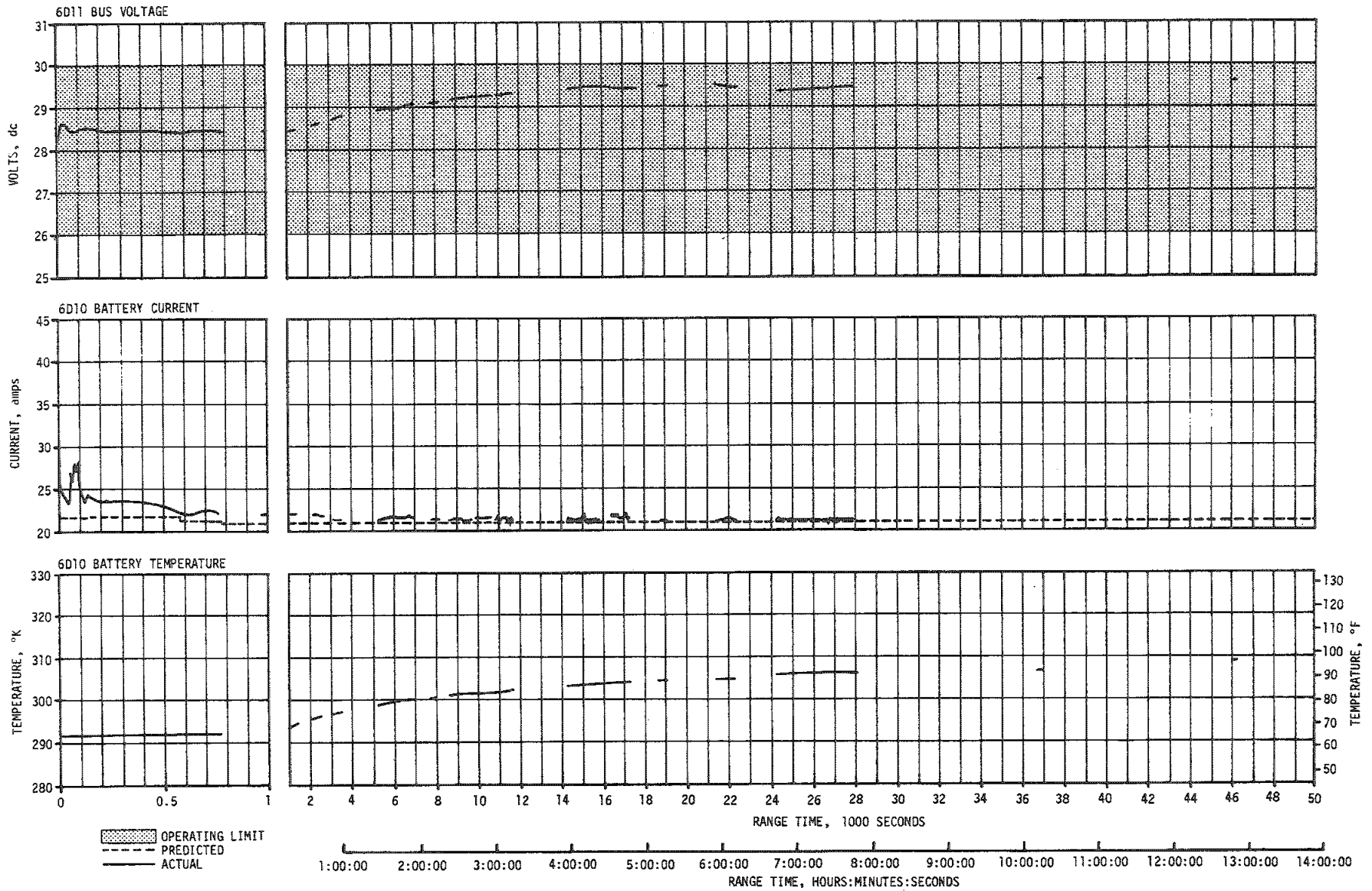


Figure 13-11. IU Battery 6D10 Voltage, Current and Temperature

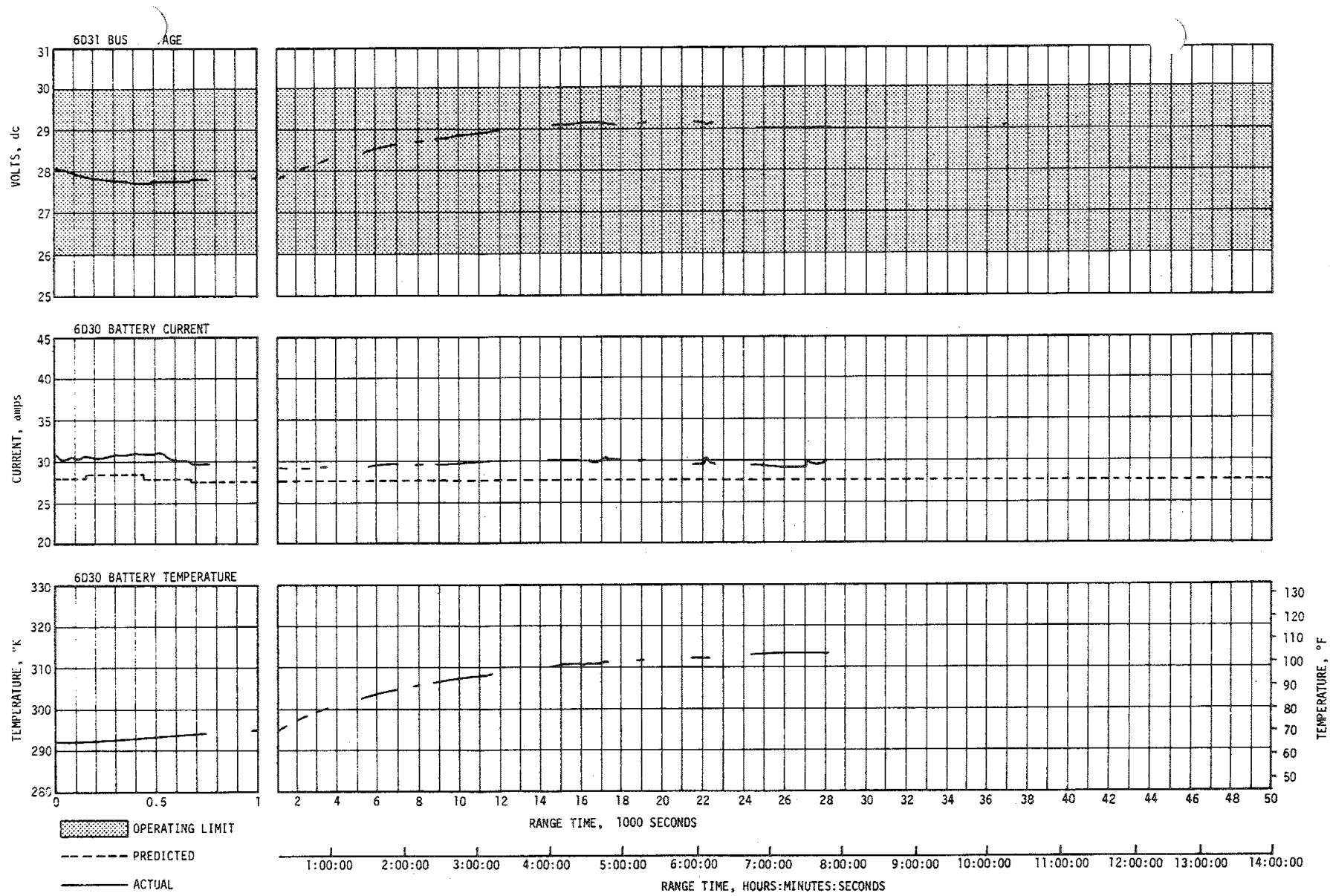


Figure 13-12. IU Battery 6D30 Voltage, Current and Temperature

13-24

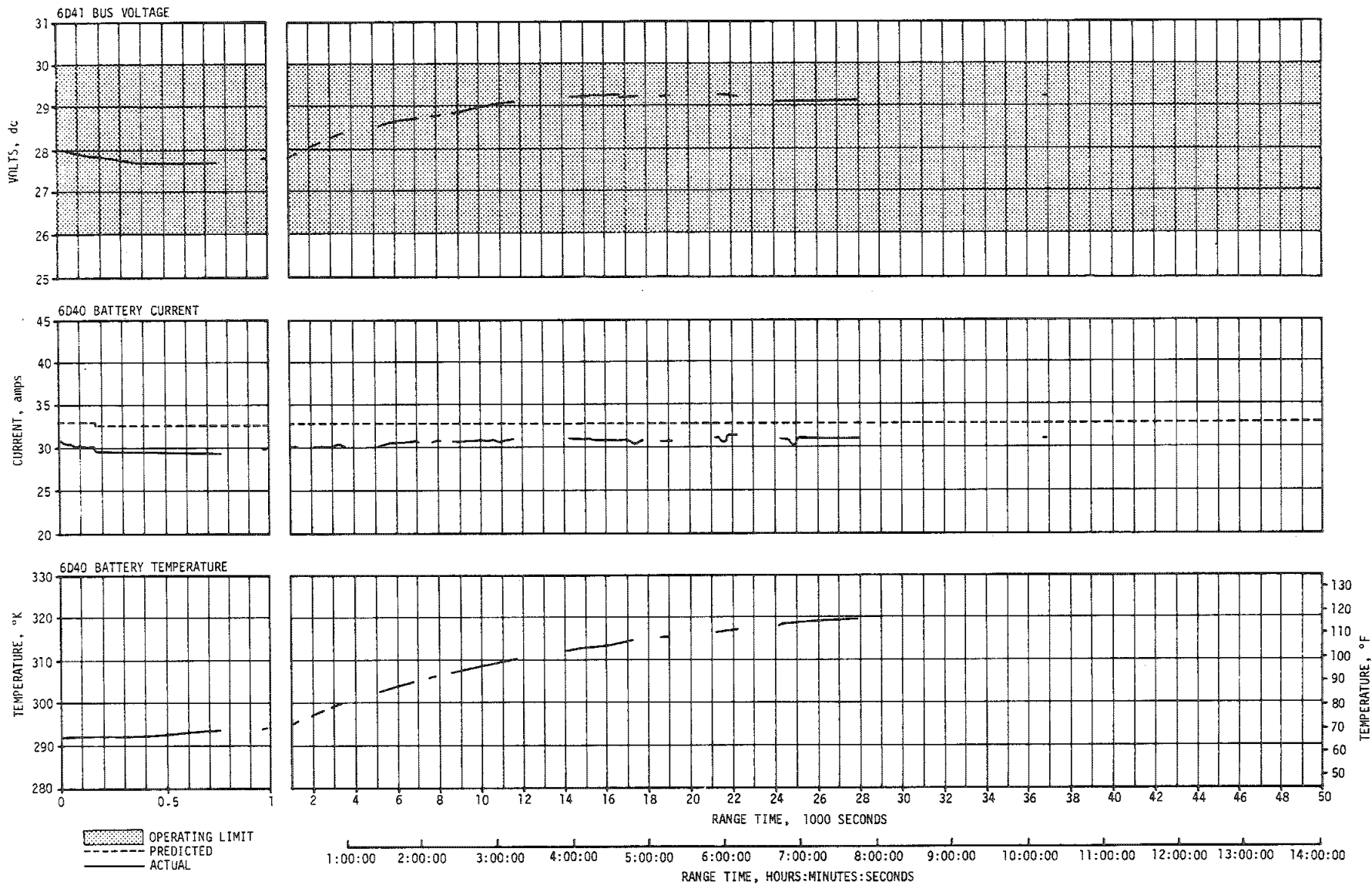


Figure 13-13. IU Battery 6D40 Voltage, Current and Temperature

Table 13-4. IU Battery Power Consumption

BATTERY	CAPACITY (AMP-HR)	AVERAGE CURRENT (AMPS)	POWER CONSUMPTION	
			EST FLIGHT TIME OF 100 PERCENT (HOURS)	PERCENT OF CAPACITY*
6D10	350	21.5	16.1	78.7
6D30	350	29.8	12.7	108
6D40	350	30.6	12.5	109

\*Battery conditions based on 12.8 hours of flight data

The 56-volt power supply supplies voltage to the gyro, accelerometer servo-loops and accelerometer signal conditioner. All indications are that this supply performed normally and its output remained well within the  $56 \pm 2.5$  volts dc limits. The 5-volt measuring reference voltage supply maintained a constant voltage of 5.00 volts and performance remained nominal.

Data indicate that the IU switch selector performed nominally throughout the flight.

## SECTION 14

### RANGE SAFETY AND COMMAND SYSTEMS

#### 14.1 SUMMARY

Data indicated that the redundant Secure Range Safety Command Systems (SRSCS) on the S-IC, S-II, and S-IVB stages were ready to perform their functions properly on command if flight conditions during the launch phase had required vehicle destruct. The system properly safed the S-IVB SRSCS on command transmitted from Bermuda (BDA). The performance of the Command and Communications System (CCS) in the Instrument Unit (IU) was satisfactory, except during the time period from 22,066.4 seconds (06:07:46.4) to 23,418.8 seconds (06:30:18.8) when a CCS power amplifier output was degraded.

#### 14.2 RANGE SAFETY COMMAND SYSTEMS

The SRSCS provides a means to terminate the flight of the vehicle by radio command from the ground in case of emergency situations in accordance with range safety requirements. After successful insertion into earth orbit, the system is deactivated (safed) by ground command. Each powered stage of the vehicle was equipped with two command receivers/decoders and necessary antennas. The SRSCS in each stage was completely independent of those in other stages.

Three types of SRSCS commands were programmed for this manned flight as follows:

- a. Arm/fuel cutoff - Charging of the Exploding Bridge Wire (EBW) firing unit and thrust termination.
- b. Destruct - Propellant dispersion by firing of the EBW.
- c. Safe - Command system switched off.

During flight, telemetry indicated that the command antennas, receivers/decoders, and destruct controllers functioned properly and were in the required state of readiness if needed. Since no arm/cutoff or destruct commands were required, all data except receiver signal strength remained unchanged during the flight. At 685 seconds the safing command was initiated, deactivating the system. Both S-IVB stage systems, the only systems in operation at this time, responded properly to the safing command.



Radio Frequency (RF) performance aspects of the system are discussed in Section 19, paragraph 19.5.3.1.

### 14.3 COMMAND AND COMMUNICATION SYSTEM

The performance of the command section of the CCS was satisfactory. A total of 45 known commands were transmitted from the ground stations. All commands were accepted by the onboard equipment, although one data word, sent at 23,172.8 seconds, had to be transmitted three times before verification. The command system did not receive the first two transmissions because of a command subcarrier dropout, caused by low signal strength. However, the third transmission of the command was received and accepted.

A terminate command was transmitted from the ship Vanguard to verify that the Launch Vehicle Digital Computer (LVDC) tag bit problem (Sections 10.5.4 and 19.3.4) did not impact the command capability. Since the command system was not enabled at this time, no computer reset pulse was transmitted, causing the ground station to automatically retransmit the command three times. The address verification pulses were received for each of these transmissions.

The restart enable commands for second and third S-IVB stage burns were accepted.

Commands were sent to open the LOX and LH<sub>2</sub> valves to dump propellant after S-IVB third burn and were accepted by the command system. These commands were sent after the valves failed to respond to the nominal onboard programmed commands.

Table 14-1 gives a summary of all transmitted commands. All commands were verified.

A CCS power amplifier gave a degraded output from 22,066.4 seconds (06:07:46.4) to 23,418.8 seconds (06:30:18.8) and recovered thereafter. This degraded output caused loss of data on the CCS down link, but did not impair capability to receive and act upon commands transmitted from ground stations, and a total of 10 commands were successfully transmitted during this period. Verifications for these commands were received through the DP-1 VHF link and the DP-1A UHF link and did not affect successful accomplishment of this mission.

RF performance aspects of the system are discussed in Section 19, paragraph 19.5.3.2.

Table 14-1. Command and Communications System,  
Commands History, AS-504

RANGE TIME		STATION	COMMAND	NUMBER OF WORDS
SECONDS	HR:MIN:SEC			
6497.5	01:48:17.5	VAN	Terminate	4
8794.8	02:26:34.8	CRO	IU Command System Enable	3
8821.9	02:27:01.9	CRO	Terminate	1
15,834.7	04:22:14.7	HAW	Remove Inhibit Maneuver No. 4	2
16,453.8	04:34:13.8	RED	S-IVB Restart Enable	1
20,418.3	05:40:18.3	CRO	S-IVB Restart Enable	1
20,594.9	05:43:04.9	CRO	Set Antenna Low Gain	1
21,709.0	06:01:49.0	GWM	Chill S/O Valve Closed On	3
21,728.3	06:02:08.3	GWM	LH2 Chill Pump Off	3
21,729.1	06:02:09.1	GWM	LOX Chill Pump Off	3
21,952.0	06:05:52.0	GWM	Chill S/O Valve Open	3
21,952.8	06:05:52.8	GWM	Prevalves Open	3
21,953.5	06:05:53.5	GWM	Engine Cutoff Off	3
21,954.3	06:05:54.3	GWM	Engine Ready Bypass On	3
21,986.5	06:06:26.5	GWM	Engine Start On	3
22,976.0	06:22:56.0	GWM	Engine Mainstage Control Valve Open Off	3
22,976.8	06:22:56.8	GWM	Engine Helium Control Valve Open Off	3
22,992.7	06:23:12.7	GWM	Passivation Enable	3
22,993.5	06:23:13.5	GWM	Engine Mainstage Control Valve Open On	3
22,994.3	06:23:14.3	GWM	Engine Helium Control Valve Open On	3
23,155.3	06:25:55.3	GWM	Engine Ignition Phase Control Valve Open Off	3
23,156.1	06:25:56.1	GWM	Engine Helium Control Valve Open Off	3
23,171.5	06:26:11.5	GWM	Passivation Enable	3
23,172.4	06:29:32.4	GWM	Engine Ignition Phase Control Valve Open On	5
23,174.1	06:39:34.1	GWM	Engine Helium Control Valve Open On	3
24,075.0	06:41:15.0	TEX	Engine Ignition Phase Control Valve Open Off	3
24,075.9	06:41:15.9	TEX	Burner LOX Shutdown Valve Closed Off	3
24,093.7	06:41:33.7	TEX	Passivation Enable	3
24,094.6	06:41:34.6	TEX	Engine Ignition Phase Control Valve Open On	3
24,095.5	06:41:35.5	TEX	Engine Helium Control Valve Open On	3
24,328.0	06:45:28.0	TEX	Passivation Enable	3
24,328.9	06:45:28.9	TEX	Engine Helium Control Valve Open On	3
24,769.1	06:52:49.1	TEX	S-IVB Engine Cutoff Off	3
24,769.9	06:52:49.9	TEX	Engine Ready Bypass	3
24,770.9	06:52:50.9	TEX	Prevalves Close Off	3
24,771.8	06:52:51.8	TEX	S-IVB Engine Start On	3
27,009.7	07:30:09.7	GDS	Set Antennas Omni	1
27,108.7	07:31:48.7	GDS	Set Antennas High Gain	1
27,162.4	07:32:42.4	GDS	Set Antennas Low Gain	1
27,189.8	07:33:09.8	GDS	C-Band No. 1 Inhibit	3
27,213.5	07:33:33.5	GDS	C-Band No. 2 Inhibit	3
27,243.4	07:34:03.4	GDS	S-IVB Ullage Engine No. 1 On	3
27,244.6	07:34:04.6	GDS	S-IVB Ullage Engine No. 2 On	3
28,108.1	07:48:28.1	GDS	CCS Inhibit	3
30,604.9	08:30:04.9	GDS	CCS Enable	3

SECTION 15  
EMERGENCY DETECTION SYSTEM

15.1 SUMMARY

The AS-504 Emergency Detection System (EDS) configuration was essentially the same as on the AS-503 vehicle. The performance of the system was nominal; no abort limits were exceeded.

15.2 SYSTEM EVALUATION

15.2.1 General Performance

The EDS provided for automatic abort during S-IC burn by monitoring two parameters; two or more S-IC engines out and excessive angular rates. In addition various parameters were displayed to the crew for manual abort cues, as discussed later.

EDS differences between AS-504 and AS-503:

- a. One discrete input signal from the EDS distributor to the Launch Vehicle Data Adapter (LVDA)/Launch Vehicle Digital Computer (LVDC) was deleted. This discrete functioned as a spacecraft separation signal on AS-503 and was not required on AS-504.
- b. The rate gyro timer, a 20-second timer which performed no function on AS-503, was not installed on AS-504.

All launch vehicle EDS parameters remained well within acceptable limits during the AS-504 mission. No overrate signals or unscheduled engine-out discretes were received by the EDS distributor. Sequential events and discrete indications occurred as expected.

15.2.2 Propulsion System Sensors

The S-IC stage utilizes three thrust OK sensors on each F-1 engine. If two of these three switches indicate a thrust drop below the mainstage nominal level, an abort indication is given to the flight crew. From liftoff until deactivation, either by the crew or the switch selector, an indication of two or more engines-out results in an automatic abort. The switch selector deactivated the two engines-out automatic abort at 133.4 seconds.

The S-II and S-IVB stages utilize two thrust OK sensors on each J-2 engine. When both switches indicate low thrust an abort indication is given to the crew, as already described for the S-IC stage.

Operation of all thrust OK sensors and associated logic was as expected. Refer to Table 15-1 for a summary of thrust OK pressure switch closing and opening times.

S-IVB LOX and LH<sub>2</sub> tank ullage pressures are displayed to the flight crew. Tank pressure abort limits are based on the differential pressure across the common bulkhead and apply only during orbital operations. Tank pressures stayed below the limits of 24.8 and -17.9 N/cm<sup>2</sup> (36 and -26 psid) for P<sub>LOX</sub>-P<sub>LH<sub>2</sub></sub> during AS-504 orbital operations.

### 15.2.3 Flight Dynamics and Control Sensors

Nine (three per axis) control rate gyros sense angular overrate for the EDS. When two or more gyros in any axis sense a rate in excess of pre-set limits, a discrete indication is given in the Command Module (CM) and from liftoff until the overrate automatic abort is deactivated, either by the flight crew or the switch selector, an automatic abort is initiated. The switch selector command which deactivates the overrate automatic abort also changes the rate limit settings. This command was given at 133.8 seconds. Table 15-2 tabulates the rate limits and maximum measured rates for both the overrate automatic abort and manual abort modes.

The angle-of-attack dynamic pressure is sensed by a redundant Q-ball located atop the launch escape tower. One Q-ball vector sum output is displayed in the CM; the other is telemetered from the Instrument Unit (IU). The maximum delta pressure measured on AS-504 was approximately 0.69 N/cm<sup>2</sup> (1.0 psid) between 75 and 85 seconds. This was only about 30 percent of the recommended manual abort limit of 2.2 N/cm<sup>2</sup> (3.2 psid).

Failures of the launch vehicle stabilized platform result in discrete indications in the spacecraft. No such platform failure indications were initiated on the AS-504 flight.

Circuitry to provide engine cutoff in the event of abort is enabled by a switch selector command and a timer. Launch vehicle engines EDS cutoff enable occurs approximately 30 seconds after liftoff. The switch selector command for AS-504 was given at 30.0 seconds, and the timer command at 31.7 seconds after liftoff. The timer is set for 30 +2, -0 seconds after liftoff.

All discrete events and discrete indications to the crew occurred as expected. See Table 15-3 for a compilation of EDS associated discretetes.

Table 15-1. Performance Summary of Thrust OK Pressure Switches

STAGE	ENGINE	SWITCH	TIME CLOSED (RANGE TIME, SEC)	TIME OPENED (RANGE TIME, SEC)
S-IC	1	1	-1.8	163.0
	1	2	-1.8	163.0
	1	3	-1.8	163.0
	2	1	-1.5	163.0
	2	2	-1.5	163.0
	2	3	-1.5	163.0
	3	1	-1.8	163.0
	3	2	-1.8	163.0
	3	3	-1.8	163.0
	4	1	-1.3	163.0
	4	2	-1.4	163.0
	4	3	-1.4	163.0
	5	1	-2.2	134.6
	5	2	-2.2	134.6
5	3	-2.2	134.6	
S-II	1	1	167.0	536.3
	1	2	167.0	536.3
	2	1	167.0	536.4
	2	2	167.0	536.4
	3	1	167.0	536.4
	3	2	167.0	536.4
	4	1	167.0	536.3
	4	2	167.0	536.3
	5	1	167.0	536.4
	5	2	167.0	536.4
S-IVB 1ST BURN	1	1	542.0	664.9
	1	2	542.0	664.9

Table 15-2. Maximum Angular Rates

PHASE	PITCH	YAW	ROLL
Liftoff to 133.8 sec	1.0 (4) deg/s	0.6 (4) deg/s	1.3 (20) deg/s
133.8 sec to SC Separation	1.2 (9.2) deg/s	0.3 (9.2) deg/s	1.0 (20) deg/s
Note: Abort limits are shown in parentheses.			

Table 15-3. EDS Associated Discretes

DISCRETE MEASUREMENT	DISCRETE EVENT	RANGE TIME
K73-602 On	EDS or Manual Cutoff of LV Engines Armed (Switch Selector)	30.7
K74-602 On	EDS or Manual Cutoff of LV Engines Armed (Timer)	31.7
K81-602 On	EDS S-IC One Engine Out	134.6
K82-602 On	EDS S-IC One Engine Out	134.6
K57-603 Off	Q-Ball On Indication (+6D21)	151.5
K58-603 Off	Q-Ball On Indication (+6D41)	151.5
K79-602 On	EDS S-IC Two Engines Out	163.0
K80-602 On	EDS S-IC Two Engines Out	163.0
K88-602 Off	S-IC Stage Separation	163.6

## SECTION 16

### VEHICLE PRESSURE AND ACOUSTIC ENVIRONMENT

#### 16.1 SUMMARY

The vehicle internal, external, and base region pressure environments were monitored by a series of differential and absolute pressure gages. These measurements were used in confirming the vehicle external, internal, and base region design pressure environments. The flight data were generally in good agreement with the predictions and compared well with previous flight data. The pressure environment was well below design levels.

The vehicle internal and external acoustic environment was monitored by a series of microphones positioned to measure both the rocket engine and aerodynamically induced fluctuating pressure levels. The measured acoustic levels were generally in good agreement with the liftoff and inflight predictions, and with data from previous flights.

#### 16.2 SURFACE PRESSURES AND COMPARTMENT VENTING

##### 16.2.1 S-IC Stage

External and internal pressure environments on the S-IC stage were recorded by 12 measurements located on and inside the engine fairings, aft skirt, intertank, and forward skirt. Representative data from a portion of these instruments are compared with previous flight data in Figures 16-1 through 16-3. Static pressure is presented as the difference between measurement pressure and free stream static pressure ( $P_{int} - P_{amb}$ ). Pressure loading is the difference between structural internal and external pressures defined such that a positive loading is in the outward direction.

The AS-504 S-IC engine fairing compartment pressure differentials, shown in Figure 16-1, agree very well with previous flight data.

The S-IC engine and intertank compartment pressure differentials are shown in Figure 16-2. The AS-504 engine compartment pressure differential agrees well with previous data. The delay in the peak of the AS-504 intertank pressure differential was caused by the slower trajectory of this flight. However, the trends and magnitudes of the AS-504 data show good agreement with previous data.

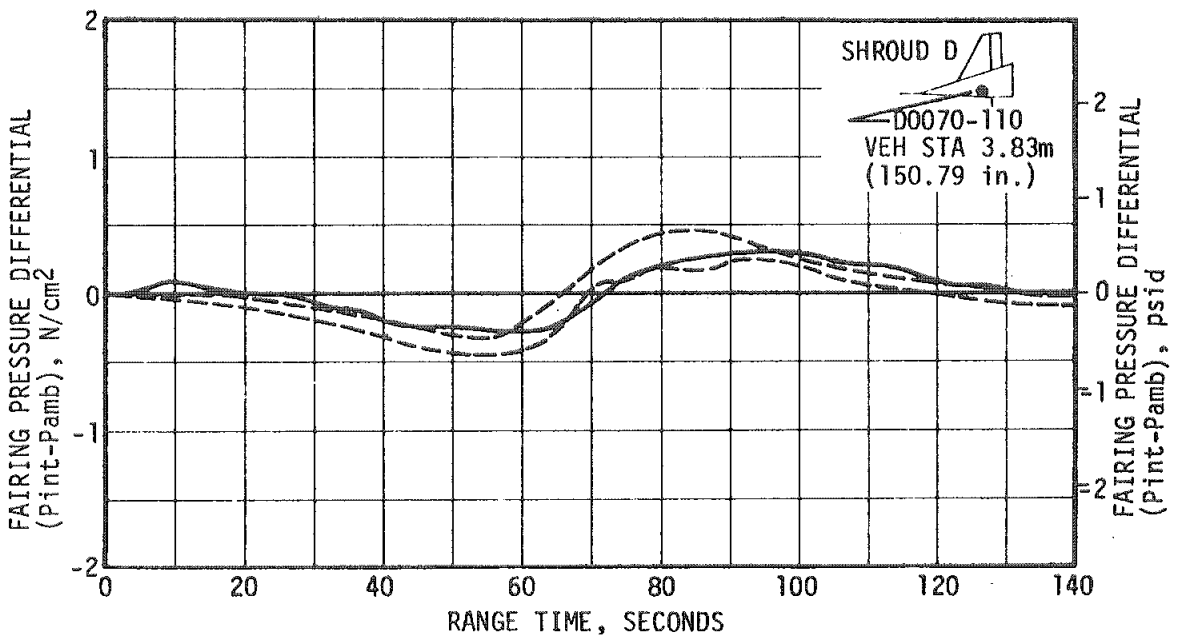
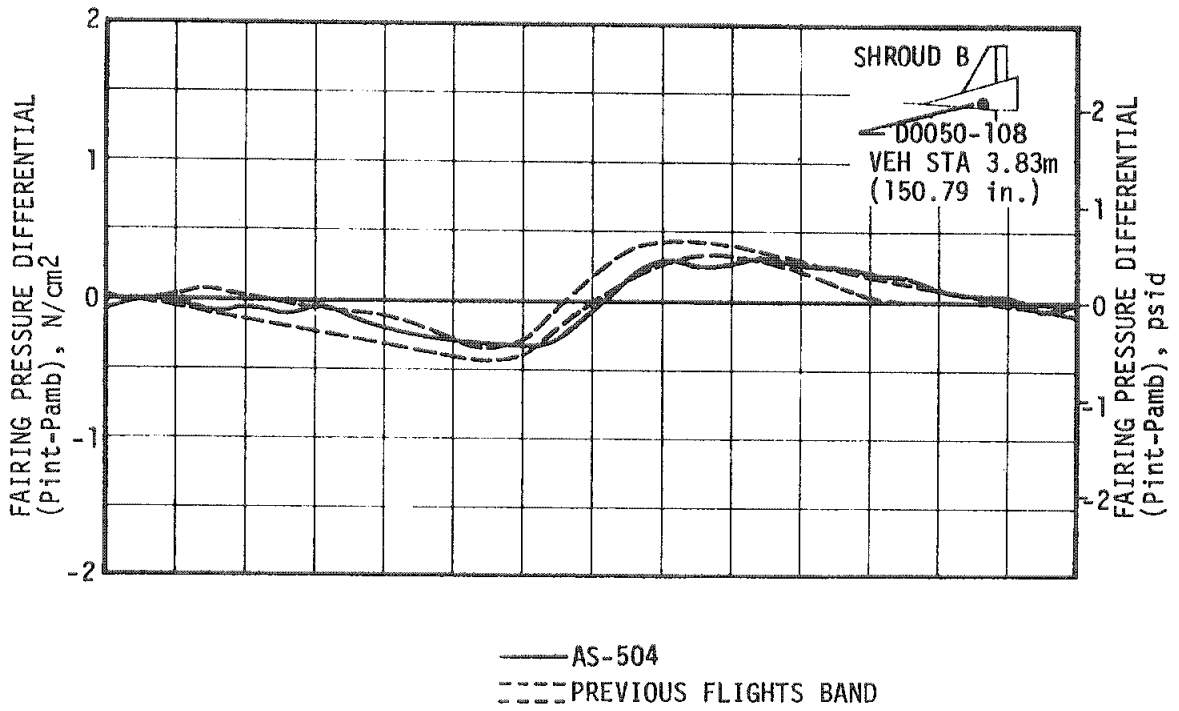


Figure 16-1. S-IC Engine Fairing Compartment Pressure Differential



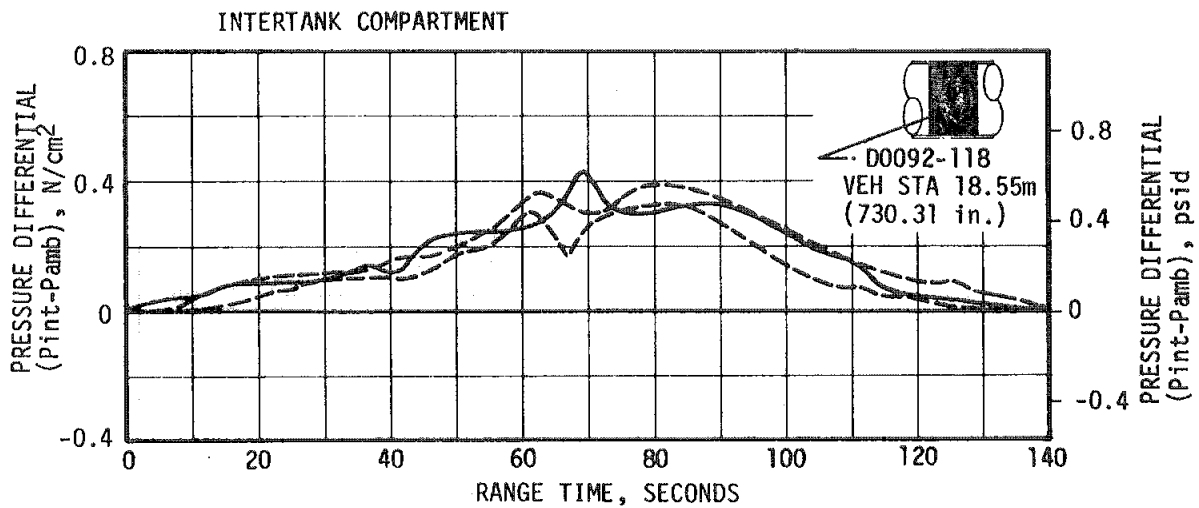
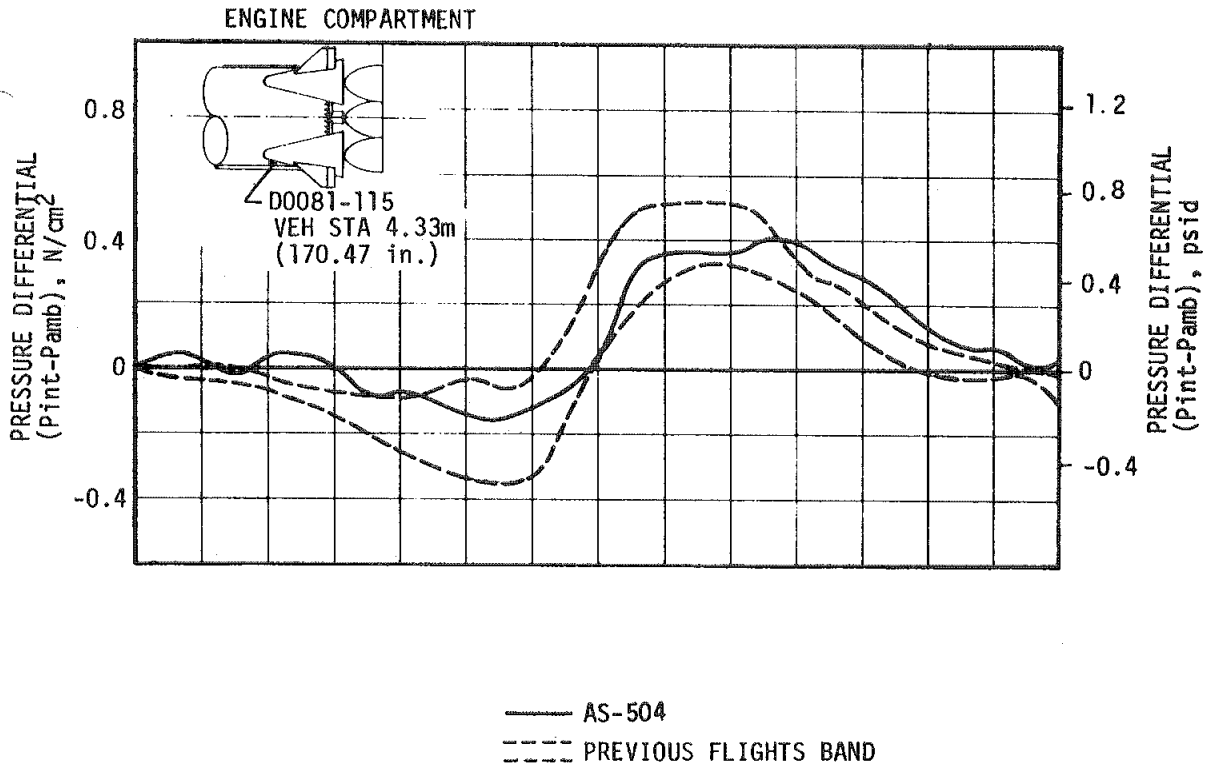


Figure 16-2. S-IC Compartment Pressure Differentials

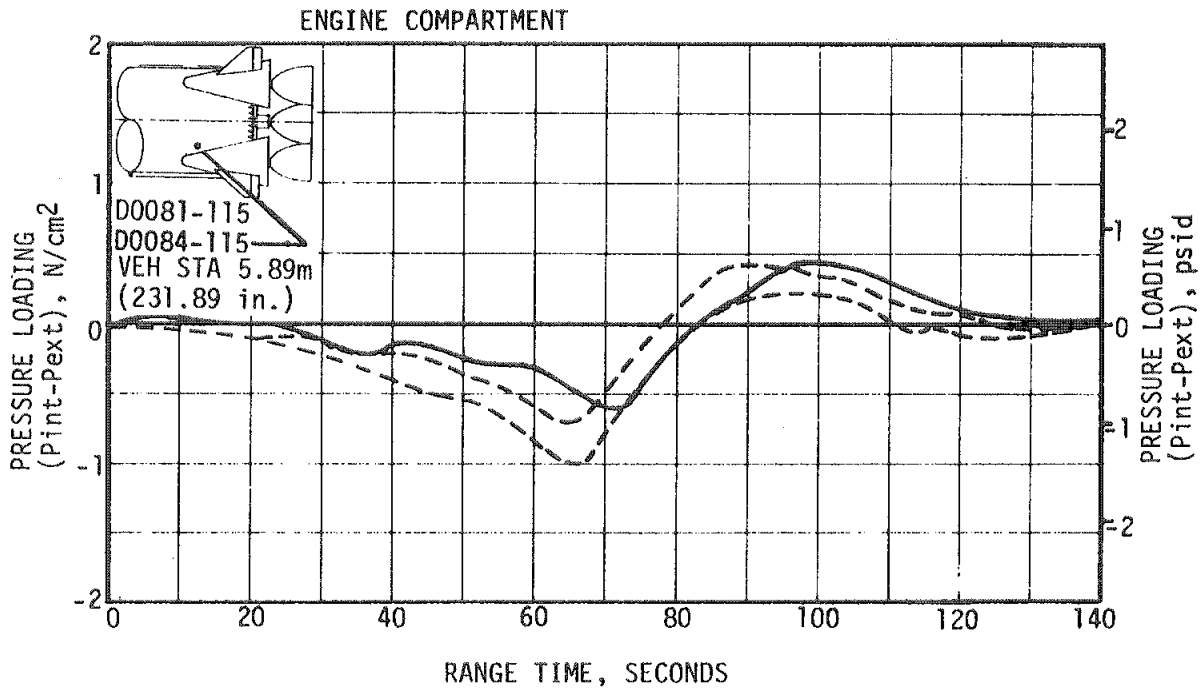
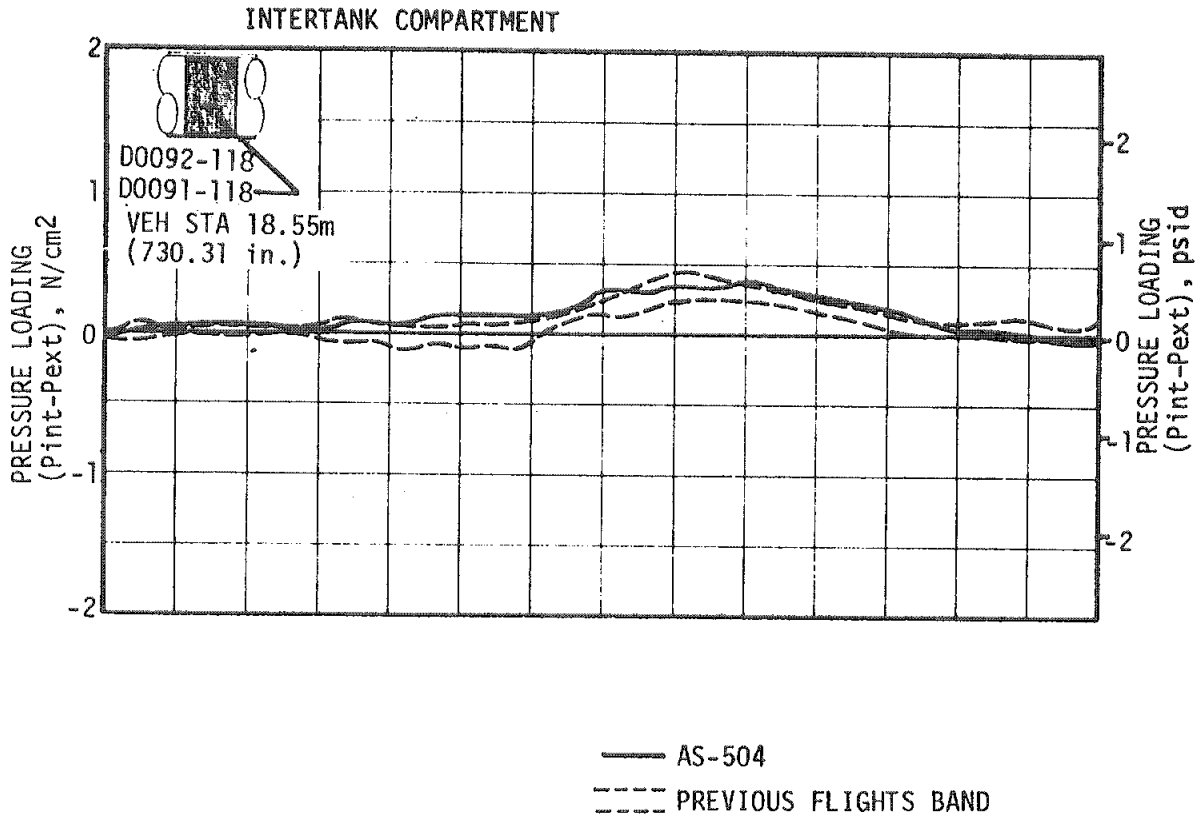


Figure 16-3. S-IC Compartment Pressure Loading

Figure 16-2 shows that the pressure differential experienced the characteristic drop as the vehicle passed through Mach 1. On previous flights, Mach 1 occurred between 60 and 62 seconds, while on AS-504 Mach 1 occurred at 68 seconds. This resulted in a higher peak pressure differential for the AS-504.

The engine and intertank compartment pressure loadings are shown in Figure 16-3. The intertank compartment pressure loading agrees well with previous data. The AS-504 engine compartment pressure loading agreed in magnitude and trend with previous flight data. However, the slower trajectory flown on AS-504 delayed the data peak by 10 seconds.

### 16.2.2 S-II Stage

The pressure loading on the forward skirt of the S-II stage was determined by 14 external absolute pressure measurements (one of which failed), and one internal absolute pressure measurement.

A plot of the pressure loading acting across the forward skirt wall is presented in Figure 16-4. The AS-504 flight data and postflight prediction data are presented in the form of maximum-minimum data bands. The AS-501 through AS-503 flight data bands are also shown for comparison. Both flight and predicted pressures were obtained from the difference between the external pressure values and a single representative internal pressure. The forward skirt pressure loading flight data were well within the design limits and agree with predicted values and previous flight data.

## 16.3 BASE PRESSURES

### 16.3.1 S-IC Base Pressures

Static pressures on the S-IC base heat shield were recorded by four measurements, two of which were heat shield differential pressures. Representative AS-504 data are compared with a band of previous flight data.

S-IC base pressure differential is shown in Figure 16-5 as a function of altitude. In general, the agreement is good between AS-504 base pressure data and previous flight data.

S-IC base heat shield pressure loading is shown in Figure 16-6 as a function of altitude. AS-504 data falls well within the band of previous flight data. The heat shield pressure loading was well within the  $1.38 \text{ N/cm}^2$  (2.0 psid) design differential.

### 16.3.2 S-II Base Pressures

The S-II stage heat shield and thrust cone pressure environment was determined by 6 absolute pressure measurements located on the aft face

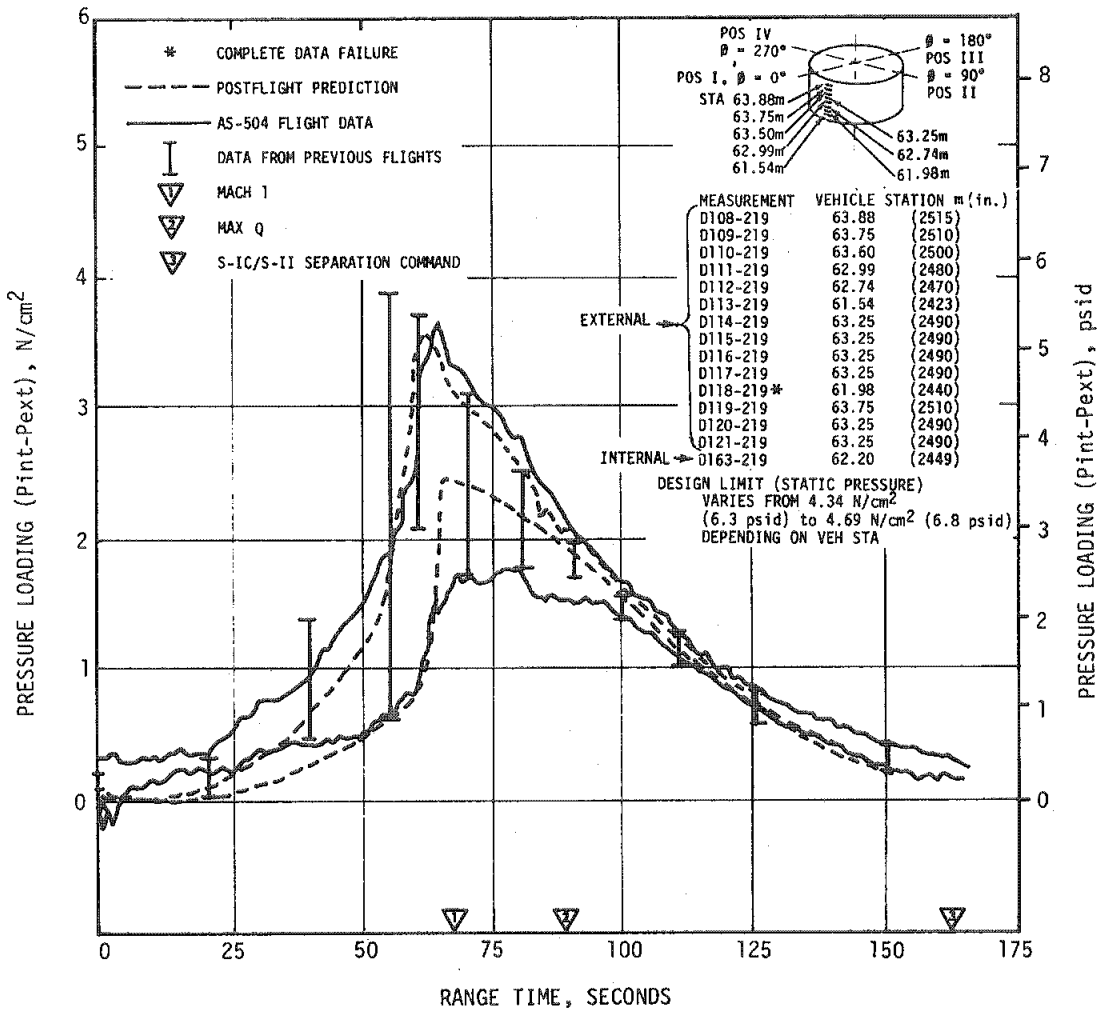


Figure 16-4. S-II Forward Skirt Pressure Loading

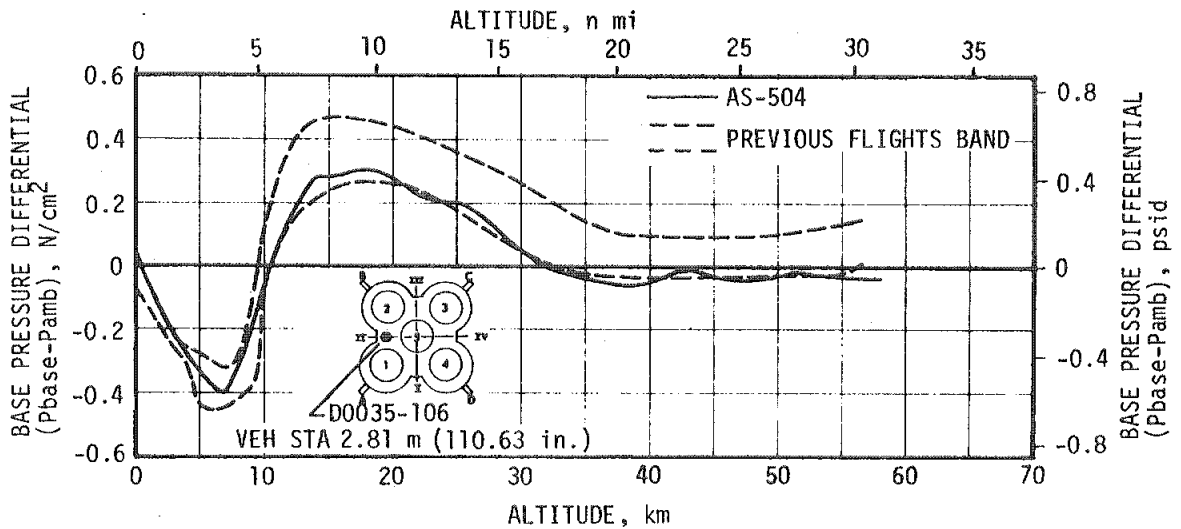


Figure 16-5. S-IC Base Pressure Differential

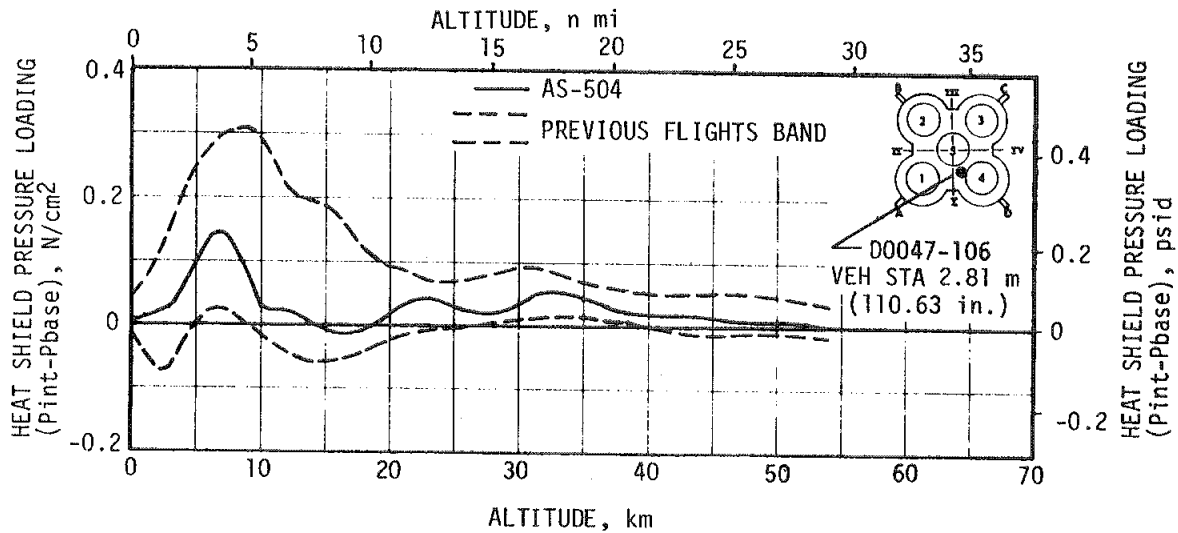


Figure 16-6. S-IC Base Heat Shield Differential Pressure

of the heat shield; by 4 absolute pressure measurements located on the forward face of the heat shield (3 of which failed), and by a single absolute pressure measurement located on the thrust cone.

Figure 16-7 shows the static pressure variation with range time on the forward face of the heat shield and in the thrust cone region. The AS-504 flight static pressure in this region is approximately the same as that measured during previous flights. The pressure peaks observed on previous flights during interstage separation are also present in the AS-504 flight data. The predictions are based on the AS-501 through AS-503 flight data.

Figure 16-8 compares the AS-504 flight heat shield aft face static pressure data with predicted values and prior flight data. In general, the analytical predictions are in fair agreement with the flight data from S-II Engine Start Command (ESC) (164.17 seconds) to Engine Mixture Ratio (EMR) shift (452.5 seconds).

The slow decay of static pressure after interstage separation noted during previous flights was also observed during this flight. The cause of this trend is under investigation.

The pressure increases, observed over the aft surface of the heat shield during S-II aft interstage separation, are probably due to engine exhaust plume impingement on the interstage which causes increased reverse flow and hence increased pressure.

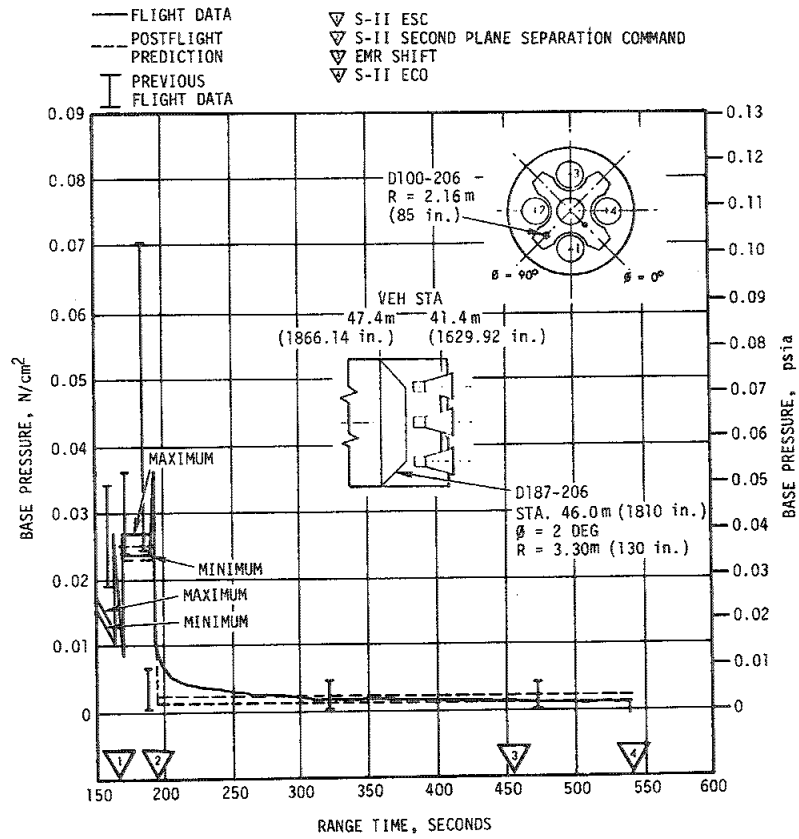


Figure 16-7. S-II Thrust Cone and Base Heat Shield Forward Face Pressures

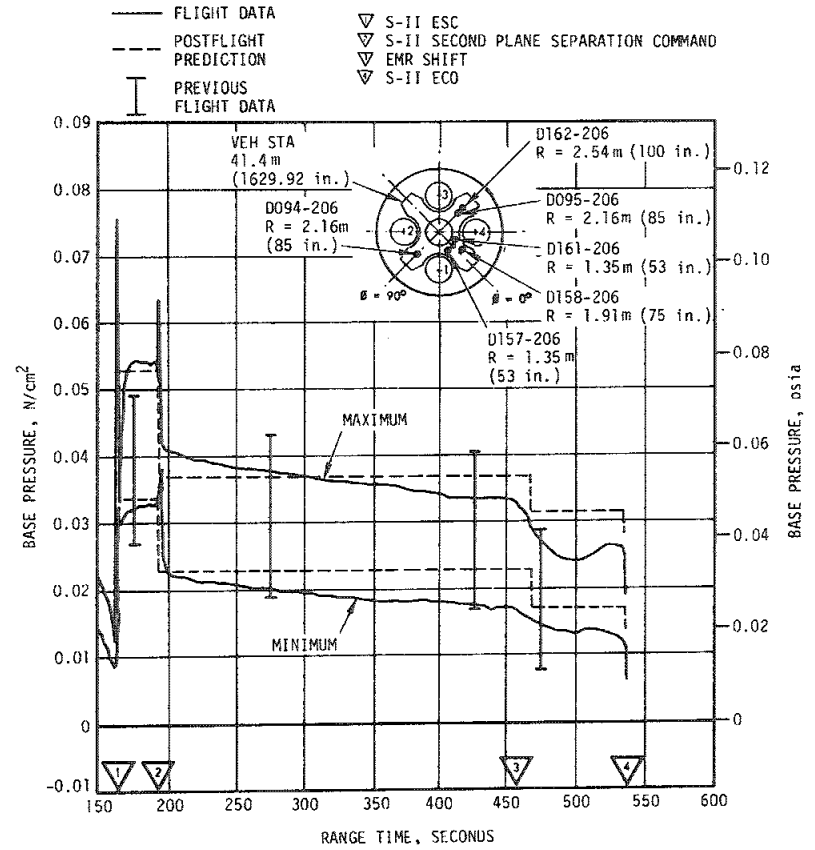


Figure 16-8. S-II Heat Shield Aft Face Pressures

## 16.4 ACOUSTIC ENVIRONMENT

### 16.4.1 External Acoustics

AS-504 external fluctuating pressures were measured at six vehicle stations located on the S-IC aft skirt, Fin D, S-IC intertank, S-II aft skirt, and S-II forward skirt. All recorded data appear valid from liftoff through S-IC boost.

Figure 16-9 presents liftoff sound pressure levels as a function of vehicle body station. The S-II pressure levels show excellent agreement between AS-504 and AS-503. The data scatter between these and AS-501 and AS-502 levels was due to changes in radial position at a fixed vehicle station. S-II data indicate the highest levels were experienced at Position IV, and the lowest at Position II. A significant amount of data scatter is evident only in S-IC measurements. A review of upper stage and S-IC liftoff power spectra shows the only significant variation occurs in high frequency content. A high frequency source, primarily affecting the S-IC, is the supersonic core of the exhaust flow between the engine exit planes and exhaust flow deflectors. In this flow region, small thrust variations between flights may alter the total produced acoustic energy more substantially than in the deflected flow, resulting in larger deviations in high frequency data. A second factor in S-IC data scatter is the time at which overall levels and spectra are computed. Spectra computed at 1 to 3 seconds after liftoff show increases below 200 hertz. This increase may be caused by some turbulent mixing beneath the Launch Umbilical Tower (LUT) deck due to vehicle motion and the related development of low frequency sources. The AS-504 S-IC intertank data computed from 1 to 2 seconds, showed this effect and it is responsible

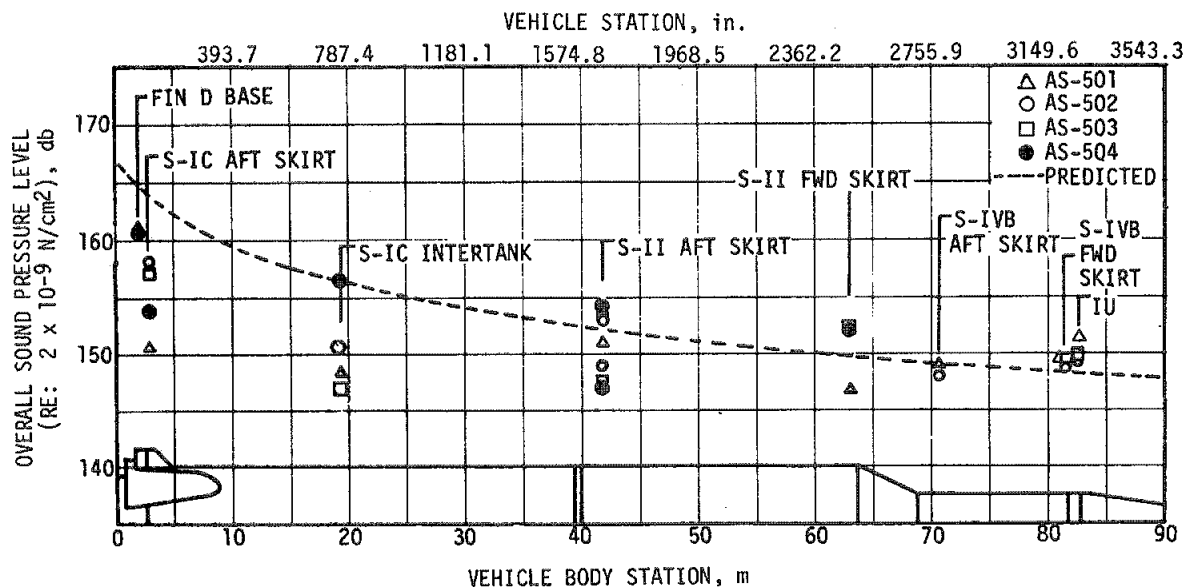


Figure 16-9. Vehicle External Overall Sound Pressure At Liftoff

for some of the level increase from previous flights which was computed 1 to 2 seconds earlier.

Figures 16-10 through 16-12 present AS-504 overall fluctuating pressure time histories for S-IC boost. A representative time history from previous flights is also presented for comparison. Any significant changes in the various flights are represented in the included time histories. AS-504 overall time histories generally display a reduction in level and maximum levels occur later in flight due to the slower AS-504 trajectory. Significant deviations, 5 to 6 decibels, from previous flights occurred at the S-IC intertank and at Position II on the S-II aft skirt. S-IC intertank data differ significantly in level from 0 to 35 seconds, and after 60 seconds of flight. The first period of level increase was expected, due to the slowness of the AS-504 trajectory since engine noise impingement is essentially a function of vehicle motion. The increased levels after 60 seconds are unaccountable. The level variation between AS-503 and AS-504 at Position II on the S-II aft skirt appears to be caused by trajectory differences. The measurement on the rear of fin D (B0004-114) was exposed to direct light fluctuation

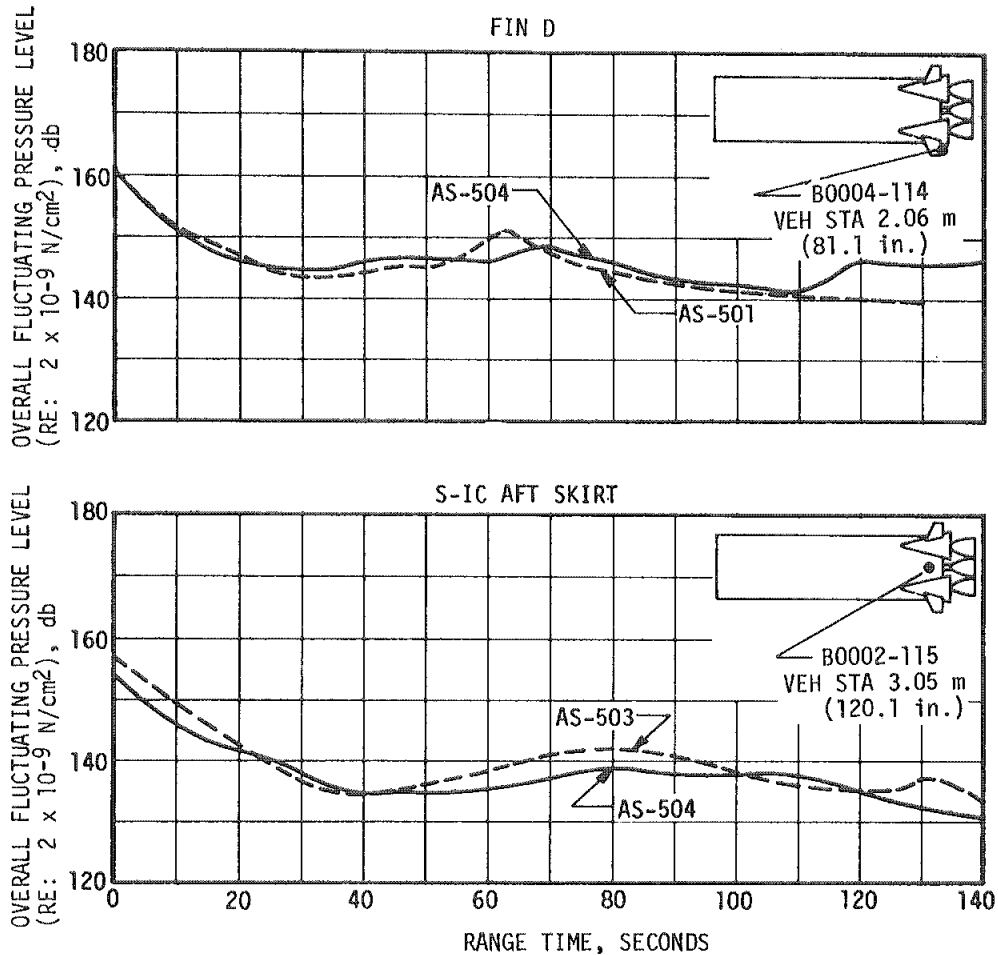


Figure 16-10. S-IC External Overall Fluctuating Pressure Level



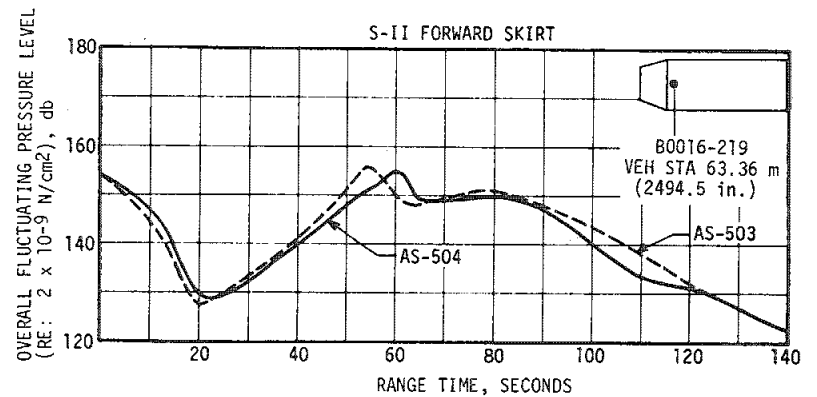
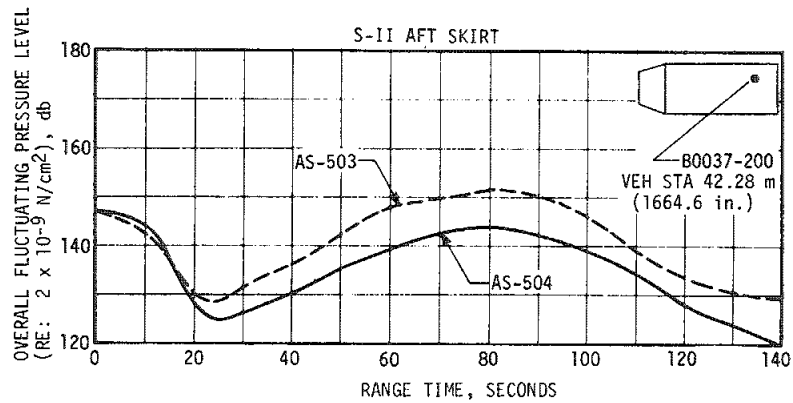
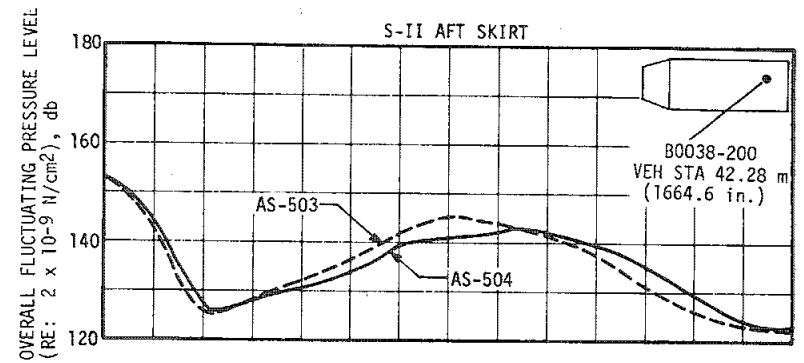
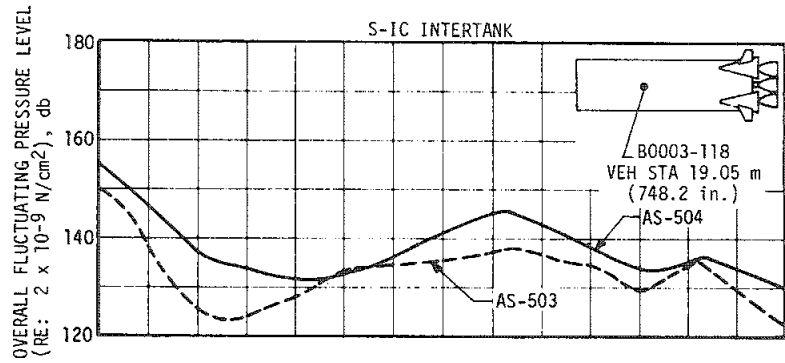


Figure 16-11. S-IC and S-II External Overall Fluctuating Pressure Level

Figure 16-12. S-II External Overall Fluctuating Pressure Level

from the exhaust flow. Since microphones are sensitive to light variations, such effects may be indistinguishable from signals of acoustic origin.

#### 16.4.2 Internal Acoustics

16.4.2.1 S-IC Stage. Internal acoustics were measured at two locations on the S-IC stage. One measurement was located in the intertank section and the other in the thrust structure above the heat shield. The acoustic data at these locations are shown in Figures 16-13 and 16-14. Data from both measurements agree with previous flight data except that the sound pressure level in the intertank was lower in the Mach 1 and Max Q periods than on previous flights.

16.4.2.2 S-II Stage. The two internal microphones used on the S-II stage are located on the forward skirt and thrust cone. Figure 16-15 presents the internal overall acoustic levels versus range time for AS-504. Previous flight data are also shown for comparison. The internal acoustics show good agreement with previous flight data during liftoff. AS-504 internal and external acoustics are shown in Table 16-1 and compared with data from previous flights. The differentials between corresponding external and internal acoustic levels are approximately 15 to 18 decibels at liftoff. The differentials for Mach 1 and Max Q conditions are 18 decibels or higher because the greater high frequency contents are more attenuated across the vehicle skin.

MEASUREMENT	MAXIMUM SPL <span style="font-size: small;">(1)</span>		OVERALL SPL LIMIT	LEGEND
	PREVIOUS FLIGHT DATA	AS-504		
B005-106	144.6 at -1.0	144.8 at 0	169.0	--- PREVIOUS FLIGHT DATA — AS-504 FLIGHT DATA

(1) SPL in db referenced to  $2 \times 10^{-5}$  N/m<sup>2</sup>

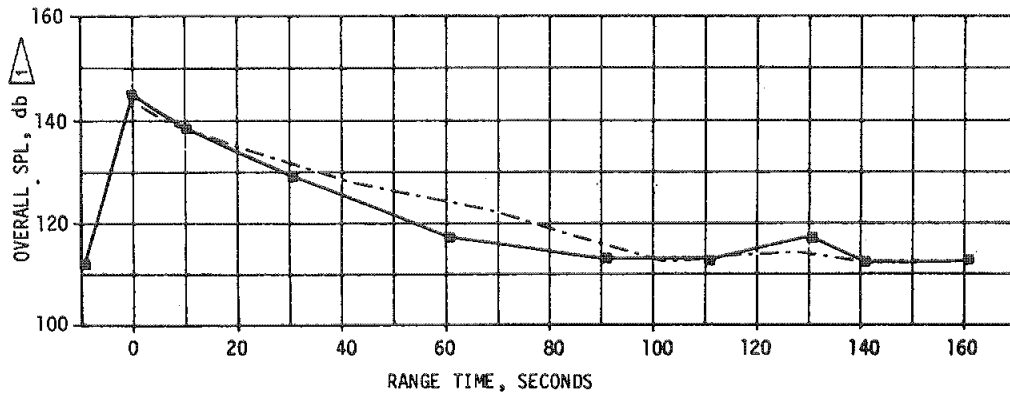




Figure 16-13. S-IC Heat Shield Panels Internal Acoustic Environment

MEASUREMENT	MAXIMUM SPL		OVERALL SPL LIMIT	LEGEND
	PREVIOUS FLIGHT DATA	AS-504		
B001-118	142.3 at 0.5	144.7 at 0	157	 PREVIOUS FLIGHT DATA ENVELOPE  AS-504 FLIGHT DATA

 SPL in db referenced to  $2 \times 10^{-5} \text{ N/m}^2$

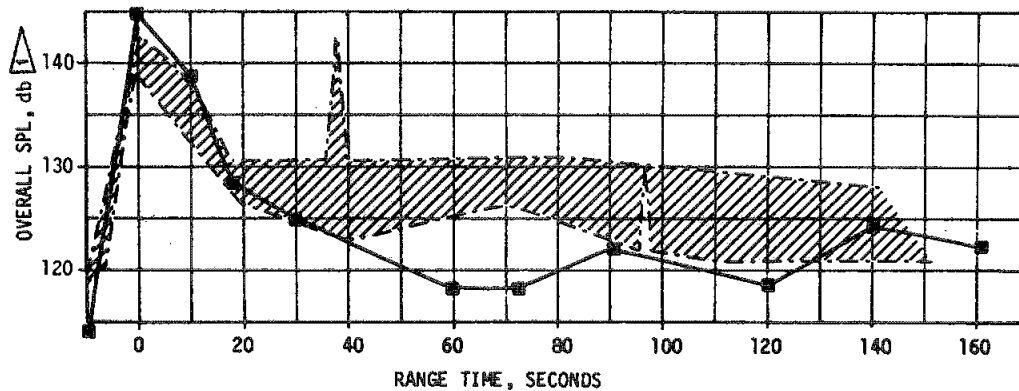
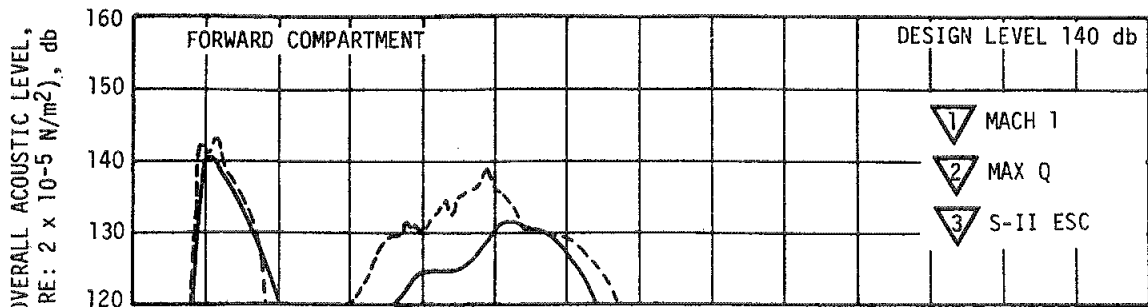


Figure 16-14. S-IC Intertank Internal Acoustic Environment



— AS 504  
 - - - AS 502, AS 503

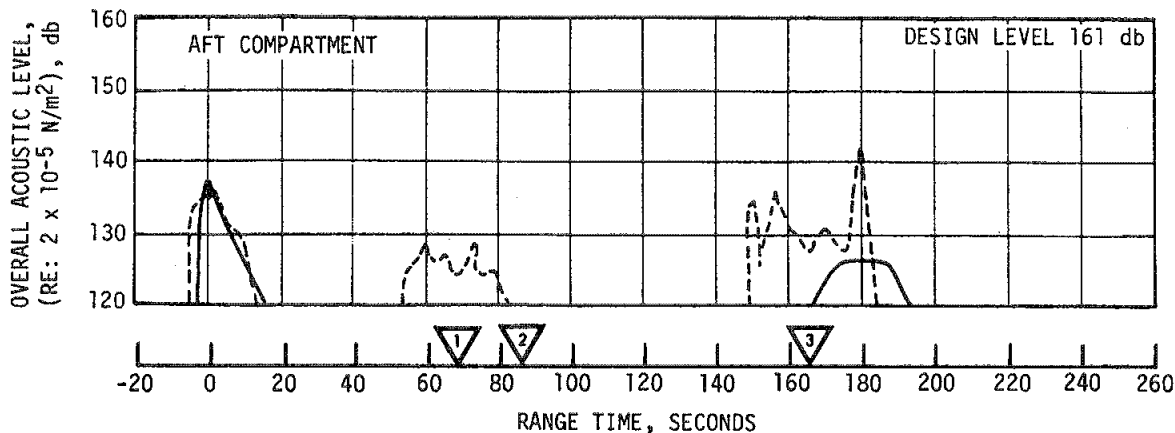


Figure 16-15. S-II Internal Acoustics History

Table 16-1. Sound Pressure Level Comparison of AS-504  
With AS-501, AS-502 and AS-503 Data

EVENT	Maximum Overall db							
	Forward Compartment				Aft Compartment			
	External (B016-219)		Internal (B017-219)		External (B037-200 & B038-200)		Internal (B039-206)	
	AS-504	AS-501/ 503	AS-504	AS-501/ 502/503	AS-504	AS-501/ 503	AS-504	AS-501/ 502/503
Liftoff	154.0	152.9	139.1	142.0	153.7	152.7	135.1	137.5
Transonic	154.2	156.5	125.5	133.0	140.9	147.8	109.8	129.0
Max Q	149.9	151.2	131.6	138.0	143.7	152.2	114.1	129.0

NOTE: AS-503 and AS-504 acoustic measurement locations were different from previous flights.

## SECTION 17

### VEHICLE THERMAL ENVIRONMENT

#### 17.1 SUMMARY

The AS-504 S-IC base region thermal environment was similar to that experienced on earlier flights with the exception of minor changes due to trajectory differences. Since altitude was not gained as rapidly as for previous flights and the total burn time was longer, there was a small increase in total radiant heating. However, heat shield temperatures and structural temperatures forward of the heat shield were generally within the bands of previous data and well below design allowances. Reversed flow of engine exhaust reached the heat shield 5 to 10 seconds later than for previous flights, and the radiant heating peak was displaced a proportionate amount; both are functions of altitude. As has occurred on all flights to date, loss of M-31 insulation material was again noted. Combined vibration and thermal ground testing has indicated that loss of M-31 is not detrimental to vehicle performance.

S-IC forward skirt skin temperatures were higher during flight and separation than on previous flights, due to removal of insulation from this area. However, these increases were small and presented no problems.

Base thermal environments on the AS-504 S-II stage were similar to those measured on previous flights and were well below design limits. The base region probe temperatures and base heat shield heating rates were lower than corresponding AS-503 values. The assessed cause was that the AS-504 S-II stage engines were toed out slightly more than for previous flights.

The aeroheating rates on the AS-504 S-II stage interstage, body structure, and fairings, though slightly lower, were similar to those on previous flights.

#### 17.2 S-IC BASE HEATING AND SEPARATION ENVIRONMENT

##### 17.2.1 S-IC Base Heating

Thermal environments in the base region of the S-IC stage were recorded by 29 measurements which were located on the heat shield and F-1 engines.

This instrumentation included 6 radiation calorimeters, 16 total calorimeters, and 7 gas temperature probes. Representative data from these instruments are compared with the AS-502 and AS-503 flight data band in Figures 17-1 and 17-2. AS-501 flight data, which was significantly different from subsequent flight data because of flow deflector effects, is not shown.

AS-504 S-IC base thermal environments are similar in magnitude and show the same trends as those measured during the AS-502 and AS-503 flights, as shown in Figures 17-1 and 17-2. AS-504 radiation heating rates were slightly higher than on AS-503, but agree more closely with AS-502. Maximum values of radiation and total heating rate occur at altitudes between 15 and 20 kilometers (8.1 and 10.8 n mi). The maximum total heating rate measured in the AS-504 base region was  $35 \text{ watt/cm}^2$  ( $30.84 \text{ Btu/ft}^2\text{-s}$ ) recorded on the nozzle lip of engine 101. Center engine cutoff (CECO) on AS-504 produced a spike in environmental data with a magnitude and duration similar to previous flight data at CECO. AS-504 base gas temperatures show good comparison with AS-502 and AS-503 flight data. In Figures 17-1 and 17-2, the thermal environments are shown versus altitude to minimize trajectory differences. Similar comparisons of heating rate versus flight time (not shown) illustrate very clearly the trajectory differences between AS-504 and previous flights. At a given time in flight, AS-504 was at a lower altitude than previous flight vehicles. Therefore, initial gas recirculation into the base (resulting from plume expansion and impingement which is principally a function of altitude) occurred at a later range time and produced a corresponding shift in the time of peak heating. AS-504 peak heating rates agree closely with AS-502 in magnitude but occurred 5 to 10 seconds later than AS-502 because of the trajectory difference.

The available heat shield temperature data is compared to previous flight data in Figures 17-3 and 17-4. Instrumentation has been reduced since AS-503. The two forward surface measurements, shown in Figure 17-3, are generally within the band of previous data. However, C038-115 (3.05 meters (120 in.) from the center on Position Line II) exceeded all previous data for the last 30 seconds of flight. This is attributed to higher radiant heating than that experienced during prior flights. C042-115 (Figure 17-5) is substantially cooler than C038-115 because it is located in an area less exposed to radiant heating than surfaces on the position lines where maximum heating occurs. In Figure 17-4, one bondline measurement, C029-106, shows thermal response attributed to local M-31 loss. The reconstructed curve was calculated, assuming 0.407 centimeter (0.16 in.) of M-31 was lost at 100 seconds, using the flight gas temperature from C052-106, flight radiation data from C151-106, and the design heat transfer coefficients. M-31 loss has occurred on every flight to date. However, extensive combined vibration and thermal tests indicate that M-31 loss during flight is not detrimental to vehicle performance. The two other measurements were as expected.

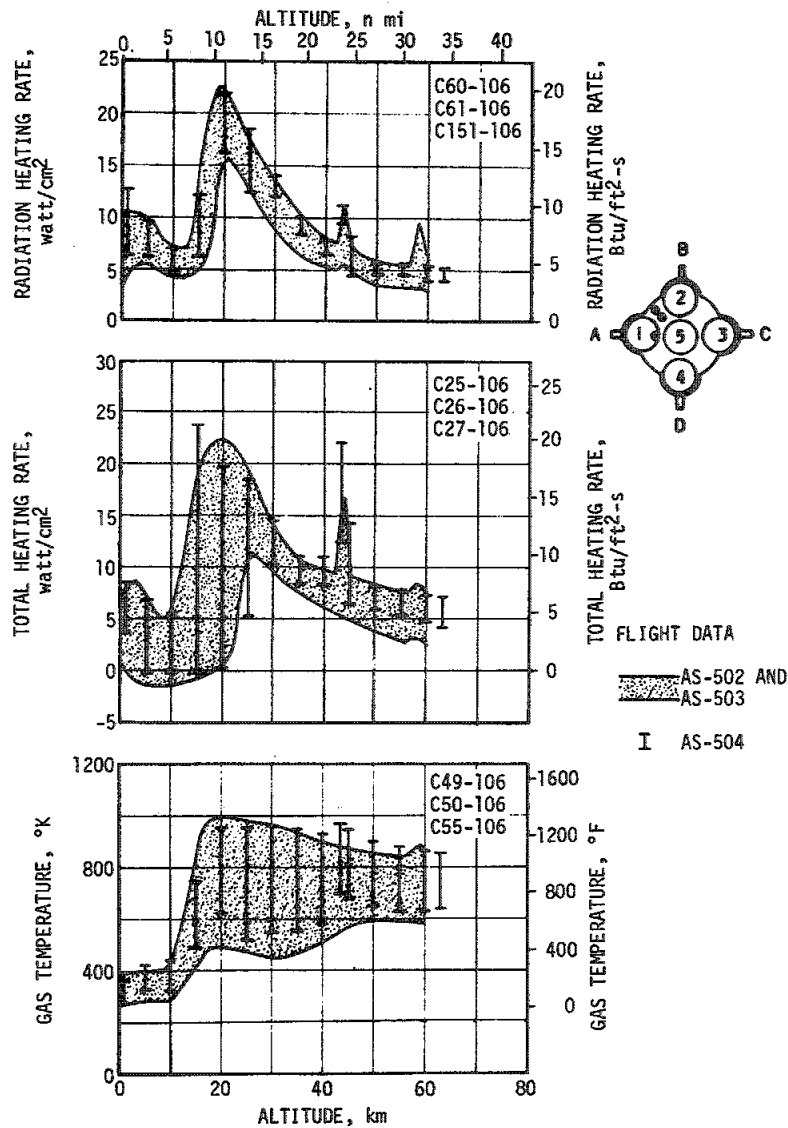


Figure 17-1. S-IC Base Heat Shield Thermal Environment

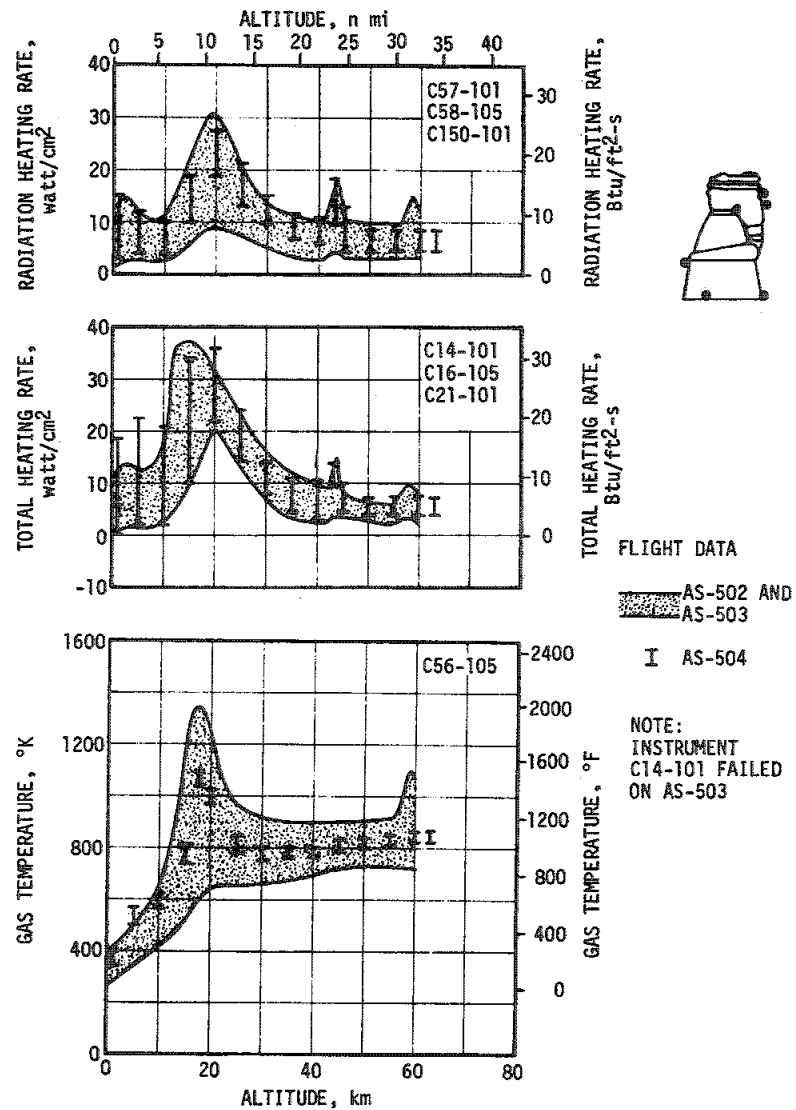


Figure 17-2. F-1 Engine Thermal Environment

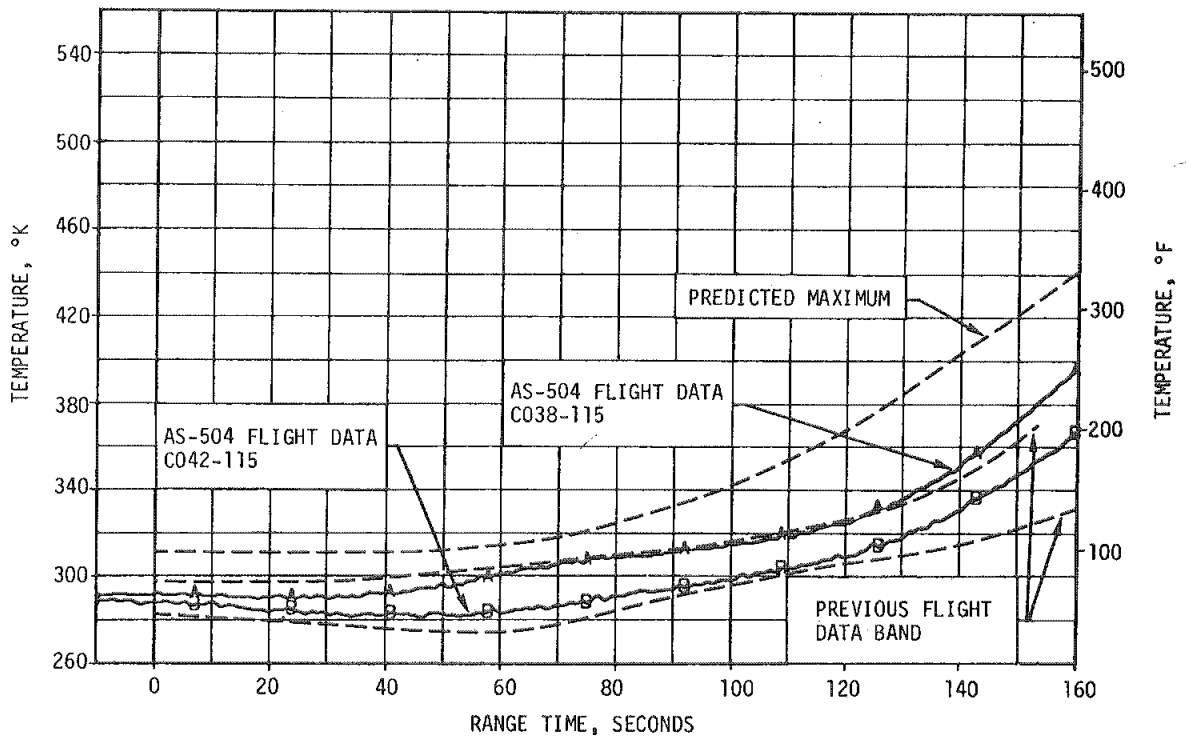


Figure 17-3. S-IC Heat Shield Forward Surface Temperature

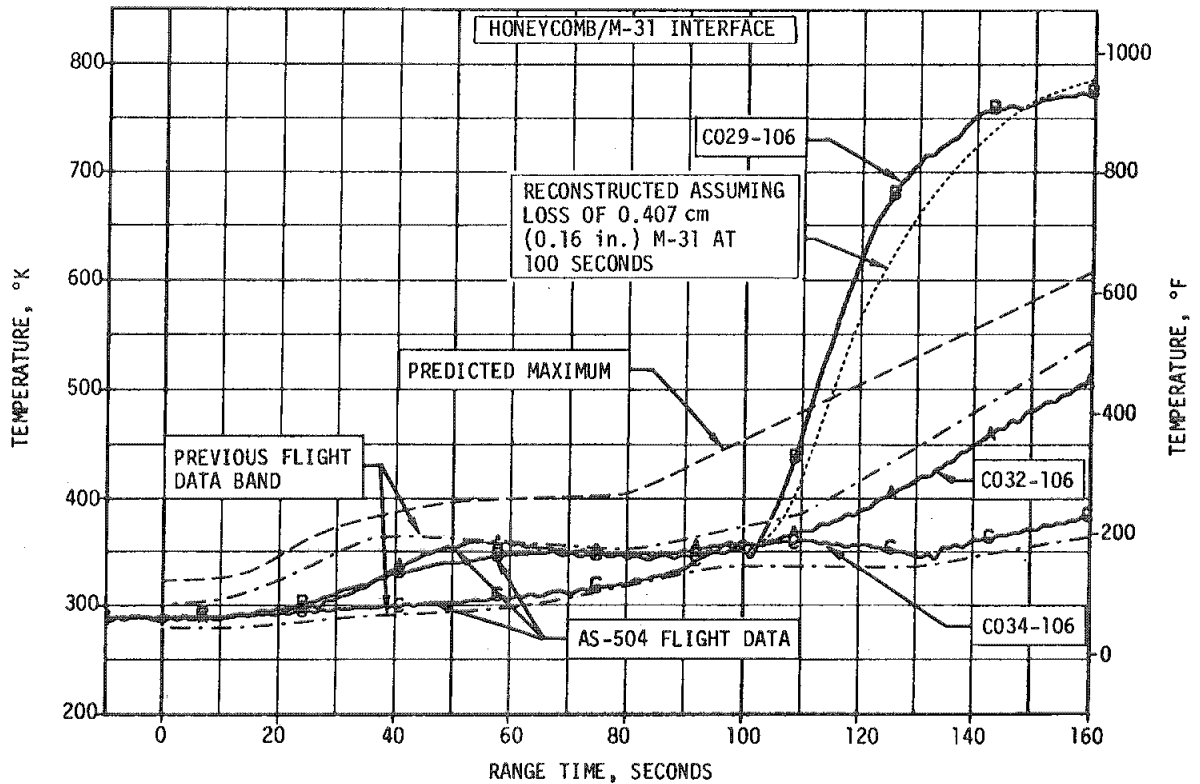


Figure 17-4. S-IC Heat Shield Bondline Temperature



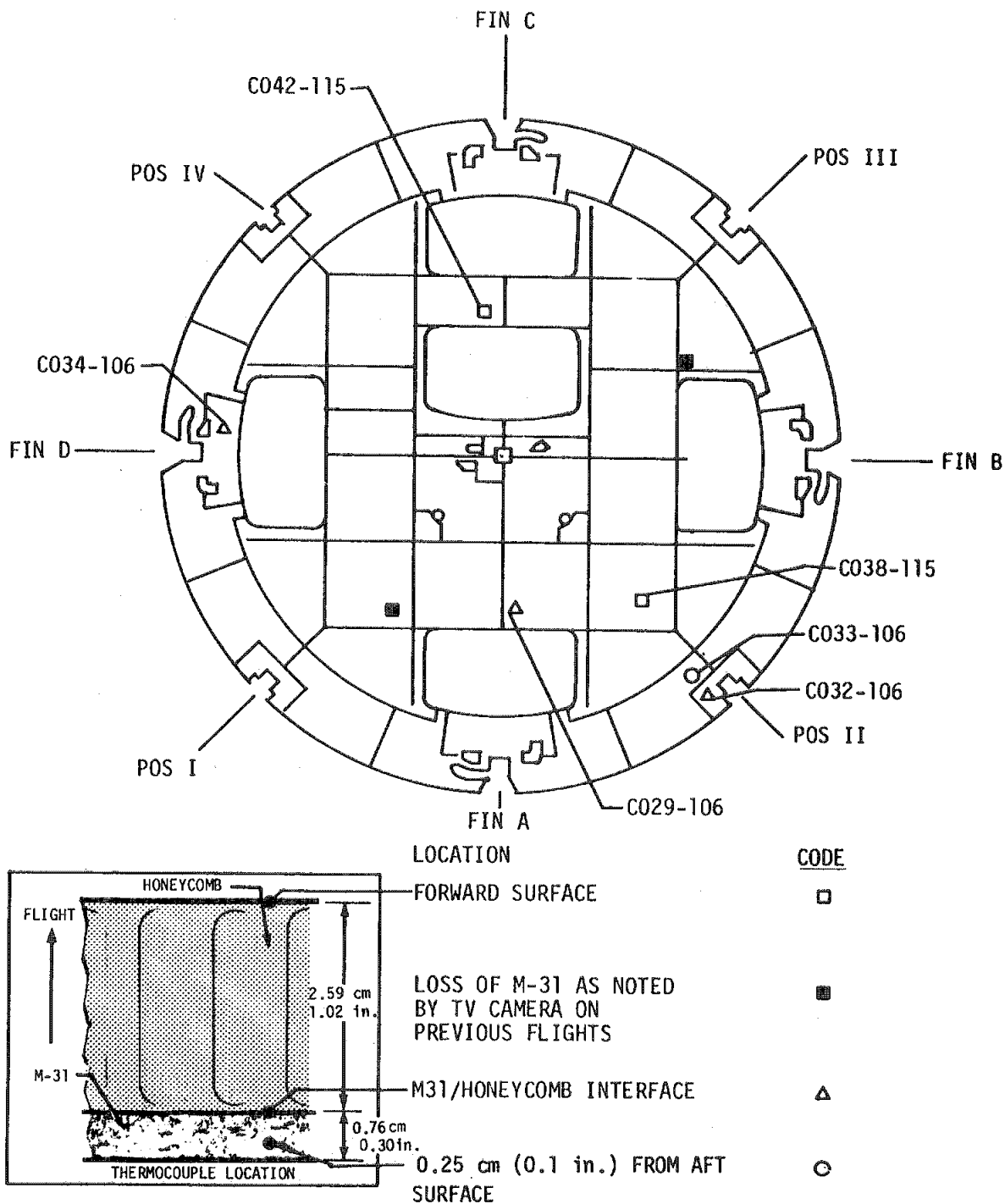


Figure 17-5. S-IC Base Heat Shield Measurement Locations

Engine temperature data was normal. The thermal response of the turbine exhaust manifold, under the insulation on the inboard side of engine No. 1, is shown in Figure 17-6. The measurement trace falls within the band of previous flight data. Temperatures under the insulation on the gimbal actuator and on the fuel discharge line were well below design allowables, while gas temperature under the engine cocoons remained within the band of previous flight data.

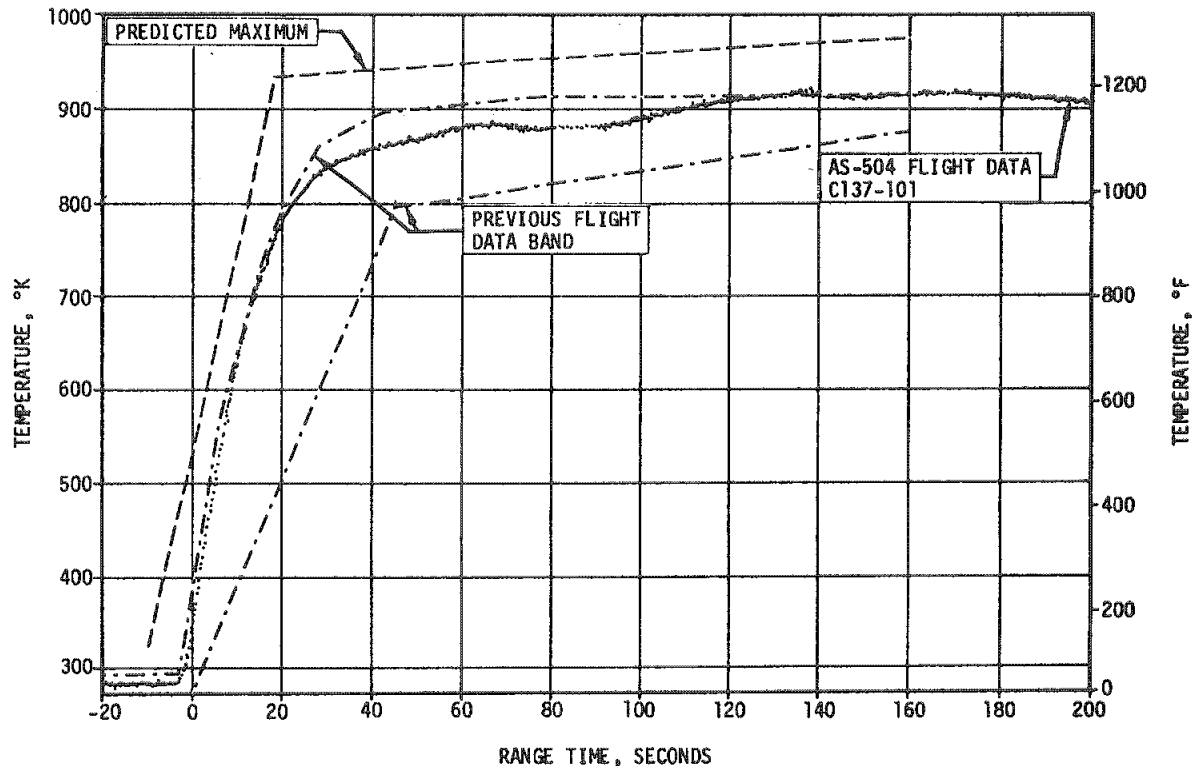


Figure 17-6. S-IC Temperature Under Insulation, Inboard Side Engine No. 1

### 17.2.2 S-IC/S-II Separation Environment

Forward skirt compartment gas temperatures, shown in Figure 17-7, were similar to those encountered during separation on previous flights. Two spikes in the gas temperature were noted. The first spike was due to the S-II ullage motor burn and the second spike was due to J-2 engine plume. Peak temperatures, due to J-2 engine plume, 3.8 seconds after separation may have reached slightly higher peaks than those shown, since data at this point exceeded the upper limit of the transducers requiring extrapolation between 3.5 and 4.5 seconds after separation.

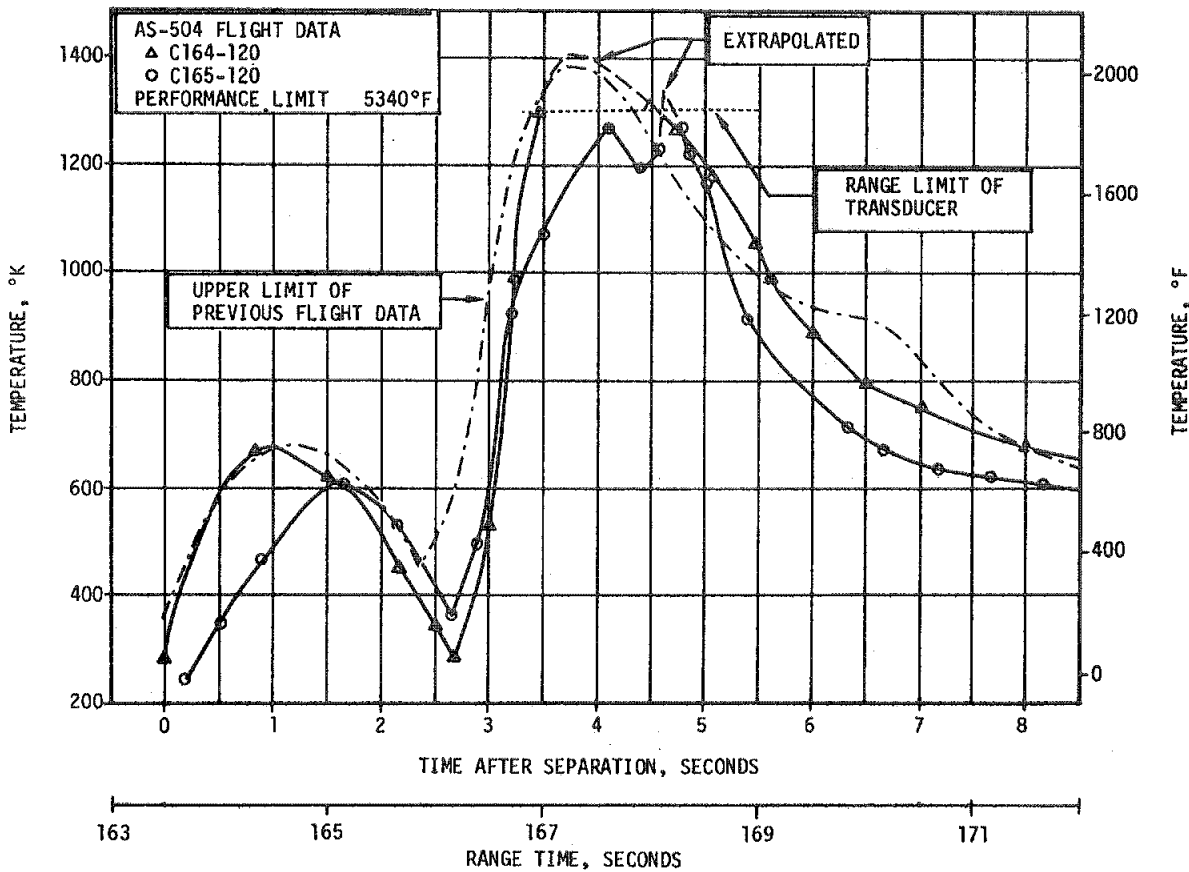


Figure 17-7. S-IC Upper Compartment Ambient Air Temperature During S-IC/S-II Stage Separation

### 17.3 S-II BASE HEATING AND SEPARATION ENVIRONMENT

Figure 17-8 presents total heating rate data recorded throughout S-II boost by calorimeters located on the aft face of the base heat shield. The postflight heating rate predictions and AS-501 through AS-503 flight data are shown for comparison. As shown in Figure 17-8, the AS-504 flight data are in good agreement with the analytical predictions and with previous flight data. The decrease in Engine Mixture Ratio (EMR) at 452.5 seconds range time resulted in a reduction of about 25 percent in heating rate on the aft face of the base heat shield. The ASI line modifications, first installed on the AS-503 vehicle, were again verified for the AS-504 vehicle.

Heating rates on the base heat shield, shown in Figure 17-8, indicate that the AS-504 flight data maximums were lower throughout S-II boost than during previous flights. This reduction in base heating rates is believed due to the fact that the AS-504 S-II stage engines were toed out slightly more than were the S-II stage engines during previous flights. The initial engine precant angle employed, coupled with the degree of structural compliance of the stages in question, caused this condition.

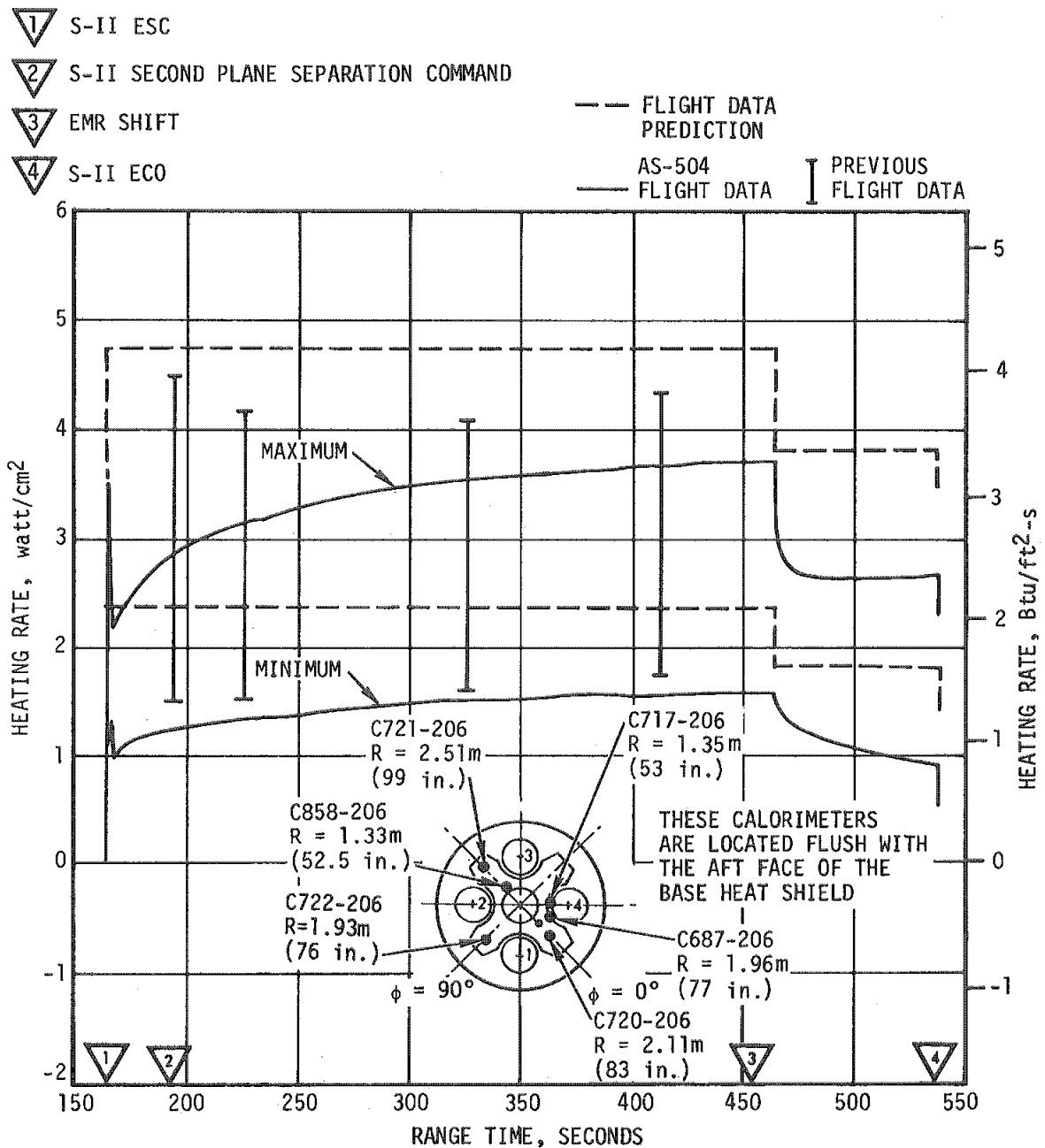


Figure 17-8. S-II Heat Shield Base Region Heating Rates

The total heating rates measured on the thrust cone region are presented in Figure 17-9. Predicted values together with AS-501 through AS-503 flight data maximum and minimum values are shown for comparison. The AS-504 flight data agree well with the analytical predictions and previous flight data, except as follows. As shown in Figure 17-9, the data band of total heating rates for AS-501 through AS-503 flights is wider prior to interstage separation when compared with the present flight data.

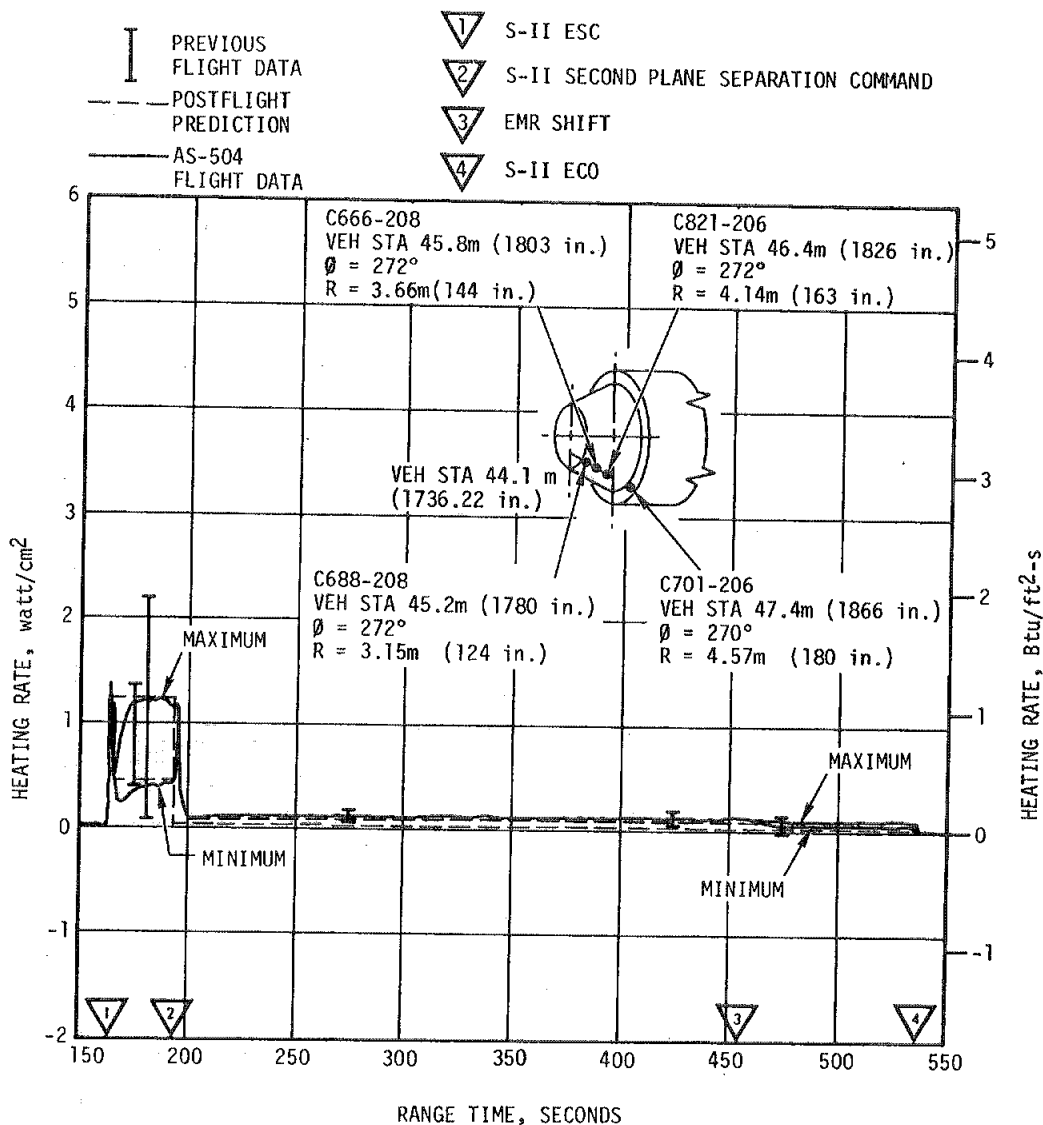


Figure 17.9. S-II Thrust Cone Heating Rate

The AS-504 flight base region gas recovery temperature-probe temperature time history is shown in Figure 17-10 together with AS-503 minimum and maximum values. Note that the flight values are the probe temperatures and not the gas recovery temperatures. The corresponding predicted probe temperature histories are also shown in Figure 17-10. The predicted gas recovery temperature was calculated based on the above probe temperatures and the measured base heat shield total heating rates. The recovery temperature of the reversed flow gas was determined to be 822°K (1020°F) prior to EMR stepdown, and 783°K (950°F) after EMR stepdown. The AS-504 flight indicated probe temperatures were slightly lower than the corresponding AS-503 values. This was due to the reduction in base region total heating rates previously discussed.

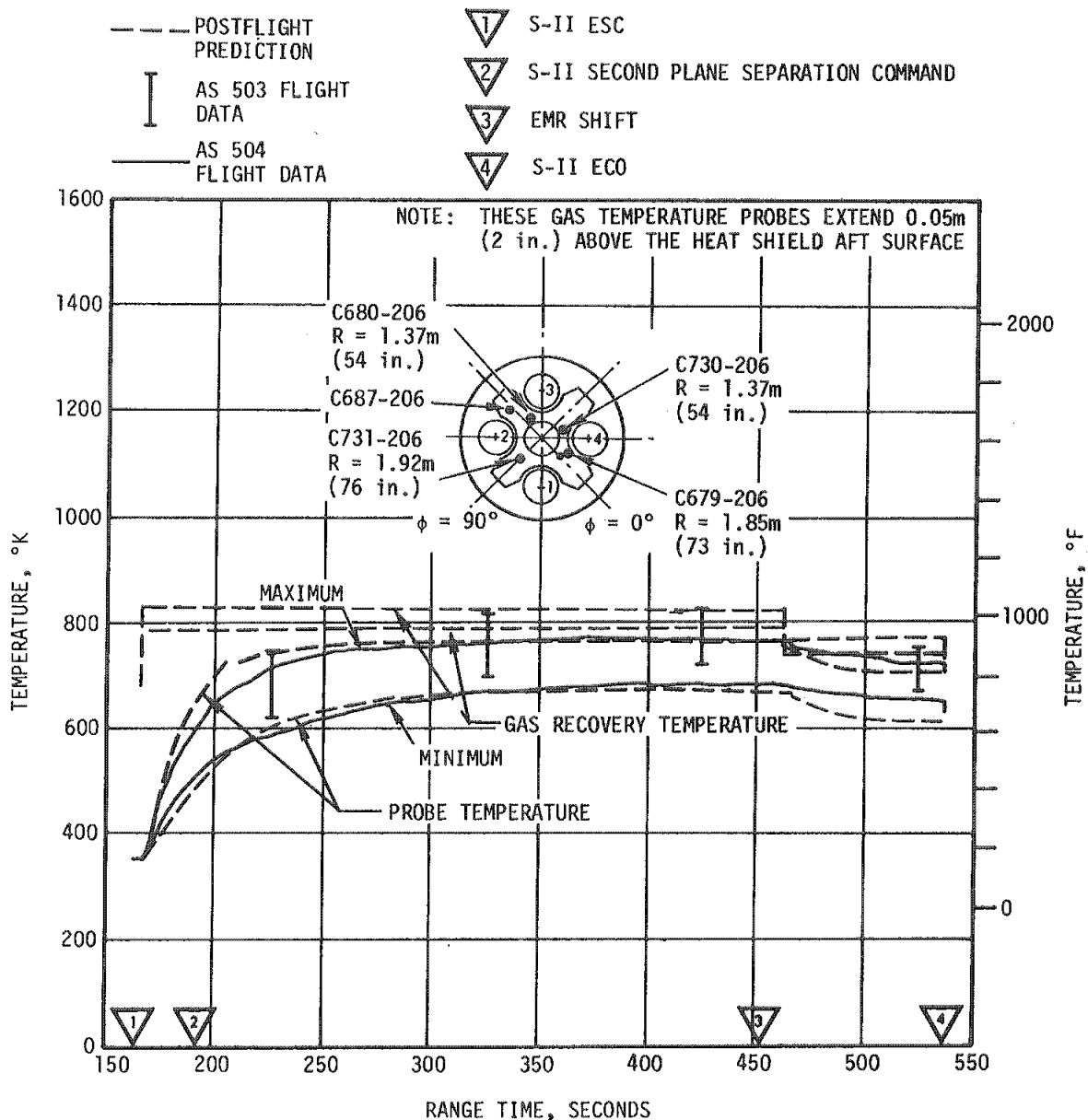
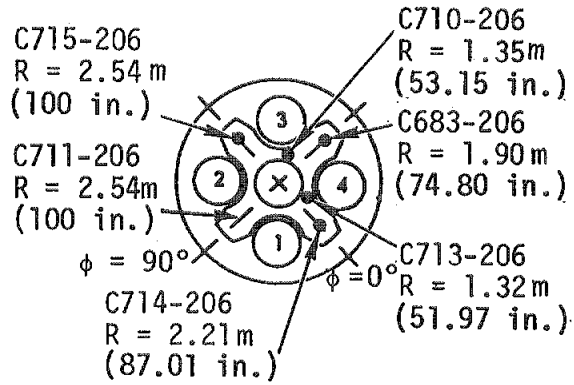


Figure 17-10. S-II Base Gas Temperature

Temperatures recorded on the aft face of the base heat shield during the AS-504 flight were well below design values, and compared favorably with temperatures from previous flights. Figure 17-11 presents a comparison of AS-504 flight data with data from previous flights and design temperatures. The maximum AS-504 temperature of 745°K (880°F) occurred at 452.5 seconds (EMR Shift), and was slightly lower than the previously recorded maximum of 764°K (915°F). The design temperatures were calculated using the maximum design environment.

THESE SURFACE TEMPERATURE MEASUREMENTS ARE LOCATED FLUSH WITH THE AFT FACE OF THE HEAT SHIELD



- DESIGN PREDICTION
- PREV FLIGHT DATA
- AS-504 FLIGHT DATA

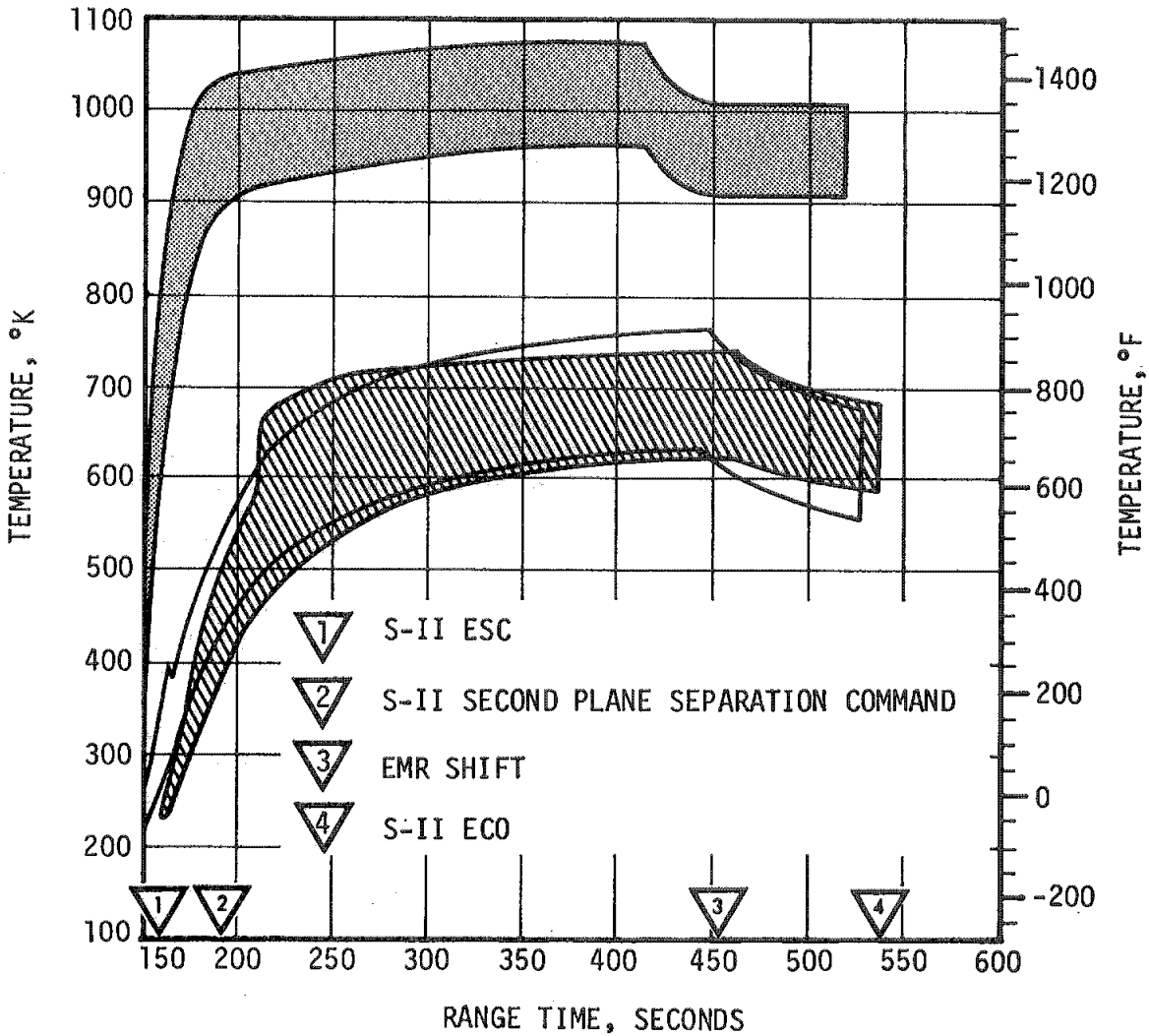


Figure 17-11. S-II Heat Shield Aft Face Temperatures

The effectiveness of the heat shield and flexible curtains as a thermal protection system was demonstrated by the relatively low temperatures of the heat shield (forward surface) thrust cone, center engine beam and equipment container when compared to the high temperature on the heat shield aft surface. The range of heat shield forward surface temperatures measured on AS-504 was below design and similar to the range of temperatures measured on previous flights, as shown in Figure 17-12. Maximum AS-504 temperatures of 285°K (50°F), 274°K (30°F) and 343°K (155°F) were recorded on the thrust cone, center engine beam, and 208 equipment container, respectively. These temperatures are in good agreement with previous flight data and are well below their respective design values.

## 17.4 VEHICLE AEROHEATING THERMAL ENVIRONMENT

### 17.4.1 S-IC Stage Aeroheating Environment

Aerodynamic heating environments were measured with thermocouples attached to the backside of the structural skin on the S-IC forward skirt and intertank. Generally, the aerodynamic heating environments were within previous flight data bands, with the exception of skin temperature measurements on the AS-504 uninsulated forward skirt. The forward skirt skin temperature measurements were, however, below design limits.

Measured skin temperatures and derived heating rates for the S-IC intertank are shown in Figure 17-13. Postflight simulations of skin temperatures and heating rates are also presented. These simulations are based on analytically determined heat-transfer coefficients and recovery temperatures until flow separation reaches the intertank. During the period of flow separation a radiation heating environment, determined from previous flight data (AS-502 and AS-503), is used in the simulation. Good correlation was obtained between the flight data and the simulations.

The S-IC forward skirt skin temperatures and derived heating rates are presented in Figures 17-14 and 17-15. Insulation was not installed on the AS-504 S-IC forward skirt skin surface; therefore, skin temperatures recorded by measurements C64-120, C322-120 and C323-120 were higher than recorded on previous flights (AS-501, AS-502 and AS-503). Postflight simulations of skin temperatures and heating rates are presented in Figure 17-15 for measurements C322-120 and C323-120. These measurements were located in a wake area downstream of the S-II ullage fairing. The simulations are based on analytically determined heat-transfer coefficients and recovery temperatures and protuberance factors, where applicable, from wind tunnel test data. Protuberance heating effects on the S-IC forward skirt could not be determined from the available flight data.

Flow separation on the AS-504 flight was observed, from Airborne Light Optical Tracking System (ALOTS) data, to occur at approximately 118 seconds. The forward point of flow separation versus flight time is plotted in Figure 17-16. The flow separation region dropped back and re-established at a lower level after CECO. The effects of CECO on the separated flow region during AS-504 flight were the same as observed on AS-503.



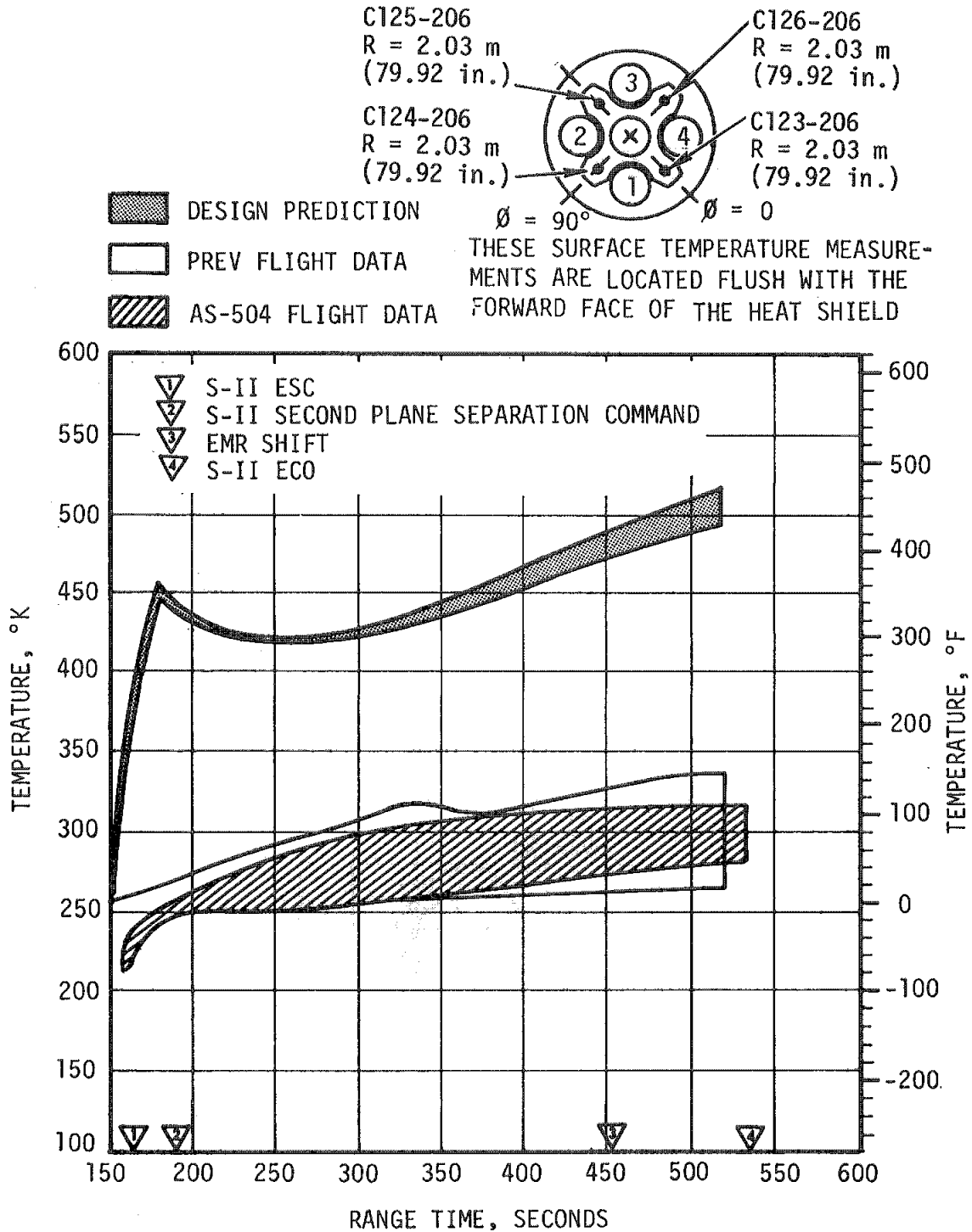


Figure 17-12. S-II Heat Shield Forward Face Temperature

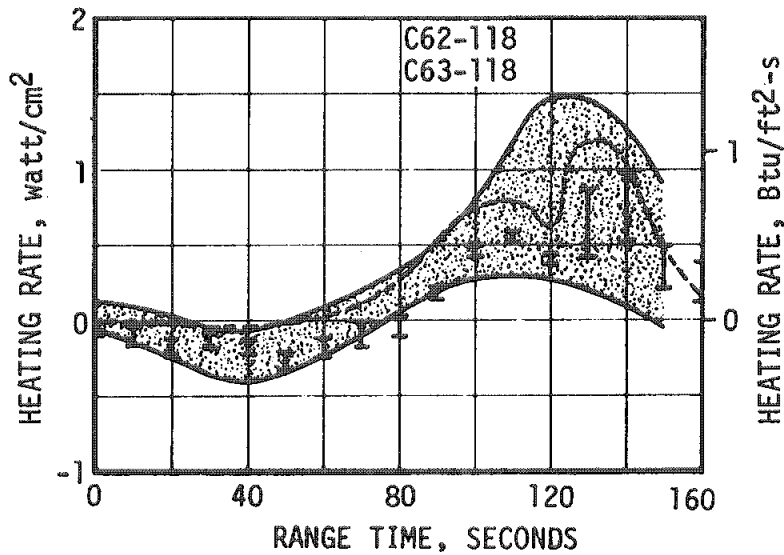
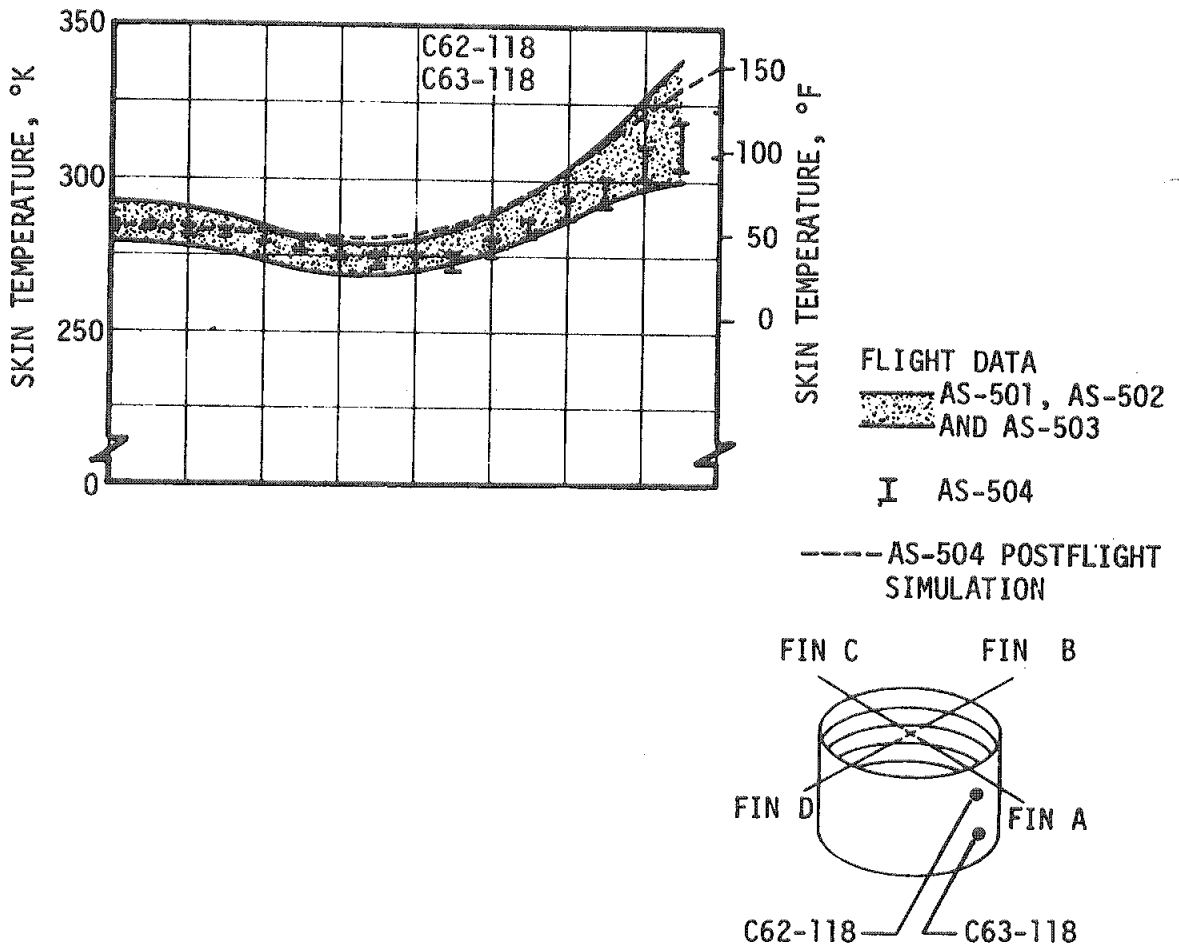


Figure 17-13. S-IC Intertank Aerodynamic Heating

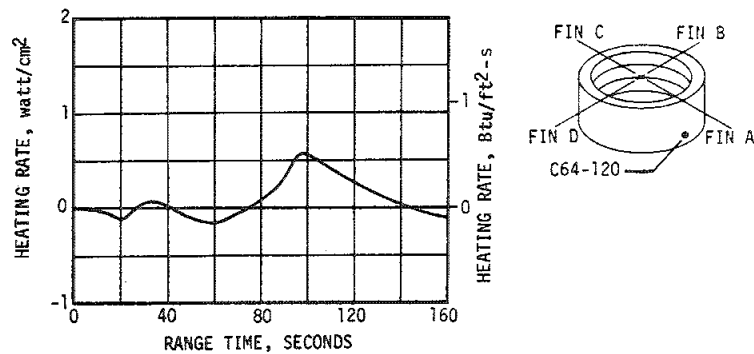
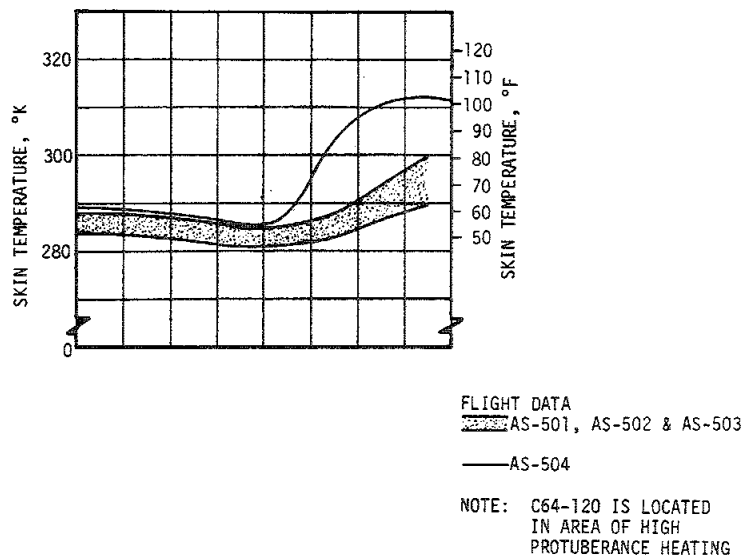


Figure 17-14. S-IC Forward Skirt Aerodynamic Heating - Measurement C64-120

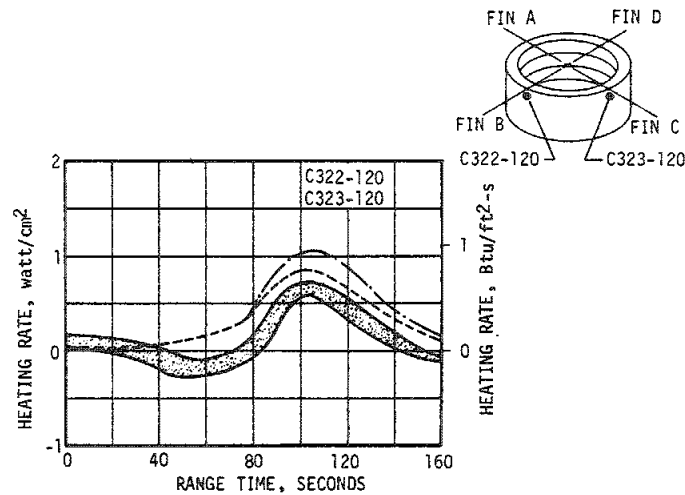
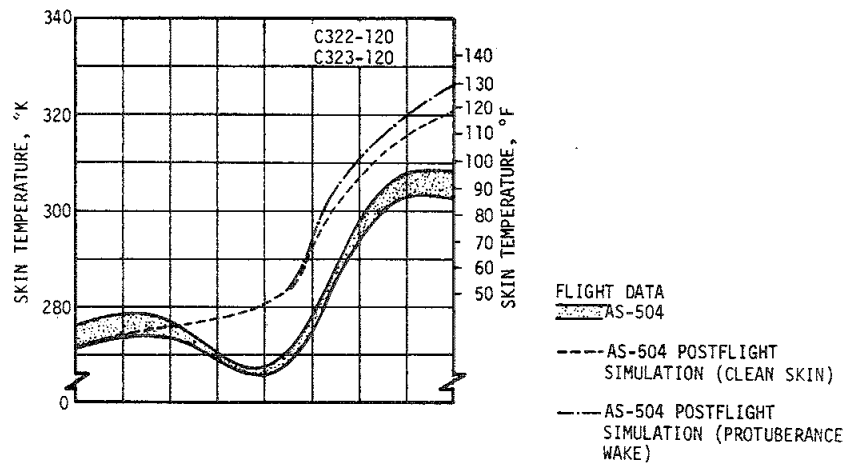


Figure 17-15. S-IC Forward Skirt Aerodynamic Heating - Measurements C322-120 and C323-120

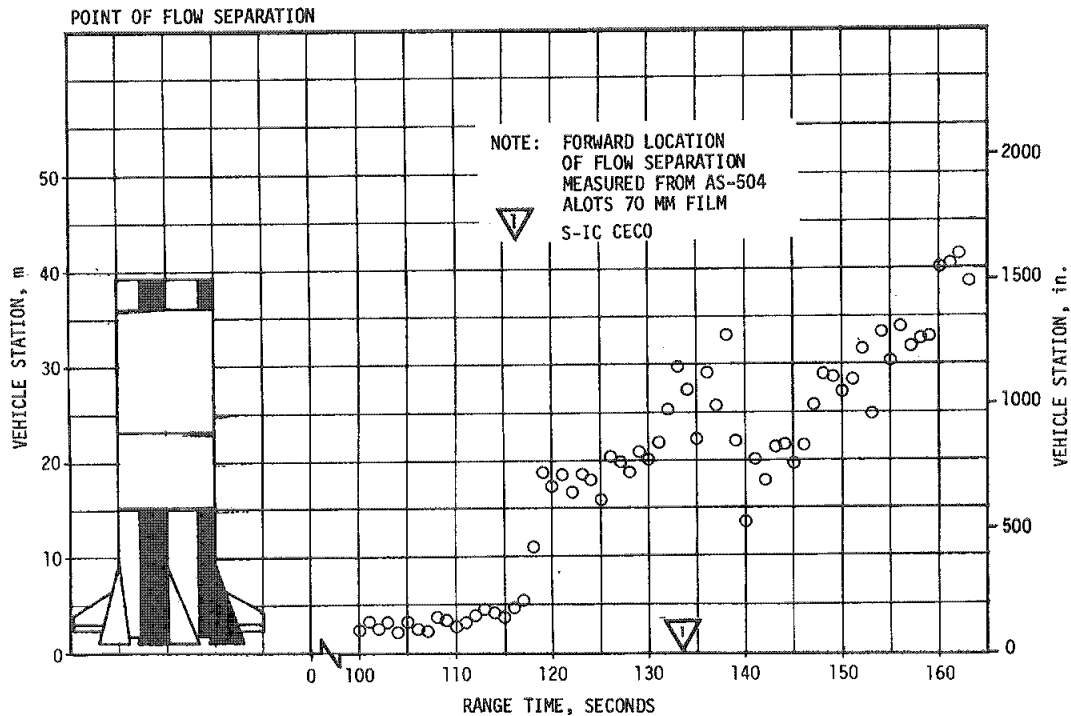


Figure 17-16. Forward Location of Separated Flow

LOX tank skin temperatures were well below the predicted maximum throughout flight, as shown in Figure 17-17. There was a noticeable measurement response when the LOX level passed corresponding thermocouples, which was to be expected.

Fuel tank skin temperatures were well below the predicted maximum until the end of flight when a significant increase in temperature was noted. A maximum temperature of 344.82°K (161°F) was reached at the end of flight, as shown in Figure 17-18. These temperatures were within structural capability and caused no concern.

Intertank skin temperatures were below predicted maximum throughout flight and within the previous flight data band, as shown in Figure 17-19.

As shown in Figure 17-20, the forward skirt skin temperatures were higher than on previous flights. This was due to the removal of insulation from the forward skirt of the S-IC stage. However, temperatures were well below the predicted maximum throughout flight and reached a maximum of 313.15°K (104°F) at S-IC Outboard Engine Cutoff (OECO).

#### 17.4.2 S-II Stage Aeroheating Environment

Aeroheating rates on the S-II stage were analyzed using the AS-504 postflight trajectory and angle-of-attack data obtained from Q-ball

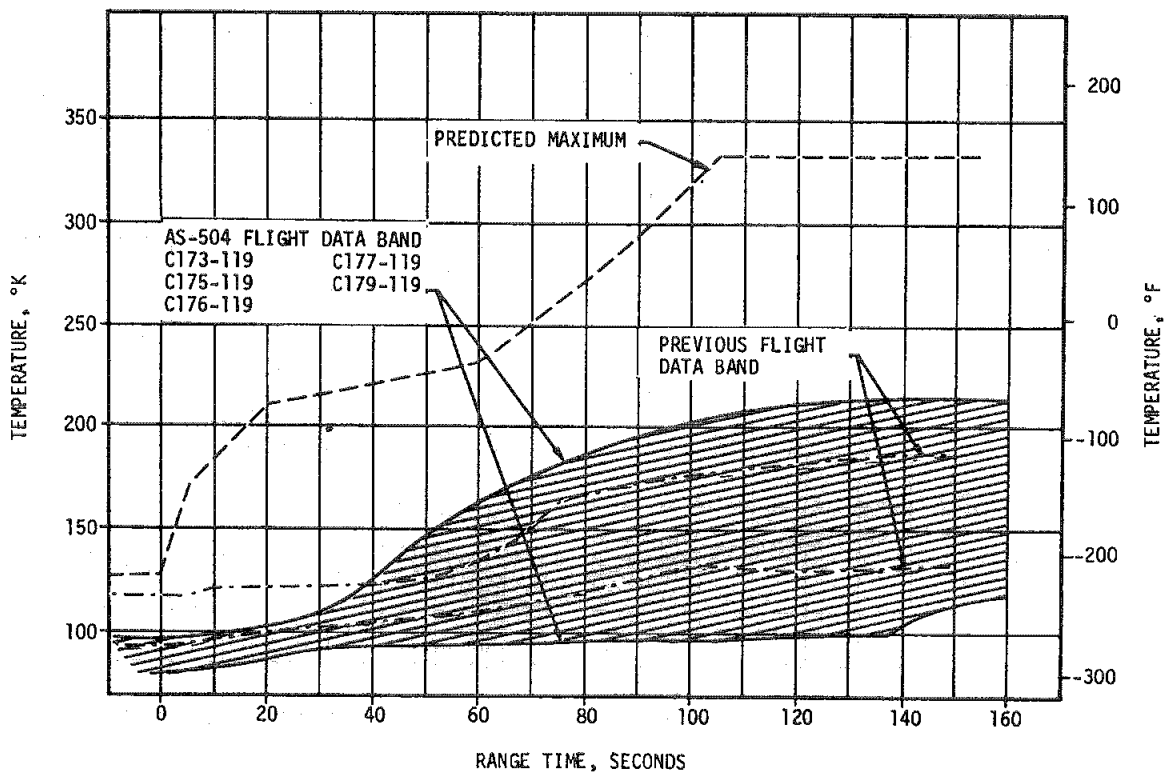


Figure 17-17. S-IC LOX Tank Skin Temperature

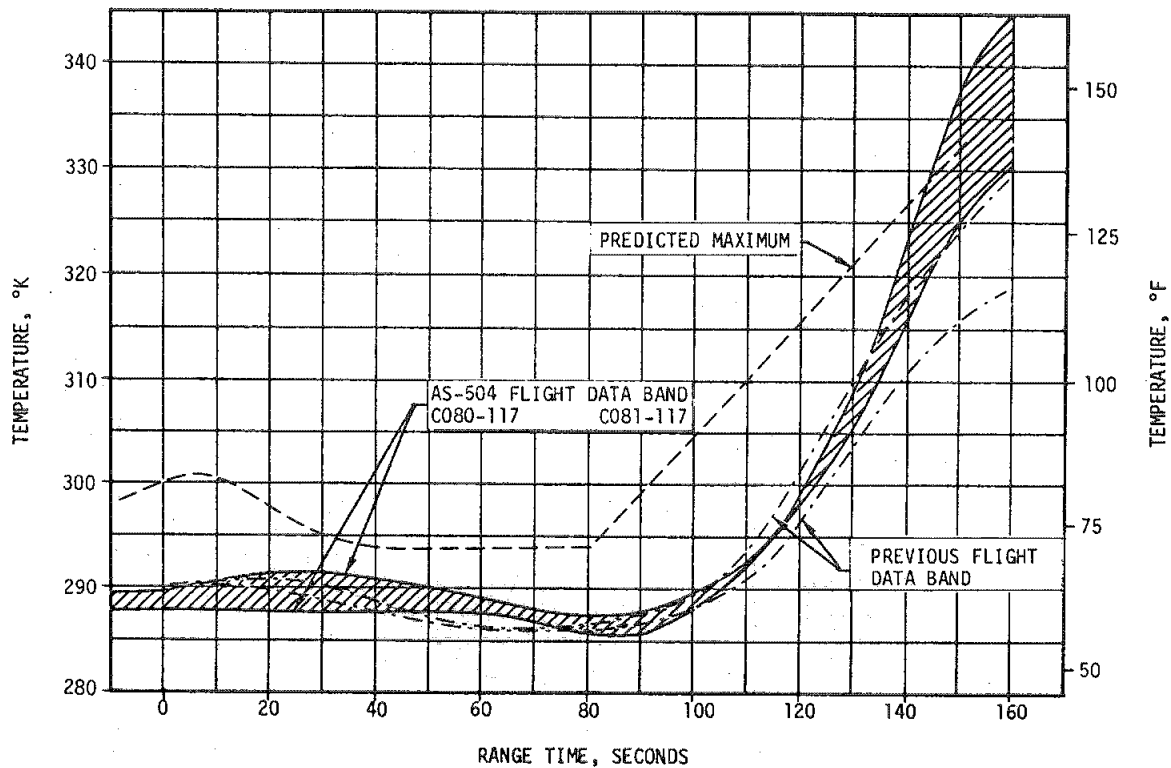


Figure 17-18. S-IC Fuel Tank Skin Temperature

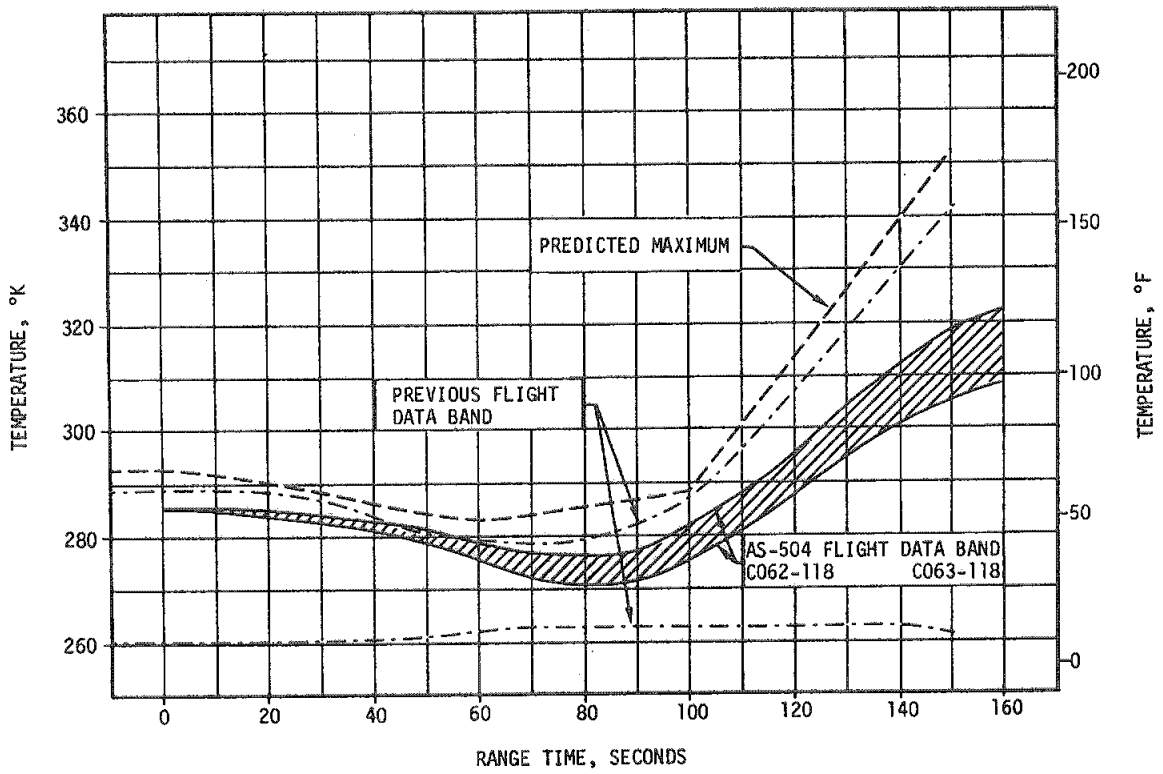


Figure 17-19. S-IC Intertank Skin Temperature

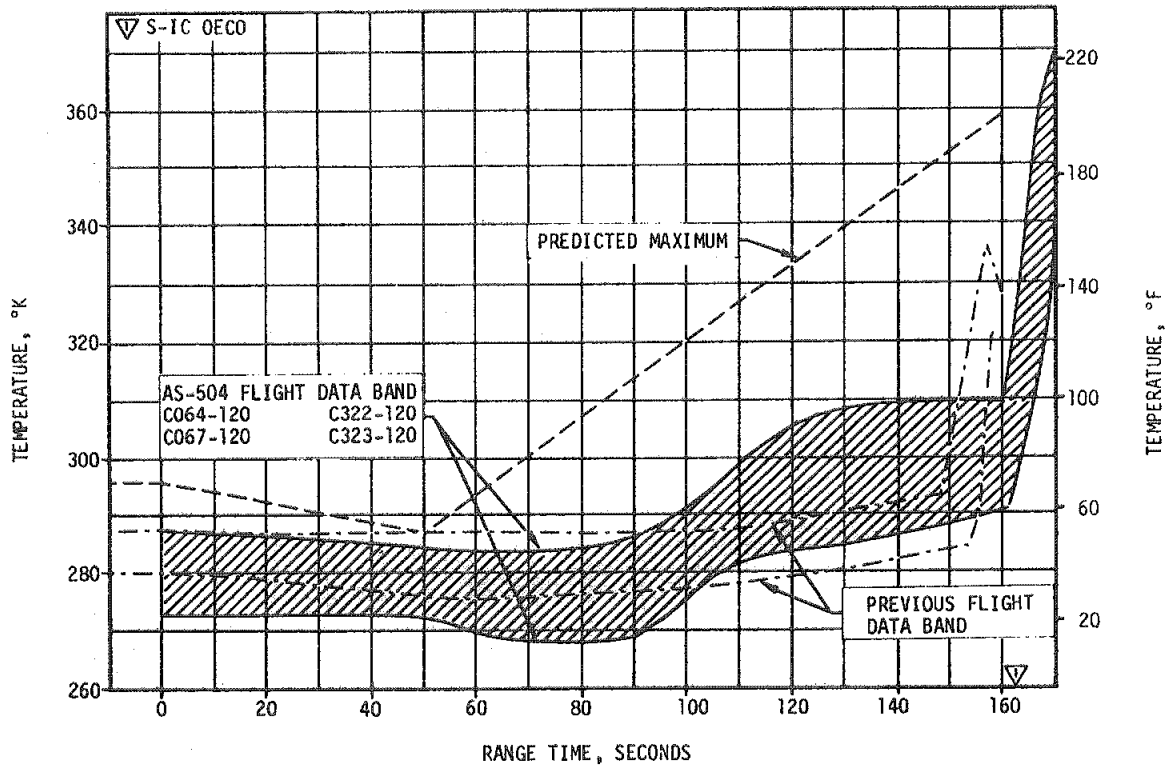


Figure 17-20. S-IC Forward Skirt Skin Temperature

measurements. Atmospheric data were obtained from the final Meteorological Data Tape. The aeroheating rates were then calculated by means of a digital computer program. These predicted rates were corrected to calorimeter conditions for purposes of direct comparison with flight data.

Predicted heating rates to calorimeters located on the S-II aft interstage are compared to AS-504 flight data in Figure 17-21. The agreement of flight data with predicted values and previous flight data is good. The heating rate spike shown at 162 seconds is due to the S-II ullage motor plume. The heating pulses indicated at 30 and 138 seconds are under investigation.

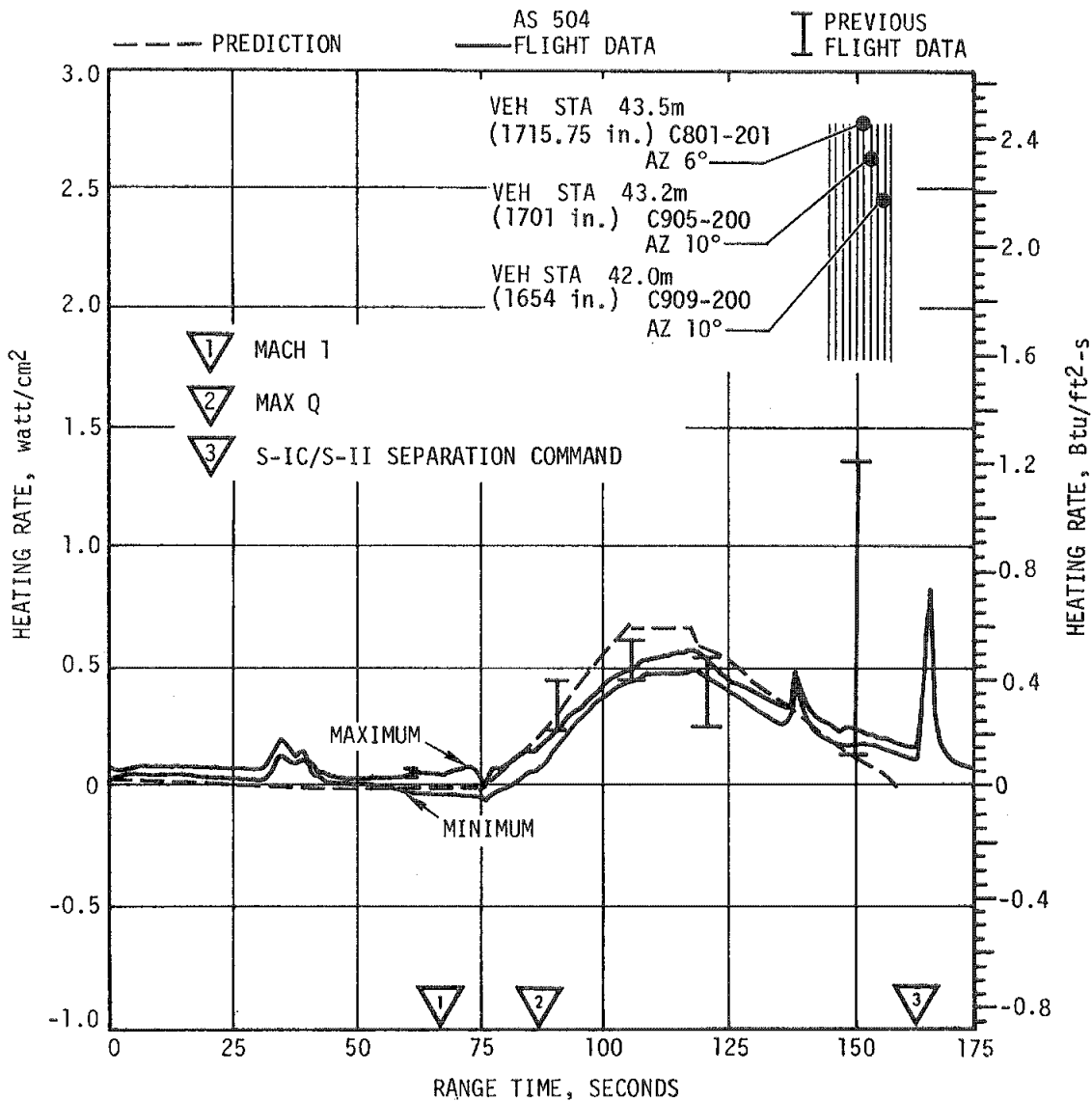


Figure 17-21. S-II Aft Interstage Aeroheating Environment

The heating rates on the forward conical fairing of an ullage motor on the S-II aft interstage are shown in Figure 17-22. Agreement between predicted values and AS-504 flight data is very good, except for the period from 100 to 140 seconds range time. As on previous flights, the flight data is somewhat lower than the prediction for this time period. The ullage motor fairing in question is located aft of the LOX vent valve fairing, and displaced 11 degrees in azimuth. Depending on the varying flow direction of the boundary layer over the ullage motor fairings, cold gases from within the LOX vent valve fairing could lower the calorimeter disk temperature and thus falsely indicate reduced heating rates. These cold gases could result from boundary layer flow, under the aft portion of the LOX vent valve fairing, being cooled by contact with the cold valve components.

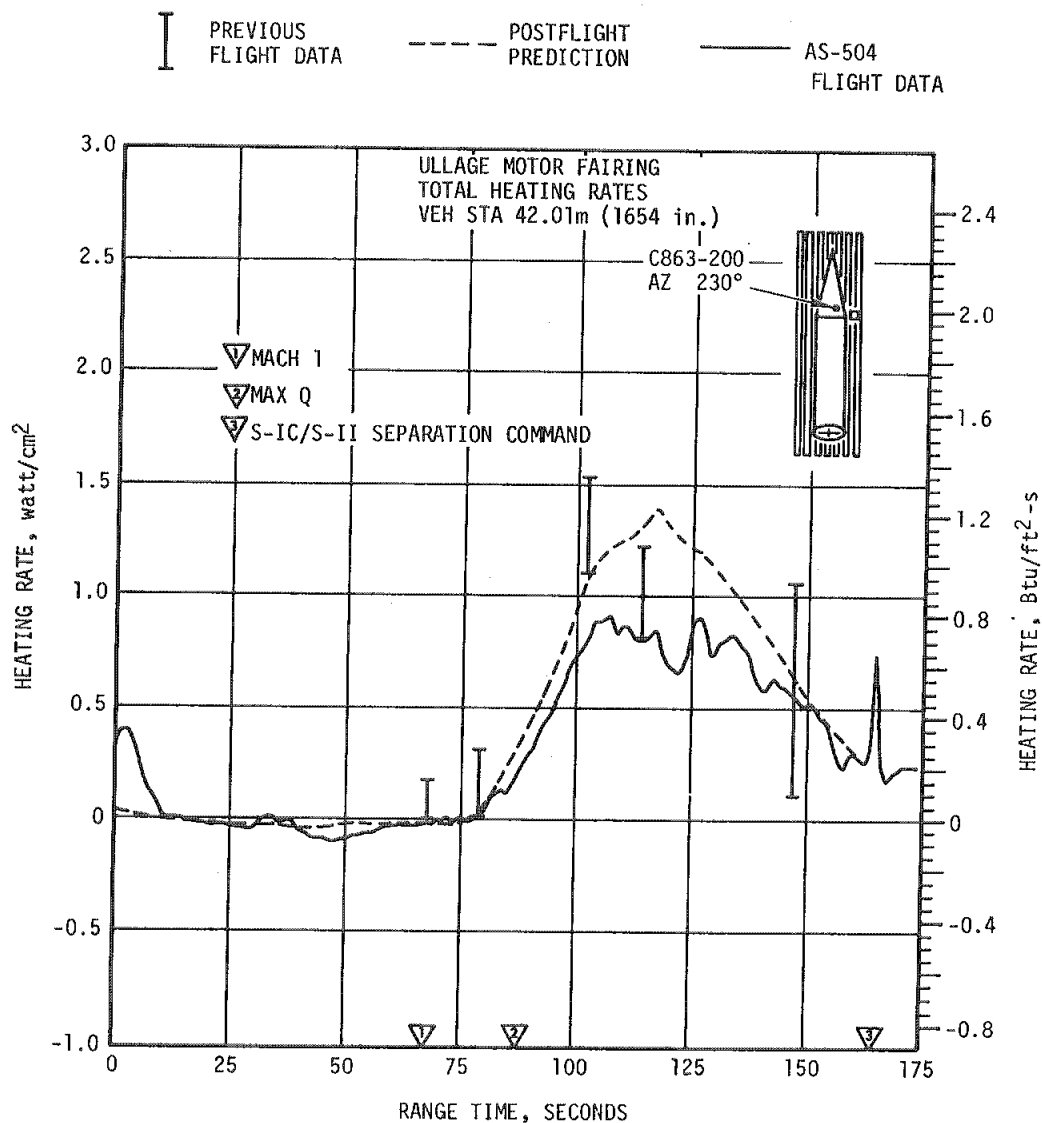


Figure 17-22. S-II Aft Interstage Aeroheating Environment, Ullage Motor Fairing



The heating rate pulse at liftoff, as shown in Figure 17-22, is assumed to be due to radiation from the S-IC engines exhaust. The spike at about 162 seconds is due to radiation from the S-II ullage motor plume. The pulses at 30 and 138 seconds range time are under investigation.

The heating rates sensed by calorimeters located on the aft boattail of an LH<sub>2</sub> feedline fairing are shown in Figure 17-23. The heating rate sensed by calorimeter A, located just downstream of the cylindrical portion of the feedline fairing, is considerably lower than that sensed by calorimeter B, located further downstream on the aft conical fairing.

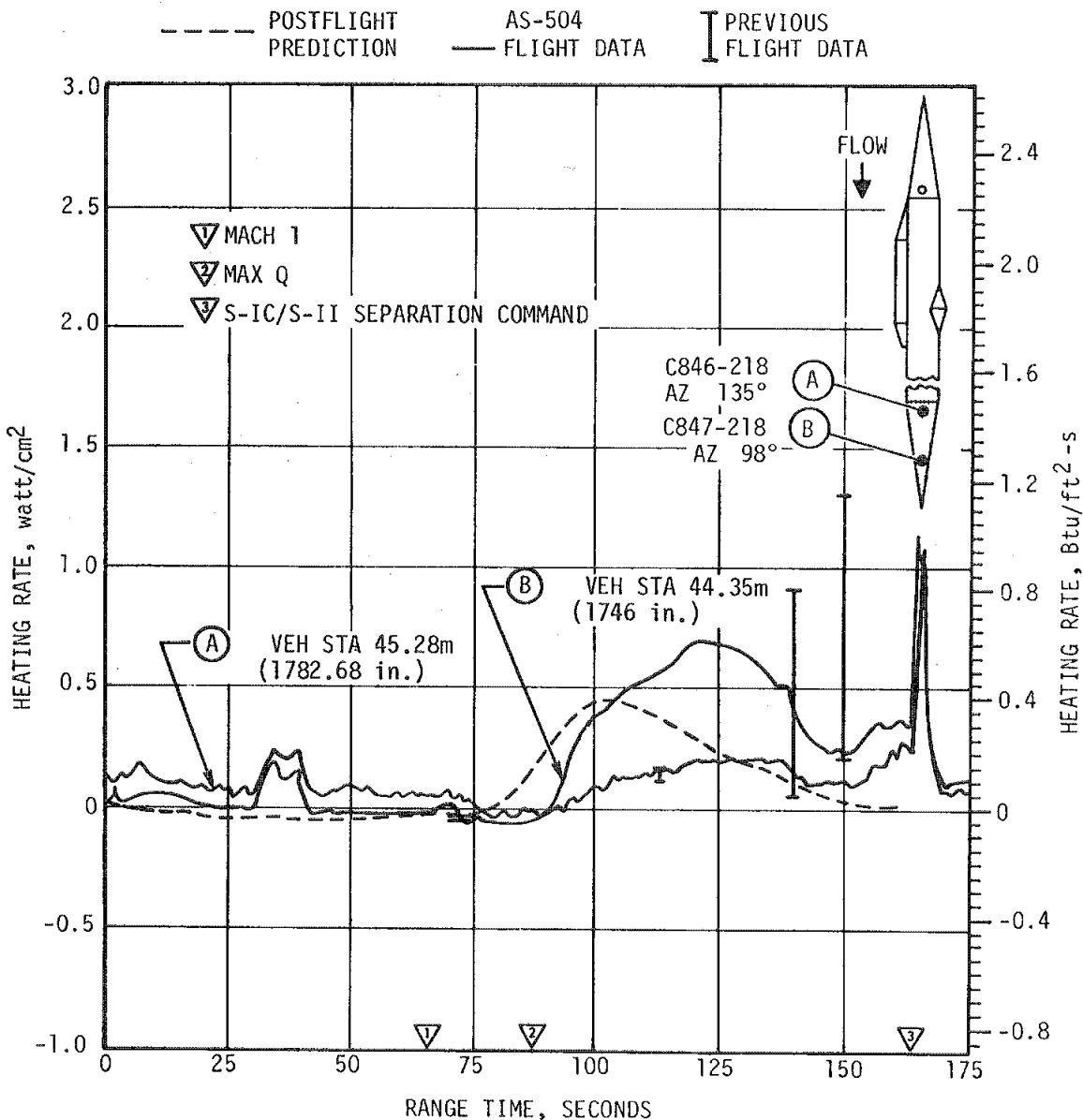


Figure 17-23. S-II LH<sub>2</sub> Feedline Aft Fairing Heating Rates

This is due to the fact that calorimeter B is in a higher heating area downstream of the reattachment shock, aft of the fairing joggle. The predicted heating rate value for this location does not include the effects of the reattachment shock. As a result, the flight data for calorimeter B is higher than the prediction. The cause of low heating rates sensed by calorimeter A, during the time period from 75 to 125 seconds, is possibly due to cool gases from within the fairing being driven out of the aft joggle of the fairing, due to the rapidly lessening pressure outside of the fairing.

The high heating rates indicated by both calorimeters between 150 and 162 seconds could be due to S-IC engine exhaust gas flowing forward along the vehicle skin into this low pressure region. This phenomenon is presently under investigation. The heating effects that would be due to the exhaust gas are not accounted for in the predicted heating rate values. Due to the short duration of additional heating, the added heat flux does not raise the structural temperature significantly; about 2.78°K (5°F).

Good agreement is seen between the AS-504 flight data, predicted values, and previous flight data for heating rates to calorimeters located on the forward conical portion of the LH<sub>2</sub> feedline fairing, as shown in Figure 17-24.

The heating rates to calorimeters located on the forward skirt of the S-II stage are presented in Figure 17-25. Good agreement exists with previous flight data and with predicted values. The heating rate spike due to the S-II ullage motor plume is apparent in Figure 17-25, at about 162 seconds.

Representative AS-504 structural and fairing temperature data are shown in Figures 17-26 through 17-28. In general, the AS-504 temperature data agree well with previous flight data and with postflight predictions. Flight data are compared with predicted values of forward skirt skin temperatures in Figure 17-26. Ullage motor fairing temperatures are shown in Figure 17-27. LH<sub>2</sub> tank insulation surface temperature data and predicted values are shown in Figure 17-28.

17-23

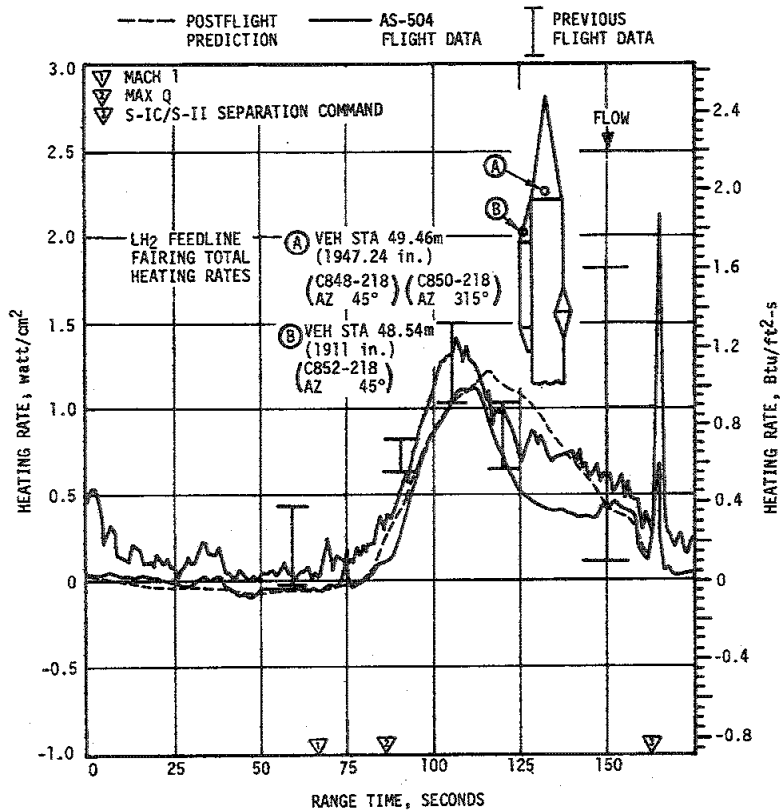


Figure 17-24. S-II LH<sub>2</sub> Feedline Forward Fairing Heating Rates

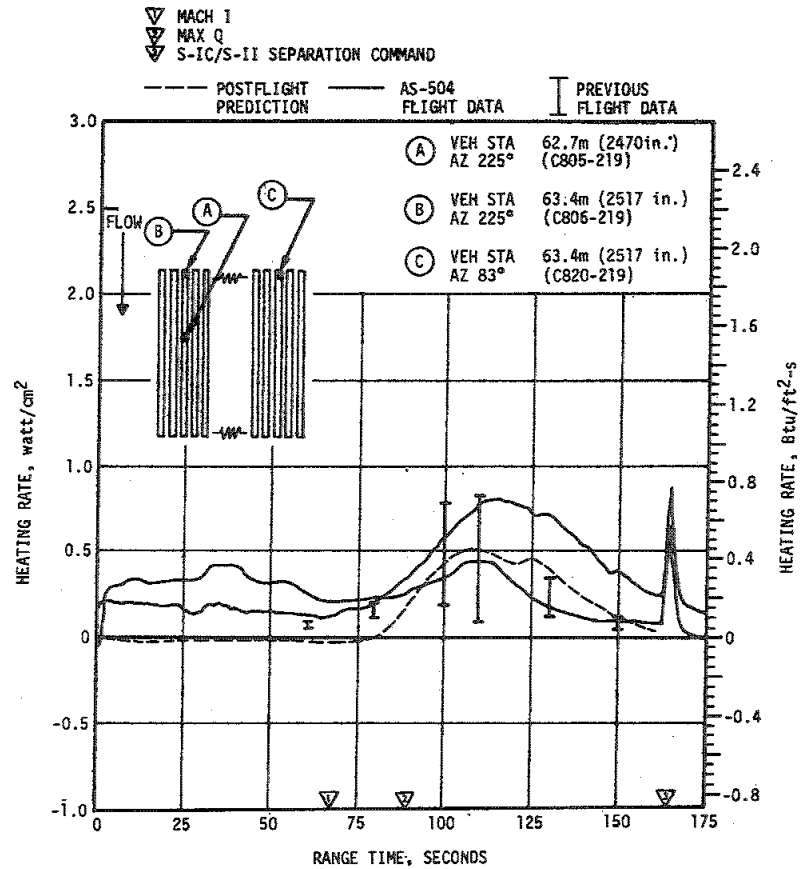


Figure 17-25. S-II Body Aeroheating Environment, Forward Skirt

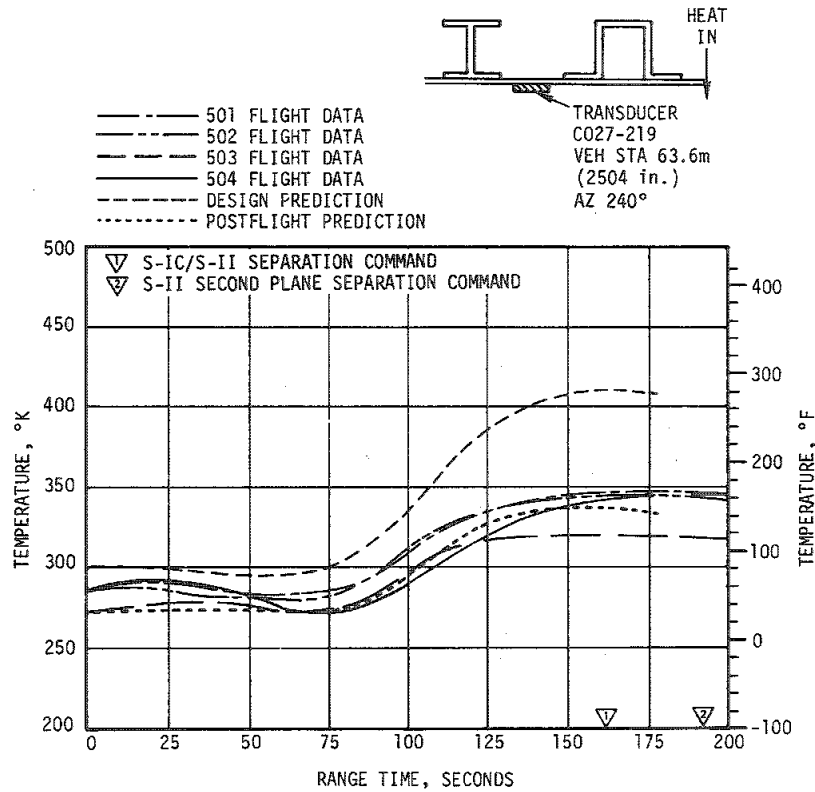


Figure 17-26. S-II Body Structural Temperature, Forward Skirt Skin

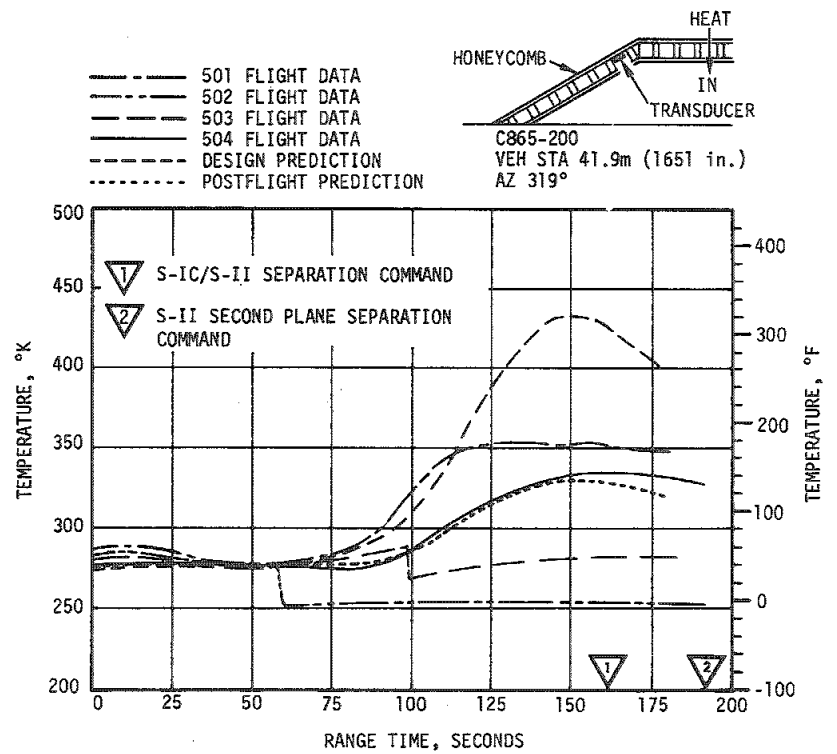
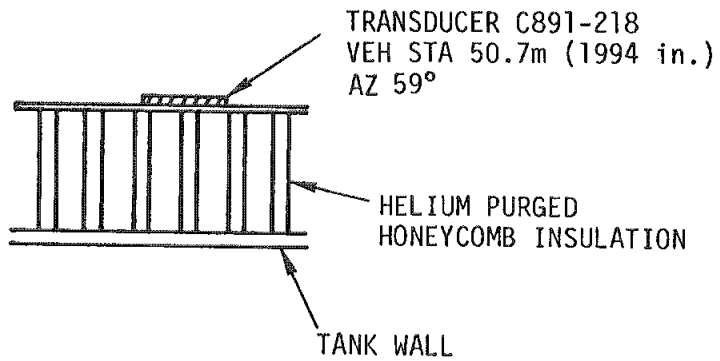


Figure 17-27. S-II Aft Interstage Structural Temperature, Ullage Motor Fairing



- 1 S-IC/S-II SEPARATION COMMAND
- 2 S-II SECOND PLANE SEPARATION COMMAND

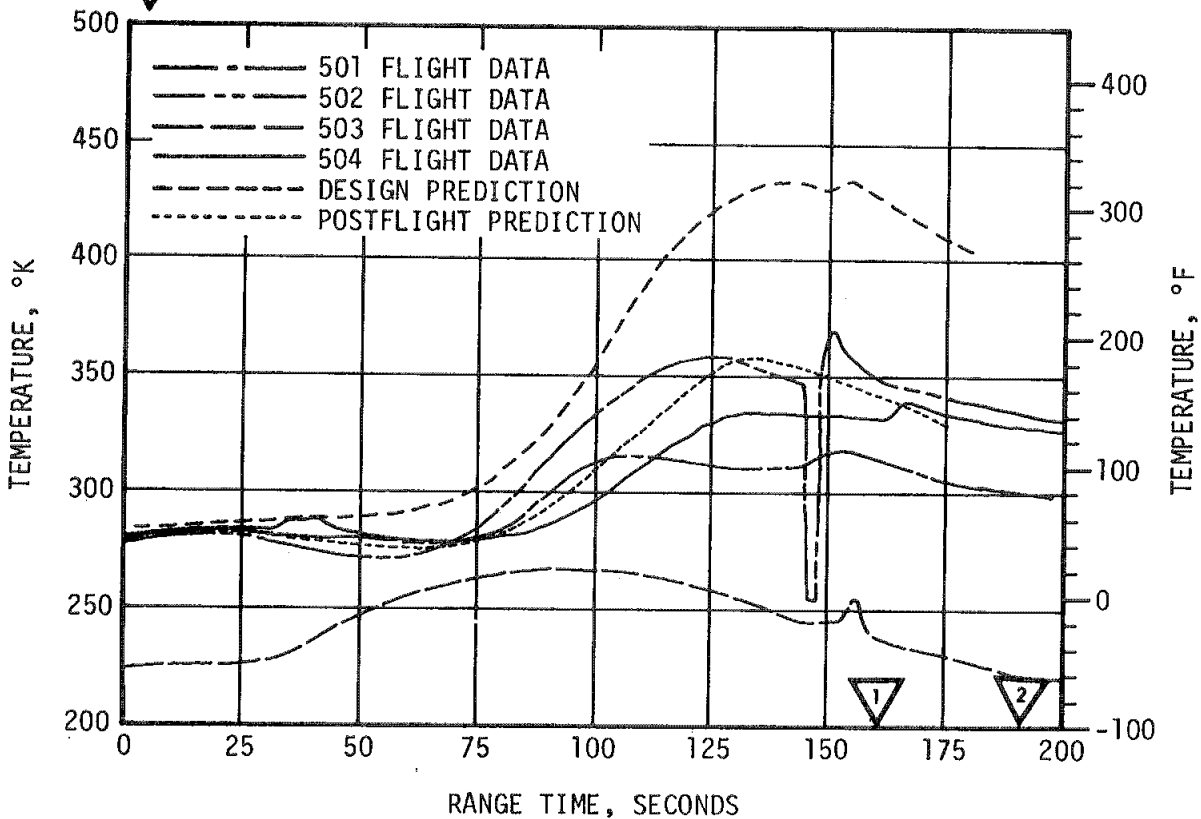


Figure 17-28. S-II Body Structural Temperature,  
LH<sub>2</sub> Tank Insulation Surface

SECTION 18  
ENVIRONMENTAL CONTROL SYSTEM

18.1 SUMMARY

The S-IC canister conditioning system and the aft environmental conditioning system performed satisfactorily during the AS-504 countdown.

The S-II thermal control and compartment conditioning system maintained temperatures within the design limits throughout the prelaunch operations.

The IU Environmental Control System (ECS) exhibited satisfactory performance throughout the flight. Coolant temperatures, pressures and flowrates were continuously maintained within the required ranges and design limits. The gas bearing pressure differential drifted  $0.28 \text{ N/cm}^2$  (0.4 psid) above the  $10.69 \text{ N/cm}^2$  (15.5 psid) maximum, and the platform internal ambient pressure remained above the  $8.27 \pm 1.03 \text{ N/cm}^2$  ( $12.0 \pm 1.5$  psia) specification range for most of the mission. These conditions had no detrimental effect on the mission or other IU systems.

18.2 S-IC ENVIRONMENTAL CONTROL

The ambient temperatures of the 10 canisters in the S-IC forward skirt compartment must be maintained at  $299.8 \pm 11.1^\circ\text{K}$  ( $80 \pm 20^\circ\text{F}$ ) during equipment operation prior to J-2 engine chilldown, and between  $324.8$  to  $277.6^\circ\text{K}$  ( $125$  to  $40^\circ\text{F}$ ) during J-2 engine chilldown. No canister conditioning is required after S-IC forward umbilical disconnect.

The ambient temperatures within the canisters remained within the required limits during the countdown, as shown in Figure 18-1. Canister No. 6 recorded the lowest temperature,  $290.6^\circ\text{K}$  ( $63.3^\circ\text{F}$ ), during prelaunch. The lowest canister temperature measured in flight was  $277.5^\circ\text{K}$  ( $39.7^\circ\text{F}$ ) in canister No. 2, as shown in Figure 18-1.

During J-2 engine chilldown, the thermal environment is at the most critical point. Within this period the ambient temperature in the forward skirt compartment dropped, as shown in Figure 18-2. The lowest temperature,  $131.2^\circ\text{K}$  ( $-223.6^\circ\text{F}$ ), was recorded at instrument C207-120 which is located under a J-2 engine nozzle and received the maximum effect of the cold helium. All other ambient temperatures were above the  $205.4^\circ\text{K}$  ( $-90^\circ\text{F}$ ) design minimum.

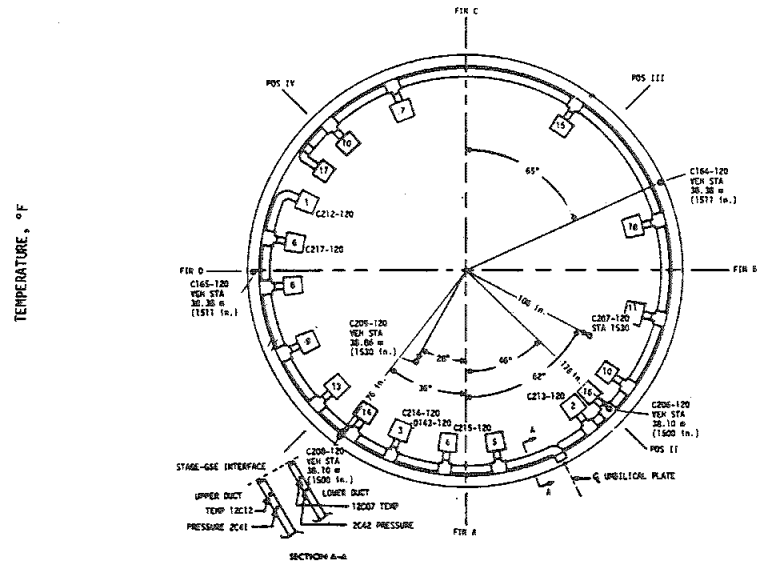
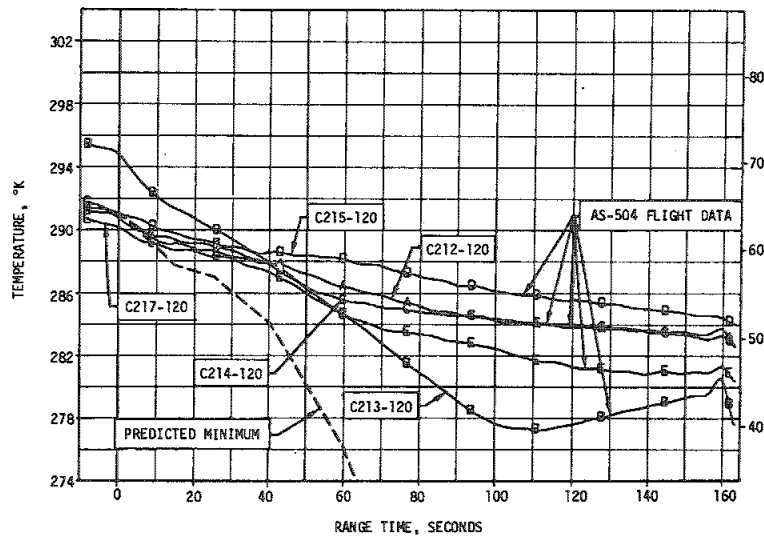
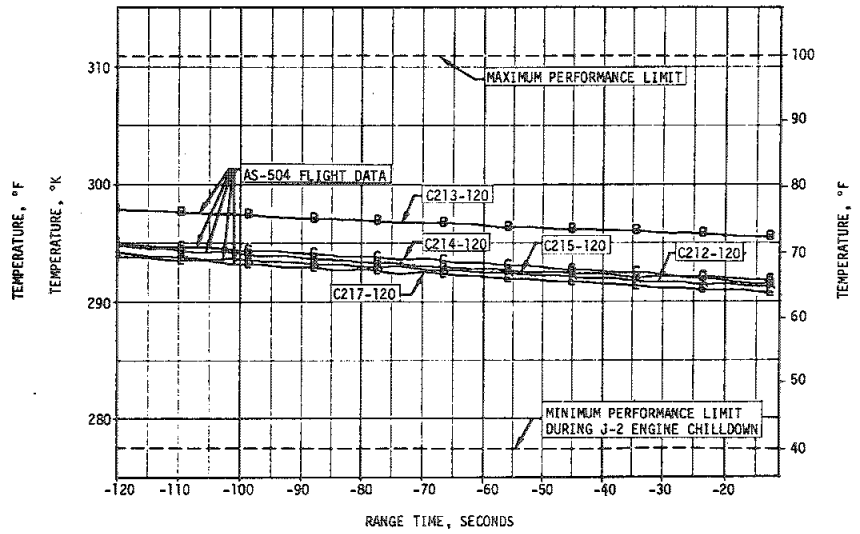
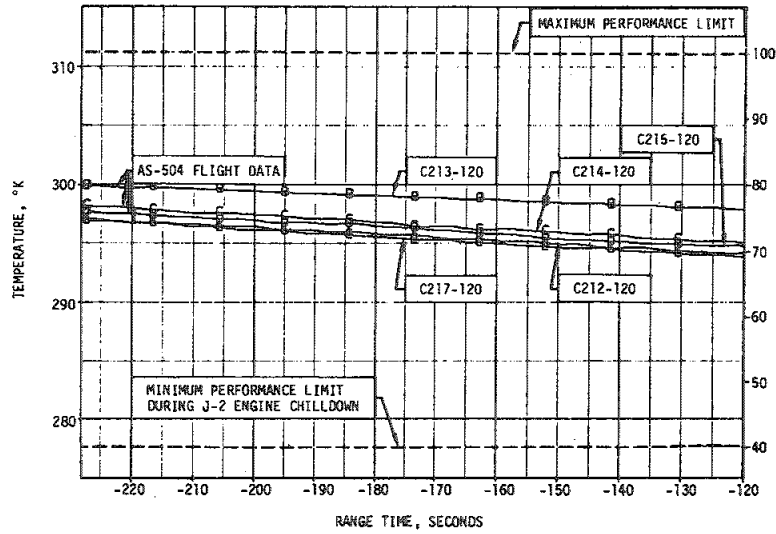


Figure 18-1. S-IC Forward Compartment Canister Temperature

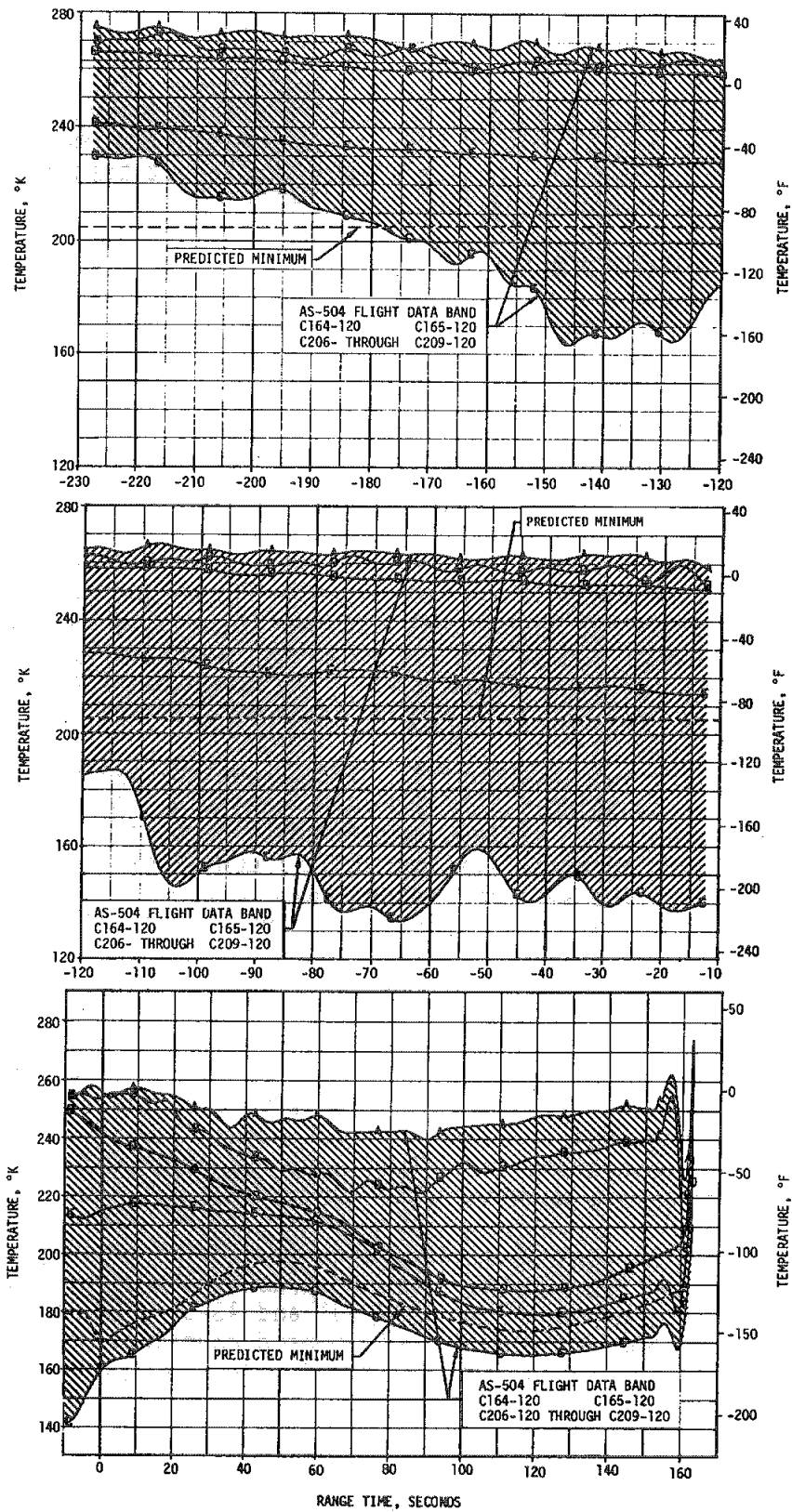


Figure 18-2. S-IC Forward Compartment Ambient Temperature



The design requirements for the aft compartment are that the prelaunch temperature be maintained at  $299.7 \pm 8.3^\circ\text{K}$  ( $80 \pm 15^\circ\text{F}$ ). Aft compartment prelaunch temperatures are shown in Figure 18-3. The lowest prelaunch temperature recorded was  $290.4^\circ\text{K}$  ( $62.9^\circ\text{F}$ ) at instrument C203-115. Although this measurement was  $1.2^\circ\text{K}$  ( $2.1^\circ\text{F}$ ) below the minimum requirement, no problem was experienced. During flight the lowest temperature was  $270.4^\circ\text{K}$  ( $37.0^\circ\text{F}$ ) at instrument C107-115.

### 18.3 S-II ENVIRONMENTAL CONTROL

The S-II stage Environmental Control System consists of two parts described as follows:

- a. The engine compartment conditioning system is designed to maintain an inert and controlled temperature in the S-II/S-IC interstage when propellants are on board. The system consists of lightweight plastic ducting which distributes facility supplied  $\text{GN}_2$  throughout the compartment. The purge gas exits from the interstage through vent holes at vehicle stations above the thrust cone, immediately below the thrust cone, and in the S-IC forward skirt. The purge gas temperature is controlled by the launch pad facility to produce an average ambient temperature of  $278 \pm 2.8^\circ\text{K}$  ( $40 \pm 5^\circ\text{F}$ ) as indicated by four thermistors located on the S-II thrust cone. The purge gas flow rate is controlled by facility valving to a nominal rate of  $3.78 \text{ kg/s}$  ( $8.33 \text{ lbm/s}$ ).
- b. Two similar, but independent, thermal control systems consisting of fiberglass containers, distribution manifold, and umbilical disconnect are employed. One system, with 3 containers, is located in the forward interstage; the other system, with 11 containers, is located in the aft interstage. The systems are designed to provide a controlled temperature and inert atmosphere for electronic equipment located in the containers. Conditioned air for cooling during ground checkout prior to propellant loading, and warm  $\text{GN}_2$  for inerting and heating after propellant loading are supplied through umbilical disconnects from the launch pad facility. The conditioned gas is distributed from the disconnects to each container by manifolds and flow control orifices. The gas exhausts from the containers to the interstage through vent holes in the container walls. Continuous flow is maintained until umbilical separation at liftoff. During flight, the equipment temperatures are maintained by thermal inertia and container insulation.

The environmental control system performed satisfactorily throughout the launch countdown and flight. Temperatures in the forward thermal control system were similar to those of AS-501 and AS-502, and were generally warmer than AS-503. The only instrumented container in the aft system indicated temperatures nearly identical with previous vehicles. Ambient

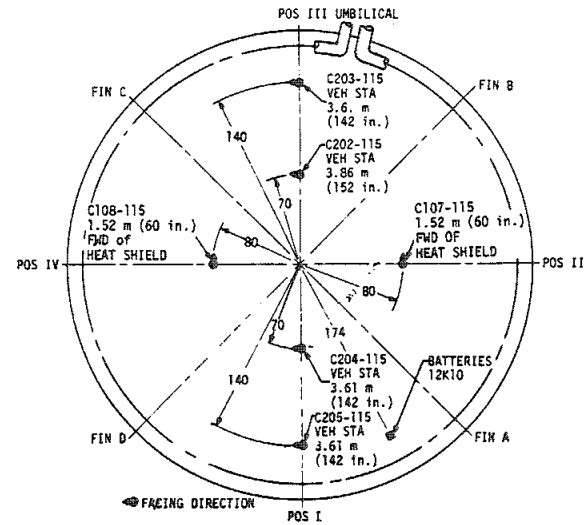
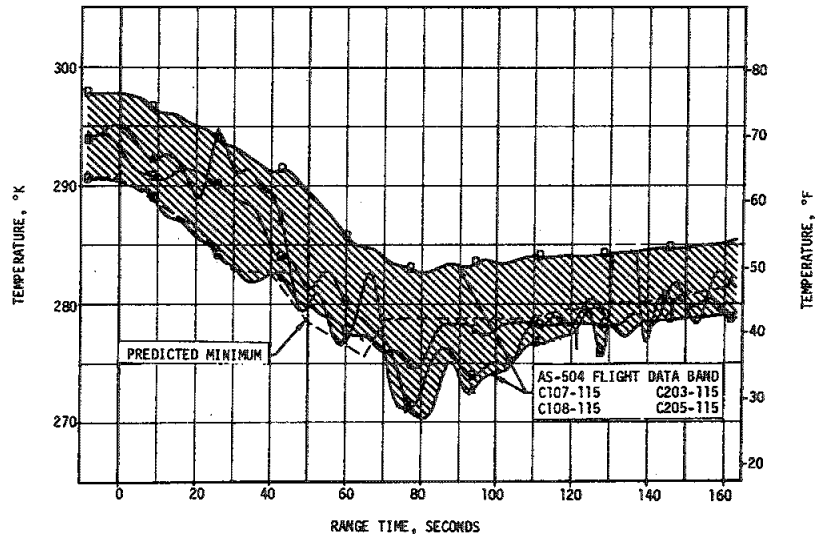
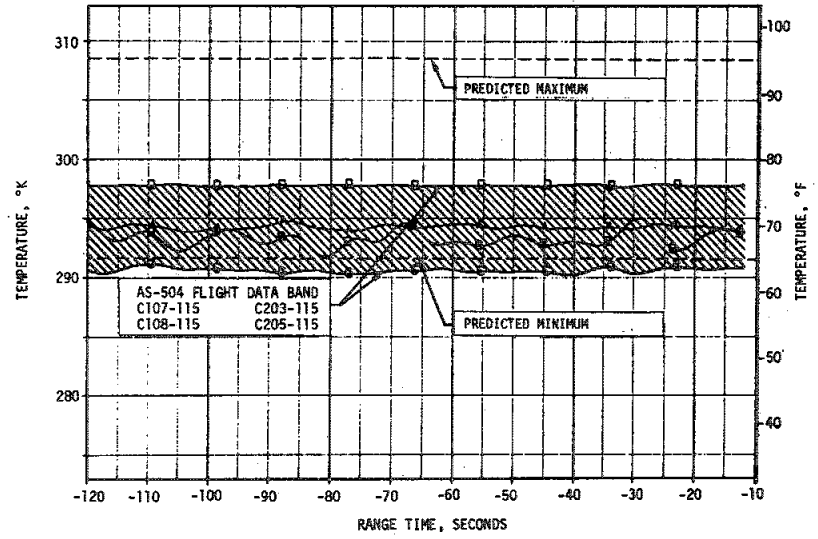
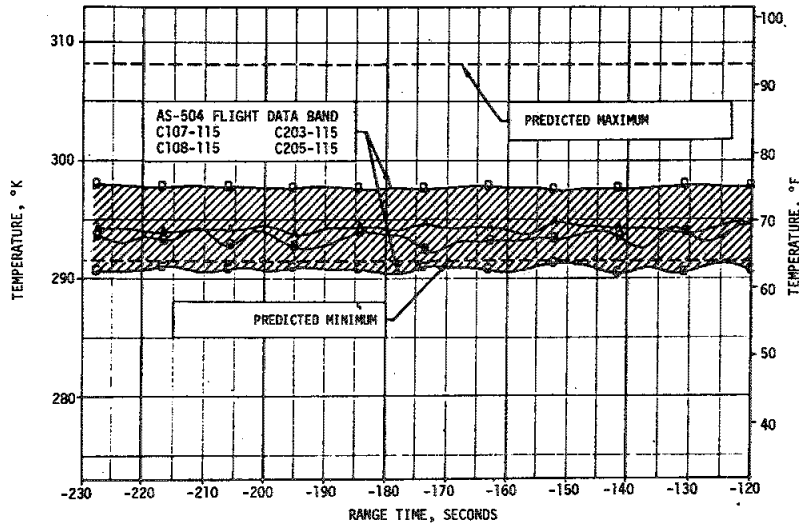


Figure 18-3. S-IC Aft Compartment Temperature Range

temperatures in the S-II/S-IC interstage prior to initiation of thrust chamber chill were generally warmer but more uniform than those of the AS-503. At liftoff and through early boost phases, the temperatures were similar to previous vehicles. There were no indications of hydrogen or oxygen in the S-II/S-IC interstage throughout the countdown.

#### 18.4 IU ENVIRONMENTAL CONTROL

The ECS maintained acceptable operating conditions for components mounted within the Instrument Unit (IU) and the S-IVB stage forward skirt during preflight and flight operations. The ECS is composed of a Thermal Conditioning System (TCS) and a Gas Bearing Supply System (GBS). A preflight purge subsystem provided compartment conditioning prior to launch.

##### 18.4.1 Thermal Conditioning System

The IU TCS, shown in Figure 18-4, Methanol/Water (M/W) coolant control temperature cycled within the required 280.3 to 293.1°K (45 to 68°F) temperature band, as shown in Figure 18-5. Initial sublimator startup and sublimator performance parameters during ascent are shown in Figure 18-6. Immediately after liftoff the Modulating Flow Control Valve (MFCV) began driving toward the full heatsink position, as commanded, which was achieved at approximately 30 seconds. The water valve opened by switch selector command at 184 seconds, allowing water to flow to the sublimator. Immediate cooling was evidenced by the rapid decline in the coolant fluid temperature. At the first thermal switch sampling, the coolant temperature was still above the actuation point and the water valve remained open. The second thermal switch sampling, at approximately 778 seconds, resulted in closing of the water supply valve. Coolant flowrates and pressures were well within required ranges as indicated in Table 18-1.

Table 18-1. TCS Coolant Flowrates and Pressures

PARAMETER	REQUIREMENT	MINIMUM OBSERVED	MAXIMUM OBSERVED
IU Coolant Flowrate F9-602 m <sup>3</sup> /s (gpm)	6.06 x 10 <sup>-4</sup> (9.6 Minimum)	6.25 x 10 <sup>-4</sup> (9.9)	6.44 x 10 <sup>-4</sup> (10.2)
S-IVB Coolant Flowrate F10-601 m <sup>3</sup> /s (gpm)	49.2 ± 2.52 x 10 <sup>-5</sup> (7.8 ± 0.4)	4.92 x 10 <sup>-4</sup> (7.8)	5.17 x 10 <sup>-4</sup> (8.2)
Pump Inlet Pressure D24-601 N/cm <sup>2</sup> (psia)	10.80 to 11.72 (15.7 to 17.0)	11.03 (16.0)	11.51 (16.7)
Pump Outlet Pressure D17-601 N/cm <sup>2</sup> (psia)	28.89 to 33.23 (41.9 to 48.2)	30.06 (43.6)	32.40 (47.0)

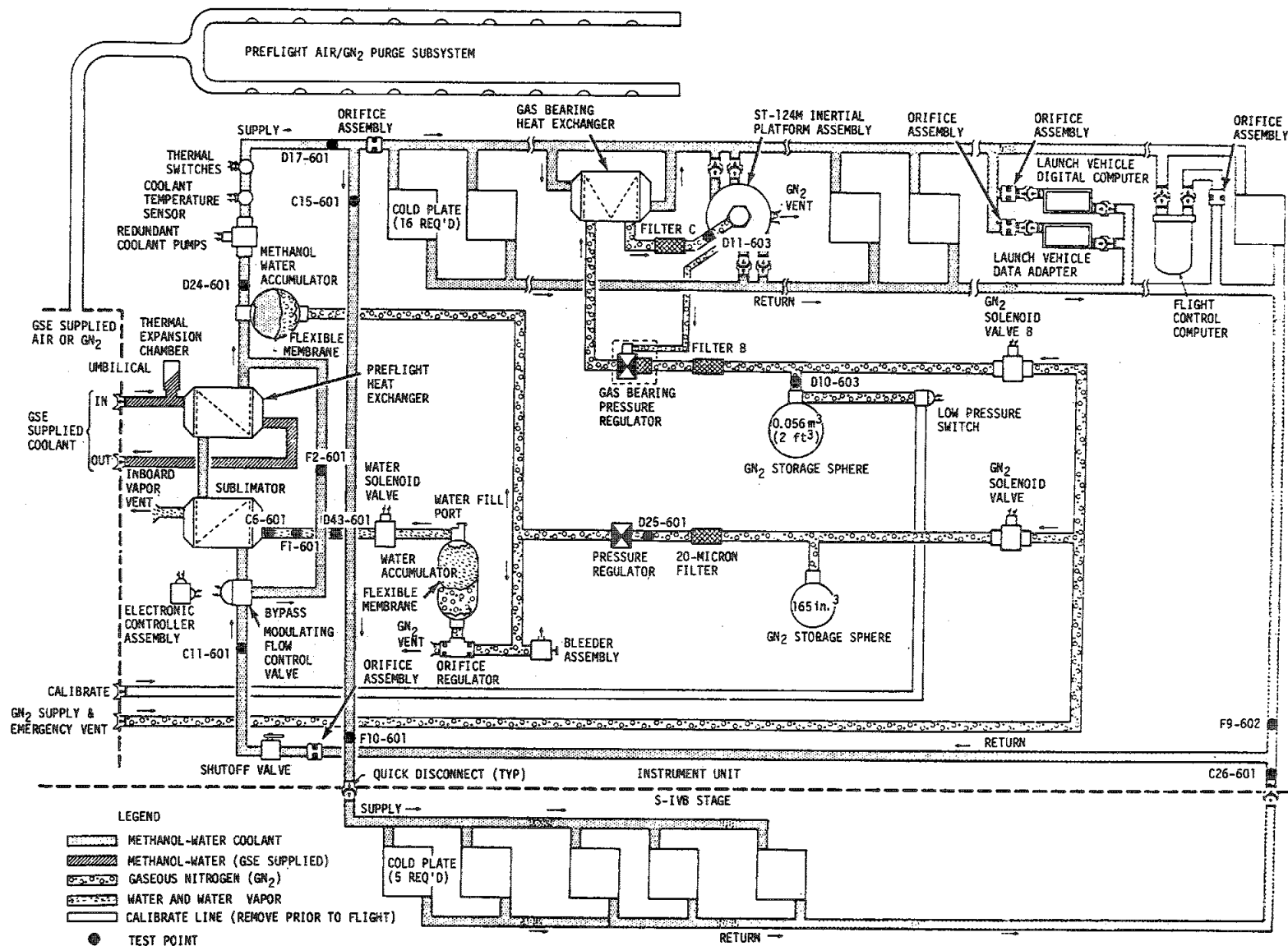


Figure 18-4. IU Environmental Control System Schematic

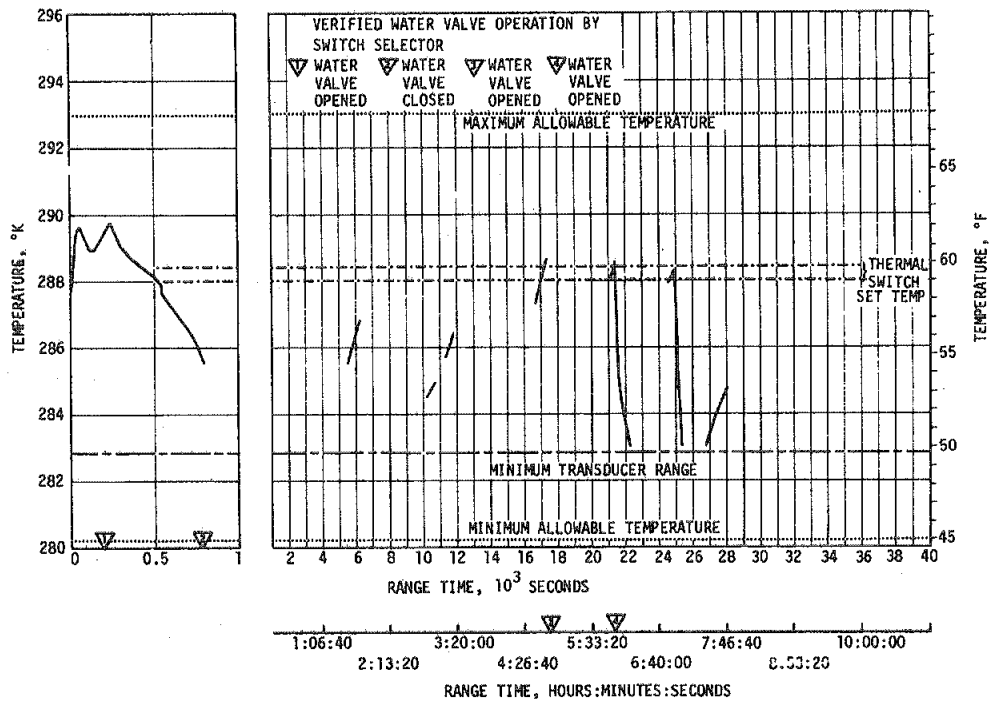


Figure 18-5. Thermal Conditioning System Methanol/Water Control Temperature

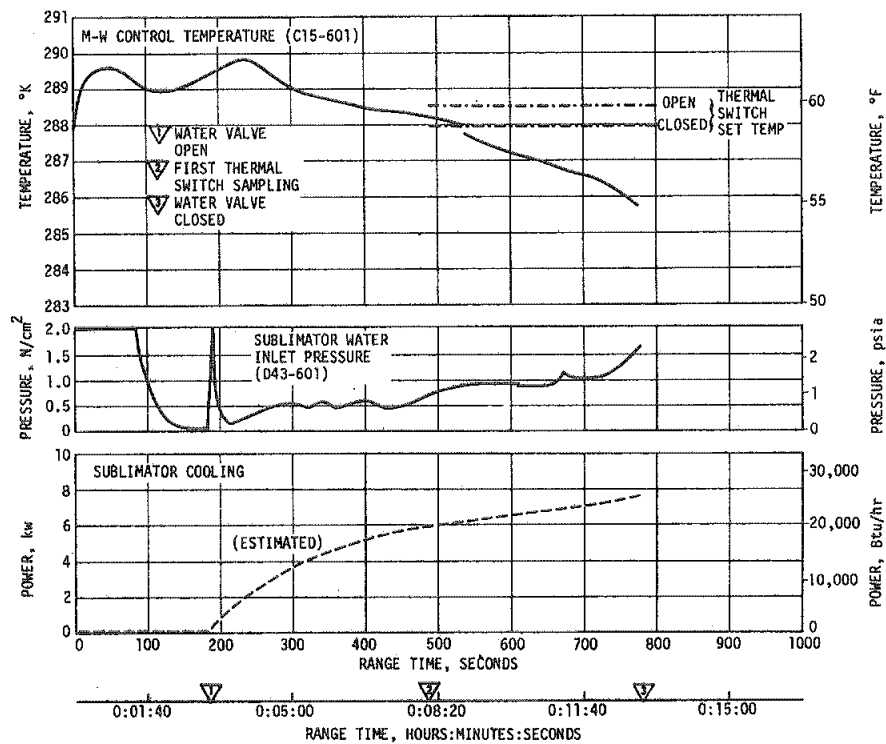


Figure 18-6. IU Sublimator Performance During Ascent

The TCS GN<sub>2</sub> sphere pressure decay, which is indicative of the GN<sub>2</sub> usage rate, was approximately as expected for the nominal case, as shown in Figure 18-7. The rapid drop in the first 1000 seconds, though not predicted, is not considered an abnormal condition.

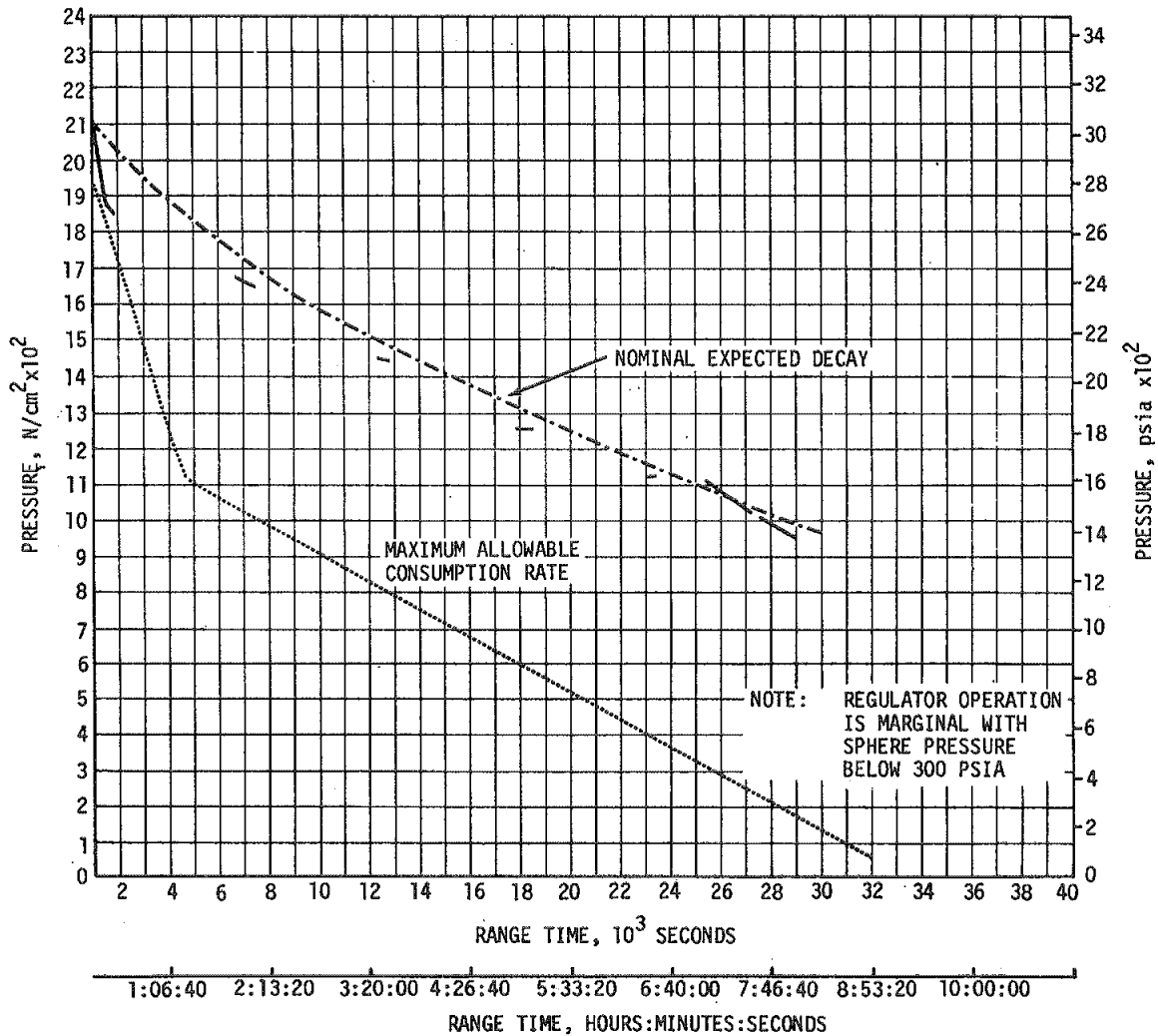


Figure 18-7. Thermal Conditioning System GN<sub>2</sub> Pressure

Selected component temperature curves are shown in Figure 18-8. All temperatures of the platform and its associated equipment were nominal with the exception of the inertial gimbal (C34-603). This temperature began to decrease from 315.7°K (108.6°F) immediately after liftoff, and fell below the specified limit of 316 ± 3°K (109.1 ± 5.4°F) between 6000 and 11,000 seconds. The temperature continued to decline steadily, reaching 309.2°K (96.9°F) at 26,449 seconds. Investigation has failed to reveal a specific

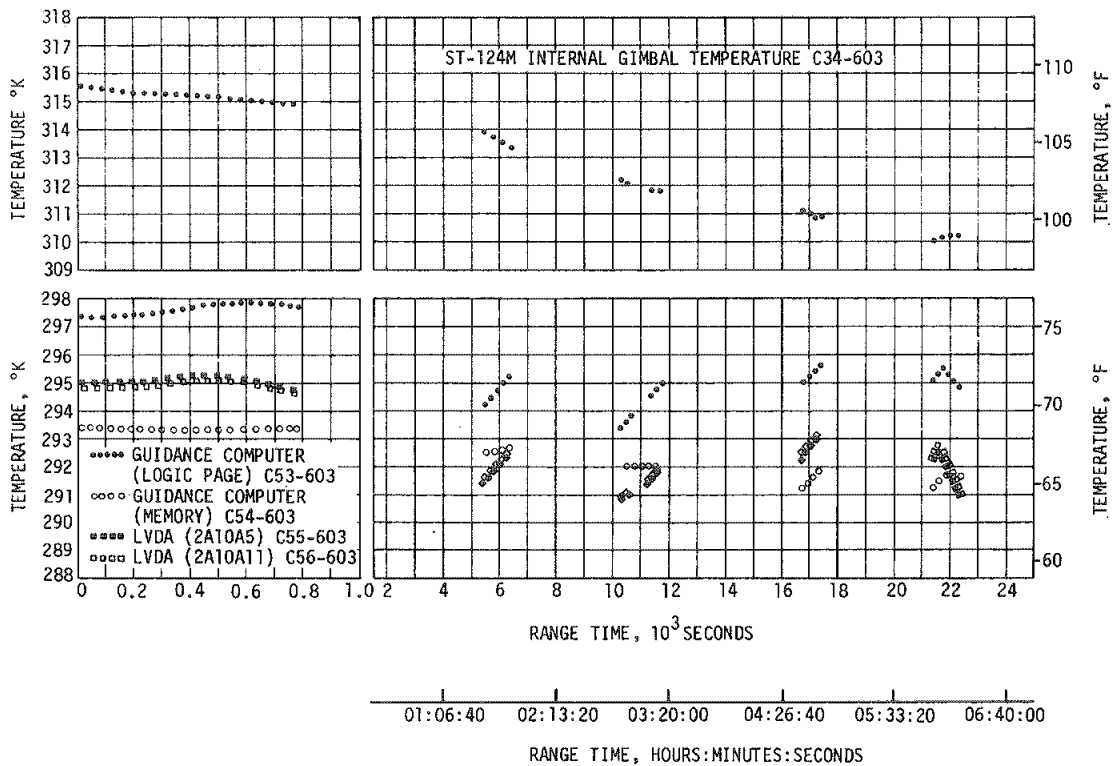
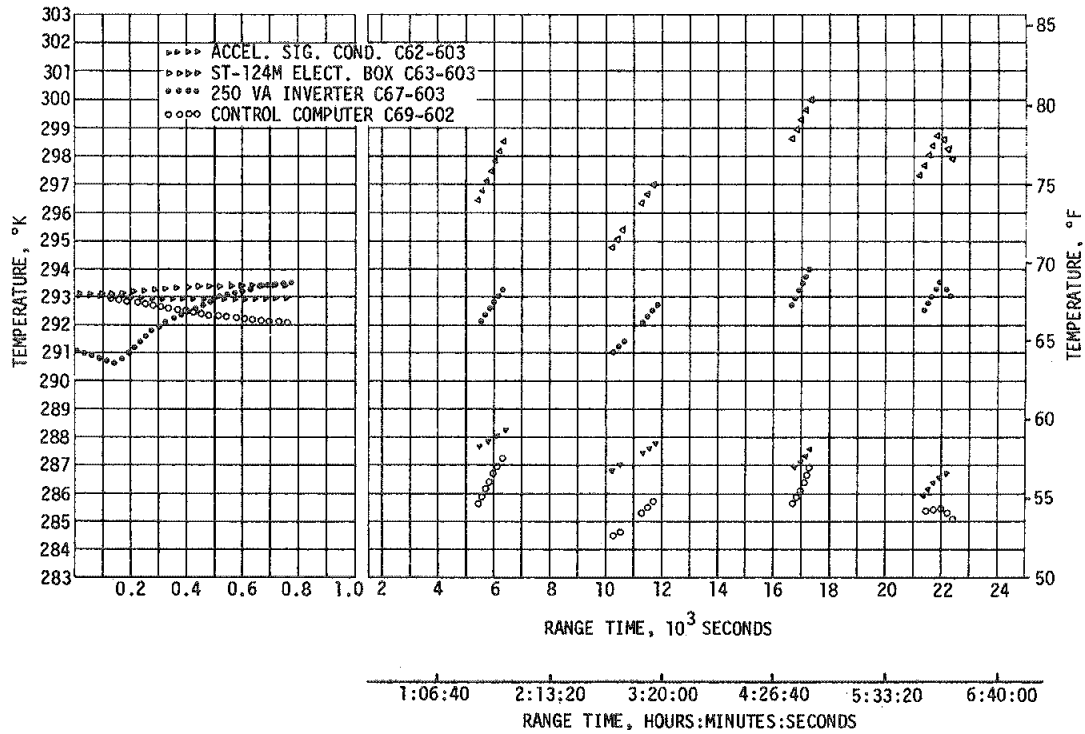


Figure 18-8. Selected Component Temperatures

cause for this deviation. However, the probable cause was very likely due to response to lower than expected environment which is not of a serious nature and will be observed on future flights. The AS-504 platform had a newly designed M/W flow configuration in the spherical covers, and used axial blowers (low flow). However, calculations indicate that the cooling rate should be nearly identical to that of previous cover configurations. It should be noted that AS-201 flight cooled even more rapidly than AS-504 during boost, and it used axial blowers (high flow).

During preflight testing, the inertial gimbal temperature periodically failed to rise to the specified minimum limit. This did not significantly affect the platform accuracy, and a waiver of the temperature requirement was obtained before launch.

#### 18.4.2 Gas Bearing Supply System

The gas bearing pressure regulator is required to maintain a GN<sub>2</sub> pressure differential across the platform bearing of  $10.34 \pm 0.34$  N/cm<sup>2</sup> (15.0  $\pm$  0.5 psid). As shown in Figure 18-9, the pressure differential drifted from the initial value of  $10.48$  N/cm<sup>2</sup> (15.2 psid) at liftoff to a value of  $10.96$  N/cm<sup>2</sup> (15.9 psid) at 22,000 seconds. The upper limit of the specification value of  $10.69$  N/cm<sup>2</sup> (15.5 psid) was exceeded sometime between 6000 and 11,000 seconds. The platform internal ambient pressure remained above the  $8.27 \pm 1.03$  N/cm<sup>2</sup> (12.0  $\pm$  1.5 psia) specification range for most of the mission. Although similar occurrences have taken place on the four previous missions, the phenomenon of gradual increase of the pressure differential is, for the most part, unexplained. The probable cause was possibly due to regulator drift which is not of a serious nature. The planned corrective action will be defined in IU Specifications and Criteria document (0.3.5.3.3). The past occurrences of a slightly high pressure differential have not been considered as an unacceptable condition, as no serious detrimental effect on platform operation has been identified.

The GBS GN<sub>2</sub> sphere pressure decay is shown in Figure 18-10 and is as nominally expected. This is an indication of normal GN<sub>2</sub> consumption by the GBS.



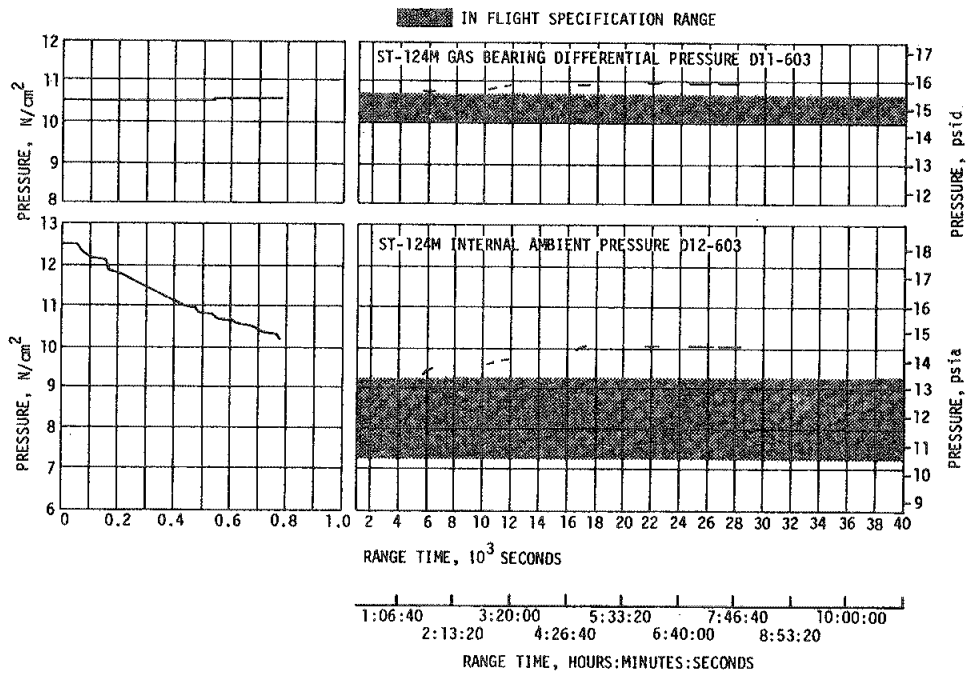


Figure 18-9. Inertial Platform GN<sub>2</sub> Pressures

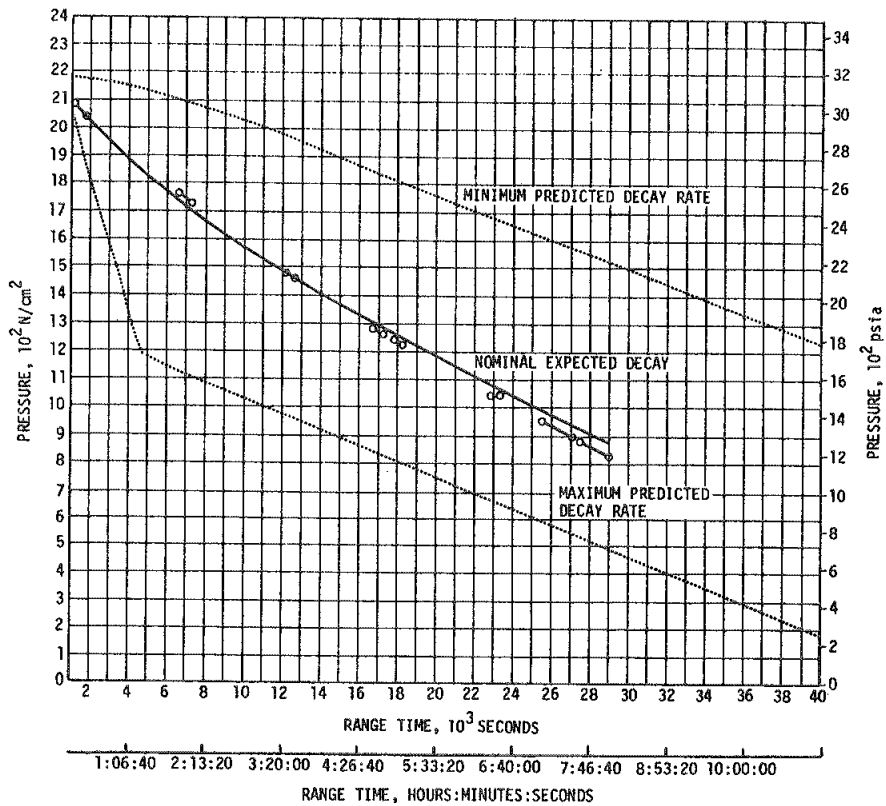


Figure 18-10. Gas Bearing System GN<sub>2</sub> Pressure

## SECTION 19

### DATA SYSTEMS

#### 19.1 SUMMARY

The data system for the AS-504 launch vehicle consisted of 2179 active flight measurements, 17 telemetry links, 3 tape recorders and tracking by Offset Frequency Doppler (ODOP), C-Band and Command Communication System (CCS). This was the first flight on which airborne film cameras were not utilized. All elements of the data system performed satisfactorily except for 4 telemetry deviations, discussed in paragraph 19.3. A degraded CCS power amplifier output is also discussed in paragraph 19.5.3.2 which did not adversely affect required data.

The propagation of Radio Frequency (RF) transmissions from the vehicle was satisfactory. Good tracking data were received and data indicate satisfactory performance of the CCS except for the degraded power amplifier output. Final loss of the Very High Frequency (VHF) telemetry RF signal occurred at 39,260 seconds (10:54:20). The Ultra High Frequency (UHF) telemetry signal was reported lost by Goldstone (GDS) at 37,758 seconds (10:29:18). The C-Band radar was commanded off at 27,213.5 seconds (7:33:03.5) and final loss of CCS signal was reported by GDS to have occurred at 48,066 seconds (13:21:06).

The 87 ground engineering cameras provided good data during the launch. However, dense cloud coverage precluded the acquisition of tracking camera data between 30 and 50 seconds.

#### 19.2 VEHICLE MEASUREMENTS EVALUATION

The AS-504 launch vehicle had 2194 measurements scheduled for the flight. A summary of these measurements, number per stage and overall performance may be found in Table 19-1. Prior to the start of automatic countdown, 15 measurements were waived as a flight requirement (see Table 19-2); three, however, provided valid flight data. Of the remaining 2179 measurements which were active, 23 were judged to be total failures and 19 others partially failed (see Table 19-3). In addition, 2 were improperly ranged (see Table 19-4) and 11 remain questionable (see Table 19-5). Flight measurement reliability for the launch vehicle was 98.9 percent, which compares very favorably with the 99.0 percent obtained on AS-503.

Table 19-1. AS-504 Flight Measurement Summary

MEASUREMENTS CATEGORY	S-IC STAGE	S-II STAGE	S-IVB STAGE		INSTRUMENT UNIT	TOTAL VEHICLE
			PHASE I *	PHASE II*		
Scheduled	666	1018	288	288	222	2194
Waived	2	10	3	3	0	15
Failures	5	13	2	5	0	23
Partial Failures	14	5	0	0	0	19
Improper Range	2	0	0	0	0	2
Questionable	7	4	0	0	0	11
Reliability, Percent	99.2	98.7	99.3	98.2	100.0	98.9

- \*Notes: 1. S-IVB Phase I period of performance is from liftoff to parking orbit insertion.  
 2. S-IVB Phase II period of performance for AS-504 was from liftoff until initiation of restart preparations for S-IVB third burn, T<sub>8</sub>, which occurred at 21,581 seconds.

#### 19.2.1 S-IC Stage Measurement Analysis

There were 666 flight measurements scheduled for the S-IC stage. Two of these measurements were waived prior to the start of automatic countdown and provided no useful flight data (see Table 19-2). Of the remaining 664 active flight measurements, 5 were total failures and 14 partially failed (see Table 19-3). In addition, 2 were improperly ranged (see Table 19-4) and 7 remain questionable (see Table 19-5). The flight measurement reliability was 99.2 percent.

#### 19.2.2 S-II Stage Measurement Analysis

There were 1018 flight measurements scheduled for the S-II stage. Ten measurements were waived prior to the start of automatic countdown of which one provided valid data during the flight (see Table 19-2). Of the remaining 1008 active flight measurements, 4 provided questionable data (see Table 19-5), 13 were considered to be total failures and 5 partially failed (see Table 19-3). The flight measurement reliability was 98.7 percent.

Table 19-2. AS-504 Flight Measurements Waived Prior to Launch

MEASUREMENT NUMBER	MEASUREMENT TITLE	NATURE OF FAILURE	REMARKS
S-IC STAGE			
C009-104	Temperature, Engine Gimbal System Return, Pitch Actuator	Wires shorted in transducer cable	Waiver LIA-I-51
E085-117	Vibration, LOX Inboard Tunnel	Measurement saturated full scale negative	Waiver LIA-I-50
S-II STAGE			
D030-201	LH <sub>2</sub> Recirculation Pump Discharge Pressure	Transducer Failure	Installation
D030-202	LH <sub>2</sub> Recirculation Pump Discharge Pressure	Transducer Failure	Installation
D030-203	LH <sub>2</sub> Recirculation Pump Discharge Pressure	Transducer Failure	Installation
D030-204	LH <sub>2</sub> Recirculation Pump Discharge Pressure	Transducer Failure	Installation
D030-205	LH <sub>2</sub> Recirculation Pump Discharge Pressure	Transducer Failure	Installation
D152-202	LH <sub>2</sub> Recirculation Pump Inlet Pressure	Transducer Failure	Installation
C714-206	Heat Shield Aft Surface Temperature	Transducer Grounded	
C052-203	E3 LOX Return Line Temperature	Transducer Grounded	(NR Waiver No. 4-12)
C121-218	LH <sub>2</sub> Tank Insulation Surface Temperature	Transducer Intermittent	Provided Valid Data During Flight
N051-228	TLM Power Out Fwd Coupler #2	Low Power Indication	Coupler Component Leakage (Waiver I-N-504-6)
S-IVB STAGE			
C0001-401	Temp-Fuel Turbine Inlet	Erratic During CDDT and Offscale Low During Countdown	Valid Data During Flight
C0007-401	Temp-Engine Control Helium	Erratic During CDDT and Launch Countdown	All Flight Data Questionable
C0159-424	Temp-LOX Circ Ret Line Tank Inlet	Erratic During CDDT and Launch Countdown	Valid Data During Flight

Table 19-3. AS-504 Measurement Malfunctions

MEASUREMENT NUMBER	MEASUREMENT TITLE	NATURE OF FAILURE	TIME OF FAILURE (RANGE TIME)	DURATION SATISFACTORY OPERATION	REMARKS
TOTAL MEASUREMENT FAILURES, S-IC STAGE					
E041-102	Vibration, Fuel Pump Flange, Longitudinal	Data contained high amplitude, low frequency noise throughout	Ignition	None	Caused by system saturation due to high level vibration (high frequency)
E042-102	Vibration, Fuel Pump Flange, Radial	Data contained high amplitude, low frequency noise throughout	Ignition	None	Caused by system saturation due to high level vibration.
E042-103	Vibration, Fuel Pump Flange, Radial	Data contained high amplitude, low frequency noise throughout	Ignition	None	Caused by system saturation due to high level vibration.
E042-104	Vibration, Fuel Pump Flange, Radial	Data contained high amplitude, low frequency noise throughout	Ignition	None	Caused by system saturation due to high vibration.
E042-105	Vibration, Fuel Pump Flange, Radial	Data contained high amplitude, low frequency noise throughout	Ignition	None	Caused by system saturation due to high level vibration.
TOTAL MEASUREMENT FAILURES, S-II STAGE					
C730-206	Heatshield Gas Recovery T at 225°F	Limited to low side of range	0 sec	None	Transducer failure.
D099-206	Heatshield Forward Face P	Full range until 123 sec. Minimum range after 138 sec.	138 sec.	None	Transducer failure.
D102-206	Heatshield Forward Face P	Full range until 44 sec. Zero range after 44 sec.	44 sec.	None	Transducer failure.
D118-219	Forward Skirt Static P	Constant pressure until 41 sec.	0 to 41 sec.	After 41 seconds.	Response not as predicted during first 41 seconds.
E001-201	E1 Long Vib Combustion Dome	Noise spikes throughout flight	0 sec.	None	Intermittent connector contacts suspected.
E001-202	E2 Long Vib Combustion Dome	Appears to be acoustic data during S-IC burn; low amplitude data during S-II burn.	0 sec.	None	
E001-204 *	E4 Long Vib Combustion Dome	Very low amplitude signal with high noise level throughout flight.	0 sec.	None	Isolated time slices where spectrum indicates possibility of valid data.
E002-201	E1 Radial Vib LOX Pump	Noise spikes throughout flight	0 sec.	None	Intermittent angle saturation suspected.
E002-204 *	E4 Radial Vib LOX Pump	Very low amplitude signal with high noise level throughout flight	0 sec	None	Isolated time slices where spectrum indicates possibility of valid data.
E003-201	E1 Radial Vib Fuel Pump	Excessive noise during S-II burn	0 sec.	None	Cause unknown.
E003-204	E3 Radial Vib Fuel Pump	Excessive noise during S-II burn	0 sec.	None	Cause unknown.
E336-206	Rad Vib LOX Sump/Prevalve	Excessive noise during S-II burn		None	Intermittent connector contacts suspected.
E341-203	Rad Vib LH2 Prevalve/FDLN	No RACS calibration data and no flight data detectable.	0 sec.	None	Failure of channel signal conditioner suspected.
*Contractor considers measurement to be a partial failure based on PSD's run at Contractor's facility.					

Table 19-3. AS-504 Measurement Malfunctions (Continued)

MEASUREMENT NUMBER	MEASUREMENT TITLE	NATURE OF FAILURE	TIME OF FAILURE (RANGE TIME)	DURATION SATISFACTORY OPERATION	REMARKS
TOTAL MEASUREMENT FAILURES, S-IVB STAGE, PHASE I					
C0133-401	Temp - Oxidizer Pump Discharge	Erratic except during second burn.	Prior to liftoff	Appeared normal only during second burn.	Faulty connector suspected.
K0005-401	Event - Mainstage Control - Sol En	Cycled during engine spark igniter operation.	During spark igniter operation	Before and after spark igniter operations.	Susceptible to spark igniter operation.
TOTAL MEASUREMENT FAILURES, S-IVB STAGE, PHASE II (TO 21,581 SEC)					
C0392-403 **	Temp - Helium heater support - 1	Offscale high at 18,100 sec. On scale but erratic at 18,250 sec.	18,100 sec.	Prior to 18,100 sec.	Partially open transducer suspected.
C2015-401 **	Temp-Crossover Duct External Wall #1	Did not respond properly to heat increase.	During second burn	Prior to second burn..	Sensor debonded.
C2016-401 **	Temp-Crossover Duct External Wall #2	Did not respond properly to heat increase.	During second burn.	Prior to second burn.	Sensor debonded.
NOTE: Phase I failures not relisted.					
MEASUREMENT ANOMALIES, S-IVB STAGE, POST-PHASE II (AFTER 21,581 SEC)					
C0010-403	Temp-Engine Area Ambient	Offscale high at 22,045 sec., returned onscale at 29,480 but later drifted offscale high.	22,045 sec.	Prior to 22,045 sec.	Sensor may have partially opened during third burn.
C0199-401	Temp-Thrust Chamber Jacket	Went offscale high at 22,150 sec.	22,150 sec.	Prior to 22,150 sec.	Sensor may have pulled loose from thrust chamber.
C0200-401	Temp-Fuel Injection	Went offscale high at 22,040 sec.	22,040 sec.	Prior to 22,040 sec.	Sensor may have partially opened.
D003-403	Press-Oxidizer Pump Inlet	Data drops from 43 to 10 psia at 22,069 sec. Offscale low at 22,290.	22,069 sec.	Prior to 22,069 sec.	Damage to transducer wiper arm suspected.
D0104-403	Press-LH <sub>2</sub> Press Module Inlet	Went offscale high at 22,237 sec.	22,237 sec.	Prior to 22,237 sec.	Possible open transducer.
G003-401	Position-Main Oxidizer Valve	Erratic during third burn.	During third burn.	Prior to third burn.	Potentiometer wiper may have failed.
G0004-401	Position-Main Fuel Valve	Erratic during third burn.	During third burn.	Prior to third burn.	Potentiometer wiper may have failed.
K0157-401	Event-Mainstage OK Press Switch 2	Continuous switch chatter from 22,103 sec to 22,107 sec.; dropped out at 22,107 sec.	22,103 sec.	Prior to 22,103 sec.	Possible transducer cable damage.
K0159-401	Event-M/S OK Press Switch 2 Depress	Continuous switch chatter from 22,083 to 22,101 sec.; picked up at 22,101 sec. and dropped out at 22,107 sec.	22,083 sec.	Prior to 22,083 sec.	Possible transducer cable damage.
**These measurements failed between the end of the MDAC defined Phase II Period (spacecraft separation), and the end of the NASA defined Phase II Period (TB <sub>g</sub> initiated).					

Table 19-3. AS-504 Measurement Malfunctions (Continued)

MEASUREMENT NUMBER	MEASUREMENT TITLE	NATURE OF FAILURE	TIME OF FAILURE (RANGE TIME)	DURATION SATISFACTORY OPERATION	REMARKS
PARTIAL MEASUREMENT FAILURES, S-IC STAGE					
A001-118	Acceleration, Longitudinal	Data offscale negative at ignition.	0 sec.	151 sec.	Data valid after 12 sec.
B004-114	Acoustic, Rear, Fin D	System had high amplitude, low frequency noise.	15 sec.	15 sec.	Caused by system saturation due to high vibration level.
C003-104	Temperature, Turbine Manifold	Measurement failed at 28 sec.	28 sec.	28 sec.	Probable transducer failure.
C013-104	Temperature, Helium Heat Exchanger Outlet	Measurement noisy after 30 sec.	30 sec.	30 sec.	Probable open transducer.
C132-101	Temperature, Heat Exchanger Bellows	Data shifts at 14 sec.	14 sec.	14 sec.	Probable transducer attachment weld failure.
C138-101	Temperature, Aft Nozzle, External	Data low throughout flight.	Ignition	Partial	Probable transducer attachment failure.
C177-119	Temperature, LOX Tank Skin	Data noisy from 60 to 120 sec.	60 sec.	100 sec.	Probable transducer bond failure.
C179-119	Temperature, LOX Tank Skin	Data noisy from 45 to 75 sec.	45 sec.	130 sec.	Probable transducer bond failure.
D009-103	Pressure, Gas Generator Combustion Chamber	Measurement failed at 12 sec.	12 sec.	12 sec.	Probable transducer failure.
D151-115	Pressure, LOX Pump Inlet	Measurement failed at 65 sec.	65 sec.	65 sec.	Transducer failure.
D180-119	Pressure, LOX Tank Lower Bulkhead	Data reads high throughout flight.	Ignition	Partial	Data offset high but can be corrected.
E041-101	Vib Fuel Pump Flange Long.	Transients and data dropouts throughout flight.	Ignition	Partial	Scattered useful data.
L018-117	Fuel Slosh Positions 2 and 4	Probes appear to be connected backwards.	Ignition	Partial	Data usable but reversed.
L019-117	Fuel Slosh Positions 2 and 4	Probes appear to be connected backwards.	Ignition	Partial	Data usable but reversed.
PARTIAL MEASUREMENT FAILURES, S-II STAGE					
C003-205	E5 Fuel Turbine Inlet T	Excessive noise.	477 sec.	477 sec.	Possible open transducer
C683-206	Heat Shield Aft Surf T	Maximum value at 212 sec. Minimum value from 223 to 520 sec.	210 sec.	210 sec.	Possible transducer failure. Response not as predicted after 210 sec.
C711-206	Heat Shield Aft Surf T	340°F temp. drop at 258 sec.	258 sec.	258 sec.	Response as predicted after 258 sec. except for indicated bias.
C859-200	Ullage Rocket 2 Fair Surf T	Dropped to minimum value at 69 sec. and remained constant.	69 sec.	69 sec.	Transducer failure.
C861-200	Ullage Rocket 4 Forward Fair Q	Dropped to 0,005 BTU/ft <sup>2</sup> and remained constant.	107 sec.	107 sec.	Heat rate not as predicted after 107 sec.

Table 19-4. AS-504 Flight Measurements With Improper Range

MEASUREMENT NUMBER	MEASUREMENT TITLE	NATURE OF OUTPUT	TIME	REMARKS
S-IC STAGE				
F047-115	Flowrate, Joint Leakage	Offscale High	0 to 55 sec	Data valid after T+55 sec
L004-119	LOX Level, Position IV	Exceeded Full-scale	100 sec 124 sec	Data valid at other times

Table 19-5. AS-504 Questionable Flight Measurements

MEASUREMENT NUMBER	MEASUREMENT TITLE	REASON QUESTIONED S-IC STAGE	REMARKS
E037-101	Vibration, LOX Pump Inlet Flange, Longitudinal	Measurements E037-101 and E038-101 appear to be reversed at the transducer	Unknown
E038-101	Vibration, LOX Pump Inlet Flange, Radial		
E036-101 E036-102 E036-103 E036-104 E036-105	Vibration, Combustion Chamber Dome, Longitudinal	All 5 measurements read approximately 60 percent of predicted	Unknown
S-II STAGE			
C803-200	Forward Skirt Heat Rate Q	0.15 BTU/Sq ft spike at 65 sec, low amplitude at max heating time	0 output at 110 sec not as high as predicted, (about 1 to 2 BTU/sq ft)
C811-216	Systems Tunnel Heat Rate Q	4.6 BTU/Sq ft spike at 65 sec, low amplitude at max heating time	0.1 BTU/Sq ft output at 110 sec, not as high as predicted (about 1 to 2 BTU/Sq ft)
D101-206	Heat Shield Forward Face P	Read full range until 369.5 sec. Approximately 0.02 psia after 370 sec	Response not as predicted between 150 and 200 sec
E336-206	Rad vib LOX sump/prevalve	Relative low signal output during first half of S-II burn. Signal on O'graph responds to environment except for additional spikes during second half of S-II burn	PSD plots are not as predicted. Spectrum contour and GRMS (high) does not agree with previous patterns

### 19.2.3 S-IVB Stage Measurement Analysis

The performance of the S-IVB stage flight measurements for AS-504 was evaluated for two phases of flight. Phase I performance period was from liftoff to parking orbit insertion, and Phase II was from liftoff to initiation of restart preparations for S-IVB third burn which occurred at 21,581 seconds. A summary of the measurement performances for these two phases of flight is listed in Table 19-1. The scheduled flight measurements numbered 288. Three measurements were waived prior to the start of automatic countdown (see Table 19-2), two of which provided



valid flight data. Of the remaining 285 active flight measurements, there were 2 total failures during Phase I and 5 during Phase II (see Table 19-3). The respective measurement reliabilities for Phase I and Phase II performance periods were 99.3 and 98.2 percent.

After Phase II an additional 9 measurements either malfunctioned or went offscale during the third burn. All of these measurement problems are believed to be attributable to the unusual conditions which prevailed during the third burn. These measurement anomalies are listed in Table 19-3.

#### 19.2.4 IU Measurement Analysis

There were 222 flight measurements scheduled for the IU. All of the scheduled measurements were active at the start of automatic countdown and provided valid data during the flight. The flight measurement reliability was 100.0 percent.

### 19.3 AIRBORNE TELEMETRY SYSTEMS

The AS-504 launch vehicle contained a total of 17 telemetry links including the CCS link. A listing of these links, stage assignment and brief performance summary is shown in Table 19-6. Performance of all telemetry systems was satisfactory except for four malfunctions as described in subsequent sections. The AS-2 transmitter power amplifier apparently developed a failure at approximately 180 seconds. A gating problem in the S-IVB DP-1B0 multiplexer occurred at liftoff. The IU data from the Launch Vehicle Data Adapter (LVDA) incurred a temporary failure

Table 19-6. AS-504 Launch Vehicle Telemetry Links

LINK	FREQUENCY (MHZ)	MODULATION	STAGE	FLIGHT PERIOD (RANGE TIME, SEC)	PERFORMANCE SUMMARY	
AF-1	240.2	PAM/FM/FM	S-IC	0-403	Satisfactory except AS-2 failed at 180 sec	
AF-2	252.4	PAM/FM/FM		0-403	Data Dropouts	
AF-3	231.9	PAM/FM/FM		0-403	Range Time (sec)	Duration (sec)
AP-1	244.3	PCM/FM		0-403	163.45	1.1
AS-1	235.0	SS/FM		0-403	166.8	1.7
AS-2	256.2	SS/FM		0-403		
BF-1	241.5	PAM/FM/FM	S-II	0-762	Satisfactory	
BF-2	234.0	PAM/FM/FM		0-762	Data Dropouts	
BF-3	229.9	PAM/FM/FM		0-762	Range Time (sec)	Duration (sec)
BP-1	248.6	PCM/FM		0-762	163.45	5.0
BS-1	227.2	SS/FM		0-762		
BS-2	236.2	SS/FM		0-762		
CP-1	258.5	PCM/FM	S-IVB	Flight Duration	Satisfactory	
					Data Dropouts	
					Range Time (sec)	Duration (sec)
					163.45	1.0
DF-1	250.7	FM/FM/FM	IU	Flight Duration	Satisfactory	
DP-1	245.3	PCM/FM		Flight Duration	Data Dropouts	
DP-1A	2277.5	PCM/FM		Flight Duration	Range Time (sec)	Duration (sec)
DP-1B	2282.5	PCM/FM		Flight Duration	163.45	1.0

of a computer word bit in the "on", or "1" condition. A degraded power amplifier output in the CCS downlink resulted in the loss of CCS telemetry data during 3rd burn and part of the final coast. Except for a 2-second S-II data dropout at approximately 64.5 seconds, all data dropouts were of a predictable nature.

#### 19.3.1 S-IC Stage Telemetry System

The S-IC stage telemetry system consisted of 3 PAM/FM/FM, 1 PCM/FM and 2 SS/FM links. Except for the AS-2 single sideband link, which exhibited a large power loss at approximately 180 seconds, the telemetry system performance was satisfactory. Though the exact cause of the AS-2 power loss is unknown, a transmitter power amplifier filament failure is suspected. The only data dropouts noted were caused by the S-IC retro motor firing at 163.45 seconds and S-II main engines effect at 166.8 seconds. These dropouts had durations of 1.1 and 1.7 seconds, respectively. Data lost from the AF-1 and AF-2 links during these predicted RF blackout periods were later recovered from the airborne tape recorder.

Two programmed inflight calibrations were performed and evaluations indicate that all telemetry calibrations were within specification.

#### 19.3.2 S-II Stage Telemetry System

The telemetry system for the S-II stage consisted of 3 PAM/FM/FM, 2 SS/FM, and 1 PCM/FM links. Performance of the telemetry system was satisfactory. Only one complete data dropout occurred during the 762 seconds of operation. This dropout occurred during S-IC retro motor firing at 163.45 seconds and lasted for approximately 5 seconds.

The PCM link, BP-1, experienced two other intermittent data dropouts at approximately 64.5 seconds and 193 seconds. Synchronization word inversions and faulty synchronization commands to the time division multiplexers were found. High electrical noise can cause this type of problem though signal strength data does not exhibit noise transients at these times. Investigations of this problem are continuing.

Four programmed inflight calibrations were performed, and evaluations indicate that the telemetry calibrations were within specifications.

#### 19.3.3 S-IVB Stage Telemetry System

The S-IVB stage contained only one telemetry link, PCM/FM, on the AS-504 flight. From evaluations of received data, performance of the telemetry system was satisfactory. However, a problem associated with the DP-1B0 multiplexer developed at liftoff. Measurement D0002-403, Pressure-Fuel Pump Inlet, exhibited a large reduction in pressure at liftoff, as received from the IU telemetry link DP-1. However, the same measurement is redundantly telemetered through the CP-1B0 multiplexer and indicated

no change in pressure. It is suspected that a gating problem developed in the DP-1B0 multiplexer at liftoff which affected only the one measurement. Investigations of the problem are continuing.

### 19.3.4 IU Telemetry System

The IU telemetry system consisted of 1 FM/FM/FM and 3 PCM/FM links. Performance of the telemetry links was satisfactory with two exceptions. A failure developed in the circuitry which conditions data from the LVDA for the DP-1 telemetry link. At S-II/S-IVB separation, word 2 bit 10 of the 40 bit computer word failed in the "1" position and remained in this state until spacecraft separation when it returned to normal. This failure affected only the telemetry data. As shown in Figure 19-1, the 40 bit computer word is divided into 4 10-bit words for telemetry. The flow of this data from the LVDA to the telemetry system model 301 PCM assembly is illustrated in Figure 19-2.

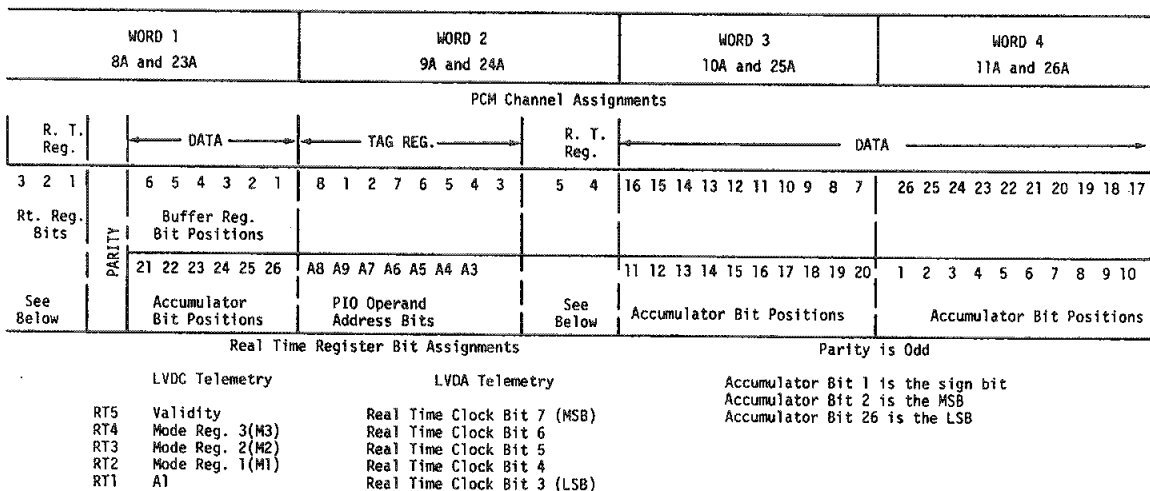


Figure 19-1. Telemetry Format

Investigations indicate that it is possible for the fault to have resulted by a foreign particle in one transistor in the 410 Remote Digital Multiplexer (RDM) of the DP-1 telemetry link. If the failure was in the 410 multiplexer, it was an isolated case as there is no previous history of failure. No corrective action is contemplated. See paragraph 10.5.4 for possible failure modes within the LVDA.

At approximately 22,066.4 seconds the second problem developed. Both Guam and Carnarvon lost lock with the CCS, DP-1B, downlink at this time and did not regain solid lock until 23,471 seconds. During this period all CCS downlink data was lost. This deviation is believed to have been caused by a temporary degraded power amplifier output. Further discussions of this problem may be found in paragraphs 14.3 and 19.5.3.2.

The only other data dropout noted on this flight occurred at S-IC retro motor firing, at 163.45 seconds, for a duration of 1.0 second.

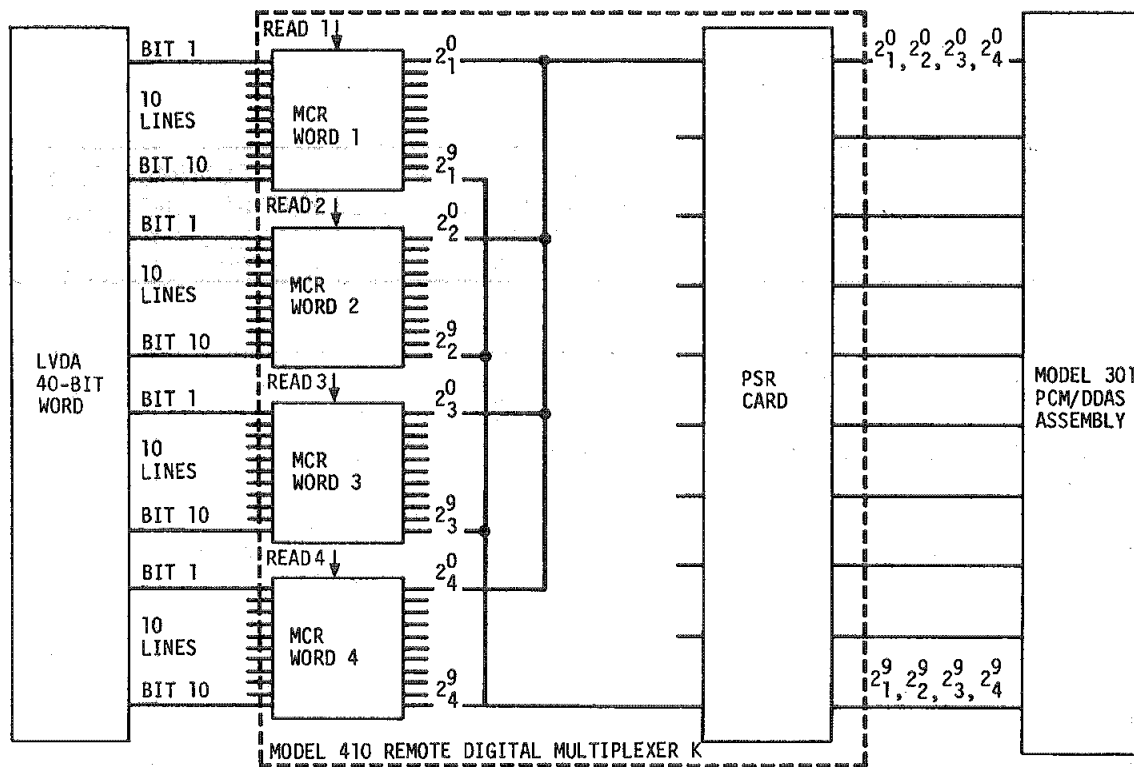


Figure 19-2. LVDC/LVDA Computer Word Flow

#### 19.4 AIRBORNE TAPE RECORDERS

Three tape recorders were installed on the AS-504 launch vehicle to record real time data during predicted RF blackout periods. Recorder assignments and their periods of performance are listed in Table 19-7. The performance of all recorders was satisfactory.

##### 19.4.1 S-IC Stage Recorder

The single tape recorder installed on the S-IC stage recorded data from the AF-1 and AF-2 telemetry links from 134.34 to 188.10 seconds. Evaluation of the played-back data indicates that the tape recorder performance was satisfactory and that all programmed data were received and acceptable.

##### 19.4.2 S-II Stage Recorders

Two tape recorders were installed on the S-II stage to record telemetry links BF-1, BF-2 and BF-3 and multiplexer BT-1. These data were recorded from 74.63 to 174.66 seconds and from 495.25 to 559.44 seconds. All recorded data were recovered during playback. An evaluation of played-back data indicates that performance of the tape recorders was satisfactory with all data acceptable.

Table 19-7. Tape Recorder Summary

RECORDER	LINK RECORDED	RECORD TIME (RANGE TIME, SECONDS)		PLAYBACK TIME (RANGE TIME, SECONDS)	
		START	STOP	START	STOP
LAUNCH PHASE					
S-IC Recorder	AF-1,AF-2	134.34	188.10	188.10	242.04
S-II Recorder No. 1	BF-1,BF-2	74.63 495.25	174.66 559.44	559.44	724.31
S-II Recorder No. 2	BF-3,BT-1	74.63 495.25	174.66 559.44	559.44	723.70

#### 19.5 RF SYSTEMS EVALUATION

The launch vehicle RF systems provide telemetry, tracking, and command system transmission and reception. Not all of the data required to perform a detailed RF analysis were available for this evaluation. Based on available data, the overall performance of launch vehicle RF systems was satisfactory and measured flight data, with few exceptions, agreed favorably with expected trends. Telemetry propagation was good, as was tracking performance. Data received indicate that the CCS performance was satisfactory except for a degraded CCS power amplifier output occurring during S-IVB third burn.

Final loss of VHF telemetry signals occurred at approximately 39,260 seconds (10:54:20) at Hawaii (HAW). The last usable data were recorded at HAW at 31,500 seconds (8:45:00). Signal levels during the time period from 31,500 seconds (8:45:00) to Loss of Signal (LOS) were at threshold 90 percent of the time. UHF telemetry data were recorded at GDS until 37,758 seconds (10:29:18). The C-Band radar was commanded off at 27,214 seconds (7:33:34). Final CCS signals were received at GDS at 48,066 seconds (13:21:06). Other stations viewing the vehicle during those time periods lost signal at earlier times.

### 19.5.1 Telemetry System RF Propagation Evaluation

The RF performance of all 15 VHF telemetry links was excellent and generally agreed with predictions. Main engine flame effects causing 15 to 25 Decibel (db) attenuation were observed from 110 to 150 seconds at Cape Telemetry 4 (TEL 4) and Central Instrumentation Facility (CIF). No significant effects were noted at Grand Bahama Island (GBI). Several short periods of low RF signal strength on the S-IC VHF telemetry links were experienced at TEL 4 and CIF between 133.6 and 138.6 seconds, causing severe data degradation during this time period. Effects at GBI were minor. These periods of low signal strength are similar to those which caused RF dropouts on AS-501 and AS-502 shortly after center engine cutoff, however, total RF dropout was not experienced on AS-504.

Effects due to staging at 163.5 seconds were as expected with all telemetry link signals dropping to threshold at all sites. The duration of the blackout period was approximately 1.1 seconds for the S-IC stage, 1.0 second for the S-II stage, and 1.0 second for the S-IVB stage and 1.0 second for the IU. All VHF telemetry data were lost at this time except for that which could be recovered by onboard tape recorder playback.

S-II stage ignition at 165.2 seconds caused S-IC VHF telemetry signal strength to drop to threshold for a period of 1.7 seconds. The S-II, S-IVB and IU links experienced 20 to 25 db attenuation at this time. All links continued to experience periods of low signal strength with antenna recovery occurring at approximately 175 seconds for S-IC links AF-1, AF-2 and AF-3, 173 seconds for AS-1, AS-2 and AP-1, 170 seconds for the S-II links and 168 seconds for the S-IVB and IU links. No significant data were lost, however, since the antenna systems recovered in sufficient time to obtain good recorder playback data.

S-II second plane separation at 193.5 seconds caused 20 to 25 db attenuation on all upper stage VHF telemetry links at TEL 4 and CIF. GBI data were not affected.

The performance of the S-IVB and IU VHF telemetry systems during orbit, second burn, intermediate coast, third burn, and final coast was satisfactory. The right hand polarized DF-1 link received at HAW during the second revolution dropped to threshold for 0.5 second at 10,365.5 seconds (2:52:45.5). Both the DP-1 and CP-1 links, right and left hand polarization, averaged -75 to -87 dbm during this time period and for most of the pass. During the AS-503 flight, all links dipped to or near threshold for 10 seconds about this time frame. Further analysis will be necessary to correlate these events.

HAW provided VHF telemetry coverage during final coast to 31,500 seconds (8:45:00). Links CP-1, DP-1 and DF-1 were recorded to 39,260 seconds (10:54:20), but the signals were at threshold 90 percent of the time.

The performance of the UHF telemetry system was satisfactory. UHF telemetry was used to provide backup to the IU VHF telemetry and became the primary acquisition system after VHF range limits were exceeded.

UHF signal strength degradation observed during the launch phase were as expected and related effects are identified as follows:

- a. Main engine flame effects caused approximately 7 db attenuation between 124 and 141 seconds.
- b. Signal strength dropped to threshold for approximately 0.3 second due to S-IC/S-II staging at 163.5 seconds.
- c. There were no observable effects at S-II stage engine ignition.
- d. Signal strength dropped approximately 50 db for 1.5 seconds due to S-II second plane separation at 193.5 seconds.

The performance of the UHF telemetry system during orbit, second burn, intermediate coast, third burn and final coast was satisfactory. Last UHF data were recorded at Goldstone at 37,758 seconds (10:29:18).

A summary of telemetry coverage from launch to approximately 39,600 seconds is shown in Figure 19-3.

#### 19.5.2 Tracking Systems RF Propagation Evaluation

Sufficient data were not received to provide a complete assessment of the ODOP and C-Band tracking systems. Based upon the limited data available, however, RF performance of these systems appears to have been satisfactory.

19.5.2.1 ODOP. The ODOP transponder was carried on the S-IC stage of the vehicle, therefore, ODOP tracking was limited to the flight of the first stage only. Signal strength data for the ODOP ground stations were not available for analyses, so evaluation was limited to performance as indicated by the onboard data from the MARGO interrogating station.

S-IC main engine flame attenuation on the ODOP transponder uplink signal strength seen onboard occurred from 80 seconds to S-IC/S-II separation. Center engine cutoff effects caused the ODOP transponder to lose phase lock at approximately 135 seconds, and remained out of lock until 148 seconds. This same effect was noted on AS-503, however, on AS-504 the transponder remained out of lock for approximately 10 seconds longer. At S-IC/S-II separation, occurring at 163.5 seconds, the transponder again lost phase lock and did not recover until 180 seconds.

19.5.2.2 C-Band Radar. Available data indicate that the C-Band radar performed satisfactorily during this flight although several ground stations experienced tracking problems due to antenna nulls and phase front disturbances.

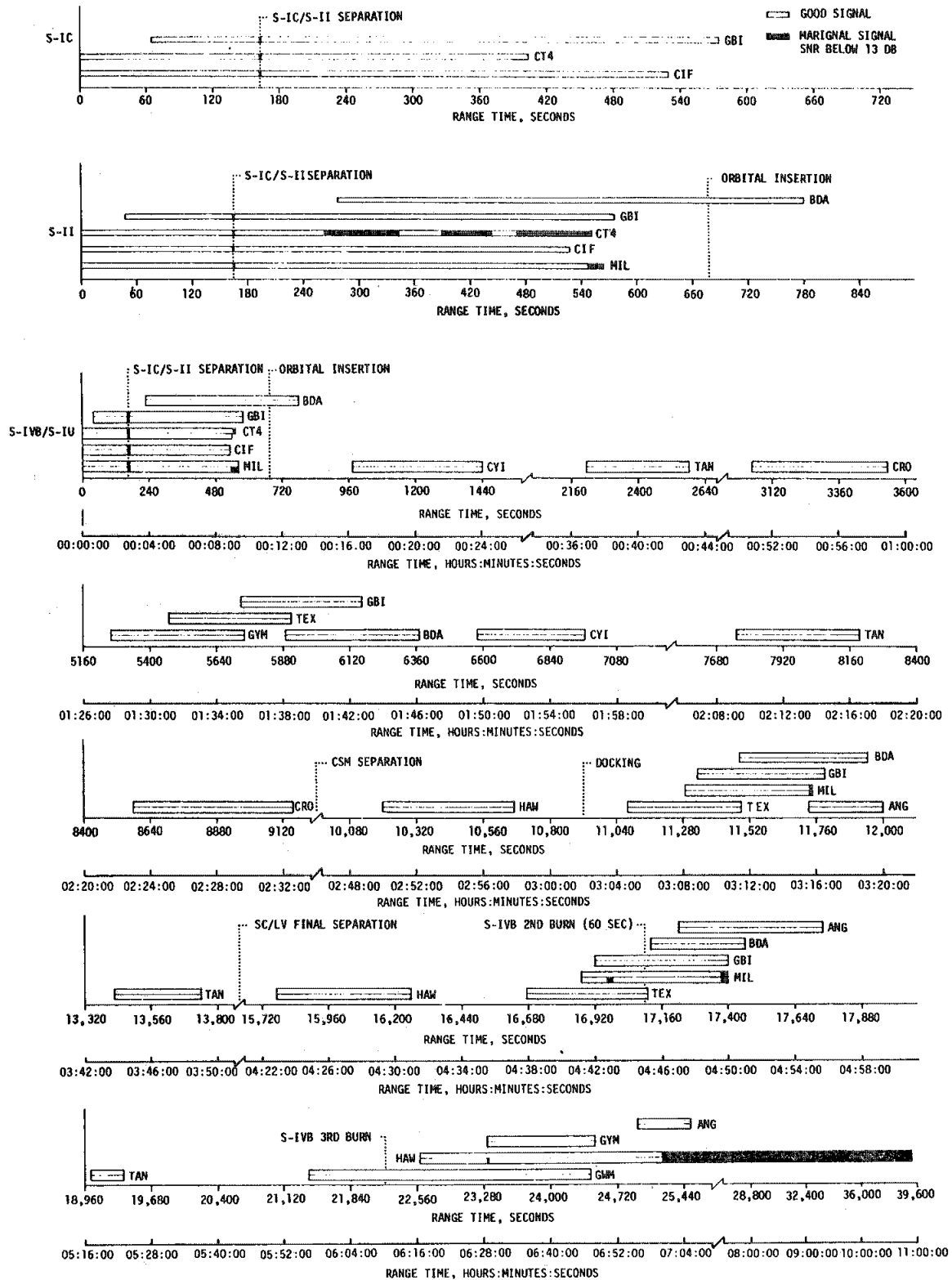


Figure 19-3. VHF Telemetry Coverage Summary



Merritt Island Launch Area (MILA) operators log indicated that a switch between beacon track and skin track had to be made several times due to weak beacon response. A tracking problem was experienced at 162 seconds due to a balance point shift (distorted beacon return) which produced antenna pointing errors.

A data dropout from 306 to 324 seconds was reported by the station operators at GBI. This dropout was attributed to balance point shifts.

Strip chart data from Bermuda (BDA) indicate that a strong signal was received during the launch phase. During the second revolution a low Signal-To-Noise Ratio (SNR) was observed at both BDA stations from 6147 (1:42:27) to 6166 seconds (1:42:40) due to high elevation angles. During this period the vehicle was almost overhead and the required antenna azimuth tracking rate exceeded the equipment capability. During revolution 3, the BDA FPQ-6 station reported transmitter shutdown at Acquisition of Signal (AOS) for 30 seconds. No reason was given for the shutdown. During this pass the FPQ-6 antenna physically obscured the FPS-16 antenna resulting in 35 seconds of data loss at the FPS-16 site. On the fourth revolution, both BDA stations locked on a side lobe at AOS due to lack of pointing information. The FPS-16 station acquired the main lobe using Unified S-Band (USB) for designation. The FPQ-16 station used FPS-16 and USB for designation. Once the main lobe was acquired, good signal was received.

White Sands (WHS) strip chart data indicated a 1 second dropout, during the second revolution, at 11,179 seconds (03:06:19) followed by a low SNR until 11,196 seconds (03:06:36). This was due to high elevation angle and an indicated attitude maneuver which occurred during this interval.

Preliminary data indicate that C-Band Systems I and II were commanded off at 27,189.9 (7:33:09.9) and 27,213.5 seconds (7:33:03.5), respectively. The SNR at HAW at this time was approximately 12 db.

The C-Band radar tracking coverage from launch to 27,217 seconds (7:33:22) is shown in Figure 19-4.

19.5.2.3 CCS Tracking. There is no mandatory tracking requirement of the CCS; however, the CCS transponder has turnaround ranging capabilities and provides a backup to the Command and Service Module (CSM) transponder used for tracking in case of failure or desire for a cross check. Since the same transponder is used for all CCS functions, discussion of the tracking performance of this system is included in the general discussion of the CCS RF evaluation.

### 19.5.3 Command Systems RF Evaluation

The AS-504 command systems consisted of the Secure Range Safety Command System (SRSCS) and the CCS. All indications were that these systems

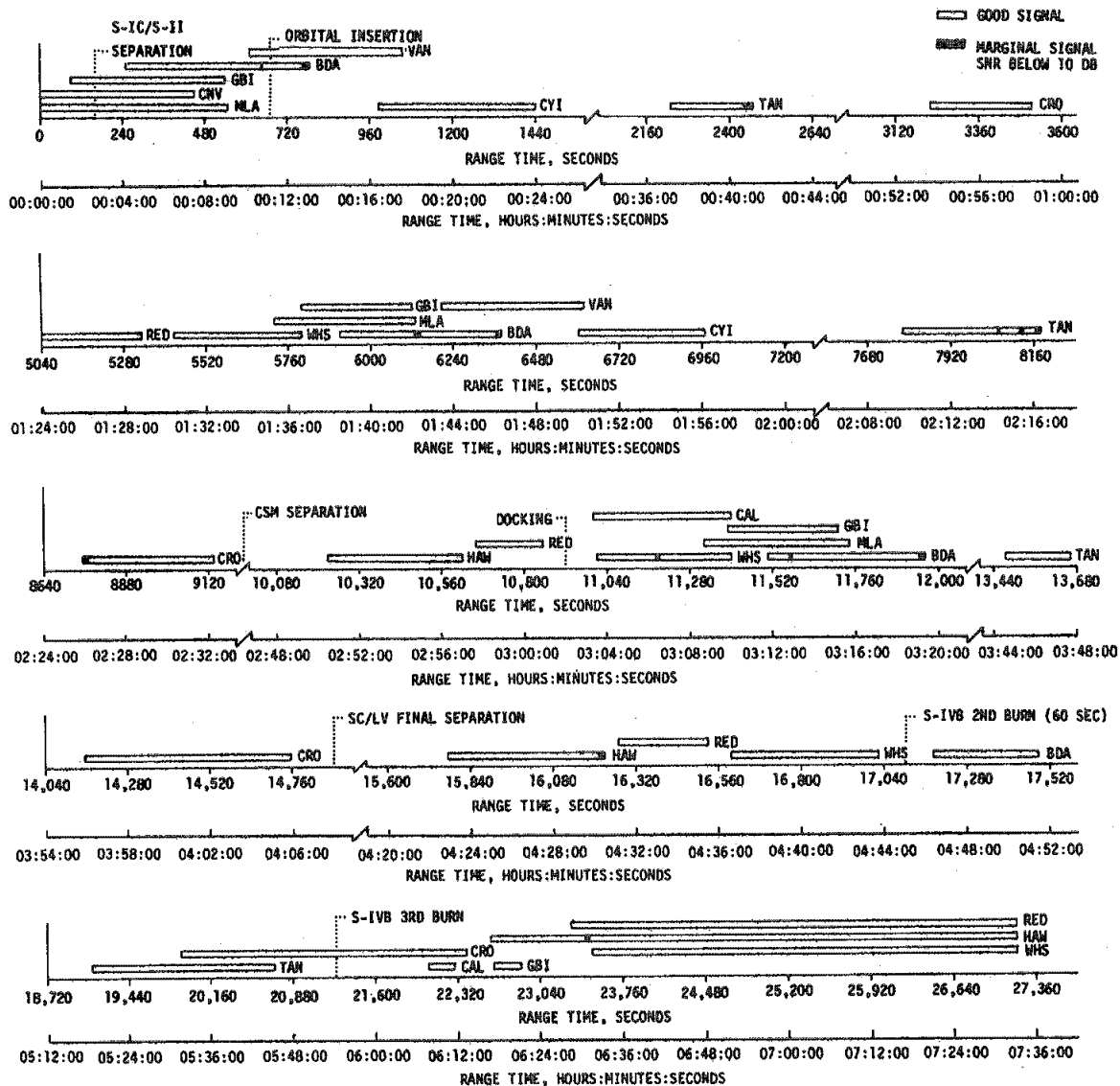


Figure 19-4. C-Band Radar Coverage Summary

performed satisfactorily, except for a degraded CCS power amplifier output discussed below.

19.5.3.1 Secure Range Safety Command System. VHF telemetry measurements received by the ground stations from the S-IC, S-II and S-IVB stages indicated that the SRSCS RF subsystems functioned properly. Canaveral (CNV) and BDA were the command stations used for this flight. The carrier signal was turned off at CNV at 396 seconds. At BDA the carrier was turned on at 392 seconds and turned off at 745 seconds. The system was safed at 684 seconds.

A 0.5 second RF dropout occurred on the S-IC carriers at 161 seconds. This dropout is similar to one which occurred at 116 seconds on AS-503 and is due to the CNV station switching transmitting antennas at these times.

The S-IVB systems experienced 0.7 second of dropout at 163.45 seconds due to S-IC/S-II staging. Momentary signal strength decreased to approximately 3.0 volts on Range Safety Receiver No. 1 at 288 and 293 seconds. These signal strength decreases may be due to an unfavorable look angle condition (Range Safety No. 1 antenna may have been obscured at these times). Range Safety Receiver No. 2 signal strength shows no decrease at these times.

19.5.3.2 Command and Communications System. Available data indicated satisfactory CCS performance with the exception of degraded CCS power amplifier output from approximately 22,066.4 seconds (06:07:46.4) to 23,418.8 seconds (06:30:18.8). A 1.5 second data dropout was experienced due to S-IC/S-II staging at 163.45 seconds. An intermittent data dropout of 11 seconds duration was experienced at 195.5 seconds due to S-II second plane separation. During handover from MILA to BDA at 332 seconds, approximately 5 seconds of data were lost. Vanguard (VAN) ship data were not available to assess handover from BDA to VAN.

MILA reported side lobe tracking problems during the second revolution. Carnarvon (CRO) reported tracking through the mechanical keyhole on the first revolution, as did HAW on the second revolution. No problems, however, were experienced. The "Remove Restart Enable Inhibit" command, necessary to enable restart preparations for the second S-IVB burn, was scheduled to be transmitted from HAW at 16,200 seconds (04:30:00). The command could not be sent at this time due to loss of signal at HAW. The command was transmitted from Redstone (RED) ship at 16,454 seconds (04:34:14).

The second burn phase was covered by MILA, GBI, and BDA with no anomalies noted.

Prior to the second S-IVB stage restart, CRO data were noisy, necessitating a switch to low gain antennas at 20,595 seconds (05:43:15), 7 minutes earlier than scheduled for this switch. The third burn of the S-IVB stage was covered by CRO and Guam (GWM). The final coast period, after S-IVB third cutoff was observed by GWM, Corpus Christi (TEX), GDS and CRO in entirety or when not tracking the CSM.

The most significant CCS problem was experienced during S-IVB third burn and final coast, and was caused by a degraded CCS power amplifier output which occurred at 22,066.4 seconds (06:07:46:4). A 40 percent drop in the power amplifier helix current was noted at this time and the current remained low until 23,418.8 seconds (06:30:18.8) when it increased to its

original level. GWM and CRO, the stations tracking the CCS at this time lost downlink lock when the current level dropped. The vehicle went over the horizon from CRO before the amplifier resumed proper operation resulting in CRO never re-establishing a downlink lock. GWM re-established intermittent downlink lock from 22,783.0 seconds (06:19:43.0) to 22,806.5 seconds (06:20:06.5), then lost lock again. Solid lock was established again at 23,471.0 seconds (06:31:11.0). No valid CCS downlink data were received during this period, however data were received from the redundant DP-1 VHF and DP-1A UHF links. The CCS transponder did not appear to be affected by the degraded power output and remained in uplink lock throughout most of this time period using telemetry antenna pointing data. The degraded CCS power amplifier output did not affect the successful accomplishment of this mission, however, since 10 commands (30 words) were successfully transmitted and verified by DP-1 VHF and DP-1A UHF telemetry data during this time period. On future missions the UHF telemetry is deleted therefore loss of the CCS telemetry during portions of trans-lunar injection beyond VHF range would result in loss of data necessary to verify commands and inability to maintain uplink lock.

Starting at 27,010 seconds (07:30:10) a signal strength test was conducted with GDS. Both the CCS and UHF telemetry antennas were switched and the signal strength for each antenna position was recorded as shown in Table 19-8. This test was performed at the altitude where LM ejection would occur during a lunar mission. At 27,162 seconds (07:32:42) the antennas were set to low gain and remained in this position through the remainder of the mission.

Table 19-8. Signal Strength at Goldstone

ANTENNA POSITION	SIGNAL STRENGTH (DBM)	
	CCS	UHF
Omni	-106	-106
Low Gain	-93	-98
High Gain	-88	-90

The planned CCS transmitter inhibit occurred at 28,108 seconds (07:48:28). The system was re-enabled at 30,605 seconds (08:30:05) to assist Goddard in tracking the S-IVB/IU and remained active throughout the lifetime of the IU batteries.

The final signals were received at GDS and TEX at 48,066 seconds (13:21:06) and 48,060 seconds (13:21:00), respectively. The elevation angles at this time were 10 degrees for TEX and 25 degrees for GDS.

The CCS coverage from launch to 48,066 seconds (13:21:06) is shown in Figure 19-5.

#### 19.6 OPTICAL INSTRUMENTATION

There was no onboard camera coverage on AS-504. In general ground camera coverage was very good. Eighty-seven items were received from Kennedy Space Center (KSC) and evaluated. One camera provided unusable data due to bad time. Three cameras malfunctioned and one film was overdeveloped in processing. As a result of the 5 failures listed above, system efficiency was 94 percent.

Due to the extreme cloud coverage at launch, tracking cameras did not acquire the vehicle between 30 and 50 seconds. Four long range tracking items were not able to acquire at all.

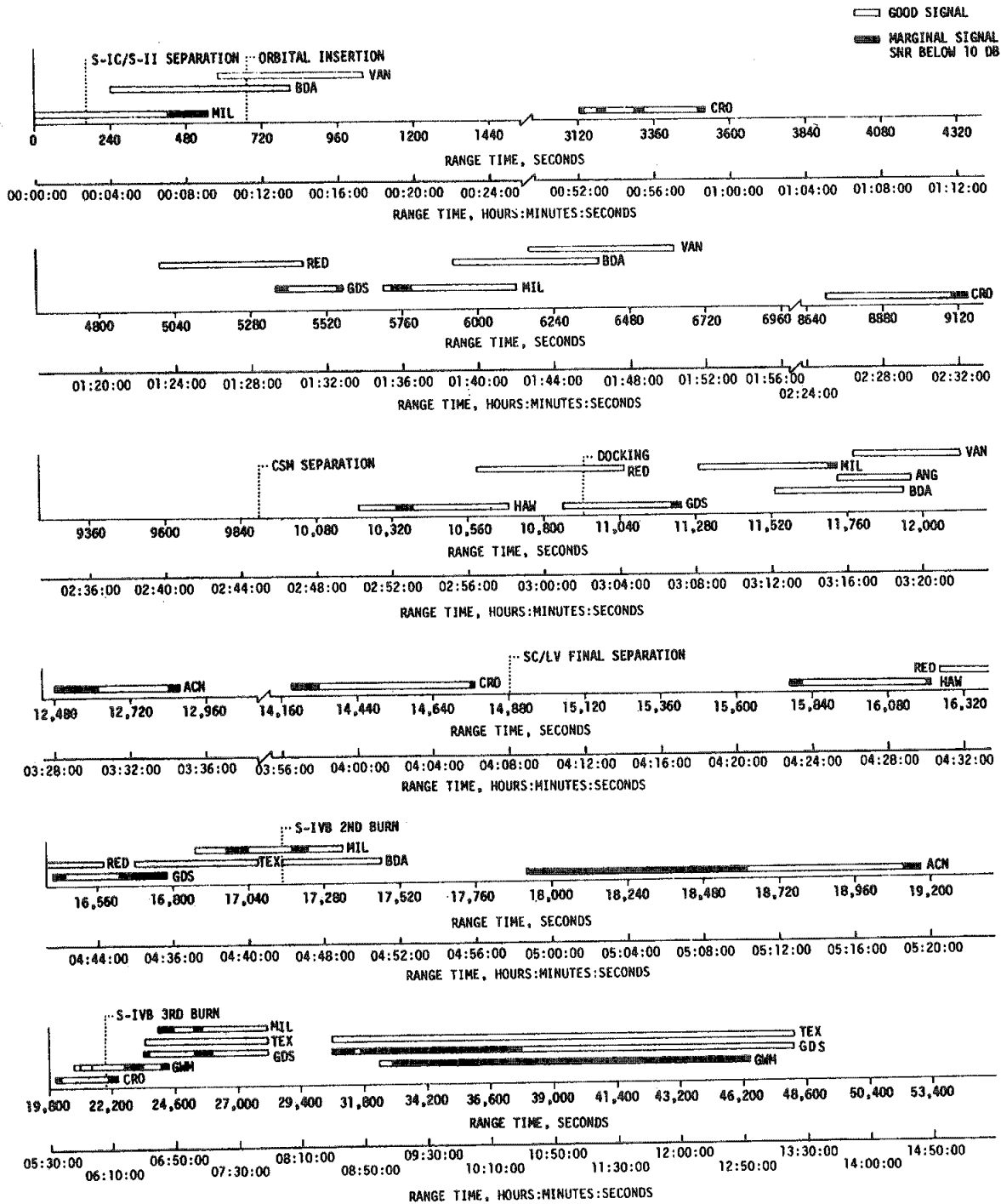


Figure 19-5. Command and Communication System Coverage Summary

## SECTION 20

### VEHICLE AERODYNAMIC CHARACTERISTICS

A base differential pressure, static stability, and fin loading analysis was not made on the AS-504 vehicle. The AS-504 had two base pressure static measurements whereas the AS-503 had six valid measurements. Because of the lack of instrumentation, a base differential pressure analysis was not performed. However, the two available measurements were in close agreement with previous flight data. This suggests that the base differential pressures fell within acceptable limits.

The AS-504 vehicle, like prior Saturn vehicles, flew at very low angles-of-attack during the period of interest. Because of this, a reliable stability analysis could not be made.

A fin pressure loading analysis was not made due to the removal of instrumentation on this vehicle.

## SECTION 21

### MASS CHARACTERISTICS

#### 21.1 SUMMARY

Postflight analysis indicates that vehicle mass during S-IC and S-II boost phases was higher than predicted. The deviations are attributed primarily to inexact initial propellant loads and greater than predicted residuals at the end of S-IC burn. A longer than predicted S-IVB first burn phase resulted in the vehicle mass at cutoff being less than expected. The vehicle mass remained lower than predicted through spacecraft separation, second S-IVB burn, and during third S-IVB burn until the engine performance decrease occurred. Vehicle mass at third burn completion was 8839 kilograms (19,487 lbm) or 34.70 percent higher than predicted.

#### 21.2 MASS EVALUATION

Postflight mass characteristics are compared with the final predicted mass characteristics (MSFC Memorandum R-P&VE-VAW-69-22) which were used in the determination of the final operational trajectory (MSFC Memorandum R-AERO-FMT-20-69).

The postflight mass characteristics were determined from an analysis of all available actual and reconstructed data from S-IC stage ignition through S-IVB stage third burn cutoff. Dry weights of the launch vehicle were based on actual stage weighings and evaluation of the weight and balance log books (MSFC Form 998). Propellant loading and utilization was evaluated from propulsion system performance reconstructions. Spacecraft data were obtained from the Manned Spacecraft Center (MSC).

Deviations from predicted in dry weights of the inert stages and the loaded spacecraft were all within 1.02 percent which is well within the 3-sigma deviation limits. Major items that contributed to these small deviations were as follows:

- a. Actual weight of vehicle components were slightly different from predicted weight.



b. Vehicle insulation modifications.

c. Deletion of an Azusa transponder and filter from the Instrument Unit (IU).

During S-IC stage powered flight, mass of the total vehicle was determined to be 1534 kilograms (3382 lbm) or 0.05 percent higher than predicted at ignition and 8826 kilograms (19,457 lbm) or 1.07 percent higher at S-IC/S-II separation. The mass above the S-IC stage contributed 933 kilograms (2056 lbm) to the higher than predicted ignition mass. The mass deviation at S-IC/S-II separation was caused mainly by the S-IC propellant residuals being 8039 kilograms (17,724 lbm) greater than predicted. S-IC burn phase total vehicle mass is shown in Tables 21-1 and 21-2.

During S-II burn phase, the total vehicle mass varied from 887 kilograms (1956 lbm) or 0.13 percent higher than predicted at start command to 668 kilograms (1472 lbm) or 0.32 percent higher than predicted at S-II/S-IVB separation. The initial mass deviation was due mainly to excess propellant loads on both the S-II and S-IVB stages. The LOX step pressurization sequence initiated during S-II burn resulted in an additional 337 kilograms (741 lbm) of LOX tank pressurant gas. This sequence was not included in the mass prediction. Total vehicle mass for the S-II burn phase is shown in Tables 21-3 and 21-4.

During S-IVB stage first burn, the total vehicle mass ranged from 488 kilograms (1076 lbm) or 0.30 percent higher than predicted at start command to 2405 kilograms (5302 lbm) or 1.77 percent lower than predicted at the beginning of orbital coast. Excess propellants and a slightly heavier than predicted spacecraft caused the initial mass deviation. A longer than predicted first burn phase resulted in the vehicle mass at cutoff being less than expected. S-IVB first burn phase total vehicle mass is shown in Tables 21-5 and 21-6. Vehicle mass during the spacecraft docking and separation maneuver is given in Tables 21-7 and 21-8. During S-IVB second and third burn phases, the total vehicle mass deviated from 2271 kilograms (5007 lbm) or 2.50 percent lower than predicted at second start command to 8839 kilograms (19,487 lbm) or 34.70 percent higher than predicted at end of third burn thrust decay. The engine performance decrease during third burn is the primary cause of this large deviation. Tables 21-9 through 21-12 show total vehicle mass from second S-IVB ignition through third burn thrust decay.

A summary of mass utilization and loss, actual and predicted, from S-IC stage ignition through S-IVB stage third burn is presented in Table 21-13. A comparison of actual and predicted mass, center of gravity, and moment of inertia, is shown in Table 21-14.

Table 21-1. Total Vehicle Mass - S-IC Burn Phase - Kilograms

EVENTS	GROUND IGNITION		HOLDDOWN ARM RELEASE		CENTER ENGINE CUTOFF		OUTBOARD, ENGINE CUTOFF		S-IC/S-II SEPARATION	
	PRED	ACT	PRED	ACT	PRED	ACT	PRED	ACT	PRED	ACT
RANGE TIME--SEC	-6.34	-6.34	0.26	0.26	134.27	134.34	159.96	162.76	160.68	163.45
S-IC STAGE DRY	133900.	133568.	133900.	133568.	133900.	133568.	133900.	133568.	133900.	133568.
LOX IN TANK	1478717.	1476286.	1447345.	1445057.	190678.	209574.	1039.	2033.	961.	1307.
LOX BELOW TANK	21000.	21115.	21737.	21874.	21720.	21793.	16705.	18483.	14596.	17232.
LOX ULLAGE GAS	187.	207.	207.	217.	2565.	2611.	3034.	3232.	3040.	3232.
RPI IN TANK	641889.	645072.	631691.	635089.	91599.	103898.	8357.	13256.	7262.	12306.
RPI BELOW TANK	4313.	4327.	5996.	6010.	5996.	6010.	5958.	5972.	5958.	5972.
RPI ULLAGE GAS	33.	73.	33.	75.	208.	245.	238.	283.	238.	283.
N2 PURGE GAS	36.	29.	36.	29.	20.	20.	20.	20.	20.	20.
HELIUM IN BOTTLE	288.	288.	288.	287.	114.	117.	84.	79.	83.	79.
FROST	635.	635.	635.	635.	340.	340.	340.	340.	340.	340.
RETROMOTOR PROP	1027.	1027.	1027.	1027.	1027.	1027.	1027.	1027.	1027.	1027.
OTHER	239.	239.	239.	239.	239.	239.	239.	239.	239.	239.
TOTAL S-IC STAGE	2282265.	2282866.	2243135.	2244107.	448407.	479441.	170943.	178532.	167667.	175605.
TOTAL S-IC/S-II IS	5291.	5258.	5291.	5258.	5291.	5258.	5291.	5258.	5258.	5224.
TOTAL S-II STAGE	482908.	483378.	482908.	483378.	482649.	483120.	482649.	483120.	482649.	483120.
TOT S-II/S-IVB IS	3665.	3628.	3665.	3628.	3665.	3628.	3665.	3628.	3665.	3628.
TOTAL S-IVB STAGE	117553.	118003.	117553.	118003.	117507.	117912.	117507.	117912.	117507.	117912.
TOTAL INSTRU UNIT	1948.	1942.	1948.	1942.	1948.	1942.	1948.	1942.	1948.	1942.
TOTAL SPACECRAFT	47098.	47188.	47098.	47188.	47098.	47188.	47098.	47188.	47098.	47188.
TOTAL UPPER STAGE	658462.	659396.	658463.	659396.	658159.	659047.	658159.	659047.	658126.	659014.
TOTAL VEHICLE	2940728.	2942262.	2901593.	2903503.	1106566.	1138488.	829102.	837579.	825793.	834619.

Table 21-2. Total Vehicle Mass - S-IC Burn Phase - Pounds Mass

EVENTS	GROUND IGNITION		HOLDDOWN ARM RELEASE		CENTER ENGINE CUTOFF		OUTBOARD ENGINE CUTOFF		S-IC/S-II SEPARATION	
	PRED	ACT	PRED	ACT	PRED	ACT	PRED	ACT	PRED	ACT
RANGE TIME--SEC	-6.34	-6.34	0.26	0.26	134.27	134.34	159.96	162.76	160.68	163.45
S-IC STAGE DRY	295200.	294468.	295200.	294468.	295200.	294468.	295200.	294468.	295200.	294438.
LOX IN TANK	3260012.	3254653.	3190849.	3185805.	420373.	462032.	2290.	4482.	2119.	2841.
LOX BELOW TANK	46296.	46550.	47921.	48225.	47884.	48045.	36828.	40748.	32178.	37989.
LOX ULLAGE GAS	411.	456.	456.	478.	5654.	5756.	6689.	7126.	6702.	7126.
RPI IN TANK	1415122.	1422139.	1392639.	1400132.	201942.	229055.	18424.	29224.	16010.	27131.
RPI BELOW TANK	9509.	9539.	13219.	13249.	13219.	13249.	13136.	13166.	13136.	13166.
RPI ULLAGE GAS	73.	151.	73.	165.	458.	540.	524.	623.	525.	623.
N2 PURGE GAS	80.	63.	80.	63.	43.	43.	43.	43.	43.	43.
HELIUM IN BOTTLE	636.	636.	636.	632.	251.	257.	185.	174.	184.	174.
FROST	1400.	1400.	1400.	1400.	750.	750.	750.	750.	750.	750.
RETROMOTOR PROP	2264.	2264.	2264.	2264.	2264.	2264.	2264.	2264.	2264.	2264.
OTHER	528.	528.	528.	528.	528.	528.	528.	528.	528.	528.
TOTAL S-IC STAGE	5031532.	5032858.	4945266.	4947410.	988567.	1056987.	376863.	393596.	369641.	387143.
TOTAL S-IC/S-II IS	11665.	11591.	11665.	11591.	11665.	11591.	11665.	11591.	11592.	11518.
TOTAL S-II STAGE	1064629.	1065657.	1064629.	1065667.	1064059.	1065097.	1064059.	1065097.	1064059.	1065097.
TOT S-II/S-IVB IS	8081.	7998.	8081.	7998.	8081.	7998.	8081.	7998.	8081.	7998.
TOTAL S-IVB STAGE	259159.	260151.	259159.	260151.	259059.	259951.	259059.	259951.	259059.	259951.
TOTAL INSTRU UNIT	4295.	4281.	4295.	4281.	4295.	4281.	4295.	4281.	4295.	4281.
TOTAL SPACECRAFT	103834.	104031.	103834.	104031.	103834.	104031.	103834.	104031.	103834.	104031.
TOTAL UPPER STAGE	1451663.	1453719.	1451663.	1453719.	1450993.	1452949.	1450993.	1452949.	1450920.	1452876.
TOTAL VEHICLE	6483195.	6486577.	6396929.	6401129.	2439561.	2509936.	1827857.	1846545.	1820561.	1840019.

Table 21-3. Total Vehicle Mass - S-II Burn Phase - Kilograms

EVENTS	S-IC IGNITION		S-II IGNITION		S-II MAINSTAGE		S-II ENGINE CUTOFF		S-II/S-IVB SEPARATION	
	PRED	ACT	PRED	ACT	PRED	ACT	PRED	ACT	PRED	ACT
RANGE TIME--SEC	-6.34	-6.34	162.39	165.17	164.38	167.17	531.16	536.22	532.00	537.20
S-IC/S-II IS SMALL	614.	614.								
S-IC/S-II IS LARGE	4061.	4033.	4061.	4033.	4061.	4033.				
S-IC/S-II IS PROP	617.	611.	313.	308.						
TOTAL S-IC/S-II IS	5291.	5258.	4374.	4342.	4061.	4033.				
S-II STAGE DRY	38374.	38243.	38374.	38243.	38374.	38243.	38374.	38243.	38374.	38243.
LOX IN TANK	371452.	371891.	371452.	371891.	370904.	371537.	644.	665.	480.	506.
LOX BELOW TANK	737.	737.	737.	737.	800.	800.	800.	800.	800.	800.
LOX ULLAGE GAS	189.	165.	189.	165.	192.	167.	1925.	2268.	1931.	2268.
LH2 IN TANK	71658.	71864.	71659.	71854.	71423.	71635.	1416.	1406.	1346.	1340.
LH2 BELOW TANK	105.	105.	105.	105.	128.	128.	128.	128.	128.	129.
LH2 ULLAGE GAS	77.	67.	77.	67.	79.	70.	692.	682.	693.	685.
INSULATION PURGE	54.	54.								
FROST	204.	204.								
START TANK GAS	14.	14.	14.	14.	2.	2.	2.	2.	2.	2.
OTHER	34.	34.	34.	34.	34.	34.	34.	34.	34.	34.
TOTAL S-II STAGE	482908.	483378.	482641.	483111.	481937.	482617.	44016.	44228.	43789.	44006.
TOT S-II/S-IVB IS	3665.	3628.	3665.	3628.	3665.	3628.	3665.	3628.	3665.	3628.
TOTAL S-IVB STAGE	117553.	118003.	117507.	117912.	117507.	117912.	117507.	117912.	117505.	117910.
TOTAL INSTRU UNIT	1948.	1942.	1948.	1942.	1948.	1942.	1948.	1942.	1948.	1942.
TOTAL SPACECRAFT	47098.	47188.	47098.	47188.	47098.	47188.	43075.	43165.	43075.	43165.
TOTAL UPPER STAGE	170265.	170760.	170219.	170669.	170219.	170669.	166196.	166646.	166194.	166644.
TOTAL VEHICLE	658463.	659396.	657233.	658122.	656216.	657320.	210211.	210875.	209983.	210651.

Table 21-4. Total Vehicle Mass - S-II Burn Phase - Pounds Mass

EVENTS	S-IC IGNITION		S-II IGNITION		S-II MAINSTAGE		S-II ENGINE CUTOFF		S-II/S-IVB SEPARATION	
	PRED	ACT	PRED	ACT	PRED	ACT	PRED	ACT	PRED	ACT
RANGE TIME--SEC	-6.34	-6.34	162.39	165.17	164.38	167.17	531.16	536.22	532.00	537.20
S-IC/S-II IS SMALL	1353.	1353.								
S-IC/S-II IS LARGE	8952.	8892.	8952.	8892.	8952.	8892.				
S-IC/S-II IS PROP	1360.	1346.	690.	680.						
TOTAL S-IC/S-II IS	11665.	11591.	9642.	9572.	8952.	8892.				
S-II STAGE DRY	84600.	84312.	84600.	84312.	84600.	84312.	84600.	84312.	84600.	84312.
LOX IN TANK	818911.	819879.	818911.	819879.	817702.	819098.	1420.	1466.	1058.	1115.
LOX BELOW TANK	1625.	1625.	1625.	1625.	1764.	1764.	1764.	1764.	1764.	1764.
LOX ULLAGE GAS	416.	364.	415.	364.	423.	369.	4243.	4999.	4258.	4979.
LH2 IN TANK	158000.	158432.	157981.	158412.	157461.	157929.	3120.	3099.	2968.	2904.
LH2 BELOW TANK	231.	231.	231.	231.	282.	282.	282.	282.	282.	282.
LH2 ULLAGE GAS	169.	148.	169.	148.	173.	154.	1525.	1504.	1528.	1510.
INSULATION PURGE	120.	120.								
FROST	450.	450.								
START TANK GAS	30.	30.	30.	30.	5.	5.	5.	5.	5.	5.
OTHER	76.	76.	76.	76.	76.	76.	76.	76.	76.	76.
TOTAL S-II STAGE	1064629.	1065667.	1064040.	1065077.	1062488.	1063989.	97037.	97507.	96539.	97017.
TOT S-II/S-IVB IS	8081.	7998.	8081.	7998.	8081.	7998.	8081.	7998.	8081.	7998.
TOTAL S-IVB STAGE	259159.	260151.	259059.	259951.	259059.	259951.	259059.	259951.	259054.	259947.
TOTAL INSTRU UNIT	4295.	4281.	4295.	4281.	4295.	4281.	4295.	4281.	4295.	4281.
TOTAL SPACECRAFT	103834.	104031.	103834.	104031.	103834.	104031.	94964.	95162.	94964.	95162.
TOTAL UPPER STAGE	375369.	376461.	375269.	376261.	375269.	376261.	366399.	367392.	366394.	367388.
TOTAL VEHICLE	1451663.	1453719.	1448951.	1450910.	1446709.	1449142.	463436.	464899.	462933.	464405.

Table 21-5. Total Vehicle Mass - S-IVB First Burn Phase - Kilograms

EVENTS	S-IC IGNITION		S-IVB IGNITION		S-IVB MAINSTAGE		S-IVB ENGINE CUTOFF		S-IVB END DECAY	
	PRED	ACT	PRED	ACT	PRED	ACT	PRED	ACT	PRED	ACT
RANGE TIME--SEC	-6.34	-6.34	535.16	540.82	537.66	543.32	648.73	664.66	649.91	665.90
S-IVB STAGE DRY	11476.	11380.	11453.	11357.	11453.	11357.	11392.	11296.	11392.	11296.
LOX IN TANK	85520.	85874.	85520.	85874.	85368.	85735.	62300.	60339.	62242.	60266.
LOX BELOW TANK	166.	166.	166.	166.	180.	180.	180.	180.	180.	180.
LOX ULLAGE GAS	17.	23.	17.	23.	23.	24.	90.	78.	91.	78.
LH2 IN TANK	19715.	19804.	19711.	19800.	19659.	19753.	15399.	14942.	15389.	14928.
LH2 BELOW TANK	22.	22.	26.	26.	26.	26.	26.	26.	26.	26.
LH2 ULLAGE GAS	21.	18.	21.	18.	22.	19.	54.	59.	54.	59.
ULLAGE MOTOR PROP	54.	54.	10.	0.						
APS PROPELLANT	286.	298.	286.	298.	286.	298.	285.	296.	285.	296.
HELIUM IN BOTTLES	203.	200.	203.	200.	202.	200.	185.	180.	185.	180.
START TANK GAS	2.	2.	2.	2.	0.	0.	3.	3.	3.	3.
FROST	45.	136.	0.	45.	0.	45.	0.	45.	0.	45.
OTHER	25.	25.	25.	25.	25.	25.	25.	25.	25.	25.
TOTAL S-IVB STAGE	117553.	118003.	117441.	117835.	117244.	117662.	89938.	87470.	89872.	87364.
TOTAL INSTRU UNIT	1948.	1942.	1948.	1942.	1948.	1942.	1948.	1942.	1948.	1942.
TOTAL SPACECRAFT	47098.	47188.	43075.	43165.	43075.	43165.	43075.	43165.	43075.	43165.
TOTAL UPPER STAGE	49046.	49130.	45023.	45107.	45023.	45107.	45023.	45107.	45023.	45107.
TOTAL VEHICLE	166599.	167132.	162464.	162942.	162267.	162768.	134961.	132576.	134895.	132490.

Table 21-6. Total Vehicle Mass - S-IVB First Burn Phase - Pounds Mass

EVENTS	S-IC IGNITION		S-IVB IGNITION		S-IVB MAINSTAGE		S-IVB ENGINE CUTOFF		S-IVB END DECAY	
	PRED	ACT	PRED	ACT	PRED	ACT	PRED	ACT	PRED	ACT
RANGE TIME--SEC	-6.34	-6.34	535.16	540.82	537.66	543.32	648.73	664.66	649.91	665.90
S-IVB STAGE DRY	25300.	25089.	25249.	25038.	25249.	25038.	25114.	24904.	25114.	24904.
LOX IN TANK	188539.	189319.	188539.	189319.	188203.	189013.	137347.	133024.	137220.	132864.
LOX BELOW TANK	367.	367.	367.	367.	397.	397.	397.	397.	397.	397.
LOX ULLAGE GAS	37.	50.	37.	50.	49.	52.	199.	172.	200.	173.
LH2 IN TANK	43465.	43661.	43455.	43651.	43341.	43547.	33948.	32941.	33928.	32910.
LH2 BELOW TANK	48.	48.	58.	58.	58.	58.	58.	58.	58.	58.
LH2 ULLAGE GAS	47.	40.	47.	40.	47.	41.	118.	130.	118.	131.
ULLAGE MOTOR PROP	118.	118.	22.	0.						
APS PROPELLANT	630.	657.	630.	657.	630.	657.	628.	652.	628.	652.
HELIUM IN BOTTLES	447.	441.	447.	441.	445.	440.	407.	397.	407.	396.
START TANK GAS	5.	5.	5.	5.	1.	1.	7.	7.	7.	7.
FROST	100.	300.	0.	100.	0.	100.	0.	100.	0.	100.
OTHER	56.	56.	56.	56.	56.	56.	56.	56.	56.	56.
TOTAL S-IVB STAGE	259159.	260151.	258912.	259782.	258479.	259400.	198279.	192838.	198133.	192648.
TOTAL INSTRU UNIT	4295.	4281.	4295.	4281.	4295.	4281.	4295.	4281.	4295.	4281.
TOTAL SPACECRAFT	103834.	104031.	94964.	95162.	94964.	95162.	94964.	95162.	94964.	95132.
TOTAL UPPER STAGE	108129.	108312.	99259.	99443.	99259.	99443.	99259.	99443.	99259.	99443.
TOTAL VEHICLE	367288.	368463.	358171.	359225.	357738.	358843.	297538.	292281.	297392.	292091.

Table 21-7. Total Vehicle Mass - At Spacecraft Separation - Kilograms

EVENTS	CSM SEPARATED		CSM DOCKED		SPACECRAFT SEPARATED	
	PRED	ACT	PRED	ACT	PRED	ACT
RANGE TIME--SEC	9583.00	9650.00	10423.00	10929.00	14983.00	14889.00
S-IVB STAGE DRY	11392.	11296.	11392.	11296.	11392.	11296.
LOX IN TANK	62242.	60216.	62242.	60211.	62242.	60189.
LOX BELOW TANK	166.	166.	166.	166.	166.	166.
LOX ULLAGE GAS	91.	128.	91.	134.	91.	155.
LH2 IN TANK	14522.	13998.	14522.	13895.	14089.	13497.
LH2 BELOW TANK	22.	22.	22.	22.	22.	22.
LH2 ULLAGE GAS	80.	106.	80.	111.	93.	131.
APS PROPELLANT	234.	250.	234.	250.	234.	250.
HELIUM IN BOTTLES	185.	180.	185.	180.	185.	180.
START TANK GAS	3.	3.	3.	3.	3.	3.
FROST	0.	45.	0.	45.	0.	45.
OTHER	25.	25.	25.	25.	25.	25.
TOTAL S-IVB STAGE	88962.	86437.	88962.	86339.	88541.	85961.
TOTAL INSTRU UNIT	1948.	1942.	1948.	1942.	1948.	1942.
TOTAL SPACECRAFT	15155.	15212.	41900.	42026.	640.	681.
TOTAL UPPER STAGE	17104.	17154.	43848.	43968.	2589.	2623.
TOTAL VEHICLE	106066.	103591.	132810.	130307.	91130.	88584.



Table 21-8. Total Vehicle Mass - At Spacecraft Separation - Pounds Mass

EVENTS	CSM SEPARATED		CSM DOCKED		SPACECRAFT SEPARATED	
	PRED	ACT	PRED	ACT	PRED	ACT
RANGE TIME--SEC	9583.00	9650.00	10423.00	10929.00	14983.00	14889.00
S-IVB STAGE DRY	25114.	24904.	25114.	24904.	25114.	24904.
LOX IN TANK	137220.	132754.	137220.	132742.	137220.	132695.
LOX BELOW TANK	367.	367.	367.	367.	367.	367.
LOX ULLAGE GAS	200.	283.	200.	295.	200.	342.
LH2 IN TANK	32016.	30861.	32016.	30633.	31060.	29755.
LH2 BELOW TANK	48.	48.	48.	48.	48.	48.
LH2 ULLAGE GAS	176.	233.	176.	245.	205.	289.
APS PROPELLANT	515.	552.	515.	552.	515.	552.
HELIUM IN BOTTLES	407.	396.	407.	396.	407.	396.
START TANK GAS	7.	7.	7.	7.	7.	7.
FROST	0.	100.	0.	100.	0.	100.
OTHER	56.	56.	56.	56.	56.	56.
TOTAL S-IVB STAGE	196127.	190561.	196127.	190345.	195200.	189511.
TOTAL INSTRU UNIT	4295.	4281.	4295.	4281.	4295.	4281.
TOTAL SPACECRAFT	33412.	33536.	92374.	92652.	1412.	1502.
TOTAL UPPER STAGE	37707.	37817.	96669.	96933.	5707.	5783.
TOTAL VEHICLE	233834.	228378.	292796.	287278.	200907.	195294.

Table 21-9. Total Vehicle Mass - S-IVB Second Burn Phase - Kilograms

EVENTS	S-IVB IGNITION		S-IVB MAINSTAGE		S-IVB ENGINE CUTOFF		S-IVB END DECAY	
	PRED	ACT	PRED	ACT	PRED	ACT	PRED	ACT
RANGE TIME--SEC	17149.74	17155.54	17152.24	17158.04	17212.34	17217.60	17213.40	17218.70
S-IVB STAGE DRY	11392.	11296.	11392.	11296.	11392.	11296.	11392.	11296.
LOX IN TANK	62067.	60156.	61926.	60023.	51291.	49397.	51243.	49334.
LOX BELOW TANK	166.	166.	180.	180.	180.	180.	180.	180.
LOX ULLAGE GAS	241.	193.	243.	194.	258.	226.	259.	227.
LH2 IN TANK	13643.	13295.	13592.	13254.	11408.	11076.	11400.	11061.
LH2 BELOW TANK	26.	26.	26.	26.	26.	26.	26.	26.
LH2 ULLAGE GAS	118.	151.	118.	139.	135.	181.	136.	182.
APS PROPELLANT	182.	205.	182.	205.	181.	202.	181.	202.
HELIUM IN BOTTLES	173.	168.	172.	167.	163.	159.	159.	158.
START TANK GAS	2.	2.	0.	0.	3.	3.	3.	3.
FROST	0.	45.	0.	45.	0.	45.	0.	45.
OTHER	25.	25.	25.	25.	25.	25.	25.	25.
TOTAL S-IVB STAGE	88036.	85730.	87858.	85557.	75064.	72817.	75004.	72740.
TOTAL INSTRU UNIT	1948.	1942.	1948.	1942.	1948.	1942.	1948.	1942.
TOTAL SPACECRAFT	640.	681.	640.	681.	640.	681.	640.	681.
TOTAL UPPER STAGE	2589.	2623.	2589.	2623.	2589.	2623.	2589.	2623.
TOTAL VEHICLE	90625.	88353.	90446.	88180.	77653.	75441.	77592.	75363.

Table 21-10. Total Vehicle Mass - S-IVB Second Burn Phase - Pounds Mass

EVENTS	S-IVB IGNITION		S-IVB MAINSTAGE		S-IVB ENGINE CUTOFF		S-IVB END DECAY	
	PRED	ACT	PRED	ACT	PRED	ACT	PRED	ACT
RANGE TIME--SEC	17149.74	17155.54	17152.24	17158.04	17212.34	17217.60	17213.40	17218.70
S-IVB STAGE DRY	25114.	24904.	25114.	24904.	25114.	24904.	25114.	24904.
LOX IN TANK	136835.	132621.	136523.	132329.	113077.	108901.	112971.	108762.
LOX BELOW TANK	367.	367.	397.	397.	397.	397.	397.	397.
LOX ULLAGE GAS	531.	425.	534.	428.	569.	498.	570.	500.
LH2 IN TANK	30077.	29311.	29965.	29219.	25150.	24418.	25132.	24385.
LH2 BELOW TANK	58.	58.	58.	58.	58.	58.	58.	58.
LH2 ULLAGE GAS	260.	334.	261.	307.	298.	400.	298.	401.
APS PROPELLANT	402.	452.	402.	452.	400.	446.	400.	446.
HELIUM IN BOTTLES	381.	370.	380.	369.	360.	350.	350.	349.
START TANK GAS	5.	5.	1.	1.	7.	7.	7.	7.
FROST	0.	100.	0.	100.	0.	100.	0.	100.
OTHER	56.	56.	56.	56.	56.	56.	56.	56.
TOTAL S-IVB STAGE	194087.	189003.	193693.	188620.	165487.	160535.	165355.	160365.
TOTAL INSTRU UNIT	4295.	4281.	4295.	4281.	4295.	4281.	4295.	4281.
TOTAL SPACECRAFT	1412.	1502.	1412.	1502.	1412.	1502.	1412.	1502.
TOTAL UPPER STAGE	5707.	5783.	5707.	5783.	5707.	5783.	5707.	5783.
TOTAL VEHICLE	199794.	194786.	199400.	194403.	171194.	166318.	171062.	166148.

Table 21-11. Total Vehicle Mass - S-IVB Third Burn Phase - Kilograms

EVENTS	S-IVB IGNITION		S-IVB MAINSTAGE		S-IVB ENGINE CUTOFF		S-IVB END DECAY	
	PRED	ACT	PRED	ACT	PRED	ACT	PRED	ACT
RANGE TIME--SEC	22032.79	22039.26	22035.29	22041.76	22275.33	22281.32	22276.33	22282.32
S-IVB STAGE DRY	11392.	11296.	11392.	11296.	11392.	11296.	11392.	11296.
LOX IN TANK	51201.	49242.	51061.	49109.	8358.	15265.	8306.	15202.
LOX BELOW TANK	166.	166.	180.	180.	180.	180.	180.	180.
LOX ULLAGE GAS	321.	295.	321.	295.	359.	340.	359.	341.
LH2 IN TANK	11038.	10642.	10988.	10627.	2169.	4034.	2161.	4020.
LH2 BELOW TANK	26.	26.	26.	26.	26.	26.	26.	26.
LH2 ULLAGE GAS	142.	209.	142.	212.	208.	290.	208.	291.
APS PROPELLANT	122.	171.	122.	171.	122.	156.	122.	156.
HELIUM IN BOTTLES	136.	136.	135.	136.	99.	100.	99.	100.
START TANK GAS	2.	2.	0.	0.	3.	3.	3.	3.
FROST	0.	45.	0.	45.	0.	45.	0.	45.
OTHER	25.	25.	25.	25.	25.	25.	25.	25.
TOTAL S-IVB STAGE	74571.	72256.	74393.	72124.	22942.	31762.	22881.	31686.
TOTAL INSTRU UNIT	1948.	1942.	1948.	1942.	1948.	1942.	1948.	1942.
TOTAL SPACECRAFT	640.	681.	640.	681.	640.	681.	640.	681.
TOTAL UPPER STAGE	2589.	2623.	2589.	2623.	2589.	2623.	2589.	2623.
TOTAL VEHICLE	77159.	74879.	76982.	74747.	25531.	34385.	25470.	34309.

21-13

Table 21-12. Total Vehicle Mass - S-IVB Third Burn Phase - Pounds Mass

EVENTS	S-IVB IGNITION		S-IVB MAINSTAGE		S-IVB ENGINE CUTOFF		S-IVB END DECAY	
	PRED	ACT	PRED	ACT	PRED	ACT	PRED	ACT
RANGE TIME--SEC	22032.79	22039.26	22035.29	22041.76	22275.33	22281.32	22276.33	22282.32
S-IVB STAGE DRY	25114.	24904.	25114.	24904.	25114.	24904.	25114.	24904.
LOX IN TANK	112878.	108560.	112570.	108266.	18427.	33654.	18311.	33515.
LOX BELOW TANK	367.	367.	397.	397.	397.	397.	397.	397.
LOX ULLAGE GAS	708.	650.	708.	651.	790.	750.	790.	751.
LH2 IN TANK	24333.	23462.	24223.	23429.	4782.	8893.	4764.	8863.
LH2 BELOW TANK	58.	58.	58.	58.	58.	58.	58.	58.
LH2 ULLAGE GAS	312.	460.	313.	468.	459.	640.	459.	641.
APS PROPELLANT	269.	376.	269.	376.	269.	344.	269.	344.
HELIUM IN BOTTLES	299.	300.	298.	300.	219.	220.	219.	220.
START TANK GAS	5.	5.	1.	1.	7.	7.	7.	7.
FROST	0.	100.	0.	100.	0.	100.	0.	100.
OTHER	56.	56.	56.	56.	56.	56.	56.	56.
TOTAL S-IVB STAGE	164400.	159298.	164008.	159006.	50578.	70023.	50444.	69856.
TOTAL INSTRU UNIT	4295.	4281.	4295.	4281.	4295.	4281.	4295.	4281.
TOTAL SPACECRAFT	1412.	1502.	1412.	1502.	1412.	1502.	1412.	1502.
TOTAL UPPER STAGE	5707.	5783.	5707.	5783.	5707.	5783.	5707.	5783.
TOTAL VEHICLE	170107.	165081.	169715.	164789.	56285.	75806.	56151.	75639.

21-14

Table 21-13. Flight Sequence Mass Summary

MASS HISTORY	ACTUAL		PREDICTED	
	KG	LSM	KG	LSM
S-IC STAGE, TOTAL	2282866.	5032858.	2282265.	5031532.
S-IC/S-II INTERSTAGE-SMALL	614.	1353.	614.	1353.
S-IC/S-II INTERSTAGE-LARGE	4644.	10238.	4677.	10312.
S-II STAGE, TOTAL	483378.	1065667.	482908.	1064629.
S-II/S-IVB INTERSTAGE	3628.	7998.	3665.	8081.
S-IVB STAGE, TOTAL	118003.	260151.	117553.	259159.
VEHICLE INSTRUMENT UNIT	1942.	4281.	1948.	4295.
SPACECRAFT INCLUDING LES	47188.	104031.	47098.	103834.
1ST FLT STG AT IGN	2942262.	6486578.	2940728.	6483196.
S-IC THRUST BUILDUP	-38758.	-85448.	-39129.	-86267.
1ST FLT STG HOLDDOWN ARM REL	2903504.	6401130.	2901598.	6396929.
S-IC FROST	-294.	-650.	-294.	-650.
S-IC MAINSTAGE PROPELLANT	-2064244.	-4550882.	-2070872.	-4565495.
S-IC N2 PURGE	-8.	-20.	-16.	-37.
S-IC INBD ENGINE T.D. PROP	-840.	-1855.	-821.	-1812.
S-IC INBD ENG EXPENDED PROP	-184.	-408.	-184.	-408.
S-II INSULATION PURGE GAS	-53.	-120.	-53.	-120.
S-II FROST	-203.	-450.	-203.	-450.
S-IVB FROST	-90.	-200.	-44.	-100.
1ST FLT STAGE AT S-IC OECOS	837579.	1846545.	829103.	1827858.
S-IC OTBD ENGINE T.D. PROP	-2926.	-6453.	-3275.	-7222.
S-IC/S-II ULLAGE RKT PROP	-32.	-73.	-32.	-73.
1ST FLT STAGE AT SIC/S-II SEP	834619.	1840019.	825793.	1820562.
S-IC STAGE AT SEPARATION	-175604.	-387143.	-167666.	-369642.
S-IC/S-II INTERSTAGE SMALL	-613.	-1353.	-613.	-1353.
S-IC/S-II ULLAGE RKT PROP	-82.	-184.	-82.	-184.
2ND FLT STAGE AT S-II SSC	658316.	1451339.	657429.	1449383.
S-II T.B. PROPELLANT	-490.	-1083.	-700.	-1546.
S-II START TANK	-10.	-25.	-10.	-25.
S-IC/S-II ULLAGE RKT PROP	-493.	-1089.	-499.	-1103.
2ND FLT STAGE MAINSTAGE	657320.	1449142.	656216.	1446708.
LAUNCH ESCAPE SYSTEM	-4022.	-8869.	-4022.	-8870.
S-IC/S-II INTERSTAGE LARGE	-4032.	-8892.	-4060.	-8952.
S-II MAINSTAGE + VENTING	-438388.	-966482.	-437920.	-965450.
2ND FLT STAGE AT S-II C.O.S.	210875.	464899.	210211.	463436.
S-II T.D. PROPELLANT	-221.	-490.	-226.	-500.
S-IVB ULLAGE PROPELLANT	-1.	-4.	-1.	-5.
2ND FLT STG AT S-II/S-IVB SEP	210651.	464405.	209983.	462933.
S-II STAGE AT SEPARATION	-44005.	-97017.	-43788.	-96539.
S-II/S-IVB INTERSTAGE-DRY	-3146.	-6938.	-3184.	-7021.
S-II/S-IVB IS PROP	-480.	-1060.	-480.	-1060.
S-IVB AFT FRAME	-21.	-48.	-21.	-48.
S-IVB ULLAGE ROCKET PROP	-1.	-4.	-0.	-3.
S-IVB DET PACKAGE	-0.	-3.	-0.	-3.
3RD FLT STG AT 1ST SSC	162992.	359335.	162504.	358259.
S-IVB ULLAGE ROCKET PROP	-49.	-110.	-39.	-88.
S-IVB FUEL LEAD LOSS	0.	0.	0.	0.
3RD FLT STG AT 1ST S-IVB IGN	162942.	359225.	162464.	358171.
S-IVB ULLAGE ROCKET PROP	0.	0.	-9.	-22.
S-IVB START TANK	-1.	-4.	-1.	-4.
S-IVB T.B. PROPELLANT	-170.	-378.	-183.	-406.
3RD FLT STG AT MAINSTAGE	162768.	358843.	162267.	357738.
S-IVB ULLAGE ROCKET CASES	-60.	-134.	-60.	-135.
S-IVB MAINSTAGE PROP	-30128.	-66423.	-27243.	-60062.
S-IVB APS PROPELLANT	-1.	-5.	-0.	-2.
3RD FLT STG AT 1ST S-IVB COS	132576.	292281.	134961.	297538.
S-IVB T.D. PROPELLANT	-85.	-190.	-65.	-145.

Table 21-13. Flight Sequence Mass Summary (Continued)

MASS HISTORY	ACTUAL		PREDICTED	
	KG	LBM	KG	LBM
3RD FLT STG AT END 1ST TD	132490.	292091.	134895.	297393.
S-IVB ENG PROP EXPENDED	-17.	-40.	-17.	-40.
S-IVB APS PROPELLANT	-44.	-100.	-50.	-113.
S-IVB FUEL TANK LOSS	-882.	-1947.	-840.	-1854.
JETTISON SLA PANELS	-1138.	-2510.	-1174.	-2590.
S/C LESS LEM AND SLA	-26814.	-59116.	-26744.	-58962.
START TRANS/DOCK	103591.	228378.	106065.	233834.
S/C TRANSPOSED	26815.	59116.	26745.	58962.
S-IVB FUEL TANK LOSS	-97.	-216.	0.	0.
END TRANS/DOCK	130307.	287278.	132810.	292796.
S/C TRANSPOSED	-26814.	-59116.	-26744.	-58962.
LEM	-14529.	-32034.	-14514.	-32000.
S-IVB FUEL TANK LOSS	-377.	-834.	-419.	-927.
LAUNCH VEH AT S/C SEP	88584.	195294.	91130.	200907.
S-IVB FUEL TANK LOSS	-168.	-372.	-415.	-918.
S-IVB LOX TANK LOSS	0.	0.	-20.	-46.
S-IVB APS PROPELLANT	-44.	-100.	-50.	-113.
S-IVB START TANK	-0.	-2.	-0.	-2.
S-IVB O2/H2 BURNER	-6.	-16.	-6.	-16.
3RD FLT STG AT 2ND SSC	88362.	194804.	90633.	199811.
S-IVB FUEL LEAD LOSS	-7.	-18.	-7.	-18.
3RD FLT STG AT 2ND SIVB IGN	88353.	194786.	90625.	199793.
S-IVB START TANK	-1.	-4.	-1.	-4.
S-IVB T.B. PROPELLANT	-171.	-379.	-175.	-389.
3RD FLT STG AT MAINSTAGE	88180.	194403.	90446.	199400.
S-IVB MAINSTAGE PROP	-12735.	-28079.	-12792.	-28203.
S-IVB APS PROPELLANT	-2.	-6.	-0.	-2.
3RD FLT STG AT 2ND SIVB COS	75441.	166318.	77652.	171194.
S-IVB T.D. PROPELLANT	-76.	-169.	-54.	-122.
3RD FLT STG AT END 2ND T.D.	75364.	166149.	77597.	171072.
S-IVB ENG PROP EXPENDED	-17.	-40.	-17.	-40.
S-IVB FUEL TANK LOSS	-367.	-812.	-338.	-748.
S-IVB LOX TANK LOSS	-22.	-50.	-2.	-7.
S-IVB APS PROPELLANT	-31.	-70.	-58.	-131.
S-IVB START TANK	-0.	-2.	-0.	-2.
S-IVB O2/H2 BURNER	-6.	-16.	-6.	-16.
3RD FLT STG AT 3RD SSC	74915.	165159.	77168.	170126.
S-IVB FUEL LEAD LOSS	-34.	-78.	-8.	-19.
3RD FLT STG AT 3RD SIVB IGN	74879.	165081.	77159.	170107.
S-IVB START TANK	-1.	-4.	-1.	-4.
S-IVB T.B. PROPELLANT	-130.	-288.	-174.	-386.
3RD FLT STG AT MAINSTAGE	74747.	164789.	76982.	169716.
S-IVB MS PROP 3RD BURN	-40347.	-88951.	-51450.	-113429.
S-IVB APS PROPELLANT	-14.	-32.	0.	0.
3RD FLT STG AT 3RD SIVB COS	34385.	75806.	25531.	56286.
S-IVB T.D. PROPELLANT	-75.	-167.	-60.	-135.
3RD FLT STG AT END 3RD T.D.	34309.	75639.	25470.	56152.
S-IVB ENG PROP EXPENDED	-17.	-40.	-17.	-40.
S-IVB APS PROPELLANT	0.	0.	-2.	-6.
SLA NOT JETTISONED	-680.	-1502.	-639.	-1412.
VEHICLE INSTRUMENT UNIT	-1941.	-4281.	-1947.	-4295.
S-IVB STAGE	-31667.	-69815.	-22860.	-50399.

Table 21-14. Mass Characteristics Comparison

EVENT	MASS		LONGITUDINAL C.G. (X STA.)		RADIAL C.G.		ROLL MOMENT OF INERTIA		PITCH MOMENT OF INERTIA		YAW MOMENT OF INERTIA	
	KILO POUNDS	O/O DEV.	METERS INCHES	DELTA	METERS INCHES	DELTA	KG-M2 X10-6	O/O DEV.	KG-M2 X10-6	O/O DEV.	KG-M2 X10-6	O/O DEV.
S-IC STAGE DRY	PRED		9.479		0.0708							
	ACTUAL		9.504	0.025	0.0683	-0.0024						
S-IC/S-II INTER-STAGE TOTAL	PRED		1638.9		6.2369		0.134		0.081		0.081	
	ACTUAL		1638.8	-0.002	6.1584	0.0000	0.134	-0.62	0.080	-0.62	0.081	-0.50
S-II STAGE DRY	PRED		48.143		0.1115							
	ACTUAL		48.107	-0.035	0.1093	-0.0021						
S-II/S-IVB INTER-STAGE TOTAL	PRED		2616.2		2.3537		0.065		0.044		0.044	
	ACTUAL		2616.0	-0.005	2.2561	-0.0024	0.064	-1.02	0.043	-1.02	0.044	-1.02
S-IVB STAGE DRY	PRED		72.534		0.1898							
	ACTUAL		72.534	0.000	0.1898	0.0000						
VEHICLE INSTRUMENT UNIT	PRED		82.415		0.4058							
	ACTUAL		82.415	0.000	0.3837	-0.0220						
SPACECRAFT TOTAL	PRED		3601.6		4.3011		0.085		1.542		1.549	
	ACTUAL		3601.7	0.002	4.3600	0.0588	0.085	-0.18	1.538	-0.24	1.546	-0.15
1ST FLIGHT STAGE AT IGNITION	PRED		30.249		0.0039							
	ACTUAL		30.235	-0.014	0.0038	-0.0001						
1ST FLIGHT STAGE AT HOLDDOWN ARM RELEASE	PRED		1190.9		0.1562		3.785		864.873		864.782	
	ACTUAL		1190.2	-0.005	0.1500	-0.0062	3.776	-0.23	867.918	4.98	867.753	4.97
1ST FLIGHT STAGE AT QUIBOARD ENGINE CUTOFF SIGNAL	PRED		30.179		0.0040							
	ACTUAL		30.179	-0.015	0.0040	0.0000						
1ST FLIGHT STAGE AT SEPARATION	PRED		1822.0		0.5440		3.771		434.234		434.147	
	ACTUAL		1822.1	0.001	0.5325	-0.0115	3.763	-0.20	445.408	2.57	445.247	2.56
2ND FLIGHT STAGE AT START SEQUENCE COMMAND	PRED		2190.4		0.5799		1.017		131.771		131.787	
	ACTUAL		2190.9	0.013	0.0147	0.0000	1.014	-0.30	132.041	0.20	132.057	0.20
2ND FLIGHT STAGE AT MAINSTAGE	PRED		2190.9		0.5799		1.005		131.650		131.666	
	ACTUAL		2191.4	0.011	0.0147	0.0000	1.002	-0.28	131.930	0.21	131.946	0.21



Table 21-14. Mass Characteristics Comparison (Continued)

2ND FLIGHT STAGE AT CUTOFF SIGNAL	PRED	210211.	70.694	0.0443								
		463436.	2783.2	1.7448			0.901	43.975		43.991		
ACTUAL		210875.	70.679	-0.015	0.0435	-0.0007						
		464892.	2782.6	-0.59	1.7149	-0.0299	0.899	-0.24	44.218	0.55	44.233	0.55
		KILO	O/O	METERS	METERS		KG-M2	O/O	KG-M2	O/O	KG-M2	O/O
		POUNDS	DEV.	INCHES	DELTA	INCHES	DELTA	X10-6	DEV.	X10-6	DEV.	X10-6
2ND FLIGHT STAGE AT SEPARATION	PRED	209983.	70.722	0.0443								
		462933.	2784.3	1.7448			0.901	43.826		43.842		
ACTUAL		210651.	70.706	-0.016	0.0438	-0.0005						
		464405.	2783.7	-0.63	1.7249	-0.0199	0.899	-0.24	44.072	0.56	44.088	0.56
3RD FLIGHT STAGE AT 1ST START SE- QUENCE COMMAND	PRED	162504.	76.923	0.0366								
		358259.	3028.4	1.4413			0.191	12.740		12.742		
ACTUAL		162992.	76.927	0.003	0.0366	0.0000						
		359335.	3028.6	0.13	1.4447	0.0033	0.191	-0.08	12.771	0.25	12.775	0.25
3RD FLIGHT STAGE AT 1ST IGNITION	PRED	162464.	76.924	0.0366								
		358171.	3028.5	1.4413			0.191	12.739		12.741		
ACTUAL		162942.	76.929	0.004	0.0366	0.0000						
		359225.	3028.7	0.18	1.4447	0.0033	0.191	-0.08	12.769	0.24	12.773	0.25
3RD FLIGHT STAGE AT 1ST MAINSTAGE	PRED	162267.	76.923	0.0366								
		357738.	3028.4	1.4413			0.191	12.737		12.740		
ACTUAL		162768.	76.926	0.003	0.0366	0.0000						
		358843.	3028.5	0.12	1.4447	0.0033	0.191	-0.08	12.768	0.25	12.772	0.25
3RD FLIGHT STAGE AT 1ST CUTOFF SIG- NAL	PRED	134961.	77.705	0.0436								
		297538.	3059.2	1.7191			0.190	12.061		12.064		
ACTUAL		132576.	77.810	0.104	0.0448	0.0012						
		292281.	3063.3	4.10	1.7670	0.0478	0.190	-0.10	12.007	-0.44	12.010	-0.43
3RD FLIGHT STAGE AT 1ST END THRUST DECAY, START COAST	PRED	134895.	77.708	0.0436								
		297393.	3059.3	1.7191			0.190	12.059		12.061		
ACTUAL		132490.	77.813	0.105	0.0448	0.0012						
		292091.	3063.5	4.13	1.7670	0.0478	0.190	-0.10	12.004	-0.44	12.007	-0.44
CSM SEPARATED	PRED	106069.	73.564	0.0267								
		233834.	2896.2	1.0519			0.138	3.167		3.166		
ACTUAL		103591.	73.597	0.032	0.0270	0.0003						
		228378.	2897.5	1.27	1.0655	0.0136	0.138	-0.10	3.172	0.17	3.170	0.11
CSM DOCKED	PRED	132810.	77.400	0.0571								
		292796.	3047.2	2.2506			0.182	11.024		11.022		
ACTUAL		130307.	77.504	0.104	0.0575	0.0004						
		282728.	3051.3	4.10	2.2671	0.0165	0.181	-0.11	10.973	-0.45	10.969	-0.47
SPACECRAFT SEP- ARATED	PRED	91130.	71.744	0.0277								
		200907.	2824.6	1.0941			0.111	0.976		0.974		
ACTUAL		88584.	71.727	-0.017	0.0287	0.0010						
		199294.	2823.9	-0.70	1.1337	0.0395	0.111	-0.15	0.982	0.60	0.978	0.43
3RD FLIGHT STAGE AT 2ND START SE- QUENCE COMMAND	PRED	90623.	71.729	0.0278								
		199811.	2824.0	1.0960			0.110	0.967		0.964		
ACTUAL		88362.	71.726	-0.003	0.0288	0.0009						
		194804.	2823.8	-0.12	1.1353	0.0393	0.110	-0.12	0.978	1.13	0.974	1.09
3RD FLIGHT STAGE AT 2ND IGNITION	PRED	90625.	71.728	0.0278								
		199793.	2823.9	1.0960			0.110	0.967		0.964		
ACTUAL		88359.	71.725	-0.003	0.0288	0.0009						
		194786.	2823.8	-0.12	1.1353	0.0393	0.110	-0.12	0.978	1.15	0.974	1.11
3RD FLIGHT STAGE AT 2ND MAINSTAGE	PRED	90446.	71.716	0.0279								
		199400.	2823.4	1.1013			0.110	0.961		0.958		
ACTUAL		88180.	71.712	-0.003	0.0288	0.0008						
		194403.	2823.3	-0.15	1.1353	0.0339	0.110	-0.12	0.972	1.10	0.968	1.07
3RD FLIGHT STAGE AT 2ND CUTOFF SIGNAL	PRED	77653.	71.620	0.0324								
		171194.	2819.6	1.2762			0.110	0.903		0.900		
ACTUAL		75441.	71.629	0.009	0.0332	0.0008						
		166318.	2820.0	0.26	1.3102	0.0340	0.110	-0.14	0.918	1.59	0.914	1.55
3RD FLIGHT STAGE AT 2ND END THRUST DECAY	PRED	77597.	71.619	0.0324								
		171072.	2819.6	1.2762			0.110	0.903		0.900		
ACTUAL		75364.	71.629	0.009	0.0332	0.0008						
		166149.	2820.0	0.38	1.3102	0.0340	0.110	-0.14	0.917	1.56	0.914	1.51

Table 21-14. Mass Characteristics Comparison (Continued)

3RD FLIGHT STAGE		PRED	77168.	71.602	0.0316								
AT 3RD START SEQUENCE COMMAND			170126.	2818.9	1.2455	0.109	0.894	0.892					
ACTUAL			74915.	71.612	0.009	0.0328	0.0012						
			165159.	-2.91 2819.3	0.38 1.2932	0.0476	0.109	0.21	0.909	1.70	0.906	1.62	
3RD FLIGHT STAGE		PRED	77159.	71.600	0.0316								
AT 3RD IGNITION			170107.	2818.9	1.2455	0.109	0.894	0.891					
ACTUAL			74879.	71.608	0.007	0.0328	0.0012						
			165081.	-2.94 2819.2	0.31 1.2932	0.0476	0.109	0.21	0.909	1.65	0.905	1.58	
3RD FLIGHT STAGE		PRED	76982.	71.593	0.0316								
AT 3RD MAINSTAGE			169716.	2818.6	1.2455	0.109	0.891	0.889					
ACTUAL			74747.	71.604	0.011	0.0328	0.0012						
			164789.	-2.89 2819.0	0.44 1.2932	0.0476	0.109	0.21	0.907	1.78	0.904	1.71	
3RD FLIGHT STAGE		PRED	25531.	72.472	0.0922								
AT 3RD CUTOFF SIGNAL			56286.	2853.2	3.6305	0.109	0.702	0.699					
ACTUAL			34385.	72.018	-0.453	0.0688	-0.0233						
			75806.	34.68 2835.3	-17.86 2.7104	-0.9200	0.109	0.09	0.774	10.19	0.771	10.16	
3RD FLIGHT STAGE		PRED	25470.	72.478	0.0923								
AT 3RD END THRUST DECAY			56152.	2853.4	3.6360	0.109	0.702	0.699					
ACTUAL			34309.	72.021	-0.456	0.0691	-0.0231						
			75639.	34.70 2835.4	-17.99 2.7242	-0.9118	0.109	0.09	0.773	10.21	0.770	10.19	

## SECTION 22

### MISSION OBJECTIVES ACCOMPLISHMENT

Table 22-1 presents the MSFC AS-504 detailed test objectives as defined in the Saturn V Mission Implementation Plan, Mission D. An assessment of the degree of accomplishment of each objective is shown. Discussion supporting the assessment can be found in the indicated sections of the Saturn V Launch Vehicle Flight Evaluation Report - AS-504, Apollo 9 Mission.

The one principal and nine of the eleven secondary detailed test objectives were completely accomplished. The other two test objectives, S-IVB 80-minute restart and LOX/LH<sub>2</sub> dump, were partially accomplished. The out-of-specification restart conditions (an experimental start) is the most probable cause for incomplete accomplishment.

Table 22-1. Mission Objectives Accomplishment Summary

NO.	DETAILED TEST OBJECTIVES		DEGREE OF ACCOMPLISHMENT	DISCREPANCIES	PARAGRAPH IN WHICH DISCUSSED
	PRINCIPAL (P)	SECONDARY (S)			
1	Demonstrate S-IVB/IU attitude control capability during Transposition, Docking and Spacecraft (SC) Ejection (TD&E) maneuver. (P)		Complete	None	11.5.2 12.6
2	Confirm launch vehicle longitudinal oscillation environment during S-IC stage burn period. (S)		Complete	None	9.2.3 9.3.1.1
3	Verify that modifications incorporated in the S-IC stage suppress low frequency longitudinal oscillations. (S)		Complete	None	5.9 9.2.3 9.3.1.1
4	Confirm J-2 engine environment in S-II stage. (S)		Complete	None	17.3
5	Verify J-2 engine modifications. (S)		Complete	None	6.3
6	Demonstrate O <sub>2</sub> /H <sub>2</sub> burner repressurization system operation. (S)		Complete	None	7.6
7	Demonstrate S-IVB restart capability. (S)		Complete	None	7.6
8	Demonstrate O <sub>2</sub> /H <sub>2</sub> burner restart capability. (S)		Complete	None	7.10
9	Demonstrate dual repressurization capability. (S)		Complete	None	7.6 7.10
10	Demonstrate 80-minute restart capability. (S)		Partial	The experimental start was achieved and accomplished the planned S-IVB third burn. However, rough combustion, a gas generator spike at ignition, and control oscillations resulted in low performance at start, performance loss during the burn, and loss of engine helium control regulator discharge pressure.	7.10 7.11 11.5.5
11	Demonstrate S-IVB propellant dump and safing. (S)		Partial	The S-IVB stage was adequately "safed" however propellant dump was not achieved due to loss of engine helium control regulator discharge pressure.	7.17
12	Verify the onboard Command Communications System (CCS)/ground system interface and operation in the deep space environment. (S)		Complete	None	14.3

## SECTION 23

### FAILURES, ANOMALIES AND DEVIATIONS

#### 23.1 SUMMARY

Evaluation of the launch vehicle performance during the AS-504 flight test revealed four areas of concern with a mission criticality category of three. Modifications are planned to improve these problem areas on future flights.

#### 23.2 SYSTEM FAILURES AND ANOMALIES

Table 23-1 defines the criticality categories assigned to the failures and anomalies listed in Table 23-2. Since all studies and corrective actions (ECPs) pertinent to these anomalies are not complete, Table 23-2 represents the action status of each item as of the release date of this report. This table complies with Apollo Program Directive No. 19. Reference paragraph numbers are given for sections in which the specific problem area is discussed in more detail.

Table 23-1. Hardware Criticality Categories For Flight Hardware

CATEGORY	DESCRIPTION
1	Hardware failure which results in loss of life of any crew member. This includes normally passive systems such as the Emergency Detection System (EDS), Launch Escape System (LES), etc.
2	Hardware failure which results in abort of mission but does not cause loss of life.
3	Hardware failure which will not result in abort of mission nor cause loss of life.

#### 23.3 SYSTEM DEVIATIONS

Eight system deviations occurred without any significant effects on the flight or operation of that particular system. Table 23-3 presents these deviations with the recommended corrective actions and a reference

Table 23-2. Summary of Failures and Anomalies

FAILURE/ANOMALY IDENTIFICATION							RECOMMENDED CORRECTIVE ACTION			
ITEM	VEHICLE SYSTEM	DESCRIPTION (CAUSE)	EFFECT ON MISSION	AS-504 MISSION CRITICALITY	EFFECT ON NEXT MISSION	TIME OF OCCURRENCE (RANGE TIME)	DESCRIPTION	ACTION STATUS	VEHICLE EFFECTIVITY	PARAGRAPH REFERENCE
1	S-II Propulsion/Structure	9-11 hertz structure oscillations, and 16.5 to 20 hertz oscillations in center engine pressure parameters and S-II structural parameters. (Unknown)	None	3	Under investigation	Approx. 500 sec.	Early center engine cutoff per ECP 6304. Other possibilities are under investigation for AS-506 and subs.	ECP 6304 Closed Open	AS-505 AS-506 and subs	6.3, 6.6, 9.2.3.2
2	S-IVB Auxiliary Propulsion System	APS Module No. II helium supply pressure decay. (One or more teflon seals leaking in high pressure system upstream of regulator.)	None. Leak was not pronounced enough to effect mission.	3	Potential loss of attitude control during operation and/or coast.	Beginning at approx. 4:25:00	Change of teflon seal material has been approved (ECP 3160) and an additional leak check at KSC implemented.	ECP 3160 Closed	AS-505 and subs	7.16
3	S-IVB Stage Propulsion	Stage pneumatic regulator reading high prior to lift-off. (Possible contamination or marginal poppet to seat mating.)	None	3	None	-3:07:00	Modification to regulator on subsequent vehicles.	ECP 3158 Closed	AS-505 and subs	7.15
4	S-IVB Propulsion and Controls	Third burn performance variations from nominal 1. Main chamber pressure oscillations which probably resulted in partial failure of engine pneumatic system and subsequent loss of engine performance. 2. Gas generator pressure spike at start which possibly damaged gas generator. 3. Abnormal yaw and pitch control system oscillation during third burn. (Out-of-specification start conditions which were experimental).	Low performance during third burn and as a result lower than predicted cutoff velocity. Failure to dump LOX and LH <sub>2</sub> through the engine.	3	None for normal start conditions.	22,039.26 seconds	Modification of mission rules for contingency start.	Closed	AS-505 and subs	7.10 7.11 7.17
			Loss of performance.		None		22,039 seconds			
			None. Greater than normal yaw and pitch disturbances during first 100 seconds of third burn.		None anticipated		22,039 to 22,141 seconds			

to the paragraphs containing further discussion of the deviation. These deviations are of no major concern, but are presented in order to complete the summary of deviations experienced on AS-504.

Table 23-3. Summary of Deviations

VEHICLE SYSTEM	DEVIATIONS	PROBABLE CAUSE	CORRECTIVE ACTION BEING CONSIDERED	PARAGRAPH REFERENCE
S-IC Propulsion	Unexpected performance increase of Engine No. 1 (within $3\sigma$ tolerance) beginning at 85 seconds.	Loss of lead from fuel pump front wear ring due to inadequate bonding.	Double inspection process, by engine mfr to assure proper lead bonding. Incorporated on Engines No. 3 and 4 for AS-504 and all subsequent F-1 engines.	5.3
Vehicle Structures	Slow damping rate of longitudinal oscillations after S-IC Center Engine Cutoff (CECO).	Low structural damping and coincidental tuning of engine cutoff rate with 1st longitudinal structural mode.	None anticipated. AS-504 oscillations considered to be worst case.	9.2.3.1
S-IC Propulsion	Unexpected decrease of fuel ullage pressure at engine start which caused Helium Flow Control Valve (HFCV) No. 5 to cycle.	Orifices erroneously interchanged on HFCV No. 1 and No. 2 producing a different He flow.	AS-505 flow test. Configuration has been verified.	5.6.1
S-IC Propulsion	Engine No. 5 LOX suction duct pressure decayed unexpectedly after CECO.	Under investigation. LOX leak below pre valve is suspected.	None anticipated	5.6.2
S-IC/S-II Separation	Apollo 9 astronauts reported negative acceleration at S-IC/S-II separation. At 163.57 seconds the oscillating characteristics reached -0.8 g peak amplitude, at 5.2 hertz.	Separation appears nominal and the dynamics apparently are characteristic of the vehicle.	None anticipated.	12.2
IU (LVDA/Telemetry)	H60-603 telemetry bit erroneously set on from 537.2 to 9676 seconds. All data recovered with bit affecting telemetry only.	Launch Vehicle Data Adapter (LVDA) telemetry driver model 410K multiplexer or interconnecting circuitry.	Real time data handling procedural change.	10.5.4 19.3.4
IU ST-124M-3 Platform	ST-124M-3 platform inertial gimbal temperature was below specification.	Very likely due to response to lower than expected ambient environment (not of serious nature).	Will be observed during AS-505 launch and will determine if further action is warranted.	18.4.1
IU ST-124M-3 Platform	ST-124M-3 air bearing differential and ambient pressure exceeded specification.	Possible regulator drift (not of serious nature).	Test defined in IU Specifications and Criteria, paragraph 0.3.5.3.3, to correct problem. Effective for AS-505.	18.4.2
IU Command and Communication Systems (CCS)	A degraded CCS power amplifier output occurred between 22066.4 and 23418.8 seconds causing loss of down link lock.	Under Investigation.	Under Investigation.	14.3 19.3.4 19.5.3.2

SECTION 24  
SPACECRAFT SUMMARY

All spacecraft systems performed essentially as planned. Thermal characteristics of both spacecrafts varied within acceptable limits. Consumables usage was maintained at acceptable levels. Communications quality was generally satisfactory with two television transmissions from the Lunar Module (LM).

Following a nominal launch phase, the spacecraft and S-IVB stage were inserted into an orbit of 184.61 by 186.57 kilometers (99.68 by 100.74 n mi). After postinsertion checkout was completed, the Command and Service Modules (CSM) were separated from the S-IVB, transposed, and docked with the LM. The docked spacecrafts were separated from the S-IVB at 4:08:06. Four service propulsion firings lasting 5.1, 110.0, 279.6, and 27.9 seconds were made while the spacecraft remained docked.

At approximately 43.5 hours, the LM Pilot and the Commander transferred to the LM. A 369.7-second firing of the LM descent propulsion system was initiated about 6 hours later; the two crewmen then returned to the Command Module (CM) for the fifth service propulsion firing, which lasted 43.3 seconds. At approximately 70 hours, the LM Pilot and the Commander again transferred for the LM Pilot's 47-minute extravehicular activity.

At approximately 89 hours, the Commander and the LM Pilot returned to the LM for the third time to perform a LM-active rendezvous. The lunar module primary guidance system was used to conduct the rendezvous with backup calculations being made by the CM computer. The phasing and insertion maneuvers were performed using the descent propulsion system to set up the rendezvous. The ascent and descent stages were separated, followed by a reaction control coelliptic sequence initiation maneuver. The ascent propulsion system was fired to establish the constant delta height. The terminal phase of the rendezvous began on time, and the spacecrafts were again docked at about 99 hours. The ascent stage was jettisoned about 2.5 hours later. Shortly after, the ascent propulsion system was fired to propellant depletion. The firing lasted 350 seconds and resulted in an orbit of 6939 by 230.6 kilometers (3747 by 124.5 n mi).

The sixth service propulsion firing, to lower apogee, was delayed because the +X translation to precede the maneuver was not programmed properly. However, the maneuver was rescheduled and successfully completed in the next revolution at approximately 123.5 hours.



During the last three days, a 25-second seventh service propulsion firing was made to raise the apogee, and a multispectral photography experiment and landmark tracking were accomplished.

Unfavorable weather in the planned landing area caused the deorbit maneuver to be delayed for one revolution. The CM landed in the Atlantic Ocean near the target of 23 degrees 15 minutes north latitude, 68 degrees west longitude, as determined from the onboard computer. The total flight duration was 240 hours, 31 minutes, 14.9 seconds.

For further details on the spacecraft performance, refer to the Apollo 9 Mission Report published by the NASA, Manned Spacecraft Center at Houston, Texas.

## APPENDIX A

### ATMOSPHERE

#### A.1 SUMMARY

This appendix presents a summary of the atmospheric environment at launch time of the AS-504. The format of these data is similar to that presented in previous launches of Saturn vehicles to permit comparisons. Surface and upper winds and thermodynamic data near the launch time are given.

#### A.2 GENERAL ATMOSPHERIC CONDITIONS AT LAUNCH TIME

A low pressure disturbance southwest of Cape Kennedy, Florida, in the Gulf of Mexico, was the principal cause of overcast conditions during launch.

#### A.3 SURFACE OBSERVATIONS AT LAUNCH TIME

At launch time, skies were overcast with 7/10 stratocumulus at 1.1 kilometers (3500 ft), and 10/10 altostratus at 2.7 kilometers (9000 ft). Table A-1 summarizes surface observations at launch time. Solar radiation data are given in Table A-2.

#### A.4 UPPER AIR MEASUREMENTS

Data were used from four of the upper air wind systems to compile the final meteorological tape. Table A-3 summarizes the data systems used.

##### A.4.1 Wind Speed

Wind speed increased with altitude, reaching a speed of 76.2 m/s (148.1 knots) at 11.73 kilometers (38,480 ft). There was a second peak in the wind speed of 75.5 m/s (146.8 knots) at 63.0 kilometers (206,690 ft). See Figure A-1 for more information of the wind speeds.

##### A.4.2 Wind Direction

The surface wind was from the southeast, but changed to westerly at 4.0 kilometers (13,125 ft) altitude. Above 4.0 kilometers (13,125 ft) winds remained generally from the west as shown in Figure A-2. A northeast direction can be noted in Figure A-2 at 29 kilometers (95,145 ft). This wind direction is assumed to be in error, due to the inaccuracy of tracking the rawinsonde balloon at low elevation angles.

#### A.4.3 Pitch Wind Component

The pitch wind speed component was in the same direction as the bias wind used for the vehicle (50-percentile wind) but exceeded the maximum bias wind by 34.5 m/s (67.1 knots). The maximum pitch wind speed component was a tail wind component of 74.5 m/s (144.8 knots) at 11.7 kilometers (38,390 ft). Above 11.7 kilometers (38,390 ft) the pitch wind speed component decreased until it became a slight head wind component of -13.8 m/s (-26.8 knots) at 28.75 kilometers (94,325 ft). It reverses above this altitude and becomes a tail wind with a peak speed of 75.5 m/s (146.8 knots) at 63 kilometers (206,690 ft).

#### A.4.4 Yaw Wind Component

The yaw wind speed component was usually below 20 m/s (38.8 knots) and from the left except near the surface. See Figure A-4.

#### A.4.5 Component Wind Shears

The largest component wind shear ( $\Delta h = 1000$  m) was a yaw shear of  $0.0254 \text{ sec}^{-1}$  at 14.7 kilometers (48,160 ft). The largest pitch wind shear was  $0.0248 \text{ sec}^{-1}$  at 15.1 kilometers (49,700 ft). See Figure A-5.

#### A.4.6 Extreme Wind Data in the High Dynamic Pressure Region

A summary of the maximum wind speeds and wind components is given in Tables A-4, A-5, and A-6. A summary of the extreme wind shear values is given in Tables A-7, A-8, and A-9.

### A.5 THERMODYNAMIC DATA

Comparisons of the thermodynamic data taken at AS-504 launch time with the Patrick Reference Atmosphere, 1963 (PRA-63) for temperature, density, pressure, and Optical Index of Refraction are shown in Figures A-6 and A-7 and discussed in the following paragraphs.

#### A.5.1 Temperature

Atmospheric temperature deviations were small, being less than 5 percent deviation from the PRA-63. At most altitudes, the temperature was colder than the PRA-63.

#### A.5.2 Atmospheric Pressure

The atmospheric pressure profile was less than the PRA-63 pressure profile. A maximum deviation of -5.6 percent occurred at 28 kilometers (91,860 ft).

### A.5.3 Atmospheric Density

Atmospheric density deviations were small, being approximately 5 percent deviation from the PRA-63. The extreme density deviation was -6.1 percent at 14 kilometers (45,930 ft).

### A.5.4 Optical Index of Refraction

At the surface, the Optical Index of Refraction was  $4.35 (n-1) \times 10^{-6}$  units higher than the corresponding value of the PRA-63. The deviation decreased with altitude, becoming a minimum of  $-4.05 (n-1) \times 10^{-6}$  at 12.75 kilometers (41,830 ft). Above this altitude the Optical Index of Refraction stays less than the PRA-63 values.

## A.6 COMPARISON OF SELECTED ATMOSPHERIC DATA FOR ALL SATURN LAUNCHES

Tables A-10, A-11, and A-12 show a summary of the atmospheric data for each Saturn launch.

Table A-1. Surface Observations at AS-504 Launch Time

LOCATION	TIME AFTER T-0 (MIN)	PRES-SURE N/cm <sup>2</sup> (psia)	TEM-PERATURE °K (°F)	POINT DEW °K (°F)	VISI-BILITY km (STAT MI)	SKY COVER			WIND	
						AMOUNT (TENTHS)	TYPE	HEIGHT OF BASE M (ft)	SPEED m/s (KNOTS)	DIR (DEG)
Kennedy Space Center, Station Mila, Florida	0	10.095 (14.64)	292.55 (67.0)	284.85 (53.0)	16 (10)	7 10	Strato-cumulus Alto-stratus	1070 (3500) 2740 (9000)	4.1 (8.0)	130
Cape Kennedy Rawinsonde Measurements	-285	10.091 (14.64)	285.95 (55.0)	284.15 (51.8)	--	--	--	--	3.0 (5.8)	360
Pad 39 A Lightpole SE (20.4 m)*	0	--	--	--	--	--	--	--	6.9 (13.5)	160

\* Above Natural Grade

Table A-2. Solar Radiation at AS-504 Launch Time, Launch Pad 39A

DATE	HOUR ENDING EST	TOTAL HORIZONTAL g-cal/cm <sup>2</sup> (MIN)	NORMAL INCIDENT g-cal/cm <sup>2</sup> (MIN)	DIFFUSE SKY g-cal/cm <sup>2</sup> (MIN)
3/2/69	0800	0.11	0.34	0.09
	0900	0.38	0.71	0.20
	1000	0.74	0.88	0.36
	1100	1.00	0.98	0.44
	1200	1.20	1.03	0.52
	1300	1.26	1.05	0.53
	1400	1.21	1.05	0.51
	1500	1.03	1.03	0.42
	1600	0.81	0.98	0.36
	1700	0.49	0.80	0.26
	1800	0.62	0.20	0.60
3/3/69	1900	0.02	0	0.02
	0800	0.07	0	0.07
	0900	0.21	0.06	0.19
	1000	0.48	0.24	0.38
	1100	0.27	0.01	0.26
	1200	0.26	0.01	0.25

Table A-3. Systems Used to Measure Upper Air Wind Data

TYPE OF DATA	RELEASE TIME		PORTION OF DATA USED			
	TIME (UT)	TIME AFTER T-0 (MIN)	START		END	
			ALTITUDE M (ft)	TIME AFTER T-0 (MIN)	ALTITUDE M (ft)	TIME AFTER T-0 (MIN)
FPS-16 Jimsphere	1615	15	0	15	16,500 (54,100)	70
Rawinsonde	1115	-285	16,750 (54,900)	-230	30,000 (98,420)	-187
Arcasonde	1730	90	52,500 (172,240)	90	30,250 (99,240)	100
Viper Dart	1829	149	73,000 (239,500)	149	52,750 (173,060)	151

Table A-4. Maximum Wind Speed in High Dynamic Pressure Region for Saturn 1 through Saturn 10 Vehicles

VEHICLE NUMBER	MAXIMUM WIND			MAXIMUM WIND COMPONENTS			
	SPEED m/s (KNOTS)	DIR (DEG)	ALT km (ft)	PITCH ( $W_x$ ) m/s (KNOTS)	ALT km (ft)	YAW ( $W_z$ ) m/s (KNOTS)	ALT km (ft)
SA-1	47.0 (91.4)	242	12.25 (40,200)	36.8 (71.5)	13.00 (42,600)	-29.2 (-55.8)	12.25 (40,200)
SA-2	33.6 (65.3)	216	13.50 (44,300)	31.8 (61.8)	13.50 (44,300)	-13.3 (-25.9)	12.25 (40,200)
SA-3	31.3 (60.8)	269	13.75 (45,100)	30.7 (59.7)	13.75 (45,100)	11.2 (21.8)	12.00 (39,400)
SA-4	51.8 (100.7)	253	13.00 (42,600)	46.2 (89.8)	13.00 (42,600)	-23.4 (-45.5)	13.00 (42,600)
SA-5	42.1 (81.8)	268	10.75 (35,300)	41.1 (79.9)	10.75 (35,300)	-11.5 (-22.4)	11.25 (36,900)
SA-6	15.0 (29.2)	96	12.50 (41,000)	-14.8 (-28.8)	12.50 (41,000)	12.2 (23.7)	17.00 (55,800)
SA-7	17.3 (33.6)	47	11.75 (38,500)	-11.1 (-21.6)	12.75 (41,800)	14.8 (28.8)	12.00 (39,400)
SA-9	34.3 (66.7)	243	13.00 (42,600)	27.5 (53.5)	10.75 (35,300)	23.6 (45.9)	13.25 (43,500)
SA-8	16.0 (31.1)	351	15.25 (50,000)	12.0 (23.3)	11.00 (36,100)	14.6 (28.4)	15.25 (50,000)
SA-10	15.0 (29.2)	306	14.75 (48,400)	12.9 (25.1)	14.75 (48,400)	10.8 (21.0)	15.45 (50,700)

NOTE: The vehicle numbers are presented in order of time of launch.

Table A-5. Maximum Wind Speed in High Dynamic Pressure Region for Apollo/Saturn 201 through Apollo/Saturn 205 Vehicles

VEHICLE NUMBER	MAXIMUM WIND			MAXIMUM WIND COMPONENTS			
	SPEED m/s (KNOTS)	DIR (DEG)	ALT km (ft)	PITCH ( $W_x$ ) m/s (KNOTS)	ALT km (ft)	YAW ( $W_z$ ) m/s (KNOTS)	ALT km (ft)
AS-201	70.0 (136.1)	250	13.75 (45,100)	57.3 (111.4)	13.75 (45,100)	-43.3 (-84.2)	13.25 (43,500)
AS-203	18.0 (35.0)	312	13.00 (42,600)	11.1 (21.6)	12.50 (41,000)	16.6 (32.3)	13.25 (43,500)
AS-202	16.0 (31.1)	231	12.00 (39,400)	10.7 (20.8)	12.50 (41,000)	-15.4 (-29.9)	10.25 (33,600)
AS-204	35.0 (68.0)	288	12.00 (39,400)	32.7 (63.6)	15.25 (50,000)	20.6 (40.0)	12.00 (39,400)
AS-205	15.6 (30.3)	309	14.60 (44,500)	15.8 (30.7)	12.08 (36,800)	15.7 (30.5)	15.78 (47,500)

Table A-6. Maximum Wind Speed in High Dynamic Pressure Region for Apollo/Saturn 501 through Apollo/Saturn 504 Vehicles

VEHICLE NUMBER	MAXIMUM WIND			MAXIMUM WIND COMPONENTS			
	SPEED m/s (KNOTS)	DIR (DEG)	ALT km (ft)	PITCH ( $W_x$ ) m/s (KNOTS)	ALT km (ft)	YAW ( $W_z$ ) m/s (KNOTS)	ALT km (ft)
AS-501	26.0 (50.5)	273	11.50 (37,700)	24.3 (47.2)	11.50 (37,700)	12.9 (25.1)	9.00 (29,500)
AS-502	27.1 (52.7)	255	12.00 (42,600)	27.1 (52.7)	12.00 (42,600)	12.9 (25.1)	15.75 (51,700)
AS-503	34.8 (67.6)	284	15.22 (49,900)	31.2 (60.6)	15.10 (49,500)	22.6 (43.9)	15.80 (51,800)
AS-504	76.2 (148.1)	264	11.73 (38,480)	74.5 (144.8)	11.70 (38,390)	21.7 (42.2)	11.43 (37,500)

Table A-7. Extreme Wind Shear Values in the High Dynamic Pressure Region for Saturn 1 through Saturn 10 Vehicles

$(\Delta h = 1000 \text{ m})$				
VEHICLE NUMBER	PITCH PLANE		YAW PLANE	
	SHEAR (SEC <sup>-1</sup> )	ALTITUDE km (ft)	SHEAR (SEC <sup>-1</sup> )	ALTITUDE km (ft)
SA-1	0.0145	14.75 (48,400)	0.0168	16.00 (52,500)
SA-2	0.0144	15.00 (49,200)	0.0083	16.00 (52,500)
SA-3	0.0105	13.75 (45,100)	0.0157	13.25 (43,500)
SA-4	0.0155	13.00 (42,600)	0.0144	11.00 (36,100)
SA-5	0.0162	17.00 (55,800)	0.0086	10.00 (32,800)
SA-6	0.0121	12.25 (40,200)	0.0113	12.50 (41,000)
SA-7	0.0078	14.25 (46,800)	0.0068	11.25 (36,900)
SA-9	0.0096	10.50 (34,500)	0.0184	10.75 (35,300)
SA-8	0.0065	10.00 (32,800)	0.0073	17.00 (55,800)
SA-10	0.0130	14.75 (48,400)	0.0090	15.00 (49,200)

NOTE: The Vehicle numbers are presented in order of time of launch.

Table A-8. Extreme Wind Shear Values in the High Dynamic Pressure Region for Apollo/Saturn 201 through Apollo/Saturn 205 Vehicles

(Δh = 1000 m)				
VEHICLE NUMBER	PITCH PLANE		YAW PLANE	
	SHEAR (SEC <sup>-1</sup> )	ALTITUDE km (ft)	SHEAR (SEC <sup>-1</sup> )	ALTITUDE km (ft)
AS-201	0.0206	16.00 (52,500)	0.0205	12.00 (39,400)
AS-203	0.0104	14.75 (48,400)	0.0079	14.25 (46,800)
AS-202	0.0083	13.50 (44,300)	0.0054	13.25 (43,500)
AS-204	0.0118	16.75 (55,000)	0.0116	14.00 (45,900)
AS-205	0.0113	15.78 (48,100)	0.0085	15.25 (46,500)

Table A-9. Extreme Wind Shear Values in the High Dynamic Pressure Region for Apollo/Saturn 501 through Apollo/Saturn 504 Vehicles

(Δh = 1000 m)				
VEHICLE NUMBER	PITCH PLANE		YAW PLANE	
	SHEAR (SEC <sup>-1</sup> )	ALTITUDE km (ft)	SHEAR (SEC <sup>-1</sup> )	ALTITUDE km (ft)
AS-501	0.0066	10.00 (32,800)	0.0067	10.00 (32,800)
AS-502	0.0125	14.90 (48,900)	0.0084	13.28 (43,500)
AS-503	0.0103	16.00 (52,500)	0.0157	15.78 (51,800)
AS-504	0.0248	15.15 (49,700)	0.0254	14.68 (48,160)



Table A-10. Selected Atmospheric Observations for Saturn 1 through 10 Vehicle Launches at Kennedy Space Center, Florida

VEHICLE NUMBER	VEHICLE DATA			SURFACE DATA						INFLIGHT CONDITIONS		
	DATE	TIME (EST) NEAREST MINUTE	LAUNCH COMPLEX	PRESSURE N/cm <sup>2</sup>	TEMPERATURE °C	RELATIVE HUMIDITY PERCENT	WIND* SPEED m/s	DIRECTION deg	CLOUDS	MAXIMUM ALTITUDE m	WIND IN 8-16 km LAYER SPEED m/s	DIRECTION deg
SA-1	27 Oct 61	1006	34	10.222	26.2	64	6.4	65	8/10 cumulus	12.25	47.0	242
SA-2	25 Apr 62	0900	34	10.205	24.6	59	3.5	180	1/10 cumulus, 3/10 cirrostratus	13.50	33.6	261
SA-3	16 Nov 62	1245	34	10.193	23.9	54	4.0	250	2/10 cumulus, 4/10 cirrus	13.75	31.3	269
SA-4	28 Mar 63	1512	34	10.176	23.9	71	6.0	40	1/10 stratocumulus, 1/10 cirrus	13.00	51.8	253
SA-5	29 Jan 64	1125	37B	10.278	17.8	59	9.0	38	4/10 stratocumulus, 2/10 cirrus	10.75	42.1	268
SA-6	28 May 64	1207	37B	10.142	28.7	64	7.0	150	1/10 cumulus, 1/10 cirrus	12.50	15.0	96
SA-7	18 Sep 64	1123	37B	10.173	29.5	55	5.0	70	1/10 cumulus, 5/10 altocumulus, 1/10 cirrus	11.75	17.3	47
SA-9	16 Feb 65	0937	37B	10.244	23.3	74	6.0	125	1/10 stratocumulus	13.00	34.3	243
SA-8	25 May 65	0235	37B	10.186	22.8	93	4.4	140	1/10 cumulus	15.25	16.0	351
SA-10	30 Jul 65	0800	37B	10.163	24.7	86	10.7	185	1/10 cumulonimbus, 2/10 altostratus, 5/10 cirrus	14.75	15.0	306

\* Instantaneous readings from charts at T-0 from anemometers on poles at 19.5 m (63.9 ft) on launch complex 34, 20.7 m (68.1 ft) on launch complex 37B. Heights of anemometers are above natural grade.

Table A-11. Selected Atmospheric Observations for Apollo/Saturn 201 through Apollo/Saturn 205 Vehicle Launches at Kennedy Space Center, Florida

VEHICLE NUMBER	VEHICLE DATA			SURFACE DATA						INFLIGHT CONDITIONS		
	DATE	TIME (EST) NEAREST MINUTE	LAUNCH COMPLEX	PRESSURE N/cm <sup>2</sup>	TEMPERATURE °C	RELATIVE HUMIDITY PERCENT	WIND* SPEED m/s	WIND* DIRECTION deg	CLOUDS	MAXIMUM WIND IN 8-16 km LAYER ALTITUDE m	SPEED m/s	DIRECTION deg
AS-201	26 Feb 66	1112	34	10.217	16.1	48	6.5	330	Clear	13.75	70.0	250
AS-203	5 Jul 66	0953	37B	10.173	30.2	70	6.3	242	8/10 cumulus, 1/10 cirrus	13.00	18.0	312
AS-202	25 Aug 66	1216	34	10.166	30.2	69	4.1	160	1/10 cumulus, 1/10 altocumulus, 1/10 cirrus	12.00	16.0	231
AS-204	23 Jan 68	1748	37B	10.186	16.1	93	4.2	45	3/10 cumulus	12.00	35.0	288
AS-205	11 Oct 68	1003	34	10.180	28.3	65	11.5	90	3/10 cumulonimbus	15.60	14.6	309

\* Instantaneous readings from charts at T-0 from anemometers on poles at 19.5 m (59.4 ft) on launch complex 34, 20.7 m (63.1 ft) on launch complex 37B. Heights of anemometers are above natural grade.

A-9

Table A-12. Selected Atmospheric Observations for Apollo/Saturn 501 through Apollo/Saturn 504 Vehicle Launches at Kennedy Space Center, Florida

VEHICLE NUMBER	VEHICLE DATA			SURFACE DATA						INFLIGHT CONDITIONS		
	DATE	TIME (EST) NEAREST MINUTE	LAUNCH COMPLEX	PRESSURE N/cm <sup>2</sup>	TEMPERATURE °C	RELATIVE HUMIDITY PERCENT	WIND* SPEED m/s	WIND* DIRECTION deg	CLOUDS	MAXIMUM WIND IN 8-16 km LAYER ALTITUDE m	SPEED m/s	DIRECTION deg
AS-501	9 Nov 67	0700	39A	10.261	17.6	55	8.0	70	1/10 cumulus	11.50	26.0	273
AS-502	4 Apr 68	0600	39A	10.200	20.9	83	5.4	132	5/10 stratocumulus	13.00	27.1	255
AS-503	21 Dec 68	0751	39A	10.207	15.0	88	1.0	360	4/10 cirrus	15.22	34.8	284
AS-504	3 Mar 69	1100	39A	10.095	19.6	61	6.9	160	10/10 strato-cumulus	11.73	76.2	264

\* Instantaneous readings from charts at T-0 from anemometers on launch pad at 18.3 m (60.0 ft) on launch complex 39 A. Heights of anemometers are above natural grade.

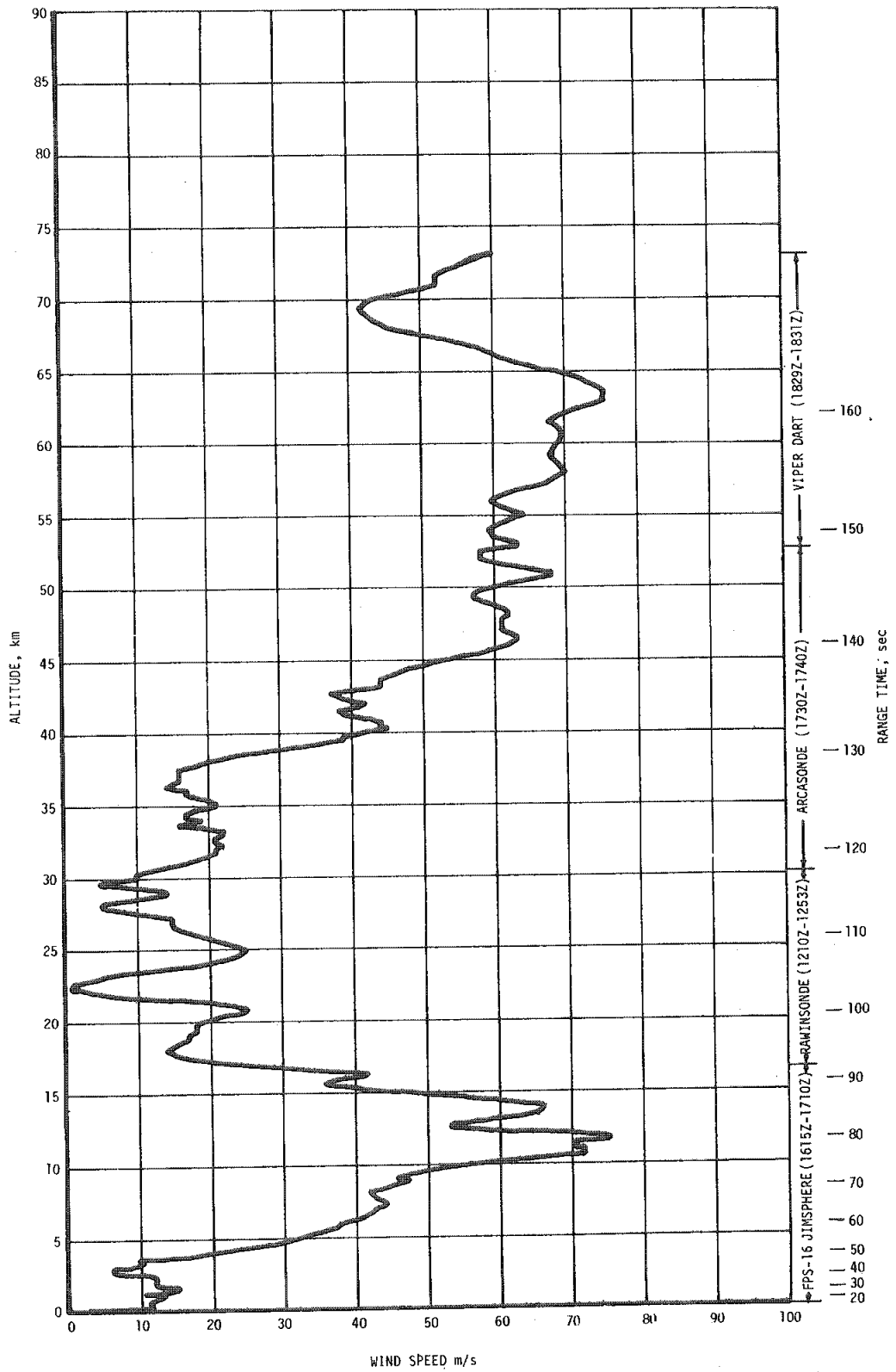


Figure A-1. Scalar Wind Speed at Launch Time of AS-504

A-10

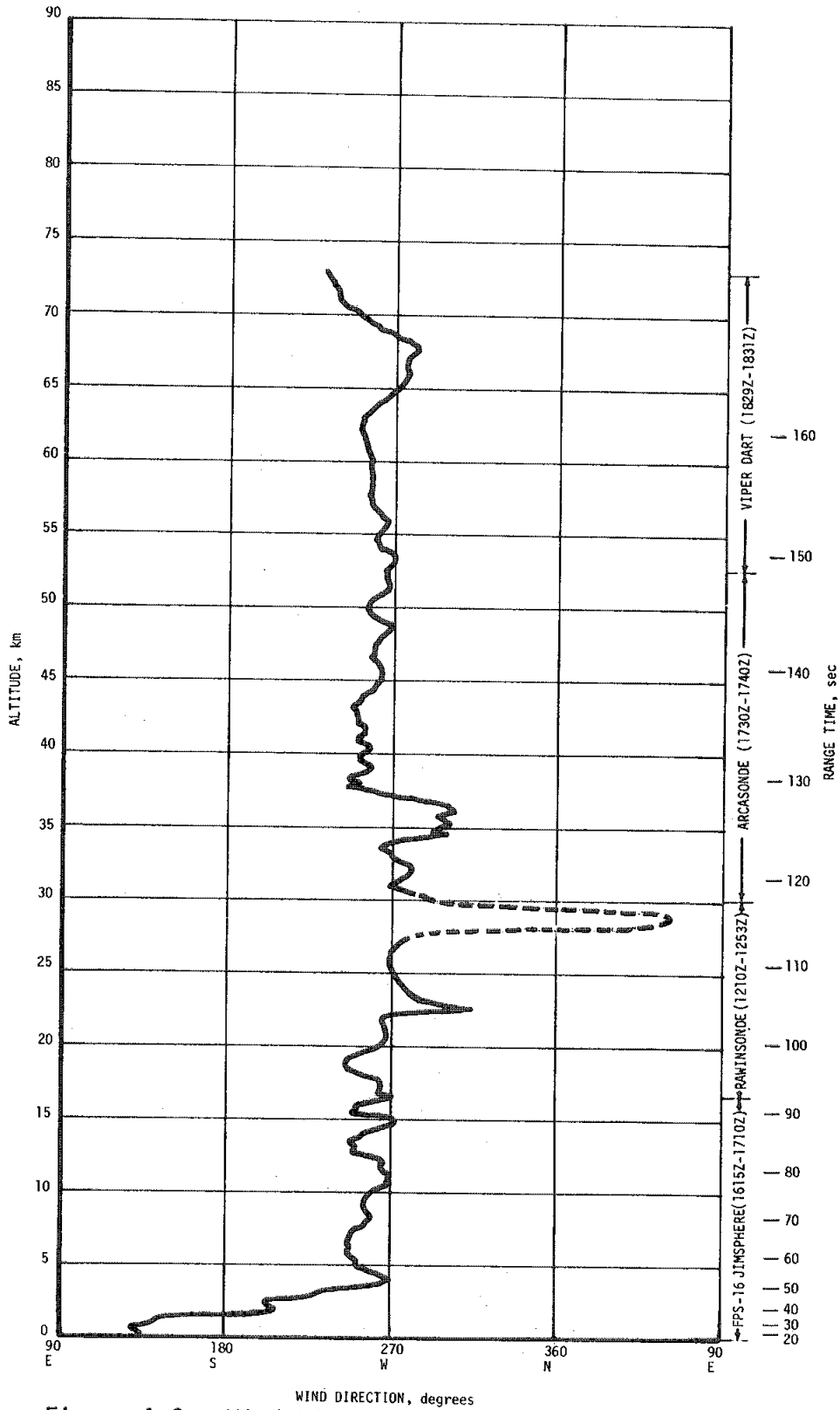


Figure A-2. Wind Direction at Launch Time of AS-504

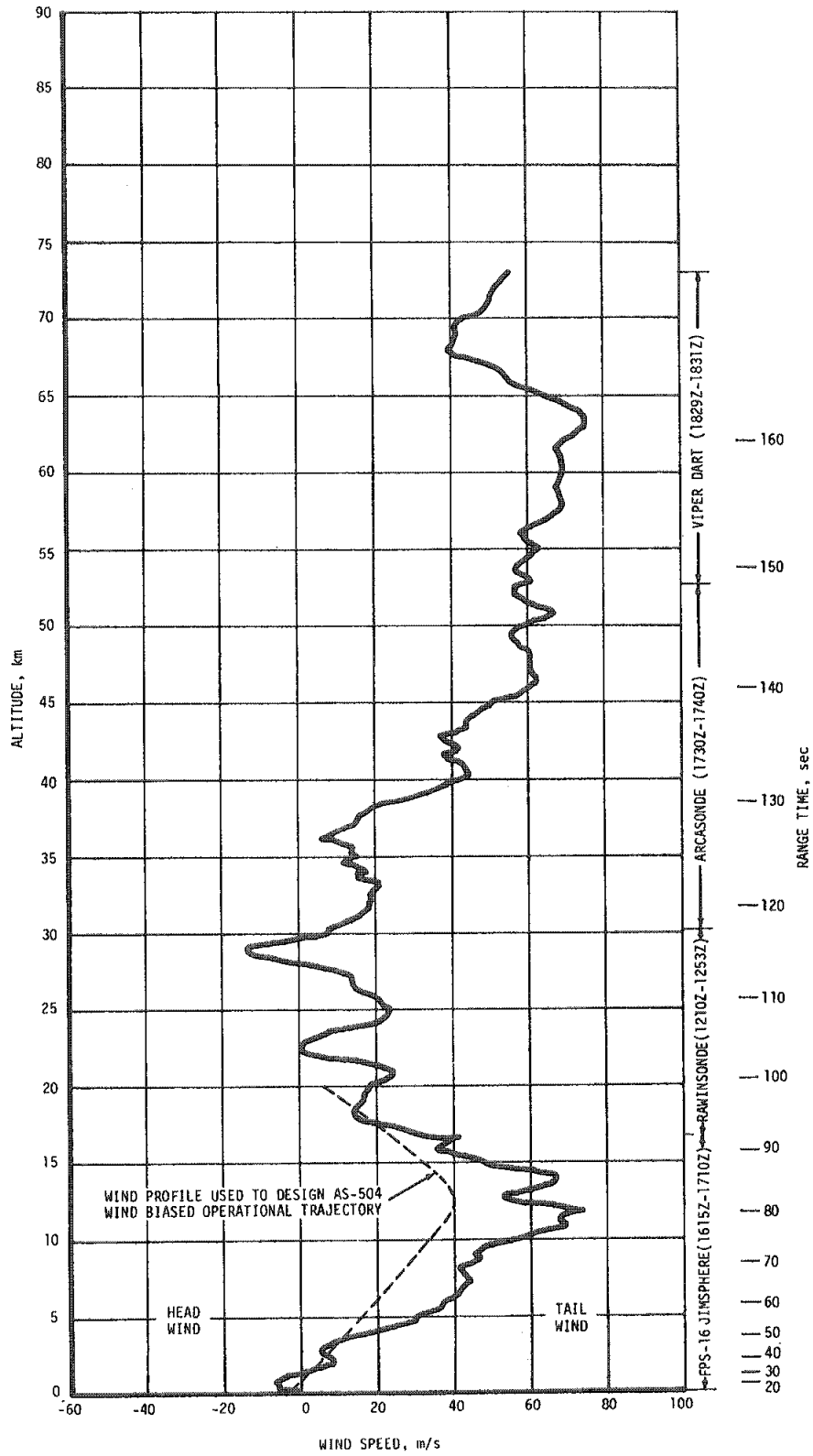


Figure A-3. Pitch Wind Speed Component ( $W_x$ ) at Launch Time of AS-504

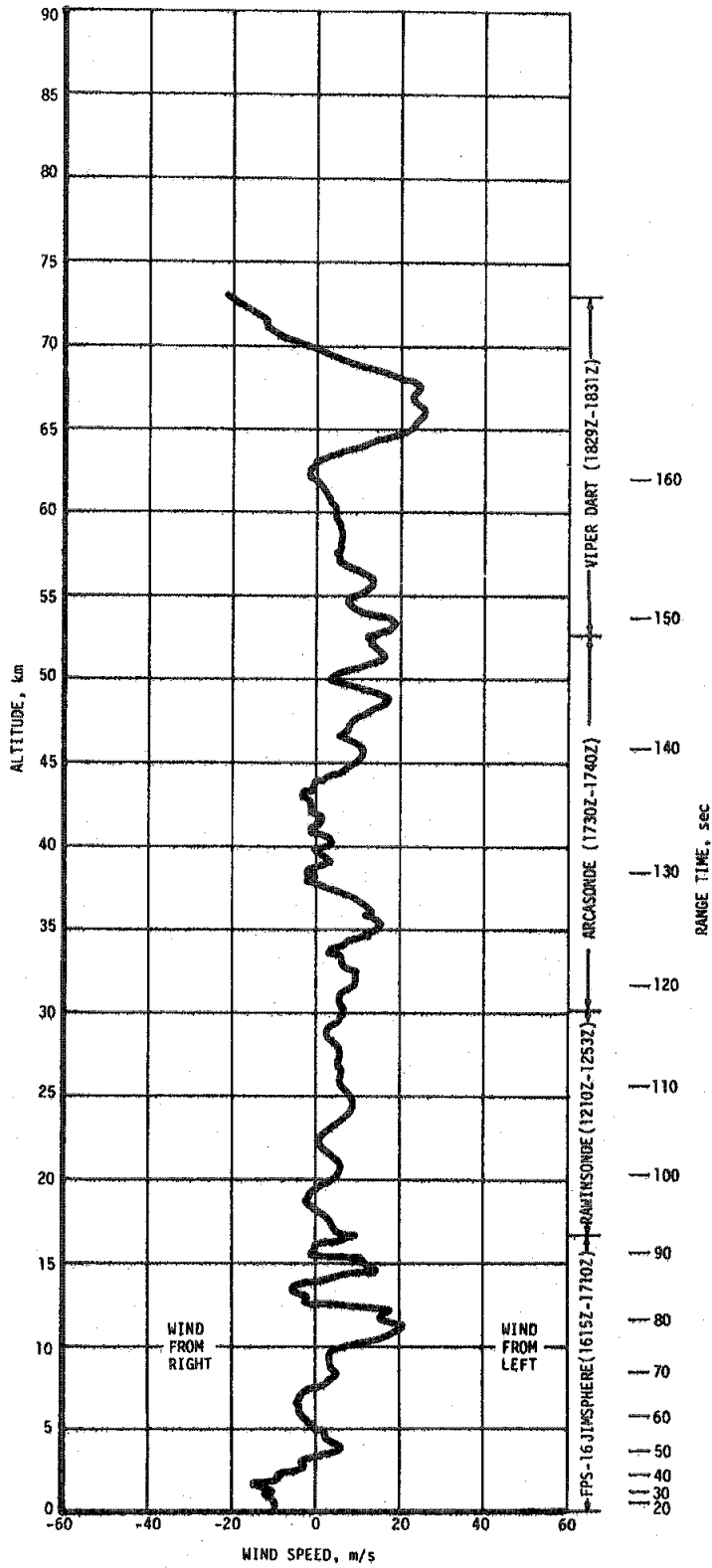


Figure A-4. Yaw Wind Speed Component at Launch Time of AS-504

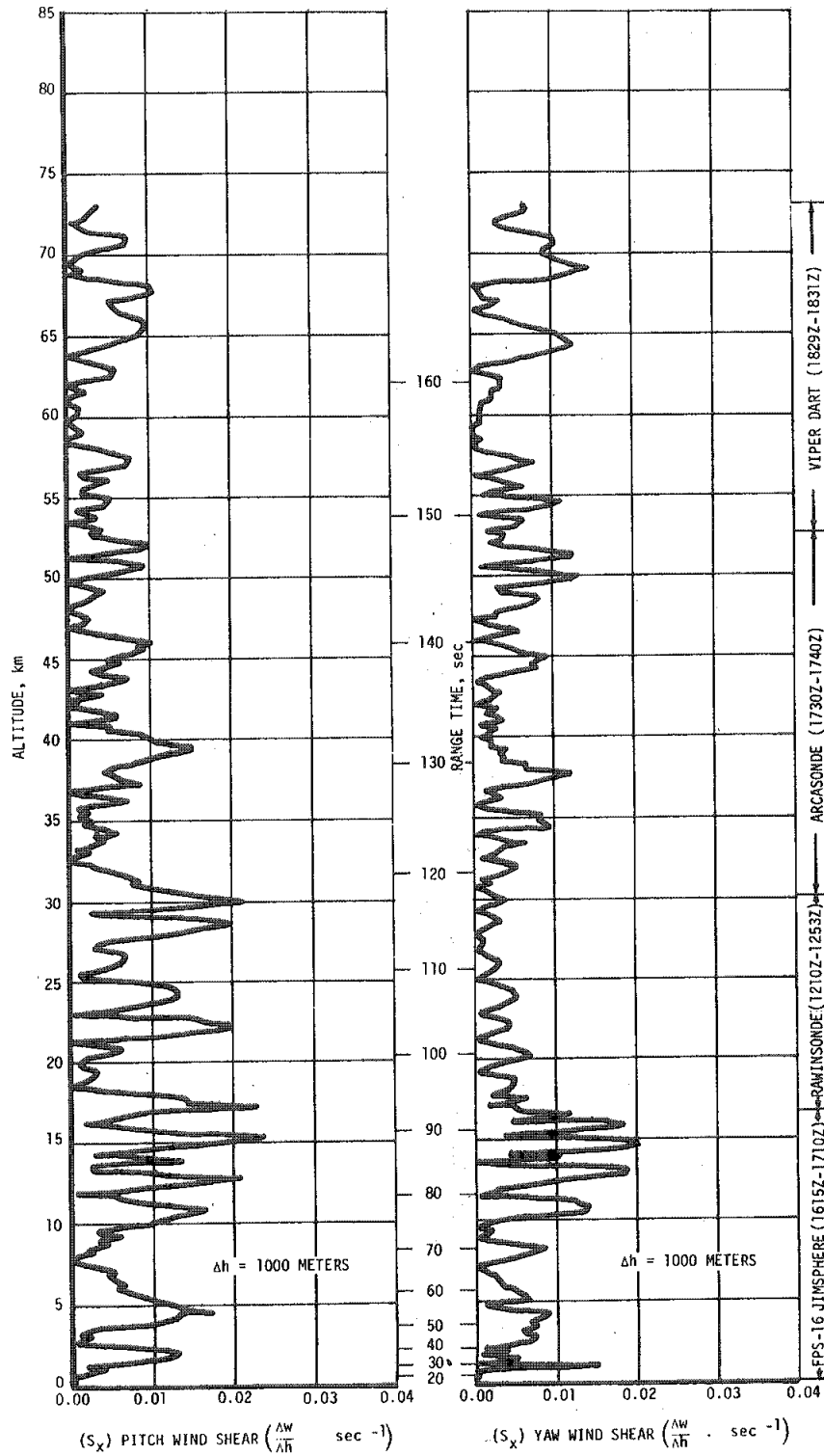


Figure A-5. Pitch ( $S_x$ ) and Yaw ( $S_y$ ) Component Wind Shears at Launch Time of AS-504

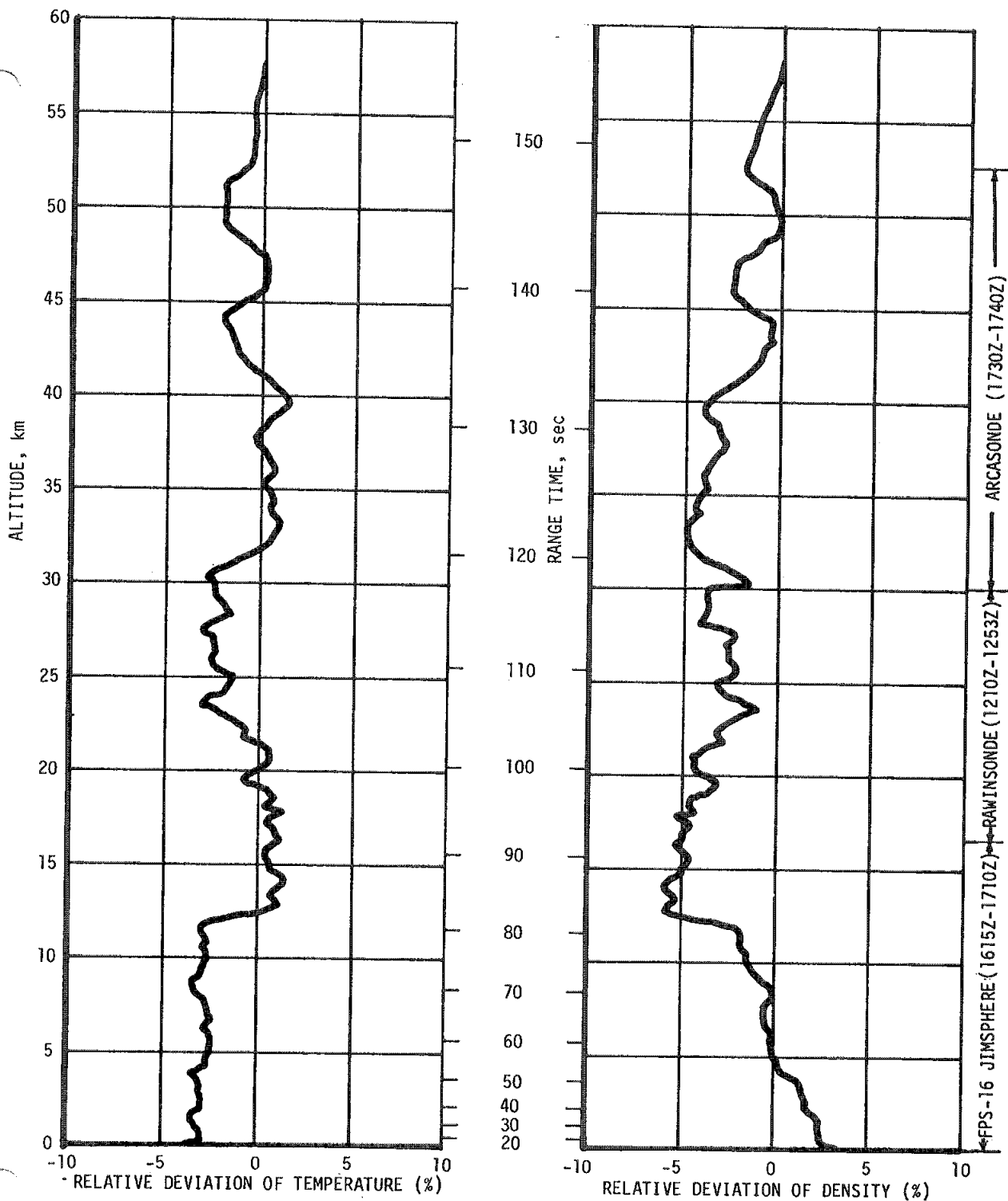


Figure A-6. Relative Deviation of Temperature and Density from PAFB (63) Reference Atmosphere, AS-504



## APPENDIX B

### AS-504 VEHICLE DESCRIPTION

#### B.1 SUMMARY

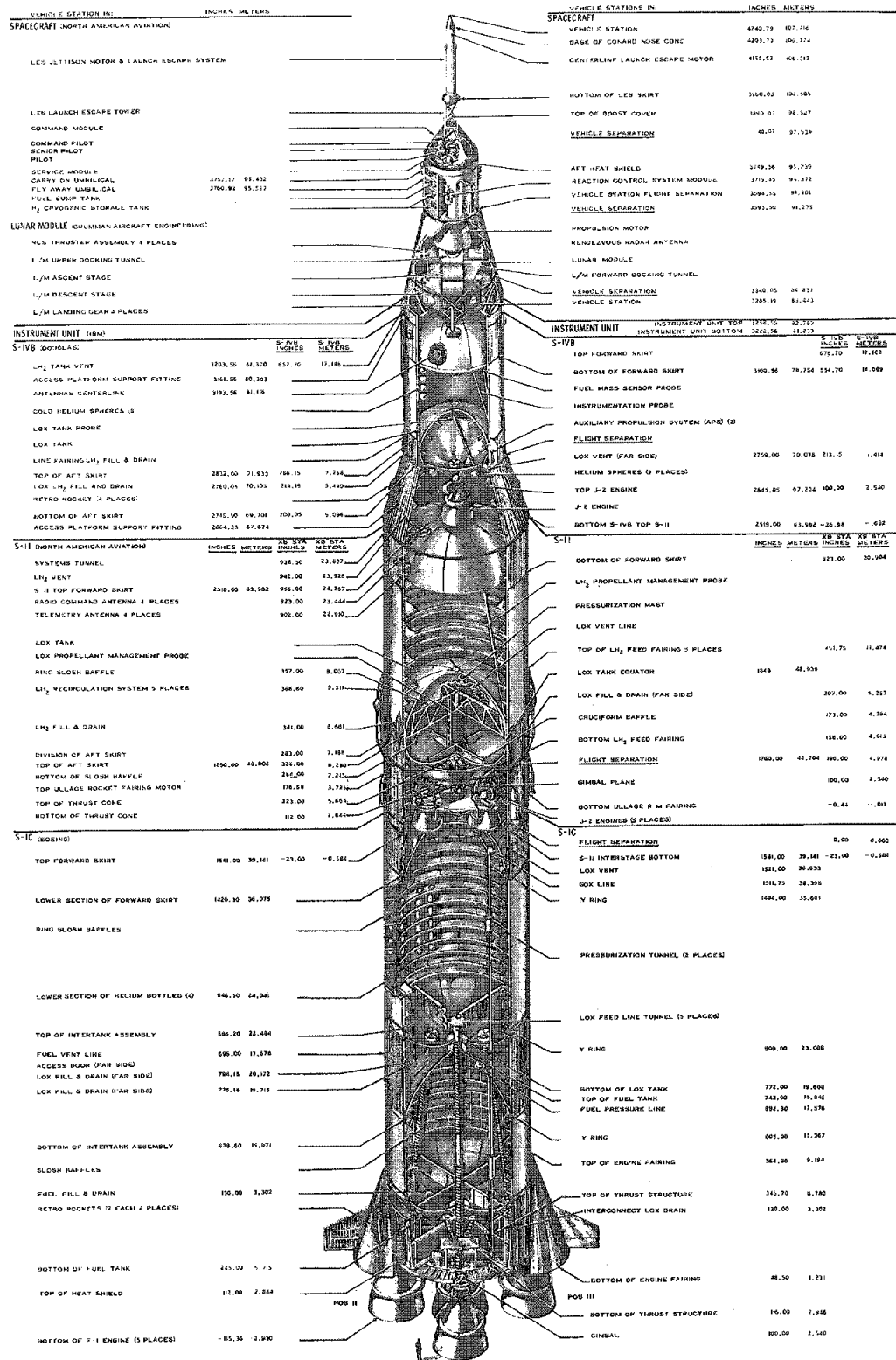
AS-504, fourth flight of the Saturn series, was the second manned Apollo Saturn V vehicle. The Apollo spacecraft was completely configured and included, for the first time, the Lunar Module (LM). The vehicle consists of five major units. From bottom to top they are: S-IC stage, S-II stage, S-IVB stage, Instrument Unit (IU), and the Spacecraft. The Saturn V Apollo vehicle is approximately 110.6 meters (363 ft) in length. See Figure B-1 for a pictorial description of the vehicle.

#### B.2 S-IC STAGE

##### B.2.1 S-IC Configuration

The S-IC stage, as shown in Figure B-2, is a cylindrical structure designed to provide the initial boost for the Saturn V Apollo vehicle. This booster is 42.1 meters (138 ft) long and has a diameter of 10.1 meters (33 ft). The basic structures of the S-IC are the thrust structure, fuel (RP-1) tank, intertank section, LOX tank, and the forward skirt. Attached to the thrust structure are the five F-1 engines which produce a combined nominal sea level thrust of 33,850,000 Newtons (7,610,000 lbf). Four of these engines are spaced equidistantly about a 9.243 meters (30.33 ft) diameter circle. The four outboard engines are attached so they have a gimbaling capability. Each outboard engine can move in a 5 degree, 9 minute square pattern to provide pitch, yaw, and roll control. The fifth engine is fixed mounted at the stage centerline. In addition to supporting the engines, the thrust structure also provides support for the base heat shield, engine accessories, engine fairings and fins, propellant lines, retro motors, and environmental control ducts. The intertank structure provides structural continuity between the LOX and fuel tanks, which provide propellant storage; and the forward skirt provides structural continuity with the S-II stage.

Propellants are supplied to the engine turbopumps by 15 suction ducts: 5 from the LOX tank, and 10 from the fuel tank. The fuel tank is a semimonocoque cylindrical structure closed at each end by an ellipsoidal



NOTE: S-1C STAGE ROTATED 45° COUNTER CLOCKWISE FOR CLARITY

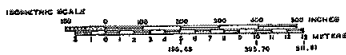


Figure B-1. Saturn V Apollo Configuration

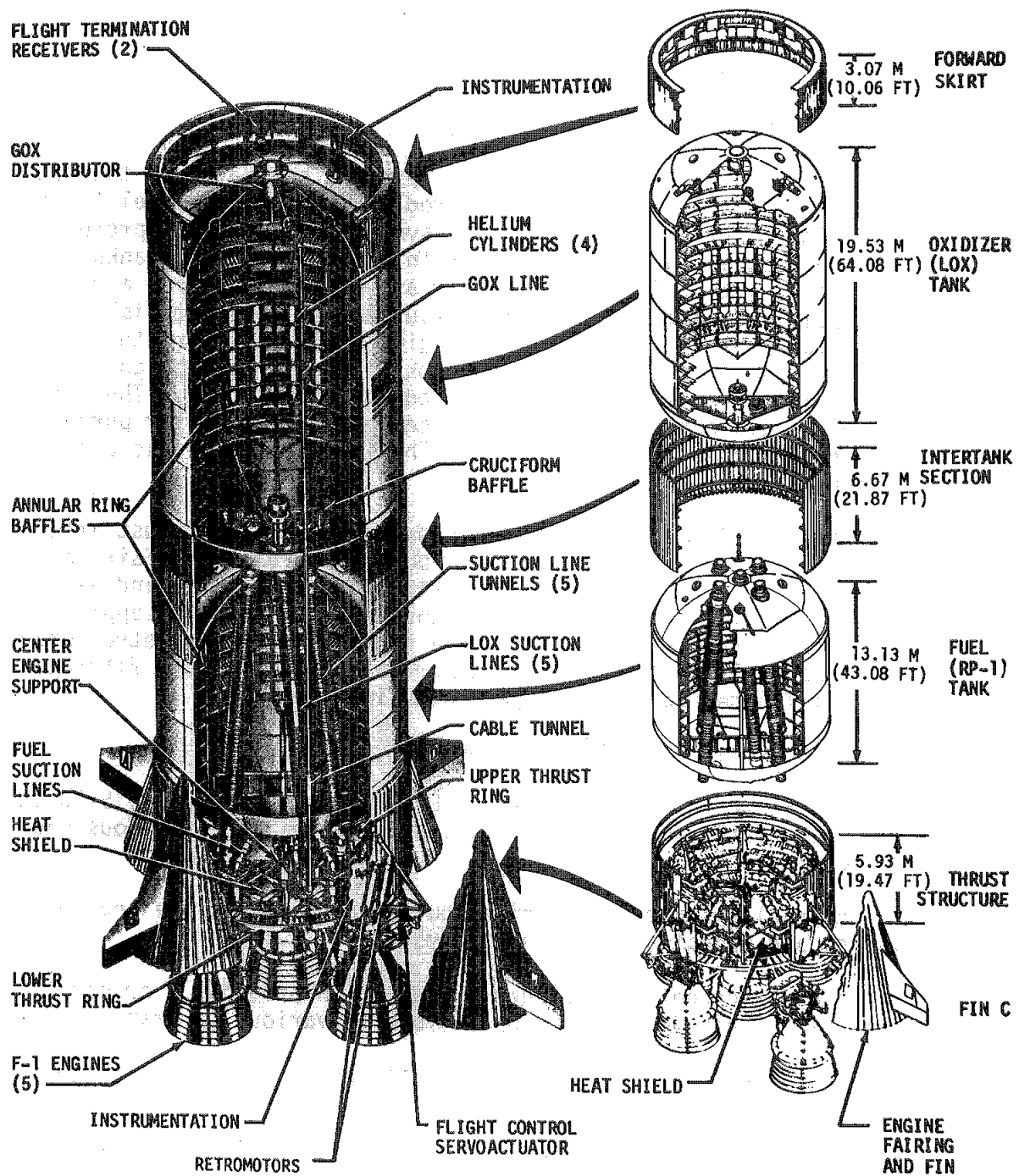


Figure B-2. S-IC Stage Configuration

bulkhead. Antislosh ring baffles are located on the inside wall of the tank, and an antivortex cruciform baffle is located in the lower bulkhead area. The configuration of the LOX tank is basically the same with the exception of capacity. The LOX tank will provide storage for 1342 m<sup>3</sup> (47,405 ft<sup>3</sup>) including ullage. The fuel tank will hold approximately 827 m<sup>3</sup> (29,221 ft<sup>3</sup>) including ullage. The mixture ratio between LOX and RP-1 is approximately 2.27:1 (LOX to RP-1).

The LOX and fuel pressurization systems provide and maintain the Net Positive Suction Pressure (NPSP) required for the LOX and fuel turbopumps during engine start and flight. These systems also provide protection from high pressures, which might occur in the LOX and fuel tanks. Before engine ignition, the LOX and fuel tanks are pressurized from a ground helium supply. During flight, LOX pressurization is accomplished by gaseous oxygen obtained by using F-1 engine heat exchangers to convert oxygen from liquid to gas. The fuel tank is pressurized by gaseous helium supplied by helium bottles located in the LOX tank. The LOX and fuel feed systems contain LOX and fuel depletion sensors for purposes of outboard engine cutoff during flight. The inboard engine was cutoff by an IU signal.

Eight solid propellant retro motors provide separation thrust after S-IC burnout. They are located inside the four outboard engine fairings and are attached externally to the thrust structure. The S-IC and S-II stages are severed by linear shaped charges, and the retro motors supply the necessary acceleration force to provide separation. Each retro motor is pinned securely to the vehicle support and pivot support fittings at an angle of 7.5 degrees from stage centerline.

Additional systems on the S-IC include:

- a. The Environmental Control System (ECS) which protects the S-IC stage from temperature extremes, excessive humidity, and hazardous gas concentrations.
- b. The hydraulic system which distributes power to operate the engine valves and thrust vector control system.
- c. The pneumatic control pressure system which provides a pressurized nitrogen supply for command operations of various pneumatic valves.
- d. The electrical system which distributes and controls the stage electrical power.
- e. The instrumentation system which monitors functional operation of the stage systems and provides signals for vehicle tracking during S-IC burn.

- f. The POGO suppression system. This system provides gaseous helium to a cavity in each of the LOX prevalves of the four outboard engine suction lines. These gas filled cavities act as a "spring" and serve to lower the natural frequency of the feed system and thereby prevent coupling between engine thrust oscillations and the first longitudinal mode of the vehicle structure.

The more significant configuration changes between AS-503 S-IC and AS-504 S-IC are shown in Table B-1.

Table B-1. S-IC Significant Configuration Changes

SYSTEM	CHANGE	REASON
Propulsion	F-1 engine qualification configuration thrust chamber injector incorporated.	To improve combustion stability and specific impulse.
	Minimum ullage volume and maximum propellant load in LOX and fuel tanks.	To increase payload capability of launch vehicle.
	Early termination of LOX replenishing system. Replenishing will be terminated at the beginning of automatic sequence (-187 seconds) rather than the start of LOX prepressurization (-72 seconds).	To accommodate Kennedy Space Center (KSC) launch operations.
	Adjustment of engine hydraulic control orifices.	Optimize engine thrust decay transient.
	Helium and LOX heat exchanger by-pass lines re-orificed.	To raise outlet temperature to within model specification limits throughout flight.
Structures	LOX delivery system center engine standpipe increased by approximately 88.9 cm (35 inches).	Originally, to prevent vehicle maximum acceleration from exceeding 4.37 g's. Subsequent to incorporation of this change, LOX depletion has become a secondary mode of center engine shutdown. The primary mode is by IU command and limits the vehicle maximum acceleration to 4.0 g's.
	LOX tank tapered skins replace stepped skins. Cantilever baffle web thickness reduced. Seventy-two radial T stiffeners removed. Chord cross section area for three baffles near helium bottles reduced. Y-rings scalloped.	To decrease weight of launch vehicle.
	Forward skirt insulation not installed.	Aerodynamic heating from AS-504 trajectory is lower than that from previous flights and permits the insulation deletion while still maintaining the thermal stress safety factor of 1.4.
Data	Deleted separation and LOX tank film cameras, base region Television (TV) camera, and associated hardware such as batteries and purge systems.	R&D instrumentation which is no longer required.
	Measurements reduced from 893 to 666. All telemetry system strain gages were deleted.	

## B.3 S-II STAGE

### B.3.1 S-II Configuration

The S-II stage shown in Figure B-3 provides second stage boost for the Saturn V launch vehicle. The S-II stage has a cylindrical structure, 24.8 meters (81.5 ft) long and 10.1 meters (33 ft) in diameter. Propulsive power is provided by five J-2 engines with a combined nominal thrust of 5,115,455 Newtons (1,150,000 lbf) at an oxidizer to fuel ratio of 5.5:1. The approximate weight of the basic stage is 38,238 kilograms (84,300 lbm) dry. Approximate weight of the aft interstage (including ullage motors) is 5,307 kilograms (11,700 lbm). The total nominal propellant load is approximately 442,253 kilograms (975,000 lbm). The approximate weight of the fully loaded S-II vehicle is 485,797 kilograms (1,071,000 lbm).

The S-II airframe consists of a body shell structure (forward and aft skirt and interstage), a propellant tank structure, and a thrust structure.

Each of the shell structure units are of basically the same construction consisting of a semimonocoque cylindrical shell fabricated from aluminum alloy material. These units are stiffened by external hat-section stringers and internal ring frames. These units provide structural continuity between adjacent stages.

The thrust structure is a semimonocoque conical shell which tapers from the stage diameter down to a 5.5 meters (18 ft) diameter. It is constructed in the same manner as the skirt section and is fabricated from aluminum alloy material. Four pairs of thrust longerons (two at each outboard engine location) and a center engine support beam distribute the thrust loads of the five J-2 engines. A fiberglass honeycomb heat shield, supported from the lower portion of the thrust structure protects the stage base area from excessive temperatures during S-II boost.

Propellants are supplied to the J-2 engines from the LH<sub>2</sub> and LOX tanks. The LH<sub>2</sub> tank is a cylindrical shell with the ends closed by a forward elliptical bulkhead and an aft reversed elliptical bulkhead. The tank, 17.1 meters (56 ft) long and 10.1 meters (33 ft) in diameter, has a capacity of 1069 m<sup>3</sup> (37,737 ft<sup>3</sup>). The tank wall is composed of six cylindrical sections which incorporate longitudinal and circumferential stiffeners. Wall sections and bulkheads are fabricated from 2014 aluminum alloy joined by fusion welding. The LOX tank is of ellipsoidal shape. It has a volume of 361 m<sup>3</sup> (12,745 ft<sup>3</sup>). The tank is 6.7 meters (22 ft) long and 10.1 meters (33 ft) in diameter. The bottom of the fuel tank is common to both tanks and serves as the forward end of the LOX tank.

B-7

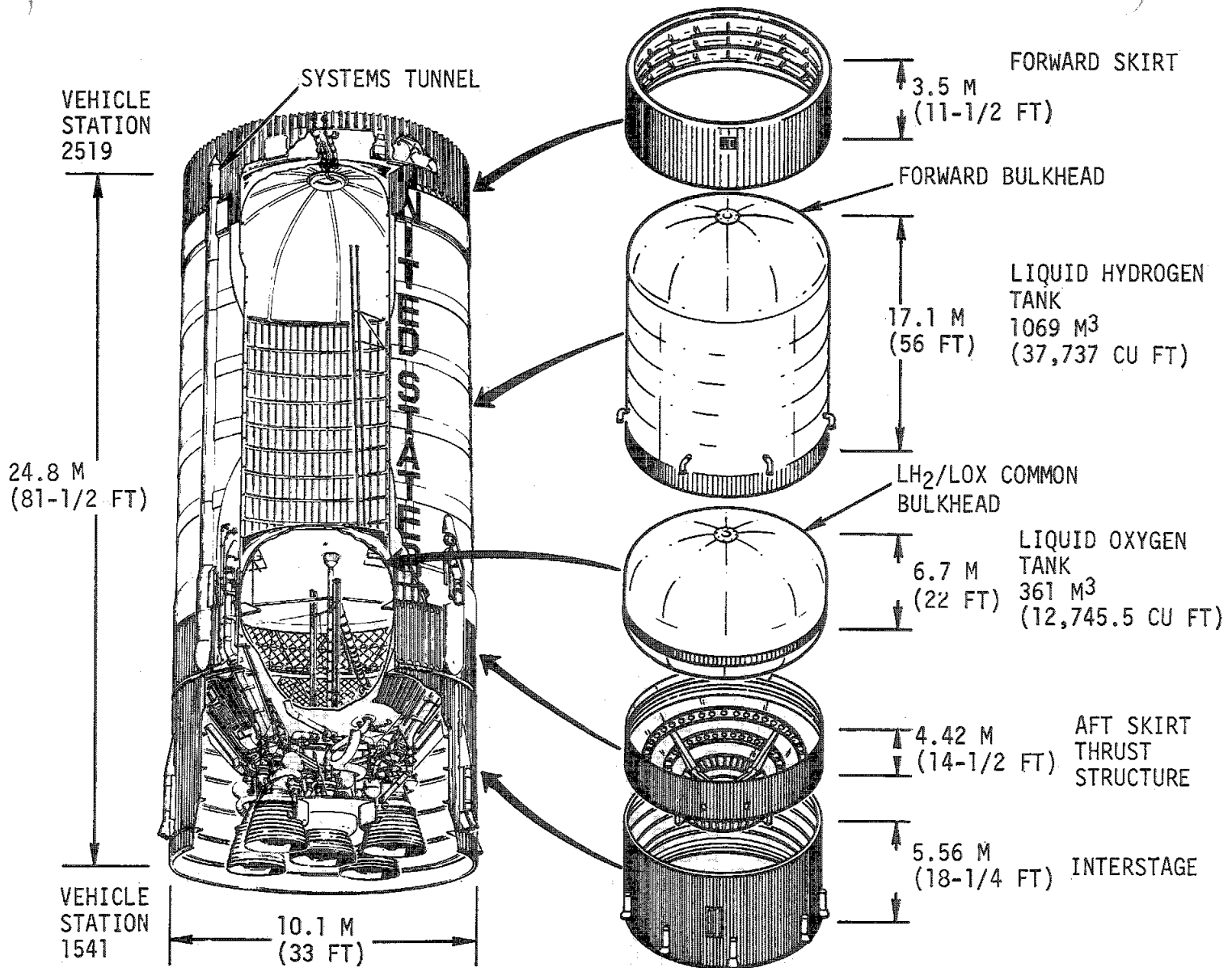


Figure B-3. S-II Stage Configuration

This common bulkhead is a sandwich structure composed of aluminum facing sheets and a fiberglass/phenolic honeycomb core. The fore and aft halves of the LOX tank are formed from waffle-stiffened gore segments fabricated from aluminum alloy. The stage propulsion system consists of five single start J-2 engines utilizing LOX and LH<sub>2</sub> for propellants. Each engine attains a nominal thrust of 1,023,091 Newtons (230,000 lbf) at an oxidizer to fuel ratio of 5.5:1. The four outboard J-2 engines are mounted with gimbal bearings and hydraulic powered actuator rods to provide thrust vector control. The fifth engine is mounted on stage centerline and is not gimbaleed.

The J-2 engine is a high performance, high altitude engine employing a tubular walled, one-and-one-half pass, regeneratively cooled thrust chamber. Propellants are fed through two independently driven turbopumps. The ratio of fuel to oxidizer is controlled by bypassing LOX from the discharge side of the oxidizer turbopump back to the inlet side through a Propellant Utilization (PU) valve.

The propellant tanks are prepressurized from a ground regulated helium source prior to liftoff to provide the turbopump inlet pressure required for engine start. Prepressurization is terminated 30 seconds prior to liftoff for both tanks. During the engine burn period, the LOX tank is pressurized by flowing LOX through the heat exchanger in the oxidizer turbine exhaust duct and the LH<sub>2</sub> tank is pressurized by GH<sub>2</sub> from the thrust chamber fuel manifold. Both the LOX and LH<sub>2</sub> propellant tanks have vent valves for over-pressure protection.

Inflight separation of the S-IC/S-II stages is accomplished by a dual-plane separation system. Both separation events are controlled by the flight program stored in the Launch Vehicle Digital Computer (LVDC) which is located in the IU stage. First plane separation, occurring at vehicle station 39.73 meters (1564 in.), is initiated by an ordnance train. This train consists of an Exploding Bridge Wire (EBW) firing unit, an EBW detonator, and a linear shaped charge which severs the tension plates around the periphery of the stage at the separation plane. Four ullage motors on the S-II stage are fired to provide a propellant settling force and retro motors on the S-IC stage are fired to provide positive separation of the two stages. Second plane separation occurs about 30 seconds later at vehicle station 44.7 meters (1760 in.) using the same type of ordnance train.

Additional S-II stage systems perform as follows:

- a. The leak detection and insulation purge system detects hydrogen, oxygen, or nitrogen leaking into the LH<sub>2</sub> tank insulation or LH<sub>2</sub> feedline elbows and provides a means for purging and diluting any leakage into the insulation prior to liftoff.



- b. The ECS provides protection against hazardous gas concentrations and also provides temperature control in the engine compartment and equipment containers prior to liftoff.
- c. The pneumatic control pressure system provides the actuating force for the prevalves, recirculation valves, and propellant fill and drain valves.
- d. The propellant utilization system is used for propellant management during propellant loading operations and S-II boost.
- e. The engine actuation system provides engine gimbaling. The hydraulic actuators, which are part of the engine actuation system, receive the gimbaling commands from the flight control system in the IU.
- f. The electrical system is used for supplying and distributing electrical power to the various systems.
- g. The Emergency Detection System (EDS) supplies engine mainstage OK and LH2 ullage pressure signals to the IU and spacecraft.
- h. The engine preconditioning (recirculation) system recirculates LOX and LH2 and provides LOX helium injection prior to S-II engine start.
- i. The data system is used for obtaining and transmitting data for stage performance evaluations.
- j. The propellant dispersion system is provided for range safety.
- k. The propellant feed system supplies propellants to the engines.
- l. The propellant level monitoring system uses liquid level monitoring devices to provide propellant low level cutoff signals to the engines and also provides backup propellant loading information.

A major structural change between this and previous S-II stages is the use of "light weight" structure on all major airframe sections.

No new systems were added for AS-504. The significant S-II stage configuration changes between AS-503 and AS-504 are listed in Table B-2.

#### B.4 S-IVB STAGE

##### B.4.1 S-IVB Configuration

The S-IVB stage, as shown in Figure B-4, is a bi-propellant tank structure designed to withstand the loads and stresses incurred on the ground and during launch, preignition boost, ignition, and all flight phases. The S-IVB stage has nominal dimensions of 18.0 meters (59 ft) in length and 6.6 meters (21.6 ft) in diameter. The basic airframe consists of the

Table B-2. S-II Significant Configuration Changes

SYSTEM	CHANGE	REASON
Structures	Incorporate light weight structural design on fwd skirt, LH <sub>2</sub> tank, LOX tank, thrust structure, aft skirt and interstage. Modify the cork insulation on the aft skirt and interstage.	Weight reduction.
Separation	Modify design of fasteners used on separation plane tension plates.	Improve installation procedures and reliability.
Insulation	Use wet lay-ups for close-out strips on LH <sub>2</sub> tank insulation (was rubber doublers).	Minimize cracking, purge gas leaks, and repair operations that might delay launch.
Propellant Management	Time delay from LOX low level sensors dry indication to engine cutoff command is changed to 1.5 seconds (was zero seconds).	Increase stage performance by minimizing propellant residuals at engine cutoff.
	Increase total nominal propellant load to 442,253 kg (975,000 lbm) from 421,841 kg (930,000 lbm).	Increase payload capability of vehicle.
	Incorporate PU computer valve drive circuit redesign.	Improve reliability.
Propellant Feed	Use PU system closed loop mode (was open loop mode on AS-503).	Improve efficiency of propellant control.
	Install Parker prevalues (was LAD prevalues).	Improve reliability. Parker prevalues are fully qualified.
Electrical	Added instrument bus power for engine cutoff signal (was main bus power only).	Permits early staging of S-II/S-IVB by alternate flight sequence Time Base 4a (T4a) if main battery fails.
Engines	J-2 engine nominal thrust uprated to 1,023,091 Newtons (230,000 lbf) from 1,000,850 Newtons (225,000 lbf).	Increase payload capability of vehicle.

aft interstage, thrust structure, aft skirt, propellant tanks, and forward skirt. The aft interstage assembly provides the load supporting structure between the S-IVB stage and the S-II stage. The thrust structure assembly is an inverted truncated cone attached at its large end to the aft dome of the LOX tank and at its small end to the engine mount. This structure provides support for engine piping, wiring and interface panels, ambient helium spheres, and some of the LOX tank and engine instrumentation. The aft skirt assembly is the load bearing structure between the LH<sub>2</sub> tank and aft interstage. The propellant tank assembly consists of a cylindrical tank with a hemispherical shaped dome at each end. Contained within this assembly is a common bulkhead which separates the LOX and LH<sub>2</sub>.

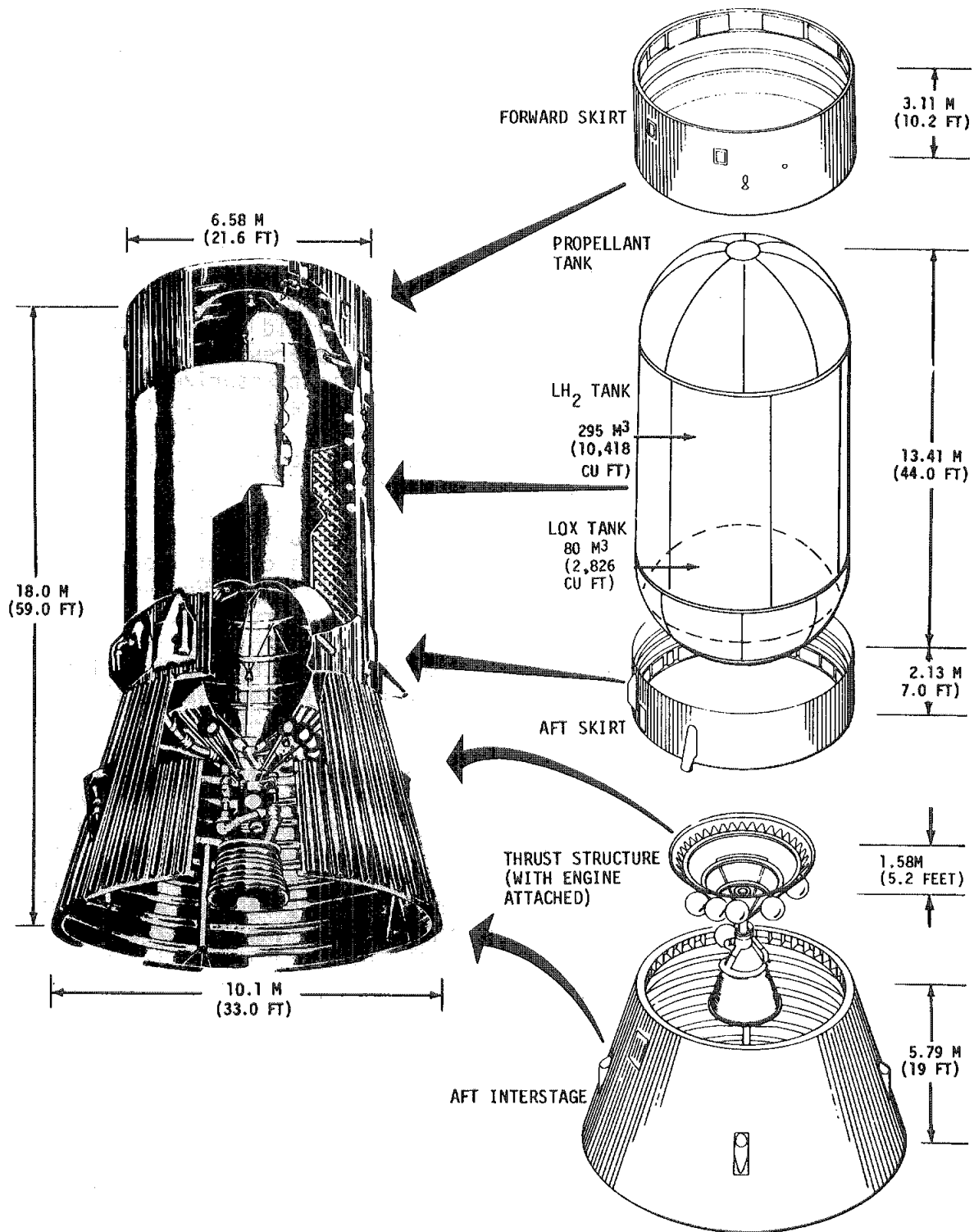


Figure B-4. S-IVB Stage Configuration

The forward skirt assembly extends forward from the intersection of the LH<sub>2</sub> tank sidewall and the forward dome providing a hard attach point for the IU.

The S-IVB is powered by one J-2 engine similar to those on the S-II stage. The engine attains a nominal thrust of 1,023,091 Newtons (230,000 lbf) at a 5.5:1 oxidizer to fuel mixture ratio. The S-IVB J-2 engine also has multiple restart capabilities. LOX is supplied to the engine from the LOX tank by a 6-inch diameter low pressure duct. LH<sub>2</sub> is supplied from the LH<sub>2</sub> tank by a vacuum-jacketed low pressure 10-inch diameter duct. Prior to liftoff, both the LH<sub>2</sub> tank and the LOX tank are pressurized by ground supplied helium. During S-IVB J-2 engine burn periods, GH<sub>2</sub> is bled from the thrust chamber hydrogen injector manifold for LH<sub>2</sub> tank pressurization. GHe, extracted from the storage spheres located in the LH<sub>2</sub> tank, is warmed by a heat exchanger and used to pressurize the LOX tank. Second burn (first restart) propellant tank repressurization is accomplished utilizing the O<sub>2</sub>-H<sub>2</sub> burner as a primary mode. The burner supplies energy to the GHe, extracted from the GHe spheres located in the LH<sub>2</sub> tank, to provide LOX and LH<sub>2</sub> repressurization. Ambient helium spheres are available for backup pressurization if required. The ambient helium spheres are used for LOX and LH<sub>2</sub> tank repressurization preceding the third burn (second restart). The O<sub>2</sub>-H<sub>2</sub> burner is operated prior to the third burn to demonstrate its restartable capability. However, it is not used for propellant tank repressurization for third burn.

Pitch and yaw control of the S-IVB is accomplished during powered flight by gimbaling the J-2 engine and roll control is provided by operating the Auxiliary Propulsion System (APS).

The APS provides three axis stage attitude control and main stage propellant control during coast flight. The ullage engines are necessary for the propellant seating which is required for engine restart. The APS modules are located on opposite sides of the S-IVB aft skirt at positions I and III. Each module contains its own oxidizer system, fuel system, and pressurization system. Nitrogen Tetroxide (N<sub>2</sub>O<sub>4</sub>) is used as the oxidizer and Monomethyl Hydrazine (MMH) is the fuel for these engines.

Additional systems on the S-IVB are:

- a. The hydraulic system which gimbals the J-2 engine.
- b. Electrical system which supplies and distributes power to the various electrical components.
- c. Thermoconditioning system which thermally conditions the electrical/electronic modules in the forward skirt area.

- d. Data acquisition and telemetry system which acquires and transmits data for stage evaluation.
- e. A set of ordnance systems used for rocket ignition, stage separation, ullage motor jettison and range safety.

The more significant configuration changes between AS-503 S-IVB and AS-504 S-IVB are shown in Table B-3.

Table B-3. S-IVB Significant Configuration Changes

SYSTEM	CHANGE	REASON
Instrumentation	AS-502 anomalies instrumentation package not installed.	Program requires AS-502 anomalies instrumentation on AS-503 and AS-505 stages only.
Propellant Utilization	Capability to command, through the switch selector, propellant utilization mixture ratios of 4.5:1, 5.0:1 and 5.5:1 (AS-503 mixture ratio was 4.5:1 and 5.0:1).  Modify PU valve by rotating the flow baffle 30 degrees.	Provide fixed mixture ratios of propellants to the J-2 engine for specific periods of time in place of closed-loop propellant utilization mixture ratio control.  Reduce in-run thrust shifts.
Structure	Anti-flutter kit not installed.	Kit was on AS-501 and AS-503. Not required for AS-504.
Propulsion	Revise LOX vent and relief valve pressure setting: Crack 30.0 to 31.4 N/cm <sup>2</sup> (43.5 to 45.5 psia) Total range 29.3 to 31.4 N/cm <sup>2</sup> (42.5 to 45.5 psia).  Revise LOX Non Propulsive Vent (NPV) latching valve pressure setting: Crack 28.6 to 30.0 N/cm <sup>2</sup> (41.5 to 43.5 psia) Total range 27.9 to 30.0 N/cm <sup>2</sup> (40.5 to 43.5 psia).  Three S-IVB J-2 engine burns. First restart propellant tank repressurization performed by O <sub>2</sub> -H <sub>2</sub> burner with ambient spheres as backup and second restart propellant tank repressurization performed by ambient spheres. O <sub>2</sub> -H <sub>2</sub> burner will be activated prior to second restart to demonstrate burner restart capability but not to repressurize propellant tanks.  Third S-IVB J-2 engine burn will be preceded by a 53 second fuel lead (in lieu of 8 seconds). Chill-down operation will not occur prior to third burn.	Eliminate propulsive relief venting during separation of Command Service Module (CSM), CSM/LM docking, and CSM/LM ejection.  Eliminate propulsive relief venting during separation of CSM, CSM/LV docking and CSM/LM ejection.  Demonstrate S-IVB dual restart capability.  Demonstrate S-IVB stage flexibility.

## B.5 INSTRUMENT UNIT (IU)

### B.5.1 IU Configuration

The IU, as shown in Figure B-5, is basically a short cylinder fabricated from an aluminum alloy honeycomb sandwich material. The IU has a diameter of 6.6 meters (21.6 ft) and a length of 0.9 meter (3 ft). The cylinder is manufactured in three 120 degree segments which are joined by splice plates into an integral load bearing unit. The top and bottom edges of the cylinder are made from extruded aluminum channels bonded to the honeycomb sandwich material. Cold plates are attached to the interior of the cylinder which serve both as mounting structure and thermal conditioning units for the electrical/electronic equipment.

Other systems included in the IU are:

- a. The Environmental Control System (ECS) which maintains an acceptable environment for the IU equipment.
- b. The electrical system which supplies and distributes electrical power to the various systems.
- c. The Emergency Detection System (EDS) which senses onboard emergency situations for automatic abort or display in the spacecraft.
- d. The navigation, guidance, and control system which guides the launch vehicle to its programmed inertial position and velocity.
- e. The measurements and telemetry system which monitors and transmits signals to ground monitoring stations.
- f. The flight program which controls the LVDC from seconds before liftoff until the end of the launch vehicle mission.

The more significant configuration changes between AS-503 IU and AS-504 IU are shown in Table B-4.

## B.6 SPACECRAFT

### B.6.1 Spacecraft Configuration

The Apollo 9 mission was the first to use the design configuration of all spacecraft components. The spacecraft, as shown in Figure B-6 includes a Launch Escape System (LES), a Command Module (CM), a Service Module (SM), a Spacecraft Lunar Module Adapter (SLA), and a LM. From the bottom of the SLA to the top of the LES, the spacecraft measures approximately 24.9 meters (81.8 ft). The LES and SLA were essentially unchanged from the Apollo 8 configurations. The CM and SM were also unchanged from the Apollo 8 configurations, except for those items required to accommodate operations with the LM. These changes notably included the addition of

B-15

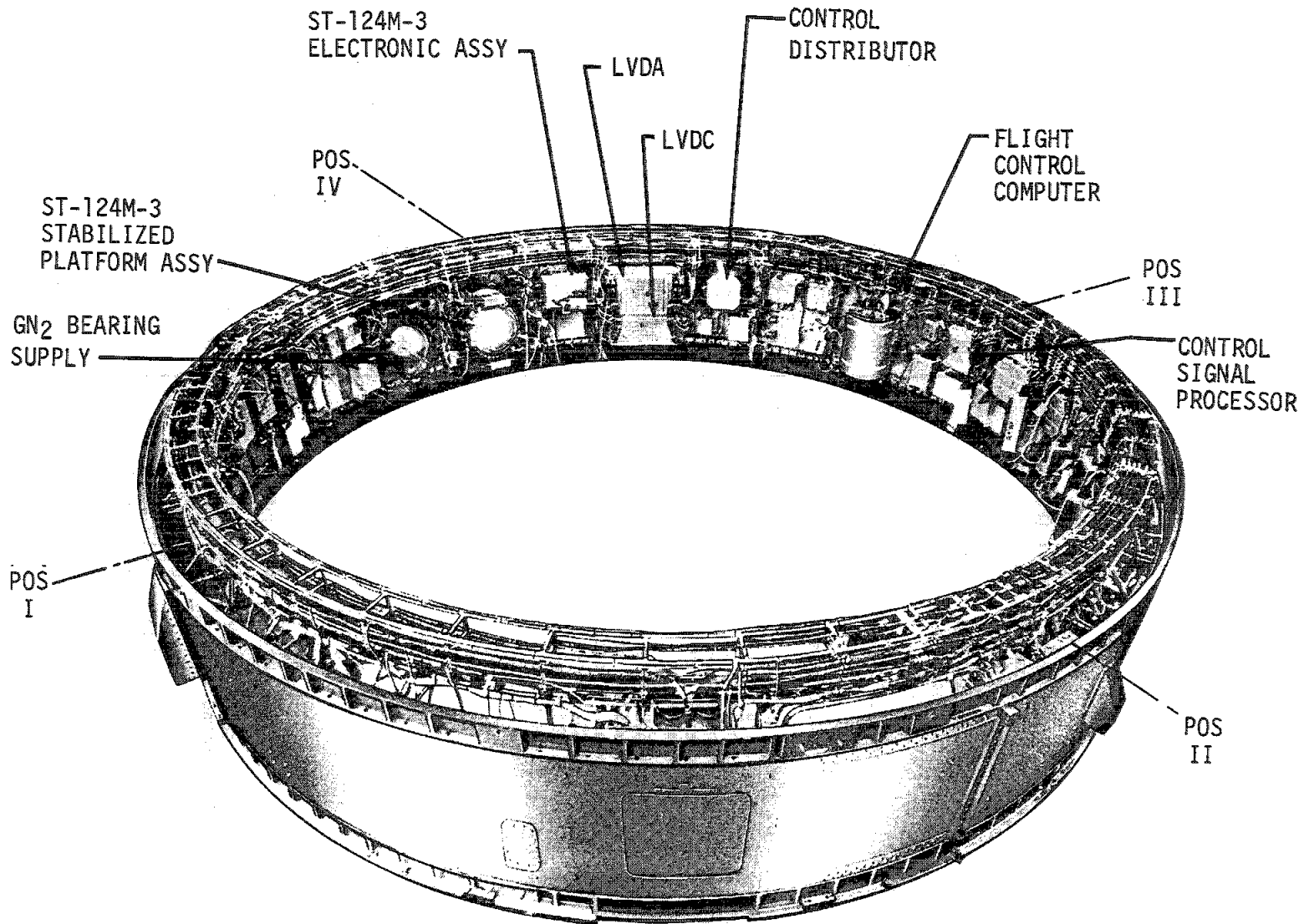


Figure B-5. Instrument Unit Configuration

Table B-4. IU Significant Configuration Changes

SYSTEM	CHANGE	REASON
Electrical Subsystem	Removed 6 measuring racks, 1 measuring distributor, and 1 battery. Calbe quantity reduced from 182 to 126.	Reduction in telemetry in going from Research and Development (R&D) to Operational Vehicle.
	Flight Control Computer (FCC) Power removed from 6D41 Bus.	The 1KHz oscillators in the FCC susceptible to coolant pump noise.
	Command and Communications System (CCS) input power moved from 6D11 to 6D41	CCS generated noise affecting FCC pitch and yaw outputs to actuators.
Instrumentation and Communications Subsystems	Removed 32 S-IVB Strain measurements, 6 LTA and 2 Launch Escape Tower acceleration measurements, and associated wires.	Required for AS-503 only.
	Measurements reduced from 377 to 222. S1 and F2 Telemetry Links and associated components removed. Removed Tape Recorder and VSWR assembly, and added a directional coupler.	Reduction in telemetry in going from R&D to Operational Vehicle.
	R4-602, R5-602 and R6-602 have capability of switching to a higher gain. (Capability only but not used on AS-504 because the system uses a latching relay. Second and third burns would probably exceed the range using the higher gain.)	During coast the rates are so low that a higher gain is desired to make the measurements useful.
Environmental Control Subsystem	7 heaters removed. Cold plate thermal isolators added.	Same net result using more desirable, permanent approach.
	Methanol/Water (M/W) pump pressure switch setting changed from 25.5 ±0.7 N/cm <sup>2</sup> (37 ±1 psia) to 22.8 ±0.7 N/cm <sup>2</sup> (33 ±1 psia). (Other ESE changes).	Help resolve AS-503 problem of Switching to pump number 2 at power transfer.
	M/W accumulator enlarged from 3090 cm <sup>3</sup> (189 in <sup>3</sup> ) to 6125 cm <sup>3</sup> (374 in <sup>3</sup> ) with improved design.	Allows filling earlier in countdown.
Emergency Detection System	20 second timer has been physically removed.	No longer required. Not active on AS-503.
Flight Program	Inclusion of third S-IVB burn capability. Digital Command System (DCS) required to remove inhibit for 2nd and 3rd burns which are at fixed attitudes and for fixed durations.	
	Deletion of variable azimuth requirements.	



Table B-4. IU Significant Configuration Changes (Continued)

SYSTEM	CHANGE	REASON
Flight Program (Continued)	<p>Inclusion of DCS navigation update capability.</p> <p>Modification of orbital attitude timeline.</p> <p>Switch Selectors for PU shift deleted due to Closed Loop PU operation (S-II only).</p> <p>Real time telemetry is executed continuously in orbit.</p> <p>Programmed sequence to close LH<sub>2</sub> continuous vents is entered in the event of an O<sub>2</sub>-H<sub>2</sub> burner malfunction.</p>	
I&C	DPI TM link deleted from CCS RF link and CPI TM link added to CCS RF link.	AS-504 only.
Navigation Guidance and Control	The ST-124M Platform end bell housings (outer gimbal pivots) were smaller than on previous vehicles. Blowers changed from mini cube to axial low flow.	This was part of the platform assembly redesign (spherical cover change effective on AS-503) involving the outer pivots, torque motors and slip ring assemblies.

a probe and latching mechanism in the command module docking tunnel to permit rigid docking and crew transfer to the LM.

The Launch Escape Tower (LET) is the forward most part of the Saturn V Apollo space vehicle. Basic configuration of the LET consists of an integral nose cone Q-ball, three rocket motors, a canard assembly, a structural skirt, a titanium-tube tower, and a boost protective cover. The purpose of the three rocket motors is tower jettison, escape, and pitch control. The LET is jettisoned shortly after S-II stage ignition in normal flight.

The CM is designed to accommodate the three astronauts. The CM is a conically shaped structure consisting of an inner pressure vessel (crew compartment) and an outer heat shield. The CM is approximately 3.39 meters (11.15 ft) long. Aluminum honeycomb panels and aluminum longerons are used to form the pressure tight crew compartment. Stainless steel honeycomb covered with an ablative material is used to construct the outer heat shield. The unified side hatch is hinged to the vehicle and provides quick opening and improved egress/ingress capabilities.

The SM is a cylindrical aluminum honeycomb shell with fore and aft aluminum honeycomb bulkheads. Six aluminum radial beams divide the SM into sectors. These beams have a triangular truss between the CM and SM

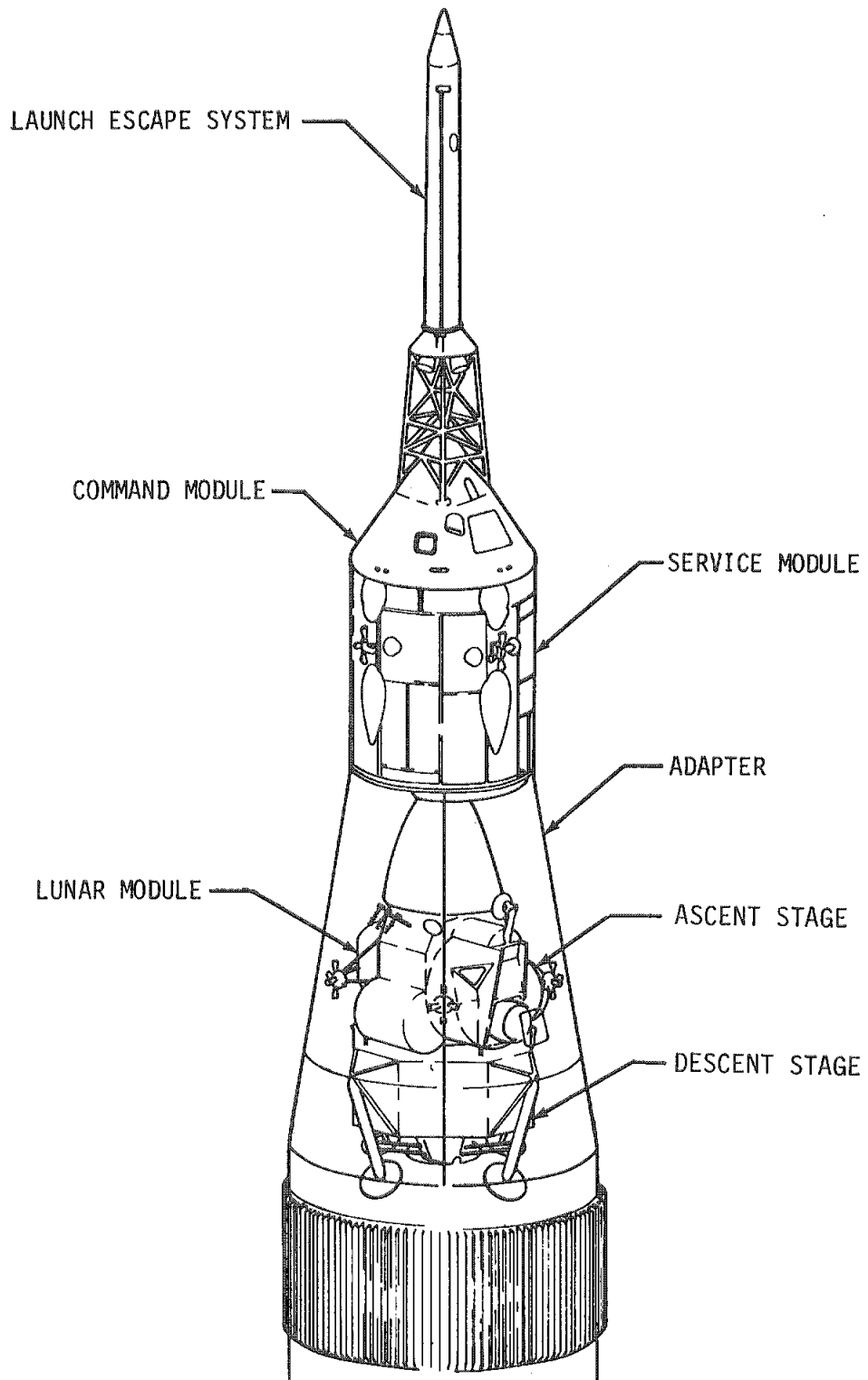


Figure B-6. Apollo Spacecraft

with pads at the apex to support the CM. The SM also houses the Service Propulsion System (SPS) which includes an engine and propellant tanks.

The SLA is a simple truncated cone measuring approximately 8.5 meters (28.0 ft) long and having forward and aft diameters of 3.9 meters (12.83 ft) and 6.6 meters (21.6 ft), respectively. There are four attachment points in the aft section of the SLA for the LM. The SLA is constructed in two sets of four panels, the panels being made from aluminum honeycomb. At CSM/S-IVB separation the forward section panels are jettisoned by a mild detonating explosive train.

The LM is a two-stage vehicle designed to descend two astronauts to the lunar surface, carry equipment for lunar exploration and return the crew to orbit through a rendezvous flight sequence. The lunar module (LM-3) was the first to accommodate inflight manned operations, and therefore differed considerably from the Apollo 5 (LM-1) configuration. The complete environmental control system was installed, whereas only those components necessary for equipment cooling had been installed for Apollo 5. The major changes to this system were therefore the addition of the suit environmental circuits, oxygen supplies, and water management subsystem. The entire complement of crew provisions, including the extravehicular mobility unit, were included. The guidance and navigation system included the abort guidance section and associated electronics and incorporated computer software necessary for rendezvous navigation and control. The landing gear was installed for the first time, together with the associated deployment pyrotechnics and circuitry, and the mission programmer functions required for the unmanned LM-1 mission were deleted. The drogue mechanism, which interfaces with the command module docking probe, was installed to permit passive docking after transposition.

APPROVAL

SATURN V LAUNCH VEHICLE FLIGHT EVALUATION REPORT

AS-504, APOLLO 9 MISSION

By Saturn Flight Evaluation Working Group

The information in this report has been reviewed for security classification. Review of any information concerning Department of Defense or Atomic Energy Commission programs has been made by the MSFC Security Classification Officer. The highest classification has been determined to be Unclassified.



Stanley L. Fragge  
Security Classification Officer

This report has been reviewed and approved for technical accuracy.



J. P. Lindberg  
Chairman, Saturn Flight Evaluation Working Group



Hermann K. Weidner  
Director, Science and Engineering



Lee B. James  
Saturn Program Manager

DISTRIBUTION:

MSFC:

Dr. von Braun, DIR  
 Mr. Shepherd, DIR  
 Dr. Rees, DEP-T  
 Mr. Goman, DEP-M  
 Dr. Stuhlinger, ADIR-S

E

Mr. Maus, E-DIR  
 Mr. Smith, E-S

PA

Mr. Slattery, PA-DIR

PM

Gen. O'Connor, PM-DIR  
 Dr. Mrazek, PM-DIR  
 Mr. Andressen, PM-PR-CM  
 Col. Teir, PM-SAT-IB-MGR  
 Mr. Huff, PM-SAT-E  
 Dr. Speer, PM-MO-MGR (4)  
 Mr. Belew, PM-AA-MGR  
 Mr. Brown, PM-EP-MGR  
 Mr. Smith, PM-EP-J  
 V. J. Norman, PM-MO  
 Mr. Stewart, PM-EP-F  
 Mr. L. James, PM-SAT-MGR  
 Mr. Bramlet, PM-SAT-MGR  
 Mr. Godfrey, PM-SAT-MGR  
 Mr. Burns, PM-SAT-T  
 Mr. Bell, PM-SAT-E  
 Mr. Rowan, PM-SAT-E  
 Mr. Moody, PM-SAT-Q  
 Mr. Webb, PM-SAT-P  
 Mr. Uraub, PM-SAT-S-IB/S-IC  
 Mr. Lahatte, PM-SAT-S-II  
 Mr. McCullough, PM-SAT-S-IVB  
 Mr. Duerr, PM-SAT-IU  
 Mr. Smith, PM-SAT-G  
 Col. Montgomery, PM-KM  
 Mr. Peters, PM-SAT-S-IVB  
 Mr. Wier, PM-SAT-IU  
 Mr. Ferrell, PM-EP-EJ  
 Dr. Constan, PM-MA-MGR  
 Mr. Riemer, PM-MA-OP  
 Mr. Balch, PM-MT-MGR  
 Mr. Auter, PM-MT-T  
 Mr. Sparks, PM-SAT-G  
 Mr. Ginn, PM-SAT-E  
 Mr. Haley, PM-SAT-S-IB/S-IC  
 Mr. Higgins, PM-SAT-S-IVB  
 Mr. Odom, PM-SAT-S-II  
 Mr. Stover, PM-SAT-S-II  
 Mr. Reaves, PM-SAT-Q  
 Mr. Wheeler, PM-EP-F  
 Mr. Johnson, PM-SAT-T  
 Mr. Cushman, PM-SAT-T (10)

S&E

Mr. Weidner, S&E-DIR  
 Mr. Richard, S&E-DIR  
 Dr. Johnson, S&E-R  
 Mr. Messer, S&E-P  
 Mr. Hamilton, MSC-RL

PD

Dr. Lucas, PD-DIR  
 Mr. Williams, PD-DIR (2)  
 Mr. Driscoll, PD-DIR  
 Mr. Goerner, PD-DO

S&E-AERO

Dr. Geissler, S&E-AERO-DIR  
 Mr. Jean, S&E-AERO-DIR  
 Mr. Dahm, S&E-AERO-A (2)  
 Mr. Holderer, S&E-AERO-A  
 Mr. Dunn, S&E-AERO-ADV  
 Mr. Elkin, S&E-AERO-AT  
 Mr. Wilson, S&E-AERO-AT  
 Mr. Jones, S&E-AERO-AT  
 Mr. Reed, S&E-AERO-AU  
 Mr. Guest, S&E-AERO-AU  
 Mr. Horn, S&E-AERO-D  
 Mr. Cremin, S&E-AERO-DA  
 Mr. Ryan, S&E-AERO-DD  
 Mr. Lindberg, S&E-AERO-F (33)  
 Mr. Baker, S&E-AERO-G  
 Mr. Hagood, S&E-AERO-P (3)  
 Mr. Jackson, S&E-AERO-P  
 Mr. Cummings, S&E-AERO-Y  
 Mr. O. E. Smith, S&E-AERO-Y

S&E-CSE

Dr. Haeussemann, S&E-CSE-DIR  
 Mr. Hoberg, S&E-CSE-DIR  
 Dr. McDonough, S&E-CSE-A  
 Mr. Aberg, S&E-CSE-S  
 Mr. Fichtner, S&E-CSE-G  
 Mr. Vann, S&E-CSE-S  
 Mr. Mack, S&E-CSE-I  
 Mr. Hammers, S&E-CSE-I

S&E-ASTR

Mr. Moore, S&E-ASTR-DIR  
 Mr. Digesu, S&E-ASTR-A  
 Mr. Stroud, S&E-ASTR-EA  
 Mr. Robinson, S&E-ASTR-ESA  
 Mr. Erickson, S&E-ASTR-ESA  
 Mr. Darden, S&E-ASTR-F  
 Mr. Justice, S&E-ASTR-FA  
 Mr. Vallely, S&E-ASTR-FO  
 Mr. Mink, S&E-ASTR-FR  
 Mr. Mandel, S&E-ASTR-G  
 Mr. Thomason, S&E-ASTR-G  
 Mr. Ferrell, S&E-ASTR-GSA  
 Mr. Powell, S&E-ASTR-I  
 Mr. Avery, S&E-ASTR-IM  
 Mr. Kerr, S&E-ASTR-IR  
 Mr. Threlkeld, S&E-ASTR-IT  
 Mr. Boehm, S&E-ASTR-M  
 Mr. Moore, S&E-ASTR-N  
 Mr. Lominick, S&E-ASTR-NFS  
 Mr. Nicaise, S&E-ASTR-NGI  
 Mr. Taylor, S&E-ASTR-R  
 Mr. Wolfe, S&E-ASTR-S

S&E COMP

Dr. Hoelzer, S&E-COMP-DIR  
 Mr. Prince, S&E-COMP-DIR  
 Mr. Fortenberry, S&E-COMP-A  
 Mr. Cochran, S&E-COMP-RR  
 Mr. Houston, S&E-COMP-RRM  
 Mr. Craft, S&E-COMP-R

S&E-ME

Mr. Siebel, S&E-ME-DIR  
 Mr. Wuencher, S&E-ME-DIR  
 Mr. Orr, S&E-ME-M  
 Mr. Franklin, S&E-ME-T

S&E-ASTN

Mr. Heimburg, S&E-ASTN-DIR  
 Mr. Hellebrand, S&E-ASTN-DIR

Mr. Palaoro, S&E-ASTN-DIR  
 Mr. Edwards, S&E-ASTN-DIR  
 Mr. Stein, S&E-ASTN-A  
 Mr. Kingsbury, S&E-ASTN-M  
 Mr. Earle, S&E-ASTN-P  
 Mr. Reilmann, S&E-ASTN-P  
 Mr. Thompson, S&E-ASTN-PA  
 Mr. Fuhrmann, S&E-ASTN-PM  
 Mr. Cobb, S&E-ASTN-PP (2)  
 Mr. Black, S&E-ASTN-PPE  
 Mr. Wood, S&E-ASTN-PT  
 Mr. Hunt, S&E-ASTN-S  
 Mr. Beam, S&E-ASTN-SLA  
 Mr. Blumrich, S&E-ASTN-SA  
 Mr. Katz, S&E-ASTN-SER  
 Mr. Showers, S&E-ASTN-SL  
 Mr. Frederick, S&E-ASTN-SS  
 Mr. Furman, S&E-ASTN-SJ  
 Mr. Green, S&E-ASTN-SVM  
 Mr. Grafton, S&E-ASTN-T  
 Mr. Marmann, S&E-ASTN-VAW  
 Mr. Lutonsky, S&E-ASTN-VAW  
 Mr. Devenish, S&E-ASTN-VNP (2)  
 Mr. Sells, S&E-ASTN-VOO  
 Mr. Schulze, S&E-ASTN-V (2)  
 Mr. Rothe, S&E-ASTN-XA  
 Mr. Griner, S&E-ASTN-XSJ  
 Mr. Boone, S&E-ASTN-XEK

S&E-QUAL

Mr. Grau, S&E-QUAL-DIR  
 Mr. Chandler, S&E-QUAL-DIR  
 Mr. Henritze, S&E-QUAL-A  
 Mr. Rushing, S&E-QUAL-PI  
 Mr. Klaus, S&E-QUAL-J  
 Mr. Brooks, S&E-QUAL-P (3)  
 Mr. Landers, S&E-QUAL-PC  
 Mr. Peck, S&E-QUAL-QVS  
 Mr. Brien, S&E-QUAL-R  
 Mr. Smith, S&E-QUAL-R  
 Mr. Wittmann, S&E-QUAL-T

S&E-SSL

Mr. Heller, S&E-SSL-DIR  
 Dr. Sieber, S&E-SSL-S

MS

MS-H  
 MS-I  
 MD-IP  
 MS-IL (8)  
 MS-D

CC-P

Mr. Wofford, CC-P

KSC

Dr. Debus, CD (5)  
 Adm. Middleton, AP  
 Mr. Petrone, LO  
 Dr. Gruene, LV  
 Mr. Rigell, LV-ENG  
 Mr. Sendler, IN  
 Mr. Mathews, AP  
 Dr. Knothe, EX-SCI  
 Mr. Edwards, LV-INS  
 Mr. Fannin, LV-MEC  
 Mr. Pickett, LV-TMO  
 Mr. Rainwater, LV-TMO  
 Mr. Bell, LV-TMO-3  
 Mr. Lealman, LV-GDC  
 Mr. Preston, DE  
 Mr. Mizell, LV-PLN-12  
 Mr. O'Hara, LV-TMO  
 Mr. Brown, AP-SVO-3  
 Mr. Smith, AP-SVO

EXTERNAL

Headquarters, National Aeronautics & Space Administration  
Washington, D. C. 20546

Dr. Mueller, M  
Gen. Phillips, MA  
Gen. Stevenson, MO (3 copies)  
Mr. Hage, MO  
Mr. Schneider, MO-2  
Capt. Freitag, MC  
Capt. Hoicomb, MAO  
Mr. White, MAR (2 copies)  
Mr. Day, MAT (10 copies)  
Mr. Wilkinson, MAB  
Mr. Kubat, MAP  
Mr. Wagner, MAS (2 copies)  
Mr. Armstrong, MB  
Mr. Mathews, ML (3 copies)  
Mr. Lord, MT  
Mr. Lederer, MY

Director, Ames Research Center: Dr. H. Julian Allen  
National Aeronautics & Space Administration  
Moffett Field, California 94035

Director, Flight Research Center: Paul F. Bikle  
National Aeronautics & Space Administration  
P. O. Box 273  
Edwards, California 93523

Goddard Space Flight Center  
National Aeronautics & Space Administration  
Greenbelt, Maryland 20771  
Attn: Herman LaGow, Code 300

John F. Kennedy Space Center  
National Aeronautics & Space Administration  
Kennedy Space Center, Florida 32899  
Attn: Technical Library, Code RC-42  
Mrs. L. B. Russell

Director, Langley Research Center: Dr. Floyd L. Thompson  
National Aeronautics & Space Administration  
Langley Station  
Hampton, Virginia 23365

Lewis Research Center  
National Aeronautics & Space Administration  
21000 Brookpark Road  
Cleveland, Ohio 44135  
Attn: Dr. Abe Silverstein, Director  
Robert Washko, Mail Stop 86-1  
E. R. Jonash, Centaur Project Mgr.

Manned Spacecraft Center  
National Aeronautics & Space Administration  
Houston, Texas 77058  
Attn: Director: Dr. Robert R. Gilruth, AA  
Mr. Low, PA  
Mr. Arabian, ASPO-PT (15 copies)  
Mr. Pauls, FC-5  
J. Hamilton, RL (MSFC Resident Office)

Director, Wallops Station: R. L. Krieger  
National Aeronautics & Space Administration  
Wallops Island, Virginia 23337

Director, Western Operations Office: Robert W. Kamm  
National Aeronautics & Space Administration  
150 Pico Blvd.  
Santa Monica, California 90406

Scientific and Technical Information Facility  
P. O. Box 5700  
Bethesda, Maryland 20014  
Attn: NASA Representative (S-AK/RKT) (25 copies)

Jet Propulsion Laboratory  
4800 Oak Grove Drive  
Pasadena, California 91103  
Attn: Irl Newlan, Reports Group (Mail 111-122)  
H. Levy, CCMTA (Mail 179-203) (4 copies)

Office of the Asst. Sec. of Defense for Research  
and Engineering  
Room 3E1065  
The Pentagon  
Washington, D. C. 20301  
Attn: Tech Library

Director of Guided Missiles  
Office of the Secretary of Defense  
Room 3E131  
The Pentagon  
Washington, D. C. 20301

Central Intelligence Agency  
Washington, D. C. 20505  
Attn: OCR/DD/Publications (5 copies)

Director, National Security Agency  
Ft. George Mead, Maryland 20755  
Attn: C3/TDL

U. S. Atomic Energy Commission, Sandia Corp.  
University of California Radiation Lab.  
Technical Information Division  
P. O. Box 808  
Livermore, California 94551  
Attn: Clovis Craig

U. S. Atomic Energy Commission, Sandia Corp.  
Livermore Br., P. O. Box 969  
Livermore, California 94551  
Attn: Tech Library

Commander, Armed Services Technical Inf. Agency  
Arlington Hall Station  
Arlington, Virginia 22212  
Attn: TIPCR (Transmittal per Cognizant Act  
Security Instruction) (5 copies)

Commanding General  
White Sands Proving Ground  
New Mexico 88002  
Attn: ORD BS-OMT10-TL (3 copies)

Chief of Staff, U. S. Air Force  
The Pentagon  
Washington, D. C. 20330  
1 Cpy marked for DCS/D AFDRD  
1 Cpy marked for DCS/D AFDRD-EX

Commander-In-Chief  
Strategic Air Command  
Offutt AFB, Nebraska 68113  
Attn: Director of Operations, Missile Division

Commander  
Arnold Engineering Development Center  
Arnold Air Force Station, Tennessee 37389  
Attn: Tech Library (2 copies)

Commander  
Air Force Flight Test Center  
Edwards AFB, California 93523  
Attn: FTOTL

Commander  
Air Force Missile Development Center  
Holloman Air Force Base  
New Mexico 88330  
Attn: Tech Library (SRLT)

Headquarters  
6570th Aerospace Medical Division (AFSC)  
U. S. Air Force  
Wright-Patterson Air Force Base, Ohio 45433  
Attn: H. E. Vongierke

Systems Engineering Group (RTD)  
Attn: SEPIR  
Wright-Patterson, AFB, Ohio 45433

AFETR (ETLLG-1)  
Patrick AFB, Florida 32925

EXTERNAL (CONT.)

Director  
U. S. Naval Research Laboratory  
Washington, D. C. 20390  
Attn: Code 2027

Chief of Naval Research  
Department of Navy  
Washington, D. C. 20390  
Attn: Code 463

Chief, Bureau of Weapons  
Department of Navy  
Washington, D. C. 20390  
1 Cpy to RESI, 1 Cpy to SP,  
1 Cpy to AD3, 1 Cpy to REW3

Commander  
U. S. Naval Air Missile Test Center  
Point Mugu, California 93041

AMSMI-RBLD; RSIC (3 copies)  
Bldg. 4484  
Redstone Arsenal, Alabama 35809

Aerospace Corporation  
2400 East El Segundo  
El Segundo, California 90245  
Attn: D. C. Bakeman

Aerospace Corporation  
Reliability Dept.  
P. O. Box 95085  
Los Angeles, California 90045  
Attn: Don Herzstein

Bellcomm, Inc.  
1100 Seventeenth St. N. W.  
Washington, D. C. 20036  
Attn: Miss Scott, Librarian

The Boeing Company  
P.O. Box 1680  
Huntsville, Alabama 35807  
Attn: S. C. Krausse, Mail Stop AD-60  
(30 copies)  
J. B. Winch, Mail Stop JA-52  
(1 copy)

The Boeing Company  
P.O. Box 58747  
Houston, Texas 77058  
Attn: H. J. McClellan, Mail Stop HH-05  
(2 copies)

The Boeing Company  
P.O. Box 29100  
New Orleans, Louisiana 70129  
Attn: S. P. Johnson, Mail Stop LT-84  
(10 copies)

Mr. Norman Sissenwine, CREW  
Chief, Design Climatology Branch  
Aerospace Instrumentation Laboratory  
Air Force Cambridge Research Laboratories  
L. G. Hanscom Field  
Bedford, Massachusetts 01731

Lt/Col. H. R. Montague  
Det. 11, 4th Weather Group  
Eastern Test Range  
Patrick Air Force Base, Florida 33564

Mr. W. Davidson  
NASA Resident Management Office  
Mail Stop 8890  
Martin Marietta Corporation  
Denver Division  
Denver, Colorado 80201

Chrysler Corporation Space Division  
Huntsville Operation  
1312 N. Meridian Street  
Huntsville, Alabama 35807  
Attn: J. Fletcher, Dept. 4830  
M. L. Bell, Dept. 4830

McDonnell Douglas Astronautics Company  
Missile & Space Systems Division/SSC  
5301 Bolsa Avenue  
Huntington Beach, California 92646  
Attn: R. J. Mohr (40 copies)

Grumman Aircraft Engineering Corp.  
Bethpage, Long Island, N. Y. 11714  
Attn: NASA Resident Office  
John Johansen

International Business Machine  
Mission Engineering Dept. F103  
150 Sparkman Dr. NW  
Huntsville, Alabama 35805  
Attn: C. N. Hansen (15 copies)

Martin Company  
Space Systems Division  
Baltimore, Maryland 21203  
Attn: W. P. Sommers

North American Rockwell/Space Division  
12214 S. Lakewood Blvd.  
Downey, California 90241  
Attn: R. T. Burks (35 copies)

Radio Corporation of America  
Defense Electronic Products  
Data Systems Division  
8500 Balboa Blvd.  
Van Nuys, California 91406

Rocketdyne  
6633 Canoga Avenue  
Canoga Park, California 91303  
Attn: T. L. Johnson (10 copies)

Foreign Technology Division  
FTD (TDPSSL)  
Wright-Patterson Air Force Base, Ohio 45433

Mr. George Mueller  
Structures Division  
Air Force Flight Dynamics Laboratory  
Research and Technology Division  
Wright-Patterson Air Force Base, Ohio 45433

Mr. David Hargis  
Aerospace Corporation  
Post Office Box 95085  
Los Angeles, California 90045

Mr. H. B. Tolefson  
DLA-Atmospheric Physics Branch  
Mail Stop 240  
NASA-Langley Research Center  
Hampton, Virginia 23365

Mr. Chasteen  
Sperry Rand  
Dept. 223  
Blue Spring Road  
Huntsville, Ala.

EXTERNAL (CONT.)

J. E. Trader  
NASA Resident Manager's Office  
McDonnell Douglas Astronautics Corp.  
5301 Balsa Avenue  
Huntington Beach, California 92646

L. C. Curran  
NASA Resident Manager's Office  
North American Rockwell/Space Division  
12214 Lakewood Blvd.  
Downey, California 90241

L. M. McBride  
NASA Resident Manager's Office  
North American Rockwell/Rocketdyne  
6633 Canoga Avenue  
Canoga Park, California 91303

C. M. Norton  
NASA Resident Manager's Office  
International Business Machines  
150 Sparkman Drive  
Huntsville, Alabama 35804

N. G. Futral  
NASA Resident Manager's Office  
North American Rockwell/Space Division  
69 Bypass NE  
McAlester, Oklahoma 74501

C. Flora  
McDonnell Douglas Astronautics Corp.  
Sacramento Test Center  
11505 Douglas Avenue  
Rancho Cordova, California 95670